

BOARD OF DIRECTORS, 1957

- *J. T. Henderson, *President*
- Yasujiro Niwa, *Vice-President*
- *W. R. G. Baker, *Treasurer*
- *Haraden Pratt, *Secretary*
- *D. G. Fink, *Editor*
- *J. D. Ryder, *Senior Past President*
- *A. V. Loughren, *Junior Past President*

1957

- J. G. Brainerd (R3)
- J. F. Byrne
- J. J. Gershon (R5)
- A. N. Goldsmith
- A. W. Graf
- W. R. Hewlett
- R. L. McFarlan (R1)
- *Ernst Weber
- C. F. Wolcott (R7)

1957-1958

- H. R. Hegbar (R4)
- E. W. Herold
- K. V. Newton (R6)
- A. B. Oxley (R8)
- F. A. Polkinghorn (R2)
- J. R. Whinnery

1957-1959

- D. E. Noble
- Samuel Seely

**Members of Executive Committee*

George W. Bailey,
Executive Secretary

- Evelyn Benson, *Assistant to the Executive Secretary*
- John B. Buckley, *Chief Accountant*
- Laurence G. Cumming, *Technical Secretary*
- Emily Sirjane, *Office Manager*

EDITORIAL DEPARTMENT

- Alfred N. Goldsmith,
Editor Emeritus
- D. G. Fink, *Editor*
- E. K. Gannett,
Managing Editor
- Helene Frischauer,
Associate Editor

ADVERTISING DEPARTMENT

- William C. Copp,
Advertising Manager
- Lillian Petranek,
Assistant Advertising Manager

EDITORIAL BOARD

- D. G. Fink, *Chairman*
- E. W. Herold, *Vice-Chairman*
- E. K. Gannett
- Ferdinand Hamburger, Jr.
- T. A. Hunter
- A. V. Loughren
- W. N. Tuttle

Authors are requested to submit three copies of manuscripts and illustrations to the Editorial Department, Institute of Radio Engineers, 1 East 79 St., New York 21, N. Y.

Responsibility for the contents of papers published in the PROCEEDINGS OF THE IRE rests upon the authors. Statements made in papers are not binding on the IRE or its members.



Change of address (with 15 days advance notice) and letters regarding subscriptions and payments should be mailed to the Secretary of the IRE, 1 East 79 Street, New York 21, N. Y. All rights of publication, including foreign language translations are reserved by the IRE. Abstracts of papers with mention of their source may be printed. Requests for republication should be addressed to The Institute of Radio Engineers.

PROCEEDINGS OF THE IRE®

Published Monthly by

The Institute of Radio Engineers, Inc.

VOLUME 45

September, 1957

NUMBER 9

CONTENTS

Ronald L. McFarlan, Director, 1956-1957.....	1184
Poles and Zeros	1185
Scanning the Issue	1186
6189. Electronics and the IRE—1967..... <i>Donald G. Fink</i>	1187
6190. A History of Some Foundations of Modern Radio-Electronic Technology..... <i>J. H. Hammond and E. S. Purington</i>	1191
6191. Description and Operating Characteristics of the Platinotron—A New Microwave Tube Device..... <i>William C. Brown</i>	1209
6192. The Role of Stratospheric Scattering in Radio Communication..... <i>H. G. Booker and W. E. Gordon</i>	1223
6193. Carrier Generation and Recombination in P-N Junctions and P-N Junction Characteristics..... <i>C. T. Sah, R. N. Noyce, and W. Shockley</i>	1228
6194. Digital Compensation for Control and Simulation..... <i>Julius Tou</i>	1243
6195. Postcast Control of Damped Oscillatory Systems..... <i>Otto J. M. Smith</i>	1249
6196. Synchronization of Oscillators by Periodically Interrupted Waves..... <i>Donald W. Fraser</i>	1256
6197. Theory and Operation of Crystal Diodes as Mixers..... <i>G. C. Messenger and C. T. McCoy</i>	1269
Correspondence:	
6198. Semantic Constraints in the Analysis of Communication Systems..... <i>A. Hauptschein and L. S. Schwartz</i>	1284
6199. Microwave Power Measurements Employing Electron Beam Techniques..... <i>W. J. Hoskin</i>	1285
6200. Hysteresis Heating of Microwave Ferrites..... <i>W. N. Honeyman and R. S. Cole</i>	1285
6201. Application of the Potential Analog in Multicavity Klystron Design and Operation..... <i>Sriramamurti V. Yadavalli</i>	1286
6202. Superregenerative Masers..... <i>P. F. Chester and D. I. Bolef</i>	1287
6203. Maximum Efficiency of the Solid-State Maser..... <i>H. Heffner</i>	1289
6204. The Phase-Shift Method of Single-Sideband Signal Reception..... <i>Harold M. Lewis</i>	1289
6205. A Third Method of Generation and Detection of Single-Sideband Signals..... <i>Harold M. Lewis</i>	1289
6206. Radar Echoes from Overdense Meteor Trails under Conditions of Severe Diffusion..... <i>G. S. Hawkins and D. F. Winter</i>	1290
6207. The Theoretical Sensitivity of the Dicke Radiometer..... <i>L. D. Storn</i>	1291
6208. Prediction of Semiconductor Surface Response to Ambients by Use of Lewis Acid-Base Theory..... <i>C. G. Peattie and J. R. Macdonald</i>	1292
6209. Nonreciprocal Two-Port Measurement Based on an Averaging Technique..... <i>Helmut M. Altschuler</i>	1293
6210. Signal Flow Graphs..... <i>William W. Happ</i>	1293
6211. Napierian Logarithms..... <i>M. S. Corrington</i>	1294
Contributors	1294
IRE News and Radio Notes	
Calendar of Coming Events.....	1297
Available Back Issues of IRE Transactions.....	1299
Obituaries.....	1300
Technical Committee Notes.....	1301
6212. Books	1302
Professional Groups.....	1302
Sections and Subsections.....	1302
Programs.....	1305
6213. Abstracts of IRE Transactions.....	1311
6214. Abstracts and References.....	1313

ADVERTISING SECTION

Meetings with Exhibits.....	6A	News—New Products..	24A	Notes.....	106A
Professional Group		Membership.....	32A	Positions Wanted....	134A
Meetings.....	10A	IRE People.....	62A	Positions Open.....	136A
Section Meetings.....	22A	Industrial Engineering		Advertising Index....	197A



THE COVER—The Natalia, an experimental boat operated by the Hammond Laboratory, was used in 1914-1915 for developing some of the earliest forms of automatic pilot, radio control and target seeking devices. These and other important developments during the early days of radio, which remained undisclosed for many years because of military security, are disclosed for the first time in a paper of unusual historical significance on page 1191 of this issue.

Copyright: © 1957, by the Institute of Radio Engineers, Inc.



Ronald L. McFarlan

DIRECTOR, 1956–1957

Ronald L. McFarlan was born on March 8, 1905 in Cincinnati, Ohio. He attended the University of Cincinnati and subsequently the University of Chicago, from which latter institution he received the Ph.D. in physics in 1930. His next two years were spent as a National Research Council Fellow in physics at Harvard University, and were followed by three more years as an instructor at Harvard.

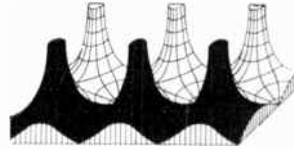
Dr. McFarlan's industrial career has included positions as chief physicist of the United Drug Company, and later the B. B. Chemical Company, and also as director of research for the Bulova Watch Company. For about eight years he was executive assistant to the director of equipment engineering, Raytheon Manufacturing Company, and is presently a consultant to the DATAmatic Corporation and the Raytheon Manufacturing Company.

Dr. McFarlan's early professional work was in

the fields of X-ray diffraction and scattering, ultraviolet spectroscopy, and electronic instrument design and navigation. He has been associated with the management of projects including electronic digital computers, radar, automatic guidance and control, microwave communication, sonar echo ranging, and depth sounding equipment. He is the holder of several patents, and the author of a number of articles in the electronic and optical fields.

Dr. McFarlan is a member of Sigma Xi, the American Physical Society, the American Chemical Society, the Institute of the Aeronautical Sciences, and the American Society of Naval Engineers. He has been Vice-Chairman and Chairman of the Boston Chapter of the Professional Group on Engineering Management, Chairman of the Boston Section, and a Senior Member of the IRE since 1951.

Poles and Zeros



Declassified. This issue contains a most interesting historical paper by John Hays Hammond, Jr. and E. S. Purington (page 1191). We think it significant that this paper presents, in part, technical information not heretofore published because, as the authors state, the work was performed under wraps of military security before, during, between and after World Wars I and II. The span of the story covers 50 years, and the fact the security measures could have been operative over such a period of time is food for uneasy thought. We do not claim that security classification has actually prevented until now the publication of information on, say, radio-controlled torpedo developments carried out in 1925. But it is obvious that classification has impeded the dissemination of knowledge by impounding information in files and requiring a lot of effort, not to say a change of heart, to dig it out, get it declassified and published. There are, of course, many excellent cases of early and rapid declassification, of which the M.I.T. Radiation Laboratory Series is a prime example. But these are exceptional.

Several months ago, we had the privilege of attending the first Army Science Conference at West Point. There we found the classification problem in particularly sharp focus. The conference was planned particularly to provide an opportunity, not otherwise available, for engineers and scientists in Army laboratories to present papers on their work, the majority of them classified. Attendance was by invitation only, and the strictest measures were taken to prevent the information from reaching the ears of any but the 416 invitees. Of the 101 papers presented, 29 were in the field of electronics and several others bordered on it. The papers were of high calibre and many of them commanded particular attention because of the "sensitive" subjects with which they dealt. Examples: (titles unclassified) "A Method of Locating Nuclear Detonations," "Detection and Tracking of Missiles by Infrared Techniques," "Ionospheric Effects of Nuclear Explosions," "Radar Observation of Atomic Clouds." The last named paper, by D. M. Swingle of the U. S. Army Signal Engineering Laboratories, won a prize of \$500 and \$3,500 in other prizes were awarded for papers in the fields of medicine, armor, ballistics, meteorology and missiles. All in all, the Army did itself proud. We don't quarrel with the present necessity of classifying papers presented at this conference. But we can't help wondering whether the paper on observation of atomic clouds must be forbidden to the PROCEEDINGS for the next 50 years.

All of which reminds us that the Institute, by the terms of the first paragraph of its Constitution, is committed to the dissemination of technical information and must, therefore, stand apart from sponsorship of

classified meetings. The policy is well stated in the Professional Groups Manual. In essence, it requires that inclusion of classified sessions within the framework of the IRE-sponsored conferences must be avoided as a matter of principle. However, classified meetings sponsored by another organization may be held in conjunction with IRE conferences, provided that the program and publicity make it clear that the IRE does not sponsor the classified meeting.

WESCON Record. We are pleased to announce a new Institute publication, the *IRE WESCON Convention Record*, which will appear late this fall and annually thereafter. The WESCON Record will follow closely the format of the National Convention Record and its purpose is identical. The program of technical papers at WESCON has grown amazingly in recent years; 225 papers were presented last month in six simultaneous sessions—a close second to the 280 papers in eight concurrent sessions which were presented in New York last March.

The footsore and brainweary conventioneer may well wonder how to encompass such programs, and many of us long for the good old days when one set of ears and eyes sufficed to take in the whole show. But industrial growth and a proliferating technology cannot be gainsaid. The IRE has 26 Professional Groups and the engineers inhabiting them are right in insisting on the privilege of hearing reports on the frontiers of their special fields of interest.

The suggestion that simultaneous sessions might be avoided by holding many smaller single-program conventions is not without merit. IRE participates in many such as the Radio Fall Meeting and the Cincinnati Television Conference. The many-little-get-togethers proposal fails to take account, however, of the up-and-coming youngsters and many busy oldsters who cannot afford time or train fare for more than one or two shows in a year. These numerous brethren want maximum exposure to papers and exhibits when they go to the big city. The fact that maximum exposure often means a decision among three or four equally interesting papers all presented at once is uncomfortable, but not fatal if assurance is given that substantially all the papers will be published shortly after the convention closes. This is the assurance that the two Convention Records give.

The presence henceforth of two sister Convention Records offers the blessings of competition. By pitting one against the other in the matters of completeness and promptness of publication, we expect to better the already excellent record. Full information on how to order any or all of the ten parts of the WESCON Record is given on page 1310 of this issue.—D.G.F.

Scanning the Issue

Electronics and the IRE—1967 (Fink, p. 1187)—This month the IRE STUDENT QUARTERLY is carrying an absorbing talk, presented at several IRE meetings last spring, in which a leading engineer and observer of the scene looks ahead at electronics in the next decade and forecasts the most promising and challenging areas for new technical developments. The author also has some important things to say about the role of the IRE in the years ahead. Because of the keen interest with which the talk was received by many members, the text is reprinted in this issue in the belief that it will be of widespread interest to the membership.

A History of Some Foundations of Modern Radio—Electronic Technology (Hammond and Purington, p. 1191)—The PROCEEDINGS presents this month a major contribution to the early history of radio. The authors describe for the first time important pioneering work carried out in the Hammond Laboratories during the period 1912–1928 which, because of its military nature, has not previously been disclosed. This work, which began with radio-controlled ships and torpedoes, led to a number of notable original developments in the realm of control and homing devices, nondetector applications of the triode, intermediate-frequency type systems and FM and related circuitries, which in retrospect could be viewed as the precursors of many of our modern radio-electronic techniques. Equally important, this paper sheds additional light on the early work of many major pioneers of radio. In particular, it brings out hitherto untold important contributions of Fritz Lowenstein in converting de Forest's grid-audion detector into an amplifier prior to 1912 and in getting a triode to oscillate early in 1912.

Description and Operating Characteristics of the Platinotron—A New Microwave Tube Device (Brown, p. 1209)—The platinotron is a new type of high-power microwave tube that has been developed for radar applications. Physically it is quite similar to a magnetron, the principal difference being that the RF circuit within the device, instead of forming a closed loop with one external connection to it, is brought out to two separate input and output terminals. This difference results in a device with completely different performance features. Since it is a two-terminal device, it can be operated as an amplifier as well as an oscillator, and in fact operates as a passive network when the signal direction is reversed. The broad bandwidth and high efficiency of the platinotron mark it as a substantial contribution to the microwave field.

The Role of Stratospheric Scattering in Radio Communication (Booker and Gordon, p. 1223)—It is well established that there are two distinctly different types of scatter transmission of radio waves: tropospheric, which is useful at frequencies above 100 mc at distances less than 600 miles, and ionospheric, at frequencies of 25 to 60 mc and distances of 600 to 1200 miles. This paper reveals that a third type of scattering occurs in the stratosphere, the region between the troposphere and the ionosphere extending from about 7 to 25 miles above the earth. It is shown that stratospheric scattering becomes pronounced at ranges above 400 miles, predominating over tropospheric scattering at the higher frequencies and playing an important role even at some of the lower frequencies associated with ionospheric transmission. This work makes a fundamental contribution and highly important extension to the theory of scatter transmission at long ranges.

Carrier Generation and Recombination in P - N Junctions and P - N Junction Characteristics (Sah, *et al.*, p. 1228)—The ideal theory that has been developed for a p - n junction, while it accounts quite well for the electrical characteristics of germanium p - n junctions at room temperatures, does not agree with some of those measured for silicon junctions, especially with respect to their current characteristics. This paper pre-

sents an important new theory of p - n junctions that does away with these discrepancies by taking into account the high recombination and generation of carriers in the space-charge or transition region lying between the p region and n region of the junction.

Digital Compensation for Control and Simulation (Tou, p. 1243)—In a digital or sampled-data system, it is possible to make the output signal equal the input at the sampling instants. Thus, if the sampling rate is kept high, an almost perfect control system can be obtained. This paper is concerned with such a system which utilizes a digital computer to detect the error between the output and input signals and to compensate the system accordingly. The author presents an interesting technique for designing a suitable program for the computer which improves the stability and reduces the error of digital control systems.

Posicast Control of Damped Oscillatory Systems (Smith, p. 1249)—The subject of feedback control systems again comes up for discussion, but from a different approach than in the preceding paper. Here the situation considered is analogous to a man holding a weight suspended from a string, who is asked to move it from point A to point C and bring it to rest there as quickly as possible. The solution proposed by the author is for the man to move his hand, not to C , but to some intermediate point B . The weight will swing beyond B and then start to return. Point B is so chosen that at the instant the weight starts to return, it is at point C . If at this same instant the man quickly moves his hand from B to C , the weight will remain at C without any subsequent oscillations. The time taken for the operation is only one-half the natural period of the system. The author then embellishes on this two-step method and develops a three-step approach in which the input pulse is broken into a positive, then a negative, and finally a positive pulse. This brings the response time of one-half cycle down to one-quarter cycle or less. Thus to achieve the quickest response time, one simply adjusts the system for the shortest possible cycle, *i.e.*, the maximum possible resonant frequency, and then applies the three-step control to completely remove the oscillatory component in the output.

Synchronization of Oscillators by Periodically Interrupted Waves (Fraser, p. 1256)—This study concerns a subject which occurs very commonly but is not generally well understood—the direct synchronizations of oscillators. Previous analyses have not described adequately the action that takes place within the pulling region, and have not considered at all the problem of synchronization when the signal is other than a cw signal. It is shown in this paper that using a cw signal that is periodically interrupted produces a form of synchronization such that the average frequency of the oscillator is identically equal to the fundamental component of the synchronizing signal or to any selected sideband. This results in interesting crystal-saving techniques in which one oscillator may be synchronized by any of ten or more sidebands. This work also suggests the possibility of further novel developments in the realm of frequency division and multiplication.

Theory and Operation of Crystal Diodes as Mixers (Messenger and McCoy, p. 1269)—A comprehensive study of the fundamental aspects of germanium and silicon diodes is presented which interrelates their physical and electrical properties to their operating characteristics at uhf and microwave frequencies. These considerations lead to a good understanding of the factors effecting conversion loss, noise temperature and noise figure, which in turn can be applied to improve the sensitivity of receivers. Because it ties together the physics of the semiconductor with the circuit application, this work will be of value both to those in radar and uhf communications and to semiconductor device manufacturers and users.

Electronics and the IRE—1967*

DONALD G. FINK
Editor, Institute of Radio Engineers

It is customary at the March annual meeting of the Institute to have a keynote speech by one of our more distinguished members. This year, the talk was given by our Editor, Mr. Donald G. Fink; those who heard him were outspoken in their praise of a bold, inspiring, and stimulating preview of the Institute's next ten years. With appropriate modesty, and perhaps the caution which comes from experience in prophecy, Don hesitated to suggest publication. Several of us connected with editorial matters felt that the entire Institute would wish to read what he said and to retain it for reference.—*Vice-Chairman, Editorial Board*

THE PURPOSE of this review is to examine certain trends in electronics and to forecast the role of the Institute of Radio Engineers in furthering the aims and interests of its members during the next ten years. This next decade has more promise for engineers in electronics and the allied arts than any similar period in history, but it is not so clear that the IRE will grow and prosper in proportion to the opportunities presented to its members as individuals.

The uncertainty arises from the fact that the IRE embraces many distinct and separate technical disciplines and is moving into many new fields and extending its authority over old ones. It faces, therefore, two difficult problems which may be classed loosely as competition: first, competition with other societies; and second, competition within itself, as each professional group strives for an increased share of the Institute's resources.

First, what is the justification for the statement that the next ten years are full of promise for the confederation of technical workers known as the IRE? The key words are *communications*, *automation*, and *nuclear power*.

Radio communications, in the broad sense that includes broadcasting and aids to navigation, is the technology for which the IRE was founded. But today only a minority of the members of IRE would claim that "radio engineer" best describes their calling. In fact the word "radio" does not appear once among the names of the IRE Professional Groups, and only one half of the Group organizations have any direct interest in radio frequency techniques as such.

Does this mean that we have just about pumped dry the well of radio communications and that the best opportunities for IRE members lie in fields outside the radio arts? No, I think not. There are solid opportunities not merely to extend existing radio systems to wider fields but also to devise wholly new techniques.

In predicting new areas of technical work, it is wise to base the prediction on a fundamental need. In radio

the growing shortage of space in the spectrum, gives rise to an urgent need to find better ways of using the spectrum space we now have. What is needed is a really potent technique of compressing the information content of radio signals, a technique which information theory gives us every hope to achieve. When it is achieved, we can expect the wholesale abandonment of many forms of existing communications systems and a vast market for new equipment.

Last December the PROCEEDINGS OF THE IRE was wholly devoted to one big step in the direction of better spectrum usage, the single-sideband technique. Already in use in vestigial form in television and in highly refined form in point-to-point radio telephony, SSB is about to invade the mobile communications field and there is at least an open chance that it may ease the burdens of standard broadcasting (a compatible form of single-sideband transmission has been under test by AM station WMGM in New York.)

This opportunity is clearly just ahead, due for a vast extension in the next decade. So is the opportunity to reduce interference by the use of highly directional systems, and to remove many classes of traffic from the open-space spectrum altogether by building cable, wire, and waveguide transmission systems of vastly greater capacity than they now possess.

It has often been supposed that the long-term opportunity in spectrum conservation lies in Shannon's law governing noise and bandwidth in communication systems, which states that a given excellence of transmission can be achieved on as small a bandwidth as we choose so long as the signal is properly encoded and sufficient power is provided in the transmitted signal. But this law offers almost no hope of relieving the spectrum shortage because the required increase in power becomes enormous as the bandwidth is reduced even slightly. For example, using the optimum method of coding, the theory states that to cut off two megacycles out of the four in the video spectrum now used in transmitting a television picture, while preserving the customary 40-db signal-to-noise ratio, the transmitter power would have to be increased by 10,000 times. Such

* Original manuscript received by the IRE, May 9, 1957. Reprinted from the IRE STUDENT QUARTERLY, September, 1957.

power now completely eludes us, and even if we knew how to generate it, the power bill for the television station would increase from about \$25 dollars per day to several hundred thousand dollars per day, and this would put the broadcaster into receivership in the first week.

So we can be pardoned perhaps for removing the power-bandwidth exchange from any expectation of substantial realization in the next decade. But one way or another we must find ways of communicating intelligence more efficiently over limited channels. Herein lies the challenge and the opportunity for communications engineers.

The second key word is automation, more particularly the electronic aspects of automation. Automation may be defined as the automatic performance by machinery of duties which would otherwise demand the active cooperation of the senses, muscles, and minds of human beings—duties which occupy the working hours of the world's population. The overwhelming majority of human wage earning is so largely repetitive that sooner or later it generates a massive sense of boredom. Fortunate indeed is the man who finds each working day a new and stimulating challenge. He is perhaps one in ten thousand, or even a hundred thousand, workers. All the others have had to make an adjustment to the repetitive boredom of earning a living.

We have indeed come a long way in transferring dangerous and heavy tasks to automatic machinery. But for the most part we still assign the control of machines to human beings, and in so doing have actually added to boredom by dehumanizing the worker's function. To correct this situation we need a machine to control the machine. This supermachine must be capable of performing a particular function which up to now has demanded human control—the ability to exercise judgment, such as that performed in inspecting the quality of a product. Until recently, inspection of any but the simplest kind has been considered outside the range of machine operations; it has demanded the keen eye, the sharp ear, or the delicate sense of touch of a human operator.

Today we now accept the proposition that such tasks can be performed by machine, given an intelligent redesign of the product and processes. The only question is economic: will it pay to convert to automated production? Thus far, in the vast majority of the cases attempted, it has paid off. And it will pay off increasingly in the next decade. One possibility is that the labor content of goods and services will thereby be so reduced that, by 1967, we will have achieved a four-day work week.

But the big challenge in automation, like the challenge of bandwidth in communications, lies a step ahead of automatic production and inspection. The big step ahead is to automatic reasoning and the making of decisions. This is a function of the brain that borders so closely on the creative that computer specialists are by

no means certain that it falls within the capabilities of machines, however intricate. But we have reason to believe that what passes for reasoning in making many decisions is in reality a series of very rapid trial-and-error comparisons of causes and their effects. When an executive makes a decision, at least the types of decisions needed in the day-to-day operation of many industrial and commercial establishments, he does so by examining possible alternatives and matching the imagined outcome with the desired result. This process of reasoning is carried out without the reasoner being aware of it, and at such high speed that it can be explained only by assuming that millions of synaptic processes have been brought into play in the course of a second.

When we try to imagine a machine capable of such goings on, we find that speed and the number of synaptic processes are not the limiting factors. Computers having speed and complexity equal to that of the brain are in principle possible. The difficulty lies in the enormous adaptability of the human brain, particularly the ease with which it devises its own programming, applies the appropriate inputs, and recognizes the outputs. The electronic computer can be programmed readily for repetitive tasks like payroll accounting and inventory control. But can it be programmed for such intricate mental processes as market analysis, competitive strategy, and the motivation of personnel?

The answer to this question is shrouded in our ignorance of the mental process itself. Despite this ignorance, we can be sure that the next decade will bring us a much better understanding not only of the principles of rapid and flexible programming of computers, but also of the processes employed by the brain in the higher levels of mental activity. This understanding will set the stage for a whole new chapter in automation—the reduction of the waste and inefficiency which results from faulty planning and ill-advised execution of business activity.

The third key word is nuclear power. There is only one IRE Professional Group (that on Nuclear Science) directly interested in this field, and it might well appear that other groups, such as the physicists in AIP and the power engineers in AIEE would have primary cognizance of developments in this field. However, the opportunity for electronic specialists in IRE is much greater than is generally realized, for it now appears that the long-range future of generation of power from nuclear energy lies in a very special form of gaseous discharge, which since the invention of the gas rectifier and thyatron has been a matter of primary interest to the electron device specialist.

The background of this subject is to be found in a most significant paper by Post.¹ He points out that pow-

¹ R. F. Post, "Controlled fusion research—an application of the physics of high-temperature plasmas," *Rev. Mod. Phys.*, vol. 28, pp. 338-362; July, 1956. Reprinted in *Proc. IRE*, vol. 45, pp. 134-160; February, 1957.

er generation from fossil fuels (oil, gas, and coal) and from fissionable materials (uranium, thorium, and plutonium) or by conversion of solar energy, is not likely to meet the demands of civilization a century hence. In contrast, the production of power from fusionable materials such as deuterium (by the "hydrogen bomb" reaction) is not only potentially much cheaper in energy per pound of fuel, but the reserves of deuterium in the oceans are so vast as to meet the foreseeable demands for a billion years. With this prospect before us, it is no wonder that the nations of the world are engaged in a competitive race to solve the problems of controlled fusion, an activity which in this country goes under the code name of Project Sherwood.

The controlled production of energy from deuterium involves the reproduction on earth of conditions like those at the center of the sun and the stars, where temperatures of hundreds of millions of degrees and pressures of hundreds of millions of pounds per square inch exist, but where the particle densities are so small as to approximate the vacuum of an electron tube. Only under such conditions can we expect the deuterium atoms to be sufficiently energetic to overcome the repelling forces in the nucleus and to transmute themselves to helium and thus release the vast energy of fusion. Under such conditions the fusionable material exists as a completely ionized gas, which the physicists call a plasma after the term suggested many years ago by the great contributor to electronics, and past president of the IRE, Dr. Irving Langmuir.

Thus far, the only known method of generating the superhigh temperatures needed for fusion consists of passing a very high current through the fusionable material in gaseous form. Matter at such temperatures tends to expand with explosive force so there is need to confine the reaction, but it is hard to imagine material which could contain the fusion reaction without itself being immediately vaporized. Fortunately, the very current which is looked to for production of the necessary high temperatures produces an intense magnetic field and this nonmaterial agent produces a self-constriction of the current-carrying ions. This phenomenon, known as the "pinch effect," offers in principle the means of confining fusion reaction in such fashion that an enormous excess of energy, over and above that required to maintain the current, would be produced.

It may well be argued that, despite the high interest among all technical people in controlled nuclear fusion, its connection with IRE affairs is somewhat tenuous and that the myriad obstacles to reproducing the energy-producing mechanism of the sun can hardly be expected to be overcome here on earth within the ten-year span under consideration here. The weight of these doubts I fully admit. But since the stakes are so high, and the welfare of our great-grandchildren is so directly affected, I doubt if we will feel happy at leaving the quest for inexhaustible power entirely to other groups. The fact is that within the membership of the IRE we have the

talent and organization to make a substantial contribution to this quest.

Before turning to the ten-year future of the IRE, let me illustrate a present reality which is an index to future events. I have here a transistorized portable radio receiver, tunable over the standard broadcast band, which operates entirely through the agency of external electromagnetic fields without benefit of dry battery or power-line connection. One of the fields has a frequency of about one megacycle and is supplied by a local broadcast station in the usual way. The other is a flux of infrared energy centered at a frequency of about 300 million megacycles and having an intensity about equal to that of sunlight, which is provided by this photoflood lamp. As I turn on the lamp, the receiver goes into operation. Six solar battery cells on top of the case made of highly refined silicon, develop the necessary three volts at full load current of 75 milliamperes.

The significance of this demonstration is that the radio reception is obtained with no process of depletion, no chemical erosion in batteries, no gradual loss of emission from a cathode, and (when power is provided by sunlight) no exhaustion of fuel in power generation. In fact, we may expect that such a radio would operate day after day, so long as a sun shines, for the next decade without any attention whatever—which adds up to well over 20,000 hours and at least 100,000 commercials!

What does all this mean for the future of The Institute of Radio Engineers? One fact is abundantly clear: the number of prospects for IRE membership will increase during the next decade in striking fashion. The Institute now has over 60,000 members and has been growing over the past three years at a rate of better than 15 per cent per year. It takes no electronic computer to compound this growth and to conclude that by 1967 the IRE will have over 200,000 members, if the present trend continues. This would amount to no less than one IRE member for every thousand of population in the United States.

We may well doubt that an additional 140,000 technical people qualified for IRE membership will appear in a mere ten years, particularly with the present rate of producing engineers and scientists. But it seems certain that this extrapolation is optimistic by no more than a factor or two. A potential of at least 100,000 IRE members by 1967 is clearly in the cards, by all the trends we have just examined. The question is whether the IRE can assimilate any such addition to its membership without suffering from such severe growing pains that fractures develop.

This is no idle threat. At the last Annual Convention we acknowledged our debt to a man who saw this threat several years ago, when we presented the Founders Award to R. A. Heising for his part in founding the IRE Professional Group System. Without the Professional Group System the IRE would already be coming apart at the seams, because large numbers of specialists would

have deserted it to join other organizations or to form their own.

The PG system is in good hands and it is prospering. But the affairs of each Professional Group are by no means free of vexing questions which arise in its relationship to the IRE parent organization and to other professional groups. This is the threat of internal competition mentioned at the start of this talk.

Let me cite two concrete examples: the Group Affiliate plan, and advertising in the Professional Group TRANSACTIONS. For many months, several Groups have argued that many technical workers in their special fields have little interest in the over-all IRE organization, do not want and would not regularly read the PROCEEDINGS, and balk at paying the full membership fee. Last January, the IRE Board of Directors approved the Group Affiliate plan, whereby a member of another accredited technical society but not of IRE would pay the Group assessment plus an additional sum to cover the full cost of his association with the Group, but would not pay IRE dues as such. He would receive the TRANSACTIONS but not the PROCEEDINGS, would hold appointive but not elective office in the Group, and would be free to contribute his knowledge in his special field as if he were a full IRE member.

Question: How many potential members of IRE, who have a primary interest in a special field and might join IRE primarily to gain access to the Group in that field, will decide in favor of the less expensive Group Affiliate status? This possibility must be watched carefully. For, if the loyalty turns out to be directed toward the Group and away from the parent IRE, IRE is in for trouble.

Careful thought has been given to this problem and many of the Directors are convinced that no such trend would develop—that, in fact, more members in the long run would be attracted to full IRE membership through initial exposure through Group Affiliation than would be lost. But it takes more than a Board of Directors to make IRE tick. *Every member must have his own conviction that the IRE is, and should continue to be, more than a mere holding company for Professional Group assets.* It seems abundantly clear that a strong and healthy central organization can with a flexible and enlightened outlook contribute far more to the support of Group activities than the Group can possibly lose by its association with IRE and the other Groups.

Consider, as a second example, the question of advertising in the Professional Group TRANSACTIONS. In the past, except for Institutional Listings, no advertising has been permitted in these publications, since such advertising might severely reduce the over-all income to the Institute by encouraging advertisers to transfer their pages from the PROCEEDINGS to the TRANSACTIONS, at the lower rates which the smaller Group circulations would normally command. Since a half of the operating expense of the Institute is paid by PROCEED-

INGS advertisers, this prospect is not to be taken lightly.

Many Groups, in need of additional income to publish more papers, feel that certain advertisers would be glad to pay a high rate to reach the concentrated audience of the Group membership. If this is so, the advertising income of the Institute as a whole would not be lowered. So permission has recently been granted to solicit TRANSACTIONS advertising, subject to the usual IRE standards, at a rate per page substantially greater than the PROCEEDINGS rate. It is too early to know whether advertisers will in fact accept the offer, but it seems likely that many, particularly those engaged in recruiting special types of engineers and scientists, will do so. If so, the IRE is the stronger for it. By such carefully considered actions, we can encourage and strengthen the Groups without pulling the IRE apart.

Finally, I would point to another potentially disruptive tendency which must be curbed during the years ahead: competition with other societies. The Group Affiliate plan is a form of cooperation with other societies which can do much to cement relations and avoid excessive duplication of technical effort. But this cooperative effort should not be left to the Groups; it must also be undertaken by the IRE as a whole. To be concrete, let me cite our relations with the American Institute of Electrical Engineers, the organization which has the largest area of technical activity overlapping that of the IRE. We cannot shut our eyes to the intersociety problem posed by the increasing interest of straight electrical engineers in electronic techniques. The group of electronics-oriented engineers common to the IRE and AIEE is increasing rapidly and the problems of duplication and cross-purposes in committee effort, conferences, and student activities are growing proportionately. These are problems to which the officers and directors of the two societies must address themselves. Should IRE and AIEE affairs in communications and electronics be amalgamated? If so, how is this to be done? We urgently need an answer to these questions, and they will no doubt be forthcoming in the next ten years, hopefully, early in that time.

These are but three illustrations of the need for wisdom in guiding the Institute in the decade ahead. Many other examples might have been chosen, such as striking the optimum balance in editorial service as between professional and nonprofessional members, taking a more active part in the recruiting of students and upgrading of technical people, and finding some effective and acceptable means of increasing by concerted action the economic and social rewards of a career in electronic science. All of us as individual members of IRE, not merely the officers of the IRE and its Groups, must make these questions matters of personal concern. If we do, the Institute will surely contribute its important share to the opportunities for all of us that lie just ahead.

A History of Some Foundations of Modern Radio-Electronic Technology*

J. H. HAMMOND, JR.†, SENIOR MEMBER, IRE, AND E. S. PURINGTON†, SENIOR MEMBER, IRE

Summary—Experiments with high-speed boats at Gloucester, Mass, in 1910–12, resulted in sustained governmental interest in radiodynamic torpedoes from 1912 to 1931. This culminated in the successful radio control of the course of a modified standard naval torpedo throughout a 9000 yard run at an operating depth of 12 feet. Many developments by the Hammond Laboratory established basic principles used in modern airborne guided missiles, including the stabilizing, security, bat, proximity, and homing principles. Needs for improved devices and circuitries for control purposes stimulated the early development of principles used in modern communications. The Hammond Laboratory sponsored the first nondetector applications of the filamentary type triode for linear amplification and for transmitter and heterodyne purposes in 1911–12. The intermediate frequency principle for selectivity purposes was developed in 1912, stemming from the heterodyne principle of Fessenden and the two-channel security principle of Tesla. At a conference at Gloucester in October, 1912, disclosure of these developments led immediately to the Alexanderson development of the tuned radio frequency principle and to the accelerated development of the high-vacuum triode by Langmuir and White. The first military application of the intermediate-frequency principle was to the solution of a World War I problem of mitigating the interference of enemy spark type transmitters upon communications from front line infantry. The receiver of the system was structurally of the most general superheterodyne type for continuous-wave reception. With the advent of broadcasting, the early 1912 conference had paved the way for the commercialization of the modern receiver with its IF basis for selectivity, its trf basis for sensitivity, and its hard tube basis for reliable practicability. Additionally, the unicontrol feature for operational simplicity of the superheterodyne stemmed from military designs of 1917–18. In the early record, there are suggestions in the fields of automatic volume control, remote cutoff triodes, and feedback for improving signal fidelity. Special early applications of the IF principle were in the fields of multiplex signaling and of privacy systems for radio telegraphy and telephony. In the field of frequency modulation, the principle that fm and AM transmissions may be independently in the same wave band was established in 1912. The technique of gathering a complete signal element from both ends of a transmitted fm spectrum was practiced in a wide-band single-shot system of security control in 1914. Researches in 1921, established the all-electronic method of fm transmission for telephony; in 1922, led to the development of a wide-band noise-reduction system for telephony having fm properties and using dual-channel noise-cancelling dual-detection reception, in 1927, provided for the possible development of wide-band artificial fm transmission with a stabilized carrier, developed from quasi-phase modulation produced from AM by a 90° carrier phase shift.

I. INTRODUCTION

DURING the period of the founding of The Institute of Radio Engineers, the radio-electronic art was in a transitional stage. This art had its beginnings with the utilization of the Edison effect in the Fleming diode detector, and a highly important advance was the invention of the de Forest triode which pro-

vided an electrically controlled impedance. But radio receivers for spark type transmitters usually comprised a coupled-circuit tuner with a simple detector and headphones; sometimes the detector was an audion triode which, because of the operating cost, was used only when the simpler devices were just insufficiently sensitive. Continuous wave receivers for arc and rotary type wave generators were of similar nature but with a device before the detector to produce a local modulation of the incoming signal; this was usually a rotary tikker to chop the continuous wave whenever present or an arc driven heterodyne to create a tonally modulated signal.

The Hammond Laboratory was privately and personally organized during this period with the immediate objective of developing radio and other remote control systems for waterborne missiles. The laboratory, Fig. 1,



Fig. 1—The Hammond Laboratory, 1912–1928.

was located on the westerly shore of the outer harbor at Gloucester, Mass., at the entrance to Freshwater Cove. Here from 1912 to 1928, many electronic and allied devices and circuitries, developed at first for radio control purposes, formed the basis of important developments in communications and other fields of application. Since most of these developments were with military and naval applications in mind, publication of technical and historical information was highly limited by governmental and self-imposed restrictions.

The purpose of the present paper, therefore, is to make available a better understanding of the background of some of the most important developments of radio-related electronics. For clarity, the report is not on an integrated chronological basis, but rather discusses different aspects in turn. After a discussion of

* Original manuscript received by the IRE, February 11, 1957; revised manuscript received, June 5, 1957.

† Hammond Research Corp., Gloucester, Mass.

radiodynamic torpedoes, attention is given to the triode tube and its fundamental nondetector applications, to the beginnings of the modern intermediate-frequency type transmitter and receiver systems, and to the development of frequency modulation and related transmitter and receiver circuitries.

II. THE RADIODYNAMIC TORPEDO

A radiodynamic torpedo is a carrier of high explosives for a military target, the course of which is alterable dynamically by radiant energy from a distance. The radiant energy may be of any form: compressional wave, light beam, or from a radio antenna. The torpedo may have the form of a surface boat, an underwater craft, or an airborne guided missile. The history of such torpedoes began in 1897, when E. Wilson¹ and C. J. Evans controlled slowly moving boats by radio waves on the Thames river. Almost simultaneously, N. Tesla then became the pioneer in the United States² and in 1898, built a working model which he successfully demonstrated at the Auditorium in Chicago. In 1905, the Quintard Iron Works in Boston actually built four radio-controlled torpedoes according to designs by H. Shoemaker. These were hybrid devices, having the form of an underwater naval torpedo rigidly suspended from a surface float which supported the receiving antenna. In the United States, these were not considered to have military merit, and they were sold to the Japanese Navy. Preliminary work by Hammond³ from 1910 to 1912, with the "Pioneer" and the "Radio" in Gloucester Harbor resulted in the development of the automatic course stabilization principle for high-speed waterborne and airborne torpedoes. This and contributions to the security of control firmly established U. S. governmental interest leading to the modern developments.

The U. S. Army had long since expressed a desire for a coast defense torpedo controllable from the shore and had experimented with a cable linkage from the control point to the torpedo. In the late fall of 1912, Brig. General E. M. Weaver and Col. R. P. Davis, the Chief and the Assistant Chief of Coast Artillery, came to Gloucester and witnessed the successful radio control of the 33-knot "Radio."⁴ In May, 1913, General Weaver detailed Capt. F. J. Behr⁵ to the Hammond Laboratory as an observer, with twelve technical sergeants to assist with 60-inch searchlights and other Coast Artillery materiel. After he had assisted in establishing the direction of the developments along desirable military

lines, Capt. Behr was relieved by Lieut. S. M. Decker.⁶

General Weaver believed that high-speed motorboats with depth charges could constitute a serious menace when directed against enemy ships. That he was right was proven in World War II when the Italians sent in their high-speed explosive boats at Suda Bay in Crete, on March 25, 1941, and sank *H.M.S. York* and other British ships. And during the Philippine actions at Lingayen, the Japanese on January 10, 1945, attacked our LCI's and LST's by manned explosive motor boats with great effect. At Kwajalein, the U. S. Navy improvised radio-controlled boats called "Stingray" to attack Japanese positions. Better results were obtained by the American forces with radio-controlled drone boats against the Germans on the Riviera.

History has therefore vindicated the early judgment of the Coast Artillery and its chief. However, as is the case with most radically new weapons, the remote control torpedo was to encounter the usual diversities of opinions which are enjoyed by the different military services.

The principles of modern radio missile guidance developed in the total pioneering period of 1910 to 1914, were as follows.

Automatic Course Stabilization

In the absence of a control signal, the torpedo should be stabilized as to course by automatic mechanisms within itself. Course stabilization had been practiced in naval torpedoes by a gyroscope energized only at the start of a run. But in 1912, the Sperry Gyroscope Company and the U. S. Navy were developing a precise and reliable motor-driven gyrocompass with remote repeaters. Accepting this as a best possible basis,⁷ the Hammond Laboratory engineered the modification of one of these devices so that the repeater controlled not a compass indicator, but the operation of a steering engine. The first navigational application of this automatic pilot principle was to the third boat, the *Natalia* of Fig. 2; the system was first put into long period operation on March 25, 1914, throughout a 60-mile run from Gloucester to Boston and return. Here, of course, the gyro setting was changed manually from time to time.

Radio Control of Gyro Setting

Directional changes of the missile should be accomplished by applying control signals to alter the course setting of the automatic stabilization device. The gyroscope for the *Natalia*, therefore, was fitted with electromagnetic solenoids to step the course setting backwards or forwards by a definite number of compass points in response to each control signal. Differentiation as to sense was by the timing pattern of a few dashes applied to a

¹ U. S. Patent 663,400 (1898-1900) to Wilson and Evans. Note: Filing and issue years are both given.

² U. S. Patent 613,809 (1898-1898) to N. Tesla.

³ The early radio-control developments were popularly described by C. Moffett, *McClure's Mag.*, vol. 42, pp. 27-39; March, 1914, and vol. 44, pp. 21-31, March, 1915.

⁴ "Fortifications Appropriation Bill, 1917," Hearings conducted by the Subcommittee (Swager Sherley, Chairman) of the Committee on Appropriations, House of Representatives, in charge of the Fortifications Appropriation Bill, pp. 288-298, 301-304; January 24 to February 10, 1916.

⁵ *Ibid.*, pp. 306-314.

⁶ *Ibid.*, pp. 314-324.

⁷ U. S. Patents 1,418,788-789-790 (all 1913-1922) to Hammond. The original sketches were made during a transatlantic crossing on the "President Grant," on July 21, 1912.



Fig. 2—The *Natalia* leaving pier for tests, 1914.

primary control relay in response to suitably transmitted signals from one or from two antennas located somewhat southerly from the laboratory building.⁸ Other dash patterns controlled various other operations, such as engine speed, searchlight shutter opening, and laying of mines.

Security of Radio Control

The control system should provide security both against control and against interference upon control by such countermeasures as are currently available to a potential enemy. This principle is of special radio-electronic interest and involves the application of several subprinciples.

First, the gyro radio principle of control contributed greatly to security since it reduced the number of control signals required during a run and made the analysis of the signal pattern much more difficult. Second, the nature of the control signals could be changed⁹ even during a run, and irrelevant signals introduced, so that the proper control officer would have a far superior statistical advantage in any radiant energy battle for guidance. Third, after the missile had received its main course corrections, the gyro setting could be locked against all

countermeasures, providing conventional stabilized course control during the final approach to the target. Fourth, as an alternative to locking the course, the missile at the end of the run could be converted to a target-seeking type to home upon the countermeasure interference, still with gyro stabilization. Fifth, undesired control could be minimized by adoption of a suitable timing pattern for different frequency radiations, obviating ready analysis and duplicative synthesis.

The remote control system used mainly with the *Natalia* was of a dual channel type. Tesla had already proposed a security system based upon the coincidental transmission on two channels: a forerunner of the “and” principle¹⁰ of modern computers. Two receivers with rectifying detectors operated two corresponding output relays, the simultaneous closure of which operated a third relay for actuating the control pattern analyzing and distributing system. The Hammond system for the *Natalia*¹¹ transmitted dual channels not simultaneously but in quick sequence from the same transmitter. Thus, to produce a control dash in the receiver, a Poulsen arc transmitter¹² was made to send a first half-dash on one frequency and the second on another greatly different frequency. Control response was only after reception of both ends of the spectrum of this single-shot frequency modulated wave. The receiver was tuned normally to the frequency of the first half-dash; reception of this part of the spectrum retuned the receiver to the frequency for the second half-dash, with the first half-dash held in storage. If the second half-dash was received within a given time limit, coincidence between the second and the stored first parts registered a complete dash, for control operation. The system restored to normal, regardless of whether the first half was signal or interference, to await further signals. This was the first example of security systems using both time and frequency diversity.

The target-seeking feature of the *Natalia* provided for homing both upon an enemy searchlight and upon enemy interference. Using the principle of the “Electric Dog,” Fig. 3, which would follow a moving light, two selenium cells mounted on the foremast operated differentially to alter the gyro setting until the boat was headed toward the controlling light source. Radio homing was by the same general principle,¹³ using crossed loops both tuned to the wave length necessary for interference. Fig. 4 shows schematically the essentials of this guidance system, practiced with special duo-triode tubes to improve the permanence of differential balance. Technical developments, of course, led to better application of the differential output to the gyro system and to satisfactory freedom from course overshoot and

¹⁰ U. S. Patents 723,188 and 725,605 (both 1900–1903) to N. Tesla.

¹¹ U. S. Patent 1,486,885 (1915–1924) to Hammond.

¹² Poulsen arc equipment from the Federal Telegraph Co. was installed with the personal attention of L. de Dorest in 1913.

¹³ U. S. Patents 1,370,688 (1914–21); 1,467,154 (1912–23); 1,513,108 (1914–24); re: 16,181 (1914–25) to Hammond.

⁸ The location of these antennas at Point Radio is marked by a bronze plaque on the grounds of the present estate at 160 Western Ave., Gloucester, Mass.

⁹ U. S. Patent 1,420,257 (1910–1922) to Hammond.

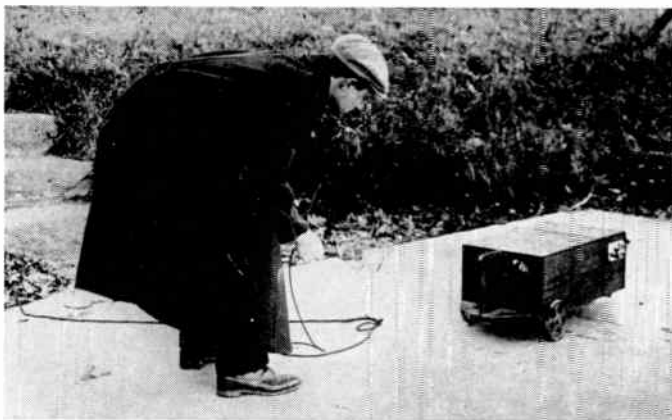


Fig. 3—The "Electric Dog" with light-controlled guidance, 1912

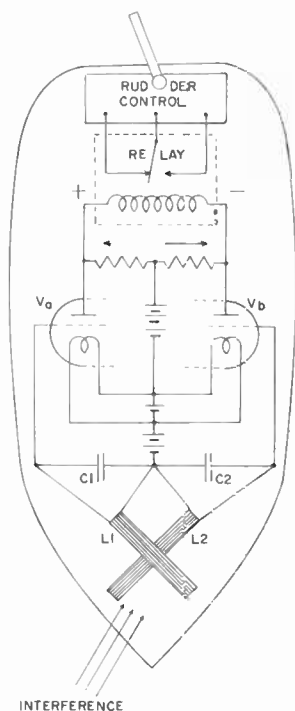


Fig. 4—Radio homing guidance system, 1914.

hunting. Homing by the differential control from two and even more channels has many modern military applications.

Practical interference tests were made with the cooperation of the *U.S.S. Dolphin*, fitted with the then latest types of communication equipment. These were made in Gloucester Harbor, October 6, 1914, during which the *Natalia* was controlled by the single-shot fm system using 118 and 1000-kc frequencies. The *Dolphin*, using in turn signals of 1000, 600, 400, and 300 kc, was at no time able to exercise control and could not block control by paralysis of the *Natalia's* rectifying detectors until she had been worked to within 250 feet of the target. Thereupon, the *Natalia* could have been operated with the gyro locked for the final fixed course, or could have been converted automatically to a target-seeking torpedo under guidance from the interference.

After demonstrations to the Government on November 16 and 24, 1914, it was officially considered the work was through its experimental stage and steps were taken toward the development of a service weapon. The original plans were to establish the first radiodynamic torpedo base at Fisher's Island off New London, Conn.; this was submitted to Congress in 1915, too late for action. Extensive hearings¹⁴ were held on the broad subject of "Radiodynamic Torpedoes," and on March 23, 1916, Hammond submitted a "Proposal Z" to the War Department. This in turn was presented to the 64th Congress, which¹⁵ on July 6, 1916, provided for a special executive board of three Army and three Navy officers to be appointed by the President with a provisional appropriation of \$1,167,000. Subject to the recommendation of the Board after a satisfactory demonstration of radiodynamic control of a torpedo, the main part of this fund was to be used for the development and procurement of a complete sample service equipment and for the acquisition of complete rights then expressed by patents and applications placed in the secret archives of the Patent Office, not open to disclosure even in cases of interference.

During its existence as a continuing body, the Torpedo Board made various changes in the requirements defining the nature of the demonstration necessary to result in a favorable recommendation. Initially, the Army members had one concept which was that of the Chief of Coast Artillery; the Navy members had another which was that of the Chief of Naval Operations. In the Congressional hearings, special interest had been expressed in the use of an airplane for controlling the torpedo far from the shore as a weapon of offense. The pilot of the plane could simultaneously observe the course of the torpedo toward its target and correct the course by radio signals preferably sent directly from the plane to the torpedo. Proceeding on this basis with preliminary work in Gloucester Harbor, official demonstrations were made to the Board on August 23, 1918, using the fourth and final surface boat, the *II-4*, shown in Fig. 5. The control was exercised directly from a plane at altitudes up to 5000 feet and at distances up to 5 miles, with the *II-4* moving through the intricate wartime shipping of Hampton Roads off Norfolk, and Fortress Monroe, Va. Since it had appeared that the final service weapon might be a submarine-like torpedo to which radio waves might not be able to penetrate, demonstrations were also successfully made of control by underwater radiosonic compressional waves. For the possible nontorpedo use of radiodynamic control, demonstrations were made with the *II-4* functioning as an unattended remotely controlled mine layer.

But in 1919, further experiments were conducted by the Navy at New London, with the cooperation of the

¹⁴ "Fortifications Appropriation Bill, 1917," *op. cit.*, pp. 258-357.

¹⁵ Congressional Record, 64th Congress, First Session, pp. 10873-876, 10904-907, 11667-671, 11784-792; June 13-30, 1916, Acts of Congress, July 6, 1916; March 3, 1919; June 30, 1922.

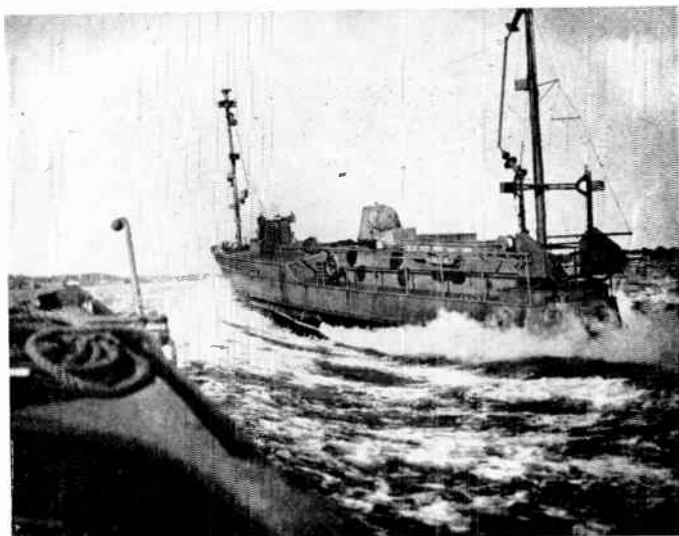


Fig. 5—The *H-4* under radio control from a plane, 1917.

Bureau of Standards, the Hammond Laboratory, and the Marconi Wireless Telegraph Company of America. The objective was to determine the essential facts of radio transmission to underwater craft. New techniques resulted as to reception on large conventional submarines, using the Bureau of Standards loop arrangement of Lowell and Willoughby with a large cross-sectional area to provide strong pickup from the magnetic component of the underwater radio field. But for small torpedo-like missiles, the antenna was required to be of the trailing wire type to minimize loss of speed and therefore of range. This antenna was to be a flexible rubber-covered wire with the trailing end sealed by a vulcanized and leakproof rubber tip and with the receiver end passing through the steel shell of the missile. Tests with a submerged submarine with such an antenna 300 feet long supported at a depth of 6 feet proved that radio control of an underwater torpedo was entirely practical with signals from a plane with 85 w continuous wave output at 188-kc frequency. It was therefore decided by the Board that the proper service weapon to meet the military requirements should be a standard naval torpedo¹⁶ modified by the addition of a midsection to house the radio control gear.

This decision to discontinue development of the surface type radiodynamic torpedo was undoubtedly made in the belief that an underwater missile of superior military value could be readily developed. Therefore, interest in the surface type lay dormant for twenty years until reawakened by the exigencies of World War II.

In December, 1921, the Board further established the quantitative requirement that the radio control of the modified naval torpedo would be considered satisfactory if, throughout a run of 9000 yards, the torpedo

was controlled at a depth of twelve feet. This increase of 6 feet over the test depth in the New London experiments was for making certain that the torpedo would be able to strike a battleship below the armor belt. After preliminary studies by the Hammond Laboratory with Navy cooperation, the Navy actively pressed the new phase of missile development when research funds appropriated by the 64th Congress became reavailable in 1925. The work was then transferred to the waters of Narragansett Bay under the direct supervision of the Naval Torpedo Station at Newport, R. I.

The problem of radio control under the stipulated conditions even from the standpoint of signal transmission was highly complex; it is along the same general lines as that of delivering energy purposely to an insulated dipole embedded in the walls of a modern waveguide. Ocean water has a conductivity of about 4.5 mho/m, a permeability the same as air, but a dielectric constant about 80 times that of air. The operating frequency must be high enough to permit a strong field to be established with E and H components parallel to the water surface at the boundary, but low enough to prevent excessive attenuation of the downwardly penetrating energy due to the conduction currents. The optimum frequency depends upon the depth at which the signal must be received, as well as the current status of the radio-electronic art; the radio band 150 to 200 kc was chosen for the purpose. At midband, the attenuation of ocean water computes to be 4.65 db per foot of depth, so that the extra 6 feet in the stipulated depth corresponded to a power ratio of about 600. Practical operation was achievable only by an increase of transmitter power in combination with improved design of the receiver system.

Then too, the field establishable parallel to the air-ocean boundary for the start of the downward flow of energy is itself small in comparison with that available for the antenna of a surface craft. Ocean water has an intrinsic impedance of about $(0.001)(1+j)$ times that of air at 175 kc operating frequency; therefore, there is about 24 db of mismatch loss for a wave directed vertically downward from a plane, just in passing from the air to the water medium. There is even greater difficulty if the energy is originally propagated horizontally from a control ship or a shore station with the H field tangential but the E field in the air medium nearly perpendicular to the air-water boundary. By the theory established by Zenneck,¹⁷ with a counterpart in modern waveguide theory, the E field tangential to the surface for the start of the downward wave computes to be at 175 kc, about $(0.001)(1+j)$ times the E field of the air wave flowing parallel to the surface. This factor is the same as the water-to-air impedance ratio, since at the boundary the H field pertains to both the air and the

¹⁶ Torpedo mechanisms were popularly described by E. F. Chandler, "The modern automobile torpedo," *Sci. Amer.*, vol. 113, p. 112; August 7, 1915.

¹⁷ The Zenneck theory is available in J. A. Fleming, "The Principles of Electric Wave Telegraphy and Telephony," Longmans, Green & Co., London, Eng., 2nd ed., pp. 729-744; 1910.

water wave. Therefore, the power flux for the downward wave even at the surface is 30 db less than that of the air wave above the surface available for antennas of surface craft. There is in effect a 30-db loss of signal energy as the wave makes a right angled turn to enter the water. Since the H field does not suffer this turning loss, it is probable that a loop antenna, if practicable, would not have the same disadvantage as a trailing wire antenna in being converted for use in the ocean.

Fig. 6, derived from a Navy release in 1930, shows the "Hammond Radio Controlled Torpedo" just after ejection from a standard tube mounted on a test barge. The addition of the radio section, bracketed by white bands, was not detrimental to the proper launching of the torpedo. When the torpedo hit the water, the filament circuits of the receiver were closed by an inertia type switch, and a reel carrying the antenna was forced from its mount behind the propellers. This reel floated to the surface after the antenna had unwound and trailed to its full operating length of 150 feet. The gyro was given a preliminary setting before launching, and the course of travel was changeable by a specific number of compass points in response to each control signal from a transmitter located at Melville, R. I. This transmitter¹⁸ was a General Electric continuous-wave type with 10-kw output rating in the 150–200 kc band, but modified as to its output circuits to provide efficient generation of two waves with as much as 10-kc separation. Control was in accordance with the time-frequency pattern fed into the power amplifier from a switchable master oscillator. Reliable operation was achieved with only occasional lapses when during a run the line from the transmitter to the torpedo antenna was at right angles to the line of torpedo travel. Final tests, meeting the requirements of the Board, were made in the early winter of 1930–31. Thereupon, by the "Hammond Patents Purchase Agreement of July 30, 1932," designation NOD 393, the Government acquired rights for radiodynamic purposes in over a hundred of the Hammond patents, including many of importance not covered by the original listing in Proposal Z.

It is believed that underwater radio-controlled torpedoes were not used in World War II; perhaps this was because of difficulties with production torpedoes in the earlier part of the war. Magnetic detonators and contact exploders were unreliable, and the depth regulation was undependable. It was not until 1944, that these difficulties were fully overcome. In the latter part of the war, torpedoes were set mostly for a 6-foot running depth to make certain that they would not under-run important targets. Under such conditions, as proven by the New London tests of 1919 and the Newport developments of 1925–31, the radio control of underwater



Fig. 6—The "Hammond radio-controlled torpedo," 1930.

torpedoes from a plane at a safe distance from the target would have been highly practicable.

An important application of the radio control of surface craft was in the contests between bombing planes and battleships. The *U.S.S. Iowa*, Fig. 7 (opposite), scheduled for scrapping in accordance with international agreements, was the first to be fitted out by the Navy as a target ship, with the General Electric Company and the Hammond Laboratory cooperating. In tests of June 29, 1921, at sea about fifty miles off the outer Maryland shore, eighty dummy bombs made of concrete were dropped in 200 minutes from 20 planes at 5000 feet elevation. It is probable that the number of hits did not exceed two near misses, and that the otherwise defenseless target ship, even with reduced speed, escaped certain theoretical destruction by the zigzag course set up by radio control from the *U.S.S. Ohio* at a safe five-mile distance.

Hammond Laboratory patents and electronic developments in the general field of remote guidance, restricted neither to the water medium nor to radio links, have been made available. Early patents necessary for application of the stabilization principle in radio control of aircraft¹⁹ were made available in 1925, to the Sperry Company for governmental developments. The government was given free use of patents and ideas with important applications in World War II and later developments of airborne missiles involving radio-electronics, although worked out originally for sound control in the water medium. Thus the Hammond statement²⁰ of the "Bat" principle is as follows: "In combination with a self-propelled body, means for automatically steering said body on a predetermined course,

¹⁸ After the completion of the Newport work in the field of radiodynamic torpedoes, the three phase power rectifier of this transmitter was incorporated into the Harvard University cyclotron, later sent to Los Alamos for research, leading to the development of warheads for guided missiles.

¹⁹ U. S. Patents 1,568,972 (1914–26); 1,568,974 (1915–26), 1,625,252 (1919–27) to Hammond and 1,772,343 (1920–30) to Dorsey and Trenor. See also U. S. Patent 1,568,973 (1915–26) at that time, in effect, optioned to the U. S. Government.

²⁰ U. S. Patent 1,892,431 (1928–32) to Hammond; claim 28.



Fig. 7—The USS Iowa under radio control, 1921.

means carried by said body for propagating energy waves, means associated therewith for receiving said waves when reflected from a distant object and means operable in response to said reflected waves for altering the course of said body.” And the statement of the “Proximity” principle²¹ is: “In a torpedo having a warhead, means for producing and radiating energy, means for receiving said energy after reflection from an outside object, and means responsive to the received energy to detonate said warhead.” The problems of the radio control of rockets²² were given inventive thought. Special research was conducted²³ in the field of security control, especially for the design of radio-guided drop bombs with partially publishable results.²⁴ And finally, a special report upon security design principles was made to the governmental agencies concerned with advanced developments to make certain that the results of the Hammond Laboratory studies in this field were fully available.

III. THE TRIODE TUBE

The Institute of Radio Engineers was created by merging the interests of two competing societies, largely through the efforts of Robert H. Marriott, Alfred N. Goldsmith, and John V. L. Hogan, Jr. Marriott was serving as the president of the Wireless Institute which was the junior society of the merger. The president of the senior Society of Wireless Telegraph Engineers was Fritz Lowenstein. Marriott and Lowenstein became the president and the vice-president, respectively, of the newly formed Institute.

In an historical paper,²⁵ Marriott has indicated that the

²¹ U. S. Patent 2,060,198 (1932-36) to Hammond; claim 18.

²² U. S. Patent 2,413,621 (1944-46) to Hammond.

²³ Partly under NDRC-OSRD Contract OEMSR-694.

²⁴ U. S. Patents 2,424,900 (1944-47); 2,449,819 (1944-48); 2,465,925 (1944-49); 2,480,338 (1944-49); 2,510,139 (1944-50); 2,522,893 (1945-50); 2,635,228 (1948-53) to Purington.

²⁵ R. H. Marriott, “United States radio development,” Proc. IRE, vol. 5, p. 184; June, 1917.

“Audion” three-electrode form of detector “was used to some extent as early as 1906, but apparently in very small numbers until about 1912 when the amateurs became active in its use. . . .” In early 1912, Lee de Forest indicated²⁶ that Dr. L. W. Austin of the Navy had “found the sensitiveness of the Audion 1.5 that of the electrolytic detector, which ranked more sensitive than any other including the magnetic detector and the crystals.” The nature of the potential figure of merit of the de Forest triode is establishable from curves given by J. H. Morecroft²⁷ for a tube that was later well evacuated and baked to remove the gaseous irregularities. For a central working condition of 45 v on the anode with 0.8 ma current at 4 v grid bias, the amplification constant was about $\mu = 2.3$ and the internal impedance was about $r_p = 36,000$ ohms. Commercially, the de Forest audion detector circuit in a cabinet with three spare bulbs retailed at \$125.00; replacement bulbs were \$5.00 each with a rated but unguaranteed life expectancy of 40 to 60 days.

Thus it would appear that at the time of the founding of the Institute of Radio Engineers, de Forest triodes were applicable only in the limited field of receiver circuitry and in the even more limited field of detectors to cause amplitude variations of radio signals to be revealed audibly. After five years of public availability, there were no other established applications in the electronic art, nor had the wire communication or other nonradio electrical companies in the United States initiated researches for the purposes of developing the potentialities.

In the preliminary work in radio control, the first relays were operated from the output of conventional detectors, with dc rectified outputs of the order of 0.1 ma. Lowenstein, as a power engineer, had been interested in the development of mercury vapor and other ionic devices for power applications. He had recognized²⁸ that while transmitters with Duddell and Poulsen arcs depended for operation upon the negative resistance characteristics of two-terminal devices, similar results might be possible with positive resistance devices through magnetic or electrical control of the current stream. As a consultant of the Hammond Laboratory, Lowenstein on May 11, 1911, undertook in New York the development of the three element “ion controller” for relay-operating rectifier-detector purposes, and also for the nondetector purposes more obviously related to amplification. Starting with power applications with a motor generator of 1000 v, $\frac{1}{2}$ kw dc rating shortly thereafter replaced by a battery, Lowenstein reported by a letter of September 19, 1911: “So far the experiments . . . were without results, but . . . will advise you immediately upon obtaining the repetition of experiments which I made some years ago. The probable cause of

²⁶ Letter of L. de Forest to Hammond, January 6, 1912.

²⁷ J. H. Morecroft, “Principles of Radio Communication,” John Wiley & Sons, New York, N. Y., p. 402; 1921.

²⁸ Lowenstein Notebook entry on October 5, 1909.

failure so far seems to lie in the degree of vacuum. . . . I have ordered from the same glassblower who made my tubes five years ago a tube of the same dimensions, and I trust to good luck that he will get as good vacuum now as he did then." But on October 7, 1911, "I have concentrated my efforts on reproducing the telephone tests of last winter, but have not succeeded as yet. . . . I am convinced that only a systematic investigation of the influence of the vacuum, the brightness of the cathode and of the screen potential will assure permanent success." Finally on November 13, 1911, Lowenstein reported upon the first application of the Class A triode amplifier: "At last a test over actual long distances. When I heard your voice I fairly jumped in delight; it came in so clear with every shade of its personal characteristics. . . . Your low voice spoken one foot from the transmitter came in as loud as conversation carried on between two extension phones on the same switchboard."

Prior to securing protection by a patent application filed in April, 1912, Lowenstein demonstrated his amplifier invention to the American Telephone and Telegraph Company, with the circuitry hidden in a "black box"; even subsequently he was reluctant to make a complete technical disclosure. In Gloucester, in late October, de Forest disclosed the achievement of an amplifier gain of 120 times, using three audions in cascade; that his system worked both ways for telephony and was highly regarded by John Stone-Stone; that he was asking the Bell people \$50,000 for his invention as applied to telephone work alone. Established histories indicate that including the stated amount for repeater work, the Telephone Company paid de Forest a total of \$250,000 for their use of his triode inventions. And Lowenstein, after the issuance of his patent,²⁹ in 1918 sold the entire Class A grid-bias invention to the Telephone Company for \$150,000; the validity of the patent was sustained in later infringement procedures. After the telephone repeater demonstrations of 1912, by Lowenstein, de Forest, and Stone (the three presidents of the Bostonian Society of Wireless Telegraph Engineers), the Telephone Company carried forward its own developments under the competent direction of Dr. H. D. Arnold.

The creation of interest in the triode by a hitherto noncommunications company of development and production competence was on a more simple and direct basis. In September, 1912, the Hammond Laboratory obtained for radio control work seven of the latest designed de Forest triodes. But these were deficient as to reliability, uniformity, and amount of dc change of rectified output in a given test setup.

But already in early 1912, Dr. Irving Langmuir of the General Electric Company, had a very active interest³⁰

in the flow of current in two-electrode tubes due to the Edison effect; the immediate objective was improvement of incandescent lamps and the potential objective was the development of high-voltage X-ray tubes. There were those who believed that a gaseous content was necessary and desirable for space flow applications. But attracted by the simplicity of the Richardson theory of 1903, as to the source of the current-carrying charges, Langmuir and Sweetser, by August 23, 1912, were already obtaining currents in a thermionic two-electrode tube of 3 to 5 ma at 200 to 250 v with the current limited by space charge and unaffected by gaseous ionization. By November, Dr. Langmuir had completed the work upon which the Coolidge X-ray tube development was based and announced commercially a year later. Langmuir's experiments of November 19, 1912, had shown that pure electron flow in two-terminal tubes could be influenced by electric charges placed upon the glass walls; he immediately recognized that large amounts of power could be controlled by the application of the small amount required for establishing an electric field. Thus the systematic investigation of the influence of the vacuum and the brightness of the filamentary cathode, indicated by Lowenstein as necessary for permanent success in October, 1911, had been independently made for two-electrode tubes by the end of 1912.

At the same time, Dr. Ernst F. W. Alexanderson, also of the General Electric Company, was developing rotary machines³¹ for use by operating companies in continuous-wave transmitters. In October, 1912, Dr. Alexanderson was at Gloucester discussing special designs of alternators for radio-control purposes. He was then familiarized with the difficulties with the de Forest triodes, and was briefed as to the Lowenstein developments. It appears³² that the General Electric Company received one of its first de Forest triodes by February, 1913, and by February 7, 1913, had received the views of the Hammond group as to the proper triode design. These were expressed in four sheets of sketches prepared by Dr. G. W. Pierce of Harvard University, as a consultant to the Hammond Laboratory. The first sheet of specifications, as shown in Fig. 8, based upon the originals, called for a straight tungsten filament held taut by a spring, a nickel spiral grid, and a nickel cylindrical plate. Other sheets referred to a tube with a conical spiral grid, a tube with a lime-coated platinum strip cathode at a dull red heat, and a tube with the de Forest linear flow structure but with grids and plates on both sides of the filament.

By the middle of February, 1913, W. C. White was transferred to assist Dr. Langmuir in the development

³¹ U. S. Patents 1,008,577 (1909-11); 1,042,069 (1911-12) to E. F. W. Alexanderson.

³² Hearings before the Committee on Interstate Commerce, U. S. Senate, 71st Congress, 1st Session, on S6, a Bill to provide for the regulation of the transmission of intelligence by wire or wireless, pp. 1360-1371.

²⁹ U. S. Patent 1,231,764 (1912-17) to Lowenstein.

³⁰ U. S. Patent Office Interference 40,380, Arnold vs Langmuir; Subject: Electron Tubes; Langmuir's Record.

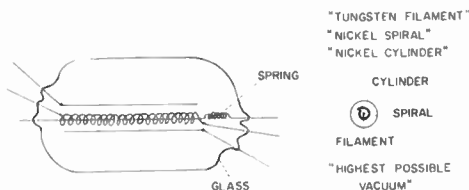


Fig. 8—Hammond-Pierce design for a high vacuum triode, 1913.

of the triode, to test the current de Forest designs, and to follow through with designs according to Langmuir sketches. In his earlier experiments, Langmuir had studied the flow between a cold and a hot tungsten filament, both having been previously heated in the process of eliminating gases and vapors before pumping. Therefore, the early General Electric triodes³³ followed neither the de Forest nor the Hammond-Pierce structural designs, but all three electrodes were of a filamentary nature. Comparative tests between the prototype General Electric and de Forest types for radio control applications were made by Langmuir and Pierce at the Hammond Laboratory on May 19, 1913. The test circuit as recorded by Capt. F. J. Behr of the Coast Artillery, and redrawn in Fig. 9, shows the Lowenstein in-

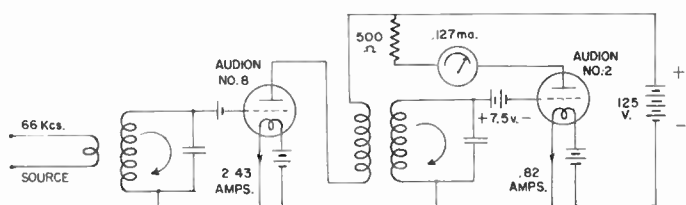


Fig. 9—Langmuir-Pierce test circuit for audion triodes, 1913.

fluence with the negative bias of the first tube as a repeater, the Lowenstein-Hammond influence of the ultra-negative bias of the second tube as a potentially operated rectifier detector, and the Alexanderson influence with the tuned cascaded circuits with electronic isolation. For this setup, the de Forest design was considered to be more suitable for control work, but the General Electric tube operated at 200 v with greater future promise. With researches on the relations between triode structure and performance, and with development of new methods of heat treatment for anode plates, Langmuir and White then developed the modern triodes for transmitter and receiver purposes, more closely along the design of the Hammond-Pierce structural specifications.

There is ample evidence from separate sources that Lowenstein developed a radio-frequency oscillator using the low-power triodes of 1911-12. Thus along with discussion of other matters,³⁴ the Federal Telegraph Company was advised: "Our method is far more reliable and simpler than the Poulsen arc method or the high-fre-

quency alternator method as used by Fessenden and others. . . . In experiments we have found that our method is highly suitable for wireless telephony, as there is absolutely no sound produced whatsoever as in the arc or H.F. alternator. . . . I am quite familiar with the art in Europe and during my recent trip to Germany found that most of the companies had abandoned the arc method of oscillation production. It is for this reason that I believe there is quite a future in the development of the work which we are carrying on."

Possibly the first recorded application of the de Forest triode as an oscillator was in the development of the final circuits of a special security control system,³⁵ as shown in Fig. 10. This is based upon a report of B. F.

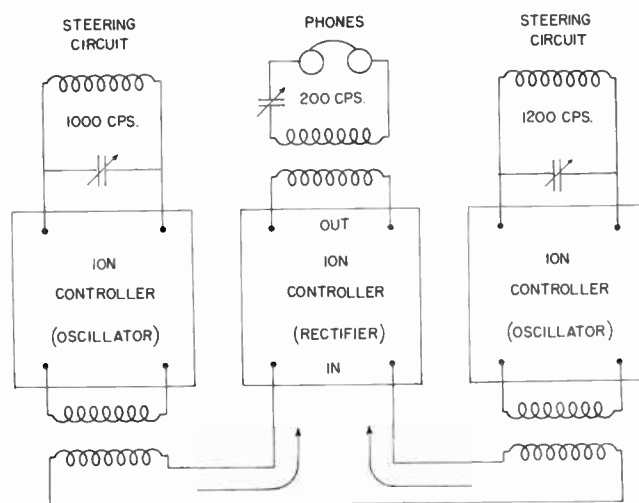


Fig. 10—Hammond selective heat system, with Lowenstein oscillating triodes, 1912.

Miessner on the work at the Lowenstein Laboratory, dated February 18, 1912. Here two triodes, or "ion controllers" by the Lowenstein designation, were fitted with "steering circuits" to generate currents with frequencies of 1000 and 1200 cps. The exact nature of the ionic devices and the manner of operation are not known. The joint outputs were fed to a third ion controller operating as a rectifier, and the resulting 200-cycle output was selectively applied to headphones in lieu of a second rectifier and a control relay.

It is possible that because he was unable to produce a triode transmitter to take the contemplated 500-watt input, or because of previous experience with triodes with mercury pool cathodes, Lowenstein did not consider his triode oscillator work of inventive importance. At any rate, in February, 1912, he turned to the development of his well-known 5-kw spark transmitters for the Navy, but cooperated in making his special knowledge and opinions available to the General Electric Company.

While awaiting the development of hard tubes with

³³ J. A. Fleming, *op. cit.*, 3rd ed., p. 873; 1916, Fig. 7.

³⁴ Letter of Hammond to B. Thompson, January 25, 1912.

³⁵ U. S. Patent 1,491,772 (1912-24) to Hammond, Fig. 5.

sufficient sensitivity and power output, the control work of the Hammond Laboratory continued with de Forest triodes and with a mercury triode later commercialized in thyratron circuitry. Such triodes would be biased just below the threshold of firing and would be triggered by the incoming signal. For de Forest types, the tube would be restored several times during a signal dash by a plate or a filament chopper³⁶ with power delivered to the output relay mainly during the triggered blue-glow condition of gaseous conduction. Restoration of the Pierce mercury type circuit³⁷ was automatic by use of an alternating plate supply. With close adjustments, the single tube circuit of Fig. 11 provided powerful relay operation even from transatlantic signals. Improvements by Dr. E. L. Chaffee,³⁸ with special care in aging the interior of the tube during the pumping process and in properly thermostating the tube with an oil bath at 70° C, permitted the device to be used in improved types of radio control circuits.³⁹ The General Electric Company acquired rights to the Pierce tube and circuitry by way of Cooper-Hewitt and Hammond. When hard tubes for power amplification purposes became available, they were of course utilized. Thus, in the final torpedo work, the control signal was built up to a high level so that with a special ac-dc converter system, the first electromagnetic mechanism in the chain operated from a triode with 10-w dc output. The development of the triode for transmitter and high level purposes was the step necessary for providing reliable circuitry in the radio-control field in which the need for improved electronic devices was early appreciated.

IV. MODERN INTERMEDIATE FREQUENCY CIRCUITRY

Intermediate-frequency circuits carry power of a frequency range intermediate between that used in conveying the information to the receiver and the audio frequency used to operate the receiver indicator. They were developed from consideration of the phenomena of beats, long established in the physics of sound, but first applied for radio purposes by Fessenden in heterodyning a keyed continuous wave to produce an audio current for signal indication purposes. As previously indicated, Tesla had proposed security of radio control by simultaneous transmission of two high-frequency signals and coincidental operation of relays after individual reception and rectification. If this Tesla method were practiced with continuous waves, beats would exist in the signal medium, but nowhere would there be any physical current of the beat frequency. In 1912, it was therefore proposed⁴⁰ that, as before, the two continuous

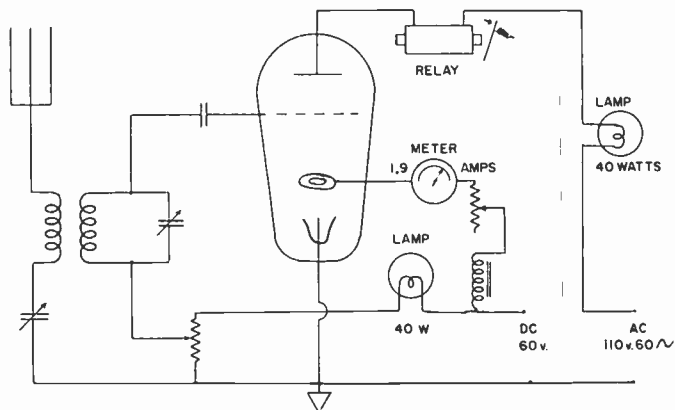


Fig. 11—Pierce mercury triode receiving circuit, 1914.

waves should be individually received to yield some degree of security, but that this security then be increased by applying the two tuner outputs to a common detecting circuit and tuning the detected output to the difference or beat frequency. For control purposes, this new ac signal in turn, could be applied to a rectifier to drive a dc relay. Or for communication purposes, if the beat frequency also was too high for direct operation of headphones, it could be applied to a conventional continuous wave type receiver of the Fessenden type. Or if the system was conveying telephony with the beat frequency itself modulated, the signal would be recoverable by a second detection, as by the condenser type headphones of the period that served both as detectors and as indicators.

Even greater security was proposed⁴¹ in which the two radio waves were amplitude modulated at different frequencies. In this manner, the transmitter to exercise control was required to have not two but four frequency generators of precision. It was in the working out of this system that the triode oscillators of Fig. 10 were used to simulate the two modulating frequency signals as recovered by first rectifier detections.

It was planned to practice these inventions for radio control by use of two Alexanderson alternators, using both of the Point Radio antennas; for the second method, the alternators were to be modulated by currents applied to the field windings.⁴² But the applications of beat selectivity in communications were also of importance. Quickly considered were double modulation with the intermediate frequency approximately the geometric mean of the radio and the signal frequencies,⁴³ and the securing of selectivity in radio telephonic communications.⁴⁴ All these advanced ideas for increased selectivity were delayed in patent prosecution and in publication during World War I.

When Dr. Alexanderson conferred in Gloucester in October, 1912, regarding the detail design of the alter-

³⁶ U. S. Patent 1,610,371 (1914-26) to Hammond.

³⁷ U. S. Patents 1,087,180; 1,112,549 (both 1913-14) to G. W. Pierce.

³⁸ U. S. Patents 1,550,877 (1916-25) and 1,627,231 (1915-27) to Chaffee.

³⁹ U. S. Patent 1,491,775 (1916-24) to Hammond, Figs. 8, 9.

⁴⁰ U. S. Patent 1,522,882 (1912-25) to Hammond.

⁴¹ U. S. Patent 1,491,772 (1912-24) to Hammond, Figs. 1, 5.

⁴² U. S. Patent 996,445 (1909-11) to E. F. W. Alexanderson.

⁴³ U. S. Patent 1,491,773 (1912-24) to Hammond, claim 4.

⁴⁴ U. S. Patent 1,491,774 (1912-24) to Hammond, claims 72-79.

nators, he was shown the general concept of selectivity in reception with a radio tuner, a first detector, an intermediate frequency selector, a second detector and an audio output circuit. Audions were shown as detecting devices, and their use as amplifiers by Lowenstein was known. Therefore, Dr. Alexanderson considered that for immediate engineering purposes,⁴⁵ the first detector should be changed to be a radio amplifier and the intermediate frequency circuit to a second radio tuner. Disturbed by the suggestion that the de Forest tubes were not sufficiently reliable and perhaps too sluggish for radio amplification, Alexanderson later proposed⁴⁶ a highly interesting diversity system, Fig. 12. Here two groups of triodes were driven from two transmission line-like arrangements. All tubes of a group were driven in phase because of the nature of the line construction. Therefore, their outputs were additive, and without blue-glow gaseous conduction the combined gain could be greatly increased. If the tubes were all detectors, then the system would be of the intermediate frequency type, but if the first were amplifiers and the second were detectors, then it would be of the new tuned-radio-frequency type with both lines of the same high frequency. Thus the October, 1912 conference not only disclosed the ultimate selective receiver with double detection but, in addition to stimulating the development of the hard triode, initiated the invention that mainly supplies the sensitivity features of modern receiver systems. This conference was, therefore, of special historical significance.

While the Alexanderson alternators, each with 2 kw, 100-kc rating, were not often used in control work, experiences in their operation were undoubtedly of value in the well-known future developments leading to the formation of the Radio Corporation of America by the General Electric Company as a result of governmental policy fostered by the Navy Department.

The intermediate frequency principle was first applied outside the laboratory⁴⁷ to the solution of a World War I communication problem of high military importance.⁴⁸ Radio-telegraphic equipment was desired for signaling from front-line infantry to barrage-laying artillery in the face of powerful interference from enemy spark-type transmitters. The Hammond solution involved a superaudible amplitude modulation of a gap-type radio transmitter with a suitable intermediate frequency receiver for producing an audio signal tone. The transmitter schematic, Fig. 13, shows⁴⁹ how the radio or "A" radiation was created by charging, at a superaudible "B" frequency rate, a capacitor which produced "A" oscillations by discharging across a special

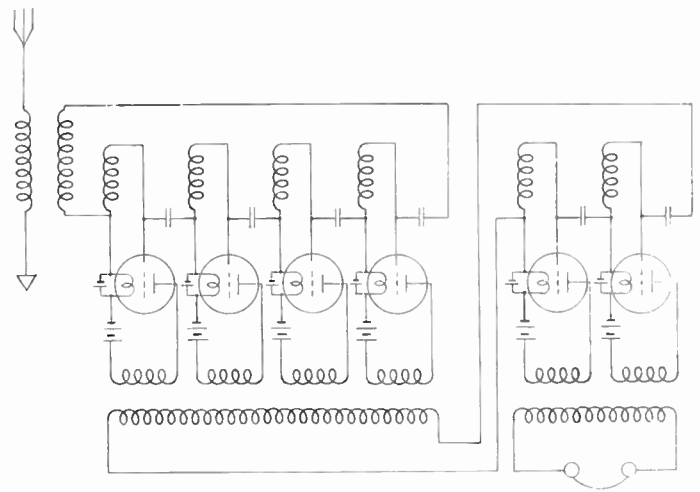


Fig. 12—Alexanderson multiple tube diversity circuit, 1912.

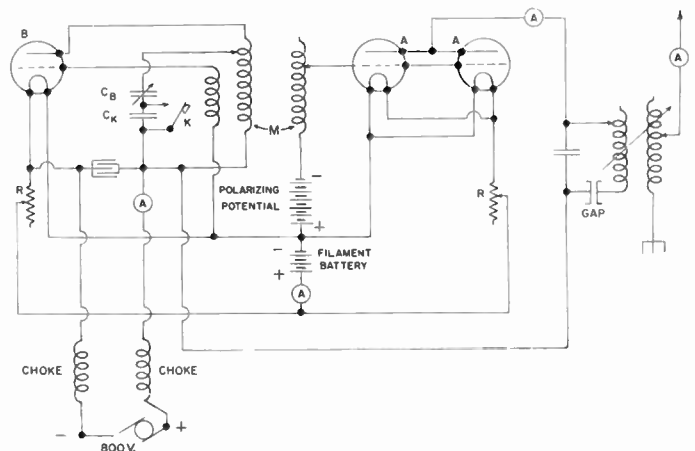


Fig. 13—Hammond-Chaffee tube-gap military transmitter, 1917.

type of spark gap. The system was of the constant energy type with signaling by key shift of the modulating frequency. While the prime purpose was selectivity, the method of keying in combination with the irregularity of the phase of the modulation at which the gap fired made the system highly secure against reception by conventional receivers. The receiver schematic, Fig. 14, shows⁵⁰ a regenerative radio tuner and first detector *X*, followed by an intermediate-frequency selector circuit *B* with an oscillatory detector *Y*, followed by an audio tuned circuit *D* with an amplifier *Z* providing audio regeneration but without causing excessive ringing. In normal operation, the first detector was nonoscillatory, but the feedback was such that the receiver was usable for single-tube continuous-wave reception. Structurally, therefore, the receiver was of the most general "superheterodyne" variety, since both detectors could be, and during adjustment often were, of an oscillatory nature. The final received signal due to the desired message was

⁴⁵ U. S. Patent 1,173,079 (1913-16) to E. F. W. Alexanderson.

⁴⁶ Letter of Alexanderson to Hammond, October 21, 1912.

⁴⁷ Signal Corps Order No. 40,105 of 1917.

⁴⁸ Even as late as October 9, 1918, this problem was recognized as "one of the most important matters connected with the war." See letter of that date, L. N. Scott, War Comm. of Tech. Soc. under Naval Consulting Board heading.

⁴⁹ U. S. Patent 1,610,425 (1918-26) to Chaffee.

⁵⁰ U. S. Patent 1,681,293 (1917-28) to Hammond; and 1,469,889 (1918-23) to Chaffee.

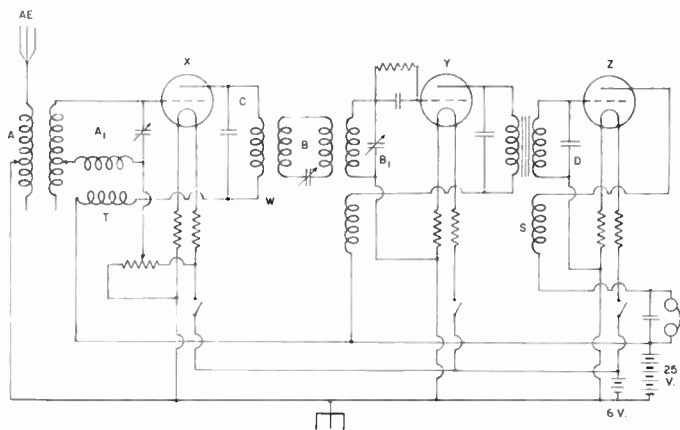


Fig. 14—Hammond-Chaffee intermediate frequency receiver, 1917.

highly free of disturbance from spark interference for a number of reasons. From a frequency domain viewpoint, the intermediate frequency circuit tuned to the fundamental of the envelope of the desired signal was not appreciably energized by the weak harmonics in the envelope of the interference. In the time domain there were lapses at the ends of the spark trains of interference during which the only signal getting to the first detector was the desired signal. Additionally, a limiter-type soft detector greatly reduced the ratio of the interference to the signal as they were both applied to the intermediate frequency circuit. The net result was that desired signals were often readily received with the interference to signal ratio at the tuner output corresponding to as much as 20 db.

This equipment was designed in accordance with military requirements as to size, weight, number of tubes, etc., and constructed by the Hammond Laboratory in 1917-18, with E. R. Cram serving as field representative of the Signal Corps. Delivered to the U. S. Army at Tours, France, by Dr. Chaffee of the Hammond group on October 10, 1918, the equipment created great interest. The performance claimed was verified by official tests directed by Capt. E. H. Armstrong of the Paris Laboratories of the Signal Corps, October 22 to November 11, 1918. Post-armistice tests were made by the British Army from whose report by Major A. C. Fuller of the Royal Engineers the schematics have been taken. This report of December 3, 1918, included the following: "The Hammond set and a 500-watt spark set were simultaneously operated on the same wavelength—710 meters—at Woolwich Common. Aerial current from Hammond set about 0.7 amp., from 500-watt set, 4.5 amps. The Hammond receiver was set up on Blackheath. The interference due to the 500-watt set was insignificant and did not prejudice reception."

In this equipment, the mean frequency of the transmitted band was 500 kc, and the bandwidth was at least twice the modulation frequency of a mean value 25 kc. While such a 10 per cent bandwidth would be intolerable for peacetime signaling merely to produce an audio tone in a receiver, this early application of intermediate

frequency circuitry provided perhaps the only possible solution of an urgent wartime problem.

The value of superaudible modulation of a gap transmitter for obtaining selectivity, sensitivity, and security continued to be demonstrated to the Army and Navy in equipments for intrafleet and plane-to-ground communications and in radio control of aircraft. But with the increase of radio services without a corresponding opening up of the higher frequency bands, the interferences by superaudibly modulated spark transmitters upon conventional communication channels became of compelling importance. Therefore, the Hammond Laboratory developed⁵¹ all-tube equipment for radiating only the minimum spectrum necessary for operating the system. Two continuous-wave equivalents of high purity were created by push-pull modulation with carrier suppression, the key-down modulation frequency determining the intermediate frequency of the receiver. Security of communications was obtained by means of an artificial frequency modulation of the carrier oscillator, using a variable capacitor wobbler in combination with key shifts with several excursions of wobble per telegraphic dot element. The total frequency swing was usually a compromise value. On the one hand, a wider swing reduced the amount of time that a given narrow-band disturbance could affect the intermediate-frequency circuit of the receiver; on the other hand, a narrower swing permitted better radio selectivity, as by coupled-circuit tuning with primary and secondary regeneration. Experiments in 1921-22, with these systems conducted by Dr. A. Hoyt Taylor and Dr. Chaffee in the Navy laboratories established points of interest regarding information theory when the interference greatly exceeds the signal. These tests proved that the nature of the detector system is of high importance in security systems based upon simple modulations. In the steady state condition, the square-law detector alone has a sensitivity for the desired signal that is not disturbed by the presence of the interference. Material pertinent to these matters has been recorded by Aiken;⁵² the need for square-law detection instead of linear is not necessarily as great in pulse systems for security control.

With the increased crowding of channels, it became evident that the important field of application of superaudible modulation was in multiplex signaling. That is, one single carrier could serve a number of sidebands, each carrying its own signal message. Laboratory and field demonstrations of August, 1925, used a carrier of 33 mc with one fixed and one variable superaudible frequency of amplitude modulation. Keying for sending messages simultaneously was by the constant energy method, with frequency shift of the amplitude modulating frequency values for minimizing cross signaling at high carrier modulation levels. These tests showed

⁵¹ U. S. Patent 1,690,719 (1922-28) to Chaffee and Purington.

⁵² C. B. Aiken, "The detection of two modulated waves which differ slightly in carrier frequency," *Proc. IRE.*, vol. 19, p. 120; January, 1931.

the practicability of sending as many as eight independent messages with the same carrier, with AM first modulations and fm second modulations. While this combination is widely used in modern practice, much radio-telephonic multiplex uses AM for both modulations with special feedback methods to linearize the modulation characteristics of the system.

While observing the performance of the two-wave system in 1922, Gen. David Sarnoff of the Radio Corporation suggested consideration be given to private radio telephony by the same general principles. This was quickly developed⁵³ with an artificially wobbled carrier that was amplitude modulated by an audio band after conversion to the supraaudible range by heterodyne methods and filtering. The receiver was of the same general type as in the telegraphic system but with the intermediate-frequency channel of speech bandwidth. The receiver heterodyne was required to be set correctly within 5 to 10 cycles for good speech quality, but more precision was required for music. This system of telephony was practiced with a transmitter on the roof of the Ministero del Interno in Rome, in 1928, to provide coverage up to 30 km with simple receivers. A later development⁵⁴ of a narrow-band system in which the speech band was not appreciably increased in width during the conversion was proposed for police work, and improvements with greater complexity were made available⁵⁵ through OSRD-NDRC for consideration in transoceanic telephony for World War II.

When the high carrier-frequency bands commenced to open up, interest again developed in the use of supraaudible modulation in simplex communications. In 1932, the Hammond Laboratory illustrated the system by transmissions at the 1-kw level from Gloucester to an Army group assembled in Washington in what is now the French Embassy. While the best monitoring facilities of the Government tuned to the Hammond band reported the radiations resembled some new kind of man-made static, the messages were received on the proper equipment with high telegraphic quality at loudspeaker level. In these tests, three-wave supersonic amplitude modulation was used with sufficient artificial frequency modulation of the carrier to yield a fairly smooth spectral energy distribution. It was noted that the signals were relatively free from selective fading, and this was considered to be due to the frequency modulation.⁵⁶ That is, during the shortest signal element not three but hundreds of spectral lines were involved in the transmission; thus the effect of selective fading was reduced as well as perhaps some noise.

Similar results were obtained in the higher frequency ranges in plane-to-ground transmissions at the 50-watt level. These transmissions were received at Washington

throughout runs to Aberdeen, Md., to Martinsburg, W. Va., and to Norfolk, Va. These tests perhaps contributed to getting military aircraft radio out of the broadcast band and to establishing better monitoring facilities for examining static-like signals coming into the Washington area.

In the field of intermediate-frequency receivers, there are four species classifiable by the different combinations of the beat and nonbeat natures of the two detectors. With both of beat nature, as is possible with Fig. 14, the receiver is applicable to continuous-wave reception; with both of the nonbeat type, the receiver is used for doubly modulated waves either in simplex or multiplex systems. For the military applications just discussed, the first detector alone is of the nonbeat type; the remaining combination with the first of the beat type and the second nonbeat is that of the familiar "superheterodyne" for reception of radio telephony as in broadcast radio.

Considering the commercial potentialities and the rigid publication restrictions upon the Hammond developments, it was probably inevitable that many others should develop parallel lines of thought. With the release from secrecy at the end of World War I, an important interference developed⁵⁷ in the patent office between R. A. Heising,⁵⁸ Hammond⁵⁹ and L. Levy⁶⁰ in the broad field of intermediate-frequency circuitry. After thorough studies of the early United States and foreign art and a clarification of the distinctions between detection and rectification, the broad subject matter in controversy was awarded Hammond, giving rights⁶¹ for the exploitation of the following word combination: "A carrier wave transmission system comprising means for receiving and detecting the energy of a modulated wave, means for selecting a component of said detected energy, and means for detecting said selected component." The entire principle of IF selectivity is expressed by the words "selecting a component" regardless of whether the unselected components were to be utilized otherwise as in multiplex reception, or were to be discarded as in simplex telephonic reception. Patent claims more specific to the superheterodyne structure for telephonic reception were awarded to Hammond in a coissued patent.⁴⁴

The commercialization of the IF principle for broadcast reception involved a somewhat different approach at first involving sensitivity rather than selectivity considerations. Observing the difficulty of amplifying short-wave signals in comparison with those of long-wave, E. H. Armstrong⁶² developed the idea of applying heterodyne conversion of the incoming signals to a lower

⁵⁷ U. S. Patent Office Interference No. 43,858.

⁵⁸ U. S. Patent Application Ser. No. 81,980, filed in 1916.

⁵⁹ U. S. Patent Application Ser. No. 175,134, filed in 1917.

⁶⁰ U. S. Patent Application Ser. No. 249,572, filed in 1918.

⁶¹ U. S. Patent 1,491,772 (1912-24) to Hammond, claim 46.

⁶² E. H. Armstrong, "A new system of short wave amplification"; *Proc. IRE*, vol. 9, p. 3; February, 1921.

⁵³ U. S. Patent 1,642,663 (1922-27) to Chaffee.

⁵⁴ U. S. Patent 2,204,050 (1938-40) to Purington.

⁵⁵ U. S. Patent 2,400,950 (1942-46) to Purington.

⁵⁶ U. S. Patent 1,761,118 (1924-30) to A. N. Goldsmith.

frequency and more readily amplifiable band, then amplifying this band before detection to produce an audio signal. Armstrong filed for a French patent on December 30, 1918. Possibly because of official knowledge of the Hammond development of IF selectivity, Armstrong discussed only the sensitivity features in his patents and technical papers. His U. S. patent claims⁶³ were later awarded to the other claimants; those pertaining to the radio-telephonic superheterodyne went to L. Levy,⁶⁴ those pertaining to the continuous-wave superheterodyne went to Alexanderson,⁶⁵ but one of these also relating to radio rebroadcast repeaters later was awarded to B. W. Kendall.⁶⁶

With the growth of broadcasting, the Alexanderson TRF system of receiver design gave way to the Hammond IF system mainly because of the requirements for superselectivity.⁶⁷ But the TRF system of cascaded selective amplification continues in preamplifiers and in IF circuits to be one of the most important elements of modern receivers.

It is noteworthy that the Hammond group additionally made other important but less basic contributions to the details of modern broadcast and receiver techniques. The principle of radio relaying by change of the carrier frequency was an early contribution.⁶⁸ An early form of automatic volume control⁶⁹ used the grid capacitor method of detection with an electronic shunting triode having a resistance that was a decreasing function of the capacitor voltage. Remote cutoff action was inherent in the Pierce proposal of 1913 to build a tube with a conical spiral grid; another solution was the use of three triodes with grids in parallel, plates in parallel, but with the cathodes at different dc potentials. There is even a suggestion in the radio-control records of the modern idea of feedback to improve fidelity of output by having the output relay of a detector rectifier discharge the grid capacitor in its input. But more positively, the Hammond group contributed to the adoption of the unicontrol superheterodyne for broadcast reception. In early models, separate controls for the radio tuner and the heterodyne oscillator provided a technically desirable flexibility. But the existence usually of two and sometimes three or more different heterodyne settings for developing the proper intermediate frequency was confusing and gave the home user a sense that the system was not selective. And in comparison with the TRF designs, the added heterodyne dial was an undesirable complication. The Hammond group, in 1917, had developed the military simplification⁷⁰ of a single-knobbed switch connected to fixed capacitors

such that the difference between the heterodyning frequency and the frequency of the selective circuit tuned to the incoming signal was independent of the switch setting. With this background, the Hammond group developed and, on April 13, 1925, was among the first to demonstrate a continuously variable unicontrol superheterodyne and to urge the adoption of this technique now almost universally used in home-instrument type receivers.

V. FREQUENCY MODULATION AND RELATED SYSTEMS

Even before the development of radio communications, some of the very basic principles of frequency modulation were discussed by Helmholtz⁷¹ in the field of sound. He indicated that when beats are formed from two unequal but substantially pure tones with slightly different pitch frequencies, "a little fluctuation in the pitch of the beating tone may be remarked." That is, a musician can hear such tones as a variation in strength and a variation of pitch of a single tone. The mathematical explanation appears to have been due to G. Gueroult⁷² who had translated Helmholtz into French, while a corresponding graphical type of explanation was provided by Taylor.⁷³ Thus the velocity of a particle vibrating under the influence of two tones was:

$$v = C \sin (mt - \epsilon)$$

where C and ϵ were slowly varying amplitude and phase functions of time. Moreover, "the pitch number of the variable tone multiplied by 2π is . . . $(m - d\epsilon/dt)$." Thus it was recognized that two unequal waves add up to the equivalent of a single wave modulated both as to amplitude and as to phase, and that the instantaneous frequency was determinable from the time derivative of the instantaneous phase. It was further shown that with the two tones unequal in strength, the instantaneous frequency would swing from within to outside the spectral limits.

In the radio field of 1912, frequency modulation was used commercially in the constant amplitude method of continuous wave transmission, without requiring a violent keyed change of the energy content of the oscillatory system. And in the Hammond Laboratory, it has been established that two independent communications could be sent in the same wave band, one by AM for telephony and one by fm for telegraphy.⁷⁴ In modern practice, the transmission of the two chrominance signals in color television is a refined example of this multiplex principle. So also to a lesser degree, in television receivers where the intermediate frequency for sound is established by the beating of the video and sound car-

⁶³ U. S. Patent 1,342,885 (1919-20) to E. H. Armstrong.

⁶⁴ U. S. Patent 1,734,038 (1918-29) to L. Levy. (See footnote reference 60.)

⁶⁵ U. S. Patent 1,508,151 (1916-24) to Alexanderson.

⁶⁶ U. S. Patent 1,734,132 (1916-29) to Kendall.

⁶⁷ See footnote reference 32, p. 278.

⁶⁸ U. S. Patent 1,313,860 (1912-19) to Hammond.

⁶⁹ U. S. Patent 1,649,778 (1917-27) to Hammond and Chaffee.

⁷⁰ U. S. Patent 1,484,605 (1917-24) to Hammond; see also U. S. Patent 1,849,651 (1924-32) to S. E. Anderson.

⁷¹ Helmholtz, "Sensations of Tone," Peter Smith, Gloucester, Mass., 6th ed., p. 165 and pp. 414-415; 1948.

⁷² *Ibid.*, footnote, p. 165.

⁷³ S. Taylor, "On variations of pitch in beats," *Phil. Mag.*, vol. 44, pp. 56-64; July, 1872.

⁷⁴ U. S. Patent 1,320,685 (1912-19) to Hammond.

riers, cross signaling between the picture tube and the speaker is minimized by this principle.

During the early development of radio, many engineers of good repute believed in the frequency modulation method of telephony, and electromechanical methods for transmission had been proposed.⁷⁵ Perhaps to a large degree such opinions were due to a then current belief that less bandwidth was required for fm than AM. As discussed under Section IV, the Hammond Laboratory was seeking means for conveying a superaudible frequency signal with a minimum of disturbance upon other channels. It was known that if a continuous-wave generator was changed periodically in frequency at a slow rate, then the tone resulting from suitable heterodyne reception was of the continuously varying siren type. In discussions, the question arose as to what happened when the rate and the extent of the frequency variation were pushed up in value. Since it was not practical to use the rotary capacitor method, the first all-electronic method of frequency modulation⁷⁶ was worked out in January, 1921. This involved setting up a triode oscillator with a plate tank circuit of high L/C ratio and with a high ratio of plate to grid feedback to yield poor frequency stability. By varying the plate and the grid dc supply voltages in phase with a proper ratio, it was found possible to produce fm with negligible AM; the oscillator could be varied about 14 kc either way from its mean 580-kc value. After checking at a slow 60-cycle modulation frequency and obtaining what was expected in a wavemeter varied as to setting, the modulation rate was pushed up to 22.5 kc. First order side frequencies were found as expected by the Fourier theory of recurrent wave forms, both by wavemeter and by beat oscillator tests. Lowering the modulation frequency to 9.5 kc, the two types of response as the swing was increased in steps from conditions 1 to 4 are as shown in Fig. 15. For the greatest swing used and the selected frequency, the carrier by both tests became smaller than the first order side frequencies. The shifting of the carrier toward the higher wavelengths with increased amount of modulation was probably due to the slight nonlinearity of the modulation characteristics.

These experiments proved that a frequency modulated signal would cause more interference upon other channels than an amplitude modulated signal for the same purpose, and the two-wave method of modulation was adopted for the immediate purposes of design. It was soon realized that a general expression for any modulated voltage wave was

$$e = A_t \cos(\omega t + \phi_t)$$

where A_t and ϕ_t are two slowly varying functions of time, and that for pure sinewave frequency modulation, the expression becomes

$$e = A \cos(\omega t + \phi_m \sin pt)$$

⁷⁵ U. S. Patents 785,803-804 (1902-05) to C. D. Ehret.

⁷⁶ U. S. Patent 1,599,586 (1922-26) to Purington.

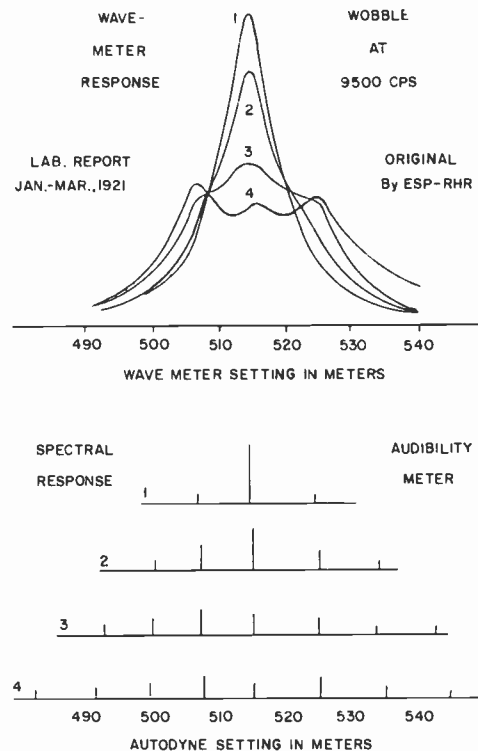


Fig. 15—Purington frequency modulator performance, 1921.

where A is a fixed amplitude value, ω and p are the angular frequencies of the carrier and modulating waves, and ϕ_m is the maximum departure of the carrier phase from mean. After the classical solution of the rotary capacitor frequency modulator by Carson,⁷⁷ expansion of the above expression by trigonometric methods confirmed the identification of the Fourier spectral amplitudes with Bessel function values. This expansion, also known to have been made by others, was first openly published by Roder.⁷⁸

But as of 1921, although consideration was given to the fm method of telephony by use of a double winding modulation transformer to provide both plate and grid voltage variation for an oscillator, it was realized that demands for channels made it imperative that broadcasting be developed first on an AM basis. Nevertheless there was some willingness to consider wider-than-necessary systems for speech telephony in the interests of reduction of noise. Fig. 16 shows one of several arrangements due to Chaffee,⁷⁹ experimentally constructed to permit examination also of another fm related idea. Here two radio carriers F_1 and F_2 were amplitude modulated in an out-of-phase manner from the same speech source, making the radiated energy at one end of the spectrum a maximum when it was a minimum at the other end. By making use of the phase

⁷⁷ J. R. Carson, "Notes on the theory of modulation," *PROC. IRE.*, vol. 10, p. 57; February, 1922.

⁷⁸ Hans Roder, "Amplitude, phase and frequency modulation," *PROC. IRE.*, vol. 19, p. 2145; December, 1931.

⁷⁹ U. S. Patent 1,776,065 (1922-30) to Chaffee.

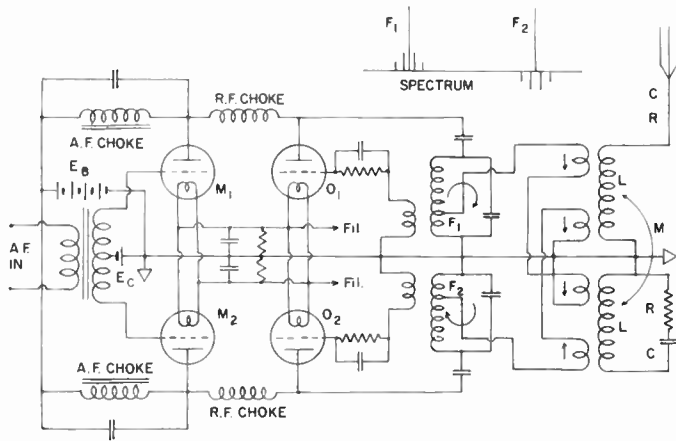


Fig. 16—Chaffee noise-reduction system transmitter, 1922.

relations of coupled circuits,⁸⁰ both modulated oscillators fed the same antenna without reactions of either source upon the other.⁸¹ This was an early form of diplexing, but with half the power from each source lost in the dummy tank circuit. The same phase principles, but with direct coupling circuitry, are used in modern frequency discriminators to perform the opposite function of distributing the two ends of a spectrum to different use circuits such as diode detectors. The receiver for this Chaffee system used individual tuners as in the Tesla two-wave procedure, but with two output transformers with secondaries connected in series in a manner to cause the two detected signals to add coherently and to provide cancellation of the noises that were common to both channels. An alternative transformerless method would develop from the differential circuit of Fig. 4 with the loops tuned to frequencies F_1 and F_2 , respectively and with the relay replaced by headphones. Patentwise, the principle was expressed in part as follows: "In a receiving system for radiant energy, a plurality of receiving channels tuned to the energy of different frequencies, respectively, means for producing currents of like frequencies but of different phases from the received energy, an indicating device, and means interposed between said channels and the indicating device for causing said currents to combine additively and to simultaneously actuate said device." Experimentally this system greatly reduced noise effects such as filament hum that were equally present as amplitude modulations in both channels. Since the Hammond group at that time was primarily concerned with high noise-to-signal ratios, no thought was given to the diversity properties of the system by which the desired signals added coherently and the random noises built up incoherently.

The relation of this system to that of modern frequency modulation is obvious. There can be no question

but that the radiation is properly receivable by an fm type receiver with a suitable line-up of the IF and discriminator circuits. But to point up the comparison more clearly, the amplitude, phase and frequency variations of a single voltage vector representing the entire radiation have been evaluated for a special case (Fig. 17, opposite). Positive and negative lines in the spectrum are representations of various cosinusoidal waves of different frequencies. For positively shown lines, the phase is zero at $t=0$, at which time the phase of a negatively shown line is π radians. The main lines of amplitude E are offset an angular frequency value δ from the reference angular frequency ω at the center of the spectrum; the signal created lines of amplitude $kE/2$ are offset by the signal angular frequency p from the main lines. The expression for the instantaneous totalized voltage is recorded. From this expression, the amplitude function A_t , the phase variation function ϕ_t , and the angular frequency deviation function $d\phi_t/dt$ are readily developed in terms of the frequency parameters δ and p and the signal modulation parameter k ; the routine procedure has been exemplified in the Helmholtz reference. With the separation parameter δ an integral multiple of the signal modulation angular frequency parameter p , these functions are recurrent in one signal cycle. Curves are shown in Fig. 17 for the conditions $\delta=3p$, $k=1$. The absolute value of the amplitude function is plotted positively to show the wave form recoverable by applying the spectrum to an ideal aperiodic linear rectifying system. The instantaneous phase and frequency curves correspondingly show the wave forms producible by applying the spectrum to ideal aperiodic phase and frequency modulation detector systems.

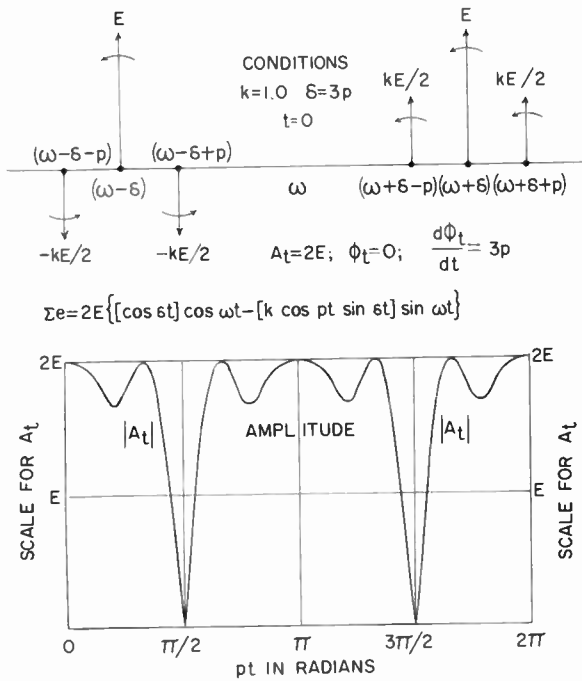
In general, the amplitude function departs mostly from uniformity at the period of the modulation cycle when the two main spectral lines and likewise the two lines of each set of signal produced lines are momentarily of opposite phase to produce cancellation. At this time, the frequency deviation is also passing through zero. While the signal distortion producible by phase modulation reception is small, that for frequency modulation reception is of course much greater. With a properly lined up fm type receiver, the Chaffee type signal would be receivable without distortion; such a receiver would of course distort a pure sinusoidal pm or fm signal. The noise reduction merits of the system in comparison with an fm system of comparable width and signal carrying capacity have not been evaluated.

The Hammond group soon developed the ultimate of spectral compactness for a two-channel system most like fm except in bandwidth. This was based upon the phase reversal of one of the sidebands of an amplitude modulated signal, or as a practical alternative, a ninety degree phase shift⁸² of the carrier with respect to the

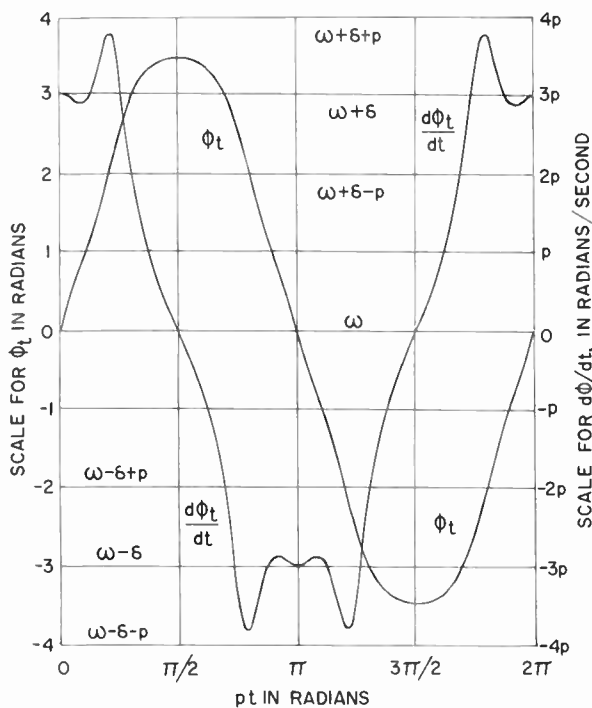
⁸⁰ U. S. Patent 1,601,109 (1922-26) to Chaffee.

⁸¹ The circuitry is discussed in E. S. Purington, "Single and coupled-circuit systems," *PROC. IRE.*, vol. 18, pp. 996-998; June, 1930.

⁸² U. S. Patents 1,935,776 (1929-33) and 1,976,393 (1929-34), to Hammond, Fig. 8.



(a)



(b)

Fig. 17—Amplitude, phase, and frequency characteristics, Fig. 16.

condition for which the carrier and sidebands would represent pure amplitude modulation.⁸³ Fig. 18 shows how the sidebands were created by a push-pull amplitude modulation, with the output of which the carrier could be combined in any desired phase in accordance

⁸³ The vector-tensor method of representing and handling an amplitude modulated wave is shown in E. S. Purington, "The Operation of the Modulator Tube in Radio Telephone Sets," Bureau of Standards, Scientific Paper No. 423; 1922.

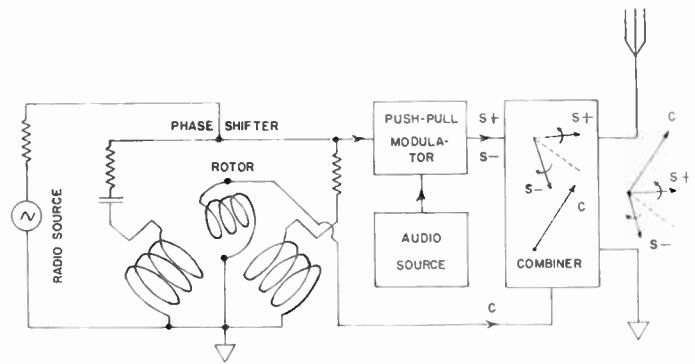


Fig. 18—Hammond "Quasi-phase" modulator, 1927.

with the setting of a rotary phase shifter. The desired radiation was produced when the rotor was so set that with a 1000-cycle signal tone, an amplitude detector of the radiation produced a 2000-cycle tone with no 1000-cycle residual. As in the reception of the previously discussed radiation, differential detection resulted in recovery of the desired signal and the reduction of noises common to both channels. This involved diverting one sideband and half the carrier to one detector and the other sideband and half the carrier to another detector.

It was quickly realized this "quasi-phase" signal could serve as the basis of an artificial frequency modulated signal with a stabilized carrier. This involved frequency multiplication and amplitude limiting together with tapering the audio signal to convert from phase modulation to frequency modulation characteristics. This process was outlined in a tutorial part of a patent⁸⁴ for consideration in commercial design when, as, and if the establishing of fm sound transmission was deemed to be in the public interest.

It has been recorded above how fm had early applications in security systems for radio control and for telegraphic and telephonic communications, and had been proposed for fading reduction in telephonic transmission. With the development of radio facsimile, fm was again proposed for fading reduction, using the principle that when the signal faded but still existed, the instantaneous frequency value could indicate the picture element tonal value desired to be recorded. Mertz⁸⁵ is considered to be the first to show this principle but in the field of wire communications. Wright and Smith⁸⁶ in Great Britain proposed it for radio-facsimile, and in the United States Hammond⁸⁷ further contributed to the art. The technique was to apply severe limiting action by clipping the received and detected fm signal to a fixed level, to feed the clipped signal through a slope filter to eliminate harmonics created by the clipping, and also to produce a signal of strength dependent solely upon the instantaneous frequency transmitted,

⁸⁴ U. S. Patent 2,020,327 (1930-35) to Purington.

⁸⁵ U. S. Patent Office Interference 61,606; U. S. Patent 1,548,895 (1923-25) to P. Mertz.

⁸⁶ U. S. Patent 1,964,375 (1926-34) to Wright and Smith.

⁸⁷ U. S. Patents 1,977,438 (1929-34) and 2,036,869 (1929-36) to Hammond.

and finally to apply the filter output to a light producing indicator. This application of fm in facsimile systems was made in the Hammond Laboratory on May 25, 1927.

The Westinghouse group was probably the first to actively press the commercialization of fm for voice transmission. A. Nyman⁸⁸ had considered improved methods of electro-mechanical frequency modulation of an oscillator. E. H. Armstrong⁸⁹ in 1927, filed upon "a new method of transmission in which the frequency of the transmitted wave (not its amplitude) is varied in accordance with the voice frequency to be transmitted." His patent claims, however, were restricted to receiver circuitry, including the combination of limiter action and dual channel detection. In interferences, the two-channel idea was credited to Conrad⁹⁰ also of the Westinghouse group, but the basic limiter idea was credited to Mertz above mentioned. However, it appears that Armstrong and later Hammond⁹¹ were among the first to realize that the distortions due to clipping the IF signal for minimizing AM effects could be mitigated by the harmonic rejection discriminator before the second detection.

As of 1927, Armstrong was uncertain as to what bandwidth should be used for fm transmission of speech and music. Thus in the patent application he indicated: "The band may be made any width desired depending on the particular conditions and the distance over which it is desired to operate. This can only be determined by experiment. In general, however, the narrower the band, the less the effect of atmospheric disturbances." This doctrine to favor narrow-band operation because of atmospheric is in accord with the accepted beliefs of the times, although irrelevant when the interferences as in

military communications and radio control were sometimes far above the atmospheric level. But in 1933, after further consideration and experimentation¹ as a freelance inventor, Armstrong indicated:⁹² "I have discovered that by imparting a greater swing to the frequency of the transmitted wave . . . a very great improvement in transmission can be produced." These discoveries were in a wave region where in general natural atmospheric disturbances were of a lessened importance, and where greater swing and channel width would by governmental protection not result in interferences from or upon most man-made radiations.

Under these conditions, fm provided a good engineering solution to the problem of providing high-quality, high-fidelity, disturbance-free music transmission at a relatively low transmitter cost. Experts in information theory revised their rules relating the possible amount of signal information to power, distance, wave frequency, bandwidth, time, and signal-to-interference ratio. Engineering developments were stimulated, resulting in improved methods of transmission and reception and the application of fm in special purpose voice communications. With the advent of television, the adoption of the highly developed fm system of sound transmission provided for the best possible cooperation between a sound channel and the basically AM system of video transmission.

VI. ACKNOWLEDGMENT

We wish to acknowledge the assistance given by Dr. E. F. W. Alexanderson, Dr. I. Langmuir, and Mr. W. Dubilier in supplying early data referred to in this history. We further express appreciation for the contributions of the many laboratory and field engineers of the Hammond staff who have participated in the little-known but highly important developments here for the first time openly recorded.

⁸⁸ U. S. Patent 1,615,645 (1920-27) to A. Nyman.

⁸⁹ U. S. Patent 1,941,447 (1927-33) to E. H. Armstrong

⁹⁰ U. S. Patent Office Interference 69,406; U. S. Patent 2,057,640 (1927-36) to Conrad.

⁹¹ U. S. Patent 1,977,439 (1929-34) to Hammond.

⁹² U. S. Patent 1,941,069 (1933-33) to Armstrong.



Description and Operating Characteristics of the Platinotron—A New Microwave Tube Device*

WILLIAM C. BROWN†, MEMBER, IRE

Summary—The term “platinotron” is the nomenclature given to a class of tube which, in general, comprises a circular, but nonreentrant, dispersive network matched at both ends over the frequency region of interest, and a reentrant electron beam originating from a continuously or nearly continuously coated cathode coaxial to the network. A dc potential is applied between the cathode and anode and a magnetic field is applied parallel to the axis of the cathode and transverse to the electric field between anode and cathode.

In operation, the device works within the pass band of the network and exhibits directional properties, acting as an efficient, broad-band, saturated amplifier when the signal is passed through the device in one direction and as a passive network when the signal is passed through in the reverse direction. The platinotron has no region of linear amplification and may self-oscillate if the driving signal is removed. When the platinotron is being driven from an rf source, there is little or no power flow from the platinotron toward the driver. This behavior distinguishes the device from a conventionally locked magnetron oscillator.

Desirable characteristics of the platinotron include: efficiencies of 50 to 70 per cent; high peak and average rf power outputs, electronic bandwidths of 10 per cent with nearly constant efficiency over the entire bandwidth, low-phase pushing figure, low operating voltage, nominal gain of 10 db over a ten per cent frequency range, and a simple, compact mechanical structure.

INTRODUCTION

THIS PAPER describes a new device, the platinotron,¹ and some essential performance features of this device when used as a broad-band amplifier. The broad-band amplifier, or “amplitron”² application of this new device, helps fill the need for an efficient, high-power, broad-band amplifier for microwave radar.

The platinotron device has its roots in the magnetron. It is structurally similar to a magnetron and shares many of the essential circuit and electron beam interaction features of the magnetron. However, there are enough differences between the two to establish the platinotron as a device with radically different performance features. These new performance features include operation as a saturated amplifier over an appreciable band of frequencies of the order of 10 per cent, with high efficiency and a nominal gain of 10 db, without any mechanical or electrical adjustments of either the platinotron or the modulator power supply. In addition, the amount of phase shift between input and output is relatively insensitive to changes in the power supply. Efficiencies are in the range of 50–70 per cent and are,

therefore, somewhat higher than for the conventional pulsed magnetron oscillator. The low insertion loss of the platinotron makes it possible to pass the signal received by the antenna back through the platinotron before entering the duplexer, thus permitting low-level duplexing. Relatively low operating voltages and simple mechanical construction are features shared with the magnetron.

Because of its close similarity to the magnetron in construction, it is surprising that the platinotron or a similar device has been so tardy in coming into being. It was well-known, for example, that the magnetron which was produced by the tens of thousands during World War II and which literally made microwave radar possible at that time, had a very broad-band circuit and that the circuit reentrancy was the cause of the narrow band of the device. There was indeed some modest effort expended in an attempt to make a more versatile operating device out of the conventional magnetron.³ The failure of a greater effort to develop was probably caused by both the formidable analytical problems which made the magnetron approach unattractive to many investigators, and the publishing of attractive performance characteristics from an amplifier device⁴ much more amenable to analyses. Another possible reason for the failure of the magnetron approach to mature earlier, was the failure on the part of engineers to recognize that there were important applications for a saturated amplifier of broad-band properties, quite independent of whether that device also had linear amplifier characteristics. The final emergence of the platinotron device then, is partly the result of persistence in forsaken fields and partly the result of a critical review of what performance characteristics were really fundamental and essential to a pulsed radar system.

The emergence of the platinotron may have significance other than its immediate usefulness as a broad-band amplifier: it may bring about a general consideration of reentrant beam tubes as a class. Reentrant beam tubes have a number of desirable characteristics such as high efficiency, compact size, etc., as well as presenting an opportunity for discovery of new properties.

Before proceeding further, it may be desirable to point out that the platinotron can be made into a highly frequency-stabilized self-excited oscillator by the addi-

* Original manuscript received by the IRE, March 13, 1957; revised manuscript received June 7, 1957.

† Raytheon Mfg. Co., Waltham, Mass.

¹ The platinotron device is proprietary to the Raytheon Mfg. Co. The experimental data reported in this article were obtained under a U. S. Signal Corps contract.

² Trademark.

³ Classified work sponsored by Bureau of Ships at Raytheon Mfg. Co., 1948–1950.

⁴ R. R. Warnecke, W. Kleen, A. Lerbs, O. Döhler, and H. Huber, “The magnetron-type traveling-wave amplifier tube,” *PROC. IRE*, vol. 38, pp. 486–495; May, 1950.

tion of rf feedback and the application of stabilizing circuits. The term "stabilotron"⁵ has been assigned to this device. For a given degree of frequency stability much higher circuit efficiency can be obtained in the stabilotron than in a magnetron since the stabilizing cavity can be placed at the input to the stabilotron and hence absorbs less power. Improvement in frequency stability over a conventional unstabilized magnetron can range from 5 to 100 depending upon the category of frequency stability being compared; for example, whether the frequency-pulling figure or frequency drift due to temperature change is being compared. Although the properties and theory of the stabilotron are of considerable interest, they will not be discussed further in this article.

The material which follows is organized into five separate sections. The first section describes the platinotron device physically and compares it with the conventional magnetron oscillator. The second section discusses the characteristics of the device as a circuit element. The third section presents some detailed performance characteristics of the platinotron used as an amplifier. The fourth and fifth sections relate to general design considerations and their application to the QK434 platinotron.

The reader should keep in mind that while this article represents a sizeable release of information on the platinotron, it does not present a complete theory of the device, particularly with respect to the details of interaction between the circuit and the beam. Experimental data are incomplete with respect to performance lying in frequency regions outside a 10 per cent frequency band centered at 1300 mc.

PHYSICAL DESCRIPTION OF THE DEVICE

Fig. 1 shows the QK434, an L-band platinotron, with the external permanent magnet in place. Fig. 2 shows the same platinotron with the magnet and cover removed, exposing the internal circuit and cathode. Physically the device is similar to the conventional fixed frequency magnetron oscillator. Like the magnetron the electron beam is reentrant and originates from a continuously coated cathode which is coaxial to the rf circuit. Like the magnetron, the device is placed in operation by supplying a static magnetic field parallel to the axis of the cathode and an electric potential between the cathode and the rf circuit. But unlike the conventional magnetron oscillator, the rf circuit is non-reentrant⁶ and the characteristic impedance of the rf circuit is matched at both ends of the circuit to two external rf connections over the frequency region of interest. This difference in the treatment of the rf circuit results in completely different operating behavior of the conventional magnetron oscillator and platinotron. The

⁵ Trademark.

⁶ The cutting of the straps of a strapped platinotron circuit provides a high degree of isolation between the two circuit members thus formed.

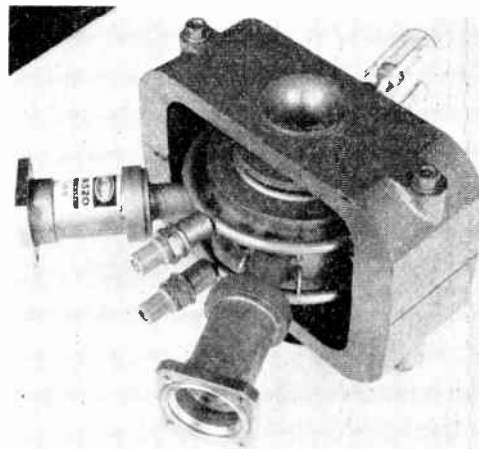


Fig. 1—Photograph of a platinotron and the permanent magnet used with it.

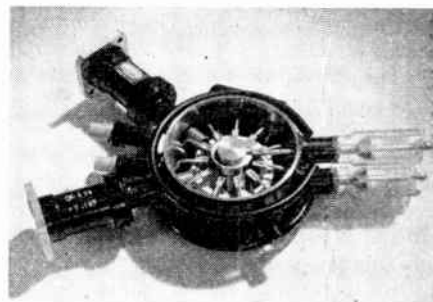


Fig. 2—Photograph of a platinotron with the magnet and one cover removed.

platinotron circuit treatment not only provides the two sets of terminals necessary for an amplifier, but it takes advantage of the natural broad-band characteristics of the rf circuit which the reentrant circuit treatment in the magnetron nullifies.

As shown in Fig. 3, the rotation of the space-charge cloud may be in either direction in the conventional magnetron oscillator without causing noticeable differences in performance, whereas in the platinotron, changing the direction of rotation relative to the input and output of the device will bring about a radical change in the behavior of the device.

Additional perspective as to the physical nature of the device may be obtained from Fig. 4 which gives a plan and cross section view of the QK434.

CHARACTERISTICS OF THE DEVICE AS A CIRCUIT ELEMENT

As a circuit element the platinotron may be best described as an active two-terminal-pair network with directional properties, as shown in Fig. 5. When an rf signal is injected into the first set of terminals, the rf level will be greatly increased at the second set of terminals. On the other hand, if the rf signal is injected into the second set of terminals, the rf level will be neither increased nor decreased at the first set of terminals. To a first approximation there will be the same phase shift θ_p of the rf signal as it traverses the device, regardless of

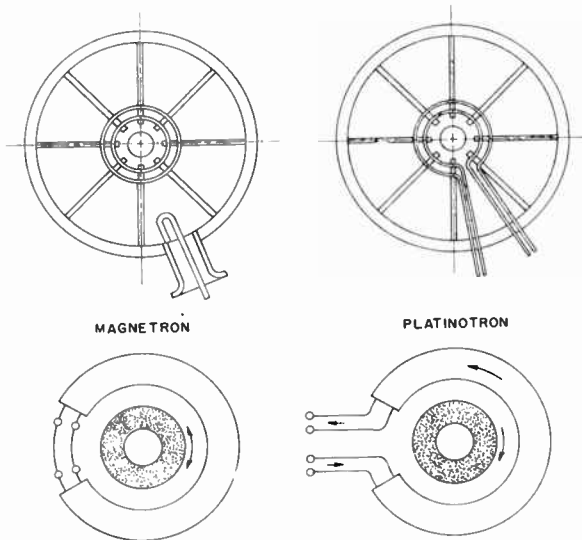


Fig. 3—Diagram illustrating the basic differences of construction and operation between the platinotron and the magnetron.

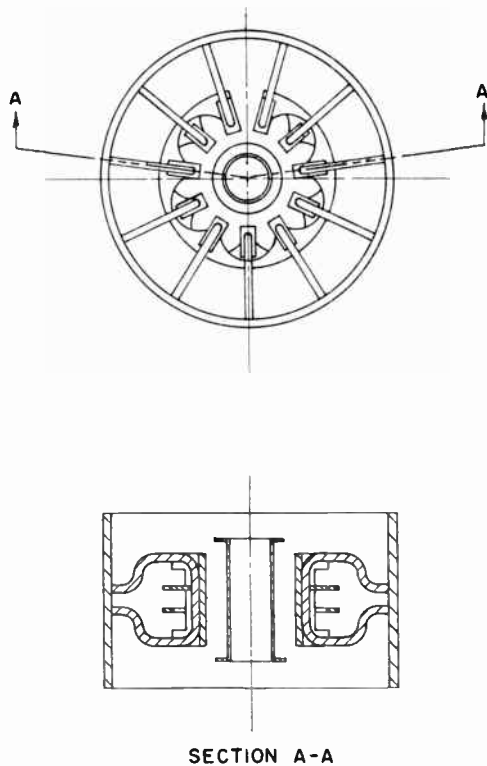


Fig. 4—Plan and cross section view of an L-band platinotron.

direction. If the direction of the magnetic field is reversed, then the directional properties of the device are also reversed.⁷

Various performance characteristics of the device based on this simplified circuit concept can now be dis-

⁷ The directional properties of the device may also depend upon the current level at which the device is operated. At very low current levels the QK434 has been found to have a forward-wave type of interaction, but at the current levels at which the QK434 would be operated as a power device, the beam-circuit interaction is of the backward-wave type. The shift occurs at a value of anode current of from two to three amperes.

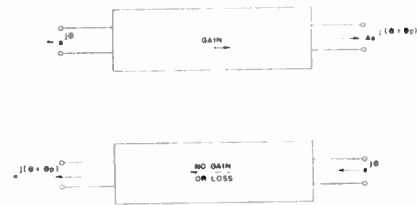


Fig. 5—The circuit element characterization of the platinotron.

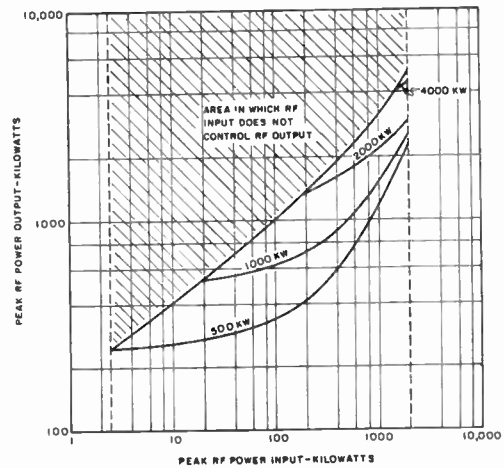


Fig. 6—The general relationship between the rf input and the rf output of the QK434 platinotron as a function of power input from the modulator.

cussed. The first characteristic to be discussed is the relationship between rf input and rf output as a function of dc power input to the device. These characteristics for the QK434 are shown in Fig. 6. Quite clearly the device behaves as a saturated amplifier. For a given dc power input level, the rf output is relatively independent of the rf drive level, departing from this independence as the magnitude of the rf drive level becomes comparable to the rf output level, and as the rf drive level becomes so low that it loses control over the frequency of the rf output. In the region in which the rf input does not control the rf output, the rf output is noisy, poorly defined, and at some other frequency than the driving signal. The transition region between the controlled and uncontrolled areas is well defined and of negligible width.

The operation of the QK434 has been explored with rf drive levels as low as 2 kw to as high as 2000 kw. Over this range of driving signal, the curve marking the separation of the controlled and uncontrolled regions of operation has been found to be approximately

$$P_{o'rf} = 145(P_{i'rf})^{0.45}$$

where

$$P_{o'rf} = \text{rf power output in kw.}$$

$$P_{i'rf} = \text{rf power input in kw.}$$

This curve also determines the maximum gain that can be obtained at any rf drive level.

$$\begin{aligned} \text{Maximum gain} &= \frac{P_{o'rf}}{P_{i'rf}} \\ &= \frac{145}{(P_{i'rf})^{0.55}} \end{aligned}$$

As indicated in the above equation and Fig. 6, power gains of 20 db may be obtained at the lower drive levels, whereas gains of only a few db may be expected at the higher drive levels. It should be noted, however, that the rf input power is conserved in the rf output power, making it possible to use efficiently the higher power but lower gain levels of the platinotron.

The rf power which is generated within the platinotron flows predominantly out of the output set of terminals only. The fraction of the generated power which finds its way to the input set of terminals and appears at those terminals as reflected or reverse-directed power is only a small fraction of the output power of the device. This behavior is distinctly different from that associated with a conventionally locked oscillator with which the platinotron is occasionally compared. The ratio of the reverse-directed power to the output power for the QK434 is shown as a function of frequency in Fig. 7. If the reverse-directed power originates from a reflection at the output of the device, however, it passes back through the tube relatively unattenuated. The manner in which this device handles the power generated within it and the manner in which it handles reflected power from the output substantiates the circuit representation of Fig. 5.

A very interesting and useful property of this device is its ability to amplify, operate efficiently, and deliver large power output over a relatively wide frequency band. A typical plot of efficiency against frequency at a fixed power input level is shown in Fig. 8. The efficiency remains relatively constant over a 10 per cent or greater frequency band. At the time this article was prepared for publication the limitations on the bandwidth capabilities of the QK434 platinotron had not been determined because of the lack of a broad-band rf driver source. It seems reasonable to expect that the frequency dependency of the phase of the reentrant electrons relative to the wave propagating on the network will be a factor which will affect the performance over a band of frequencies, but it is not clear as to how and to what extent.

Another characteristic of this device of considerable practical importance is that the phase shift across the device is nearly independent of the dc current applied to the device over a relatively wide range of currents. The term "phase pushing" has been applied to the slope of the characteristic of frequency vs current because of its relationship to the term "frequency pushing" which is descriptive of a similar phenomenon in oscillators in which the frequency is changed or "pushed" as the current is changed. In the platinotron device the phase pushing can be measured either directly by noting the

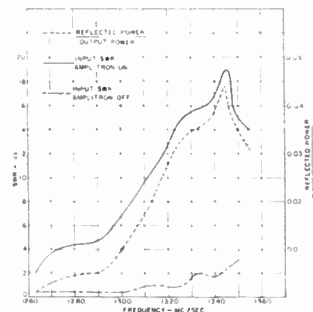


Fig. 7—Relationship between efficiency and frequency typical of platinotron performance.

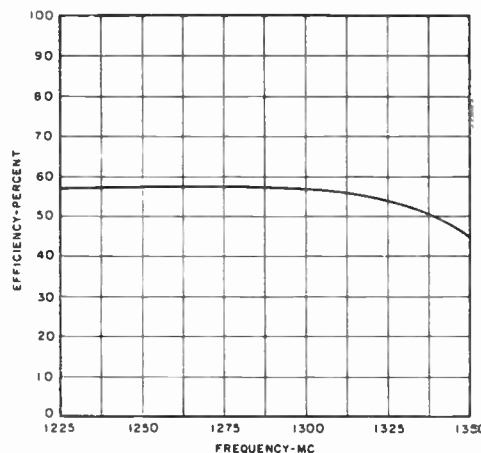


Fig. 8—Measurement of reverse-directed power at the input of the platinotron as a function of frequency with the platinotron operating into a matched load.

change in phase across the device as the current is changed, or it may be measured indirectly by using the platinotron as an oscillator and measuring the frequency change. In conventional magnetron oscillators, the frequency pushing can change from a positive value to a negative value, going through a zero value, as the current is increased. Similarly in the platinotron the "phase pushing" can obtain a value of zero. However, its value everywhere in the operating range is so low as to make quantitative measurements of phase pushing difficult. It has been necessary to note the phase change resulting from a relatively large change in current, and thereby obtain an average value of phase pushing over this current range. Fig. 9 has been prepared from such data. These data indicate that the phase pushing does go to zero and is everywhere small in value.

Considerably better data have been obtained on phase pushing by measuring the frequency pushing when the platinotron device is set up as a self-excited oscillator, its frequency being primarily controlled by the relative position of reflections deliberately placed in the input and output. Such data are shown in Fig. 10 where it is clearly seen that the slope of the frequency vs current characteristic obtains a zero value for certain values of current and magnetic field. Since an oscillator in the steady state must always maintain a total loop phase shift of some integral multiple of 2π , and since the oscil-

kv ↓ 1b →	10-20 A.	20-30 A.	30-40 A.
36	-0.8°/amp.	+0.34°/amp.	30-34 A. +0.85°/amp.
34.6	-0.45°/amp.	+0.22°/amp.	30-34 A. +0.8°/amp.
33.2	-0.44°/amp.	+0.22°/amp.	30-40 A. +0.9°/amp.
30.3	-0.6°/amp.	+0.40°/amp.	+0.8°/amp.
25.9	-0.8°/amp.	+0.60°/amp.	+0.9°/amp.

Fig. 9—Experimentally measured phase pushing characteristics in an L-band platinotron.

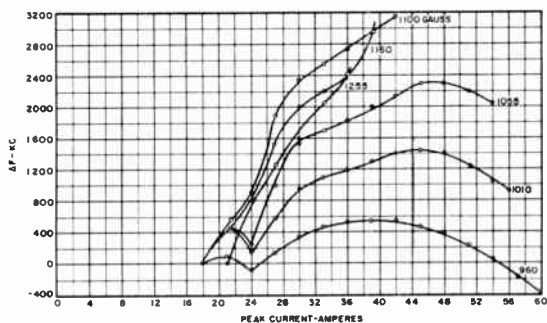


Fig. 10—Experimentally measured frequency pushing characteristics in an L-band platinotron operated as a nonstabilized oscillator.

lator is composed of elements whose phase shift is dependent upon frequency, a constant frequency can only be obtained if the phase shift remains constant. If the frequency of such an oscillator remains constant as the current is varied, the conclusion may be drawn that the phase shift also remains constant over the current region.

The possibility of obtaining zero or small phase pushing in an amplifier is of considerable significance in the design of many radar systems in which it is desired to hold the phase shift across the device constant while still making the modulator as simple and compact as possible.

The relationships between anode voltage, anode current, frequency, and magnetic field are of primary importance. These relationships are similar to those for a magnetron device, and will be developed later in this article. Representative data giving the relationship between anode voltage, anode current, and magnetic field, with the frequency held constant are shown in Fig. 11. The platinotron is a relatively low input impedance device, ranging from 500 to 1000 ohms depending upon the operating point which is selected.

DETAILED PERFORMANCE CHARACTERISTICS OF THE PLATINOTRON USED AS AN AMPLIFIER—THE "AMPLITRON"

Although the platinotron device itself has been described as an amplifier, it is possible to use it as a self-

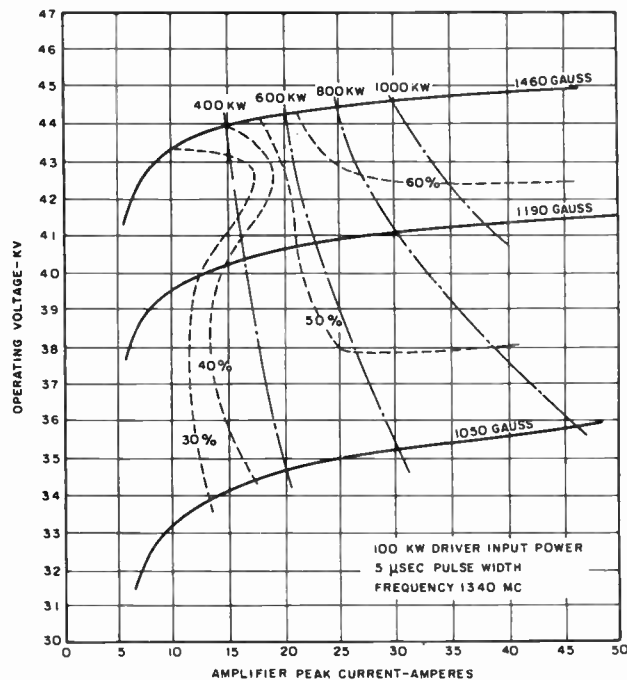


Fig. 11—Typical performance chart of an L-band platinotron (QK434). The relationship between anode current and applied anode potential for a particular value of magnetic field is given by the curves of constant magnetic field. Curves of constant rf power output and efficiency are shown.

excited oscillator, either stabilized or unstabilized. The term "amplitron"⁸ has been assigned to the use of a platinotron in those applications where it is intended to drive it with an rf signal. The following material, therefore, describes the characteristics of the platinotron when it is used as an amplifier, and the term amplitron will, therefore, be used.

The Presentation of Amplitron Operating Data

In evaluating the performance of an amplifier, there is natural major concern as to the quality of the reproduction of the input signal. From the standpoint of evaluating the quality of reproduction, the usual ordinary measurements of efficiency, power output, gain, etc. are not enough. It is desirable to take each point of data in such a manner that a measure of the quality of the reproduction of the input signal is available. This is accomplished by photographing the input and output frequency spectra presented on a voltage basis on a spectrum analyzer. The voltage spectra are particularly useful as critical measurements, for the spectrum side-lobe structure is very sensitive to any reproduction change. As a further enhancement of critical evaluation, a relatively long pulse duration of 5 μsec is used. This results in a spectrum bandwidth of 400 kc between the first null points of the spectrum.

For amplitron tests, obtaining a good driver spectrum posed considerable difficulty. This problem was solved finally by using a stabilotron as the driver. Because

⁸ Trademark.

spectrum analyzers of sufficient resolving power and stability were not generally available, a special analyzer was developed for the purpose of taking spectral data.

The amplitron tested was designated the QK520. Fig. 12 is a photograph of the actual amplitron test setup that was used. Fig. 13 is a schematic diagram of the amplitron test setup. Separate modulators for the driver and the amplitron were used but the trigger of one was slaved to the other. The times of the start of the two pulses and the pulse widths were made as nearly identical as possible. In the rf circuit, a resistive pad was inserted between the driver and the amplitron, primarily for the purpose of reducing the power output of the driver down to a usable input signal level for the amplitron. The pad served a second function in that it effectively isolated the driver from the amplitron. Such isolation is of particular importance when the amplitron is operated into a mismatched load.

The measurement of amplitron efficiency requires definition and discussion. In a nominal gain device where the input power appears as an appreciable percentage of the output power, a conservative definition of efficiency must make provision for the subtraction of this input power from the output power. Consequently, in all the data presented in this paper, the following conservative definition of efficiency is used:

amplitron efficiency

$$= \frac{\text{rf power output} - \text{rf power input}}{\text{modulator power input to amplitron}} \quad (1)$$

The definition of amplitron gain is, of course,

$$\text{amplitron power gain} = \frac{\text{power output}}{\text{power input}} \quad (2)$$

Although the amplitron efficiency should be defined as above, it should be remembered that the input power is not lost but appears as part of the output power. The effective over-all efficiency of a chain of amplitrons can, therefore, remain very high.

In evaluating this device we must consider the effects of varying the parameters of anode voltage, anode current, magnetic field, level of rf drive, frequency of rf drive, and the load into which the tube operates. Over a very wide variation of these parameters the spectra reproduction should remain satisfactory throughout the region and not vary discontinuously in any manner. Therefore, the spectrum was photographed at frequent intervals of the parameters that were being varied.

Matched-Load Performance as a Function of Anode Current, Anode Voltage, Magnetic Field, Frequency, and Input RF Level

These data are presented in the same manner that magnetron data are often presented. The relationship between anode voltage and anode current is determined by the magnetic field strength, as indicated in Fig. 14

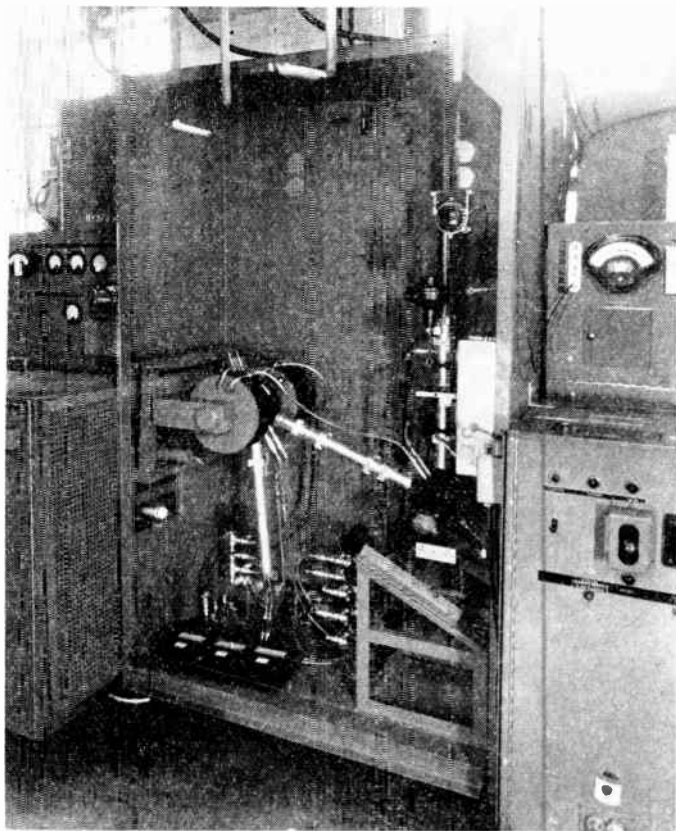


Fig. 12—Photograph illustrating the test setup for the amplitron. Stabilotron driver is on the right, the amplitron on the left surrounded by the test electromagnet.

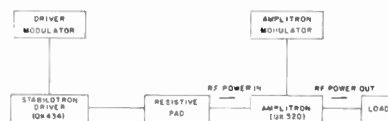
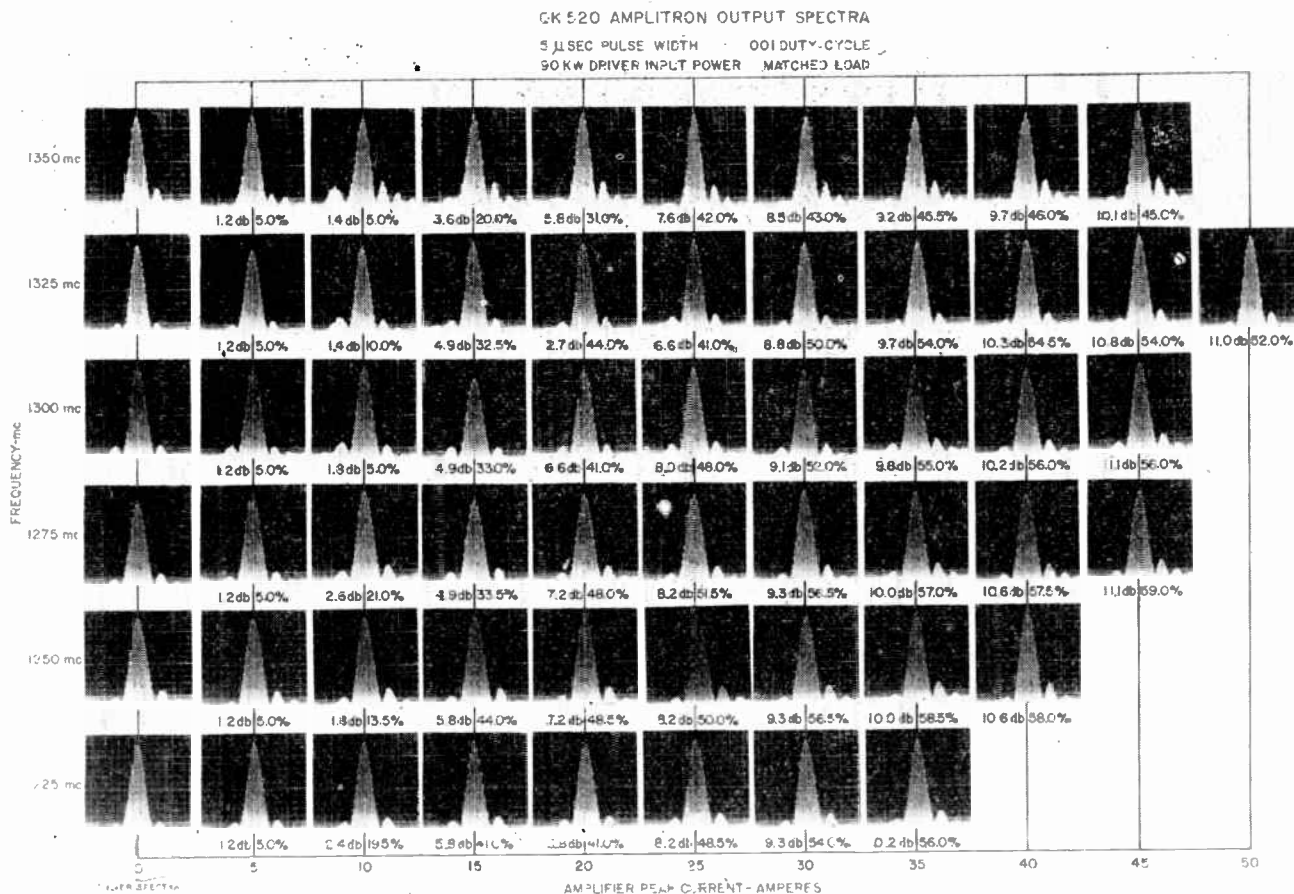


Fig. 13—Schematic diagram for the testing of the amplitron.

(opposite) by the three "Gauss" lines. The reproduction of the input spectrum is indicated at 5-ampere increments along each Gauss-line. Over the region of the graph in which spectra data are shown, the quality of the spectra is good and there are no regions of poor spectra. The highest current values, for which spectra are shown, mark the limits of amplification of the amplitron and indicate that good spectrum quality is maintained as the upper current boundary is approached. If the upper current boundary is exceeded, there is complete failure of amplifier action.

Power output, efficiency, and gain are shown below each spectrum photograph. The particular data shown in Fig. 14 and Fig. 11, which were derived from the data of Fig. 14, indicate increasing efficiency with increasing current and magnetic field. Efficiencies in the range of 60–65 per cent are attained.

These particular data were taken with an rf input power of 100 kw. Similar data taken at 10 kw and 50 kw of rf drive indicate no discontinuities of spectra quality over wide variation of the parameters of magnetic field



(a)

a wide range of frequency and current. Fig. 15(a) and 15(b) show such data taken with an rf input of 90 kw. Spectrum photographs were taken at 5-ampere increments of current and 25-mc increments of frequency to cover a 10 per cent frequency range. By means of these data it is possible to determine the gain level and efficiency with which it is possible to cover the 10 per cent frequency band while keeping the current constant. It may be noted that the efficiency exceeded 50 per cent at a 9.5-db gain level over most of the band. Similar data have been taken at lower rf drive levels. With a 10-kw drive level an amplification of 15.5 db with good reproduction over an 8 per cent frequency band was obtained.

Variable-Load Performance as a Function of Frequency and Drive Level

To be practical, an amplifier must be capable of operating into a mismatched load of arbitrary phase and standing wave ratio of at least 1.5 in voltage and preferably higher. To examine the ability of the amplitron to meet these requirements, spectrum photographs and other essential data were taken for representative mismatches and plotted on load diagrams similar to that shown in Fig. 16. Spectra were taken for eight equally spaced phase positions of a 2.5/1 vswr and 1.5/1 vswr, and at the match point. The shape and quality of the

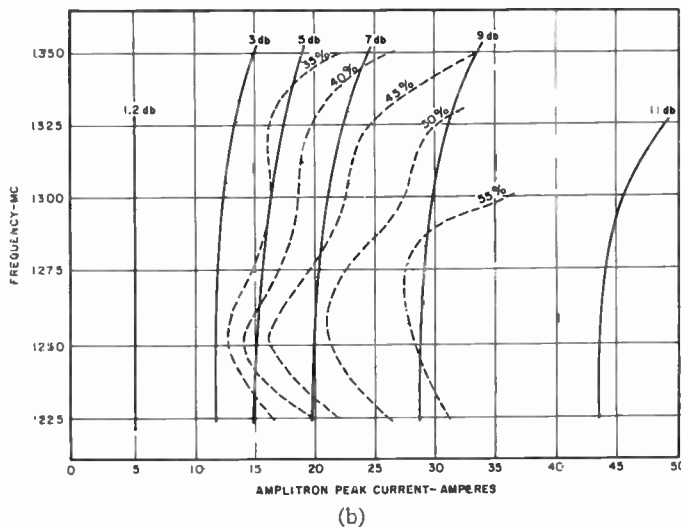


Fig. 15—(a) Amplitron matched-load performance as a function of anode current and frequency at an rf input level of 90 kw and with the magnetic field held constant. Output spectra photographed at increments of five amperes of anode current and 25 mc of frequency. Output spectra at zero anode current is identical to input spectra. (b) Data of (a) replotted to indicate contours of constant efficiency and power output.

spectrum varied a negligible amount under these varying conditions of load. The data of Fig. 16 are particularly interesting since the drive power of only 10 kw permits a gain of 16 db at the match point. The re-

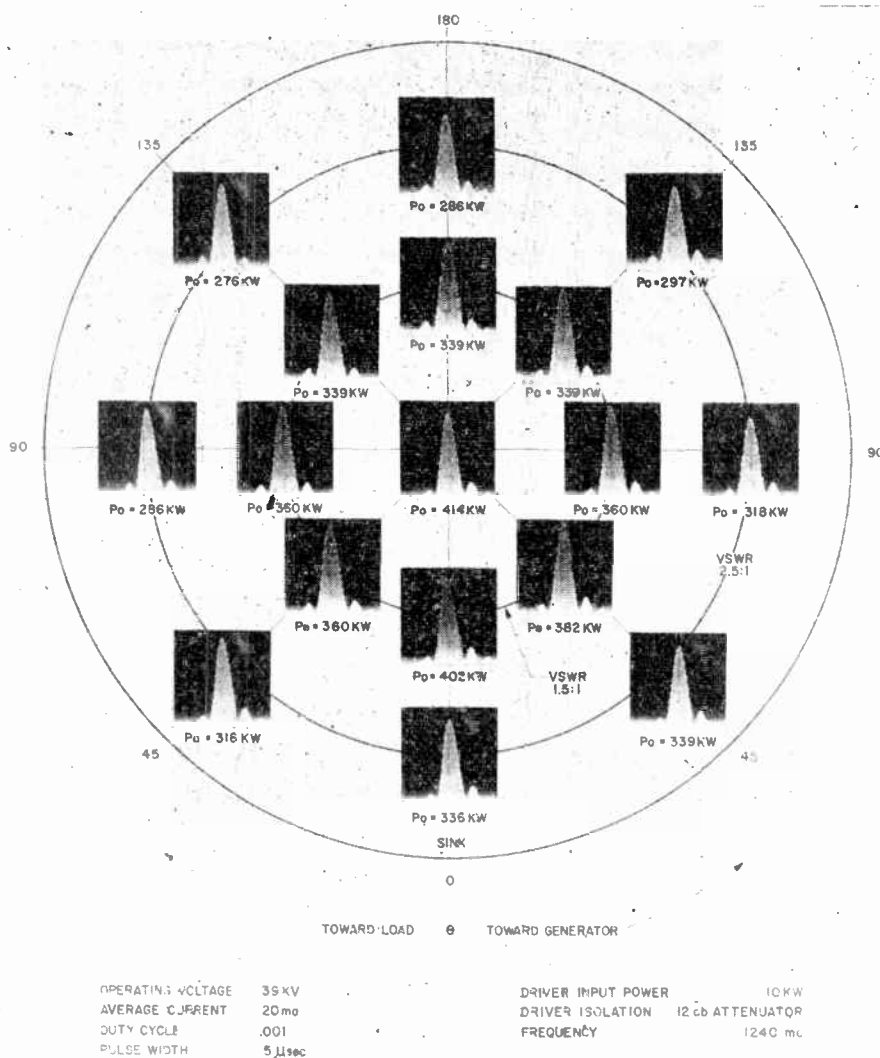


Fig. 16—Amplitron performance as a function of load at 1240 mc and with an rf input level of 10 kw.

reflected power from a 2.5/1 vswr, therefore, represents a reflected power of over seven times the input power. The bulk of this reflected power is absorbed in the input pad between the driver and the amplatron. The data are of further interest in that they were taken at 1240 mc which is very near one frequency edge of the band. Similar data have been taken at 1290 mc and 1340 mc, respectively.

High-Efficiency Operation

The fact that all the input power appears in the output power of the amplatron, and is, therefore, not wasted, gives rise to consideration of the use of amplitrons at relatively low gains, if there is any practical benefit in doing so. For example, the paralleling of two tubes is often used as a device to double the power; it may be just as desirable to run two amplitrons in cascade to produce increased power although the gain of the second tube may be only 3 db.

Experimental study of high-level drive of the QK520 amplatron reveals that the advantages of extremely high efficiency and extremely high-power output are to be

gained through high-level drive, low-gain operation of these tubes. Efficiencies of amplitrons run under these conditions were measured very carefully by the heat-balance method in which anode-dissipation power as well as output power are calorimetrically measured. These results were then checked against efficiency computed by the usual method of dividing the calorimetrically measured rf power output by the modulator power output. It was concluded that measured efficiencies were not less than 71.3 nor greater than 76 per cent for several operating conditions where the power exceeded 1600 kw. Observed data are tabulated in Fig. 17.

DESIGN CONSIDERATIONS FOR THE PLATINOTRON

It has been determined that the QK434 platinotron in the power range where performance characteristics have been described, operates in a backward-wave mode, that is, there is interaction between a backward-wave space harmonic of the circuit and the rotating electron beam.

To examine this interaction quantitatively it is necessary to examine the relationship between the circuit

Magnetic field Gauss	Anode potential kv	Anode current ma	Total aver. power output watts	Amplif- tron aver. power output watts	Amplif- tron anode dissipation watts	Effi- ciency meth- od A* per cent	Effi- ciency meth- od B** per cent
1260	39	26	1370	760	312	75	71
1260	39.6	31	1560	950	356	77.5	72.8
1260	40.9	36	1710	1100	445	75.0	71.3
1260	42.7	41	1920	1310	535	75.5	71.3
1330	42.1	31	1600	990	338	76.0	74.5
1395	44.7	31	1640	1030	356	74.7	74.5

* Method A—efficiency =
$$\frac{\text{(rf power out - rf power in)}}{\text{(modulator kv) (modulator aver. current)}}$$

**Method B—efficiency =
$$\frac{\text{(rf power out - rf power in)}}{\text{(rf power out - rf power in) + anode dissipation}}$$

Conditions of operation

- Duty cycle —0.001
- Pulse duration —5 μsec
- RF drive power—610 kw
- Frequency —1300 mc
- Load condition —matched.

Note: Input drive power was measured at output of amplif- tron with amplif- tron turned off. Use of same power meter to measure both power output and power input minimized any effect of an error in the carefully calibrated calorimetric power meter upon efficiency.

Fig. 17—QK520 amplif- tron high-efficiency data under conditions of high rf drive.

properties of the network, the electric potential and magnetic field applied to the platinotron, and the dimensions of the interaction area between cathode and anode. The assumption that there is synchronism between the rotating space-charge and the phase velocity is basic to this relationship.

The Phase and Characteristic Impedance Properties of the Platinotron Circuit

The phase shift vs frequency characteristic of the platinotron is necessary in the determination of the phase velocity of the space harmonic interacting with the electrons. But in the examination of the circuit for this characteristic, it will be convenient to discuss the characteristic impedance of the platinotron circuit as well. The strapped structure, common in magnetrons and in many of the platinotron structures which have been built, will be discussed, with the full realization that similar expressions can be developed for other structures.

Fig. 18 shows a section of the strapped circuit. If we regard the two straps as a parallel transmission line with the platinotron cavities representing impedances hung across the transmission line as loading, we obtain an equivalent circuit as shown in Fig. 18, where L_s represents the strap inductance between cavity sections, C_s the capacity between the two straps, and Z_c , the input impedance to the cavity across the points of strap connection, for example, points A-D. Z_c may be considered as nearly purely reactive. This equivalent circuit

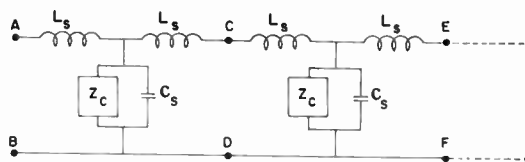
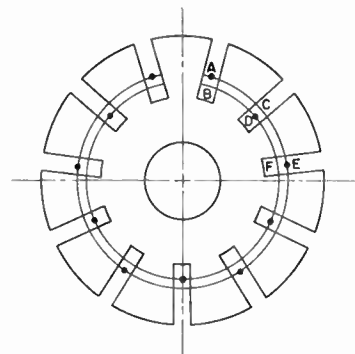


Fig. 18—The platinotron circuit and its two-terminal-pair network representation.

behaves as a two-terminal-pair network with band-pass characteristics. The lower cutoff of the pass band occurs at a frequency where Z_c and C_s resonate in parallel, that is, where $Z_c = -j/\omega C_s$ and the upper cutoff occurs when

$$\frac{2Z_c}{1 - j\omega C_s Z_c} = -j\omega L_s.$$

From network theory the phase shift function is given as

$$\theta_p = \cos^{-1} \left(\frac{Z_{11}}{Z_{12}} \right) = \cos^{-1} \left(\frac{j\omega L_s + \frac{Z_c}{1 - j\omega C_s Z_c}}{\frac{Z_c}{1 - j\omega C_s Z_c}} \right) \tag{3}$$

$$\theta_p = \cos^{-1} \left\{ \frac{j\omega L_s \left[\left(1 - \left(\frac{\omega}{\omega_c} \right)^2 \right) \right] + 1}{Z_c} \right\} \tag{4}$$

where ω_c is defined as the lower cutoff frequency, that is, $\theta_p = 0$. The characteristic impedance function is given as

$$Z_p = \sqrt{Z_{11}^2 - Z_{12}^2} \tag{5}$$

$$Z_p = \sqrt{j\omega L_s \left(j\omega L_s + \frac{2Z_c}{1 - j\omega C_s Z_c} \right)}. \tag{6}$$

The phase shift and the characteristic impedance functions are shown in Fig. 19 for a particular choice of circuit parameters in which Z_c is assumed to consist of a

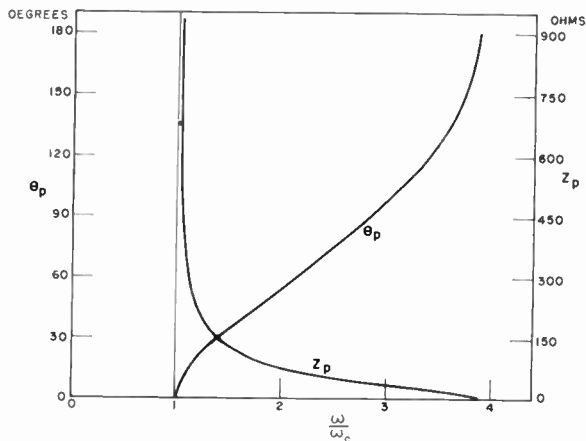


Fig. 19—Theoretical phase shift and characteristic impedance functions typical of the network representation of Fig. 18.

lumped inductance and capacity. In general Z_C will not be a simple function of frequency.⁹ The phase shift across the network will be zero at the lower cutoff frequency and π radians at the upper cutoff frequency. There will usually be a substantial range in which the phase shift is nearly linear with frequency. The characteristic impedance is infinite at the lower cutoff frequency and zero at the upper cutoff frequency.

Conditions for Synchronism Between the Circuit Wave and the Electron Stream

Having obtained the phase shift θ_p as a function of frequency for the network, it is possible to investigate the synchronism relationship between the electron beam and the traveling wave on the circuit. Fig. 20 indicates a section of the network in which the direction of power flow in the circuit is indicated as being toward the left and the direction of the beam toward the right. The reversed directions of electron motion and power flow in the circuit are necessary conditions for backward-wave interaction. The phase shift per network section, as given by (4) is in the direction of power flow. This phase shift is along the straps. To convert this to a phase shift in the interaction area it is necessary to add or subtract π radians because of the manner in which the vanes are connected to the straps. Since θ_p is always less than π , the subtraction of π radians from θ_p will mean a phase shift in the interaction area in the direction of the beam.

If d is the distance between vane tips, then

$$\lambda_s = \frac{2\pi d}{\pi - \theta} = \text{distance of one rf cycle} \quad (7)$$

$$v = \frac{\omega d}{\pi - \theta} = \text{phase velocity.} \quad (8)$$

⁹ Suitable expressions of Z_C for some common tube geometries are given by G. B. Collins, "Microwave Magnetrons," McGraw-Hill Book Co., Inc., New York, N. Y., pp. 49-65; 1948.

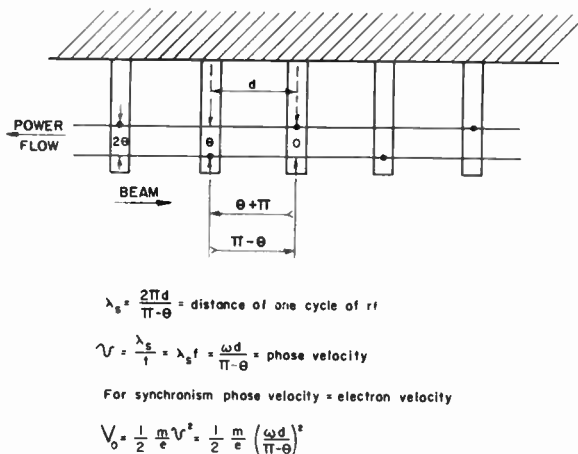


Fig. 20—Diagram illustrating conditions for interaction of the beam with a wave traveling in a direction opposite to that of the beam.

Then for synchronism the electron velocity must match the phase velocity and we have

$$V_0 = \frac{1}{2} \frac{m}{e} \left(\frac{\omega d}{\pi - \theta} \right)^2 \quad (9)$$

which gives the voltage through which the electrons must be accelerated to reach the required velocity.

Interrelationship of the Magnetic Field, DC Potential Applied to the Anode, and Physical Dimensions of the Interaction Region—Design Equations

In order to interrelate the magnetic field, dc potential applied to the anode, and platinotron physical dimensions, the assumption is made that there will be no interaction until synchronism between the traveling wave on the circuit and the fastest moving electrons is reached, and that further interaction will be maintained at such synchronism. However, it is not at all necessary for the electrons to be located at the tips of the vane for effective interaction and, for efficiency considerations, it is quite necessary that the synchronism condition be established early in the movement of the electron from the cathode to the anode. Eqs. (10)–(12) relate the voltage at which operation begins to the physical dimensions of the tube and value of magnetic field. These equations will be recognized as being similar to the design equations for magnetrons with the difference that $N(\pi - \theta) / 2\pi$ has been substituted for the mode number n .

$$V = V_0 \left(2 \frac{B}{B_0} - 1 \right) \text{ volts} \quad (10)$$

$$V_0 = 253,000 \left[\frac{2\pi r_a}{N(\pi - \theta)\lambda} \right]^2 \text{ volts} \quad (11)$$

$$B_0 = \frac{21,200}{N \left(\frac{\pi - \theta}{2\pi} \right) \lambda \left[1 - \left(\frac{r_c}{r_a} \right)^2 \right]} \text{ Gauss} \quad (12)$$

where

- V = threshold voltage or where operation starts,
- V_0 = value of voltage between anode and cathode, which, with a field of B_0 , causes the electrons to just graze the anode at synchronous velocity,
- B_0 = value of magnetic field for grazing of anode by electrons at synchronous velocity,
- B = value of magnetic flux in Gauss,
- r_a = radius of anode in centimeters,
- λ = operating wavelength of tube in centimeters,
- N = number of vanes (assumed equally spaced),
- θ = phase shift along straps of the network as defined in (4).

If the reader is not familiar with the principle of operation of the magnetron, he is advised to refer to one of the books¹⁰ which treats this subject. Inclusion of such material here would only be repetitious.

Limitations on Bandwidth Caused by the Electron Reentrancy

The platinotron may not operate equally well at all values of θ because of the electron reentrancy involved. Consider, for example, attempting to operate an odd numbered vane platinotron in the π mode. Fig. 21 should make it clear that in the π mode ($\theta=0$) electrons which are bunched to deliver energy to the traveling wave at the input of the network will take energy from the traveling wave at the output of the network after traversing the gap between input and output. Such a situation may not be conducive to a satisfactory interaction between electrons and a circuit traveling wave, although it is conceivable that the unfavorably bunched electrons could regroup themselves and move into a region of favorable phase.

On the other hand, if there is approximately 180° phase shift along the straps from output to input, the bunched electrons will deliver energy to the circuit on either side of the gap between output and input. This situation is favorable to the proper operation of the platinotron.

The general requirements for the electron bunches to be in phase with the traveling wave on both sides of the gap can be derived. Consider a bunch of electrons located at the output plane shown in Fig. 21 at time $t=0$. Then if t' is the time required for this group of electrons to rotate around the cathode once and come back to the output plane, the phase change at the output plane is obviously $\omega t'$. And, of course, if the electrons and the traveling wave are to have the same phase relationship at t' as at $t=0$, $\omega t'$ must be an integral multiple of 2π .

$$\omega t' = M2\pi, \text{ where } M \text{ is an integer.} \tag{13}$$

¹⁰ *Ibid.*

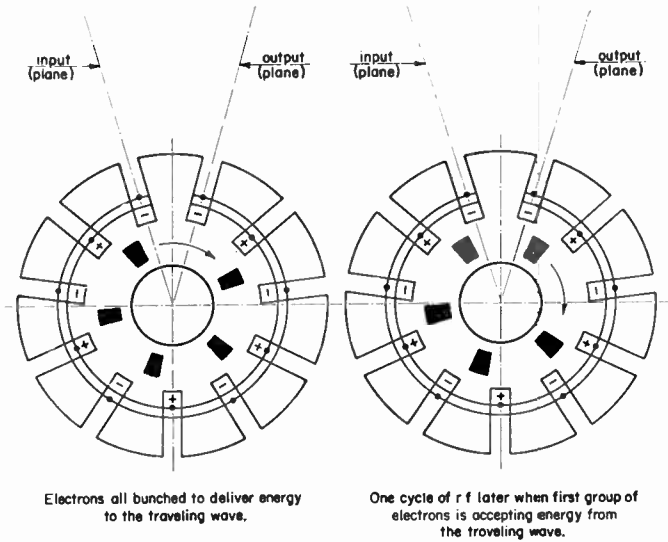


Fig. 21—Diagram illustrating poor conditions for interaction of the spokes of space-charge with the platinotron circuit.

Now t' is equal to the distance around the anode divided by the velocity of the electron bunches. This velocity is the phase velocity V given by (8).

Then

$$t' = \frac{2\pi r_a}{v} = \frac{2\pi r_a}{\frac{\omega d}{\pi - \theta}} = \frac{N(\pi - \theta)}{\omega} \text{ secs.} \tag{14}$$

Substituting the expression for t' into (13) we obtain

$$\theta = \pi \left(1 - \frac{2M}{N} \right) \text{ radians.} \tag{15}$$

If the electrons after crossing the gap are permitted to initially lead or lag the traveling wave on the circuit, additional equations may be derived to determine the corresponding phase shifts permitted on the network.

$$\theta_{\max} = \pi \left[1 - \frac{2(M - Q)}{N} \right] \tag{16}$$

$$\theta_{\min} = \pi \left[1 - \frac{2(M + Q)}{N} \right] \tag{17}$$

where

$$Q = \frac{\text{lead or lag of beam in degrees}}{360}.$$

APPLICATION OF THE CIRCUIT, SYNCHRONISM, AND BANDWIDTH ASPECTS OF PLATINOTRON DESIGN TO THE QK434

The QK434 is the experimental platinotron developed under Signal Corps contract. It was designed for use at L band and for a peak output power level of 200 to 1000 kw. A considerable amount of data have been

taken on the use of this tube both as an amplatron and a stabilotron. It is, therefore, logical to use this tube to illustrate various aspects of platinotron design and performance.

A plan and cross section view of the interaction area of the QK434 platinotron is shown in Fig. 4. Pertinent dimensions are as follows:

Number of vanes	= 11
Cathode diameter	= 0.750 inches
Anode diameter	= 1.600 inches
Vane length	= 1.500 inches.

The experimental phase shift vs frequency curve for the entire network of ten cavities of the configuration shown in Fig. 4 has been found to be as shown in Fig. 22. The formula given by (4) for a single network section is difficult to apply for vanes of this geometry because of the difficulty of determining Z_C as a function of frequency. If, however, Z_C is assumed to be the impedance of a lumped circuit element, which must be inductive in nature, it is possible to compute the value of L_C using the experimental lower cutoff frequency and one other point from the 1200–1400 mc region of the phase shift vs frequency characteristic. If the values of ωL_C so obtained are then used for Z_C in (4), the agreement between the experimental curve and that predicted by (4) will be excellent in the frequency region up to 1500 mc. Beyond this frequency, however, there is serious lack of agreement.

With the aid of the phase shift vs frequency characteristic given in Fig. 22, it is possible to apply (15)–(17) to determine the preferred frequencies of operation. The results are shown in Fig. 23. Eq. (14) may be solved for the values of the phase shift across each network section which will permit the reentrant electron beam to reenter the input side of the circuit in exact synchronism with the circuit wave. These values of phase shift are found to be 17° and 49° and higher values not shown in Fig. 23. The platinotron will operate satisfactorily at either of the two frequencies determined by the two respective phase shifts. Fig. 23 also shows in heavy shading the frequency regions determined by (16) and (17) for a 45° lag and lead of the reentrant beam, and in lighter shading the frequency regions determined by a 90° lag and lead of the reentrant beam.

It is not clear from an examination of Fig. 23 whether operation at 800 or 1300 mc is to be preferred. Because the 1300-mc region represents a frequency region of interest to radar systems, most of the experimental data have been taken in this frequency region of operation, although very efficient operation has been observed in the 800-mc region.

From the dimensions given for Fig. 4, from the phase shift and frequency as determined by (4) and Fig. 22, and from (10)–(12), it is possible to determine the relationship between anode potential and magnetic field

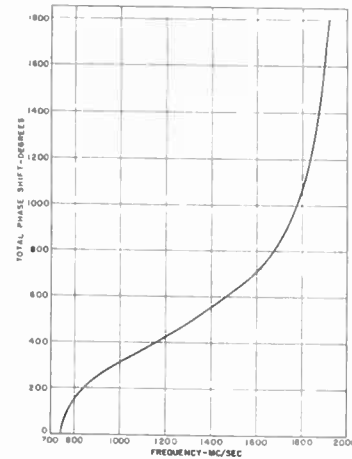


Fig. 22—Experimentally determined phase shift across the QK434 platinotron network of ten sections as a function of frequency.

PHASE SHIFT CHARACTERISTIC OF PLATINOTRON CIRCUIT SHOWING LIKELY REGIONS OF OPERATIONS

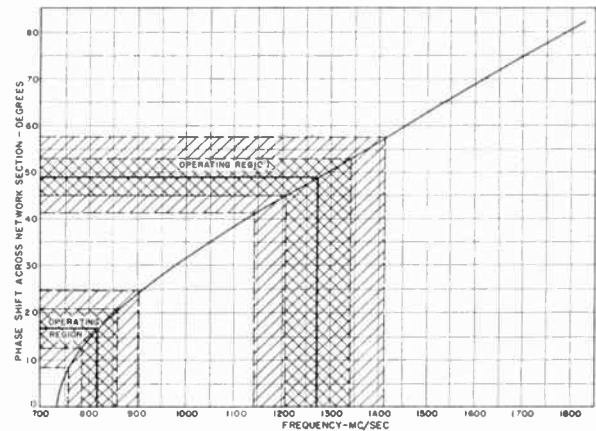


Fig. 23—Diagram illustrating regions of phase shift and frequency in which operation of the QK434 platinotron may be expected. Heavily cross-hatched regions correspond to a 45° lead or lag of the rotating spokes. Lightly cross-hatched regions correspond to a 90° lead or lag.

for the onset of operation for backward-wave interaction. The relationship between this threshold voltage and the magnetic field for a frequency of 1300 mc is given as the upper curve in Fig. 24. The lower curve in Fig. 24 indicates the predicted relationship between anode potential and magnetic field for interaction with the forward wave at 1300 mc. Eqs. (10)–(12) can be converted to predict forward-wave interaction by adding θ to π in the equations instead of subtracting it.

In the region of rf input levels over 2.5 kw, the experimentally observed values of threshold voltage appear in substantial agreement with the predicted values for backward-wave interaction. The range covered by these experimental data is also indicated on Fig. 24. However, at lower rf input levels forward-wave interaction has been observed at current levels from zero to 3 amperes.

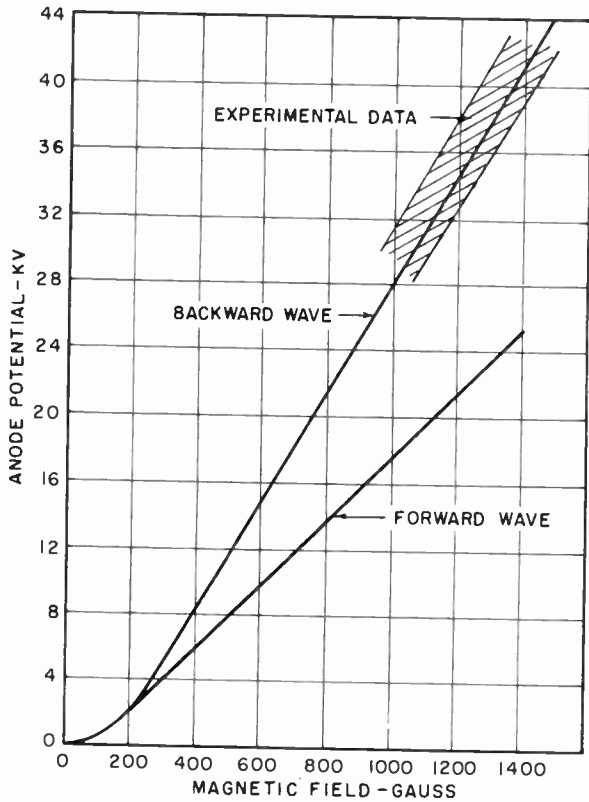


Fig. 24—Theoretically predicted and observed relationship between anode potential and magnetic field for onset of QK434 platinotron operation. Cross-hatched area contains points of experimentally observed behavior.

The proper operation of the platinotron is dependent upon a reasonable impedance match between the platinotron network and the input and output terminals over a reasonable range of frequency. For suitable tube geometries (6) may be used to compute the characteristic impedance. For the QK520 the characteristic impedance at 1300 mc was experimentally found to be 92 ohms. Although considerable work has been expended on the matching problem, such problems are common to a variety of microwave tubes, and so need not be discussed in detail here. The broad-band match, which was obtained for the QK520, is shown in Fig. 25. The vswr

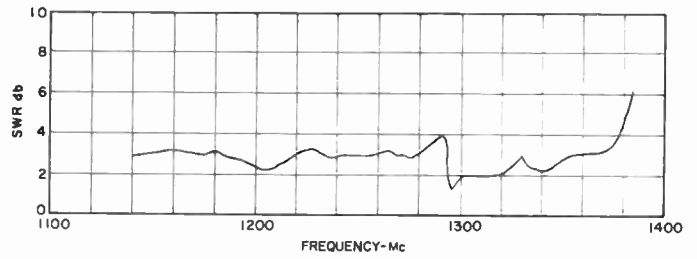


Fig. 25—Broad-band match between the external circuit and the QK434 platinotron.

as given in Fig. 25 is that vswr obtained by looking into the input to the platinotron with the output pipe looking into a matched-load.

CONCLUSION

A new microwave tube device has been described and a significant amount of data has been given to illustrate its major performance characteristics. Some information relative to design procedures has been given. All the data which has been presented is for a backward-wave mode of interaction, but this does not preclude the use of this device in a forward-wave interaction mode. Such forward-wave interaction has been noted at low rf drive levels and low anode currents.

The mechanism of interaction between the beam and circuit is not fully understood because of the complications of considering both electron reentrancy and circuit nonreentrancy simultaneously. A fuller understanding is essential to the prediction of the bandwidth and gain capabilities of this device. It is expected that analytical and experimental work in process will provide greater understanding of the beam-circuit interaction mechanism.

ACKNOWLEDGMENT

The author gratefully acknowledges the support given this development by the U. S. Signal Corps, whose support greatly accelerated development of an embryonic device into a practical device whose major characteristics and potentialities are now well recognized.



The Role of Stratospheric Scattering in Radio Communication*

H. G. BOOKER†, FELLOW, IRE, AND W. E. GORDON‡, MEMBER, IRE

Summary—On the mixing-in-gradient hypothesis of incoherent scattering of radio waves in a dry atmosphere, the intensity of the irregularities in dielectric constant depends on the excess of the temperature gradient above that appropriate to an adiabatic atmosphere. In going from the upper troposphere to the stratosphere, there is a significant increase in this gradient excess and consequently, a significant increase in the intensity of irregularities in dielectric constant. The decrease in intensity with increase of height measured by Crain in the troposphere does not, therefore, indicate reliably the intensity to be expected above the tropopause.

Calculations have been made concerning the effect of stratospheric, as distinct from tropospheric, scattering. Stratospheric scattering is expected to predominate over tropospheric scattering at ranges greater than about 600 km. At a range of 1000 km, the calculated transmission-loss due to stratospheric scattering is a few decibels greater than is indicated by observations. The effect of stratospheric scattering at a frequency of 108 mc is such that the minimum signal observed at this frequency over the path from Cedar Rapids, Iowa, to Sterling, Va., could conceivably have been stratospheric in origin, with ionospheric scattering being predominant at certain times, for example, during SID's.

INTRODUCTION

VHF AND UHF radio fields are observed with presently available equipment over distances up to about 1000 km.¹ Increases in transmitter power and antenna size will extend the useful range to distances comparable with those normally used in ionospheric scatter communications.

Since 1950, theoretical descriptions²⁻⁴ of scattering by a turbulent troposphere (the atmosphere below about 10 km), have been available to predict the scattered power received and other characteristics of the signal. The theories depend on models of turbulence in the troposphere and require numerical estimates of the intensity and scale of the dielectric constant fluctuations. At heights below about 7 km, these estimates of intensity and scale are available from direct observation with the refractometer.⁵

For ranges in excess of about 700 km, the tangent

planes of transmitter and receiver intersect above the top of the troposphere (tropopause). Extrapolation of the refractometer observations that have been made in the lower part of the troposphere to heights above the tropopause fails to predict the fields observed at 1000 km where the scatterers are at heights above the top of the troposphere. The role of the stratosphere (the atmosphere above about 10 km) is, therefore, investigated. Since refractometer observations have not yet been made in the stratosphere, nor indeed in the upper one-third of the troposphere, it is necessary to use theoretical reasoning, and this can be done by using the mixing-in-gradient hypothesis. The excess of the gradient of refractive index over that in an adiabatic atmosphere is available both from the theoretical variation of air density with height and from measurements made throughout the stratosphere by means of rockets and in other ways. The gradient excess determines the scattering coefficient and from this the power scattered to a receiver may be calculated. We shall show that the calculated values of scattering in the stratosphere agree reasonably well with the available observations for distances of the order of 1000 km.

The mixing-in-gradient hypothesis is applied to the stratosphere in the next section and the water vapor fluctuations which control the dielectric fluctuations in the lower troposphere are shown to be negligible. In the third section, the power scattered to a receiver by a turbulent stratosphere is calculated. The results are related to the customary calculations for the ionosphere in the fourth section. For communication systems certain design factors are required, including degradation of antenna gain, diversity distance, and bandwidth of the mechanism. These are derived in the fifth section and the available radio observations are compared with the theoretical predictions in the last section.

THE SCATTERING COEFFICIENT IN THE STRATOSPHERE

On the mixing-in-gradient hypothesis the fluctuations of dielectric constant are produced by the mixing or turning over of an eddy of size L immersed in a gradient of dielectric constant $d\epsilon/dz$. After turning over, an elementary volume within the eddy will have a dielectric constant that differs from the average dielectric constant of the air surrounding the eddy at the same height as the elementary volume, by an amount which is of the order of $Ld\epsilon/dz$. During the turning over process, however, the elementary volume will expand or contract adiabatically and the dielectric constant of the elementary volume will change by an amount which is of

* Original manuscript received by the IRE, March 23, 1957; revised manuscript received, June 10, 1957. This work was performed under AF contract AF33(616)-3236, Wright Air Dev. Ctr., Dayton, Ohio.

† Cornell Univ., Ithaca, N. Y.

¹ J. H. Chisholm and J. F. Roch, "Measurements of Signal Levels at UHF and SHF Propagated by the Troposphere over Paths 100 to 618 miles in Length," URSI Meeting, Washington, D. C.; May, 1956.

² H. G. Booker and W. E. Gordon, "A theory of radio scattering in the troposphere," *Proc. IRE*, vol. 38, pp. 401-412; April, 1950.

³ F. Villars and V. F. Weisskopf, "On the scattering of radio waves by turbulent fluctuations of the atmosphere," *Proc. IRE*, vol. 43, pp. 1232-1239; October, 1955.

⁴ H. Staras, "Forward scattering of radio waves by anisotropic turbulence," *Proc. IRE*, vol. 43, pp. 1374-1380; October, 1955.

⁵ C. M. Crain, "Survey of airborne microwave refractometer measurements," *Proc. IRE*, vol. 43, pp. 1405-1411; October, 1955.

the order of $L(d\epsilon/dz)_A$ where $(d\epsilon/dz)_A$ is the adiabatic gradient of ϵ . With this correction the dielectric constant of the element differs from that of the surrounding air at the same height by an amount $L[d\epsilon/dz - (d\epsilon/dz)_A]$.

To calculate the gradient excess first consider the adiabatic atmosphere. The adiabatic lapse rate is

$$\Gamma = \frac{\gamma - 1}{\gamma} \frac{g}{R} \quad (1)$$

where R is the gas constant, g the acceleration of gravity, and $\gamma = 7/5$ for a dry atmosphere. In the adiabatic atmosphere the temperature T varies with height z as

$$T = T_0 - \Gamma z. \quad (2)$$

The scale height is given by

$$H = \frac{RT}{g} \quad (3)$$

and the change of scale height by

$$\frac{dH}{dz} = -\frac{\gamma - 1}{\gamma}. \quad (4)$$

The density ρ varies with height in an adiabatic atmosphere as

$$\begin{aligned} \frac{\rho}{\rho_0} &= \left(\frac{T}{T_0}\right)^{1/(\gamma-1)} \\ &= \left(\frac{H}{H_0}\right)^{1/(\gamma-1)}. \end{aligned} \quad (5)$$

The logarithmic gradient of density in a dry adiabatic atmosphere is, therefore,

$$\begin{aligned} \frac{1}{\rho} \frac{d\rho}{dz} &= \frac{1}{\gamma - 1} \frac{1}{H} \frac{dH}{dZ} \\ &= -\frac{1}{\gamma H}. \end{aligned} \quad (6)$$

For a dry atmosphere the dielectric constant is

$$\epsilon = 1 + b \frac{\rho}{\rho_0} \quad (7)$$

where $b = 540 \times 10^{-6}$ and ρ_0 is the density at ground level. The dielectric constant gradient is

$$\frac{d\epsilon}{dz} = \frac{b}{\rho_0} \frac{d\rho}{dz}. \quad (8)$$

For a dry adiabatic atmosphere the gradient is

$$\left(\frac{d\epsilon}{dz}\right)_A = -\frac{1}{\gamma H} b \frac{\rho}{\rho_0} \quad (9)$$

and the gradient excess is, therefore,

$$\frac{d\epsilon}{dz} - \left(\frac{d\epsilon}{dz}\right)_A = b \frac{\rho}{\rho_0} \left[\frac{1}{\rho} \frac{d\rho}{dz} + \frac{1}{\gamma} \frac{1}{H} \right]. \quad (10)$$

In an isothermal stratosphere H is independent of height so that

$$\frac{1}{\rho} \frac{d\rho}{dz} = -\frac{1}{H}. \quad (11)$$

Substituting (11) in (10)

$$\begin{aligned} \frac{d\epsilon}{dz} - \left(\frac{d\epsilon}{dz}\right)_A &= b \frac{\rho}{\rho_0} \left[-\frac{1}{H} + \frac{1}{\gamma} \frac{1}{H} \right] \\ &= -\frac{(\gamma - 1)b}{\gamma H} \frac{\rho}{\rho_0} \end{aligned} \quad (12)$$

or in terms of the height z_T and density ρ_T of the tropopause

$$\frac{d\epsilon}{dz} - \left(\frac{d\epsilon}{dz}\right)_A = -\frac{(\gamma - 1)b}{\gamma H} \frac{\rho_T}{\rho_0} \exp\left(-\frac{z - z_T}{H}\right). \quad (13)$$

The above derivation neglects the contribution of fluctuations in water vapor which, in the troposphere, is the dominant factor. To evaluate the importance of water vapor fluctuations in the stratosphere, consider the extreme case of an element of volume at the saturation vapor pressure in a dry medium. This case produces a fluctuation in dielectric constant which is a few powers of 10 less than the fluctuations produced by the mixing-in-gradient process. The water vapor fluctuations, therefore, contribute negligibly.

SCATTERED POWER

Consider the power P scattered to a receiver on the assumption that the scattering volume is determined by the scattering coefficient and not by the antenna beam angles (the wide beam angle case). On the mixing-in-gradient hypothesis the ratio of this power to the power P_F appropriate to free space is

$$\frac{P}{P_F} = 0.4 \frac{(\overline{\Delta\epsilon/\epsilon})^2}{(2\pi L)^2} \frac{\lambda a^3}{d^2} \quad (14)$$

where d is the path length, λ the wavelength, and a the radius of the earth modified for any appropriate refraction. Eq. (14) is obtained by assuming $(\overline{\Delta\epsilon/\epsilon})^2(2\pi L)^2$ constant over the important scattering height rather than decreasing exponentially with height. The latter leads to a form which includes an exponential integral. The numerical results, however, are substantially the same.

As indicated previously, the dielectric constant fluctuations are

$$\overline{(\Delta\epsilon/\epsilon)^2} = \left[L \left\{ \frac{d\epsilon}{dz} - \left(\frac{d\epsilon}{dz}\right)_A \right\} \right]^2 \quad (15)$$

and this may be written in a form for direct substitution in (14) as

$$\frac{\overline{(\Delta\epsilon/\epsilon)^2}}{(2\pi L)^2} = \left[\frac{1}{2\pi} \left\{ \frac{d\epsilon}{dz} - \left(\frac{d\epsilon}{dz}\right)_A \right\} \right]^2 \quad (16)$$

and with (13)

$$\frac{(\Delta\epsilon/\epsilon)^2}{(2\pi L)^2} = \left[\frac{(\gamma - 1)b}{2\pi\gamma H} \frac{\rho_T}{\rho_0} \exp\left(\frac{z - z_T}{H}\right) \right]^2. \quad (17)$$

The scattered power relative to free-space power as given by (14) and (17) is plotted in Fig. 1 as a function of distance for distances greater than 800 km corresponding to a tropopause height of 10 km. Fig. 1 gives the scattered power for a wavelength of 1 meter. The power for other wavelengths may be found by noting in (14) that the power is directly proportional to wavelength.

Instead of assuming that the stratosphere is isothermal the gradient-excess may be computed from observations of the distribution of temperature with height made by rockets and other means.⁶ The scattered power computed from this gradient-excess is plotted in Fig. 1. Note that the powers computed from the rocket

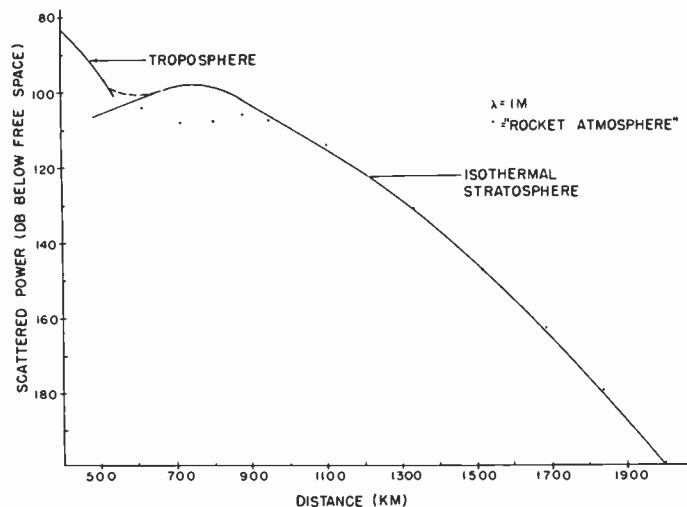


Fig. 1—Radio scattering from the troposphere and the stratosphere.

atmosphere are in agreement with the theoretical curve, except in the neighborhood of 800 km where a difference has been introduced to illustrate the following point. The curve of scattered power from the stratosphere vs distance levels off at a range that depends on the height of the tropopause. In the rocket atmosphere the tropopause is at a height of 12 km; whereas, for the theoretical curve shown in Fig. 1, the tropopause is assumed to be at 10 km. The height of the tropopause varies between about 10 and 14 km, so that large variations in signal level are expected at distances of the order of 800 km and these variations in signal level should correlate with the height of the tropopause.

There is a remarkable agreement between scattered power deduced for the rocket atmosphere and the power computed from Crain's refractometer observations at 5 to 7 km. The path lengths corresponding to scattering

at these heights are about 500 to 600 km. Note that the mixing-in-gradient hypothesis applied to a dry atmosphere at these heights produces the same scattered fields as the refractometer data.

For antennas whose beams are sufficiently narrow to control the relevant scattering volume, (14) is replaced by a formula given by Booker and deBettencourt⁷

$$\frac{P}{P_F} = \frac{64\sigma V}{d^2} \quad (\text{narrow beams}) \quad (18)$$

where the volume,

$$V = \frac{2}{\theta} \left(\frac{d}{2} \frac{\alpha_v^2}{2} \right) \left(\frac{d}{2} \frac{\alpha_H^2}{2} \right),$$

yielding with (18)

$$\frac{P}{P_F} = \frac{2Sp\lambda d\alpha_v^2\alpha_H}{\theta^6} \quad (19)$$

where $Sp = (\Delta\epsilon/\epsilon)^2(2\pi L)^{-2}$, α_v and α_H are the vertical and horizontal antenna beam angles, respectively. The ratio of powers received for the narrow beam and wide beam cases is evaluated and plotted in the section on Communication Aspects of the Received Signal.

TRANSITION REGIONS AT THE TROPOPAUSE AND IONOSPHERE

To estimate the power scattered over a path length of the order of 700 km, it is necessary to combine, by adding powers, the scattering contributed by the stratosphere and the troposphere with appropriate weighting factors determined by the portion of the scattering volume in each of the two regions.

The scattering in the troposphere is calculated from the intensities and scales reported by Crain for heights up to seven kilometers applied to the mixing-in-gradient formula, (14). These results are plotted for several wavelengths in Fig. 2 (next page). Note that the stratospheric contribution to the scattered power dominates for path length greater than about 600 km.

At sufficiently large ranges and sufficiently long wavelengths the contribution from ionospheric scattering predominates. Using Bailey's⁸ measured values at 25, 50, and 100 megacycles at 1200 km and extrapolating them in distance and frequency using a fifth power angle dependence for the low frequencies and a thirteenth power angle dependence for 100 mc and higher frequencies, the curves of Fig. 2 are obtained.

COMMUNICATION ASPECTS OF THE RECEIVED SIGNAL

To effectively employ stratospheric scattering for communications, it is necessary to know, in addition to

⁷ H. G. Booker and J. T. deBettencourt, "Theory of radio transmission by tropospheric scattering using very narrow beams," *Proc. IRE*, vol. 43, pp. 281-290; March, 1955.

⁸ D. K. Bailey, R. Bateman, and R. C. Kirby, "Radio transmission at vhf by scattering and other processes in the lower ionosphere," *Proc. IRE*, vol. 43, pp. 1181-1230; October, 1955.

⁶ W. Liller and F. J. Whipple, "Rocket Exploration of the Upper Atmosphere," Pergamon Press, London, Eng., p. 112; 1954.

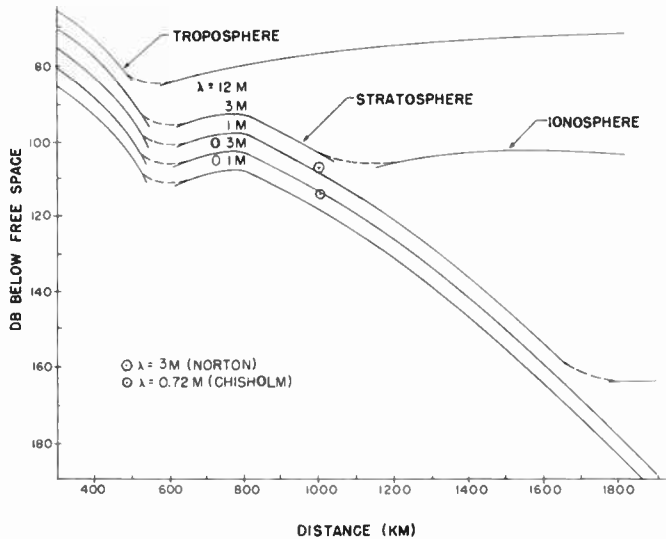


Fig. 2—Radio scattering from the troposphere, stratosphere, and the ionosphere.

the received power available, certain characteristics of the received signal such as the diversity distance, antenna-gain degradation and bandwidth limitation. These characteristics may be estimated from the size of the scattering volume.

A volume with a thickness $(\Delta X)h_0$ at a distance $d/2$ from the receiver scatters power to the receiver in a critical vertical angle α_{cv} given by

$$\alpha_{cv} = \frac{2\Delta X \cdot h_0}{d/2} \tag{20}$$

where the 2 in the numerator accounts for a perfectly reflecting ground. Similarly, the width w of the volume at a distance $d/2$ subtends a critical horizontal angle α_{ch} given by

$$\alpha_{ch} = \frac{w}{d/2} \tag{21}$$

For the mixing-in-gradient hypothesis

$$w = 0.3d^2/a \tag{22}$$

and (21) becomes

$$\alpha_{ch} = 0.6d/a. \tag{23}$$

The vertical dimension of the scattering volume is calculated by considering that the volume is composed of elementary horizontal slabs. The power contributed by the i th slab is

$$P_i \alpha \sigma_i dV_i \tag{24}$$

Including only the factors which vary with height this becomes

$$P_i \alpha \frac{x \exp - 2 \left(\frac{x}{H/h_0} \right)}{(x + 2)^5} \tag{25}$$

where

$$x = h/h_0 \text{ and } h_0 = d^2/8a.$$

The factor $(x + 2)^5$ represents the fifth power angle dependence, the exponential represents the decrease of the intensity of the fluctuations with height, and the factor x represents the increase in elementary slab volume with height. By finding the values of x for which P_i is equal to one half its maximum value, an estimate of the thickness factor Δx is obtained and is given approximately by

$$\frac{3}{2} \frac{H}{H + h_0} \tag{26}$$

The critical vertical angle is, therefore,

$$\alpha_{cv} = \frac{6H}{d} \frac{1}{(1 + H/h_0)} \tag{27}$$

From the critical beam angles a critical antenna gain can be estimated. Antennas with plane-wave gains larger than this critical value will not realize their full gain.

$$\begin{aligned} G_c &= \frac{4\pi}{\alpha_{cv} \alpha_{ch}} \\ &\doteq \frac{7}{2} \frac{a}{H} (1 + H/h_0) \\ &\doteq 4000(1 + H/h_0). \end{aligned} \tag{28}$$

Where the modified radius of the earth is taken as 7000 km and the scale height H as 6 km, $h_0 = d^2/8a$ will vary between about 10 and 40 km as d varies from 750 to 1500 km.

Corresponding to the above critical angles, the diversity distances normal to the path are

$$D_v = \lambda/\alpha_{cv} = \frac{\lambda d}{6H} (1 + H/h_0) \tag{29}$$

$$D_h = \lambda/\alpha_{ch} = 1.6 \frac{a\lambda}{d} \tag{30}$$

for the vertical and horizontal directions, respectively.

The useful bandwidth may be estimated by considering the excess path between the longest and shortest paths from transmitter to receiver through the scattering volume. There is a time delay corresponding to the excess path and the reciprocal of the delay is taken as the bandwidth. Two bandwidths are estimated; one associated with the vertical thickness, the other with the width of the volume. The lesser of the two will apply. From the thickness one obtains

$$B_1 = \frac{2.3}{d_{100}} (1 + H/h_0) \text{ mc} \tag{31}$$

where d_{100} is distance in hundreds of kilometers. From the width one obtains

$$B_2 = \frac{300}{d_{100}^3} \text{ mc} \tag{32}$$

This limitation may be avoided by using antennas whose beamwidths are smaller than the critical value, α_c given by (23) or (27), so that the scattering volume is restricted by the antenna beams. The bandwidth is then determined by the beamwidth α and is approximately

$$B_s = \frac{1.7 \text{ mc}}{\alpha d_{100}^2} \quad (33)$$

where α is the beamwidth in radians.

The bandwidth available in stratospheric scattering is equal to or greater than that which would be predicted by extrapolating the tropospheric scattering calculation.

The degradation of antenna gain for large antennas may be computed by comparing the expressions for scattered power in the case of wide and narrow beam antennas. It is assumed that identical transmitting and receiving antennas are used. Wide and narrow antenna beams are defined on the basis of the critical beam angle α_c given by (23) and (27). With this definition

$$\frac{P}{P_F} = \frac{0.4S\rho\lambda d}{\theta_0^3} \text{ for wide beam antennas,} \quad (34)$$

$$\frac{P}{P_F} = \frac{2S\rho\lambda d\alpha_v^2\alpha_h}{(\theta_0 + \alpha_v/2)^6} \text{ for narrow beam antennas.} \quad (35)$$

Letting R be the ratio of powers received for small beam relative to large beam systems,

$$R = \frac{5\theta_0^3\alpha_v^2\alpha_h}{(\theta_0 + \alpha_v/2)^6} \quad (36)$$

where $\theta_0 = d/a$. When $\theta_0 \ll \alpha_v/2$

$$10 \log R = 7 + 20 \log \alpha_v + 10 \log \alpha_h - 30 \log \theta_0. \quad (37)$$

The scattered power relative to the free-space power for a narrow beam scatter link may be obtained by adding the loss in decibels indicated by (37), using the appropriate α_v , α_h , and θ_0 , to the loss given by Fig. 2.

To summarize the communication aspects of stratospheric scattering numerical estimates of various parameters are listed in Table I for three path lengths (assuming $II = 6$ km, $a = 7000$ km).

TABLE I

Path length in kilometers	750	1000	1500
Critical beam angles in milliradians			
Elevation α_{ev}	30	27	21
Azimuth α_{eh}	64	86	129
Diversity distances in wavelengths			
Vertical D_v	33	37	48
Horizontal D_h	16	12	8
Critical gain G_c in decibels	38	37	37
Bandwidth B_1 or B_2 in kilocycles	490	310	100

Table I shows clearly that the antenna aperture should not be circular, but rather elliptical to provide maximum efficiency. The ellipticity (D_v/D_h) depends on path length, as illustrated in the table, varying from 2:1 to 6:1 with increasing range. Eqs. (29) and (30) indi-

cate the appropriate antenna dimensions for distances not included in Table I. The tabulated values of bandwidth can be approximately quadrupled by using antennas with 1 degree beamwidth as shown by (33).

COMPARISON WITH OBSERVATIONS

Radio observations at 1000 km reported by Norton⁹ ($\lambda = 3$ meters) and by Chisholm¹ ($\lambda = 3/4$ meter) are plotted on Fig. 2 and show good agreement with predicted values.

Chisholm has reported that the relative gain of 18-meter dishes compared to 9-meter dishes is realized on a 1000-km path at $\lambda = 0.72$ meter. The plane wave gains of the dishes are assumed by him to be 35 and 29 db, respectively. For this path the critical gain is 37 db and so one would expect to observe the regular difference in plane-wave gains of the two dishes. However, from diversity distance considerations, the area over which the scatter field at the receiving site behaves like a plane wave has dimensions 37λ vertically and 12λ horizontally; and since the larger dish has a diameter of 25λ , one would expect its gain to be degraded by a maximum of two decibels, assuming a uniformly illuminated aperture, while the smaller dish with diameter 12.5λ would be expected to yield its full plane wave gain. Since the gains of the two dishes are assumed, not measured, and since the degradation expected is so small, there would not seem to be any significant discrepancy between theory and experiment.

Bailey reports measurements made at 1243 km presumably associated with ionospheric scatter which at 108 mc differ from observations at lower frequencies in an unexplained way. In particular, the diurnal and seasonal variations in observed level at 100 mc are less than would be expected from the behavior of the lower frequencies. From Fig. 2 it will be noted that the contribution from stratospheric scattering is comparable to that from normal ionospheric scatter at this distance for wavelengths between 2 and 3 meters. It is suggested that the contribution from stratospheric scattering may uphold the level at 108 mc, when the ionospheric component weakens and therefore reduces the diurnal and seasonal variations.

Of the experiments suggested by this work, two in particular might be emphasized. The first is a measurement of signal vs distance in an aircraft to observe the tropospheric, stratospheric, and ionospheric components. Fig. 2 indicates that this might be accomplished using a high-power transmitter operating at about $\lambda = 3$ meters. The second is signal measurements vs time over a fixed path in which the path length is selected to be sensitive to signal variations correlated with the height of the tropopause as discussed in connection with Fig. 1.

⁹ K. A. Norton, L. Rice, and L. E. Vogler, "The use of angular distance in estimating transmission loss and fading range for propagation through a turbulent atmosphere over irregular terrain," Proc. IRE, vol. 43, pp. 1488-1526; October, 1955.

Carrier Generation and Recombination in $P-N$ Junctions and $P-N$ Junction Characteristics*

CHIH-TANG SAH†, MEMBER, IRE, ROBERT N. NOYCE†, MEMBER, IRE AND
WILLIAM SHOCKLEY†, FELLOW, IRE

Summary—For certain $p-n$ junctions, it has been observed that the measured current-voltage characteristics deviate from the ideal case of the diffusion model. It is the purpose of this paper to show that the current due to generation and recombination of carriers from generation-recombination centers in the space charge region of a $p-n$ junction accounts for the observed characteristics. This phenomenon dominates in semiconductors with large energy gap, low lifetimes, and low resistivity. This model not only accounts for the nonsaturable reverse current, but also predicts an apparent $\exp(qV/nkT)$ dependence of the forward current in a $p-n$ junction. The relative importance of the diffusion current outside the space charge layer and the recombination current inside the space charge layer also explains the increase of the emitter efficiency of silicon transistors with emitter current. A correlation of the theory with experiment indicates that the energy level of the centers is a few kT from the intrinsic Fermi level.

I. INTRODUCTION

THE VOLTAGE current characteristics of $p-n$ junctions have been studied by many authors. The ideal theory of a $p-n$ junction of Shockley accounts for the electrical characteristics of a germanium $p-n$ junction quite well at room temperatures.¹ However, it is generally observed that at room temperatures the measured electrical characteristics of silicon $p-n$ junctions deviate considerably from that predicated by the ideal theory. For example, Shockley's ideal theory predicts a saturation current for the $p-n$ junction under large reverse bias and a simple dependence of the forward current on the applied bias through the Boltzmann's factor of the full applied voltage when the forward bias is several kT/q . Usually, at room temperature the current in a silicon $p-n$ junction does not saturate at large reverse bias and increases much slower than the Boltzmann's factor to the full applied voltage under forward bias. Discrepancy has also been observed by many workers between the ideal theory for $p-n$ junction transistors and the observed characteristics of silicon $p-n$ junction transistors. In particular, the ideal theory predicts a nearly unity value for the transistor current amplification factor, alpha, at low emitter current densities, while the observed alpha usually becomes very small at low emitter current densities.^{2,3}

* Original manuscript received by the IRE, March 23, 1957; revised manuscript received, May 13, 1957.

† Shockley Semiconductor Lab., Mountain View, Calif.

¹ W. Shockley, "The theory of $p-n$ junctions in semiconductors and $p-n$ junction transistors," *Bell Sys. Tech. J.*, vol. 28, pp. 435-489; July, 1949.

² J. L. Moll, et al., "P-N-P-N transistor switches," *Proc. IRE*, vol. 44, pp. 1174-1182; September, 1956.

³ M. Tanenbaum and D. E. Thomas, "Diffused emitter and base silicon transistors," *Bell Sys. Tech. J.*, vol. 35, pp. 1-22; January, 1956.

It has been pointed out by Shockley and Read⁴ that generation of the current carriers in the space charge region or the transition layer of a $p-n$ junction may be extremely high. The essential features of the reverse characteristics of a silicon $p-n$ junction can be understood in terms of this phenomenon by using a model of single energy level uniformly distributed Shockley-Read-Hall recombination centers. Pell and Roe,⁵ and Kleinknecht and Seiler⁶ have independently used this model to account for the reverse characteristics of silicon $p-n$ junctions.

Shockley has suggested that the recombination of the carriers may also dominate in the space charge region when a $p-n$ junction is biased in the forward direction.¹ However, the importance of this effect on the $p-n$ junction and junction transistor characteristics has not been realized until recently.⁷

In this paper, we present a physical theory of $p-n$ junctions taking into account the recombination and generation of the carriers in the space charge region or the transition region.

II. SHOCKLEY-READ-HALL RECOMBINATION STATISTICS

A brief derivation is given in this section for the steady-state recombination statistics of electrons and holes in semiconductors to illustrate the method and physical principle involved. For a complete and detailed treatment of this subject, the reader is referred to Shockley and Read.⁴

The recombination and generation of electrons and holes in semiconductors may take place at some type of recombination-generation centers or traps. These sites may be crystal lattice dislocations, impurity atoms located interstitially or substitutionally in the crystal lattice, or surface defects. Recombination may also oc-

⁴ W. Shockley and W. T. Read, Jr., "Statistics of recombinations of holes and electrons," *Phys. Rev.*, vol. 87, pp. 835-842; September, 1952.

R. N. Hall, "Germanium rectifier characteristics," *Phys. Rev.*, vol. 83, p. 228; July, 1951.

R. N. Hall, "Electron-hole recombination in germanium," *Phys. Rev.*, vol. 87, p. 387; July, 1952.

⁵ E. M. Pell and G. M. Roe, "Reverse current and carrier lifetime as a function of temperature in germanium junction diodes," *J. Appl. Phys.*, vol. 26, pp. 658-665; June, 1955.

⁶ H. Kleinknecht and K. Seiler, "Einkristalle und pn Schichtkristalle aus Silizium," *Z. Physik*, vol. 139, pp. 599-618; December 20, 1954.

⁷ R. N. Noyce, C. T. Sah, and W. Shockley, "Carrier generation and recombination in the space charge region of a $p-n$ junction," *Bull. Amer. Phys. Soc. II*, vol. 1, H9, p. 382; December 27, 1956.

C. T. Sah, and W. Shockley, "Interpretation of silicon $p-n$ junction current-voltage characteristics," *Bull. Amer. Phys. Soc. II*, vol. 1, H10, p. 382; December 27, 1956.

cur directly with the emission of light or by the three (or more) particle process (Auger process) with the third carrier carrying away the energy. The radiative process is rather improbable. At present, there is no sufficient information about the Auger process in semiconductors. Thus, these processes will not be considered.

Under steady-state conditions, a single energy level recombination center is characterized by three numbers: the capture cross section for electrons, the capture cross section for holes, and the energy involved in these transitions. The cross sections are inversely proportional to the lifetimes of electrons and holes respectively, and the transition energy may be measured from one of the edges of the energy gap of the semiconductor.⁸

There are four basic processes involved in the carrier generation and recombination through the traps.⁴ If a trap is occupied by a hole, an electron may drop into the trap from the conduction band and recombine with the hole, or the trap may emit the hole to the valence band. If the trap is initially filled with an electron, the trapped electron may be emitted to the conduction band or a valence band hole may move into the trap and recombine with the trapped electron. These four processes are illustrated in Fig. 1. The direction of the arrow indicates

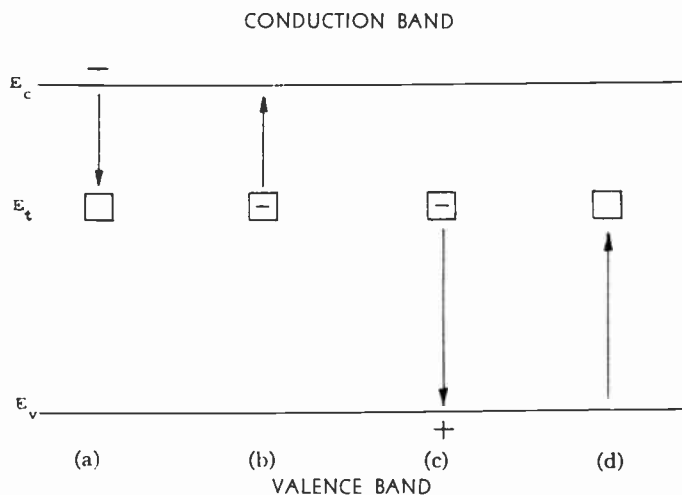


Fig. 1—The basic processes of carrier generation and recombination through traps, (a) electron capture, (b) electron emission, (c) hole capture, (d) hole emission.

the direction of transition for either a conduction or a valence band electron as the case may be.

Consider the electron capture process indicated by Fig. 1(a). The rate that the electron in the conduction band will drop into an empty trap is

$$nf_{tp}/\tau_{n0} \tag{1}$$

(See Table I for the meaning of the symbols.)

The electron emission rate indicated by Fig. 1(b) can be written as

$$af_i \tag{2}$$

⁸ The steady-state recombination statistics involving centers with more than one energy level has also been considered by the authors. (To be published.)

TABLE I
SYMBOLS

n	= density of electrons in the conduction band = $n_i \exp (F_n - E_i) / kT$
p	= density of holes in the valence band = $n_i \exp (E_i - F_p) / kT$
E_c	= energy of the highest valence band level
E_v	= energy of the lowest conduction band level
E_i	= intrinsic Fermi level = $-q\Psi$
E_t	= energy level of the recombination-generation centers or traps
ϵ_i	= $(E_i - E_t) / kT + \ln \sqrt{\tau_{p0} / \tau_{n0}}$
Ψ	= electrostatic potential = $-E_i / q$
V_D	= diffusion or built-in voltage in a p - n junction
ϕ_n	= quasi-Fermi electrostatic potential or imref for electrons = $-F_n / q$
ϕ_p	= quasi-Fermi electrostatic potential or imref for holes = $-F_p / q$
n_i	= density of electrons or holes in an intrinsic specimen
N_c	= effective density of levels for conduction band
N_v	= effective density of levels for valence band
N_t	= density of the recombination-generation centers or traps
f_{tp}	= fraction of traps occupied by holes
f_i	= fraction of traps occupied by electrons = $1 - f_{tp}$
n_i	= density of electrons in the conduction band when the Fermi level falls at $E_i = n_i \exp (E_i - E_i) / kT$
p_i	= density of holes in the valence band when the Fermi level falls at $E_i = n_i \exp (E_i - E_i) / kT$
τ_{n0}	= lifetime for electrons injected into highly p -type specimen
τ_{p0}	= lifetime for holes injected into highly n -type specimen
q	= magnitude of electronic charge
k	= Boltzmann constant
T	= absolute temperature
U_{cn}	= net electron capture rate
U_{cp}	= net hole capture rate
U	= steady-state electron or hole recombination rate
J_{rg}	= recombination-generation current density in the space charge layer
J_D	= diffusion current density outside the space charge layer

where a is a proportionality factor which includes the trap density, the total number of empty electronic states in the conduction band and the probability of electron emission from the traps. The expression for a can be obtained by a detailed balance argument for the system under the thermal equilibrium condition. Under this condition, the electron emission rate must be equal to the electron capture rate, *i.e.*, (1) and (2) are equal. Thus, if the occupancy of the traps is expressed in terms of a quasi-Fermi level⁴ (or imref) for traps F_t , then the imref for electrons, F_n , must fall at F_t at thermal equilibrium. Assuming that the semiconductor is nondegenerate, and using⁹

$$f_i = (1 + \exp (E_t - F_t) / kT)^{-1}$$

then from equating (1) and (2) we obtain

$$a \approx n_i / \tau_{n0} \tag{3}$$

The net capture rate for electrons by the traps under nonequilibrium conditions can then be written as

$$U_{cn} = (nf_{tp} - n_i f_i) / \tau_{n0} \tag{4}$$

An entirely similar treatment can be carried out for holes leading to the following equation for the net rate of capture for holes under nonequilibrium conditions.

$$U_{cp} = (pf_i - p_i f_{tp}) / \tau_{p0} \tag{5}$$

⁹ Electron spin degeneracy is included in E_i .

The rate of recombination for nonequilibrium but steady-state conditions is obtained by requiring that the net rate of capture of electrons be equal to that of holes. This condition leads to

$$U = U_{cn} = U_{cp} = (pn - n_i^2) / [(n + n_1)\tau_{p0} + (p + p_1)\tau_{n0}] \quad (6)$$

for the steady-state recombination rate for electrons or holes.

The result of these statistics is applied to the current carriers in the transition region of a *p-n* junction and in the region outside of the transition region.

III. IDEALIZED MODEL

An idealized *p-n* junction is considered in this section so that the physical processes can be readily visualized. It is assumed that there are single-level, uniformly-distributed recombination-generation centers located at the intrinsic Fermi level. Thus $p_1 = n_1 = n_i$. It is further assumed that the lifetimes, mobilities, and the densities of the minority carriers on opposite sides of the junction are equal. The recombination and generation processes are considered separately in the *p* region, the *n* region, and the transition region of a *p-n* junction.

In the *p* region shown in Fig. 2(a), the traps are mostly empty and ready to trap the injected electrons. Subsequently, the holes would move into these occupied traps and recombine with the trapped electrons. In order to preserve electrical neutrality, holes must be replenished through electron current flowing in the external circuit. Thus, with $p = p_p \gg p_1$, n_1 and n , and $n = n_p + \Delta n$, (6) reduces to

$$U = (n - n_p) / \tau_{n0} \quad (7)$$

Similarly, the recombination rate in the *n* region, shown in Fig. 2(b), is given by

$$U = (p - p_n) / \tau_{p0} \quad (8)$$

These are the usual linear recombination laws which hold when the injected minority carrier density is much smaller than the equilibrium carrier density.

If the minority carriers are rapidly moving out of a certain region of the semiconductor by electric field, the generation rates in this region would be

$$-U = n_p / \tau_{n0} \quad (7a)$$

for *p*-type region, or

$$-U = p_n / \tau_{p0} \quad (8a)$$

for *n*-type region. The edges of the space charge layer of a reversely biased *p-n* junction are precisely the regions where (7a) and (8a) prevail. On the average, a minority carrier generated in the *n* region or the *p* region within one diffusion length from the edge of the space charge layer would diffuse to the edge and slide down the potential hill of the space charge region rapidly.¹ Thus,

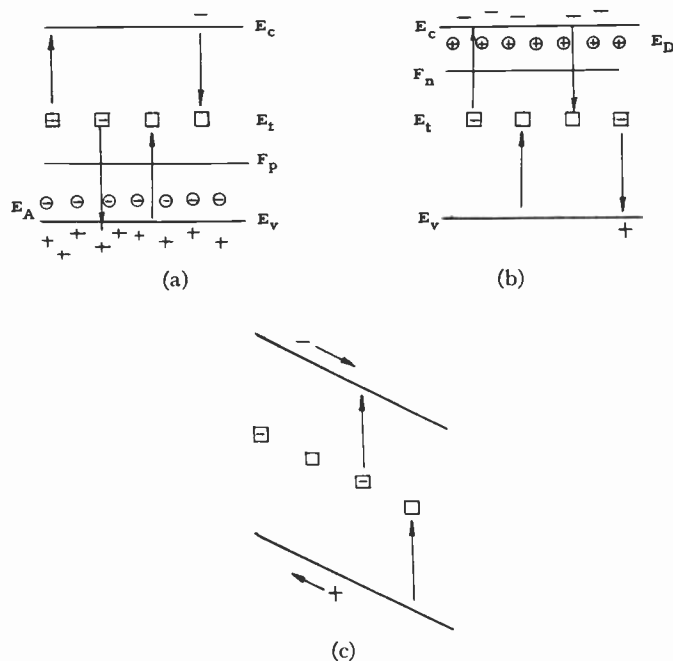


Fig. 2—Recombination and generation processes in semiconductor, (a) *p* region, (b) *n* region, (c) intrinsic with swept field.

the current which must flow in the external circuit to replenish the diffusing minority carriers is

$$J_d A = -2qn_p L_0 A / \tau_0 \quad (9)$$

where $n_p = p_n$ and $\tau_{n0} = \tau_{p0} = \tau_0$ have been used. L_0 , the diffusion length of the minority carrier, is given by $(D_0 \tau_0)^{1/2}$, and $D_0 = D_n = D_p$ is the diffusion constant of the minority carriers. A is the area of the junction.

Let us next consider the space charge region or the transition region of a reversely biased *p-n* junction. Both types of carriers are rapidly swept out of this region by the large electric field, thus their densities are small compared to n_i . The situation is shown in Fig. 2(c). For this case, the generation rate from (6) is

$$-U = n_i / 2\tau_0 \quad (10)$$

and is approximately constant over the entire space charge layer. It may be noted that the recombination effect is again unimportant here because of the presence of the large electric field. It may also be noted that the centers are about half empty and half filled in this region.

Since for every pair of carriers generated, one electron must flow in the external circuit, the current flowing in the external circuit due to this effect is

$$J_{\tau_0} A = -qWn_i A / 2\tau_0 \quad (11)$$

where W is the width of the space charge layer.

The currents generated in the *p* region and the *n* region and the current generated in the space charge layer may be compared. The ratio of these two components given by (9) and (11) is

$$J_{\tau_0} / J_d = (n_n / 4n_i) W / L_0 \quad (12)$$

A number of conclusions regarding the relative importance of these two currents can be deduced. Eq. (12) indicates that the current generated in the space charge region may be extremely large compared with the diffusion current for semiconductors with short lifetimes, low resistivities, large energy gap and at low temperatures, even if $W \ll L_0$.

For a typical example, consider a 2 ohm-cm material of one microsecond lifetime. Assuming a one micron space charge layer width, at room temperature the current ratio is about 3000 for a silicon p - n junction while it is only about 0.1 for a germanium p - n junction. Thus, the generation-recombination current in the space charge layer would greatly influence the characteristics of silicon semiconductor devices.

If the current due to generation in the space charge layer is important under the reverse bias condition, it would be expected that the reverse process, namely, recombination in the space charge layer, will be important under forward bias. However, the extension of the argument for deriving the current produced in the space charge layer must take a slightly different form from that applied to the reverse-bias case.

Under forward bias, the carrier concentrations at the center of the space charge region are equal and vary as

$$n = p = n_i \exp(qV/2kT), \quad (13)$$

since $np = n_i^2 \exp(qV/kT)$. The recombination rate at this p - n boundary is then

$$U = n_i \exp(qV/2kT)/2\tau_0 \quad (14)$$

for V greater than several kT/q , and falls exponentially with distance on either side of the p - n boundary with a characteristic length of kT/qE where E is the electric field at the junction. Thus, the recombination current density is

$$J_{r,g} = 2(kT/qE)qn_i \exp(qV/2kT)/2\tau_0, \quad (15)$$

where the factor 2 comes from the contribution on the two sides of the p - n boundary. The exact expression for this idealized case involves an additional factor of $\pi/2$, which takes into account that the recombination rate falls slower than $\exp(-qEx/kT)$ near $x=0$.

$$U = \frac{n_i}{\sqrt{\tau_{p0}\tau_{n0}}}$$

$$\frac{\sinh \frac{q}{2kT} (\phi_p - \phi_n)}{\cosh \left[\frac{q}{kT} \left(\Psi - \frac{\phi_p + \phi_n}{2} \right) + \ln \sqrt{\frac{\tau_{p0}}{\tau_{n0}}} \right] + \exp \left[\frac{-q}{2kT} (\phi_p - \phi_n) \right] \cosh \left(\frac{E_t - E_i}{kT} + \ln \sqrt{\frac{\tau_{p0}}{\tau_{n0}}} \right)} \quad (20)$$

Using a linear potential variation across the junction, the electric field can be written as

$$E = (\Psi_D - V)/W \quad (16)$$

where Ψ_D is the built-in voltage.

The sum of the diffusion current densities which flow in the p region and the n region is given by¹

$$J_D = (2qn_p L_0 / \tau_0) \exp(qV/kT) \quad (17)$$

for applied forward bias of several kT/q . The two currents can again be compared, giving a current ratio of

$$\frac{J_{r,g}}{J_D} = (n_i/n_p)(W/2L_0) [kT/q(\Psi_D - V)] \cdot \exp(-qV/2kT). \quad (18)$$

Using the same data as in (12) with a space charge layer width of 0.1 micron, the recombination current becomes equal and greater than the diffusion current at applied bias of less than 10 kT/q .

The total current per unit area is given by the sum of the diffusion and the recombination-generation current densities. The comparison given above indicates that the recombination-generation current is much greater than the diffusion current, and the total current would vary slower than the ideal rectifier formula of $\exp(qV/kT)$.

IV. THEORETICAL CALCULATION OF THE CURRENT-VOLTAGE CHARACTERISTICS

In the last section and in the literature,^{1,4} an effective lifetime, which is a function of the carrier densities, has been used to obtain the characteristics of p - n junction devices. The effective lifetime is usually obtained by experimental measurements. In order to obtain a complete theoretical relation between the current and the applied voltage, it is necessary to start with the exact expression of the steady-state recombination rate of the carriers given by (6).

Substitution of the following relations

$$p_1 = n_i \exp(E_i - E_t)/kT$$

$$n_1 = n_i \exp(E_t - E_i)/kT$$

$$p = n_i \exp(\phi_p - \Psi)/kT$$

$$n = n_i \exp(\Psi - \phi_n)/kT$$

$$E_t = (E_c + E_v - kT \ln N_c/N_v)/2 = -q\Psi \quad (19)$$

into (6) gives the following expression for the steady-state recombination rate:

The notations are identical to those used by Shockley and Read,⁴ and are listed in Table 1.

The recombination rate given above is sketched for several limiting conditions in Fig. 3.

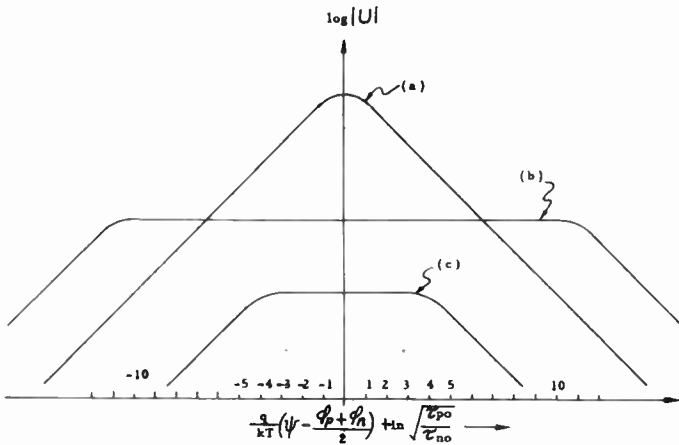


Fig. 3—Variation of the recombination rate in the p - n junction transition region; (a) forward bias $(\phi_p - \phi_n)q/2kT \gg 1$, $|(E_t - E_i)/kT + \frac{1}{2} \ln \tau_{p0}/\tau_{n0}|$, (b) reverse bias $(\phi_n - \phi_p)q/2kT \gg 1$, $|(E_t - E_i)/kT + \frac{1}{2} \ln \tau_{p0}/\tau_{n0}|$, (c) small bias $(\phi_p - \phi_n)q/2kT \approx 1$, $|(E_t - E_i)/kT + \frac{1}{2} \ln \tau_{p0}/\tau_{n0}| \approx 4$.

The recombination-generation current in the space charge layer is obtained by integrating (20) over the space charge layer. For the one-dimensional case, the total recombination-generation current density in the space charge layer is given by

$$J_{r_g} = q \int U dx, \tag{21}$$

where the integration is taken over the space charge layer.

The exact solution of this problem requires a knowledge of the imrefs ϕ_p and ϕ_n and the electrostatic potential Ψ as a function of position in the p - n junction. This is a difficult problem involving the solution of simultaneous nonlinear differential equations.¹ In this treatment, we shall follow a self-consistent approach given in Appendix I. It is convenient to consider three regions of the applied bias, the large reverse-bias region, the small bias region, and the large forward-bias region.

Large Reverse-Bias, $-q(\phi_p - \phi_n)/kT \gg 1$

For this case, the potential energy diagram for holes is shown in Fig. 4 together with the current distribution in the p - n junction. The hole current J_p shown in the lower part of Fig. 4 can be deduced from the recombination-generation rate and (21). Under large reverse-bias, the first term in the denominator of (20) is small compared with the second term, since $\phi_n - \phi_p$ is several kT/q inside the space charge layer. Thus, the recombination rate is approximately constant over the entire transition region as illustrated in Fig. 3(b). The hole current then is proportional to the distance and decreases monotonically. The total recombination-generation current for this case is then

$$J_{r_g} = qUW, \tag{22}$$

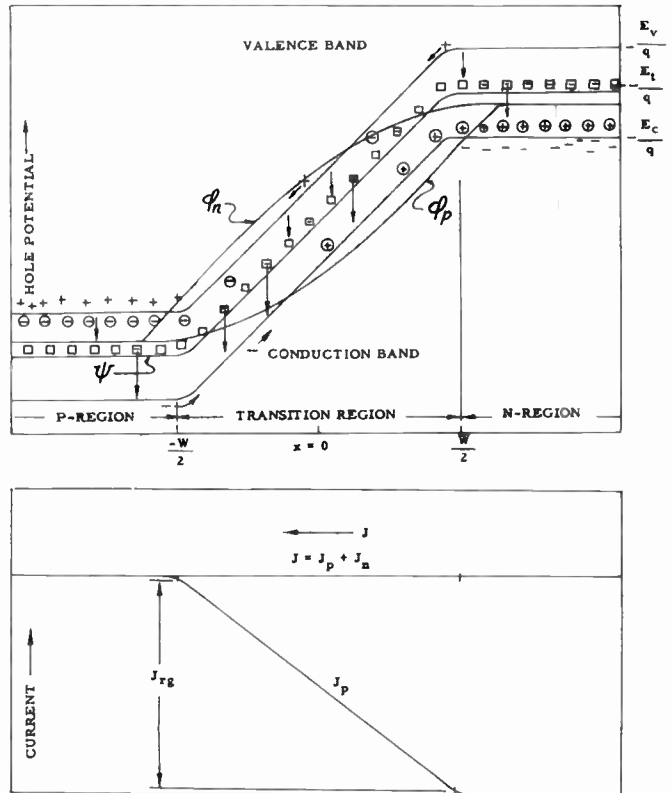


Fig. 4— p - n junction under large reverse bias.

where W is the space charge layer width and the generation rate is given by

$$-U = n_i \left[2\sqrt{\tau_{p0}\tau_{n0}} \cosh \left(\frac{E_t - E_i}{kT} + \frac{1}{2} \ln \frac{\tau_{p0}}{\tau_{n0}} \right) \right]^{-1}. \tag{23}$$

This approximation slightly overestimates the generation current since the generation rate drops exponentially to zero near the edges of the space charge layer.

The result obtained above indicates that the traps are most effective as generation centers if they are located at the intrinsic Fermi level when the lifetimes of the carriers are equal. In general, the traps are most effective if $(E_t - E_i)/kT + (1/2) \ln \tau_{p0}/\tau_{n0} = 0$. The above result also shows that the generation current cannot saturate. For the linear-graded junction this current is proportional to $\frac{1}{3}$ power of the applied voltage and for a step junction it is proportional to $\frac{1}{2}$ power of the applied voltage since the space charge layer width varies accordingly.

Although it was shown that the shapes of the imrefs have negligible effect on the calculation of the generation-recombination rate, it is instructive to deduce the shapes of the imrefs. From the relation between the hole current and the imref for holes,

$$J_p = -qn_i\mu_p \exp [(\phi_p - \Psi)q/kT] d\phi_p/dx, \tag{24}$$

it can be concluded that in the transition region, the increase of the slope of ϕ_p must be slower than the decrease

of the hole density p or the factor $\exp(\phi_p - \Psi)q/kT$ in order to give a monotonic variation of J_p . A similar consideration can be given to the electron imref variation in the transition region. These arguments lead to the potential diagram shown in Fig. 4. The drop of the imrefs is almost complete inside the space charge layer. A numerical calculation in Appendix I for a silicon junction also gives the same conclusion.

It is interesting to note that the product of the junction capacity and the space charge layer generated current is a constant under large reverse-bias and is independent of the shape of the electrostatic potential distribution inside the junction. This relation can be written as

$$CJ_{r0} = \epsilon_0 K q U, \tag{25}$$

where ϵ_0 is the permittivity of free space and K is the dielectric constant. The constancy of the product given above holds only at intermediate range of applied voltage. At reverse-bias near the avalanche breakdown, the product given by (25) increases. The lifetimes τ_{n0} and τ_{p0} may be field dependent and cause additional variation of the product with the reverse-bias.

The avalanche mechanism is considered in detail in Appendix II. The effect of the avalanche multiplication is to multiply the recombination-generation current in the same way as if it were injected into the space charge layer if the electron and hole ionization rates are equal. Thus, for large reverse-bias, the recombination-generation current is given by

$$J_{r0} = qUWM, \tag{22a}$$

where M is the avalanche multiplication factor given in Appendix II.

The thermal activation energy or the energy level of the recombination-generation centers can be obtained readily by temperature measurement of the reverse characteristics. The magnitude of the trap energy level from the intrinsic Fermi level is given by the difference of half the zero temperature energy gap width and the activation energy obtained from the slope of a plot of $\ln J_{r0} - (5/2) \ln kT$ vs $(kT)^{-1}$. The detailed calculation is given in Appendix III.

Small Applied Bias

For this case, both terms in the denominator of the expression for U are important and one has to consider the shape of the imrefs in order to obtain a good approximation to $\Psi - (\phi_p + \phi_n)/2$ in the expression for U . A similar argument for the shape of the imrefs as that given to the large reverse-bias case can be made here. This leads to the conclusion that the variation of the imrefs in the space charge layer is very small, contrary to the result of the large reverse-bias case. This is also confirmed by a numerical calculation given in Appendix

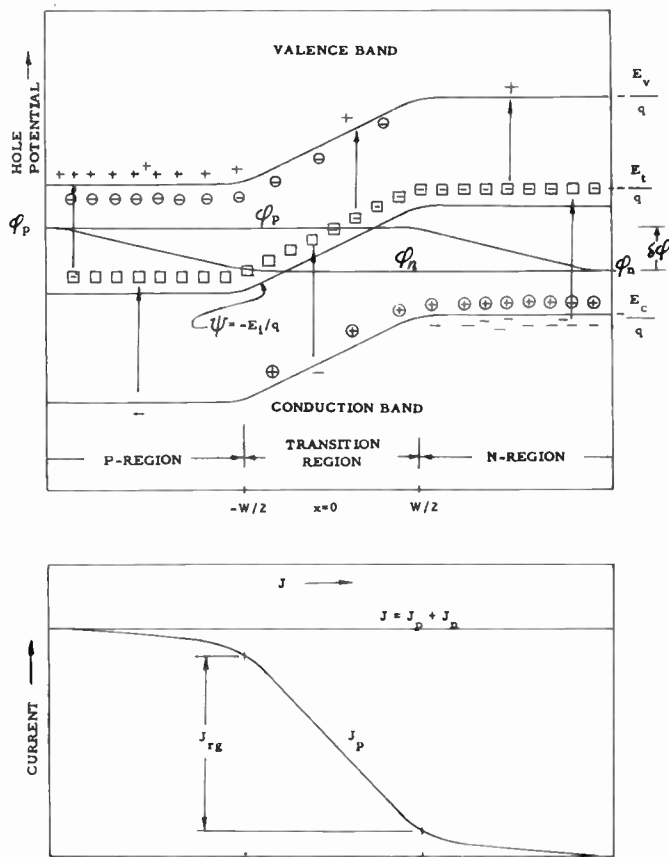


Fig. 5—*p-n* junction under forward bias.

I. Outside the space charge region the imrefs vary linearly with distance. The approximate potential energy diagram and the current distribution across the junction is shown in Fig. 5 from these conclusions. The current shown there is for a case where the recombination current is about 2.5 times higher than the total diffusion outside the space charge layer.

From Fig. 5, it can be seen that the electrostatic potential can be written approximately

$$\Psi - \frac{\phi_p + \phi_n}{2} = \frac{\Psi_D - (\phi_p - \phi_n)}{W} x - \frac{W}{2} < x < \frac{W}{2}, \tag{26}$$

where W is the total space charge layer width, $\phi_p - \phi_n$ is approximately the applied voltage and Ψ_D is the built-in voltage or the difference of the intrinsic Fermi levels on the two sides of the junction. An exact expression for the electrostatic potential variation could be obtained.¹ However, a linear approximation given by (26) will give a maximum of 50 per cent error in the slope of Ψ and will put the integral of (21) into a more tractable form.¹⁰

¹⁰ Dr. Ruth F. Schwarz of Philco Corporation has kindly sent us her more exact calculation for step junctions. The linear approximation of (26) is quite good for grown or diffused type graded-junctions.

Performing the integration, the recombination current can be written as

$$J_{r0} = \frac{qn_i}{\sqrt{\tau_{p0}\tau_{n0}}} W \frac{2 \sinh(\phi_p - \phi_n)q/2kT}{(\Psi_D - \phi_p + \phi_n)q/kT} f(b), \quad (27)$$

where

$$f(b) = \int_{z_1}^{z_2} \frac{dz}{z^2 + 2bz + 1}$$

$$b = \exp \left[-(\phi_p - \phi_n)q/2kT \right] \cdot \cosh \left[\frac{E_t - E_i}{kT} + (1/2) \ln(\tau_{p0}/\tau_{n0}) \right]$$

and the integration limits are

$$z_{1,2} = (\tau_{p0}/\tau_{n0})^{1/2} \exp \left[\mp (\Psi_D - \phi_p + \phi_n)q/2kT \right].$$

The integral given by $f(b)$ can be evaluated exactly. However, at applied voltages several kT/q less than the built-in voltage, the integration limits can be extended from zero to infinity with small error. The value of the integral and its slope is plotted in Fig. 6 for the case of $z_1=0$ and $z_2=\infty$. The variation of the slope of $\log J_{r0}$ is also plotted in Fig. 7.

There are several regions of the current-voltage characteristics for this case which need special discussion.

1) *Very Small Bias*: When the applied bias is less than kT/q , the recombination-generation current follows essentially the ohmic law. The recombination conductance at zero bias is given by

$$R_{r0}^{-1} = qn_i W f(b) / \sqrt{\tau_{p0}\tau_{n0}} \Psi_D. \quad (28)$$

A comparison of this resistance with the diffusion resistance gives the same conclusions for the relative importance of the two currents as that obtained in Section II.

2) *Medium Forward-Bias with Deep Traps*: When the traps are located near the intrinsic Fermi level, the function $f(b)$ increases slightly when the forward-bias decreases. Thus the recombination current will vary slightly faster than $\exp(qV/2kT)$ as can be seen from (27). This is in agreement with the result obtained in Section II from intuitive arguments.

3) *Small or Medium Forward-Bias with Shallow Traps*: A region of small or medium bias with values of b greater than 10 may exist, if the traps are quite shallow, i.e., the effective trap level is about $10kT$ from the intrinsic Fermi level. The integral given by $f(b)$ will vary approximately as $1/b$ and the recombination current will vary with the applied voltage approximately as $\exp(qV/kT) - 1$ shown in Fig. 7.

The result given by (27) would reduce to that given by (22) and (23). However, (27) is not accurate in the transition region between small and large reverse bias because of the error in estimating the shape of the imrefs.

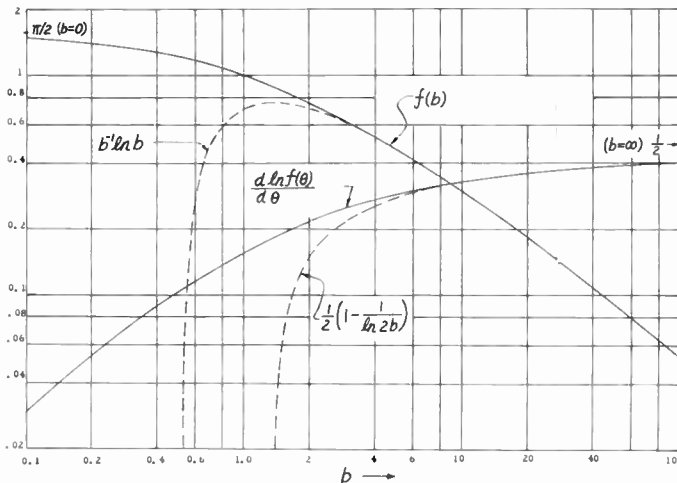


Fig. 6—The function $f(b)$ and its slope.

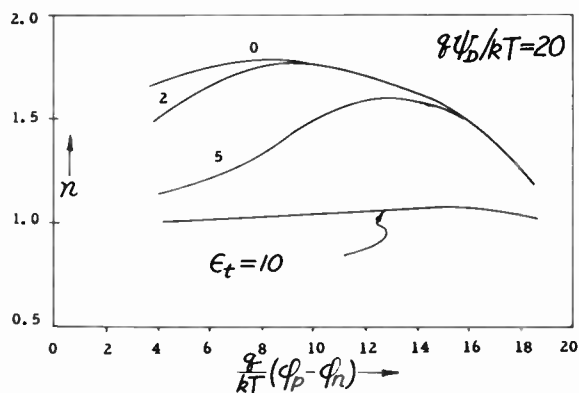


Fig. 7—Slope of $\ln J_{r0}$ vs forward applied bias.

Large Forward-Bias

At forward-bias about or greater than the built-in voltage, the width of the space charge layer is small. The recombination current in the space charge layer is negligible compared with the diffusion current due to injected carriers outside the space charge layer. We shall consider the case for which the injected carrier density is much higher than the fixed impurity charge concentration in the n region. One may assume for this case that $n \approx p$. The boundary condition at the junction becomes

$$n(0) = p(0) = n_i \exp(qV/2kT), \quad (29)$$

where V is the applied voltage less the ohmic drop. The usual diffusion formula applies and the total current is nearly equal to the hole current at the junction. Thus

$$J = J_p(0) = 2(qD_p n_i / L_0) \exp(qV/2kT), \quad (30)$$

where L_0 is an effective diffusion length given in Appendix IV. A more detailed treatment of the diffusion current is given there also. We may note that the region of $\exp(qV/2kT)$ occurs at higher applied voltage for the diffusion current than the same case for the recombina-

tion current. The case for the diffusion current has been observed for certain P^+IN diodes with very low ohmic drops.¹¹

At still higher current density or applied bias, the current will eventually be limited by the ohmic contact resistance and the bulk resistance of the material. The current voltage characteristics become linear in this range.

To summarize the theoretical calculation, the characteristics of a linearly graded junction is sketched in Fig. 8. Fig. 8(a) shows the reverse characteristics and Fig. 8(b) shows the forward characteristics including the diffusion current outside the space charge layer at large forward bias. For an actual case the regions of distinct but different slopes shown in Fig. 8(b) would merge and a varying slope of between 0.5 and 1 would be observed. From these considerations, we may also conclude here that the minority carrier concentrations at the boundary cannot vary faster than $\exp(qV/kT)$. This is in agreement with statistical mechanics considerations.

V. THE EMITTER EFFICIENCY AND THE CURRENT AMPLIFICATION FACTOR OF A $p-n$ JUNCTION TRANSISTOR

Carrier recombination in the space charge layer of a forward-biased emitter may play an important role in the determination of the emitter efficiency of a silicon junction transistor at low emitter current. This effect thus imposes a lower limit on the emitter current density for high emitter efficiency operation.

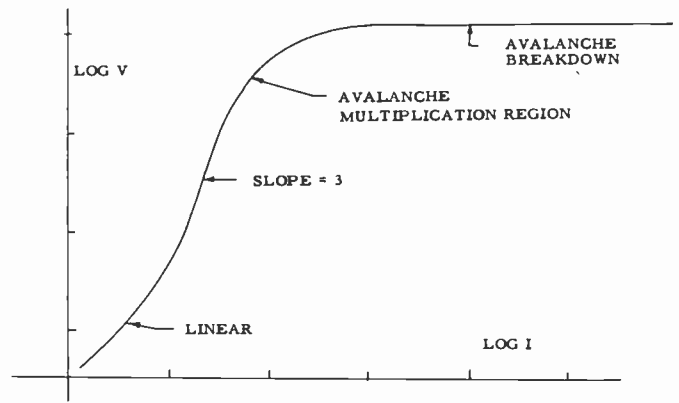
From the theoretical considerations given in the previous sections, the recombination process is dominant in a forward-biased silicon emitter junction. The portion of the emitter current due to this mechanism consists of carrier recombination in the space charge layer and thus is not available for transistor action. At high emitter current, the diffusion current dominates and the emitter efficiency increases. This phenomenon has been observed for silicon transistors.^{2,3} The recombination in the space charge layer which causes increasing transistor alpha with current is also the basis for the operation of low current $p-n-p-n$ transistor switches.²

The dc transistor current amplification factor, alpha, can be calculated by the following expression at reverse collector bias when the recombination in the emitter space charge layer is taken into consideration.

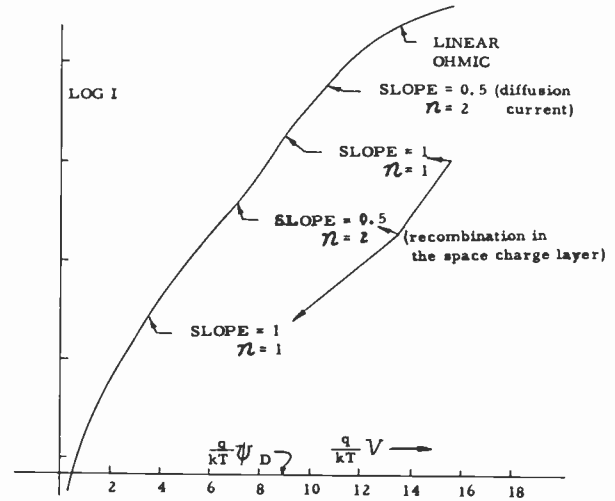
$$\alpha = \text{sech}(W_b/L_b) \{ 1 + [(J_{r0} + J_d')/J_d \tanh(W_b/L_b)]^{-1} \} \quad (31)$$

J_d and J_d' are the injected current densities flowing into the base and the emitter region respectively. L_b is the minority carrier diffusion length in the base and W_b is the base layer width. It is evident from the calculations

¹¹ R. N. Hall, "Power rectifiers and transistors," PROC. IRE, vol. 40, pp. 1512-1519; November, 1952.



(a)



(b)

Fig. 8—Characteristics of a linearly graded $p-n$ junction, (a) reverse bias, (b) forward bias.

made in the previous section that the dc transistor alpha given by (31) approaches zero at low emitter current density since $J_d \ll J_{r0}$. At large forward bias the alpha increases toward unity since $J_d \gg J_{r0}, J_d'$. At still higher emitter current densities, $J_d, J_d' \gg J_{r0}$, the emitter efficiency or the alpha decreases as pointed out by Webster.¹²

The proximity of the collector junction increases the diffusion current component and increases the alpha of the device at low emitter current densities.

Fig. 9 shows the current distribution in a $p-n$ junction transistor under various emitter bias conditions. Fig. 10 shows several calculated transistor alpha using (31) and the calculated result for the diode shown in the next section. These theoretical curves follow closely the experimental alpha of Moll² and Tanenbaum.¹³

¹² W. M. Webster, "On the variation of junction-transistor current amplification factor with emitter current," PROC. IRE, vol. 42, pp. 914-920; June, 1954.

¹³ We are indebted to J. L. Moll for pointing out a numerical error.

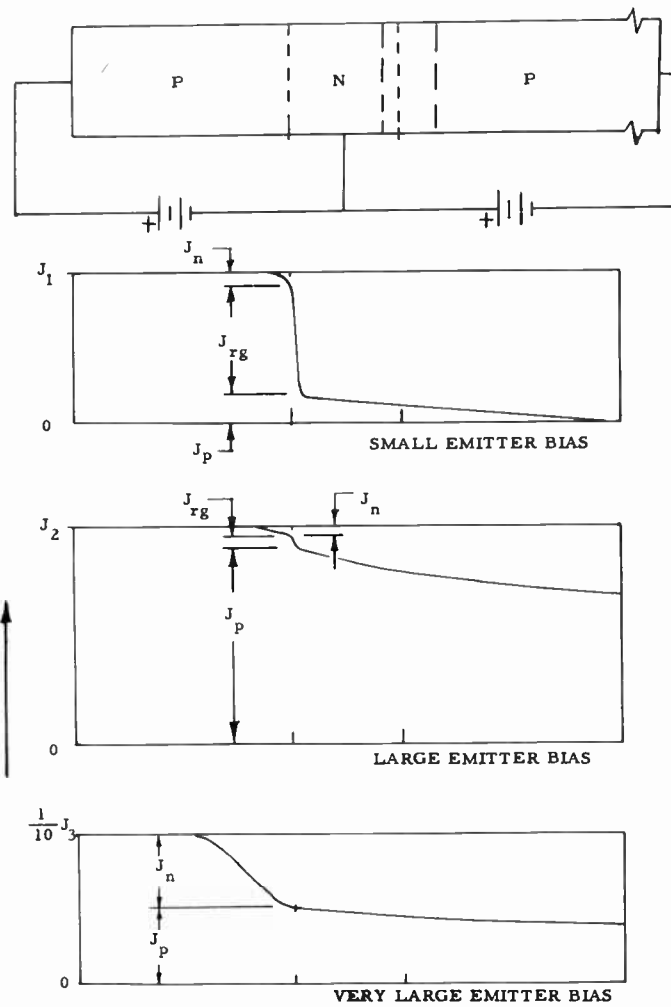


Fig. 9—Current in junction transistor with large carrier recombination in the emitter junction.

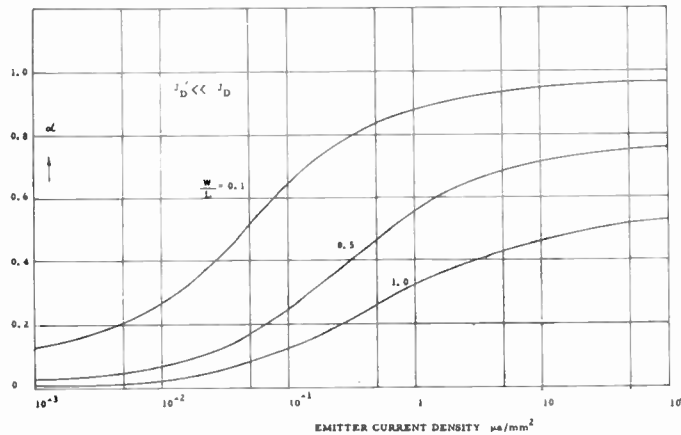


Fig. 10—*p-n-p* silicon transistor dc alpha.

VI. EXPERIMENTAL MEASUREMENTS

The experimental *p-n* junctions were produced by diffusion of boron from the gaseous phase into an *n*-type silicon of 2.4 ohm-cm resistivity at 1250°C for 80".

The following data are obtained from measurements of a typical diffused junction and from calculations.

- Bulk concentration $N_D = 2.2 \times 10^{15} \text{ cm}^{-3}$
- Surface concentration of boron $= 4 \times 10^{21} \text{ cm}^{-3}$
- $(D\tau)^{1/2}$ diffusion length of boron = 1.8 microns
- Junction depth = 11.8 microns from surface
- Breakdown voltage = 120 volts (calculated from results in Appendix II)
- Built-in voltage = 0.47 volt (see Shockley,¹ with linear graded junction approximation)
- Area of junction 0.620 mm².

In order to calculate the theoretical *p-n* junction characteristics we shall use the linear-graded junction approximation. The trap level $E_t - E_i$ and lifetimes are obtained by matching the theoretical formula and the experimental data at three points. It is most convenient to use two points at relatively small applied bias where the current from the space charge layer is dominant and one point at large forward bias where the diffusion current dominates. We choose these points to be at applied bias of $\theta = qV/kT = -4.6, 4.6, \text{ and } +18.3$. The last point corresponds to the built-in voltage at room temperature. The currents at these voltages are $2.96 \times 10^{-10}, 3.75 \times 10^{-9}, \text{ and } 1.0 \times 10^{-4}$ amperes respectively from Figs. 11 and 12.

Using (27) for the first two points and the formula for diffusion current given in Appendix IV we obtain the following results:

$$\begin{aligned} \tau_{p0} &= 1.2 \times 10^{-8} \text{ sec,} \\ \tau_{n0} &= 4.3 \times 10^{-6} \text{ sec,} \\ E_t - E_i &= 4.6kT \text{ or } 1.3 kT, \end{aligned}$$

where we have used the following constants:¹⁴

$$\begin{aligned} n_i &= 10^{-10} \text{ cm}^{-3}, \\ D_p &= 11.1 \text{ cm}^2/\text{sec}, \\ D_n &= 2.77D_p, \\ E_g &= 1.21 \text{ eV at } 0^\circ \text{ K.} \end{aligned}$$

The value of $E_t - E_i$ cannot be uniquely determined from this experiment since the results only give $\cosh [(E_t - E_i)/kT + (1/2) \ln(\tau_{p0}/\tau_{n0})]$ which makes the sign uncertain. However, the value of $E_t - E_i$ obtained is in good agreement with the result of Pell and Roe.⁵

The theoretical calculations and the experimental measurements are presented in Figs. 11 and 12. Good agreement is obtained over the entire range of more than 9 decades of junction current. In addition to the three-point-match, we have also taken into consideration the contact resistance drop which accounts for

¹⁴ Morin and Maita, "Electrical properties of silicon containing arsenic and boron," *Phys. Rev.*, vol. 96, pp. 28-35; October 1, 1954. M. B. Prince, "Drift mobility in semiconductors. II. Silicon," *Phys. Rev.*, vol. 93, pp. 1204-1206; March 15, 1954.

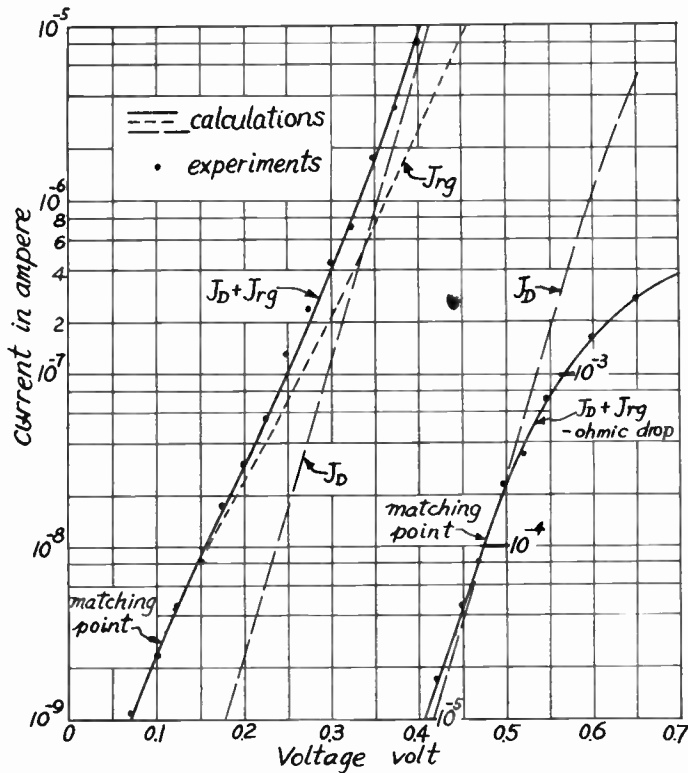


Fig. 11—Forward characteristics of a silicon *p-n* junction.

the slow increase of the large forward current. The avalanche multiplication near the avalanche breakdown voltage is also considered. In this region, the experimental measured currents were found for all cases to be always greater than the calculated values. This may be due to the dependence of the lifetimes on the electric field and due to surface breakdown.

Additional data are shown in Figs. 13(a) and (b), on the next page, for silicon diodes of different base resistivities and surface concentrations. Table II shows the calculated lifetimes and trap energy levels from the experimental data. The energy level of the recombination-generation center or trap is at about $+4kT$ from the intrinsic Fermi level. This is in fair agreement with the temperature data shown in Fig. 14.

TABLE II

Unit No.	352-10	354-3	354-4	315A12	317A18
Type	<i>P+N</i>	<i>P+N</i>	<i>P+N</i>	<i>N+P</i>	<i>N+P</i>
ρ (Ω -cm)	2.4	2.4	2.4	21	21
C_0 surface cm^{-3}	5×10^{21}	5×10^{21}	5×10^{21}	10^{22}	3×10^{18}
τ_{p0} (μsec)	0.035	0.035	0.039	0.052	0.15
τ_{n0} (μsec)	0.65	0.69	0.69	0.075	0.012
$\cosh \epsilon_t$	6.3	5.3	6.0	2.2	5.5
$((E_t - E_i)/kT)_+$	4.0	3.9	3.9	1.3	3.7
$((E_t - E_i)/kT)_-$	-1.1	-0.9	-1.0	-1.6	-1.2

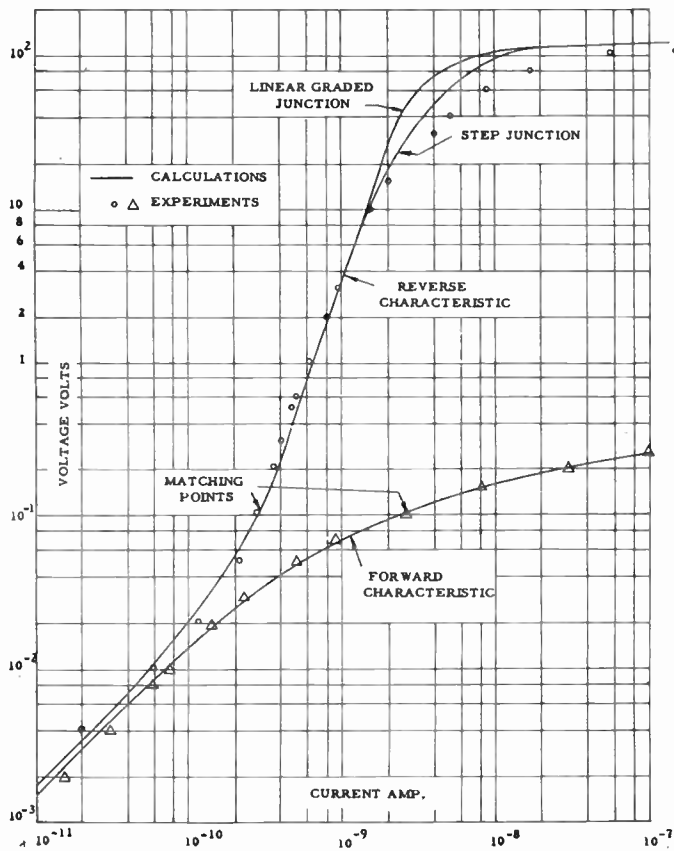


Fig. 12—Silicon *p-n* junction characteristics.

Under certain conditions, the surface leakage current may be important in silicon *p-n* junctions.^{16,16} If the surface charge is smaller than the fixed charge of the impurities, it can be shown that the surface current, produced by recombination-generation centers or surface states at the circumferential surface of the junction, will follow the same voltage dependence, namely, $V^{1/2}$ or $V^{1/3}$, under the large reverse bias condition.

In order to separate the recombination-generation current due to surface centers from that due to volume centers we have made experimental measurements on *p-n* junctions with extremely large and small ratios of junction area to circumference. The geometries are shown in Fig. 15. The results indicate that the surface current is negligible compared with bulk current for freshly etched junctions.

VII. CONCLUSION

In this paper we have used a model of the single level uniformly distributed Shockley-Read recombination-generation centers to explain the *p-n* junction characteristics. This model explains both the nonsaturable reverse characteristics and the apparent $\exp(qV/nkT)$ dependence of the forward current of typical silicon

¹⁶ M. Culter and H. M. Bath, "Surface leakage current in silicon fused junction diodes," *PROC. IRE*, vol. 45, pp. 39-43; January, 1957.

¹⁶ W. T. Eriksen, H. Stutz, and G. A. DeMars, "Excess surface currents on germanium and silicon diodes," *J. Appl. Phys.*, vol. 28, pp. 133-139; January, 1957.

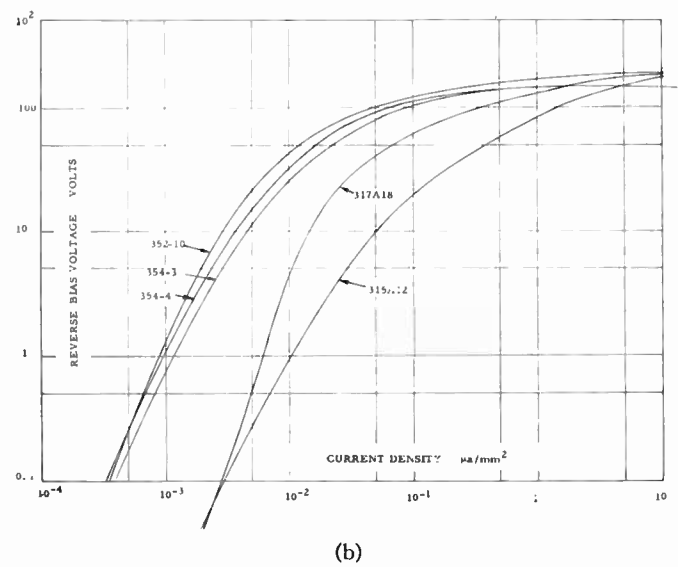
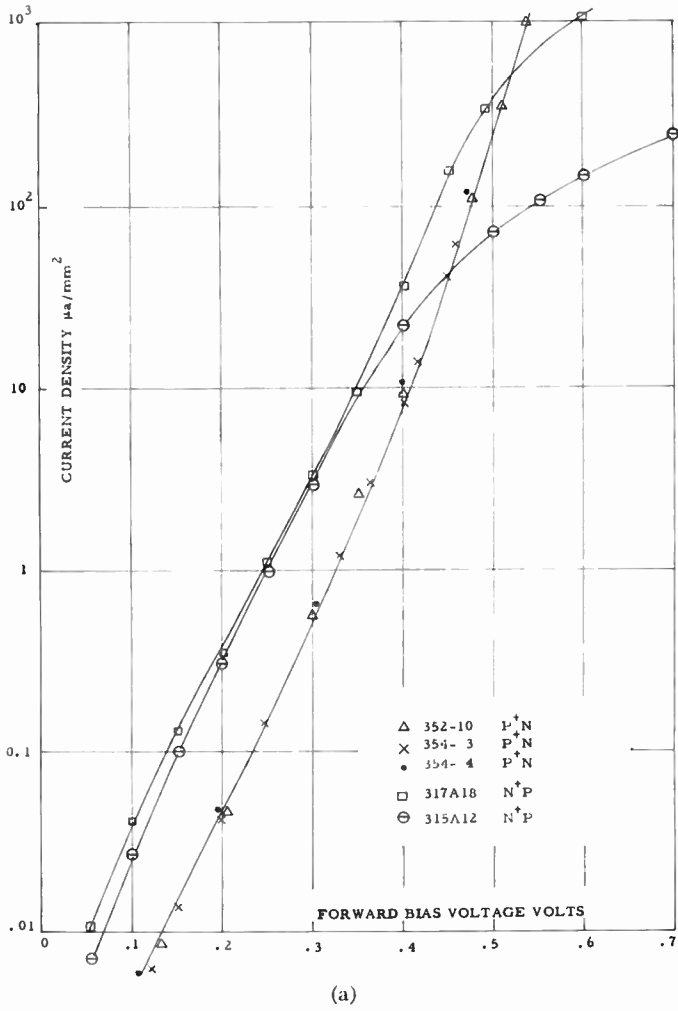


Fig. 13—(a) Experimental forward characteristics of silicon *p-n* junctions. (b) Experimental reverse characteristics of silicon *p-n* junctions.

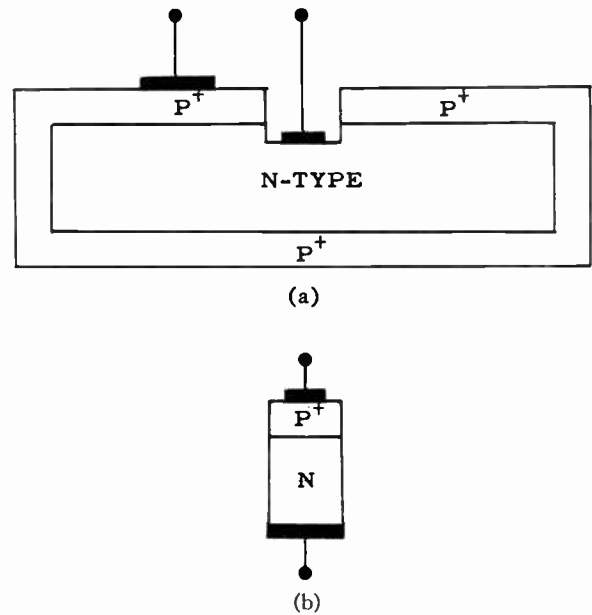
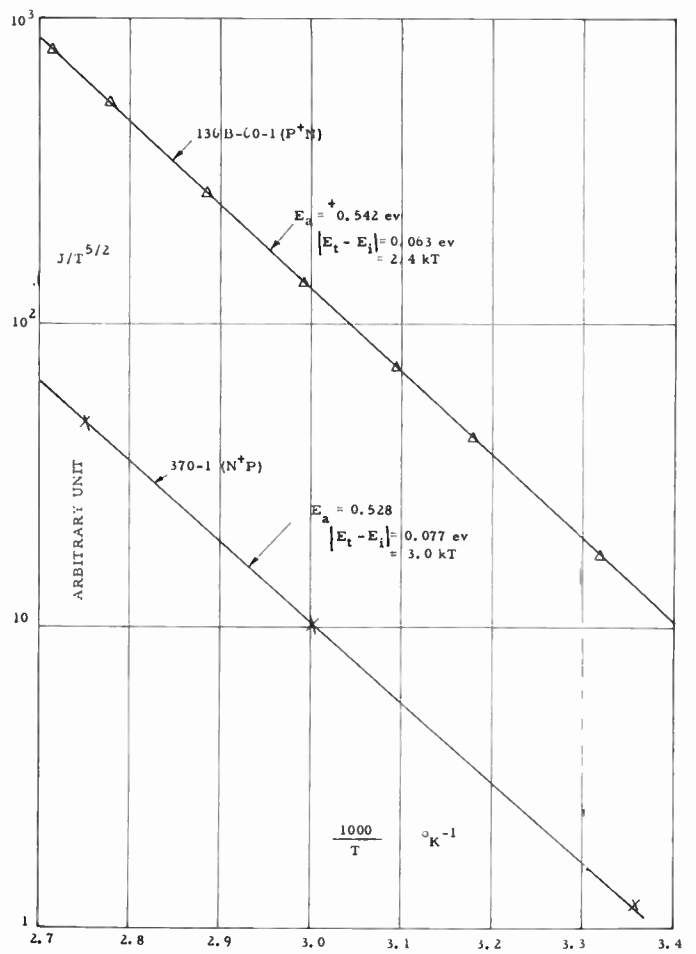


Fig. 15—Geometry for separating surface and bulk currents; (a) large junction area to circumference ratio geometry; (b) small junction area to circumference ratio geometry.

p-n junctions. The recombination of the carriers in the space charge layer also explains the variation of the current amplification factor of a silicon transistor at low emitter current density.

APPENDIX I

VARIATION OF THE QUASI-FERMI LEVELS IN THE SPACE CHARGE LAYER

The hole current can be written as

$$J_p = -q\mu_p p (d\phi_p/dx). \quad (32)$$

Substituting the expression for p from (19) into (32) the following differential equation can be obtained.

$$\frac{d}{dx} \exp \frac{q}{kT} (\phi_p - \Psi) - \frac{q}{kT} \left(\frac{d\Psi}{dx} \right) \exp \frac{q}{kT} (\phi_p - \Psi) = - \frac{J_p}{q\mu_p n_i}. \quad (33)$$

The solution of this equation is

$$\exp (q\phi_p/kT) = C - \int \exp \left(\frac{q}{kT} \Psi \right) \frac{J_p dx}{q\mu_p n_i}. \quad (34)$$

To calculate the variation of the quasi-Fermi potential across the space charge layer we use the linear approximation for the hole current density J_p , and for the electrostatic potential variation. Thus, for $-\frac{1}{2}W < x < \frac{1}{2}W$

$$J_p = J(1 - 2x/W) \quad (35)$$

and

$$\Psi = (\Psi_D - \delta\phi)x/W, \quad (36)$$

where Ψ_D is the built-in voltage, $\delta\phi$ is the applied voltage and W is the space charge layer width. By the evaluation of the integral of (34) with these approximations, the following relation is obtained for the quasi-Fermi potentials for holes at the edges of the space charge layer.

$$\begin{aligned} & \exp \frac{q}{kT} \left[\phi_p \left(\frac{W}{2} \right) + \phi_p \left(\frac{-W}{2} \right) \right] \\ & \cdot \sinh \frac{q}{2kT} \left[\phi_p \left(\frac{W}{2} \right) - \phi_p \left(\frac{-W}{2} \right) \right] \\ & = (JW/q\mu_p n_i) \left[\frac{\sinh(\theta_1/2)}{\theta_1} - \exp(-\theta_1/2) \right] / \theta_1 \end{aligned} \quad (37)$$

where $\theta_1 = (\Psi_D - \delta\phi)q/kT$.

For forward bias, θ_1 is small and (37) reduces to

$$\begin{aligned} & \exp \left[\phi_p \left(\frac{W}{2} \right) + \phi_p \left(\frac{-W}{2} \right) \right] \frac{q}{2kT} \\ & \cdot \sinh \left[\phi_p \left(\frac{W}{2} \right) - \phi_p \left(\frac{-W}{2} \right) \right] \frac{q}{2kT} = JW/2q\mu_p n_i. \end{aligned} \quad (38)$$

Thus, for a forward current of $J = 2$ amp/cm², $W = 10^{-6}$ cm and $\mu_p = 500$ for Si, the maximum drop of the quasi-Fermi potential for holes is

$$\sinh q\delta\phi_p/2kT = 0.4 \exp - \left[\phi_p \left(\frac{W}{2} \right) \frac{q}{2kT} \right].$$

The exponential factor on the right-hand side cannot be more than 1. This is easily seen from Fig. 5 if the reference potential is at $(\frac{1}{2})[\phi_p(x) + \phi_n(x)]_{x=0}$ as was implied in (36). In addition, a current less than J should be used as shown in Fig. 5. Thus the upper limit of the drop of the quasi-Fermi level in the space charge layer is about (kT/q) and is indeed very small.

For the large reverse-bias case, $\theta_1 > 5$, the situation is quite different. Eq. (37) can be approximated by

$$\begin{aligned} & \sinh \left[\phi_p \left(\frac{W}{2} \right) - \phi_p \left(\frac{-W}{2} \right) \right] \frac{q}{2kT} \\ & = \exp \left\{ - \left[\phi_p \left(\frac{W}{2} \right) + \phi_p \left(\frac{-W}{2} \right) \right] \frac{q}{2kT} \right\} \\ & \cdot \left(\frac{JW}{q\mu_p n_i} \right) \frac{e^{1/2\theta_1}}{\theta_1^2}. \end{aligned} \quad (39)$$

Thus, for $J = 10^{-6}$ amp/cm², $W = 10^{-4}$ cm and $\theta_1 = 100$, the drop of the quasi-Fermi potential is

$$\sinh (q\delta\phi_p/2kT) = \exp \left[80.7 - \phi_p \left(\frac{W}{2} \right) q/2kT \right].$$

By successive approximation it can be shown that the drop of the quasi-Fermi potential for holes is approximately equal to the applied voltage as indicated in Fig. 4.

For small bias, θ_1 is equal to the built-in voltage. For $\theta_1 = 20$, $J = 10^{-8}$ amp/cm², and $W = 10^{-5}$ cm the drop of the quasi-Fermi potential for holes is approximately

$$\sinh \delta\phi_p q/2kT = \exp (-12.5 - \delta\phi q/kT).$$

Thus the drop is appreciable only when the reverse-bias is greater than about $12.5kT/q$.

APPENDIX II

AVALANCHE MULTIPLICATION OF THE GENERATED CARRIERS IN THE SPACE CHARGE LAYER

Suppose that the *p-n* junction shown in Fig. 16 is biased in the reverse direction. Hole current density per unit area $J_p(x)$ flows toward the left, and electron current density per unit area $J_n(x)$ flows toward the right. There is also a net steady-state generation of the hole-electron pairs in the space charge region of U per unit volume per unit time from the Shockley-Read-Hall generation-

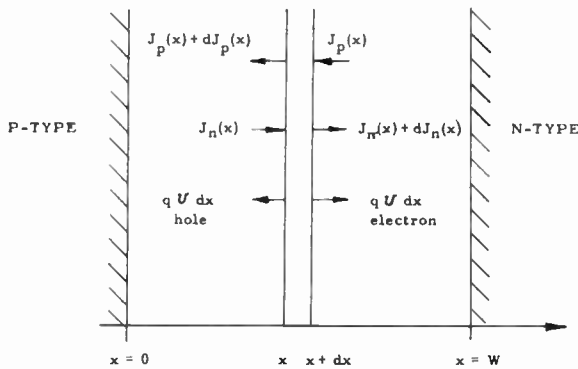


Fig. 16—Avalanche multiplication of electron and hole currents in the space charge layer of a reverse biased *p-n* junction.

recombination centers. We define, as done by McKay and Miller¹⁷ the ionization coefficients as follows:

α = no. of electron-hole pairs produced per cm travel of an electron.

β = no. of electron-hole pairs produced per cm travel of a hole.

We assume that α and β are functions of the local electric field only and neglect the past history of the carriers. We also neglect the space charge effect or the interaction between the carriers. The change of electron current in dx per unit area is

$$dJ_n(x) = \alpha J_n(x)dx + \beta J_p(x)dx + qUdx, \quad (40)$$

where the first term on the right comes from the multiplication of the electron current going into dx from the side x , and the second term comes from the electrons produced by holes going into dx from the side $x+dx$. Similarly, the change of the hole current in dx per unit area is

$$-dJ_p(x) = \alpha J_n(x)dx + \beta J_p(x)dx + qUdx, \quad (41)$$

and the sum of the two incremental currents satisfies the condition that the total current is space constant, namely

$$J = J_p(x) + J_n(x) = \text{independent of position.} \quad (42)$$

To solve the two simultaneous differential equations we use the following boundary conditions. At $x=0$, $J_n = J_{n0}$ and at $x=W$, $J_p = J_{p0}$. Substituting (42) into (40) and (41) the electron and the hole current satisfies the following equations:

$$dJ_n(x)/dx = (\alpha - \beta)J_n(x) + \beta J + qU \quad (43)$$

and

$$dJ_p(x)/dx = (\alpha - \beta)J_p(x) - \alpha J - qU. \quad (44)$$

The solutions are

$$J_n(x) = e^{-\int^x (\alpha - \beta) dx} \cdot \int_0^x (\beta J + qU) e^{\int^x (\alpha - \beta) dx} dx + J_{n0} \quad (45)$$

and

$$J_p(x) = e^{-\int^x (\alpha - \beta) dx} \int_W^x (\alpha J + qU) e^{\int^x (\alpha - \beta) dx} dx + J_{p0}. \quad (46)$$

Thus, the total current is

$$J = J_p(x) + J_n(x) = J_{p0} + J_{n0} + e^{-\int^x (\alpha - \beta) dx} \int_0^W qU e^{\int^x (\alpha - \beta) dx} dx = \frac{J_{p0} + J_{n0} + \int_0^W qU e^{\int^x (\alpha - \beta) dx} dx}{1 - \int_0^x \beta e^{\int^x (\alpha - \beta) dx} dx - \int_x^W \alpha e^{\int^x (\alpha - \beta) dx} dx}. \quad (47)$$

For $\alpha = \beta$, J reduces to

$$J = \frac{J_{p0} + J_{n0} + \int_0^W qU dx}{1 - \int_0^W \alpha dx} = M(J_{p0} + J_{n0} + \int_0^W qU dx), \quad (48)$$

where M is the current multiplication factor given by

$$M = \left(1 - \int_0^W \alpha dx\right)^{-1}.$$

Eq. (48) indicates that for $\alpha = \beta$ the generated current in the space charge layer, $\int qU dx$, acts as if it is injected into the layer as far as avalanche multiplication is concerned.

APPENDIX III

ACTIVATION ENERGY OF THE TRAPS

The thermal activation energy of the traps is obtained from the slope of a plot of the log of the reverse current as a function of the reciprocal of temperature at a constant reverse-bias.

Consider the range of $-\theta > 5$ where θ is the normalized applied bias $(\phi_p - \phi_n)q/kT$. The function $f(b)$ for this case can be approximated by $(\log 2b)/b$ and the recombination-generation current can be written as

$$\log [J_{r0}/J_0(kT)^{5/2}] = \log \left[\frac{n_i}{\theta(kT)^{5/2} \cosh \left(\frac{E_t - E_i}{kT} + \frac{1}{2} \ln \frac{\tau_{p0}}{\tau_{n0}} \right)} \right]. \quad (49)$$

Since n_i is proportional to $T^{3/2} \exp(-E_{g0}/2kT)$ and $b > 10$ for the restriction imposed on the reverse-bias, the activation energy can be obtained by differentiating (49) and is

¹⁷ K. G. McKay, "Avalanche breakdown in silicon," *Phys. Rev.*, vol. 94, pp. 877-884; May 15, 1954.

S. L. Miller, "Ionization rates for holes and electrons in silicon," *Phys. Rev.*, vol. 105, pp. 1246-1249; February 15, 1957.

$$E_a = -\frac{1}{2} E_{g0} - (E_t - E_i) \cdot \tanh\left(\frac{E_t - E_i}{kT} + \ln \sqrt{\frac{\tau_{p0}}{\tau_{n0}}}\right), \quad (50)$$

where E_{g0} is the energy gap width at zero temperature. Thus for deep traps, $E_t \doteq E_i$ and the trap energy cannot be obtained exactly unless measurements are done at low temperatures. For shallow traps, accurate energy level can be obtained in the room temperature range.

If

$$\left(\frac{E_t - E_i}{kT} + \ln \sqrt{\frac{\tau_{p0}}{\tau_{n0}}}\right)$$

is greater than about 2, the last term of (50) reduces to the absolute value of $E_t - E_i$. The energy of the traps can be obtained from

$$\pm(E_t - E_i) = E_a + E_{g0}/2. \quad (51)$$

APPENDIX IV

CURRENTS OUTSIDE SPACE CHARGE LAYER

In this appendix we shall obtain the diffusion current flowing in the n region of a forward biased $P+N$ junction. The approach here is slightly different from that given in the text but is similar to that generally used in the literature.¹⁸ We take into consideration both the nonlinear recombination rate and the high-level boundary condition.

The assumptions of this analysis are:

1) The space charge due to the divergence of the electric field E is small compared with the fixed charge N due to the impurities. This assumption implies that $n = p + N$.

2) The imrefs are approximately constant in the transition region and their difference is only slightly less than the applied voltage.

The second assumption above is a very good one at not very large current densities. At very high current densities the ohmic resistance drop in the N region becomes important. This ohmic drop can be calculated from the total drop of the electron imref in this region,

namely, $J = qD_n N \text{ grad } \phi_n$, where J is the total current density. This correction of the voltage at the junction can then be made.

The boundary condition follows from the second assumption and may be written as

$$pn = n_i^2 \exp(\phi_p - \phi_n)q/kT = n_i^2 \exp(qV/kT), \quad (52)$$

where V is V (applied) $- \delta\phi_n$ and $\delta\phi_n$ is the electron imref drop in the N region.

We shall start from the following relations:

$$\begin{aligned} K\epsilon_0 \text{ div } E &= q(p - n + N)^{++},^{19} \\ J_p &= qD_p(qEp/kT - \text{grad } p), \\ J_n &= qD_n(qEn/kT + \text{grad } n), \\ \text{div } J_p &= -qU, \\ \text{div } J_n &= qU, \end{aligned} \quad (53)$$

where the notations are defined before.

For the one-dimension case with uniform doping in the n region the above equations can be reduced to

$$d^2p/dx^2 = (D_n + D_p)U/2D_pD_n \quad (54)$$

and

$$qE/kT = \frac{J - qD_p(b - 1)dp/dx}{qD_p[p(1 + b) + bN]}, \quad (55)$$

where $b = D_n/D_p$ differs from the same symbol used previously in the text. The recombination-generation rate from (6) becomes

$$U = (\tau_{p0} + \tau_{n0})^{-1} \left[p + N - p_0 - \frac{p_0(N - p_0) + n_i^2}{p + p_0} \right] \quad (56)$$

where

$$p_0 = \frac{\tau_{p0}n_1 + \tau_{n0}p_1 + \tau_{p0}N}{\tau_{p0} + \tau_{n0}}. \quad (57)$$

We shall use the following boundary conditions derived from our assumptions.

At $x=0$, the edge of the space charge layer on the n -region side

$$p(0)n(0) = n_i^2 \exp(qV/kT)$$

and

$$n(0) = p(0) + N$$

so that

$$p(0) = [\sqrt{1 + (4n_i^2/N^2) \exp(qV/kT)} - 1]N/2. \quad (58)$$

At $x = \infty$, $p(\infty) = p_n$ and let $\text{grad } p = 0$, then

$$\frac{qE(\infty)}{kT} = \frac{J}{qD_n[N + p_n(1 + b)/b]} \quad (59)$$

¹⁹ Contribution from the traps is neglected.

¹⁸ E. S. Rittner, "Extension of the theory of the junction transistor," *Phys. Rev.*, vol. 94, pp. 1161-1171; June 1, 1954.

T. Misawa, "A note on the extended theory of the junction transistor," *J. Phys. Soc. Japan*, vol. 11, pp. 728-739; July, 1956.

W. T. Read, Jr., "Theory of the swept intrinsic structure," *Bell Sys. Tech. J.*, vol. 35, pp. 1239-1284; November, 1956.

D. A. Kleinman, "The forward characteristic of the PIN diode," *Bell Sys. Tech. J.*, vol. 35, pp. 685-706; May, 1956.

K. B. Tolpygo, "Emission capability of an abrupt $p-n$ transition and its effect upon the conductivity of a semiconductor," *J. Tech. Physics*, vol. 1, pp. 287-305 (English translation, *Am. Inst. of Phys.*)

J. A. Swanson, "Diode theory in the light of hole injection," *J. Appl. Phys.*, vol. 25, pp. 314-323; March, 1954.

and

$$J_p(x) = \frac{J p_n}{(1+b)p_n + bN}. \quad (60)$$

The gradient of the hole density can now be solved. Eqs. (54) and (56) give

$$d^2p/dx^2 = (2L_0^2)^{-1} \left[p + N - p_0 - \frac{p_0(N - p_0) + n_i^2}{p + p_0} \right], \quad (61)$$

where

$$L_0^{-2} = (D_n^{-1} + D_p^{-1})(\tau_{p0} + \tau_{n0}). \quad (62)$$

Eq. (61) can be easily integrated to give

$$(dp/dx)^2 = L_0^{-2} \left[p^2/2 - p_n^2/2 + (N - p_0)(p - p_n) - (p_0(N - p_0) + n_i^2) \ln(p + p_0)/(p_n + p_0) \right]. \quad (63)$$

We are interested in the solution at $x=0$ since at this point the relation between the total current and the hole current can be written as

$$J = J_p(0) + J_{r0}, \quad (64)$$

if the electron current in the p region is neglected. Using these results we can deduce the following relations for the total current and the hole current at $x=0$.

$$J = \frac{J_{r0}[(1+b)p(0) + bN] - qD_n[2p(0) + N]dp(0)/dx}{b[p(0) + N]} \quad (65)$$

and

$$J_p(0) = \frac{J_{r0}p(0) - qbD_p[2p(0) + N]dp(0)/dx}{b[p(0) + N]}. \quad (66)$$

Thus, (58), (65), and (66) represent the complete solution.

The asymptotic forms of the above results will be considered. The regions to be considered are the low-level case $p(0) \leq N/10$, the medium-level case $p(0) \geq N$, and the high-level case $p(0) \geq 10N$.

1) Low-Level Case, $p(0) \leq N/10$

For this case the total current is given by

$$J = J_{r0} + qp_nL_{p0}\sqrt{(1+b^{-1})/2}[\exp(qV/kT) - 1]/\tau_{p0}$$

and

$$J_p(0) = qp_nL_{p0}\sqrt{(1+b^{-1})/2}[\exp(qV/kT) - 1]/\tau_{p0}$$

where $L_{p0} = \sqrt{D_p\tau_{p0}}$. The hole current varies exponentially with distance. However, the expression for the hole current at $x=0$ given above differs from the ordinary low-level relation by a factor $\sqrt{(1+b^{-1})/2}$. This comes from the difference of the assumption made. In the ordinary low-level theory it is assumed that not only the charge neutrality holds but the electric field is also zero everywhere outside the junction. The present assump-

tion of negligible charge due to the divergence of electric field is less restrictive than the usual one.

For a one ohm-cm material with 1-microsecond lifetime the maximum range of validity of the above quantities are listed below for germanium and silicon at room temperature.

	$J_p(0)_{\max}$ amp/cm ²	V_{\max} volts
Ge	0.16	0.15
Si	0.25	0.57

2) Medium-Level Case $p(0) \geq N$

For this case the current densities cannot be reduced to simple expressions. However, the hole gradient at $x=0$ can be written as

$$\text{grad } p(0) = -[p^2(0) + 2(N - p_0)p(0)]/\sqrt{2}L_0.$$

The electric fields can be obtained approximately as

$$qE(\infty)/kT = 3/(2bL_0)$$

and

$$qE(0)/kT = 1/(2L_0),$$

thus the electric field is relatively constant over the entire n region.

For a one ohm-cm material with 1-microsecond lifetime, the following list summarizes the minimum current density and minimum applied voltage for this range at room temperature.

	J_{\min} amp/cm ²	V_{\min} volts
Ge	2.9	0.18
Si	4.6	0.6

3) High-Level Case $p(0) \geq 10N$

For this case the boundary condition becomes

$$p(0) = n_i \exp(qV/2kT)$$

and the current densities are

$$J = J_{r0}(1+b)/b + \sqrt{2}qD_p p(0)/L_0$$

and

$$J_p(0) = J_{r0}/b + \sqrt{2}qD_p p(0)/L_0.$$

It has been shown in the text that for this case the recombination current in the space charge layer is negligible compared with the diffusion current. Thus the total current is essentially equal to the hole current at $x=0$, and varies as $\exp(qV/2kT)$. This region is at a much higher current density than the similar region considered for the recombination-generation current in the space charge layer.

We need to examine the electric field and its divergence at the boundaries to verify the validity of our assumptions. At the lowest applied voltage for this case of large bias the electric fields can be obtained by using (58) and (59).

$$qE(0)/kT = (1/\sqrt{2}L_0)$$

$$qE(\infty)/kT = (1/\sqrt{2}L_0) 2p(0)/bN.$$

Thus the electric field varies about a factor of 10 at least. The gradient of the electric field can be obtained by differentiating (55). At $x = \infty$, dE/dx is zero and at $x = 0$ the electric field is about

$$(q/kT)(dE/dx) = 1/2L_0^2$$

at the lowest injection limit. This corresponds to about 25 v/cm for a 1-microsecond lifetime material at room temperature. The quantity $(K\epsilon_0/q)dEdx$ can now be compared with $p-n+N$ from (53). Using the values given above we obtain

$$p - n + N \gg 7.6 \times 10^{10} \text{ cm}^{-3},$$

which is usually satisfied since N is of the order of 10^{15} cm^{-3} for silicon of a few ohm-cm resistivity.

We shall give again a list indicating the limiting values of current density and voltage for this range.

	J_{\min} amp/cm ²	V_{\min} volt
Ge	27	0.34
Si	43	0.75

ACKNOWLEDGMENT

The authors wish to acknowledge the helpful discussions with their colleagues at the Shockley Semiconductor Laboratory. The diffused silicon materials were prepared by D. Grunwald, and some of the data were taken by Dr. S. M. Fok and M. Asemissen.

(Note added in proof: The forward characteristics of germanium $p-n$ junctions at low temperatures have recently been investigated independently by M. Bernard using the same model. "Mesures in fonction de la temperature du Courant," *J. Electronics*, vol. 2, pp. 579-596; May, 1957.)

Digital Compensation for Control and Simulation*

JULIUS TOU†, SENIOR MEMBER, IRE

Summary—This paper describes a technique for improving the performance of digital feedback control systems and operational digital simulators by making use of the computer to perform information programming or data processing. The system stability can be improved and the system error can be reduced by digital programming of the input and error signals together with digital correction computations. This technique of digital compensation is illustrated by an example.

INTRODUCTION

AMONG the many performance criteria for feedback control systems, the stability and accuracy considerations are of primary importance. Considerable amount of work has been done for improving the performance of feedback control systems and a number of methods have been published in the literature. With the rapid advance of computer design techniques and their applications, there arose a new type of system for control and simulation which involves a digital computer. Such systems are often called digital control systems and operational digital simulators.

A typical digital control system or a channel of an operational digital simulator is shown in Fig. 1, which

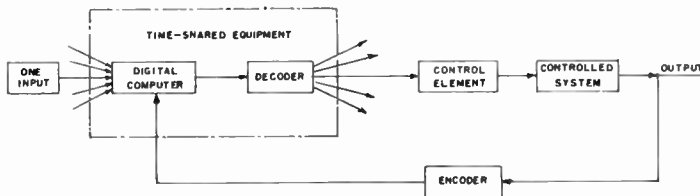


Fig. 1—A typical digital control system or a channel of an operational digital simulator.

consists of a digital computer, a decoder, an encoder and the control element and controlled system. The computer performs error detection and system compensation. The decoder converts signals in digital or sampled form into continuous form. The encoder converts continuous data into sampled form or digital code. The stability and accuracy of such control systems can be improved by designing a suitable program for the computer. The technique of digital programming compensation will be described in this paper.

One of the most powerful tools for analyzing and designing digital and sampled-data feedback control systems and simulators is the Z -transform method.^{1,2} Since this method of approach will be employed in this

* Original manuscript received by the IRE, August 13, 1956; revised manuscript received, June 11, 1957. This article is based upon the paper "High Accuracy Operational Digital Simulation" presented by the author at the first Natl. Simulation Conf., in Dallas, Tex., January, 1956.

† Purdue Univ., Lafayette, Ind. Formerly with Moore School of Elec. Eng., Univ. of Pennsylvania and the Philco Corp., Philadelphia, Pa.

¹ R. H. Barker, "The pulse transfer function and its application to sampling servo systems," *Proc. IEE*, vol. 99, pt. IV, pp. 302-317; December, 1952.

² J. R. Ragazzini and L. A. Zadeh, "The analysis of sampled-data systems," *AIEE Trans.*, vol. 71, pp. 225-232; November, 1952.

paper for the design of digital programs for system compensation, a brief review of the *Z*-transform method is given in the following section.

MATHEMATICAL BACKGROUND

A control system utilizing a computer or a digital control system is essentially a type of sampled-data control system in which the signals are in the form of some digital code. The basic component of sampled-data control systems is the sampler which converts a continuous signal into a train of amplitude-modulated narrow pulses occurring at the sampling instants as shown in Fig. 2. If the input to the sampler is $x(t)$, the output

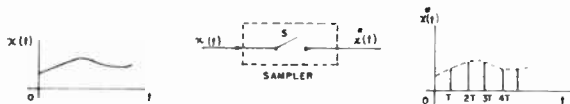


Fig. 2—Properties of an ideal sampler.

from the sampler is given by^{1,2}

$$x^*(t) = \sum_{n=-\infty}^{\infty} x(nT)\delta(t - nT). \tag{1}$$

Since $x(nT) = 0$ for $n < 0$,

$$x^*(t) = \sum_{n=0}^{\infty} x(nT)\delta(t - nT). \tag{2}$$

Taking the Laplace transform of (2),

$$X^*(s) = \sum_{n=0}^{\infty} x(nT)\epsilon^{-nTs}. \tag{3}$$

Substituting z for ϵ^{Ts} ,

$$X^*(s) \Big|_{s=(1/T)\ln z} \triangleq X(z) = \sum_{n=0}^{\infty} x(nT)z^{-n} \tag{4}$$

where

$$X(z) = Z\{x^*(t)\} \tag{5}$$

is defined as the *Z* transform of $x^*(t)$.

In a continuous system, Fig. 3(a), the output is given

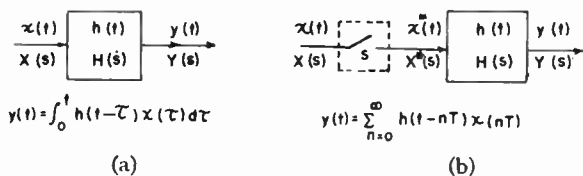


Fig. 3—Comparison of continuous and sampled-data system. (a) Continuous system (b) system with sampler

by the convolution integral

$$y(t) = \int_0^t g(t - \tau)x(\tau)d\tau \tag{6}$$

in which $x(t)$ is the output and $g(t)$ is the impulse response function of the system. In terms of the complex variable s , the output and the input are related by

$$Y(s) = G(s)X(s) \tag{7}$$

where $Y(s)$, $G(s)$ and $X(s)$ are the *L* transforms of $y(t)$, $g(t)$ and $x(t)$ respectively. With reference to Fig. 3(b), the output of an open-loop sampled-data system can be described by a convolution summation

$$y(t) = \sum_{n=0}^{\infty} g(t - nT)x(nT) \tag{8}$$

since the input to system $G(s)$ is a discrete function of time. At the sampling instant, mT ,

$$y(mT) = \sum_{n=0}^{\infty} g(mT - nT)x(nT). \tag{9}$$

The *L* transform of output $y(t)$ is

$$Y(s) = \int_0^{\infty} y(t)\epsilon^{-st}dt. \tag{10}$$

Substituting (8) into (10) and rearranging,

$$Y(s) = \sum_{n=0}^{\infty} x(nT)\epsilon^{-nTs} \int_0^{\infty} g(t - nT)\epsilon^{-(t-nT)s}dt. \tag{11}$$

Since

$$X^*(s) = \sum_{n=0}^{\infty} x(nT)\epsilon^{-nTs}$$

and

$$G(s) = \int_0^{\infty} g(t)\epsilon^{-st}dt,$$

eq. (11) becomes

$$Y(s) = G(s)X^*(s). \tag{12}$$

Eq. (12) for a sampled-data system bears a close resemblance to (7) for a continuous-data system. By definition,

$$Y(z) = Z\{y^*(t)\} = \sum_{m=0}^{\infty} y(mT)z^{-m}. \tag{13}$$

Substituting (9) into (13),

$$Y(z) = \sum_{m=0}^{\infty} \sum_{n=0}^{\infty} g(mT - nT)x(nT)z^{-m}. \tag{14}$$

Letting $m - n = k$, and rearranging,

$$Y(z) = \sum_{k=0}^{\infty} g(kT)z^{-k} \sum_{n=0}^{\infty} x(nT)z^{-n} \tag{15}$$

Since

$$X(z) = \sum_{n=0}^{\infty} x(nT)z^{-n}$$

$$G(z) = \sum_{k=0}^{\infty} g(kT)z^{-k},$$

$$Y(z) = G(z)X(z). \tag{16}$$

$G(z)$ is sometimes called the pulsed transfer function.^{1,2} In direct analogy with the L transform, the inverse Z transform of $G(z)$ is given by^{1,3}

$$g(kT) = \frac{1}{2\pi j} \oint_C G(z) z^{k-1} dz \quad (17)$$

in which the contour of integration, C , is a unit circle with center at the origin of the z plane. From the definition of $G(z)$, it can easily be derived that

$$Z\{g^*(t - T)\} = z^{-1}G(z) \quad (18)$$

and, in general,

$$Z\{g^*(t - nT)\} = z^{-n}G(z). \quad (19)$$

Eqs. (18) and (19) describe the shifting theorem of the Z transform.

ERROR COMPENSATION BY DIGITAL PROGRAMMING

The block diagram of a typical digital feedback control system is shown in Fig. 4, in which $r^*(t)$ is the input

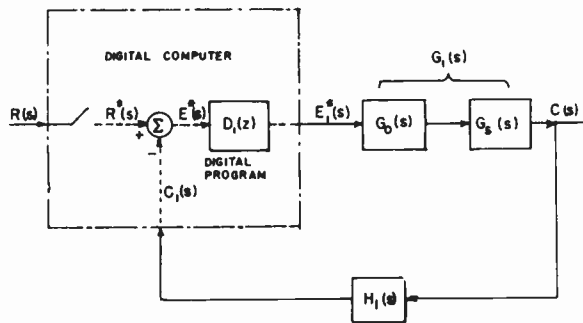


Fig. 4—A typical instrument channel of an operational digital simulator.

in sampled form; $c(t)$, the output; $e^*(t)$ the actuating error from the digital subtractor; $e_1^*(t)$, the processed error signal; $G_1(s)$, the transfer function of the decoder, the control elements and the controlled system; $H_1(s)$, the transfer function of the control elements in the feedback path and the encoder; and $D_1(z)$, the required digital programming function for error compensation. In Fig. 4, the asterisk refers to sampled-data computation, and the functions of (s) are the L transforms; for instance, $R^*(s) = L\{r^*(t)\}$. The system performance can be derived from the system over-all transfer function which is defined as the ratio of system output to system input.

Referring to Fig. 4,

$$E^*(s) = R^*(s) - C_1^*(s) \quad (20)$$

$$E_1^*(s) = D_1^*(s)E^*(s) \quad (21)$$

and

$$C_1^*(s) = \overline{G_1 H_1}^*(s)E_1^*(s) \quad (22)$$

where $D_1^*(s)$ equals $D_1(z)$ and $\overline{G_1 H_1}^*(s)$ equals $\overline{G_1 H_1}(z)$ with $z = e^{Ts}$, and $\overline{G_1 H_1}(z)$ is the Z transform of $G_1(s)H_1(s)$. From (20) and (22),

$$E^*(s) = R^*(s) - \overline{G_1 H_1}^*(s)E_1^*(s). \quad (23)$$

Eliminating $E^*(s)$ from (21) and (23), and simplifying,

$$E_1^*(s) = \frac{D_1^*(s)R^*(s)}{1 + D_1^*(s)\overline{G_1 H_1}^*(s)} \quad (24)$$

and

$$C(s) = \frac{D_1^*(s)G_1(s)}{1 + D_1^*(s)\overline{G_1 H_1}^*(s)} R^*(s) \quad (25)$$

since

$$C(s) = G_1(s)E_1^*(s). \quad (26)$$

For brevity, (25) can be written as

$$C(s) = G(s)R^*(s) \quad (27)$$

where

$$G(s) = \frac{D_1^*(s)G_1(s)}{1 + D_1^*(s)\overline{G_1 H_1}^*(s)} \quad (28)$$

is the over-all transfer function of the system. In terms of Z transforms,

$$C(z) = G(z)R(z) \quad (29)$$

and $G(z) = Z\{G(s)\}$ is the over-all pulsed transfer function of the system and is given by

$$G(z) = \frac{D_1(z)G_1(z)}{1 + D_1(z)\overline{G_1 H_1}(z)}. \quad (30)$$

Since the system error is equal to the difference between the input and the output, $e(t) = r(t) - c(t)$, a system is said to be of high accuracy if

$$c(t) = r(t) \quad (31)$$

or

$$C(s) = R(s), \quad (32)$$

i.e., the system over-all transfer function is equal to unity. Unfortunately, this condition can hardly be realized in a conventional continuous-data servo system. However, in a digital or sampled-data feedback control system, it is not difficult to make the output equal the input at the sampling instants; *i.e.*, the system error is made zero at the sampling instants. This can be done if the over-all pulsed transfer function of the system is made equal to unity by designing a suitable programming function for the computer. Thus, if the sampling rate is kept high, an almost perfect control system can be obtained. Since the over-all pulsed transfer function of the system shown in Fig. 4 is given by (30), the system error at sampling instants is zero, if

$$\frac{D_1(z)G_1(z)}{1 + D_1(z)\overline{G_1 H_1}(z)} = 1. \quad (33)$$

³ Class notes, Course EE 608, Moore School of Elec. Eng., Univ. of Penna., 1956.

In (33), both $G_1(z)$ and $\overline{G_1 H_1}(z)$ are known since $G_1(s)$ and $H_1(s)$ are given. The only unknown function is $D_1(z)$, which is required for realizing the condition for zero system error at sampling instants. From (33) it follows that

$$D_1(z) = \frac{1}{G_1(z) - \overline{G_1 H_1}(z)} \quad (34)$$

is the desired digital programming function for system-error compensation. Since both $G_1(z)$ and $\overline{G_1 H_1}(z)$ are ratios of two polynomials^{1,2} in z^{-1} , the programming function, $D_1(z)$, can be described by a ratio of two polynomials in z^{-1} also. That is, in Fig. 4,

$$D_1(z) = \frac{E_1(z)}{E(z)} = \frac{\alpha_0 + \alpha_1 z^{-1} + \alpha_2 z^{-2} + \dots + \alpha_m z^{-m}}{\beta_0 + \beta_1 z^{-1} + \beta_2 z^{-2} + \dots + \beta_n z^{-n}}. \quad (35)$$

The processed signal $e_1^*(t) = Z^{-1}\{E_1(z)\}$ is evaluated by the digital computer. Rearranging (35),

$$(\alpha_0 + \alpha_1 z^{-1} + \alpha_2 z^{-2} + \dots + \alpha_m z^{-m})E(z) = (\beta_0 + \beta_1 z^{-1} + \beta_2 z^{-2} + \dots + \beta_n z^{-n})E_1(z). \quad (36)$$

Making use of (19),

$$\begin{aligned} \alpha_0 e^*(t) + \alpha_1 e^*(t-T) + \alpha_2 e^*(t-2T) + \dots + \alpha_m e^*(t-mT) \\ = \beta_0 e_1^*(t) + \beta_1 e_1^*(t-T) + \beta_2 e_1^*(t-2T) + \dots \\ + \beta_n e_1^*(t-nT) \end{aligned} \quad (37)$$

where T is the sampling period of the system. Rearranging (37),

$$e_1^*(t) = \frac{1}{\beta_0} \left[\sum_{k=0}^m \alpha_k e^*(t-kT) - \sum_{k=1}^n \beta_k e_1^*(t-kT) \right]. \quad (38)$$

This is essentially a form of numerical quadrature formula^{4,5,6}, which is often used in digital real time simulation. The reader is referred to footnotes 4, 5, and 6 for the manipulation and application of numerical quadrature formula. The computation involved in (38) can easily be performed by a digital computer.

If it is desired to make the output of the system follow the input according to some prescribed instructions other than the requirement of zero system error and one-to-one follow-up as described in the above paragraphs, such systems can also be realized by the digital programming technique.⁷ The specified instruction can be expressed in a function of z . For instance, if it is desired to make the output and the input be related by $C(z) = G_d(z)R(z)$ with $G_d(z)$ specified, then for the system shown in Fig. 4, the required digital program for realizing this condition is given by

⁴ H. M. Gurk and M. Rubinoff, "Numerical solution of differential equations," *Proc. Eascon*, pp. 58-64; December, 1954.

⁵ L. Collatz, "Numerische Behandlung von Differentialgleichungen," Springer-Verlag, Berlin; 1951.

⁶ J. B. Scarborough, "Numerical Mathematical Analysis," John Hopkins Press; Baltimore, Md., 1950.

⁷ A. R. Bergen and J. R. Ragazzini, "Sampled-data processing techniques for feedback control systems," *AIEE Trans.*, vol. 73, pp. 236-246; November, 1954.

$$D_1(z) = \frac{G_d(z)}{G_1(z) - \overline{G_d(z)G_1 H_1}(z)}. \quad (39)$$

GENERALIZED DIGITAL COMPENSATION

In a digital feedback control system, three quantities—the input, the error, and the output—can generally be programmed in the digital computer, as shown in Fig. 5, in which

$$C(s) = G_1(s)E_1^*(s), \quad (40)$$

$$E(s) = R_1^*(s) - C_2^*(s), \quad (41)$$

$$C_2^*(s) = D_2^*(s)C_1^*(s), \quad (42)$$

$$C_1^*(s) = \overline{G_1 H_1}^*(s)E_1^*(s), \quad (43)$$

$$E_1^*(s) = D_1^*(s)E^*(s) + D_3^*(s)R_1^*(s). \quad (44)$$

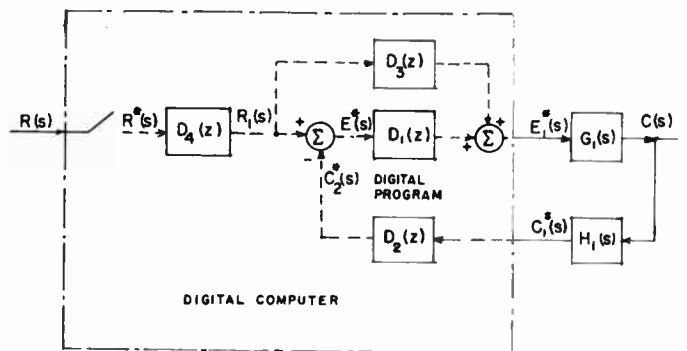


Fig. 5—Generalized digital compensation.

Solving for $E^*(s)$ from (41), (42), (43) and (44),

$$E^*(s) = \frac{1 - D_2^*(s)D_3^*(s)\overline{G_1 H_1}^*(s)}{1 + D_1^*(s)D_2^*(s)\overline{G_1 H_1}^*(s)} R_1^*(s). \quad (45)$$

Substituting (45) into (44), and simplifying,

$$E_1^*(s) = \frac{D_1^*(s) + D_3^*(s)}{1 + D_1^*(s)D_2^*(s)\overline{G_1 H_1}^*(s)} R_1^*(s). \quad (46)$$

From (40) and (46), it is obtained that

$$C(s) = G(s)R_1^*(s) \quad (47)$$

where

$$G(s) = \frac{G_1(s)[D_1^*(s) + D_3^*(s)]}{1 + D_1^*(s)D_2^*(s)\overline{G_1 H_1}^*(s)}. \quad (48)$$

Taking the Z transform of (47),

$$C(z) = G(z)R_1(z) \quad (49)$$

in which

$$G(z) = Z\{G(s)\} = \frac{G_1(z)[D_1(z) + D_3(z)]}{1 + D_1(z)D_2(z)\overline{G_1 H_1}(z)}. \quad (50)$$

From (49), if the system transfer function $G(z)$ is equal to unity, $C(z) = R_1(z)$, and $C^*(t) = r_1^*(t)$. Thus, the system error at sampling instants is null, if

$$G(z) = \frac{G_1(z)D_1(z) + D_3(z)}{1 + D_1(z)D_2(z)\overline{G_1H_1}(z)} = 1. \quad (51)$$

Solving for $D_3(z)$ from (51),

$$D_3(z) = \frac{1 + D_1(z)D_2(z)\overline{G_1H_1}(z)}{G_1(z)} - D_1(z). \quad (52)$$

From the expression of $D_3(z)$ in (52), it is clear that a quadrature formula for $e_3^*(t)$, in terms of the past information of the output of $D_3(z)$ and the present and past information of the input to $D_3(z)$, can readily be derived for the necessary computation, if $D_3(z)$ is a physically realizable program.

A digital programming function, $D_k(z)$, is physically realizable^{8,9} if the output of the network for the program does not depend upon the future information of the input signal, or mathematically, if the digital program can be written as

$$D_k(z) = \frac{\sum_{\mu=0}^m \alpha_{\mu} z^{-\mu}}{\beta_0 + \sum_{\nu=1}^n \beta_{\nu} z^{-\nu}} \quad (53)$$

where $\beta_0 \neq 0$; i.e., the expression of $D_k(z)$ about the point at infinity must contain no positive powers of z . Generally speaking, if the order of the numerator of $G_1(z)$ in z is not equal to that of the denominator, the programming function $D_3(z)$ becomes physically unrealizable. However, this difficulty could be overcome by choosing proper functions for $D_1(z)$, $D_2(z)$ and $H_1(s)$ or by introducing a fourth programming function $D_4(z)$ so as to make $D_3(z)$ physically realizable.

The characteristic equation of the system is given by

$$1 + D_1(z)D_2(z)\overline{G_1H_1}(z) = 0. \quad (54)$$

To secure system stability,^{1,2,10} the digital programming function, $D_1(z) D_2(z)$, should be designed in such a way that all the roots of the characteristic equation lie inside the unit circle of the z plane or that (54) should satisfy the Schur-Cohn Criterion.⁹ The product $D_1(z) D_2(z)$ can be considered as the system stabilizing function. After the programs $D_1(z)$ and $D_2(z)$ are determined from system stability and transient performance considerations, the programming function, $D_3(z)$, is derived from (52) for zero system error. Since $D_3(z)$ is located outside of the control loop, it does not affect the stability of the system. $D_3(z)$ is the system-error reduction function.

⁸ J. M. Salzer, "Frequency analysis of digital computers in real time," *Proc. IRE*, vol. 42, pp. 457-466; February, 1954.
⁹ M. Marden, "The Geometry of the Zeros of a Polynomial in a Complex Variable," Amer. Math. Soc., New York, N. Y., chap. 10; 1949.
¹⁰ J. Tou, "Stability criterion for digital feedback control systems," *Proc. NEC*, vol. 12, pp. 336-346; October, 1956.

ILLUSTRATIVE EXAMPLE

To illustrate the principle of digital compensation for control and simulation as described above, a simple control system shown in Fig. 6 is considered. It is assumed that the motor time constant is 0.1 second and the controller and the controlled system can be described by transfer function

$$G_s(s) = \frac{40}{s(1 + 0.1s)} \quad (55)$$

and that sampling period $T=0.2$ second. With the decoder represented by transfer function $(1 - \epsilon^{-Ts})/s$ and the encoder by conversion factor $K_e = 1$, the system can be described by the block diagram of Fig. 7, in which the digital programming functions $D_1(z)$, $D_2(z)$, $D_3(z)$ and $D_4(z)$ are introduced for improving system stability and reducing system error.

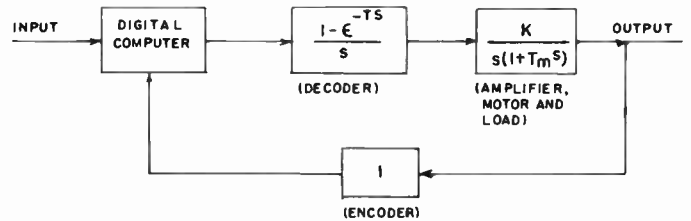


Fig. 6—Illustrative example.

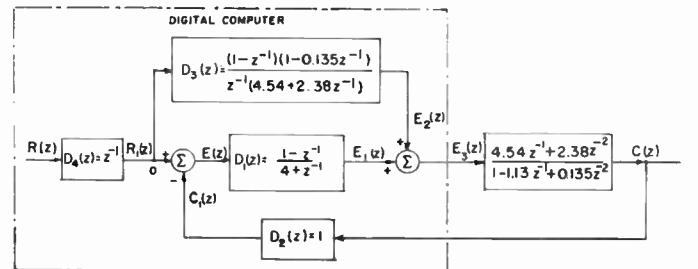


Fig. 7—System with digital compensation.

For the original uncompensated system, the open-loop transfer function is

$$A(s) = G_1(s)H_1(s) = \frac{40(1 - \epsilon^{-0.2s})}{s^2(1 + 0.1s)}. \quad (56)$$

The Z transform of (56) is

$$A(z) = \frac{4.54z^{-1} + 2.38z^{-2}}{(1 - z^{-1})(1 - 0.135z^{-1})}. \quad (57)$$

The system characteristic equation is given by

$$z^2 + 3.405z + 2.515 = 0 \quad (58)$$

which has two roots at $z_1 = -1.082$ and $z_2 = -2.322$. Evidently the original system is unstable. To meet the stability requirement, a digital program

$$D_1(z)D_2(z) = \frac{1 - z^{-1}}{4 + z^{-1}} \quad (59)$$

is introduced. Eq. (59) is derived according to the procedures outlined in footnote 10. The open-loop transfer function for the compensated system is

$$A_c(z) = D_1(z)D_2(z)A(z) = \frac{4.54z^{-1} + 2.38z^{-2}}{(4 + z^{-1})(1 - 0.135z^{-1})} \quad (60)$$

The roots of the characteristic equation for the compensated system,

$$z^2 + 1.25z + 0.561 = 0, \quad (61)$$

are $z = -0.625 \pm j0.413$, which indicates a stable system.

To meet the requirement of zero system-error at sampling instants, digital program $D_3(z)$ is introduced. If (59) is split into

$$D_3(z) = 1 \quad \text{and} \quad D_1(z) = \frac{1 - z^{-1}}{4 + z^{-1}} \quad (62)$$

then from (52),

$$D_3(z) = \frac{(1 - z^{-1})(1 - 0.135z^{-1})}{z^{-1}(4.54 + 2.38z^{-1})} \quad (63)$$

Unfortunately the digital program of (63) is not physically realizable. In order to realize (63) a digital program $D_4(z) = z^{-1}$ is introduced as shown in Fig. 7. If the take-off point a of Fig. 7 is moved ahead of element $D_4(z)$, Fig. 8, the digital program for the feed-forward element becomes

$$D_3'(z) = D_3(z)D_4(z) = \frac{(1 - z^{-1})(1 - 0.135z^{-1})}{4.54 + 2.38z^{-1}} \quad (64)$$

which is physically realizable. However, this artifice for realizing the feed-forward element has one drawback. The input signal is delayed by one sampling period and the system error referred to the delayed input is zero at sampling instants. But by sampling the signals

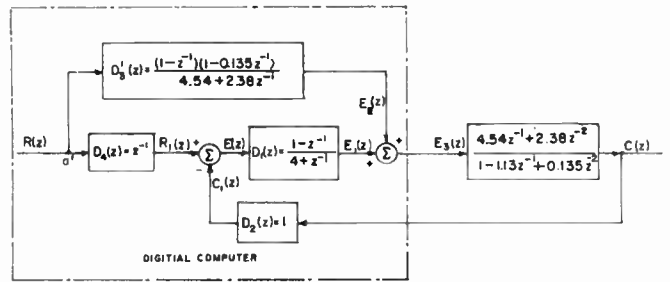


Fig. 8—Modified form of Fig. 7.

at a higher rate, the output could be made to follow the input closely. When the input data are processed in the computer before they are applied to the control system, the digital program $D_3(z)$, could be realized by arranging a suitable take-off point for the feed-forward element. From (62) and (64) it follows that the required quadrature formulas are

$$e_1^*(t) = \frac{1}{4} [e^*(t) - e^*(t - T) - e_1^*(t - T)] \quad (65)$$

and

$$e_2^*(t) = \frac{1}{4.54} [r^*(t) - 1.135r^*(t - T) + 0.135r^*(t - 2T) - 2.38e_2^*(t - T)] \quad (66)$$

respectively.

ACKNOWLEDGMENT

The author wishes to acknowledge with thanks the assistance given to him by his colleagues in the Moore School of Electrical Engineering of the University of Pennsylvania. In particular to Dr. Morris Rubinoff, he expresses his deep appreciation for many valuable suggestions. Also he wishes to thank Dr. J. G. Brainerd, the Director of the Moore School, for his encouragement and inspiration.



Posicast Control of Damped Oscillatory Systems*

OTTO J. M. SMITH†, SENIOR MEMBER, IRE

Summary—A novel method is presented for producing dead-beat response in a lightly-damped oscillatory feedback system. Complete transient response times of the order of a fraction of the natural oscillatory period can be obtained. Excellent waveshape reproduction is achieved through a linear phase lag with frequency. The method consists of exciting several transient oscillations, at closely spaced times, with magnitudes and phases so adjusted that the resultant sum of the transient oscillation phasors is zero. The steady-state output is the arithmetic sum of the excitation magnitudes.

When a step input transient is divided into two spaced excitations, one-half cycle response is obtainable. When the input transient is divided into three excitations, one-fourth period or faster transient times are realizable, depending upon the available dynamic range or signal-to-noise ratio. The principle of design is to adjust a system to the maximum possible resonant frequency, independent of the damping factor, but stable, and then to apply the Posicast control to completely remove the oscillatory component in the output. In an electrical feedback control system, the additional hardware consists of one or two artificial transmission lines.

INTRODUCTION

THE PROBLEM in a feedback control system is to change the stored energy of an object from one value to another without subsequent oscillations or overshoot. This method can be easily demonstrated by its application to the problem of changing the at-rest position of an undamped pendulum. The system input is the point of suspension. In Fig. 1, (a) is the initial position; (b) is the condition immediately after the input step has been broken into two parts and only half of the desired change has been applied to the support; (c) is the condition after one-half cycle of the natural transient period of the pendulum. At this instant, the support is suddenly moved until it is directly over the bob and (d) shows the final position. The scheduling of the motion of the support is the transference of an equalizer, which compensates for the resonant frequency of the load by introducing attenuation at the resonant frequency. This is, however, a time-domain synthesis yielding a linear time-domain equalizer.

The electrical analog of the pendulum is a capacitive load with inductance and resistance in series between the supply and the load. The input is voltage across the series RLC, and the output is voltage across the capacitor. The step response for an input voltage of magnitude A is shown in Fig. 2.

If after time $T_n/2$, the input voltage has added to it a second step of magnitude B (determined from Fig. 2), so that the sum is $(A + B)$, then at this instant the current will suddenly drop to zero, since the voltage across

* Original manuscript received by the IRE, November 12, 1956; revised manuscript received, June 12, 1957.
 † Elec. Eng. Div., Univ. of Calif., Berkeley, Calif.

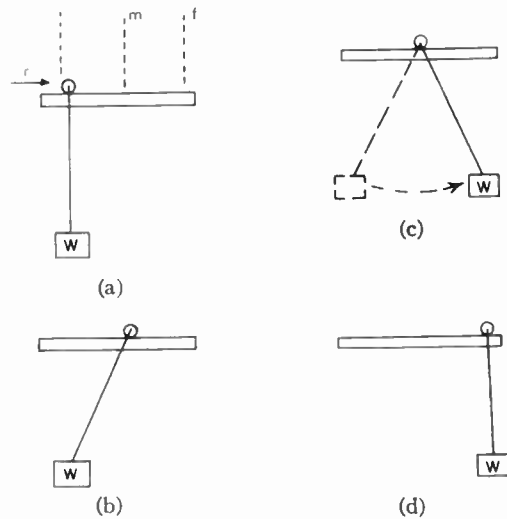


Fig. 1.

the condenser is also $(A + B)$. The steady-state condition has been suddenly achieved, and there will be no further transient.

The final value is reached just as the velocity goes to zero. This is what happens when a fisherman drops his fly in the water at the maximum-position and zero-velocity instant. Hence the descriptive name *positive-cast* or Posicast for this kind of system.

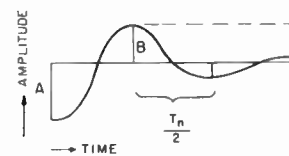


Fig. 2.

The input command was broken into two parts; the first part was applied immediately, and the second part was delayed until after one-half period of the natural transient, $T/2$. Fig. 2 shows the relative magnitudes of the two excitation functions. Amplitude A is proportional to the first excitation function, amplitude B is the magnitude of the second excitation function, and $A + B$ is the amplitude of the input driving function and of the output of the system. Mathematically, the Laplace transform of the control function is

$$[k_a + (1 - k_a)e^{-sT/2}]. \tag{1}$$

$T/2$ is the delay between the initial and the final pulse. The ratio of the first to the second pulse is a measure of the attenuation of the oscillation envelope during the transient time.

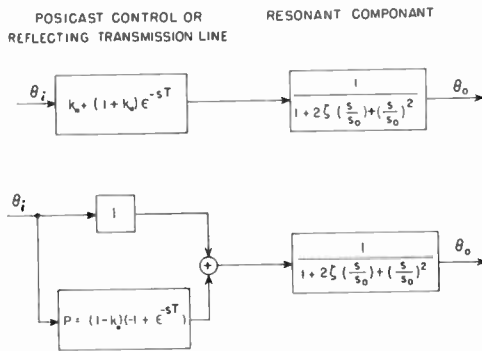


Fig. 3.

$$k = \left(\frac{k_a}{1 - k_a} \right) = \exp \left(\frac{\zeta \omega_n T_r}{\sqrt{1 - \zeta^2}} \right). \quad (2)$$

T_r is the over-all response or transient time. In this special case of half-period control, $T_r = T/2$. The natural transient radian frequency of oscillation is

$$\omega_n = 2\pi f_n = \omega_0 \sqrt{1 - \zeta^2} \quad (3)$$

ζ is the per unit dimensionless damping per undamped radian of the oscillatory system. ζ is equal to α/ω_0 , the sine of the angle between the $j\omega$ axis and the pole in the s plane. ζ_n is the tangent of the same angle, equal to α/ω_n or $\zeta/\sqrt{1 - \zeta^2}$.

Fig. 3 shows the block diagram of the half-period control of a resonant component, in which the input is broken into an initial and delayed step. This can be represented as a unity input plus a negative pulse generator, which is shown as the block P . Fig. 4 shows the gain and phase response of the system before and after compensation. Curves A are for a lightly-damped resonant component alone. Curves B are for the lightly-damped system in Fig. 3 after the application of the Posicast control. The phase lag is approximately linear with frequency. Curves C are for a highly damped resonant component alone and curves D are for the same system after the application of Posicast control. Fig. 5 shows the s -plane plot for the undamped system. The uncompensated resonance is represented by two complex poles. The Posicast component alone has two complex zeros which exactly coincide in location in the s plane with the complex poles. The cascade combination of these two has a series of complex zeros at a very high frequency only.

This system is linear, and although it contains non-minimum phase elements, the parallel branches guarantee that the over-all system will always be minimum phase.

Even though temperature changes may affect the constants of the delay line or the oscillatory system, the basic character of the response is relatively unchanged, so long as the distance between the poles and the zeros is significantly less than the distance between the poles and the $j\omega$ axis.

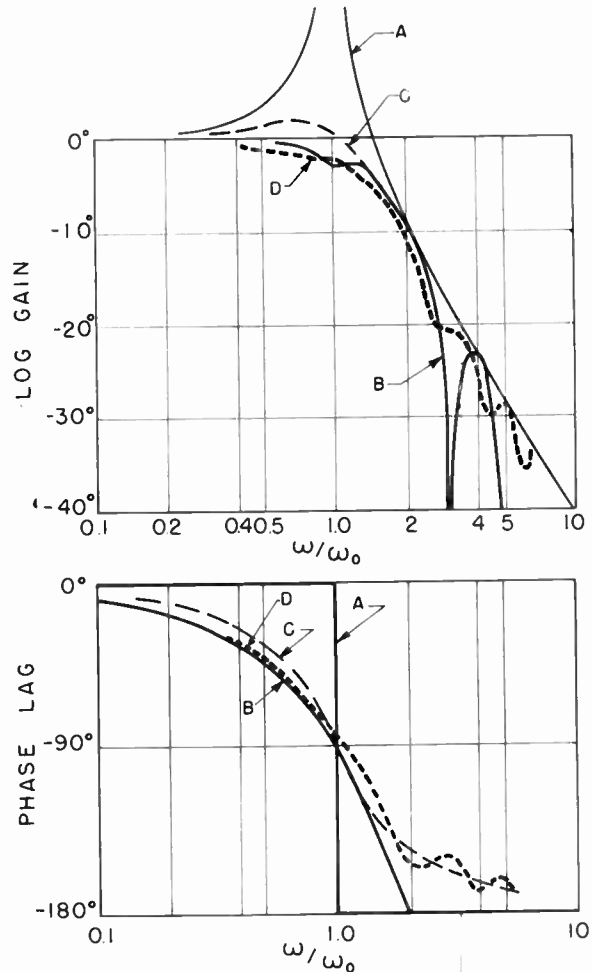


Fig. 4.

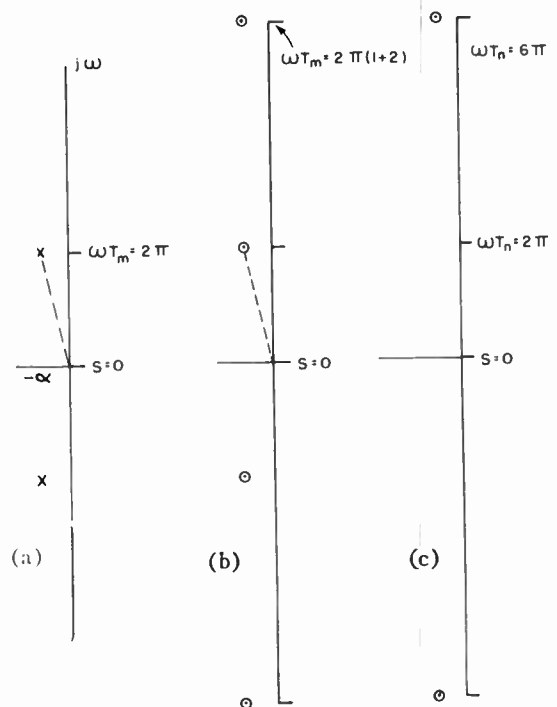


Fig. 5.—(a) $G(s)$ original lightly-damped oscillatory system, (b) $1 + P$ Posicast compensating section, (c) Resultant system, one-half period response.

It can be seen that this Posicast compensator performs the function of equalization. At the frequencies for which the system gain is high, the compensator gain is low. In the Bibliography are references to other work using delay lines as equalizers. In Wiener's work [1], a line with many taps was used to approximate an impulse response whose peak was delayed in time, in order to achieve a maximum discrimination between signal and noise. In Calvert's work, multitapped delay lines were used as equalizers to generate phase lead and to adjust the attenuation on a real frequency response basis. Exponential functions of s were converted to trigonometric form and then approximated by Taylor's series.

It is not necessary to build actual LC delay lines for low frequency systems. Servomechanisms may require delays of the order of 0.05 second. These can be achieved with RC twin-tee networks, an amplifier, and negative feedback around the whole. It is beyond the scope of this paper to discuss the design of precision delay lines [5]. Process controls may require delays of 30 seconds. These can be realized pneumatically with orifices and membrane-divided capacities in a twin-tee network, with an air amplifier and negative feedback. In the megacycle range, various network configurations will yield a circular pattern of poles and zeros, each uniformly spaced in the vertical s -plane direction, and very closely approximating a delay line.

ONE-QUARTER CYCLE RESPONSE

A resonant load can be driven by an input step to produce an output step completely realized in a very small fraction of a period. The excitation function must deliver a positive step first, a negative step after a short delay, and a final positive step. These three inputs to the resonant load excite three oscillatory transients. Each can be represented by the real part of a rotating phasor which is diminishing in magnitude at the rate $\exp(-\alpha t)$. These are called *shrinking phasors* or *shrinking vectors*. The vector sum of the three phasors at any time after the last input step must be zero for the transient response to have no overshoot and to remain constant at its steady-state value. The *arithmetic* sum of the magnitudes of the three steps is the steady-state output. For very short transient times (very-wide bandwidth), the first accelerating force and the second braking force must be very large compared to the final step and to the steady-state gain.

Fig. 6 shows the excitation function necessary to drive an undamped resonant load to achieve the best step response in one-quarter period. Fig. 6(b) is a vector diagram of the three phasors representing the three oscillation components excited by the three steps in Fig. 6(a). The first step is of magnitude 1.7 and starts a negative cosine oscillation of 1.7 amplitude. The second step is 45° later with magnitude of -2.4 . The sum of these two is a positive sine wave of 1.7 amplitude. The third step is of magnitude 1.7 and occurs when the resultant oscillation has reached unity with zero deriva-

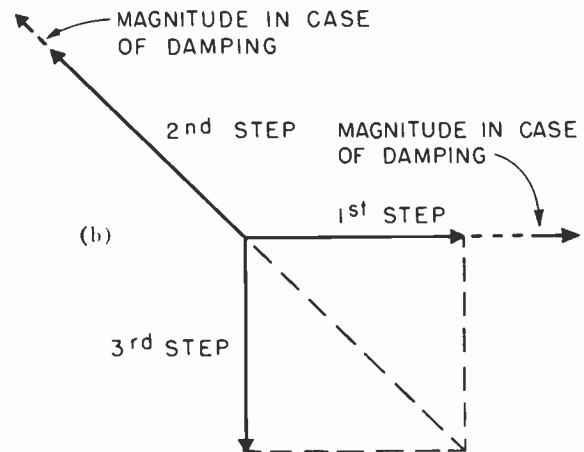
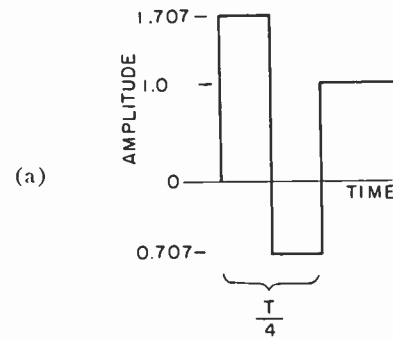


Fig. 6—(a) System input, step response of $(1+p)$. (b) Vector diagram for one-quarter-period Posicast control.

tive. The vector sum of the three is zero and the arithmetic sum is unity.

When the system has damping, the vectors diminish in magnitude with time, and so are called *shrinking vectors*. At the time instant of the last step, the three oscillations should be represented by the three solid vectors in Fig. 6(b). The magnitudes of the steps to produce these, however, should be larger for the earlier vectors, because of the damping. The original step magnitudes are shown with dotted vectors.

Fig. 7 shows the form of the output transient from the undamped resonant load when driven with the excitation of Fig. 6. It is the first 45° of a negative cosine wave attached to the last 45° of a positive cosine wave. The steps in Fig. 6 must be the center lines of these cosine waves. Fig. 8 is a practical circuit for obtaining the excitation function of Fig. 6. This is a doubly reflecting line, with each section having a delay of $1/16$ of the resonant period. A positive input step drives the output positive and starts a transient propagating down the distortionless delay line. When this transient reaches the $0.707R$ it is reflected with reversed phase and this reflection reverses the output when it arrives back at the sending end of the delay line. The transient which continues to the end of the second delay line is reflected back with a doubling of amplitude and this restores the output to a positive polarity at the end of a total delay time of one-fourth period.

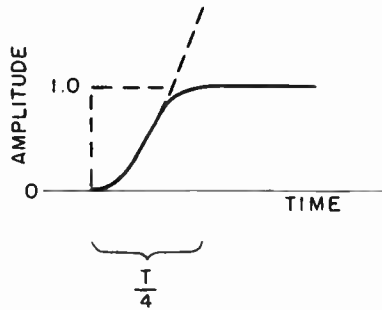


Fig. 7—System output.

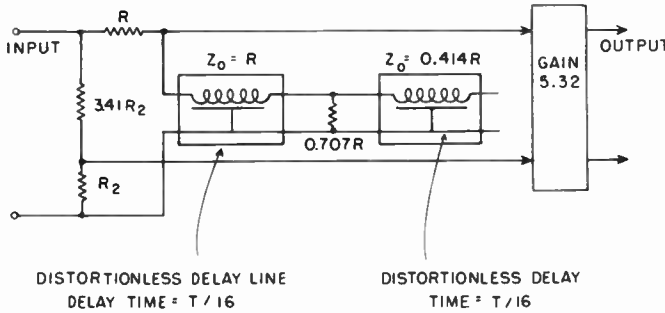


Fig. 8—Circuit for $(1+p)$.

For the complex zeros of this Posicast delay line section to cancel exactly the complex poles of a resonant component, the delay line should have the transference

$$1 + P = \frac{k - 2k^{1/2} \left(\cos \frac{\omega_n T_r}{2} \right) \epsilon^{-sT_r/2} + \epsilon^{-sT_r}}{k - 2k^{1/2} \left(\cos \frac{\omega_n T_r}{2} \right) + 1} \quad (4)$$

where k is the value previously defined. This equation is valid for all 3-step or double-pulse excitations.

The control in (4) above is derived from two restrictions on the system. For each step out of the compensator, an oscillation component is excited. After the last step, these three oscillation components can be represented by three rotating phasors. That due to the last step has a magnitude equal to the last step and a phase of zero degrees. That phasor due to the next-to-the-last step has a magnitude less than the step due to the attenuation of the oscillation, $1/\sqrt{k}$, which has occurred in the time between the middle and the last step. It has an angle of $\omega_n T_r/2$ radians, which is 45° for quarter-period control. That phasor due to the first step has a magnitude equal to the first step times $1/k$, the attenuation during the total transient period. It has an angle of $\omega_n T_r$ radians, which is 90° for quarter-period control. The sum of these three phasors must equal zero. Setting the real and imaginary parts separately equal to zero, one has two equations from which the relative magnitudes of the three steps can be calculated. These are the three numerator terms in (4).

The compensator should have unity steady-state gain, delivering a unit output for a unit input. There-

fore the arithmetic sum of the three steps of the compensator should equal unity. This yields the calibration constant shown in the denominator of (4).

It is beyond the scope of this paper to discuss the z plane and the z transform, in which the substitution $z = \epsilon^{sT}$ is used. However, for those skilled in this method, it is apparent that (4) can be changed into a ratio of polynomials in z by making the substitution above. Eq. (4) will then have a numerator quadratic, with two complex z -plane zeros. These zeros should be designed to coincide exactly with the system s -plane poles when they are plotted in the z plane (z transform of the system). This method has great mathematical rigor and simplicity.

A compensator can be built for any multiple-pole system of any order, which will have only tangential transients, with no transient components which approach the final value asymptotically. In this case, all of the poles and zeros from the s -plane plot of the complete system are transferred to the z plane and plotted there as poles and zeros (z transform). For each z -plane pole, the compensator produces a z -plane zero. The polynomial in z for all of these zeros is the Posicast compensator transference. This is applicable to two or more coupled resonant frequencies.

When one attempts to achieve extremely short response times, initial pulse must be many times larger than steady-state value. This may result in saturation of amplifiers or transducers in the system. Less than one-quarter period response is feasible primarily only in low-level applications. For high-level servo systems driven near saturation, the law of diminishing returns excludes responses faster than one-fourth-period.

FEEDBACK SYSTEMS

This method of control can be applied to any complex feedback system. With respect to the input, only a feed-forward pulse generator is needed. Fig. 9 shows the block diagram. The compensator $(1+P)$ should have unity steady-state gain. When transmission lines are used, or amplifiers to simulate lines, changes in temperature will change the gain. Therefore, high steady-state stability and accuracy are achieved by dividing the function $(1+P)$ into two parts as shown in Fig. 9(b). The unity-gain input to the system is left undisturbed. In parallel with this is introduced a pulse generator, P , capacitively- or transformer-coupled with zero steady-state gain. The pulse generator P has no steady-state gain. Fig. 10(a) shows the wiring diagram for a pulse generator of this sort. Its transference is

$$P = K_0 + K_1 \epsilon^{-sT_r/2} + K_2 \epsilon^{-sT_r} \quad (5)$$

where

$$K_0 = \frac{2k^{1/2} \left(\cos \frac{\omega_n T_r}{2} \right) - 1}{k - 2k^{1/2} \left(\cos \frac{\omega_n T_r}{2} \right) + 1} \quad (6)$$

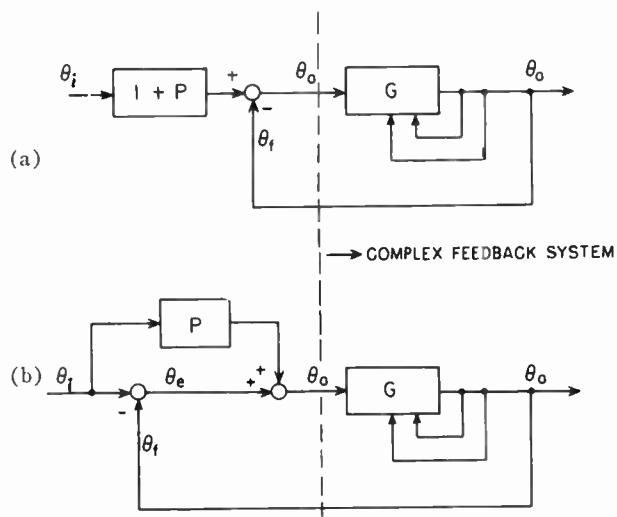


Fig. 9—(a) Statement of best control. (b) Constructional form to minimize the effects of changes in steady-state gain of p .

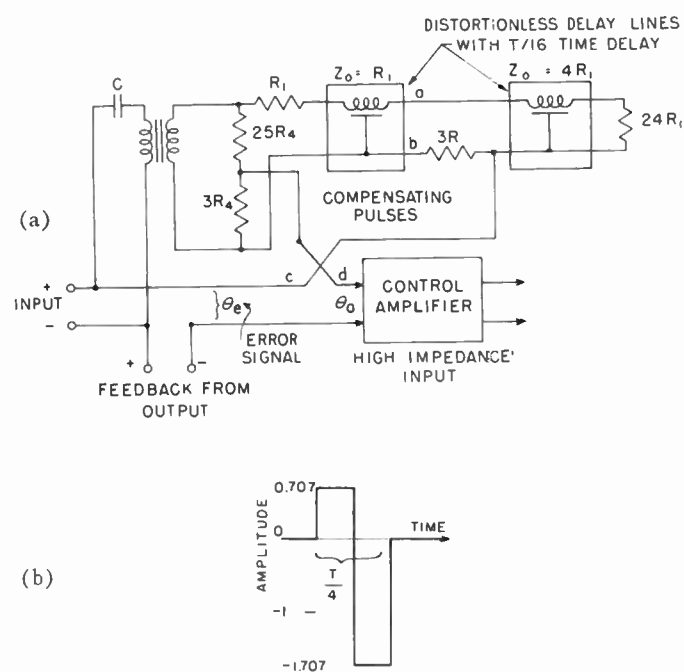


Fig. 10—(a) Circuit for p in feedforward independent of the input. (b) Step response of p alone.

$$K_1 = \frac{2k^{1/2} \left(\cos \frac{\omega_n T_r}{2} \right)}{k - 2k^{1/2} \left(\cos \frac{\omega_n T_r}{2} \right) + 1} \quad (7)$$

$$K_2 = \frac{1}{k - 2k^{1/2} \left(\cos \frac{\omega_n T_r}{2} \right) + 1} \quad (8)$$

$$K_0 - K_1 + K_2 = 0. \quad (9)$$

Fig. 10(b) shows the step-response pulse output at $c-d$ in Fig. 10(a).

COMPENSATION FOR LOAD DISTURBANCES

Fig. 11 (next page) shows a block diagram of the original uncompensated feedback system. It is desired to make the speed of response of this system as great as possible. The functions G_1 and G_2 are adjusted to make the damped resonant frequency as high as possible, with the restriction that the system always be reliably stable for the normal variations in the parameters with signal level and with temperature. A statement of the optimum realizable form of control is the block diagram in Fig. 12. This is not the block diagram for the construction but only states that the load signal should have come through a block which divided it into two or more components so phased that the transients excited by these components would cancel out. Fig. 13 is the block diagram of the actual system. This can be derived from Fig. 12 by block diagram substitutions.

The compensation block required, P_0' , is the transference P_0 with unity negative feedback. This block alone would have the transfer function

$$P_0' = \frac{P_0}{1 + P_0} = \frac{K_0 + K_1 e^{-sT_r/2} + K_2 e^{-sT_r}}{1 + K_0 + K_1 e^{-sT_r/2} + K_2 e^{-sT_r}} \quad (10)$$

P_0' is a reentrant transmission line, or a continuously reflecting transmission line, which is terminated in values other than the characteristic impedance at each end. The transference of this block can be represented by

$$P_0' = 1 - \frac{1}{1 + K_0 + K_1 e^{-sT_r/2} + K_2 e^{-sT_r}} \quad (11)$$

$$P_0' = 1 - \frac{1}{(1 + K_0)} (1 - X + X^2 - X^3 + X^4 - \dots) \quad (12)$$

where

$$X = \left(\frac{K_1}{1 + K_0} \right) e^{-sT_r/2} + \left(\frac{K_2}{1 + K_0} \right) e^{-sT_r} \quad (13)$$

This transference has both poles and zeros. However, the use of this block within the feedback system introduces a unique mode of operation in which the poles are excited for only a short time and then are quenched. A step change or disturbance of the load produces at the input to P_0' a triple step operated on by the function $1/G_1$. These three steps have the unique relationship necessary to cancel the feedback pulses from the output of P_0 , so that the input to P_0 is not a triple step, but is only a single step, operated on by the function $1/G_1$. The line, therefore, delivers only a triple-step output for a single-step load disturbance.

The function P_0' can be constructed like Fig. 10, except that the impedance values are so chosen as to produce continuous reflections back and forth down the line in accordance with (10)–(12). Or, the actual circuit of Fig. 10 can be used with an isolating amplifier providing negative feedback. Since this minor loop feedforward has only high-frequency response, it is not

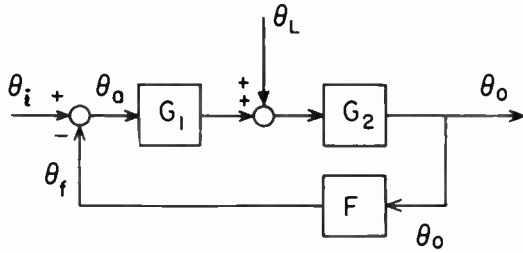


Fig. 11.

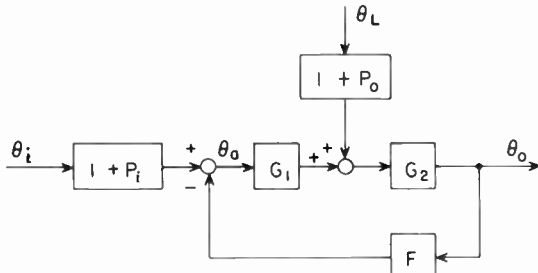


Fig. 12—Statement of best control.

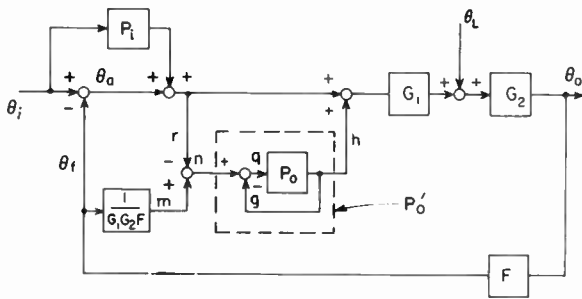


Fig. 13—Constructional arrangement for load compensator.

necessary for it to have zero frequency gain and can be transformer- or capacitively-coupled. The block $1/G_1G_2F$ is the inverse of the original system loop gain. However, this computation must be effective only for very high frequencies in the region where the loop gain is unity with a phase lag of nearly 180° .

The input of the pulse-generating line P_o can be thought of as being located at the null position of a bridge which is driven by the output of this line. Therefore, pulses generated due to the delay within the line itself do not excite the line further, but disappear into the cancellation of the load-excited oscillation.

Fig. 14 shows the s -plane pattern of the original system, the compensator $(1+P)$ alone, and the complete feedback system with compensators for one-quarter period response.

DIGITAL COMPUTER CONTROL

All of the previous systems can be adapted directly to digital computer control or periodically-sampled systems. Eq. (5) is the scheduling of the input feedforward or input computer. Eq. (10) is the scheduling of

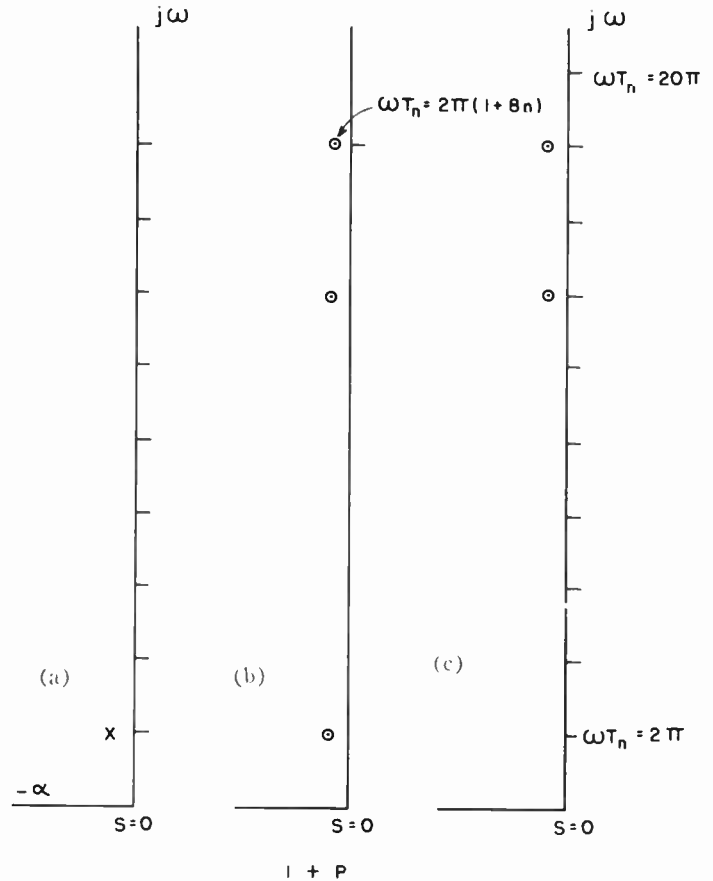


Fig. 14.—(a) Original lightly-damped system, (b) Posicast compensator for one-quarter period, (c) Final compensated system.

the minor-loop feedforward or load-compensating computer. The sampling period is $T_r/2$. In the special degenerative case represented by (1), half-period response can be achieved by setting T equal to both the half-period of the oscillation and to the sampling period, but this introduces problems in stability which are beyond the scope of this paper. The general control represented by (5) and (10) will yield a dead-beat response. In general, $T_r/2$ should be several sampling periods for good control without saturation problems.

ERROR COEFFICIENT RESTRICTIONS

This Posicast method of control can be applied to systems which have specified positional, velocity, and acceleration error coefficients. These coefficients are usually designated as k_p , k_v , and k_a , respectively. If, in addition, the system has the unalterable components of two resonant poles, we have five restrictions on the system. To fulfill these five restrictions, the control device should convert a single-step input into five step functions. The transfer function of the control device would therefore be

$$1 + P = K_0 + K_1 e^{-sT_r/4} + K_2 e^{-sT_r/2} + K_3 e^{-sT_r3/4} + K_4 e^{-sT_r} \tag{14}$$

To solve for the coefficients of this transfer function,

which is the same as the scheduling of a periodically sampled controller, one can start with the restriction that the vector sum of the five transients excited by these five steps must be zero. This yields

$$K_0 e^{4\theta(-\zeta_n + j)} + K_1 e^{3\theta(-\zeta_n + j)} + K_2 e^{2\theta(-\zeta_n + j)} + K_3 e^{\theta(-\zeta_n + j)} + K_4 = 0 \quad (15)$$

where $\zeta_n = \zeta / \sqrt{1 - \zeta^2}$ and θ is the transient phase angle corresponding to time $T_r/4$.

The arithmetic sum of the coefficients of (14) above should equal one minus the reciprocal positional error coefficient. The difference between the integral of unity for time T_r and the integral of the output of the controller, that is the integral of (14) for a step input, should be the reciprocal velocity error coefficient. In a similar manner the difference between the double integral of unity and the double integral of (14) for a step input should be the reciprocal acceleration error coefficient. Setting down these integral equations and simplifying them will yield the following three restrictions:

$$\begin{aligned} K_0 + K_1 + K_2 + K_3 + K_4 &= (1 - 1/k_p) \\ 4K_0 + 3K_1 + 2K_2 + K_3 &= 4(1 - 1/k_v T_r) \\ 4^2 K_0 + 3^2 K_1 + 2^2 K_2 + K_3 &= 16(1 - 2/k_a T_r^2). \end{aligned} \quad (16)$$

The real and the imaginary parts of (15) taken separately are two independent equations. These 5 equations are sufficient to solve for the complete schedule. This method can be extended to the control of a pair of resonant poles with any number of error coefficient restrictions.

The same technique can be applied to the control of a complex system with fairly simple error coefficient restrictions. For example, a system could have one real time constant and a pair of complex poles, and a zero positional error for constant velocity would be desired. The system real pole can be considered as an operator on the input signal. The resultant condition to be imposed is that there must be zero error for a delayed integral of an input step, after time T_r .

CONCLUSION

A method of control has been developed which eliminates the necessity for adjusting a feedback control system to have only highly damped resonant poles. It is possible to obtain significantly greater speeds of response, by adjusting the feedback system for maximum frequency of oscillation, only lightly damped, but with a reproducible and consistent closed-loop complex pole location in the s plane. The method is analogous to the race-break systems of nonlinear predictor controls, in which a large positive pulse is applied initially, a large negative pulse follows to reduce the derivative of the output, and a third steady-state step is applied permanently. These three excitations are adjusted so that the phasor sum of their phasor transients is zero after the final excitation is applied. These excitations are a mode of high-frequency control, and do not need to be included within the characteristics of the feedback system. Although this system contains nonminimum phase elements, the over-all system is minimum phase, and furthermore approaches a linear phase lag with frequency, as the original resonant poles approach zero damping. The waveshape reproduction is the best possible from any linear system with the restriction of a fixed dynamic range, or the restriction of a maximum permissible signal which will not drive the amplifiers or transducers into the nonlinear region.

BIBLIOGRAPHY

- [1] Wiener, N. *The Extrapolation, Interpolation and Smoothing of Stationary Time Series*, New York, John Wiley & Sons, Inc., 1949.
- [2] Calvert, J. F. and Ford, D. J. "The Application of Short-time Memory Devices to Compensator Design," *Applications and Industry*, No. 12 (May, 1954), pp. 88-93.
- [3] Calvert, J. F. and Gimpel, D. J. "Signal Component Control," *Transactions of the AIEE*, vol. 71, Part II (November, 1952), pp. 339-343.
- [4] Sze, T. W., and Calvert, J. F., "Short Time Memory Devices in Closed-loop System—Steady-State Response," *Transactions of the AIEE*, Part II, vol. 74 (1955), pp. 340-344.
- [5] Kuh, E. S., "Synthesis of Lumped-Parameter Precision Delay Lines," 1957 IRE NATIONAL CONVENTION RECORD, Part 2, pp. 160-174, 1957.



Synchronization of Oscillators by Periodically Interrupted Waves*

DONALD W. FRASER†, SENIOR MEMBER, IRE

Summary—This paper describes the principles, methods, circuit applications, and the theoretical basis of the synchronization of LC oscillators by interrupted wave trains. The synchronizing process is shown to depend upon the transient behavior of the phase angle between two vectors which represent, respectively, the instantaneous voltage of the oscillator and the corresponding instantaneous voltage of the injected synchronizing signal. This phasing action is employed in the derivation of formulas by means of which it is possible to define the regions of synchronization due to each of the several significant frequency components of the interrupted wave train.

The term *interrupted wave train* as used herein refers to a cw signal which is interrupted (gated) in a periodic manner. The resultant signal, as herein demonstrated by theoretical and experimental means, can produce a form of synchronization such that the average frequency of the oscillator is *identically equal* to the fundamental component of the synchronizing signal or to any selected sideband. Phase modulation of determinable magnitude is shown to exist in the synchronized oscillator and analyses are included which permit evaluation of the frequency spectrum of the output.

Particular emphasis is given to the band of synchronization due to a cw signal of the same amplitude as the interrupted signal. This band, a measure of frequency, is used as a convenient unit when comparing the synchronizing action of various forms of synchronizing signals. By choice of this unit the data required in the design of the oscillators under discussion are derived from quantities generally familiar in the art.

Illustrations are given of the application of the formulas to typical oscillators and these are coupled with experimentally obtained data which are in support of the derived equations. A practical oscillator which may be synchronized by at least ten sidebands of an interrupted wave train is described and other applications of the principle are suggested.

LIST OF SYMBOLS

- k = Duty cycle of periodically interrupted synchronizing signal.
 $K = \omega_s / \omega_c$ = Ratio of frequency difference between synchronizing and free-running frequencies to half bandwidth of synchronization.
 t = The general time variable.
 t_0 = A constant of integration, the time of initiation of a transient of phase.
 θ = Phase angle between synchronizing voltage and grid voltage of oscillator.
 V_1 = Amplitude of synchronizing voltage.
 V_g = Amplitude of oscillator voltage, grid-to-ground.
 V_R = Amplitude of feedback voltage in oscillator.
 $\omega_1 = 2\pi f_1$ = Angular frequency of synchronizing voltage.
 $\omega_{1ab} = 2\pi f_{1ab}$ = Half bandwidth of synchronization by first sideband of synchronizing signal.
 $\omega_{ci} = 2\pi f_{ci}$ = Half bandwidth of synchronization by an interrupted synchronizing signal.
 $\omega_c = 2\pi f_c$ = Half bandwidth of synchronization by a cw synchronizing signal.
 $\omega_m = 2\pi f_m$ = Angular frequency of signal which modulates (gates or interrupts) the synchronizing signal.
 $\omega_0 = 2\pi f_0$ = Angular frequency of free-running oscillator.
 $\omega_s = 2\pi f_s$ = Difference of angular frequencies of synchronizing and oscillator signals.

INTRODUCTION

THE phenomenon of synchronization has been long known to exist but only in recent years has the literature contained any definitive analyses of the mechanisms and principles involved. One of the first analyses, devoted to a mathematical interpretation of the nonlinear characteristics of an oscillator, is due to van der Pol.¹ In a later paper, Adler² combined classical theory with a physical interpretation of the action which occurs in an LC oscillator when subjected to a cw synchronizing signal. Adler derived equations which describe the transient action of the phase angle (between oscillator voltage and injected signal) during the synchronizing process. His conclusions, substantiating in principle the theories of van der Pol, were further verified by results obtained by such experimenters as Huntoon and Weiss³ and van Slooten,⁴ who used different bases of analysis but who derived formulas which are essentially identical to those of Adler.

The referenced analyses consider two types of synchronizing signals, those which are of cw form and those which are composed of periodic pulses. In each case a primary objective is the determination of the limits of synchronization and principal emphasis is given to those frequencies which lie within the band of synchronization. The immediate vicinity of the edge of the band, sometimes called the "pulling" region, is treated subjectively rather than analytically. This borderline region, important in everyday practice because of the common occurrence in the region of wanted or unwanted signals, has been analyzed by Buchanan⁵ with results appearing in precise but rather complicated form.

Quite recently another type of synchronizing signal, distinct from those two listed above, has come under consideration. Hahnel⁶ has described an oscillator in which the primary (anode) oscillatory circuit is synchronized by the action of a lower frequency grid-circuit oscillation. The grid-circuit signal consists of oscillations which are periodically damped so that there re-

¹ B. van der Pol, "The nonlinear theory of electric oscillations," *PROC. IRE*, vol. 22, pp. 1051-1086; September, 1934.

² R. Adler, "Locking phenomena in oscillators," *PROC. IRE*, vol. 34, pp. 351-357; June, 1946.

³ R. D. Huntoon and A. Weiss, "Synchronization of oscillators," *PROC. IRE*, vol. 34, pp. 1415-1423; December, 1947.

⁴ J. van Slooten, "Mechanisms of the synchronization of LC oscillators," *Philips Tech. Rev.*, vol. 14, pp. 292-297; 1953.

⁵ T. J. Buchanan, "Frequency spectrum of a pulled oscillator," *PROC. IRE*, vol. 40, pp. 958-961; August, 1952.

⁶ A. Hahnel, "Multichannel crystal control of vhf and uhf oscillators," *PROC. IRE*, vol. 41, pp. 79-81; January, 1953.

* Original manuscript received by the IRE, September 3, 1956; revised manuscript received, April 24, 1957.

† Univ. of Rhode Island, Kingston, R. I.

sults a series of "interrupted wave trains." The effect of this form of synchronizing signal is less simple than that of a cw signal because of the many frequency components involved.

In the present paper analytical means are employed to show that periodically interrupted waves have particular and peculiar properties when serving as synchronizing signals. In particular, it is shown that the frequency and duty cycle of the interrupting (gating) signal are the determining factors in predicting the frequency(s) of synchronization. In addition, it is shown that the change of phase between oscillator and synchronizing voltage is a function of the interrupting action and that this phasing action may be usefully employed in the several cases when the synchronizing frequency lies inside the band of synchronization, when it lies well outside the band, and when it lies in the borderline (pulling) region. It is further shown that the formulas which may be derived describe both the limiting conditions of synchronization and the form of the frequency spectrum of the synchronized oscillator. These derived formulas provide a reasonably precise basis for the design of oscillator circuits which may adequately utilize the various frequency components of a specific synchronizing signal.

SYNCHRONIZATION OF OSCILLATORS BY CW SIGNALS

The study of the synchronizing effects of interrupted wave trains is facilitated by reference to certain known effects of cw signals. The following analysis provides information which can be directly employed in the present study.

Consider a free-running tuned-plate oscillator, whose essential components are shown in Fig. 1(a), to which a disturbing sinusoidal voltage V_1 is applied as shown. Fig. 1(b) illustrates the phase relationships in the oscillator. The most significant quantity illustrated, from the standpoint of the analysis to follow, is the angle θ between V_1 and V_o . Adler⁷ has shown, when the oscillator has a free-running angular frequency ω_0 , that a forcing signal of angular frequency ω_1 produces a phase variation which is governed by the following equation

$$\frac{d\theta}{dt} = (\omega_1 - \omega_0) - \frac{\omega_0 V_1}{2QV_o} \sin \theta \tag{1}$$

wherein Q refers to the Q of the tuned circuit and the other quantities are as previously defined.

Eq. (1) is conveniently written

$$\frac{d\theta}{dt} = \omega_s - \omega_c \sin \theta. \tag{2}$$

Here, ω_s evidently, represents the difference between injected and free-running frequencies. Also, $\omega_c = \omega_0 V_1 / 2QV_o$, a quantity which will be found to equal one half the band of synchronization.

⁷ Adler, *op. cit.*

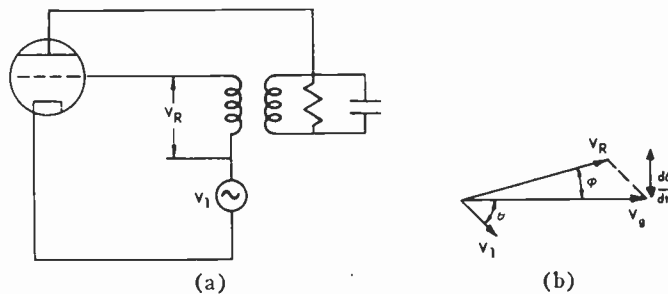


Fig. 1—Voltage relationships in a disturbed oscillator.

Inasmuch as (2) describes the relationships existing between input voltage and oscillator voltage, it is seen that synchronization is attained when $d\theta/dt$ is identically equal to zero, from which it follows that

$$\omega_s = \omega_c \sin \theta. \tag{3}$$

The maximum value of ω_s occurs when $\sin \theta = \pm 1$ at which time $\theta = \pm 90^\circ$. Two important conclusions are deduced. 1) The maximum phase angle which can exist between the input voltage V_1 and the oscillator voltage is 90° , and this condition applies when the frequency of the input signal lies at that point of the band of synchronization which is most remote from ω_0 . 2) The half-width of the band of synchronization is equal to ω_c .

Eq. (3) describes the conditions which exist during the time when actual synchronization has been achieved. During the initiation of synchronization the phase angle is constantly changing. Considerable information can be obtained from a study of the magnitude of θ itself and to that end it is necessary to integrate (2). That nonlinear equation is subject to direct integration, using formula 436.00 of Dwight's Table of Integrals.⁸ Jones⁹ has developed the results in the form

$$\theta = 2 \tan^{-1} \frac{1}{\omega_s} \left[\omega_c - \sqrt{\omega_c^2 - \omega_s^2} \tanh \frac{1}{2} \sqrt{\omega_c^2 - \omega_s^2} (t + t_0) \right], \tag{4}$$

where t is the general time variable and t_0 , a constant of integration, represents the time of initiation of the phase transient. This equation applies when $\omega_s < \omega_c$; that is, the frequency of the injected signal lies inside the band of synchronization. If one uses $K = \omega_s / \omega_c$, the equation can be written

$$\theta = 2 \tan^{-1} \left[\frac{1}{K} - \frac{\sqrt{1 - K^2}}{K} \tanh \omega_c \frac{\sqrt{1 - K^2}}{2} (t + t_0) \right]. \tag{4a}$$

When the frequency of the synchronizing signal is outside the band of synchronization $\omega_s > \omega_c$ and the equation of the phase angle becomes

⁸ H. B. Dwight, "Tables of Integrals," Macmillan Co., New York, N. Y., rev. ed.; 1947.
⁹ W. B. Jones, Jr., "Synchronized oscillators with frequency modulated synchronizing signals," unpublished thesis, Georgia Inst. of Tech., Atlanta, Georgia; 1953.

$$\theta = 2 \tan^{-1}$$

$$\left[\frac{1}{K} + \frac{\sqrt{K^2 - 1}}{K} \tan \omega_c \frac{\sqrt{K^2 - 1}}{2} (t + t_0) \right]. \quad (5)$$

The two equations, (4) and its equivalent in (5) when expressed in terms of ω_s and ω_c , illustrate the important difference between the synchronizing action of a signal which lies inside the band of synchronization ($\omega_s < \omega_c$) and one which lies outside the band ($\omega_s > \omega_c$). In the first equation, (4), which is applicable to a signal within the band, the phase angle is seen to be a function of the hyperbolic tangent of $(t + t_0)$. Since $\tanh(t + t_0)$ is known to approach unity in an asymptotic manner as t increases without limit, the angle θ will approach a final value θ_0 , where θ_0 becomes

$$\theta = 2 \tan^{-1} \frac{\omega_c - \sqrt{\omega_c^2 - \omega_s^2}}{\omega_s} \quad (6)$$

by virtue of (4) and the limiting value of $\tanh(t + t_0)$.

If the signal lies outside the band, the effect of the signal upon the phase angle is described by (5) or its equivalent in terms of ω_s and ω_c . As t increases the quantity $\frac{1}{2}\sqrt{\omega_c^2 - \omega_s^2}(t + t_0)$ will pass through $\pi/2, \dots, 3\pi/2, \dots$, etc., and the tangent of the angle will pass through $\infty, -\infty$, etc. At these instants $\theta/2$ must pass through $\pi/2, \dots, 3\pi/2, \dots$, etc. It is evident that within the band of synchronization the phasing action is well-behaved but that outside the band it can vary with great rapidity. Experimenters have found that the frequency spectrum in the latter case, at least at its most unstable point, may be so violent in fluctuation as to defy photography on presently available panoramic display systems.

EXPERIMENTAL OBSERVATIONS

An experiment which aided in understanding the factors involved in synchronization by periodically interrupted waves is now described. The equipment involved in the experiment is illustrated in Fig. 2 with the oscillator under test shown in the upper right block. A cw signal generator of variable frequency f_1 has its output interrupted (gated) by a rectangular pulse of variable frequency f_m and adjustable pulse width t_1 . The output of the gating circuit consists of several cycles of frequency f_1 which occur only during the time $0 - t_1$. This interrupted signal of total period $T = 2\pi/\omega_m$ is injected as a synchronizing signal into the oscillator under test. The output of the synchronized (or disturbed) oscillator is studied by means of a cro (utilized as a synchroscope), by a frequency counter, and by a spectrum analyzer.

In the first portion of the test the free-running frequency of the oscillator under test was set to 20,000 cps, approximately, that of the rectangular pulse generator to 500 cps, and the output of the gating circuit was ad-

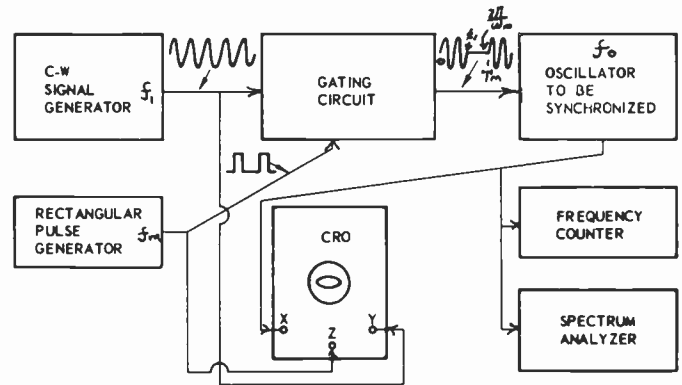


Fig. 2.—Block diagram of arrangement for synchronization by interrupted wave trains.

justed so that V_1 would be approximately $1/10$ of V_o . (See Fig. 1(b).) The frequency f_1 of the signal generator was then varied slowly from 100 cps to 100,000 cps. The following important results were observed.

1) Within certain narrow bands centered about the frequencies $f_0 \pm n f_m$ ($n = 0, 1, 2, 3, \dots$) the frequency of the output was identically equal to $f_1 \pm n f_m$. That is, the oscillator under test was synchronized to the fundamental or a sideband of the modulated (gated) signal.

2) The spectrum of the output of the oscillator contained not only the major line at the frequency of synchronization but also other lines which were separated, individually, by the frequency f_m .

In the second portion of the test the same procedure was followed except that three separate modulating frequencies were employed and the form of the output of the oscillator was studied by means of Lissajou patterns. The observed patterns, obtained with the aid of Z-axis modulation, are shown in Fig. 3. The "on" time, caption of the left column, is defined to mean that portion of the modulating (gating) cycle during which a synchronizing signal of significant amplitude is present; the "off" time represents that portion of the cycle when the signal is of zero or negligible amplitude.

The patterns observed were produced by a synchronizing signal whose fundamental frequency lies very close to the edge of the band of synchronization. In the upper portion of Fig. 3 (a), the modulating frequency is relatively high and the phase angle is seen to be very nearly 97° at all times. This condition is similar to that which is observed upon the application of a cw synchronizing signal whose frequency is at the "edge of the band of synchronization." The condition is different, however, in the remaining illustrations, Fig. 3 (b) and (c), where the modulating frequency is progressively decreased. The phase angle is found to undergo a considerable excursion, one which becomes large when the modulating frequency is low.

Four significant features are revealed in Fig. 3(c). First, the excursions of the phase angle are much greater than when the modulating period was small. Second,

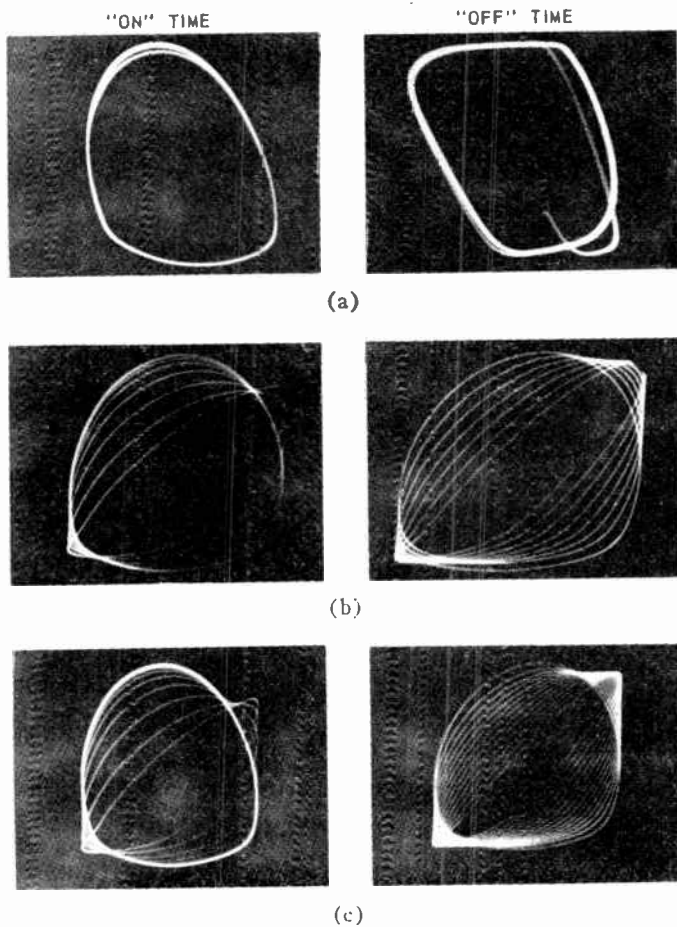


Fig. 3—Lissajou patterns illustrating phase modulation in oscillator. (a) $f_0 = 12,100$ $f_m = 1800$, (b) $f_0 = 12,100$ $f_m = 750$, (c) $f_0 = 12,100$ $f_m = 300$.

the magnitude of the total excursion during the "on" time exactly balances the total excursion during the "off" time. Third, the rate at which the phase progresses (*i.e.*, the spacing between lines) is uniform during the "off" time but is nonuniform during the "on" time. Finally, when the modulation period is long the phase angle reaches and maintains for a portion of the cycle a constant value (heavy ellipse of Fig. 3(c)). This constant value corresponds to the constant angle maintained during synchronization by a cw signal, *i.e.*, θ_0 of (6). As a final and separate observation, it will be noted that the phase varies between limits of approximately 45° – 135° .

It is possible now to form a picture of the action within the oscillator utilizing the information of Fig. 3. The phase angle oscillates during all or most of the modulation cycle, but in a manner constrained so that the *net* deviation is zero. The vector V_1 of Fig. 1(b) may be likened to a pendulum, swinging about the origin and opening and closing upon V_0 but never actually reaching a relative position of 0° or 180° when synchronized by the fundamental component of the synchronizing signal. During the "on" time the rate of change is nonlinear and is determined by (1); during the "off" time the rate is constant and is simply equal to ω_s , *i.e.*, $\omega_1 - \omega_0$.

These observations and conclusions can now be used as a direct guide in developing formulas by which to define the synchronizing action. The requirements that the total net phase per modulation cycle be a specified amount provides the criterion of synchronization which is employed in the next section of this paper.

PHASE REQUIREMENTS IN SYNCHRONIZATION

In the case of synchronization by a cw signal it has been shown that the vector voltages may be represented in the form shown in Fig. 1(b) and that $d\theta/dt = \omega_s - \omega_c \sin \theta$, where $\omega_c =$ one-half the band of synchronization $= \omega_0 V_1 / 2QV_0$. This latter quantity, it will be noted, is a constant for any given set of parameters ω_0 , V_1 , Q , and V_0 .

It has been previously stated that synchronization occurs in the cw case when $d\theta/dt = 0$; that is, when $\omega_s - \omega_c \sin \theta = 0$. Obviously the conditions for synchronization are quite different when the synchronizing signal is periodically interrupted. Referring again to Fig. 3, one recalls that the net phase deviation during any one modulation cycle is *zero*. The latter fact permits the definition of a criterion for synchronization by the fundamental component of an interrupted wave train, namely

$$\int_{t=0}^{2\pi/\omega_m} \left(\frac{d\theta}{dt} \right) dt = 0. \quad (7)$$

This basic criterion can be reduced to a more convenient form by dividing the modulation period into the "on" time and the "off" time. Assuming that the phase deviation $d\theta/dt$ obeys Adler's differential (2) during the presence of the synchronizing signal and, in a similar manner, that $d\theta/dt$ varies linearly during the absence of synchronizing signal at the rate $\omega_0 - \omega_1 = \omega_s$, the basic equation (7) may be written

$$\int_0^{t_1} (\omega_s - \omega_c \sin \theta) dt + \int_{t_1}^{2\pi/\omega_m} \omega_s dt = 0. \quad (8)$$

At this point it is convenient to reintroduce the dimensionless quantity K , where $K = \omega_s / \omega_c$. This quantity represents the ratio of the difference between synchronizing frequency and free-running frequency and the half-band of synchronization due to a cw synchronizing signal. When this ratio is employed, (8) becomes

$$\omega_c \int_0^{t_1} (K - \sin \theta) dt + \omega_c \int_{t_1}^{2\pi/\omega_m} K dt = 0. \quad (9)$$

The left integral is now evaluated by substituting the basic equation for θ (4a) and carrying out the procedures necessary to simplify the results. The steps are quite long and tedious and are not included here. The interested reader is referred to Buchanan's paper⁵ in which a basic derivation is carried out. Finally, there is obtained the transcendental equation

$$\begin{aligned}
 & 2 \tan^{-1} \left\{ \frac{1-K}{\sqrt{1-K^2}} \tanh \left[\omega_c \frac{\sqrt{1-K^2}}{2} (t+t_0) - \tanh^{-1} \frac{1-K}{\sqrt{1-K^2}} \right] \right\} \\
 & - 2 \tan^{-1} \left\{ \frac{1-K}{\sqrt{1-K^2}} \tanh \left[\omega_c \frac{\sqrt{1-K^2}}{2} t_0 - \tanh^{-1} \frac{1-K}{\sqrt{1-K^2}} \right] \right\} \\
 & = \omega_c K \left(\frac{2\pi}{\omega_m} - t_1 \right). \tag{10}
 \end{aligned}$$

Eq. (10) is probably the most important equation appearing in this paper. It will henceforth be called the *equation of synchronization*. It is the equation which must be satisfied for every condition of synchronization. The expressions on the left of the equality show the change of phase angle which occurs during the presence of the synchronizing signal while that on the right shows the change of phase angle that occurs during the absence of the synchronizing signal. These changes must be balanced if the average frequency of the output, as measured over one complete modulating cycle, is to be identically equal to a particular frequency component of the input.

In later sections of this paper references are made to the actual forms of the phase deviations which occur during the synchronization process. Since these deviations are described by (10), and inasmuch as some visualization of the phasing action is important in understanding the synchronization phenomenon, illustrations of three typical conditions are shown in Fig. 4. The phase excursions which occur during the application of the synchronizing signal are a nonlinear function of time, but the excursion which occurs during the remainder of the gating period is a linear function of time. When the modulation frequency is high (*i.e.*, the ratio of ω_m/ω_c is large) there is little error in assuming that the phase deviation is at all times a linear function of time. [See Fig. 4(c).]

An analysis of (10) is now undertaken in order to determine the relationship between its variables and parameters so that the characteristics of the oscillator may be predicted from known data. The analysis is first applied to the case when the phase deviations are assumed to be linear by employing the fact that for short modulation periods and for operation near the edge of the band of synchronization, the phase angle remains close to 90° throughout the modulation cycle.

Eq. (4a) is again referred to, and the substitution of $\theta = 90^\circ$ when $t = 0$ is made. There is then obtained

$$\omega_c t_0 = \frac{2}{\sqrt{1-K^2}} \tanh^{-1} \frac{1-K}{\sqrt{1-K^2}} \tag{11}$$

for all ω_c .

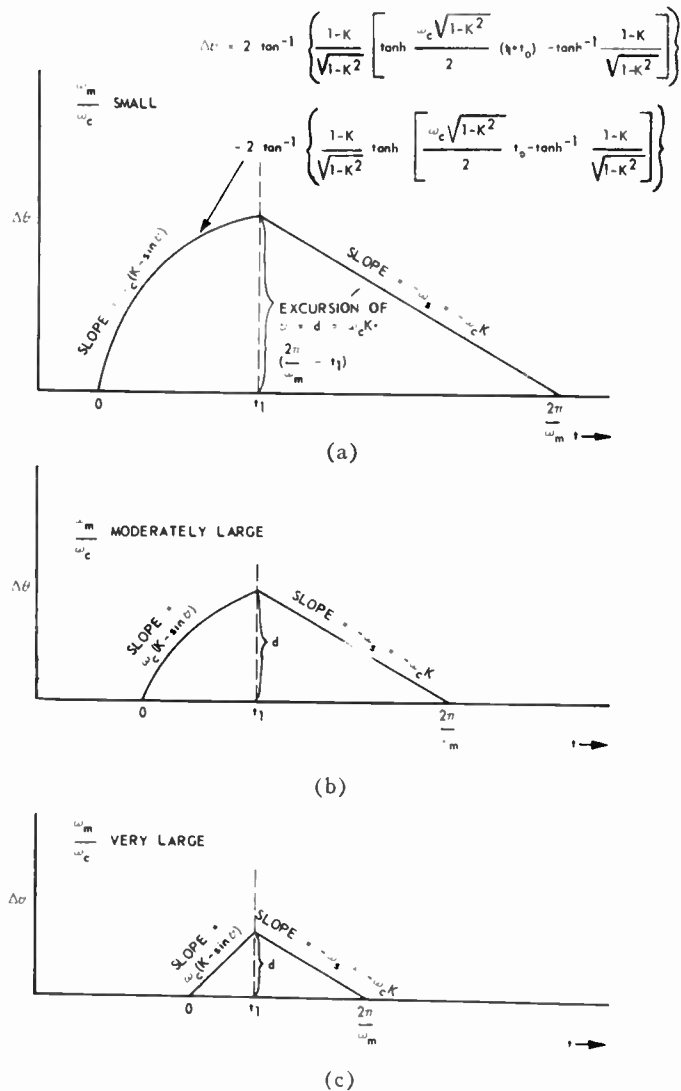


Fig. 4—Phase deviations in the synchronized oscillator.

The derived value of $\omega_c t_0$ is now substituted into the equation of synchronization (10) in order to produce considerable simplification of that equation. The simplified result is written as

$$\frac{1-K}{\sqrt{1-K^2}} \tanh \omega_c \frac{\sqrt{1-K^2}}{2} t_1 = \tan \frac{\omega_c K}{2} \left(\frac{2\pi}{\omega_m} - t_1 \right). \tag{12}$$

It is useful to introduce here the duty cycle factor, $k = t_1/T = \omega_m t_1/2\pi$. With its use, (12) becomes

$$\frac{1-K}{\sqrt{1-K^2}} \tanh \omega_c \frac{\sqrt{1-K^2}}{2} t_1 = \tan \frac{\omega_c K T}{2} (1-k). \tag{13}$$

This transcendental equation may be solved explicitly in the present case because the modulation period T is very short. Letting $x = \omega_c T$ and permitting T to approach zero, use is made of the first few terms of the series

$$\tanh x = x - x^3/3 \dots, \tan x = x + x^3/3. \tag{14}$$

When (13) is solved for $\omega_c T$ the following equation is obtained.

$$\omega_c T = \sqrt{\frac{12(K - k)}{k^3(K^3 + K - 1 - K^2) - (1 - k)^3 K^3}} \quad (15)$$

An important conclusion is deduced from (15); that is, $T \rightarrow 0$ when $K \rightarrow k$. From the physical standpoint, this signifies that when the modulating frequency ($f_m = 1/T$) is very high, the maximum frequency difference between synchronizing frequency and free-running frequency is determined by the duty cycle of the modulating (gating) signal. In particular, the quantity K , which is the quotient of this difference and the half-band of synchronization by a cw signal, approaches as a limit the numerical value of the duty cycle k .

The conclusion thus gained has a special significance in the light of a Fourier analysis of the synchronizing signal. In that analysis it is easily shown that the fundamental component of a pulse-amplitude modulated wave has an amplitude of k , the duty cycle of modulation, when the amplitude of the unmodulated wave is taken as unity. But this is exactly the limiting (maximum) half-width of the band of synchronization due to the fundamental component of the interrupted wave. Therefore, one concludes that under favorable conditions this band of synchronization due to the interrupted wave train may be calculated as though the oscillator were receiving a cw synchronizing signal whose amplitude is equal to the fundamental component of the interrupted wave train.

The above analysis applies only to the case in which the modulating frequency is high. An analysis which is applicable to all values of modulating frequency is based upon a consideration of the curves of Fig. 4. The particular item of interest which is significant to the bandwidth of synchronization is the excursion of the angle θ during the modulation period. This excursion is represented in each part of Fig. 4 by the quantity d .

It is evident that for each value of modulating period there exists some maximum value of phase excursion, d , and that the latter increases in direct proportion to the magnitude of the frequency difference, $\omega_s = \omega_1 - \omega_0$, or, representing the same thing, the ratio K . Therefore, at the edge of the band of synchronization the excursion will be a maximum and the problem evidently is that of determining the maximum possible value of d and at the same time satisfying the conditions imposed by (10).

Once K is selected, (10) can be satisfied for one, and only one, set of the quantities t_1 and t_0 . These quantities assume the status of variables in determining the excursions of phase.

Analytically, the maximum excursion of d is determined by the method of undetermined coefficients. This method includes the well-known principle that if it is desired to maximize a function $F(x_1, x_2)$ subject to the conditions that another function of the same variables is identically zero; that is, if $\phi(x_1, x_2) = 0$, then the con-

dition required to establish the maximum may be determined from

$$\frac{\partial F}{\partial x_i} + \lambda \frac{\partial \phi}{\partial x_i} = 0 \quad (i = 1, 2); \quad \phi(x_1, x_2) = 0. \quad (16)$$

In the case under discussion the variables are t_1 and t_0 . If t_1 is set equal to kT the variables become T and t_0 . These quantities appear in (10) and inasmuch as that equation is used in the analysis it is convenient to write it in the abbreviated form

$$2 \tan^{-1}(a \tanh A) - 2 \tan^{-1}(a \tanh B) = \omega_c K T (1 - k) \quad (17)$$

which has been so written by using the combined terms

$$a = \frac{1 - K}{\sqrt{1 - K^2}}, \quad b = \tan^{-1} a, \quad c = \omega_c \frac{\sqrt{1 - K^2}}{2}$$

$$A = c(t_1 + t_0) - b, \quad \text{and} \quad B = ct_0 - b. \quad (18)$$

One desires to maximize

$$F(T, t_0) = 2 \tan^{-1}(a \tanh A) - 2 \tan^{-1}(a \tanh B)$$

subject to

$$\phi(T, t_0) = 0 = 2 \tan^{-1}(a \tanh A) - 2 \tan^{-1}(a \tanh B) - \omega_c K T (1 - K).$$

The partial differentiation is carried out, employing (10) in its combined form. The most important equation evolves from the differentiation with respect to t_0 which leads to the following:

$$(\lambda + 1) \left[\frac{ac}{1 + (a^2 + 1) \sinh^2 A} \right] - \left[\frac{ac}{1 + (a^2 + 1) \sinh^2 B} \right] = 0 \quad (19)$$

which is satisfied if $A = \pm B$.

The solution $A = +B$ is trivial since the excursion of d would be zero for all values of t . If the solution $A = -B$ is employed (17) can be written

$$-4 \tan^{-1}(a \tanh B) = \omega_c K T (1 - K) \quad (20)$$

which when expressed in terms of the original parameters and variables becomes

$$-4 \tan^{-1} \left[\frac{1 - K}{\sqrt{1 - K^2}} \tanh \omega_c k T \frac{\sqrt{1 - K^2}}{4} \right] = \omega_c K T (1 - k). \quad (21)$$

This equation permits calculation of the band of synchronization for any value of the duty cycle k . It is best illustrated by an example. Assume square-wave modulation and let the scaling factor ω_c be set equal to unity. Since the duty cycle is $\frac{1}{2}$, the parameter K must be less in numerical value. Let $K = 0.35$. Then, with $k = \frac{1}{2}$ and $K = 0.35$, (21) reduces to

$$-4 \tan^{-1} (0.694 \tanh 0.174T) = 0.175T \quad (22)$$

which yields a value of T approximately 13. Then ω_m , which is $2\pi/T$, becomes 0.484. The given data and the results can more generally be stated as follows: given that the ratio of ω_m/ω_c is 0.35, it is found that the minimum permissible modulating frequency consistent with synchronized conditions in ratio to ω_c is 0.484.

Eq. (21) combined with (12) permits calculation of the band of synchronization for any prescribed condition. Data for three values of duty cycle have been computed and plotted in Fig. 5. Data for the case of square-wave modulation have been computed and plotted in Fig. 6. This latter figure also illustrates the results of experiments whose purpose was to determine the correlation of theory and practice.

An example will illustrate the quantities described in Figs. 5 and 6. Assume that an oscillator is subjected to an interrupted wave train which has a modulating frequency f_m , a duty cycle k , and frequency f_1 . The following data apply:

- f_0 = free-running frequency of oscillator = 20,000 cps.
- V_0 = grid-voltage of free-running oscillator = 1.6 v pk.
- Q = effective Q of oscillator tuned circuit = 5.
- V_1 = amplitude of synchronizing voltage = 0.2 v pk.
- k = duty cycle of interrupted wave train = $\frac{1}{2}$.

Then,

$$\omega_c = \frac{\omega_0 V_1}{2QV_0} = 500\pi \text{ rad/sec, and } f_c = 250 \text{ cps.}$$

Since the duty cycle is $\frac{1}{2}$, the value of K must be equal to or less than $\frac{1}{2}$ and f_1 must fall within the limits of $20,000 \pm \frac{1}{2} (250)$ cps. Suppose f_1 is selected to be 20,100 cps, then $K = 100/250 = 0.4$. This quantity serves as the argument which is applied on the abscissa of Fig. 6. The intersection of the vertical line $K = 0.4$ and the curve is located, and the corresponding value of the ordinate is determined. It is found that the ratio of ω_m/ω_c corresponding to this point is approximately 0.55, whence the minimum allowable value of ω_m is 275π rad/sec, or minimum $f_m = 137.5$ cps. Therefore, if synchronization is to persist under the given conditions the rate of interruption of the input signal must be equal to or greater than 137.5 cps.

The curves of Figs. 5 and 6 assume the status of boundaries between "Go-No-Go" areas. For any particular duty cycle, the region above and to the left of its applicable curve represents the area of synchronization whereas that to the right and below represents the area of no synchronization. The curve itself defines the extreme limit of synchronization and does not represent a desirable condition of operation. The index of phase modulation is large near the boundary curve but decreases as one moves up and to the left. The several

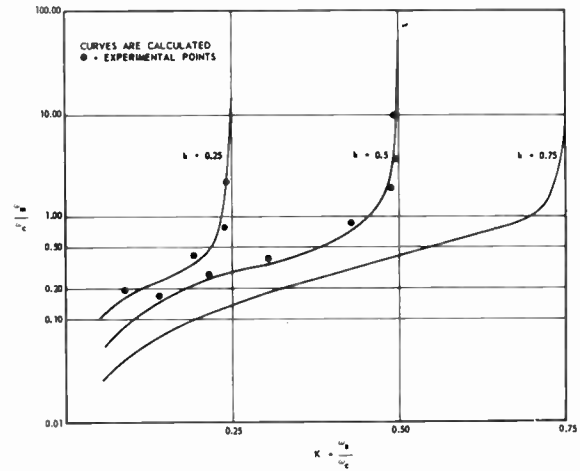
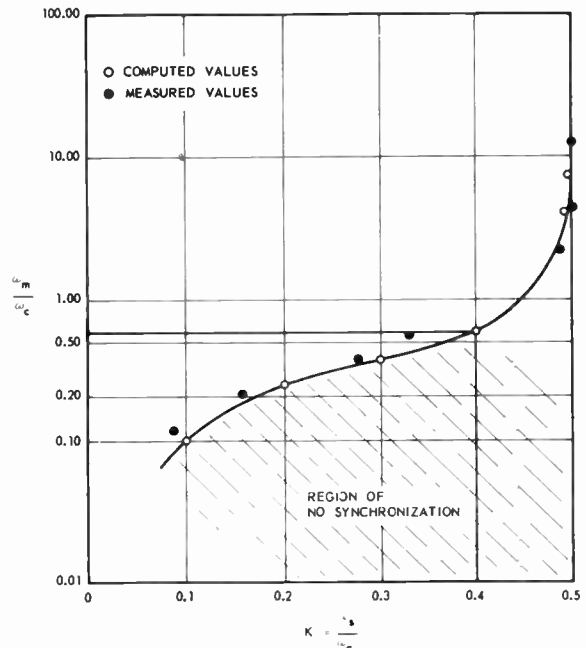


Fig. 5—Modulation frequencies required for synchronization.



Experimental Data

$f_0 = 14,600$ cps
 $2\omega_c = 2\pi \times 1000$ rad/sec.
 $2f_c = 1000$ cps.

f_m	$2f_{c1}$	$\frac{f_m}{f_c}$	$K = \frac{f_1}{f_c}$
6000	503	12	0.5
2000	502	4	0.5
1000	484	2	0.484
600	453	1.2	0.444
300	387	0.6	0.33
200	279	0.4	0.288
100	167	0.2	0.154
60	90	0.12	0.088

$2f_{c1}$ = bandwidth of synchronization when using square-wave modulated signal

Fig. 6—Modulation frequencies and bands of synchronization when signal is modulated with square wave.

magnitudes of the index of phase modulation are now employed as quantities by which to determine the frequency spectra of the synchronized oscillators.

PHASE DEVIATIONS IN THE SYNCHRONIZED OSCILLATOR

When an oscillator is synchronized by an interrupted wave train the frequency spectrum of the output will not have a simple form. A definitive approach to the determination of the spectrum is found in transient analysis and the information relative to phase variations gathered in previous paragraphs can be directly employed. A brief description of the spectrum of rectangular fm waves facilitates the analysis.

Consider the Fourier analysis of the square-wave fm signal illustrated in Fig. 7(a). Since phase is the time integral of frequency, the phase deviations corresponding to the frequency changes are as illustrated in Fig. 7(b). The instantaneous frequency is described as

$$\begin{aligned} \theta_t &= \omega_1 t + m(\pi + \omega_m t) & -\frac{\pi}{\omega_m} \leq t \leq 0 \\ &= \omega_1 t + m(\pi - \omega_m t) & 0 \leq t \leq \frac{\pi}{\omega_m} \end{aligned} \quad (23)$$

where $m = \Delta\omega/\omega_m =$ modulation index.

If the phase deviation is written as $\Delta\theta(t)$, where $\Delta\theta(t) = m(\pi \pm \omega_m t)$, then an expression for the modulated wave is

$$\begin{aligned} i &= I \sin \theta_t = I \sin [\omega_1 t + \Delta\theta(t)] \\ &= I \sin \omega_1 t \cos \Delta\theta(t) + I \cos \omega_1 t \sin \Delta\theta(t). \end{aligned} \quad (24)$$

The above function may be expanded in a Fourier series. Corrington¹⁰ has developed a general expression for the spectrum of a wave which is subject to rectangular-pulse modulation.

$$e = \frac{mE}{\pi(m-n)(mk-nk+n)} \sin k\pi(m-n) \cdot \sin(\omega + n\omega_m)t \quad (25)$$

in which k is the duty cycle, m is the modulation index, E is the amplitude of the unmodulated signal, and n is an integer.

Fundamental characteristics of the spectra resulting from square-wave fm are shown in Fig. 8. When the duty cycle is varied, results which are similar in form but which deviate in detail are found to exist.

The phase deviations shown in Fig. 7(b) are essentially the same as those found in Fig. 4(c) and are not dissimilar to the curves of Figs. 4(a) and 4(b). By defining a modulation index similar to that of (23) the tech-

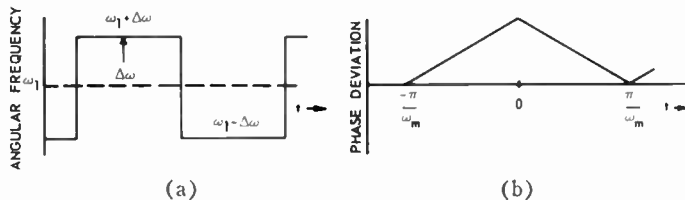


Fig. 7—Phase and frequency deviations in square wave fm.

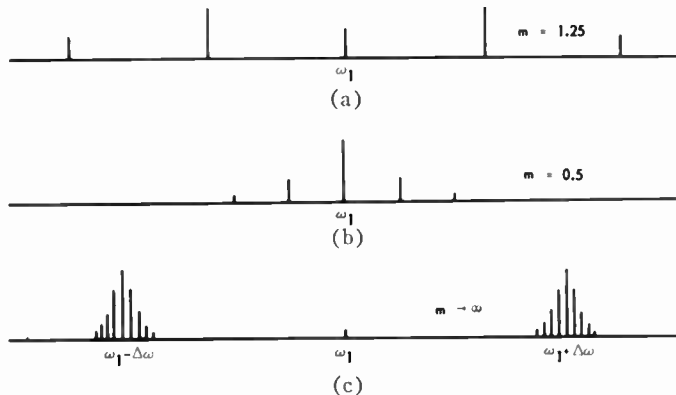


Fig. 8—Spectrum behavior of square wave fm.

niques used in developing (25) can be employed to determine the spectrum of the modulated signal illustrated in Fig. 4. When the curves of phase deviation are quite nonlinear, the Fourier analysis can be completed only by suitable methods of numerical analysis.

A modulation index similar to that introduced in (23) and one that is directly applicable to Fig. 4(c) is

$$m = \frac{\omega_s}{\omega_m} \quad (26)$$

wherein ω_s corresponds to the $\Delta\omega$ of Fig. 7.

The magnitude of the modulation index can be obtained directly from Figs. 5 and 6 because in those figures the independent variable is ω_s and the dependent variable is ω_m . Therefore each point within the area of synchronization corresponds to some specific modulation index. In the illustrative example just given, the value of ω_s was 0.4 and of ω_m was 0.55, therefore $m = 0.73$ closely.

Supporting data for this theory are given in Figs. 9 and 10. Fig. 9 shows the significant frequency content of a phase-modulated wave whose phase deviations are similar to those of Fig. 4. The data required for Fig. 9 were obtained by plotting the actual excursions of phase angle throughout a modulation cycle and then applying the methods of Fourier analysis to the resulting curves and to the curves approximated by straight lines. The spectra of Fig. 10 were obtained by experiment on synchronized oscillators. The individual frequencies of Fig. 10 correspond to those of Fig. 9, the center (largest) line representing ω_1 and the others $\omega_1 \pm \omega_m, \omega_1 \pm 2\omega_m, \text{ etc.}$

¹⁰ M. S. Corrington, "Variation of the bandwidth with modulation index in frequency modulation," PROC. IRE, vol. 35, pp. 1013-1020; October, 1947.

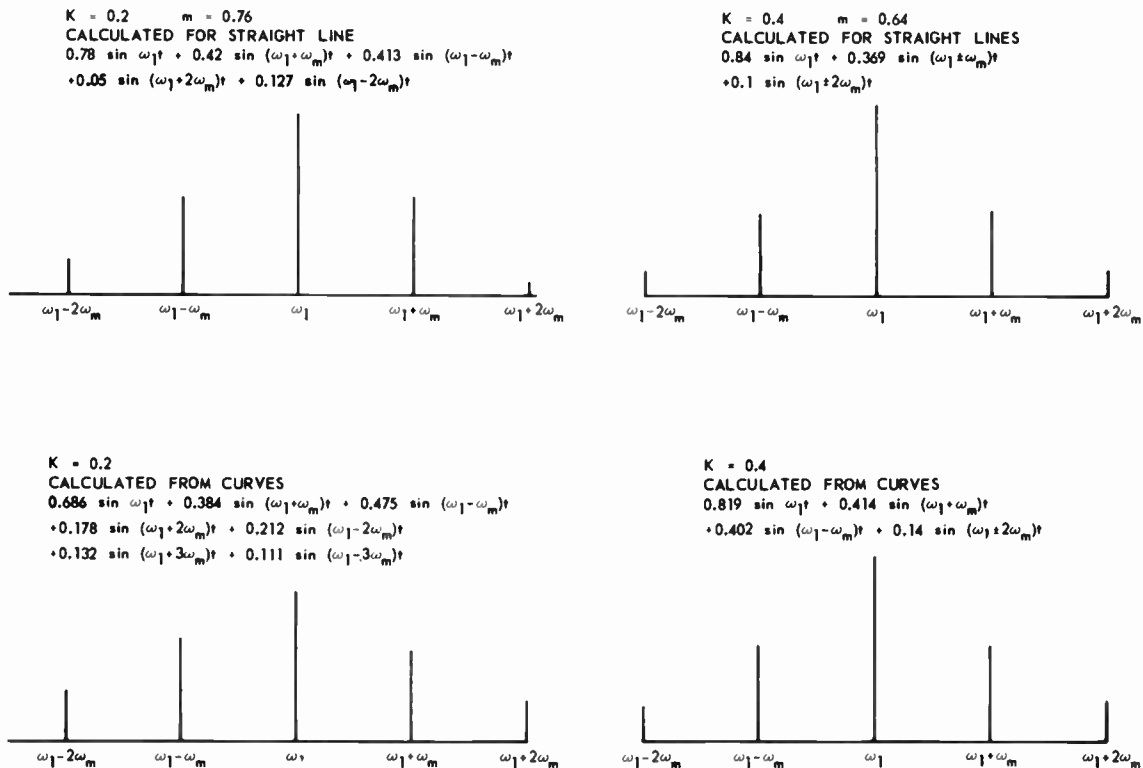


Fig. 9—Spectra of oscillator.

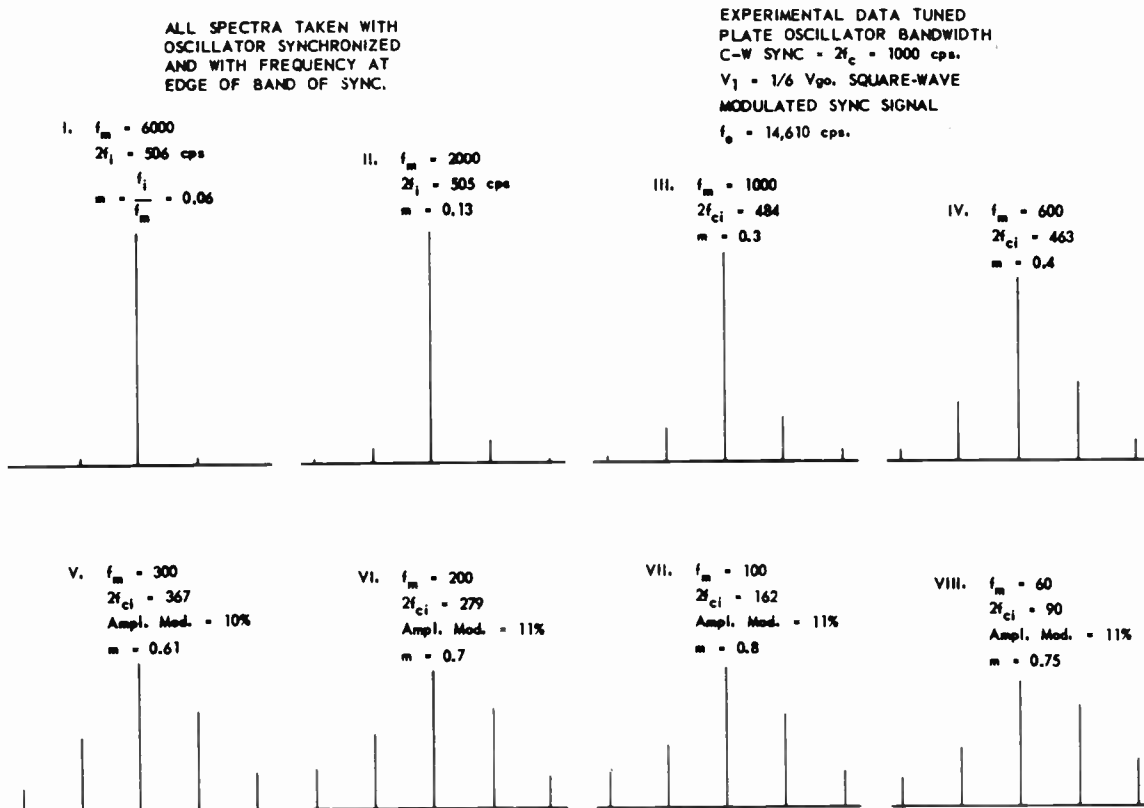


Fig. 10—Frequency spectra of oscillators synchronized by square-wave interrupted synchronized signal.

For small to moderate values of modulation index the correspondence is good. For large values of modulation index the experimentally obtained data demonstrate considerable nonsymmetry about the center frequency. This lack of symmetry is attributable in small part to the effect of amplitude modulation introduced during the modulation process but in a greater extent to a non-uniform response of the experimental oscillator about its free-running frequency. The relative effect of the amplitude modulation has been analyzed and found to be quite small but the analysis is not included for sake of brevity.

SYNCHRONIZATION BY SIDEBANDS OF INTERRUPTED WAVE TRAINS

In a preceding section an experiment was described in which it was found that an oscillator could be "locked" both to the fundamental frequency f_1 of an interrupted wave train and to the components $f_1 \pm nf_m$. The action occurring during sideband synchronization is analyzed in a manner similar to that employed for synchronization by the fundamental component. In the present case the net phase deviation may be defined by the equality

$$\int_{t=0}^{2\pi/\omega_m} \left(\frac{d\theta}{dt}\right) dt = 2N\pi \quad (N = 1, 2, 3, \dots) \quad (27)$$

which states that the "locked" condition exists between input and output if exactly N cycles are gained, or lost, per modulation cycle.

A physical illustration of the action is facilitated by a further study of Fig. 1. During synchronization by a cw signal, the vector V_1 could be thought of as an oscillating pendulum which was never permitted to gain or lose a cycle during any single modulation period. This mechanism insured that the number of cycles of the oscillator, performing as a slave, would be exactly equal to the number of cycles of the synchronizing signal, acting as a master. An equivalent mechanism is portrayed in synchronization by the first sideband of the synchronizing signal. In synchronism on the first lower sideband we may think of the slave as locked firmly to the master during the "on" time, then slipping back exactly a full cycle during the "off" time. This is a stable equilibrium in that any error will be corrected by the clamping action of the master during the "on" time.

The methods of analysis closely parallel those employed in previous sections. The equation for transient analysis becomes

$$\omega_c \int_0^{t_1} (K - \sin \theta) dt + \omega_c \int_{t_1}^{2\pi/\omega_m} K dt = 2N\pi. \quad (28)$$

In this equation θ is given by (5) rather than (4) or (4a) because the fundamental frequency of the synchronizing signal lies *outside* the band of synchronization. This is a fundamental and important difference and

should be recognized as such because, as far as known, no previous analysis has demonstrated the mechanism by which such a frequency can actually serve to synchronize an oscillator.

The integration of (28) is performed and after considerable simplification the following equation is produced.

$$\begin{aligned} & 2 \tan^{-1} \left\{ \frac{K-1}{\sqrt{K^2-1}} \tan \left[\omega_c \frac{\sqrt{K^2-1}}{2} (t_1 + t_0) \right. \right. \\ & \qquad \qquad \qquad \left. \left. - \tan^{-1} \frac{K-1}{\sqrt{K^2-1}} \right] \right\} \\ & - 2 \tan^{-1} \left\{ \frac{K-1}{\sqrt{K^2-1}} \tan \left[\omega_c \frac{K^2-1}{2} t_0 \right. \right. \\ & \qquad \qquad \qquad \left. \left. - \tan^{-1} \frac{K-1}{\sqrt{K^2-1}} \right] \right\} \\ & = 2N\pi - \omega_c K T (1 - k). \end{aligned} \quad (29)$$

Again, as in previous sections, it is necessary to determine the maximum allowable excursion of the phase angle consistent with a condition of synchronization. Using the method of undetermined coefficients, one obtains

$$4 \tan^{-1} (a \tan B) = 2N\pi + \frac{2BK}{ck} (1 - k) \quad (30)$$

in which the quantities a , B , and c are as defined in (18).

Finally, since $B = -ct_1/2 = -ckT/2$, the equation may be expressed in terms of T . Values of T have been computed using (30), square-wave modulation and various values of K . Corresponding values of ω_m have been computed ($\omega_m = 2\pi/T$), after which it has been possible to evaluate ω_{1sb} , the half-band of synchronization by the first sideband. A simple linear relationship exists among ω_0 , ω_1 , ω_m , and ω_{1sb} as may be observed in Fig. 11. This figure has been introduced as an aid in

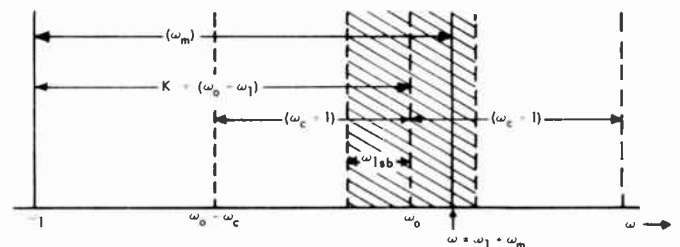


Fig. 11—Angular frequencies involved in synchronization by first sideband.

visualization of the various frequencies involved in the synchronization process. Here ω_1 has been adjusted so that its first upper sideband, $\omega_1 + \omega_m$, lies within the band of synchronization. The half-band of synchronization by a cw signal, ω_c , has been given the value of unity so

that K equals simply $\omega_0 - \omega_1$. Now, if the sideband $\omega_1 + \omega_m$ lies at the edge of the cross-hatched area it is evident that

$$\omega_{1sb} = \omega_0 - (\omega_1 + \omega_m) \tag{31}$$

and this is the relationship employed in the evaluation of ω_{1sb} .

The results of the calculations appear in Table I and in Fig. 12. The table lists the computed values and Fig. 12 illustrates the width of this "band of synchronization" by showing the ratio of ω_{1sb} to ω_c when K is varied. Values of ω_{1sb} have not been computed for magnitudes of K which are equal, or approximately equal, to unity because the synchronization equation is undefined in this immediate vicinity.

TABLE I
WIDTH OF BAND OF SYNCHRONIZATION DUE TO FIRST
SIDE BAND OF INTERRUPTED WAVE TRAIN

$K = \omega_1 - \omega_0$ (when $\omega_c = 1$)	T	$\omega_m = \pi/T$	$\omega_{1sb} = K - \omega_m$
10	0.65	9.68	0.32
9	0.725	8.67	0.33
6	1.11	5.67	0.33
3	2.38	2.64	0.36
2	3.9	1.62	0.38
0.95	12.8	0.49	0.36
0.85	13.33	0.47	0.33
0.75	13.6	0.46	0.29

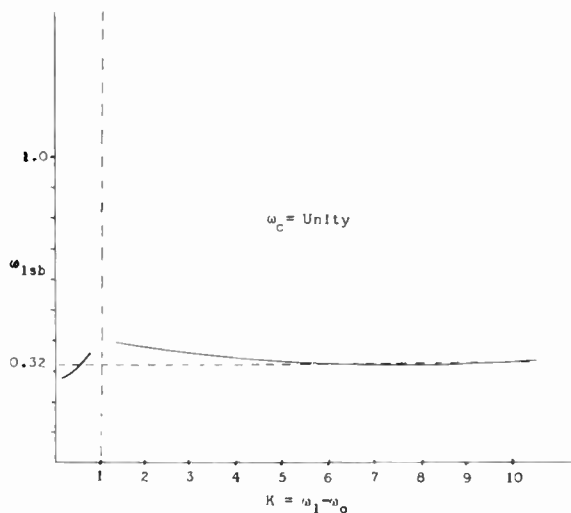


Fig. 12—Width of band of synchronization due to first sideband of interrupted wave train.

A very significant result of the computations, strikingly corroborated by experimental results, is the clustering of the calculated ratios of ω_{1sb}/ω_c about the value of 0.32. It is concluded that irrespective of the value of K (or what is the same, the position of ω_1) there always exists a band of synchronization due to the frequency $(\omega_0 - \omega_1) - \omega_m$ whose width is always a fixed fraction of

ω_c . In the example, employing square-wave modulation of the synchronizing signal, the fixed fraction is 0.32.

The significance of the ratio 0.32 follows from the Fourier analysis of a cw signal which is interrupted by a rectangular pulse. The resultant signal has a spectrum whose envelope is given by $(\sin nk\pi)/nk\pi$. This fraction always has a value of unity when n is zero, but the relative amplitudes of the sidebands ($n = 1, 2, 3, \dots$) depend upon the duty cycle. For square-wave modulation ($k = \frac{1}{2}$) the first sideband ($n = 1$) has a relative amplitude of 0.32. Therefore, comparing this figure to the mean of Table I it may be concluded from this example that: *The synchronizing action of the "first sideband" of the synchronizing signal may be computed from steady-state theory by calculating the bandwidth of synchronization due to a cw signal whose amplitude is equal to the amplitude of the first sideband of the actual synchronizing signal.* The same logic may be extended to other sidebands.

FREQUENCY SPECTRUM OF OSCILLATOR SYNCHRONIZED BY SIDE BANDS OF INJECTED SIGNAL

The frequency spectrum of an oscillator which has been synchronized by a sideband of an interrupted wave train can be computed in the same manner as was employed in the case of synchronization by the fundamental. The results of computation are illustrated in Fig. 13. The spectrum of the synchronizing signal is shown at the upper right and the spectra of the output of the oscillator, represented for various values of K , are illustrated in the other three drawings in the same figure.

The conclusions gained from the figure relate primarily to the relative amplitudes of the various frequency components as a function of the spacing between sidebands. When K is large, so that the nearest unused sideband lies remote from the band of synchronization, almost all of the oscillator energy is concentrated at the desired frequency. When K is small, so that the fundamental frequency or other undesired component lies close to the band of synchronization, considerable phase modulation occurs and the undesired components in the output become relatively large.

Experimental results are illustrated in Fig. 14, with the spectrum of the synchronizing signal shown at the top. The effects of different duty cycles are shown as well as the effects of different ratios of input voltage V_1 to free-running oscillator voltage (designated as $V_{\theta 0}$ in this figure).

The computations by which to compare exactly calculated and experimental values of the frequency components are not included for sake of brevity. However, results of tests were found to compare favorably with the derived data. In practice it has been found possible to maintain the largest undesired component at a level of about 40 db below that of the desired component.

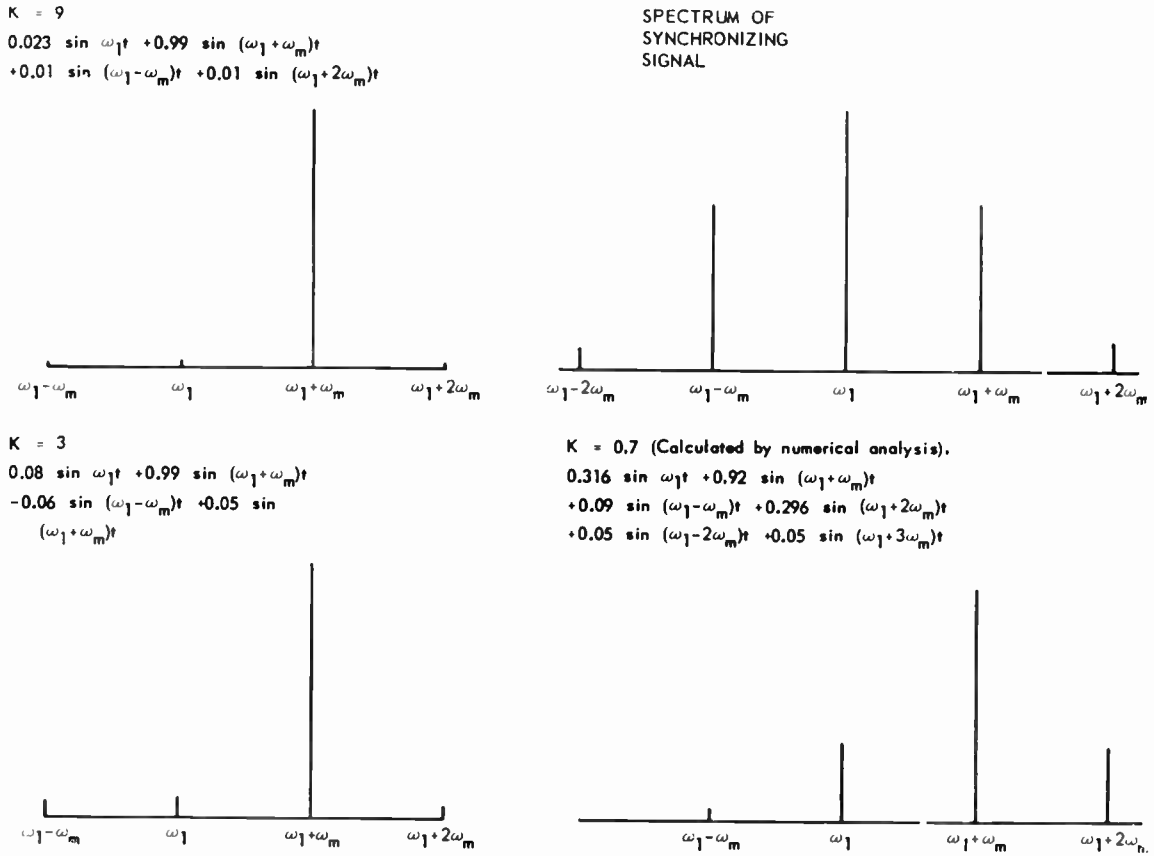


Fig. 13—Spectra of oscillator synchronized by sidebands of interrupted wave train, computed values.

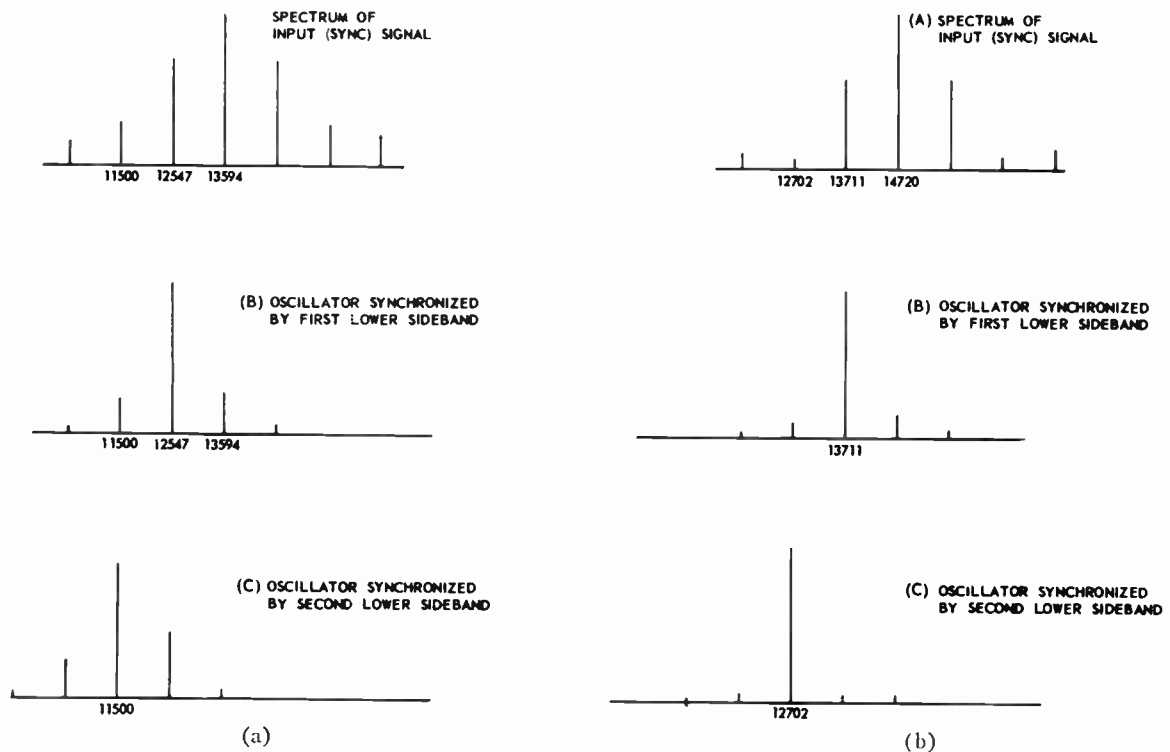


Fig. 14—Spectra of oscillator synchronized by sidebands, experimental values. (a) Duty cycle $K = \frac{1}{3}$, $V_1/V_{\theta 0} = 0.9$, $f_m = 1047$ cps. (b) Duty cycle $K = \frac{1}{2}$, $V_1/V_{\theta 0} = \frac{1}{6}$, $f_m = 1009$ cps.

APPLICATIONS OF THE SYNCHRONIZED OSCILLATOR

A number of applications of an oscillator which is synchronized by an interrupted wave train can be cited, but a device which gains considerable flexibility by the process is one which employs "detent" tuning, a step-switching procedure. In the present case, the steps controlled are steps in frequency and these have a separation which is approximately equal to the spacing between two sidebands in the spectrum of the synchronizing signal. The action of the switch is to tune the oscillator, in steps, to free-running frequencies which lie within a band of synchronization. The proper sideband of the synchronizing signal, falling within this band, then "locks" the oscillator to its prescribed frequency.

If an oscillator is to be synchronized by sidebands of an interrupted wave train, a preferred signal is one which has frequency components which are of equal magnitude, or more particularly, one in which desired components are equal in magnitude and all others are of zero amplitude. Although this form is not strictly attainable, a reasonable approximation of the ideal can be produced. The interested reader is referred to a summary of various waveforms¹¹ and their respective frequency components in which it is shown that damped oscillations of the proper decrement have spectra closely approximating the desired ideal.

A spectrum of this type has been successfully applied by the author and a colleague as a means of obtaining several crystal-controlled frequencies from one crystal. The circuit is shown in Fig. 15. In this oscillator system the synchronizing frequencies are harmonics of a 100-kc crystal-controlled oscillator. The spectrum generator is centered about the pentode whose cathode, control grid, and screen grid form the three vacuum tube elements of the crystal-controlled oscillator. The 2-mh peaking coil in the plate circuit is shock excited by the plate-current pulses but is damped by a series combination of a 1K resistor and a germanium diode. The output of the plate-circuit network consists of damped waves whose spectrum has frequency components which are multiples of 100 kc and which have nearly uniform amplitude over the range of 100 kc to 3 mc (or higher). In this particular example, frequency components 1.5, 1.6, . . . 2.4, 2.5 mc inclusive are of greatest interest because the LC oscillator associated with V_2 is adjusted to tune, in steps, over the approximate range of 1.5–2.5 mc.

The LC oscillator is step-tuned by means of appropriate capacitors in shunt with L_2 to the approximate frequencies 1.5, 1.6, . . . , etc., mc. The appropriate synchronizing component of the input from V_1 then locks the LC oscillator to the exact multiples of 100 kc. The voltage at the output (arrow) then contains the desired crystal-controlled frequency and contains in addition, but in greatly reduced amplitude (about 40 db

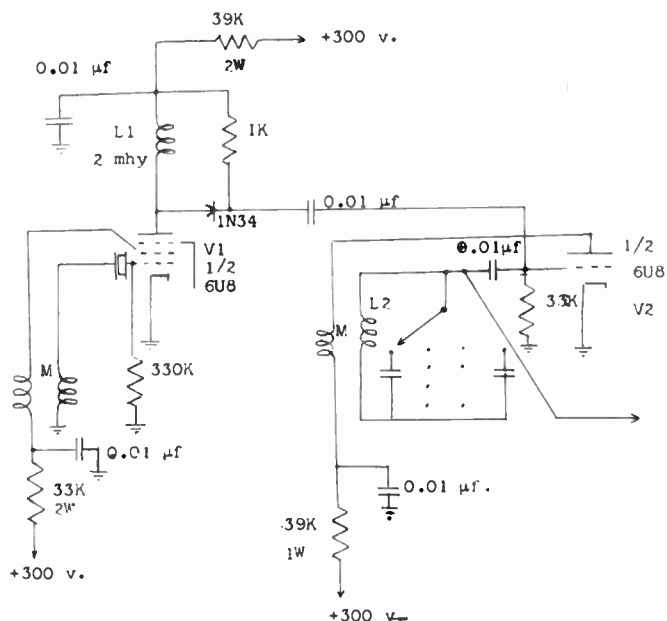


Fig. 15—Spectrum generator and synchronized oscillator.

down), the nearest undesired components. Other components are so small as to be considered negligible.

An oscillator of this type provides a convenient device for use in conjunction with "crystal-saving" techniques. If the 40-db sideband rejection noted above is found to be insufficient for certain applications, two oscillators similar to those of V_2 may be tied in tandem so as to double the apparent selectivity.

At higher frequencies it may be desirable in some cases to actually interrupt (gate) the output of a crystal-controlled oscillator by another crystal-controlled oscillator of much lower frequency. In one experiment a 6-mc crystal oscillator was gated by a 100-kc crystal oscillator and the resultant signal was employed as a synchronizing signal on a tunable LC oscillator. Synchronization was effected at frequencies of 5.7, 5.8, 5.9, 6.0, 6.1, 6.2, and 6.3 mc, respectively, these corresponding to the first three lower sidebands, the fundamental, and the first three upper sidebands of the synchronizing signal.

In conclusion, it may be stated that the phenomenon of synchronization by interrupted waves is one which can find considerable practical application. In addition to the "detent" oscillator just described, various possible but untried applications include frequency division by nonintegral numbers, frequency multiplication at extended levels, and frequency following of fm signals which have been subjected to undesired severe amplitude modulation. When the synchronizing signal is gated by a rectangular pulse, the band of synchronization and the index of phase modulation can be determined from the equations and curves of this paper. When the synchronizing signal is of less simple form, the synchronizing action can be predicted if the spectrum of the signal is known or can be measured.

¹¹ *Hewlett-Packard J.*, Hewlett-Packard Co., Palo Alto, Calif., vol. 5; November-December, 1954.

Theory and Operation of Crystal Diodes as Mixers*

G. C. MESSENGER†, ASSOCIATE MEMBER, IRE, AND C. T. MCCOY†, SENIOR MEMBER, IRE

Summary—The electrical parameters (barrier resistance, barrier capacity, and spreading resistance) of a crystal diode are quantitatively related to its fundamental physical properties and geometrical construction.

The effects of these parameters on conversion loss at uhf and microwave frequencies are discussed, with particular reference to diodes made from *n*-type germanium and *p*-type silicon.

Semiconductor materials may be compared for their mixer sensitivity potentialities, by use of the figure of merit $N^{1/2}b/\epsilon^{1/2}$ (N is carrier concentration in cm^{-3} , b is carrier mobility in $\text{cm}^2/\text{volt sec}$, ϵ is the dielectric constant) which is herein derived. It shows that *n*-type germanium is a better mixer material than *p*-type silicon. A method for minimizing the conversion loss of any given semiconductor is developed.

Application of the above method produced germanium diodes having conversion losses which attained the theoretical minimum and silicon diodes having losses 0.8 db above the minimum.

It is pointed out that the noise temperature of a mixer is dependent on the conversion loss, and that it rapidly becomes less important as conversion loss is decreased.

The optimum receiver noise figure is shown to occur quite close to the operating conditions which minimize conversion loss.

It is shown also that the temperature dependency of germanium and silicon mixer diodes are nearly the same.

The experimental application of the information in this paper resulted in an *X*-band receiver with an over-all noise figure of 6 db.

I. INTRODUCTION

THE ever-widening search for improved sensitivity in receivers at successively higher frequencies was given impetus by World War II developments in semiconductor rectifiers [1]. The "cat whisker" crystal came out of its erratic, mystic stage into a more proper scientific phase wherein the physics of superheterodyne mixer crystals became qualitatively understood. The advent of single-crystal metallurgy in germanium and of the technique for measuring receiver noise figure in absolute terms allowed for the first time the expression of a quantitative relationship between noise figure and the fundamental physical constants of semiconductors. This paper presents this theoretical relationship and its experimental verification. The application of the relationship to germanium and silicon mixer diodes or, for that matter, to any semiconductor diode, enables one to predict the lowest possible noise figure. The experimental noise-figure data have been recorded principally at *X* band and uhf bands. The accuracy of the noise-figure relationship is estimated to be about ± 0.3 db at *X* band. At frequencies higher than *X* band, the accuracy of the relationship becomes progressively poorer.

* Original manuscript received by the IRE, July 20, 1956; revised manuscript received, June 3, 1957.

† Res. Div., Philco Corp., Philadelphia, Pa.

II. NOISE FIGURE PARAMETERS

Friis [2] was one of the first to show that a superheterodyne-receiver noise figure could be broken down into three measurable parameters, phenomenological rather than hypothetical in nature, which do not explain, but divide, the problem into parts which can be attacked separately. These parameters, as well as noise figure, were defined as dimensionless and absolute. Their mutual relationship, as defined by Friis, is expressed in

$$F_r = L_x(t_x + F_{it} - 1). \quad (1)$$

F_r is receiver noise figure defined as the ratio of available signal-to-noise at the *input* of the receiver to available signal-to-noise at the *output* of the receiver. Signal and noise are measured in units of power; the ratios are dimensionless.¹

When the signal termination, G_s , and image termination, G_i , are made identical, the mixer is specifically termed *broad band* and conversion loss is given the symbol L_0 (Figs. 1 and 2). When G_i and G_s are not identical, the mixer is labelled *narrow band*. Conversion loss is symbolized by L_1 and G_i is short-circuited and L_3 when G_i is open-circuited.

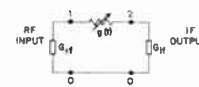


Fig. 1—Schematic representation of a mixer as a time-varying conductance between the radio-frequency input and the intermediate-frequency output terminals.

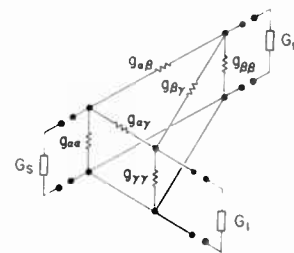


Fig. 2—The equivalent linear network of a circuit using a crystal mixer.

Simple broad-band mixer measurements allow a good evaluation of the noise-figure potentialities of a diode. The various narrow-band improvements, calculable from broad-band measurements, become significant only as broad-band performance improves. In this paper therefore, crystal physics developments are related to broad-band potentialities only.

¹ Sometimes F_r , L_0 , and F_{if} are expressed in decibels equal to ten times the common logarithm of the power ratio. In this article all values will be expressed in power ratio unless the word decibel is specifically appended.

III. CONVERSION LOSS, L_0 , IN A CRYSTAL

The barrier resistance, R_b , in a crystal diode's equivalent circuit (Fig. 3) permits the desired time-varying conductance. The undesirable, inherent parasitic elements, spreading resistance, R_s , and barrier capacity, C_b , increase conversion loss above that caused by the barrier resistance alone. They act as lossy transformations inserted between the mixer network in Fig. 2 and each of the three terminations. When each element of the equivalent circuit is quantitatively related to basic physics parameters, the conversion loss, L_0 , will also thereby be quantitatively related [4].

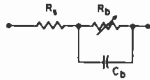


Fig. 3—Equivalent circuit for a semiconductor mixer crystal.

IV. NOISE TEMPERATURE, t_x

The mixer-noise temperature can come from two sources; tube noise accompanying the generation of the local-oscillator signal, and noise generated within the crystal diode by the mixing process.

The local-oscillator noise can be completely eliminated, both in theory and practice, by narrow band-pass filters, or with balanced mixing. This paper assumes that all local oscillator noise has been eliminated.

The spreading resistance and barrier resistance (Fig. 3) both generate noise as functions of the instantaneous current flowing through them by the action of the local-oscillator and bias voltages. For the lowest value for receiver noise figure, F_r , the effects of R_s , R_b , bias, and local-oscillator operating conditions on L_0 and t_x must be considered simultaneously. As can be seen from (1), the importance of noise temperature, t_x , depends on its magnitude relative to the excess intermediate-frequency noise figure ($F_{if}-1$). The mixer noise temperature, t_x , decreases monotonically with higher intermediate frequencies.

V. EXCESS INTERMEDIATE-FREQUENCY NOISE FIGURE ($F_{if}-1$)

Eq. (1) makes it clear that achieving a lower mixer noise temperature, t_x , and reducing the excess intermediate-frequency noise figure ($F_{if}-1$), will, in turn, reduce receiver noise figure. With the development of better tubes (having higher transconductance), ($F_{if}-1$) can be indefinitely reduced. For all tubes, ($F_{if}-1$) is in linear proportion to frequency. There is, therefore, a compromise intermediate frequency (generally near 30 mc) which minimizes the sum ($t_x + F_{if}-1$).

VI. SCOPE OF CRYSTAL PHYSICS DEVELOPMENT

It will be shown that the lowest possible value of L_0 is determined only by barrier resistance which is inherently identical for all crystal rectifiers. The least possible degradation in conversion loss above this theoret-

ical minimum is due to the two parasitic elements, spreading resistance, R_s , and barrier capacity, C_b , which are functions of crystal physical parameters. The minimum theoretical degradation will be shown to be related quantitatively to only three physical parameters, area of whisker wire contact, semiconductor carrier concentration, and carrier mobility. Though experimental verification of the theory was limited to n -type germanium and p -type silicon because of the greater body of metallurgical experience with them, the findings discussed are applicable to any semiconductor.

It will be shown in Section XI that the minimum value of mixer noise temperature can be calculated by assuming that all rectifier noise except barrier shot noise is eliminated. Shot noise taken through the mixing process produces mixer noise temperature, t_x . This, as also will be shown, is minimized simultaneously with minimization of conversion loss.

There are unnumbered metallurgical circumstances which can cause conversion loss, L_0 , and noise temperature, t_x , to be higher in experimental crystal diodes than values predicted from the mixer operating conditions and the elemental physical constants. No combination of circumstances yields values of L_0 and t_x lower than those predicted by the theory. It is a happy feature of n -type germanium that these extraneous fabrication and metallurgical problems have been largely eliminated.

From the work of previous investigators, which was confirmed by our own investigations, two conclusions were reached: 1) germanium or silicon of very low resistivity must be used in the fabrication of low-noise-figure diodes, and 2) the radius of the "point contact" must be kept small, especially at very high frequencies. The reader must therefore bear in mind that the resistivity range examined in detail was from 0.05 ohm-cm to 0.001 ohm-cm. The lower limit was determined by loss of rectification primarily due to tunneling or avalanche breakdown of the barrier. The contact radii investigated were all less than 2×10^{-3} cm. Most of the experiments used a standard radius of 4×10^{-4} cm, which was the best compromise between mechanical stability, burnout, and improved noise figure at X band.

VII. THE RELATIONSHIP BETWEEN ELECTRICAL AND PHYSICAL PARAMETERS

This section will express the relationship between the electrical elements of the mixer-crystal equivalent circuit, the area of the point-contact interface, and the properties of the bulk semiconductor. The actual equations have been derived previously elsewhere [5]. Hence, to verify their applicability to point-contact rectifiers in the extremely high range of semiconductor conductivities used in mixer crystals, only the experimental information obtained will be presented. As a by-product of this discussion, the reader will gain some familiarity with the magnitudes of capacitance and resistance in the equivalent circuit.

The performance of the mixer diode is described in terms of the following parameters of its equivalent circuit (Fig. 3):

- 1) Barrier resistance, R_b ;
- 2) Spreading resistance, R_s ;
- 3) Barrier capacity, C_b .

The value of spreading resistance, R_s , varies from about 3 to 20 ohms in germanium and from about 15 to 75 ohms in silicon. The barrier capacity, C_b , using a contact radius of 4×10^{-4} cm, is about $0.3 \mu\mu\text{f}$ at X band for both germanium and silicon. Fig. 4 is a typical i - v curve (i being the current through the crystal and v the applied voltage across it) of a germanium crystal diode from which the voltage dependence and order of magnitude of the nonlinear barrier resistance, R_b , are apparent. The components, R_b , R_s , and C_b , will now be related to the physical properties of the semiconductor and the geometry of the point contact in order to furnish a causal chain linking conversion loss to the basic electrical properties of the semiconductor.

Barrier Resistance

Eq. 2 describes barrier resistance in terms of the i - v characteristic of any semiconductor diode [6].

$$i = \frac{1}{2} \pi a^2 N q V e^{-q\Phi_0/kT} (e^{qV/kT} - 1), \quad (2)$$

Symbols are defined as follows:

- a = radius of contact, cm,
- N = carrier density, cm^{-3} ,
- q = charge on an electron, 1.6×10^{-19} coulomb,
- T = temperature, $^\circ\text{K}$,
- V = voltage across barrier, volts,
- v = electron velocity, cm/sec,
- K = Boltzmann's constant,
- Φ_0 = barrier height, volts.

The simplest empirical equation which adequately describes the dc characteristic of mixer diodes in the range of interest for mixing applications is

$$i = A(\epsilon^{\alpha(v-iR_s)} - 1) + B(\epsilon^{-\beta v} - 1) \quad (3)$$

where A , α , B , β , and R_s are empirical constants, and v is the voltage across the barrier. No attempt so far has been quantitatively successful in deriving more general, fundamental equations and/or explaining the second term in (3) by considering image lowering, quantum-mechanical tunneling [8] models of the barrier. Explanation of this equation has also been attempted in terms of minority-carrier injection; however, these arguments probably can not be extended to diodes as highly doped as mixer crystals.

In evaluating the crystals with very high carrier density, approximately $8 \times 10^{18} \text{ cm}^{-3}$, several crystals were observed which had nearly lost their ability to rectify. The i - v characteristic of one of these is shown in Fig. 5. The exponential reverse characteristic of rectification, due to tunneling of the barrier, is in the opposite

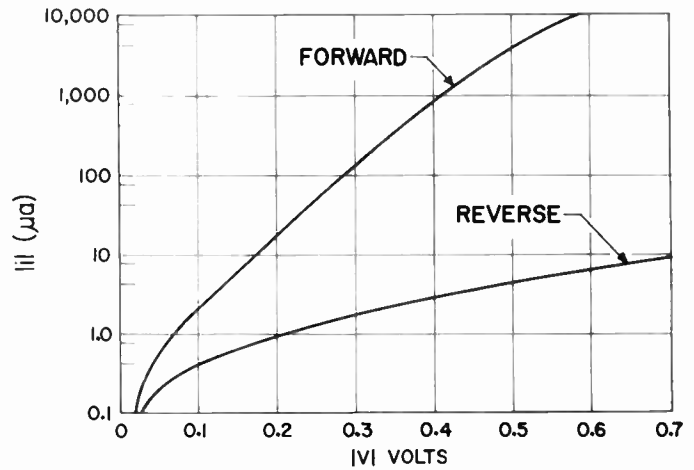


Fig. 4—Current-voltage characteristic of a 1N263 diode.

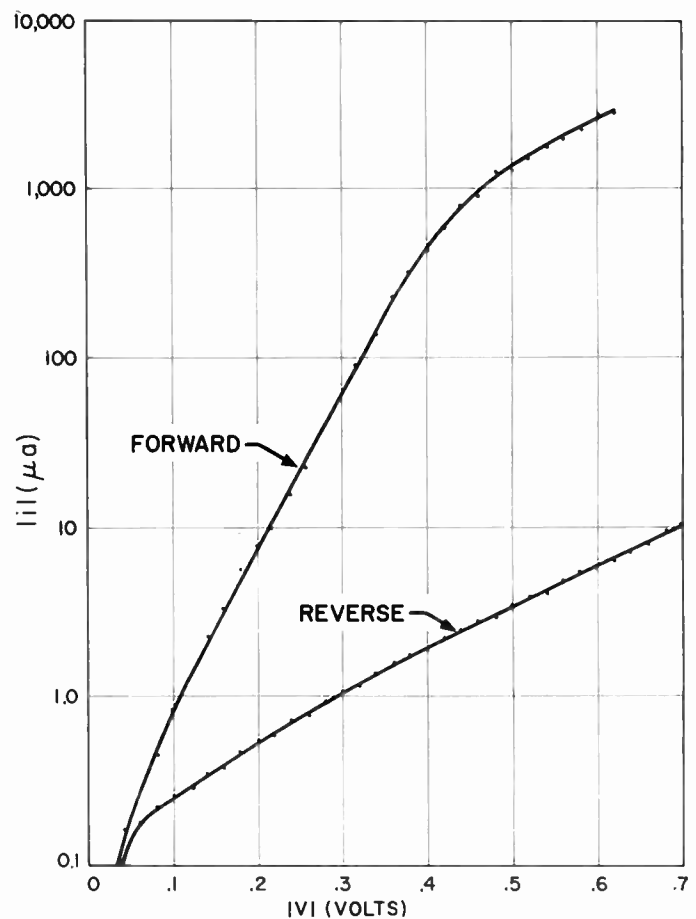


Fig. 5—Current-voltage characteristic of a highly-doped germanium crystal showing tunneling in the reverse direction

direction to normal rectification. Here the value of β , as defined by (3), is 5.3, and values as high as 9 have been observed. Attempts to make diodes with doping densities greater than 10^{19} cm^{-3} failed; apparently, a carrier density of about 10^{19} cm^{-3} is the upper limit because the barrier becomes too thin to support rectification.

The exponential form, common to both (2) and (3), contains the nonlinearity essential for conversion. The

leakage component, defined by the second term on the right side of (3), has a negligible effect on conversion loss as long as the ratio of forward to reverse current is greater than 10 at an absolute value of 0.5 volt of crystal bias. This arbitrary limit insures that extra loss due to the reverse shunt resistance will be less than a decibel [9]. Under these conditions, A , α , and R_s are determined by fitting (4) to the forward part of the i - v characteristic of Fig. 3.

$$i = A(e^{\alpha(v - iR_s)} - 1). \quad (4)$$

The curve of Fig. 4 has the fitted constants: $A = 0.30$ μ amp, $\alpha = 19$ volts $^{-1}$, $R_s = 6$ ohms. The nonlinear barrier resistance, R_b , described by (4), is determined by the empirical constants A and α and by the operating conditions (local-oscillator peak voltage, e_1 , and the dc bias, e_0).

Using (2) and (4), two useful associated equations may be written by comparing coefficients and exponents.

$$A = \frac{1}{2} \bar{v} \pi a^2 N q e^{-q\Phi_0/kT} \quad (5)$$

$$\alpha = \frac{q}{kT} = 39 \text{ volts}^{-1} \text{ at } 300^\circ \text{ K.} \quad (6)$$

A value for Φ_0 can be calculated from (5) either by direct substitution from a single measurement of A or by using a ratio at two different temperatures which reduces the number of parameters.² Both methods were used to provide a cross check, yielding a value of $\Phi_0 = 0.30$ volt for both germanium and silicon. Experimentally, (6) turns out to be an upper limit with α generally varying between 10 and 30 volts $^{-1}$ at a temperature of 300° K. Several possible explanations for this have been advanced. One is in a multicontact theory [10], another is a surface layer drop theory [11].

Spreading Resistance

The spreading resistance is constant to a good first approximation over the range of voltages, -0.5 v to $+0.5$ v , used in a typical mixer. When a point contact is made to a flat semiconductor surface, the interface is approximately circular. In this case [12],

$$R_s = \frac{1}{4\sigma a} = \frac{1}{4aNqb}, \quad (7)$$

where σ is the conductivity in ohm $^{-1}$ cm $^{-1}$, a is the contact radius in cm, N is the carrier density/cm 3 , q is the charge on the carrier (1.6×10^{-19} coulomb), and b is the carrier mobility in cm 2 /volt-sec. Eq. (7) was verified experimentally for welded-contact germanium diodes which conducted over the whole contact area. Using material with a resistivity of 0.012 ohm-cm, several diodes were made using platinum whiskers which were

pulsed to obtain alloying with negligible penetration. This method formed contact radii of 0.0010 cm. The agreement between measured and calculated values of R_s can be seen in Table I.

TABLE I
CORRELATION BETWEEN CALCULATED AND MEASURED
VALUES OF SPREADING RESISTANCE

Unit	ρ	a	R_s calc.	R_s meas.
1	0.012	0.001	3	3.5
2	0.012	0.001	3	4.0
3	0.012	0.001	3	3.0
4	0.012	0.001	3	3.0
5	0.012	0.001	3	3.5

In the doping range of less than 10^{16} carriers/cm $^{-3}$, injection effects are not negligible and (7) must be modified to include the decrease in resistivity contributed by injected holes.

In most mixer crystals, some of the crystal area under the whisker point does not conduct [13], and (7) defines the lower limit of R_s . Hence,

$$R_s > \frac{1}{4aNqb}. \quad (8)$$

When titanium wire is used on germanium or tungsten wire is used on silicon, R_s varies from one and one half to three times the value indicated by (7). One of the effects of "forming"³ in germanium crystals, and "tapping"⁴ in silicon crystals is to bring the value of R_s down nearer the lower limit indicated by (7). These procedures establish a more intimate contact between the wire and the semiconductor.

With this in mind, Fig. 6 shows the variation of R_s with resistivity ($1/Nqb$) for a contact radius, $a = 4.0 \times 10^{-4}$ cm using a formed titanium whisker on n -type germanium [14]. The position of the theoretical curve lies below the experimental curve for low values of a as ascribed to the inequality in (8).

The fact that the experimental curve lies below the theoretical curve at higher values of resistivity is ascribed to injection of minority carriers. The extent of this modification was investigated and determined to be negligible below 0.01 ohm-cm by the following experiments.

Fig. 7 shows the voltage pulse created by a constant-current 10- μ sec pulse applied to an average 1N263. This produced a plateau-voltage level of 1.1 volts. At this point, barrier resistance is negligible. The nearly flat top of the pulse proves, therefore, that the spreading resistance is not being modulated to more than 5 per cent by hole injection, at least at frequencies below 200 mc which was the upper limit of the measuring equip-

³ "Forming" is done by discharging of electrical energy through the point contact after it has been established mechanically; this improves the mixer performance.

⁴ "Tapping" is done by mechanically shocking the unit after the contact has been established to improve the mixer performance.

² $\Phi_0 = \frac{kT_2T_1}{q(T_1 - T_2)} \ln \left[\frac{A_1}{A_2} \left(\frac{T_2}{T_1} \right)^{1/2} \right]$.

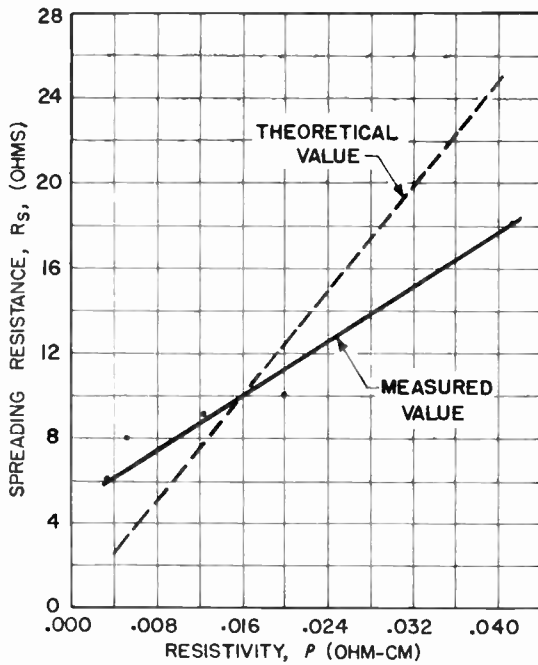


Fig. 6—Spreading resistance vs resistivity for a titanium contact on germanium.

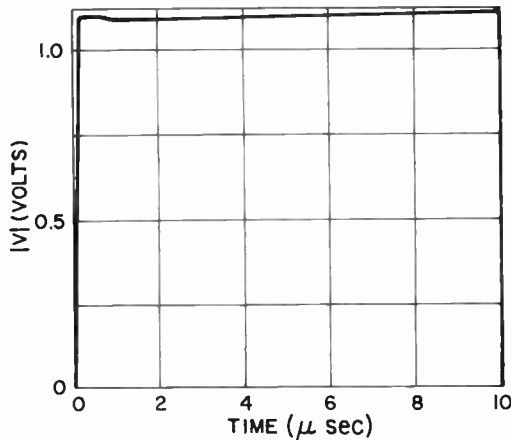


Fig. 7—Response of a 0.003-ohm-cm mixer diode to a current pulse.

ment. By comparison, Fig. 8 is a picture of a 1-ohm-cm point contact in which the modulation of R_s is apparent. Where modulation exists, the measured dc spreading resistance is much lower than the spreading resistance at radio frequencies. At radio frequency, the holes do not have time in a normal half-cycle to enter the base and modulate resistivity. For resistivities less than 0.01 ohm-cm, the range of primary importance in mixing, (7) is a reasonably correct statement of the variation of R_s with carrier density when viewed in the light of the above data.

Further indication that modulation of R_s is not present to any large extent is given by the fact that there is no measurable decrease in rectification efficiency in these diodes up to the X-band region. If injection occurred, decrease in rectification efficiency would be seen when the half-cycle time of the applied ac voltage was

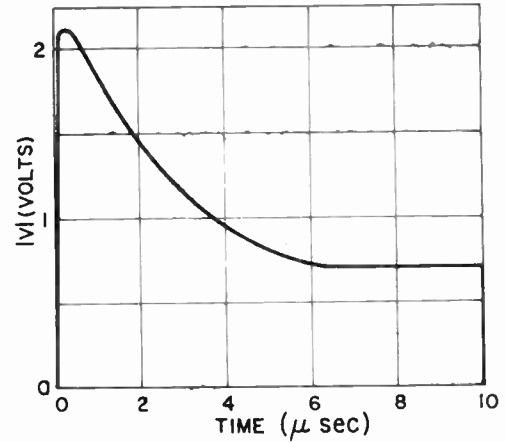


Fig. 8—Response of a normal 1-ohm-cm diode to a current pulse.

insufficient to allow for modulation of the bulk resistance by minority carrier diffusion.

Barrier Capacity

The voltage dependency of the barrier capacity is defined by

$$C_b = \frac{\pi a^2 (\epsilon q N)^{1/2}}{2(\Phi_0 - V)^{1/2}} \tag{9}$$

Here, ϵ is the dielectric constant in farads per cm, Φ_0 the height of the barrier in volts, and V the voltage across the barrier. The value of Φ_0 is 0.30 volt. This formula will set upper limits for C_b because of the probability that not all of the whisker area is in intimate contact with the crystal [17].

Measurements of capacity as a function of voltage for high-frequency diodes have been reported by Mataré [18]; they agree closely with the form of (9).

$$\text{(germanium)} \quad C_b = 2.1 \times 10^{-15} N^{1/2} a^2 \tag{10}$$

$$\text{(silicon)} \quad C_b = 1.6 \times 10^{-15} N^{1/2} a^2 \tag{11}$$

The average value of capacity for the 1N263 has also been measured and found to be $0.3 \mu\mu\text{f}$ with the diode in an unbiased condition. The value calculated from (10) for the 1N263 is $0.4 \mu\mu\text{f}$.

The value of capacity at the dc bias point was used as an average value over the local-oscillator cycle because:

- 1) It is close to the actual value obtained by averaging the changing capacity over a local-oscillator cycle.
- 2) It agrees with values deduced from the rectification efficiency method.
- 3) It is felt that this value most closely approximates the capacity which affects the operation of the mixer crystal.

This is a reasonable approximation because the resistance of the barrier decreases exponentially in the forward direction while the capacity increases as the hyperbolic square root function [19], as shown in (9).

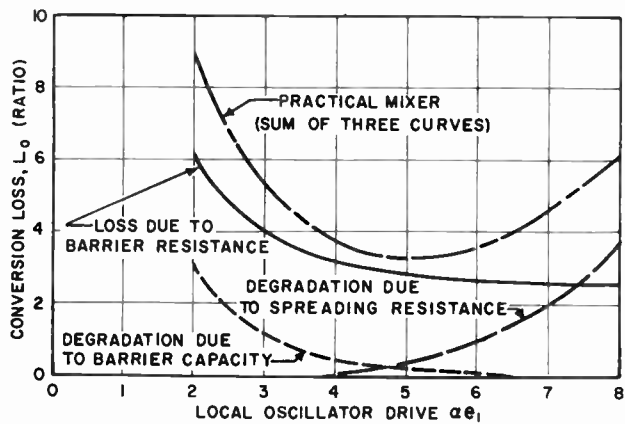


Fig. 9—Conversion loss vs local-oscillator drive for a germanium mixer having a 6-ohm spreading resistance and 0.3- μf barrier capacity with a 0.15-volt forward bias.

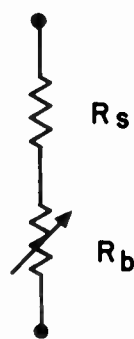


Fig. 10—UHF equivalent circuit of a crystal diode.

The cutoff frequency of the contact therefore increases as the current increases.

The added degradation in conversion loss due to capacity is a second-order correction for frequencies up to X band, as will be shown later. Thus, the voltage-varying capacity causes no more than a second-order and most probably a third-order error in the matched case with small area contacts.

VIII. EFFECT OF ELECTRICAL PARAMETERS AND OPERATING CONDITIONS ON CONVERSION LOSS

In this section, the effect on conversion loss of variations in the values of R_b , R_s , and C_b will be discussed. The theoretical background for this material is in Torrey and Whitmer [20]. The purpose of this section is to give the reader an idea of the dependence of conversion loss upon the magnitude of the parameters in the equivalent circuit, and to present experimental evidence which verifies these equations.

In the order of their importance, the three quantities which affect conversion loss are: 1) barrier resistance, R_b , 2) spreading resistance, R_s , and 3) barrier capacity, C_b .

If the equivalent circuit of a crystal diode is represented by R_b only, conversion loss decreases and approaches asymptotically a value of two (ratio) as the local-oscillator drive, αe_1 , is increased (solid line in Fig. 9). Local-oscillator drive is the product of α , the

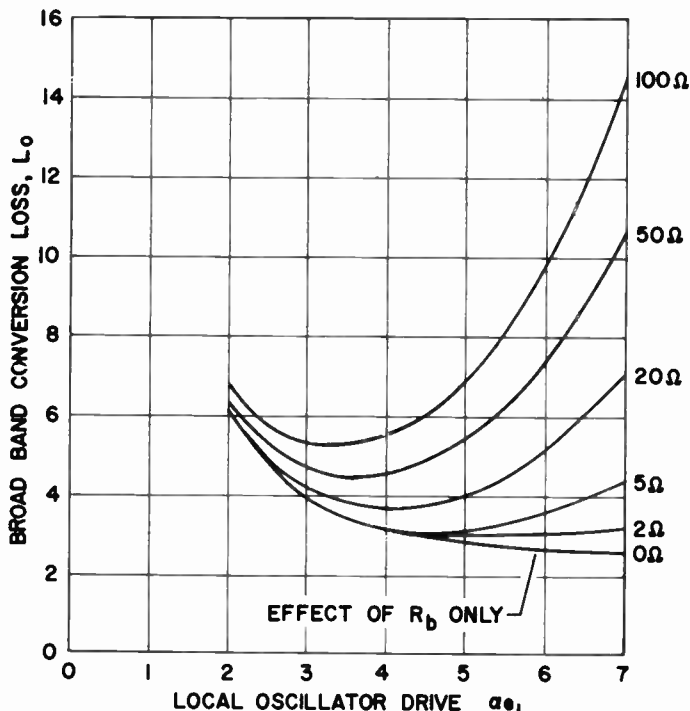


Fig. 11—Broad-band conversion loss vs local-oscillator drive as a function of various values of spreading resistance for a 0.15-volt forward bias.

log current slope of the forward $i-v$ characteristic, and e_1 , the amplitude of the local-oscillator voltage. Since the value of conversion loss depends on the product αe_1 , the actual magnitude of α itself is relatively unimportant. By adjusting e_1 , the desired value of drive may be obtained with any reasonable value of α (between 10 and 40 volts⁻¹). The apparent inference from this curve alone is that merely increasing the local-oscillator drive will reduce L_0 . However, the inclusion of the parasitic elements R_s and C_b in the equivalent circuit results in an optimum value (discussed below) of αe_1 , usually between four and seven.

The equivalent circuit at uhf of a crystal diode consists of R_b in series with R_s (Fig. 10). The effect of R_s on L_x is most pronounced at high values of local-oscillator drive; as the local-oscillator drive is increased the average value of R_b decreases, and at first L_x begins to decrease. Then, as the average value of R_b approaches R_s , more power is dissipated in R_s , and L_0 increases. The degradation of L_0 due to a fixed value of R_s (5 ohms, typical of 1N263 diode) is shown by the dotted line in Fig. 9. The effect of both R_b and R_s for various values of R_s are shown in Fig. 11, and it shows the optimum value of local oscillator drive for crystal diodes at uhf where C_b can be neglected. The effect of R_s on the location and magnitude of the minimum is apparent. The curve for $R_s=5$ ohms is typical of germanium; $R_s=20$ ohms is typical of silicon. These curves show that a germanium crystal, because of its lower spreading resistance, will have a slightly lower conversion loss than a silicon mixer.

The values of conversion loss, rectified current, and mixer impedances may be calculated from the iv characteristics of the crystal if the operating conditions, bias, and local-oscillator power are known. This has been done at uhf (850 mc) and Table II shows the agreement with experiment which was obtained. The equations necessary for the calculations are outlined in Appendix I. The accuracy of the loss measurements is ± 15 per cent, the impedance and current measurement accuracy was ± 10 per cent.

TABLE II
VALUES OF CONVERSION LOSS, RECTIFIED CURRENT, AND
MIXER IMPEDANCES

Crystal Number		L_0 ratio	L_1 ratio	I_R ma	R_{IF0} ohms	R_{IF1} ohms
A-105	Measured	3.8	3.7	1.8	180	100
A-105	Calculated	3.6	3.0	1.7	190	90
A-109	Measured	3.3	2.8	1.8	200	110
A-109	Calculated	3.5	2.9	1.7	190	95
A-134	Measured	3.2	3.0	1.9	190	90
A-134	Calculated	3.5	2.9	1.8	190	90
CP2-3	Measured	3.9	3.2	3.0	125	66
CP2-3	Calculated	3.1	3.1	2.9	127	61

L_0 is the broad-band conversion loss.

I_R is the rectified current.

R_{IF0} is the broad-band intermediate-frequency resistance.

R_{IF1} is the image-short intermediate-frequency impedance.

The calculated values for Table II were obtained by taking an iv curve from which values of A , α , and R_s were computed. The local-oscillator power and bias voltage were then chosen; the five quantities were analyzed as shown in Appendix I. Computed values for conversion loss, rectified current, and mixer impedances are compared with the experimental results in the table.

The importance of this experimental verification⁶ stems from its demonstration that the low-frequency calculations agree with measured values to within about 10 per cent.

To obtain the high-frequency (X -band) equivalent circuit of a crystal diode, C_b must be added in parallel with R_b as shown in Fig. 3. The effect of C_b on L_0 is most pronounced at low values of local oscillator drive; as this drive is decreased, the value of R_b increases, more current is shunted by C_b , and, therefore, L_0 increases. The dashed curve in Fig. 9 shows the degradation in L_0 caused by a fixed value of C_b (0.3 μmf , typical of the 1N263 diode). By adding this curve to the R_b and R_s curves, L_0 of a practical mixer is obtained as a function of drive (curve labeled *practical mixer*). The center of the minimum in the practical mixer curve occurs at $\alpha e_1 = 5.0$, which is the optimum value of drive for the 1N263 crystal. At this drive, both R_s and C_b decrease L_0 by an equal amount. A more general justification of this is readily obtained by calculating the ratio of the

power available to the average barrier resistance (the power which is converted) to the total available input power. This ratio is

$$\frac{P_b}{P_a} = \frac{1}{1 + \omega^2 C_b^2 R_b R_s + R_s/R_b} \quad (12)$$

The term R_s/R_b comes from power dissipated in the series resistance; the term $\omega^2 C_b^2 R_b R_s$ comes from power dissipated in R_s due to the magnitude of the shunt path through C_b .

If the bias and local oscillator power are used to adjust the magnitude of R_b , the maximum power delivered to the barrier occurs when the R_s/R_b term and the $\omega^2 C_b^2 R_b R_s$ term are equal, at which point $R_b = 1/\omega C_b$. This fact is used as the basis for an approximate calculation of L_0 as a function of R_s (Fig. 12). This is similar in principle to the arrangement reported by Strum [21] where the slope of the iv curve in the spreading resistance region is used as a measure of conversion loss.

Fig. 13 shows the current-voltage characteristic of a crystal diode being swept by a cycle of the local-oscillator voltage. The iv characteristic has been divided into three sections. In Section VII, the barrier resistance is greater than the reactance of the barrier capacity. In Section VIII, R_b is much smaller than X_{C_b} and much greater than R_s . In Section IX, the barrier resistance is less than the spreading resistance. Therefore, if the bias were too low, the local oscillator power would be shunted past R_b by the barrier capacity; if the bias were too high, the local oscillator power and signal power would be dissipated in the spreading resistance. From the point of view of conversion loss, the crystal should be biased between these two extremes so that the mixer acts primarily as a nonlinear barrier resistance. Silicon crystals have values of R_s about three times greater than germanium crystals. Therefore, the optimum bias for silicon should occur at a lower voltage than for germanium. In practice, silicon crystals are used without bias while germanium crystals are biased about 0.15 volt forward.

Fig. 12 shows the variation of L_0 with R_s for either silicon or germanium crystals made from material in the doping range investigated (5×10^{17} to 10^{19} carriers/cm³) with local oscillator drive and crystal bias optimized. Optimum values for both were obtained experimentally and were consistent with considerations discussed with reference to Figs. 9 and 13, respectively. To present a general expression or curve which shows the dependence of conversion loss on R_s and C_b is a very complicated problem. To eliminate it, barrier capacity is inferred from spreading resistance, because both are functions of the same variables in the semiconductor. Similarly, the X -band approximation is inferred from the low-frequency approximation, since the capacity adds a degradation of L_0 equal to that added by R_s (Fig. 12). This neglects second-order effects resulting from interaction terms, so that at frequencies progressively

⁶ The data are representative of an average of 50 CRX-3 type crystals.

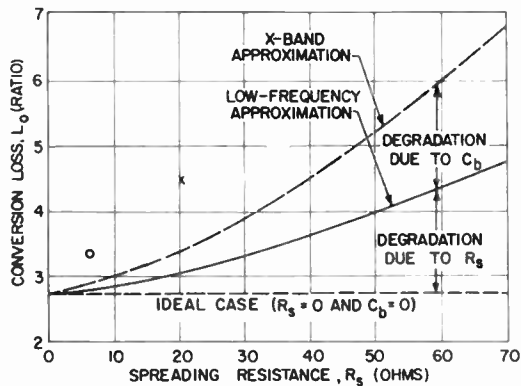


Fig. 12—Conversion loss vs spreading resistance.

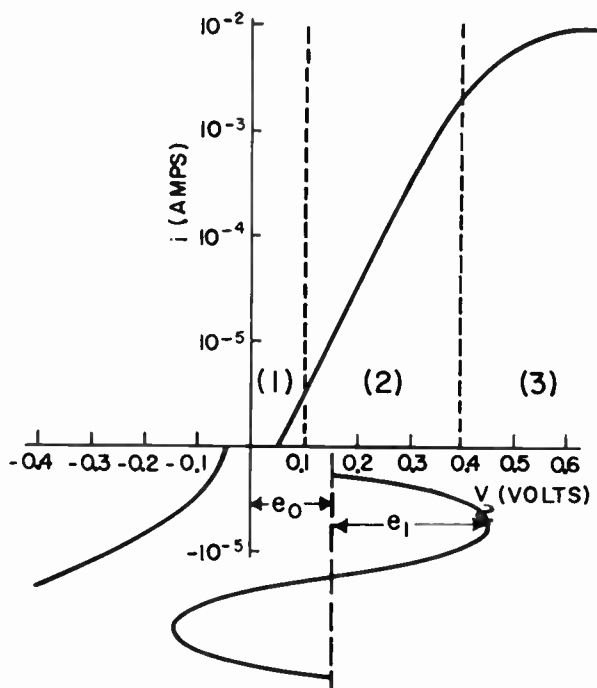


Fig. 13—Current-voltage characteristic of a mixer diode showing a cycle of the local-oscillator voltage.

further above X band, the calculation will lead to more optimistic values of L_0 . At these high frequencies, the effect of the capacity's nonlinear dependence on voltage must also be considered. No general solution to this problem has been found.

Further work is planned to determine experimentally the closeness of the approximation at frequencies above X band. The estimated accuracy of 35 mc is ± 1 db.

At X band and higher frequencies, conversion loss is a monotonically increasing function of the product of barrier capacity and spreading resistance. This will probably be intuitively evident to readers accustomed to finding products such as this in gain-bandwidth expressions and other high-frequency calculations.

The matrix for calculating the conversion loss as a function of R_s , C_b , α , and operating condition has been developed [22] and consists of the matrix of R_b alone modified by functions of R_s and $\omega C_b R_s$. The losses al-

ways increase when the product $\omega C_b R_s$ is increased for any given value of R_s . To minimize losses, R_s itself should also be kept small.

IX. MINIMIZATION OF CONVERSION LOSS

Conversion loss increases monotonically with the product $R_s C_b$. Since both R_s and C_b depends on N and b , carrier mobility in $\text{cm}^2/\text{volt-sec}$, this section will show that the product $N^{1/2} b / \epsilon^{1/2}$ can be used as a figure of merit for high-frequency mixer semiconductor material. In the course of exposition, comparison of measured values of carrier mobility with values of carrier mobility from the Conwell-Weisskopf [23] relationship as a function of carrier density will be useful to ensure the maximum carrier mobility for a given carrier density.

Minimization involves compromising the decrease in R_s with the increase in C_b as resistivity is decreased. The two cases of interest in a discussion of conversion loss minimization depend on whether or not barrier capacity is important. The low-frequency case, where capacity is not important, involves minimization of spreading resistance (Fig. 11). Eq. 7 indicates that the value of contact radius should be chosen as large as possible consistent with negligible capacity, and that the crystal should be doped as highly as possible without degrading conversion loss by losing rectification. At the limit of minimizing noise figure, however, the radius should be increased to the point where capacity and spreading resistance are equally important. The minimization of conversion loss at uhf would thus become the same as at X band except that smaller contact radii are used at X band.

At X band and higher frequencies, conversion loss is an increasing function of the product of barrier capacity and spreading resistance ($C_b R_s$). By combining (7) with (9), it can be seen that

$$C_b R_s \frac{a \epsilon^{1/2}}{N^{1/2} b} \tag{13}$$

where ϵ is the dielectric constant of the semiconductor material. The value of a is chosen as a compromise between reducing conversion loss, and maintaining adequate burnout protection and mechanical strength. A radius of 4×10^{-4} cm was used, because it was the smallest value which provided adequate protection from 2-erg energy pulses.

The concept of maximizing $N^{1/2} b / \epsilon^{1/2}$ for a given semiconductor in order to minimize the conversion loss of the mixer has led directly to the 1N263 germanium mixer diode. Careful analysis of the relationship between carrier density, N , and carrier mobility, b is worthwhile.

Thermal and ionized scattering are the two primary scattering processes which operate in a good single crystal [24]. Thermal scattering leads in n -type germanium to an electron mobility of approximately $3600 \text{ cm}^2/\text{volt-sec}$ and in p -type silicon to a hole mo-

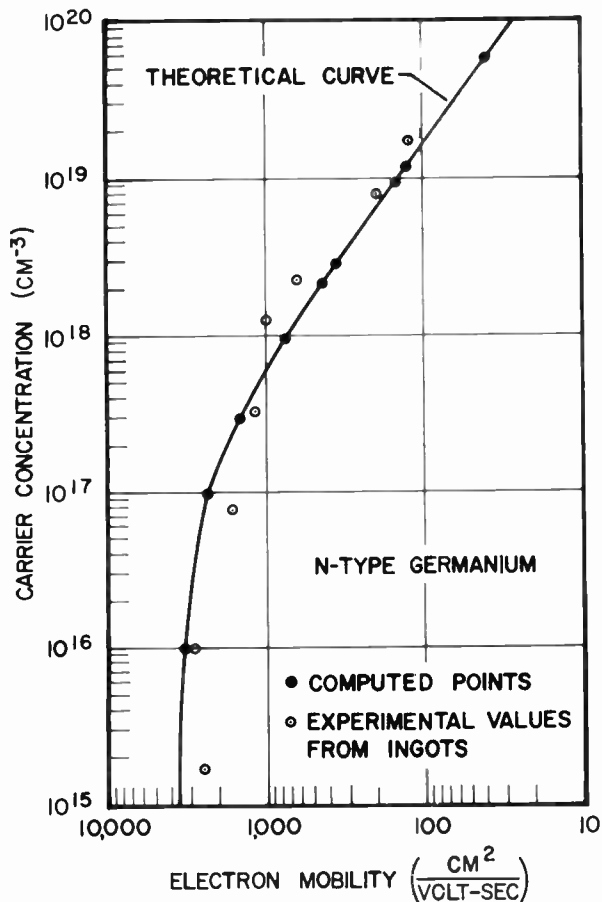


Fig. 14—Electron mobility vs carrier concentration for *n*-type germanium.

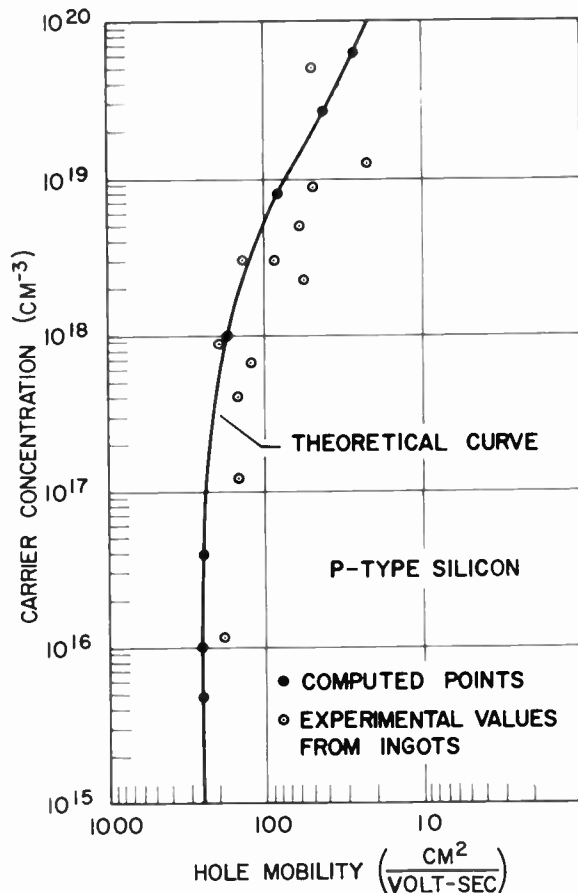


Fig. 15—Hole mobility vs carrier concentration for *p*-type silicon.

bility of approximately 250 cm²/volt-sec.⁶ Ionized scattering, as worked out by Conwell and Weisskopf [25], leads to a room-temperature carrier mobility (with effective carrier mass considered equal to electron mass) which depends on carrier concentration [26]. The product of these two mobilities divided by their sum gives actual carrier mobility (Hall mobility), which is a function only of carrier concentration, *N*. The equations used to determine Hall mobilities in germanium and silicon are given below.

$$\text{(germanium) } b_p = \frac{4.4 \times 10^{21}}{N \ln \left(1 + \frac{7.4 \times 10^{13}}{N^{2/3}} \right) + 1.2 \times 10^{13}} \quad (14)$$

$$\text{(silicon) } b_p = \frac{2.5 \times 10^{21}}{N \ln \left(1 + \frac{4.0 \times 10^{13}}{N^{2/3}} \right) + 1.0 \times 10^{19}} \quad (15)$$

Mobility vs carrier density is plotted from these equations in Figs. 14 and 15. The experimentally measured values of *b* and *N* are shown (Figs. 14 and 15) for many of the silicon and germanium ingots produced for

use in mixer crystal investigation. It will be noted that at the higher doping densities, high mobility becomes progressively more difficult to obtain. It may be seen from Figs. 14 and 15 that these curves mark an upper limit for the experimental points. An extra scattering mechanism could cause an experimental point to fall below the curve. This would reduce the product *N*^{1/2}*b* and increase conversion loss. Hence, this type of curve is a good criterion for crystal perfection. The closer the measured data comes to the theoretical value, the better the high frequency performance of the unit.

Eqs. 14 and 15 are multiplied by *N*^{1/2} to arrive at (16) for germanium and (17) for silicon.

$$\text{(germanium) } N^{1/2}b = \frac{4.4 \times 10^{21}}{N^{1/2} \ln \left(1 + \frac{7.4 \times 10^{13}}{N^{2/3}} \right) + \frac{1.2 \times 10^{18}}{N^{1/2}}} \quad (16)$$

$$\text{(silicon) } N^{1/2}b = \frac{2.5 \times 10^{21}}{N^{1/2} \ln \left(1 + \frac{4.0 \times 10^{13}}{N^{2/3}} \right) + \frac{1.0 \times 10^{19}}{N^{1/2}}} \quad (17)$$

Eqs. 16 and 17 are then differentiated with respect to *N* and set equal to zero to determine the value of *N* which

⁶ Higher values have since been reported for drift mobility, but this value represents the upper limit of measured values of Hall mobility made on material in connection with this work.

will give optimum conversion loss at high frequency. For germanium, a maximum value of $N^{1/2}b$ occurs near $N = 4 \times 10^{17}$ carriers/cm³. For silicon, the derived equation has no real roots, and the product $N^{1/2}b$ continues to rise as N is increased. The minimum conversion loss in this case occurs at the highest value of N obtainable before loss of rectification.

Using $N^{1/2}b/\epsilon^{1/2}$ as a figure of merit, different semiconductors can be compared to determine their relative merits for use as high-frequency mixer diodes. Fig. 16 shows $N^{1/2}b$ vs N for n - and p -type silicon and for n - and p -type germanium. The values of ϵ for silicon and germanium are nearly identical. Therefore, dielectric constant was neglected, and they were compared only with respect to $N^{1/2}b$. For germanium, the experimental points create a well-defined experimental maximum near 2×10^{18} . The expected minimum in L_0 for germanium having N of 2×10^{18} carriers/cm³ has been verified experimentally (Fig. 17). For silicon, the minimum L_0 is found at the value of N which causes the rectification ratio to decrease to 10 at a crystal bias of 0.5 volt. (Any further increase in doping density would lead to a loss in rectification ability.) The expected concentration, 5×10^{18} carriers/cm³, for minimum conversion loss in silicon crystals has also been experimentally verified (Fig. 17).

The concept of maximizing $N^{1/2}b/\epsilon^{1/2}$ allows the relative high-frequency potentialities of any semiconductor to be predicted from its basic physical structure. Of the well-known semiconductors, n -type germanium offers the best possibilities (Fig. 16). Several intermetallic semiconductors show promise on the basis of high values of b reported in the literature, but detailed information on mobility in the high doping range is not yet available.

Even if a semiconductor were found with the parasitic effects of R_s and C_s completely negligible at X band, the improvement in L_0 would amount only to about 0.3 db. This is understood when Fig. 9 is considered in which the primary dependence of L_0 is shown to be on R_b . The best 1N263 units have a degradation in L_0 (due to the parasitic elements R_s and C_s) of only about 0.3 db.

The ideas hitherto presented are basic and provide the theoretical minimum value of conversion loss. There are many fabrication variables (whisker material and advance, surface treatment, forming, tapping, heat treatment, etc.) which affect conversion loss. It is possible that skin effect resistance plays a role when the contact is made up of a large number of small contacts. The method of attack was to assume that some combination of fabrication variables existed which would permit the reduction of conversion loss to the minimum predictable from the basic theory. Using the value of N which maximizes $N^{1/2}b$ consistent with a barrier thick enough to support rectification (2×10^{18} cm⁻³ for germanium and 5×10^{18} cm⁻³ for silicon) and taking the smallest value of "a" compatible with minimum strength and burnout requirements (4×10^{-4} cm), a value of R_s has

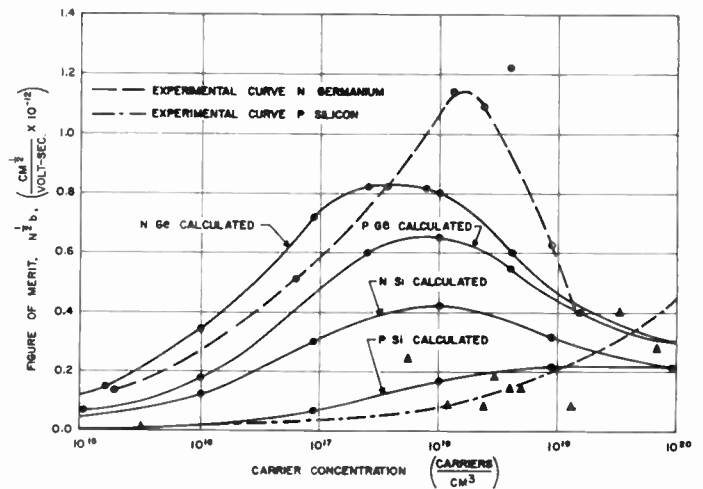


Fig. 16—Figure of merit, $N^{1/2}b$, vs carrier concentration for n - and p -type germanium and silicon.

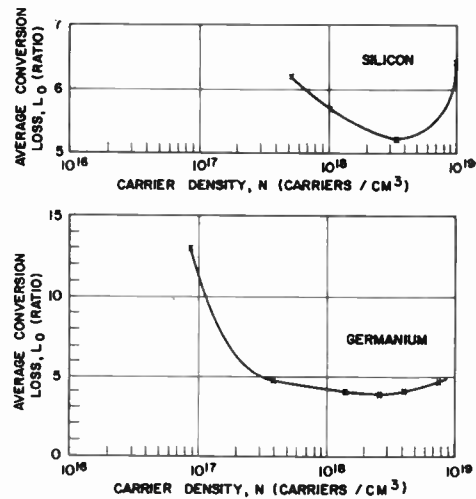


Fig. 17—Average conversion loss vs carrier density for n -type germanium and p -type silicon.

been deduced from (7). The approximate value of L_x at X band can then be found from the upper curve in Fig. 12.

The above procedure indicates a minimum conversion loss of 3.2 (ratio) for silicon and 3.0 (4.8 db) for germanium at X band. A combination of fabrication variables has been found which sometimes produces a germanium crystal with such a conversion loss. For silicon, the closest approach was 3.9 (ratio). The average value of L_x for the 1N263 crystal is less than 0.5 db above the theoretical minimum.

The reduction of conversion loss to its calculated minimum for some units indicates that a point of diminishing returns has been reached in the germanium crystal development program at X band. The degree of success attained with silicon indicates that some additional improvement is possible before this point is reached. The extent to which theory has been verified shows that n -type germanium is the better semiconductor for producing good, low-conversion-loss crystals.

Since C_b is about the same in both silicon and germanium crystals, the above conclusion is valid at all frequencies and is due to the lower value of R_s found in germanium mixer crystals. In fact, as frequency goes up the superiority of germanium should increase, since the power lost in R_s is increased because of the current flowing through R_s and C_b , and the spreading resistance contributes a greater proportion of the total power loss.

The problem of designing diodes for progressively higher frequencies can be discussed with reference to the frequency-dependent factor $\omega C_b R_s$. This is proportional to the design factor $\omega a \epsilon^{1/2} / N^{1/2} b$. To maintain the same performance in the mixer diode, the radius must be reduced in direct proportion to the increase in frequency. This, probably, will be difficult because of increased susceptibility to burnout. At higher frequencies, the compromise between noise-figure performance and protection against burnout will probably be made at higher values of noise figure.

X. EFFECTS OF NOISE TEMPERATURE ON NOISE FIGURE

In this section, noise-temperature considerations will be shown to decrease rapidly in importance as conversion loss is improved.

The contributions of shot noise and IF noise are discussed and experimental evidence indicating the magnitude of noise temperature as a function of bias is presented.

Noise temperature, t_x , is, by definition, the ratio of the noise power available from the intermediate-frequency terminals of the mixer to the noise power available from an equivalent resistor at room temperature. It has its origin in those parts of the frequency spectrum which can beat with the local-oscillator fundamental or with its harmonics to produce the intermediate frequency. The physical origin of t_x is in the shot noise of the barrier, in the Johnson noise of the spreading resistance, and in the IF noise which is a characteristic of semiconductors. Since most of the noise reaches the intermediate-frequency terminals through the primary conversion process, the noise temperature of the mixer is dependent on the conversion loss of the mixer as given by (18).

$$t_x = \bar{l} \left(1 - \frac{2}{L_0} \right) + \frac{2}{L_0} \tag{18}$$

The derivation of this equation is given in Appendix II.

Here \bar{l} is the value of noise temperature obtained by averaging the instantaneous values of crystal noise temperature over the voltage range produced by the local oscillator.

Values of t_x as low as 0.8 have been measured which indicate that \bar{l} can be less than unity. The instantaneous noise temperature of a typical germanium crystal at 30 mc is shown in Fig. 18 as a function of bias voltage.

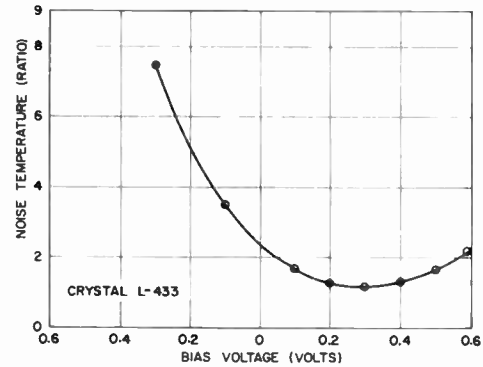


Fig. 18—Noise temperature as a function of bias voltage for a germanium crystal.

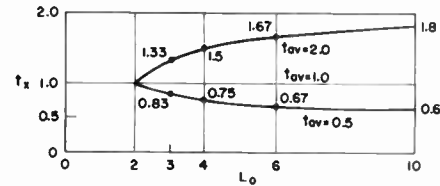


Fig. 19—Crystal noise temperature as a function of t_{0v} and L_0 .

An important aspect of (18) is that for values of \bar{l} close to unity, say between 0.5 and 1.5 and for values of L_0 less than 3, values of t_x lie between 0.85 and 1.15 (Fig. 19); thus, as conversion loss is decreased, t_x tends to approach unity more and more independently of the value of \bar{l} . Thus, in very good mixer crystals L_0 is the most important factor determining noise figure.

In general, germanium crystals exhibit lower values of t_x than silicon crystals. Whether this is a result of their lower conversion loss, as (18) would indicate, or whether it is typical of the noise mechanism in the semiconductor has not at present been resolved.

In the limit, when the noise arising from the diode is solely shot noise [27], $\bar{l} = \frac{1}{2}$. In this case, noise temperature does not depend upon bias, power or frequency. Other noise sources, particularly the IF spectrum, introduce these dependences although with good mixer crystals, using a 30-mc intermediate frequency, the variation of t_x with bias or power in the vicinity of the optimum operating point is quite small.

In computations involving expected minimum values of noise figure, t_x is taken as 1, which is the limiting value from (18). This approximation becomes progressively better as conversion loss is improved.

XI. THE MINIMIZATION OF RECEIVER NOISE FIGURE

This section will indicate the process used to minimize the over-all receiver noise figure by minimizing the sum ($t_x + F_{if} - 1$). This argument will specify the intermediate frequency which should be used for minimum noise figure.

The desired end result is a low F_r . Therefore,

$$F_r = L_0(t_x + F_{if} - 1)$$

must be minimized by choice of bias, local oscillator power, and operating intermediate frequency. Remembering that

$$t_z = \bar{i} \left(1 - \frac{2}{L_0} \right) + \frac{2}{L_0},$$

and assuming that excess crystal noise temperature is inversely proportional to frequency and that excess intermediate-frequency noise figure is proportional to frequency, then

$$(\bar{i} - 1/2) = \frac{C}{f}$$

where C is a constant and $\frac{1}{2}$ is the limiting value of \bar{i} .

$$(F_{it} - 1) = Kf$$

where K is another constant, then the optimum intermediate frequency is

$$f = \sqrt{\frac{L_0 - 2}{L_0} \left(\frac{C}{K} \right)},$$

and F_r will minimize at the operating condition which minimizes L_0 , as can be seen by combining the preceding equations to yield

$$F_r = 2 + \sqrt{CK(L_0 - 2)L_0} + (L_0 - 2)\bar{i} + K\sqrt{L_0(L_0 - 2)}\frac{C}{K}.$$

The constant C has a slight dependence upon the operating condition used to minimize L_0 . In practice, therefore, minimum F_r is usually found quite close to, rather than exactly at the combination of operating conditions which minimize L_0 .

XII. OTHER CONSIDERATIONS

Temperature Dependency

The purpose of this section is to consider the effect of temperature on the diode characteristic of mixer crystals and to disprove the common misconception the authors have encountered that germanium mixer crystals should be inferior to silicon mixer crystals at elevated temperatures.

Silicon has a larger energy gap than germanium, and therefore in junction devices the former has the better temperature stability. On the other hand, in point-contact crystal rectifiers for microwave mixing, the temperature dependence of the current vs voltage curve is determined primarily by the contact potential⁷ which is about 0.3 volt for both germanium and silicon. Fig. 20 shows the experimental dependence of the current vs voltage curve on temperature for both silicon and germanium. They are seen to be substantially the same. In actual mixer operation, a 7.5-db noise-figure receiver

⁷ An experimental determination of Φ_0 in (5) for both silicon and germanium yields a value of 0.3 ev.

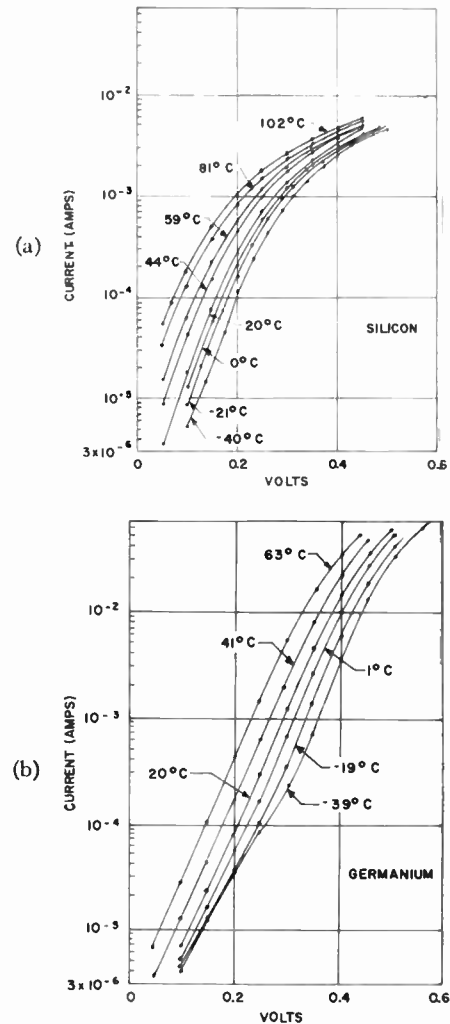


Fig. 20—Temperature dependence of typical X-band crystals.

at room temperature typically degrades about 1 db at 100°C and 2 db at 150°C for either the 1N263 (germanium) or the best 1N23D (silicon). The degradation is about half of this if the operating parameters are reset and the mixer rematched for each temperature. It is worth repeating that in microwave mixer crystals temperature dependence is small and is the same for either germanium or silicon.

Burnout

As indicated at the end of the third paragraph of Section IX, the standard short duration energy burnout criteria were used as a limit on how small the radius of contact should be for practicality. A contact radius of 4×10^{-4} cm gave a safe rating of 2 ergs without any noise-figure degradation for the 1N263. The standard energy burnout test is based on the assumption that TR energy spike leakage duration is always short compared to the crystal thermal relaxation time. Recent experiments by the University of Illinois⁸ using a high-

⁸ "TR Tube Spike Leakage Investigation," Seventh Quart. Rep., Univ. of Ill., Elec. Eng. Res. Lab., Signal Corps Contract DA-SC-039-SC 52670; May 15, 1955.

speed oscillograph have shown that spike durations of commercial TR's such as the 1B24 and 1B63 are from 6 to 15 μsec . The spike peak power was from 0.5 watt up depending on tube design, age and operating conditions. Rough tests have indicated these spike durations to be comparable to 1N263 and 1N23D thermal relaxation times, and therefore a peak watt test should be used for the burnout criteria. Using these criteria as tested both by microwave rf pulses and by condenser discharge for durations of 0.1 μsec or longer, the 1N263 withstands without noise-figure degradation about 1-watt peak.

For future improvement of the burnout from the radar system designer's viewpoint, research should be aimed toward reducing the duration of the TR spike leakage and increasing the thermal relaxation time of crystal rectifiers. This will make the energy criteria valid again and improve the effective burnout in proportion to the ratio of crystal thermal relaxation time divided by the TR leakage duration. In this case the absorbed energy density will be proportional to the square of the radius. For this reason, a slight increase in radius, which does not seriously degrade sensitivity, will lead to a much more rugged and reliable unit.

XIII. CONCLUSION

A quantitative theory has been developed which connects crystal conversion loss with the physical constants of the semiconductor and the geometry of the contact. The dependence of conversion loss on the equivalent circuit components (R_b , R_s , and C_b) was shown first; these components were then linked to the physical properties of the semiconductor and the fabrication techniques involved in producing the finished diode.

Next, the importance of conversion in determining the noise temperature of the crystal was shown. This established that the noise figure of the crystal is primarily determined by the conversion loss. A minimization of the sum of intermediate-frequency noise figure and crystal noise temperature with intermediate frequency led to an expression for F_r at the optimum intermediate frequency which depended mainly on the conversion loss of the crystal. Increase of receiver sensitivity can therefore be limited to the problem of reducing crystal conversion loss. The figure of merit for conversion loss, $N^{1/2}b/\epsilon^{1/2}$, can thus be extended to receiver noise figure.

The use of this figure of merit for high-frequency mixer crystals has shown that n -type germanium is the best semiconductor currently available. The figure of merit provides a tool for the evaluation of the mixer potentialities of new semiconductor materials.

It is indeed fortunate that n -type germanium is the preferred semiconductor for low-noise-figure diodes because it is also the most easily worked of the currently known semiconductors. The comparative ease of working with germanium has resulted in the excellent uniformity (Fig. 21) of the 1N263 crystal diode.

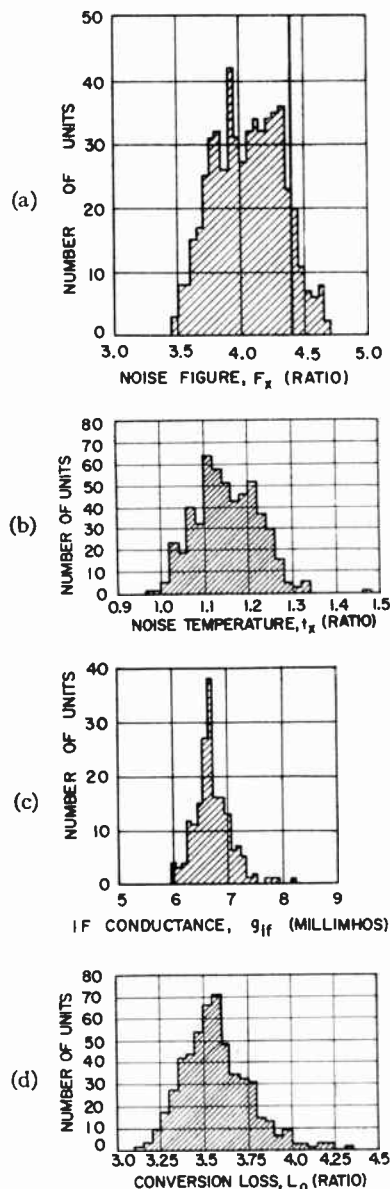


Fig. 21—Distribution of 1N263 performance parameters.

The uniformity achieved in making pilot runs promises to yield a crystal sufficiently uniform to be adaptable to more sophisticated circuitry such as narrow-band mixer circuits and harmonically reinforced local-oscillator circuits.

An improvement in values of F_r has been obtained as a result of this work. A histogram of values of F_r using germanium crystals is shown in Fig. 22, using a 30-mc intermediate frequency and a bias of 0.15 volt with a local-oscillator power of $\frac{1}{2}$ mw.

Further improvements in F_r should result from designs using narrow-band circuitry. The percentage reduction in noise figure derived from narrow-band circuits increases rapidly as the noise figure of the crystal is reduced. Noise figure may otherwise be reduced by cooling the mixer crystal to very low temperatures. This should reduce t which is proportional to temperature [28] causing a reduction of noise figure [30].

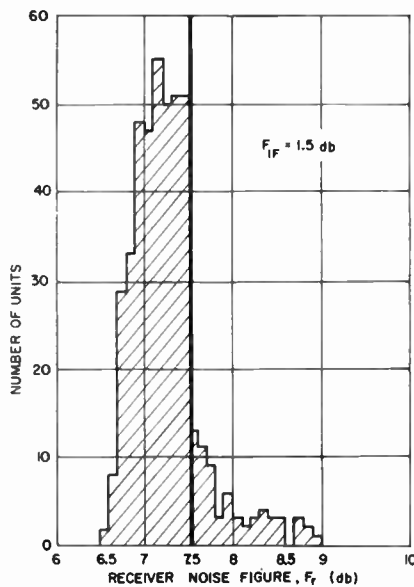


Fig. 22—Distribution of receiver noise figure.

The diode designer should realize that the possibility of the discovery of new oxide or intermetallic semiconductors having higher values of $N^{1/2}b/e^{1/2}$ could lead to mixer crystals having lower noise figures than are presently attainable.

APPENDIX I

The low-frequency equivalent circuit of a mixer crystal is composed of a fixed spreading resistance, R_s , in series with a nonlinear barrier resistance, R_b , characterized by A , the log current intercept, and α , the log slope. The performance of a crystal may be calculated from A , α , and R_s , which specify the crystal characteristics, plus the operating bias and local-oscillator power. The following equations [29] summarize the calculation.

Values of $I_0(\alpha e_1)$, $I_1(\alpha e_1)$ and $I_2(\alpha e_1)$ are obtained by solving the transcendental equation

$$e_1^2 [I_0(\alpha e_1) - I_2(\alpha e_1)] = \frac{2P_{rf}}{A\alpha^{(\alpha e_0)}} \quad (19)$$

Next, three auxiliary conductances are calculated.

$$\begin{aligned} g_0 &= A\alpha e^{(\alpha e_0)} I_0(\alpha e_1), \\ g_1 &= A\alpha e^{(\alpha e_0)} I_1(\alpha e_1), \\ g_2 &= A\alpha e^{(\alpha e_0)} I_2(\alpha e_1). \end{aligned} \quad (20)$$

Then, the actual mixer conductances as shown in Fig. 2 are calculated.

$$\begin{aligned} \Delta g_{\alpha\alpha} &= g_0 + R_s(2g_0^2 - g_1^2 - g_2^2) \\ &\quad + R_s^2(g_0^3 - g_0^2g_1 - g_0g_2^2 - 2g_0g_1^2 + 2g_1^2g_2), \\ \Delta g_{\alpha\beta} &= g_1 [1 + R_s(g_0 - g_2)], \\ \Delta g_{\alpha} &= g_2 + R_s(g_0g_2 - g_1^2), \\ \Delta g_{\beta\beta} &= g_0 + 2R_s(g_0^2 - g_1^2) \\ &\quad + R_s^2(g_0^3 - g_0g_2^2 - 2g_0g_1^2 + 2g_1^2g_2), \end{aligned} \quad (21)$$

where

$$\begin{aligned} \Delta &= 1 - 3R_s g_0 + R_s^2(3g_0^2 - 2g_1^2 - g_2^2) \\ &\quad + R_s^3(g_0^3 - g_0^2g_2 - g_0g_2^2 - 2g_0g_1^2 + 2g_1^2g_2). \end{aligned}$$

Next, two auxiliary parameters are defined.

$$\begin{aligned} E_1 &= \frac{g_{\alpha\beta}^2}{g_{\alpha\alpha}g_{\beta\beta}} \\ E_3 &= \frac{E_1}{1 - E_1} \frac{g_{\alpha\alpha} - g_{\alpha\sigma}}{g_{\alpha\alpha} + g_{\alpha\sigma}}. \end{aligned} \quad (22)$$

The conversion losses are

$$\begin{aligned} L_0 &= 2 \left(\frac{1}{E_1} + \frac{1}{E_3} - 1 \right), \\ L_1 &= \frac{1 + \sqrt{1 - E_1}}{1 - \sqrt{1 - E_1}}, \\ L_3 &= \frac{1 + \sqrt{1 - E_3}}{1 - \sqrt{1 - E_3}}, \end{aligned} \quad (23)$$

and the intermediate-frequency conductances are

$$\begin{aligned} g_{ifo} &= g_{\beta\beta} - \frac{g_{\alpha\beta}^2}{g_{\alpha\alpha}} \\ g_{ifi} &= g_{\beta\beta} - \frac{g_{\alpha\beta}^2}{2g_{\alpha\alpha} - g_{\alpha\sigma}} \\ g_{ifs} &= g_{\beta\beta} - \frac{g_{\alpha\beta}^2}{g_{\alpha\alpha} - 1/3(g_{\alpha\alpha} - g_{\alpha\sigma})} \end{aligned}$$

The rectified current is

$$I_r = Ae^{(\alpha e_0)} I_0(\alpha e_1).$$

These equations are derived by simplifying the general equation applicable when the barrier resistance is also shunted by a capacitor.

APPENDIX II

NOISE TEMPERATURE UNDER OPERATING CONDITIONS⁹

Static noise temperature, both experimental and theoretical, is defined as the ratio of noise power arising within the crystal available at the intermediate-frequency termination to kTB , the available noise power of an equivalent resistor. Under operating conditions, the former quantity has been assumed to be the time-average of the static noise characteristic. This assumption has been qualitatively verified, though it fails to account for the fact that there is contribution, under operating conditions, of noise from the radio-frequency terminations due to the conversion phenomenon. In general, the noise contribution from the radio-frequency terminations is at a temperature different from that of

⁹ The authors are indebted to Edward Chatterton for this derivation.

the crystal itself. Since the actual t_x includes the radio-frequency contribution the theory must be extended.

The noise figure of a network is defined by

$$F_x = \frac{N}{G_x k T_0 B} = \frac{t_x}{G_x}, \quad (24)$$

where N is available noise output from network, $k T_0 B$ is the noise input from generator, and G_x is network available gain. Note that t_x is defined for a network with $k T_0 B$ input, whereas t_{av} is determined from the static case where input radio-frequency terminals do not exist and therefore the noise input is zero.

Obviously, if a network and its generator are in thermal equilibrium, they may be separated without affecting the noise temperature measured at the network output. Thus, the noise temperature of the crystal with no input, t_{av} , is the same as that of the crystal connected to an input termination whose temperature is also t_{av} .

The noise figure of the crystal referred to the temperature is given by F_{T_n} :

$$T_n = t_{av} T_0, \quad (25)$$

$$F_{T_n} = \frac{N}{G_x k T_n B}. \quad (26)$$

The subscript T_n denotes the fact that the crystal and the input termination are at the same temperature

$$T_n = t_{av} T_0.$$

The available output noise power due to the network alone, at the temperature T_n , is

$$(F_{T_n} - 1) G k T_n B. \quad (27)$$

If the input termination at room temperature, T_0 , is connected to the crystal at temperature T_n , the available output noise temperature is

$$N = G k T_n B (F_{T_n} - 1) + G k T_0 B. \quad (28)$$

Since t_x referred to T_n is unity

$$F_{T_n} = \frac{t_x(T_n)}{G_x} = \frac{1}{G_x}. \quad (29)$$

Substituting (25) and (26) into (28) and dividing by $k T_0 B$ gives t_x referred to T_0 .

$$t_x = t_{av}(1 - G) + G. \quad (30)$$

The above relation applies to the case of narrow-band operation. The corresponding relation for the broad-band case is

$$t_x = t_{av}(1 - 2G) + 2G. \quad (31)$$

The effect of this phenomenon is shown in Fig. 19. The contribution from the radio-frequency terminations of unity noise temperature causes t_x to be closer to unity than t_{av} . This effect becomes more prominent as conversion loss decreases, until ideal conversion is attained, at which point t_x is totally determined by the radio-frequency termination contribution and is unity.

BIBLIOGRAPHY

- [1] Torrey, H. C., and Whitmer, C. A. *Crystal Rectifiers*. New York: McGraw-Hill Book Co., Inc., Massachusetts Institute of Technology Radiation Laboratory Series, vol. 15, ch. 5, 1948.
- [2] Friis, H. T. "Noise Figures of Radio Receivers," *PROCEEDINGS OF THE IRE*, Vol. 32 (July, 1944), pp. 419-423.
- [3] Torrey and Whitmer, *op. cit.*, Ch. 5.
- [4] Torrey and Whitmer, *op. cit.*, Ch. 5, Sec. 12.
- [5] Torrey and Whitmer, *op. cit.*, Ch. 5.
- [6] Torrey and Whitmer, *op. cit.*, Ch. 4, Sec. 3.
- [7] Bethe, H. A., *Theory of the Boundary Layer of Crystal Rectifiers*, Cambridge: Massachusetts Institute of Technology Radiation Laboratory Report No. 43-12, November 23, 1942.
- [8] Yearian, H. G. *Investigation of Crystal Rectifier DC Characteristics*. Lafayette, Ind.: Purdue University, Naval Department Research Contract No. 14-115, December 3, 1942.
- [9] Southworth, G. C. *Principles and Applications of Wave Guide Transmission*. New York: D. Van Nostrand Company, Inc., 1950. See p. 636.
- [10] Yearian, H. G., *op. cit.*
- [11] Cutler, M. "Flow of Electrons and Holes Through the Surface Barrier Ring in Point Contact Rectification," *Physical Review*, Vol. 96 (October 15, 1942), p. 255.
- [12] Torrey and Whitmer, *op. cit.*, Ch. 2, Sec. 4.
- [13] Holm, R. *Electrical Contacts*. Stockholm: Almqvist and Wiksells Akademiska Handböcker, Hugo Gerbers Förlag, 1946. See p. 7.
- [14] Matare, H. F. *Empfange Probleme in Ultrahoch Frequenz Gebiet*. Munich: R. Oldenbourg. Sec. 32a, 1951.
- [15] Torrey and Whitmer, *op. cit.*, Ch. 4, Sec. 6.
- [16] Torrey and Whitmer, *op. cit.*, Ch. 2, Sec. 4.
- [17] R. Holm, *op. cit.*, p. 7.
- [18] H. F. Matare, *op. cit.*, Sec. 329.
- [19] H. F. Matare, *op. cit.*, Sec. 329.
- [20] Torrey and Whitmer, *op. cit.*, Ch. 5.
- [21] Strum, P. "Some Aspects of Crystal Mixer Performance," *PROCEEDINGS OF THE IRE*, Vol. 41 (July, 1953), pp. 875-890.
- [22] Torrey and Whitmer, *op. cit.*, Ch. 5.
- [23] Conwell, E., and Weiskopf, V. F. "Theory of Impurity Scattering in Semiconductors," *Physical Review*, Vol. 77 (February 1, 1950), pp. 388-390.
- [24] Shockley, W. E. *Electrons and Holes in Semiconductors*. New York: D. Van Nostrand Company, Inc., Sec. 11.4, 1950.
- [25] Conwell and Weiskopf, *op. cit.*
- [26] Conwell, E. "Properties of Silicon and Germanium," *PROCEEDINGS OF THE IRE*, Vol. 40 (November, 1952), p. 1327.
- [27] Torrey and Whitmer, *op. cit.*, Ch. 6.
- [28] Nicoll, T. "Noise in Silicon Microwave Diodes," *Proceedings of the Institution of Electrical Engineers*, Part 3, (September, 1954.)
- [29] Torrey and Whitmer, *op. cit.*, Ch. 4.
- [30] Messenger, S. C. "Cooling of Microwave Mixers and Antennas," *IRE TRANSACTIONS*, Vol. MTT-5 (January, 1957), pp. 62-68.



Correspondence

Semantic Constraints in the Analysis of Communication Systems*

The Shannon theory of communications is developed from considerations of statistical data but not from concepts of value or meaning. On the other hand, Shannon has considered the influence of language statistics, and thus indirectly that of semantic constraints, on entropy. Thus, he says, "The new method of estimating entropy exploits the fact that anyone speaking a language possesses, implicitly, an enormous knowledge of the statistics of the language. Familiarity with the words, idioms, clichés and grammar enables him to fill in missing or incorrect letters in proofreading or to complete an unfinished phrase in conversation."¹ Shannon investigates this question by studying the predictability of printed English, considering the matter from the standpoint of completing an unfinished phrase in conversation. The following is a report on some preliminary measurements which purport to study the problem from the standpoint of filling in missing or incorrect letters in proofreading. Actually, the succeeding discussion has a further objective which is to emphasize that, because of semantic constraints, the reliability of communication systems which transmit a natural language such as English depends on the human decoder, just as the reliability of a system which transmits messages with artificial constraints depends on the mechanical or electronic decoder.

Experiments were conducted which simulate the transmission of English as teletype-encoded binary sequences over a channel perturbed with additive Gaussian noise. Particular systems were simulated by specifying decoding and decision mechanisms. For assumed signal-to-noise ratios, probabilities of error were computed, and these were used to alter binary digits with the aid of a table of random numbers. For example, if the computed probability of error were 0.12 and if random numbers from 00 to 99 were used, digits corresponding to the numbers from 00 to 11, or any other 12 numbers which might be prescribed, would be altered. Out of the 32 possible binary sequences, only those alterations which occurred in 26 letters and a word space were treated as permissible. Alterations in the remaining five sequences were recorded as nulls, indicating the possibility of any letter or a word space. Minimum message lengths were about 5000 digits (1000 letters) in length to insure reasonable statistical stability in the measured results. Corrupted messages were given to a group of people with instructions that they attempt to reconstruct the original message in a given time. In this experiment no use was made of the teletype code to aid in de-

coding the message; only the observer's knowledge of the English language was utilized.

Natural and artificial constraints in a message represent two elementary structural patterns, and there may also be mixtures of the two. A communication system that transmits and receives clear English text, for example, employs messages with natural constraints; one that transmits and receives with systematic codes employs artificial constraints. The systems studied can be divided into two divisions which, in this discussion, are called coded and uncoded groups; the coded group representing systems which contain natural and artificial constraints and the uncoded group natural constraints only. For both groups, Neyman-Pearson and modified sequential-sampling, decision devices were assumed.

In the following systems, p_0 is the digit error probability, u_0 is the digit null or ambiguous probability, p is the sequence or letter error probability, and u is the letter null probability.

Uncoded

1) *Binary PCM*: Five-digit binary sequences.

Signal-to-Noise Ratio = 3 db.

$p_0 = 0.08$ or $p = 0.34$.

2) *Binary PCM with Single Pulse Integration*: Five-digit binary sequences.

Effective Signal-to-Noise Ratio = 6 db.

$p_0 = 0.022$ to $p = 0.107$.

3) *Binary PCM with Null Indication*: (Two-level decision system in which observations that lie between threshold levels are designated as null readings.) Five-digit binary sequences.

Signal-to-Noise Ratio = 3 db.

$p_0 = 0.028$, $u_0 = 0.151$; p (letter error + more than 1 null digit per letter) = 0.280.

Two letters were printed for sequences with one null digit, and the null symbol was printed for sequences with more than one null. The null level was set for maximum information rate on the assumption of the transmission of independent digits.

For the following coded systems, the signal-to-noise ratio was adjusted for equal noise-free information rates for equal transmitted powers.

Coded²

4) *Wagner Code*:³ Five message digits plus one check digit.

Effective Signal-to-Noise Ratio = 3 db.

$p = 0.190$.

¹ For the coded systems, letters rather than digits were altered in accordance with random numbers, and it was assumed, for simplicity, that only single errors occurred in the binary sequences of the corresponding letters.

² R. A. Silverman and M. Balsler, "Coding for constant-data-rate systems—part I. A new error-correcting code," *Proc. IRE*, vol. 42, pp. 1428-1435; September, 1954.

5) *Hamming Single-Error-Correcting Code*:⁴ Five message digits plus four check digits.

Effective Signal-to-Noise Ratio = 1.25 db.

$p = 0.310$.

6) *Coded Null*: Five message digits, one parity check digit, and null digit indication.

Effective Signal-to-Noise Ratio = 3 db.

$p = 0.090$; $u = 0.220$.

Null level set for maximum q , the probability of printing a letter correctly. This setting closely approximates the condition for maximum information rate.

The transmission of two messages over each of the above systems was simulated by suitable alterations of digits. The altered messages were then given to observers in the College of Engineering of New York University with instructions to reconstruct the messages in not more than one hour. The results were for an average of approximately five observers per system. The measure of performance was the percentage of correctly interpreted words. The results are listed in Tables I and II.

TABLE I
TEXT—TECHNICAL

System	Average Message Decoding Time (Min)	Average Per Cent Correct Words	
		Before Decoding	After Decoding
1) Binary PCM	60	12	68
2) Integrated Binary PCM	40	45	92
3) Uncoded Null	60	11	46
4) Wagner	60	21	90
5) Hamming	60	11	56
6) Coded Null	60	11	80

TABLE II
TEXT—NOVEL

System	Average Message Decoding Time (Min)	Average Per Cent Correct Words	
		Before Decoding	After Decoding
1) Binary PCM	60	10	52
2) Integrated Binary PCM	30	43	97
3) Uncoded Null	60	11	74
4) Wagner	60	28	86
5) Hamming	60	11	63
6) Coded Null	60	12	70

Before interpreting the results, the following limitations of the method are noted.

- 1) Relatively small sampling of English text.
- 2) Relatively small number of observers.
- 3) Restriction of the message to English text.
- 4) Omission of teletype code restraints in decoding messages.

* Received by the IRE, April 15, 1957. This work has been sponsored by the Air Force Cambridge Res. Ctr., Air Res. and Dev. Command, Mass., under Contract No. AF19(604)-1049.

¹ C. E. Shannon, "Prediction and entropy of printed English," *Bell Sys. Tech. J.*, vol. 30, pp. 50-64; January, 1951.

⁴ R. W. Hamming, "Error Detecting and Error Correcting Codes," Bell Telephone System Monograph No. 1757; April, 1950.

This is analogous to disregarding the distribution of errors in the language and is exemplified by the difference between per-unit equivocation and probability of error as reliability criteria. The former considers distribution of errors by means of transition probabilities whereas the latter lumps all errors together. The effect of this on the given results should be small, since operation is predicated for small signal-to-noise ratios, so that errors should be rather uniformly distributed.

- 5) In the case of the null system, the null level was set for maximum information rate on a per symbol basis, resulting in a rather large percentage of nulls. A better criterion for setting the null level would be to determine the maximum readability as a function of null level, thus accounting for redundancy in the language.

Because of these limitations, the above results must be regarded as only tentative. Hence, the following observations must be regarded as preliminary and in no sense as final. The large improvement in the percentage of correctly interpreted words clearly results from the observer's knowledge of the language which reduces the residual uncertainty of the received message in much the same way as reliable transmission reduces equivocation. Inter-word influence and redundancy are accounted for in the decoding process. A complete experiment of this kind could be used to determine the tolerable number of letter errors and nulls in an average word length for approximately 100 per cent readability.

The Wagner code appears to be superior to the other coding systems, but several observers did as well for the coded null system. It is possible that a larger experiment might perhaps change the magnitude of the differences; and changing the criterion for setting the null level might, as already indicated, improve the performance of the null system. It is also noted that the "cost" of improved performance for the integrated binary pcm system is increased transmission time.

A. HAUPTSCHNEIN
AND L. S. SCHWARTZ
College of Engineering
New York University
New York, N. Y.

Microwave Power Measurements Employing Electron Beam Techniques*

A technique similar to that employed by Thomas in the above paper¹ has been used in the Elliott Brothers' laboratories since 1953 for the monitoring or measuring of microwave power in which a coaxial structure is

used. Part of a coaxial line forms a diode, and when power is fed along the line the potential difference developed between the center conductor and outer conductor is a measure of this rf power. The rf power is fed by a waveguide to a waveguide-to-coaxial line transformer, which is so arranged that certain components of the transformer are contained within the evacuated envelope of the diode. The power can be fed through the coaxial line to a similar coaxial line to waveguide transformer from which the power is either dissipated in a suitable load or is used to some purpose, or alternatively, the coaxial line itself may be loaded at the end. If the center conductor of the coaxial line is used as an emitter and the outer conductor as a collector then the electric field between the outer and inner conductor is given by

$$E_x = \frac{v}{x \log \left(\frac{r_a}{r_b} \right)}$$

where E_x = field at radius x , r_a is the radius of the collector, r_b is the radius of the emitter, and v is the instantaneous voltage between the emitter and collector. If space charge and thermal velocities of the electrons are ignored, the field is considered to act radially and only radial components of motion of the electrons need be considered, then

$$x'' = - \frac{e}{m} \frac{V_0 \sin(\omega t + \alpha)}{x \log r_a/r_b}$$

where V_0 = peak rf potential between collector and emitter and α is the phase of entry of an electron.

This equation has been solved for various values of α . An electron leaving early in a cycle appears to travel quickly to the collector, while an electron leaving later takes several cycles to cover the distance. An electron which leaves still later in the cycle returns to the emitter with considerable kinetic energy. If it is assumed that a secondary electron is emitted with the same initial energy as that with which the primary electron bombards the emitter, then the time of flight of this secondary electron is less than that of any primary electron and the energy of this electron on arrival at the collector is greater than that of any other electron. It has been observed in practice that the potential developed by the collector approaches very nearly that calculated from consideration of this particularly favored secondary electron. It has also been found that the diode will operate with no detectable change of output as cathode temperatures vary from 650°C to 850°C as measured optically.

A more accurate analysis of the operation can be made if the collector is assumed to have negative bias; this negative bias is chosen to be that value which the collector attains when the diode is unloaded.

Under these conditions, calculations of further electron trajectories have been made. It has been shown that for phase angles up to 106° the electron reaches the collector without reversal of direction. Above this figure, the direction of flight of the electron is reversed when it approaches the collector, although it may experience a second reversal in direction near the emitter and still reach

the collector. At about 120° the electron returns to the emitter during the first cycle. The potential finally reached by the collector must be that of the fastest electron and this depends on the magnitude of V_0 , frequency and tube geometry only.

Test results on tubes now in production agree fairly closely with values predicted from the above considerations.

Tubes have been designed for use at 8.6 mm, 3.2 cm, 8.5 cm and 10-cm bands. With the exception of the 8.6-mm band, tubes can be plugged into holders without tuning or adjustment. The resultant vswr of holder and tube is better than 1.2 over a wide band. Using an 80-ohm load, a peak power output of 100 v is obtainable for an input of 13.5 kw peak at 9500 mc and the same output for an input of 3 kw at 3000 mc. The response time of the diodes appears to be better than 0.001 μ sec. Hence, using a suitable oscilloscope, magnetron moding and other irregularities of performance can be viewed. The output from the diodes remains remarkably constant over a 1000-hour life.

The initial work on these tubes was done by the Services Electronics Research Laboratory at Baldock.² Further developments have been carried out by Elliott Brothers (London) Ltd., including the design and manufacture of a range of diodes and power measuring units which are now commercially available.

W. J. HOSKIN
Elliott Brothers (London) Ltd.
Borehamwood, Hertfordshire, Eng.

¹ P. O. Hawkins, "A diode rectifier of microwaves," *S.E.R.L. Tech. J.*, vol. 3, pp. 38-43; July, 1953.

Hysteresis Heating of Microwave Ferrites*

In the development of a high-speed sinusoidal ferrite phaser in X band, it was found that the temperature of the General Ceramics R1 ferrite used rose rapidly and melted the polystyrene support. To investigate this phenomenon, a coil was wound on a tufnol former inside which a 2-inch-length, $\frac{1}{4}$ -inch-diameter rod of ferrite was placed. A small search coil was wound round the ferrite to monitor the field, while thermocouples were attached to the ferrite and field coils to monitor their temperatures.

With an applied field of 50 oersteds (peak-to-peak) varying at 300 kc, the temperature of the ferrite rose to 150°C in a few minutes, while the field-coil temperature lagged behind. This rise was found to be dependent upon the shape of the ferrite, a fact which was attributed to demagnetising effects. Similar effects were noted with various types of experimental ferrite of MgMn and NiAl compositions.

Other workers in this field have attributed loss of efficiency of high-frequency ferrite phasers to waveguide eddy current losses. The above experiment suggests that

* Received by the IRE, May 20, 1957.

* Received by the IRE, May 2, 1957.
¹ H. A. Thomas, *PROC. IRE*, vol. 45, pp. 205-211; February, 1957.

another cause of this is due to some form of loss in the ferrite itself, probably high-field hysteresis loss.

This effect does appear to provide a serious difficulty in the design of very-high-speed continuous phasers and switches.

W. N. HONEYMAN
AND R. S. COLE
Microwave Division
E.M.I. Electronics Ltd.
Feltham, Middlesex, England

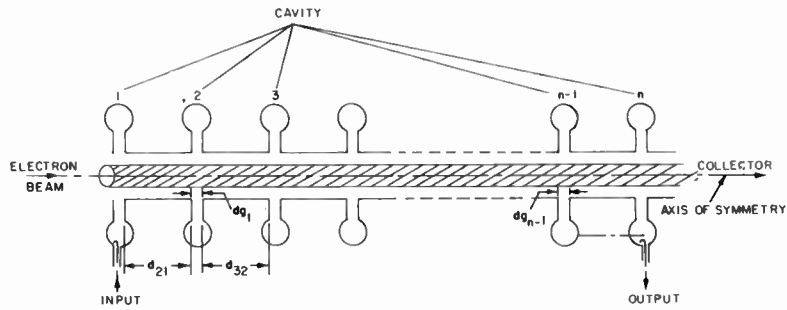


Fig. 1—General disposition of a *n*-cavity klystron amplifier.

Application of the Potential Analog in Multicavity Klystron Design and Operation*

The multicavity klystron problem can be treated analytically by one of two methods:

1) Following Webster¹ and Feenberg,² a ballistic model can be employed with some corrections to take care of space charge. This procedure yields results that are essentially valid under large signal conditions when the calculations are carried out in the manner suggested by Feenberg.

2) Using the space-charge wave theory of Hahn and Ramo³ or the Llewellyn-Peterson equations in an appropriate form.⁴

The procedure employed here involves the second approach and can be corrected to take care of some of the large signal effects. (This will be discussed at a later date.)

Making the usual assumptions, pertinent to a one-dimensional, small-signal nonrelativistic case, we can write down the following matrices expressing the relations between ac velocity *v*, and ac current *i* at two planes *a* and *b* (electron beam traveling in the direction from *a* to *b* and ac quantities are assumed to be uniform over the beam cross section).

For a drift region we have

$$\begin{bmatrix} i_b \\ v_b \end{bmatrix} = \begin{bmatrix} \cos \theta_{ba} & jg \sin \theta_{ba} \\ jg^{-1} \sin \theta_{ba} & \cos \theta_{ba} \end{bmatrix} \begin{bmatrix} i_a \\ v_a \end{bmatrix} e^{-j\psi_{ba}} \quad (1)$$

* Received by the IRE, May 13, 1957; revised manuscript received, May 23, 1957.

¹ D. L. Webster, "Cathode ray bunching," *J. Appl. Phys.*, vol. 10, pp. 501-508; July, 1939.

² E. Feenberg, "Notes on Velocity Modulation," Sperry Gyroscope Co., reprints nos. 5221-1043; 1942-1945.

³ W. C. Hahn, "Small signal theory of velocity modulated electron beams," *G. E. Rev.*, vol. 42, pp. 258-270; June, 1939.

⁴ S. Ramo, "The electronic-wave theory of velocity-modulation tubes," *Proc. IRE*, vol. 27, pp. 757-763; December, 1939.

⁵ F. B. Llewellyn and L. C. Peterson, "Vacuum-tube networks," *Proc. IRE*, vol. 32, pp. 144-166; March, 1944.

The equivalence of space-charge wave and Llewellyn-Peterson equations has been shown, for instance, by:

L. D. Smullin, "Propagation of disturbances in one-dimensional accelerated electron beams," *J. Appl. Phys.*, vol. 22, pp. 1496-1498; December, 1951.

C. K. Birdsall, "Equivalence of Llewellyn and space charge wave equations," *IRE TRANS.*, vol. ED-3, pp. 76-77; April, 1956.

where

- I* = the dc current density,
- ω = the operating angular frequency,
- $g = -\omega I / \omega_q u_0$,
- ω_q = reduced plasma angular frequency to account for the finite beam diameter,
- $= r \omega_p (\omega_p^2 = \eta I / \epsilon_0 u_0)$,
- u_0 = dc velocity of beam,
- $\eta = e/m$ (charge to mass ratio) of an electron,
- ϵ_0 = dielectric constant of vacuum,
- $\theta_{ba} = \omega_q d_{ba} / u_0$ (transit angle of region *ba* measured in terms of reduced plasma frequency),
- d_{ba} = distance between planes *a* and *b* (drifting distance), and
- $\psi_{ba} = \omega d_{pa} / u_0$.

Similarly, for a gap we may write

$$\begin{bmatrix} i_b \\ v_b \end{bmatrix} = \begin{bmatrix} 1 & 0 \\ M^2 Z(\omega) \frac{\eta}{u_0} & 1 \end{bmatrix} \begin{bmatrix} i_a \\ v_a \end{bmatrix} e^{-j\psi_g} \quad (2)$$

where

- Z*(ω) = shunt impedance (of the cavity) connected across the gap in question,
- M* = beam-coupling coefficient, a function of beam and drift tube geometry, and
- ψ_g = transit angle of gap.

The above matrices can also be written in a form analogous to the transmission-line equations as suggested by Chu some time ago.⁵

By a repeated application of the transformations given by (1) and (2), one can obtain the necessary expression for gain for any given structure consisting of drift spaces, cavities and an electron beam of given characteristics.

Suppose then that there are *n* cavities (see Fig. 1) where the different regions have different parameters. Let the voltage across the *n*th cavity be *V_n*. Then,

$$V_n = M_n Z_n i_n \quad (3)$$

where *M_n* and *Z_n* are the beam coupling coefficient and the shunt impedance of the *n*th cavity gap respectively and *i_n* current exciting the *n*th cavity. One finds that *i_n* can be written as

⁵ Such a procedure was adopted by L. D. Smullin and A. Bers of M.I.T. in a paper on multicavity klystrons presented at the Conference on Electron Tube Research, Boulder, Colo.; June, 1956.

$$i_n = -j \sum_{k=1}^{n-1} \alpha_{nk} V_k, \text{ but for a phase factor} \quad (4)$$

and

$$\alpha_{nk} = -M_k g \frac{\eta}{u_0} \sin \theta_{nk} = M_k Y_c \sin \theta_{nk} \quad (5)$$

where

$$Y_0 = -(\eta / u_0) g$$

and

θ_{nk} = transit angle between cavities *n* and *k* (*k* < *n*) measured in terms of reduced plasma frequency radians.

From (3), (4), and (5) one can write the following expression for *V_n*:

$$V_n = \left(\sum_{k=1}^{n-1} F_{nk} V_k \right) e^{-j\psi_{n1}} \quad (6)$$

where

$$F_{nk} = -j M_n Z_n \alpha_{nk}, \quad (7)$$

and ψ_{n1} is the transit angle between cavities *n* and 1.

$$\left(\psi_{n1} = \frac{\omega}{u_0} d_{n1} \right).$$

For instance, in the case of a four-cavity klystron we have

$$\frac{V_4}{V_1} = e^{-j\psi_{41}} (-jY_0)^3 [M_1 M_2^2 M_3^2 M_4 Z_2 Z_3 Z_4 \sin \theta_{43} \sin \theta_{32} \sin \theta_{21}] \cdot \left\{ 1 + \frac{j \sin \theta_{31}}{M_2^2 Z_2 Y_0 \sin \theta_{32} \sin \theta_{21}} + \frac{j \sin \theta_{42}}{Y_0 M_3^2 Z_3 \sin \theta_{43} \sin \theta_{32}} \right\} \cdot \left(1 + \frac{j \sin \theta_{41}}{Y_0 M_2^2 Z_2 \sin \theta_{42} \sin \theta_{21}} \right) \quad (8)$$

It is clear then, that we can write down the ratio of two voltages (output/input) for a multicavity klystron with arbitrary parameters by the above relations.

To investigate the methods of broad banding of multicavity klystrons, in analogy with the low-frequency IF amplifier design,⁶ we recognize that the input voltage *V₁* should be expressed in terms of a constant current generator and a number which is a function of the coupling scheme and impedance of the input cavity *Z₁*. It is convenient to express all impedances in terms of ad-

⁶ G. E. Valley, Jr. and H. Wallman, "Vacuum Tube Amplifiers," M.I.T. Rad. Lab. Ser., McGraw-Hill Book Co., Inc., New York, N. Y., vol. 18; 1948.

mittances. That is, write $Z_i = 1/Y_i$, noting that for a small amount of detuning (around 10 per cent or less) we can write

$$Y_i \approx G_i [1 + 2jQ_i \delta_i] \\ = 2G_i Q_i \left[p + \frac{1}{2Q_i} - j(1 + \delta^{(i)}) \right] \quad (9)$$

where

$$G_i = G_{Li} + G_{Bi} + G_{Ri}$$

G_{Li} , G_{Bi} , and G_{Ri} represent the contribution to the shunt conductance by the external load, beam loading, and ohmic losses, respectively,

Q_i = is over-all Q (loaded Q) of the i th cavity,

$$\delta_i = (\omega/\omega_i) - 1, \quad \delta^{(i)} = (\omega_i/\omega_0) - 1, \quad p = \sigma + j\Omega, \text{ and}$$

ω_i = resonant of the i th cavity, ω_0 = mid-band frequency of the klystron, and $\Omega = \omega/\omega_0$, the normalized frequency.

After going through the procedure suggested above, namely, expressing V_1 in terms of a constant current generator and expressing all impedances in terms of admittances, we obtain the following general expression for power gain:

$$\text{power gain} = K |f_1(Z_1, Z_2, \dots, Z_n) \cdot \{g_1(Y_2, Y_3, \dots, Y_{n-1})\}|^2 \quad (10) \\ = HZ(p), \quad (10a)$$

say where

f_1 is a function of the impedances of all the cavities,

g_1 is a function of the admittances of all the intermediate (excluding the input and output) cavities,

K is a function of the input current and the coupling scheme at the input cavity,

H is a multiplicative constant or scale factor, and

$Z(p)$ is a ratio of two polynomials in p .

It is evident that a sort of voltage gain function G_{n1} can be written in the form

$$G_{n1} = z(p) = e^{\alpha} e^{j\beta} \quad (11)$$

It is now clear that the concept of the potential analog⁷ enters in at this place, when we have written $z(p)$ as the ratio of two polynomials. As usual, we can define the transmission function $\mathcal{F}(p)$ as

$$\mathcal{F}(p) = \log z(p) = \alpha + j\beta \\ = \log K + \sum_i \log(p - p_i^0) \\ - \sum_k \log(p - p_k) \quad (12)$$

where K is a constant which may be ignored in the analysis, since its value merely changes the level or amplitude, and p_i^0 and p_k are the zeros and the poles of the transfer function $z(p)$ respectively. One recalls then

⁷ S. Darlington, "The potential analog method of network synthesis," *Bell Sys. Tech. J.*, vol. 30, pp. 315-365; April, 1951; see bibliography of this paper for additional references.

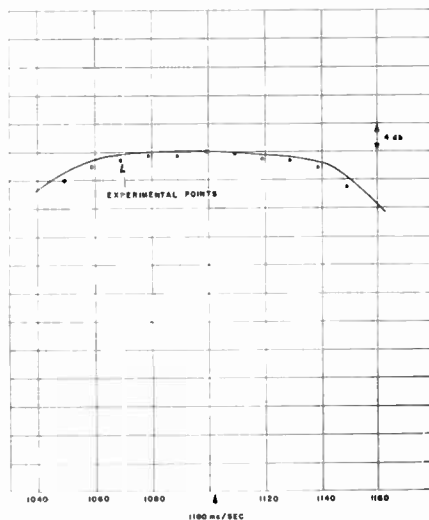


Fig. 2.—Comparison of theory and experiment.

that: 1) the zeros and poles must be either real or conjugate complex, and 2) the real parts of the poles must be negative for physical realizability.

It follows then, that

$$[\mathcal{F}(p)]^* = \mathcal{F}(-p) = \alpha - j\beta$$

where the asterisk denotes complex conjugate, since $p^* = -p$ when $p = j\Omega$.

On the real frequency axis then, we have

$$\alpha = \frac{1}{2} [\mathcal{F}(p) + \mathcal{F}(-p)] = \text{even part of } \mathcal{F} \\ j\beta = \frac{1}{2} [\mathcal{F}(p) - \mathcal{F}(-p)] = \text{odd part of } \mathcal{F}$$

A comparison of (12) with potentials due to line charges in two-dimensional potential theory clearly shows that the amplitude and phase of the output voltage can be determined in principle by simple graphical means if desired.

The following comments are in order. In the present problem of a (multi) n -cavity klystron, where the cavities are singly tuned, the transfer function has n poles and at the most $(n-2)$ zeros. If each of the cavities are m -ply tuned, then the transfer function would have nm poles and at the most $n(n-2)$ zeros.

The synthesis procedure may well follow the usual techniques; namely, Butterworth, Tchebycheff, or flat delay approximations. However, it is convenient in practice to treat each problem separately.

Fig. 2 shows a comparison of the theoretically and experimentally determined responses in the case of a particular four-cavity klystron. The agreement appears to be quite good, within 1 to 1.5 db.

It should be stated here that similar ideas have also been expressed independently by Kreuchen and others.⁸

Details of additional theoretical work and experimental verification will be reported later.

SRRAMAMURTI V. YADAVALLI
G. E. Microwave Lab,
Palo Alto, Calif.

⁸ K. H. Kreuchen, B. A. Auld, and N. E. Dixon, "A study of broadband frequency response of the multicavity klystron amplifier," *J. of Electronics*, vol. 2, pp. 529-567; May, 1957.

Superregenerative Masers*

Solid-state maser amplifiers operating at liquid helium temperatures are expected to have noise figures of the order of 0.04 db.^{1,2} If use is to be made of this low noise figure without coupling masers in series, it is necessary for the maser to have a high enough gain to work into a conventional microwave receiver. Since noise figures for the latter are commonly greater than 6 db, a gain of 25 db or more will be required in the maser. Of the two modes of operation that have so far been proposed for solid-state masers, the regenerative mode,^{3,4} in which the paramagnetic material is contained in a resonant cavity, is in principle capable of unlimited gain but in practice, considerations of gain stability and linearity set an upper limit to the realizable gain. The other mode, in which a traveling wave is amplified in a waveguide containing the paramagnetic material together with a nonreciprocal element,⁵ avoids the disadvantages of regenerative operation but introduces difficulties of its own both because of the length of guide required for reasonable gain with magnetic dipole transitions and because of cryogenic and magnetic field considerations. A third possible mode of operation, which will be examined below, makes use of superregeneration.

For any receiver in which unambiguous demodulation is required, the noise figure obtained with intermittent operation is higher than that obtained with continuous operation by a factor of the order of T/t , where t is the "on" time out of a total cycle time T . For a superregenerator the factor is T/τ where τ is the time constant for oscillation build-up. Thus, superregenerative masers or intermittent masers with poor duty factors are not likely to be advantageous for coherent signal reception. In certain fields, for example in radioastronomy and in microwave radiometry, the "signal" of interest is just microwave noise power at very low levels. In this case there is no problem of demodulation ambiguity and all the noise power received in the maser bandwidth is useful "signal." Under such conditions the "noise figure" (now defined in terms of the ratio of received noise to internally generated noise) will be about the same for a superregenerative or intermittent maser as for a similar maser operated continuously, and in this respect the former two will be at no disadvantage.

Superregeneration is more likely to be considered in two-level than in three-level masers because, in the absence of some mechanical transport of material, the former have to operate intermittently in any case to allow time for the preparation of the ampli-

* Received by the IRE, April 24, 1957.

¹ R. V. Pound, "Spontaneous emission and the noise figure of maser amplifiers," *Ann. Phys.*, vol. 1; April, 1957.

² J. P. Wittke, "Molecular amplification and generation of microwaves," *Proc. IRE*, vol. 45, pp. 291-316; March, 1957.

³ N. Bloembergen, "Proposal for a new type solid state maser," *Phys. Rev.*, vol. 104, pp. 324-327; October 15, 1956.

⁴ H. E. D. Scovil, G. Feher, and H. Seidel, "The operation of a solid state maser," *Phys. Rev.*, vol. 105, p. 762; January 15, 1957.

⁵ N. Bloembergen, invited talk presented before Amer. Phys. Soc., New York, N. Y.; January 30-February 2, 1957; unpublished.

fying state. Although most attention so far has been devoted to three-level masers there are reasons for believing that two-level masers will be developed, particularly for the fields mentioned above where intermittency is not disadvantageous. These reasons include the fact that there is a wider range of materials available for two-level operation, including some with lower power losses, higher intrinsic gain for the same electron content, and relaxation times which would permit operation at temperatures above 4°K. In addition, two-level masers have greater flexibility in frequency range and an upper frequency limit which is not determined by the availability of a local oscillator of still higher frequency. It will be appropriate to compare the characteristics of a two-level maser operated both intermittently and superregeneratively.

Any intermittently operating two-level maser will have a time cycle resembling that shown in Fig. 1(a). T_i represents the time re-

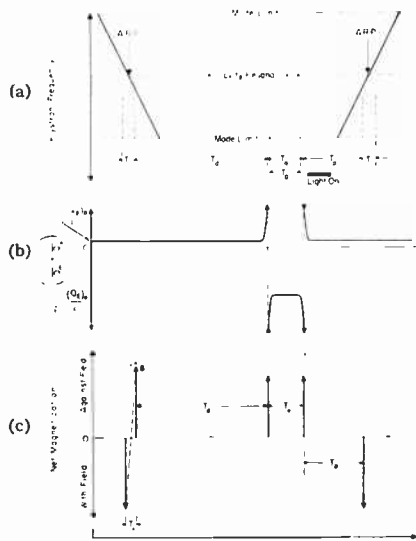


Fig. 1—(a) Time sequence showing klystron frequency and state of maser as function of time, (b) The variation of total Q , Q_i , with time for superregenerator, (c) The behavior of the net spin magnetization as a function of time. (Imperfect inversion is shown by the dashed vector.)

quired to perform the population inversion and might be the duration of a "180 pulse"² or of an "adiabatic rapid passage."² The Q which describes the paramagnetic material, Q_m ,³ becomes negative during the inversion process. During and immediately after T_i the system possesses a coherent transverse magnetic moment which precesses about the external field, but decays with a characteristic time T_2 , the spin-spin relaxation time. The coherent transverse moment gives rise to radiation in the cavity because of radiation damping⁶ and if the rate of radiation growth is faster than the rate of decay of the transverse moment the inverted population will "radiate itself away." To reduce losses of this type to an acceptable level it is necessary for Q_i , the loaded Q of the cavity, to

be much smaller than the minimum value of $|Q_m|$ both during T_i and for the period T_d after it, during which the radiation rate decreases roughly exponentially. The length of T_d is determined by the value of T_2 , by the accuracy of inversion, and by the lowest signals that will have to be amplified. For good inversion and the lowest signals it will be of the order of 10 to 15 T_2 . For amplification, it is necessary for Q_i to be made almost equal to $|Q_m|$ (regeneration) or greater than $|Q_m|$ (superregeneration), and such a change will initiate the active period T_a . Suitable means for reducing Q_i might be by switching a ferrite loading device coupled to the cavity or by changing the magnetic field so that the paramagnetic resonance frequency is shifted into the wings of the cavity resonance curve. At some time after T_a and before the start of T_i , Q_i must be reduced to a low level again. In the regenerative case T_a will be the "on" time of the amplifier and T_a/T [$= T_a/(T_i + T_d + T_a + T_p)$] will be the duty factor. In the superregenerative case, T_a will be the time during which oscillation is allowed to build up. In either case the active period may be terminated by lowering Q_i by or the process that initiates T_p , the preparation period. During T_p the electrons are brought back approximately to a Boltzmann distribution, a process that normally proceeds with a time constant T_1 , the spin-lattice relaxation time. In certain materials a very close approach to a Boltzmann distribution may be attained in a time very much shorter than T_1 by means of a suitable auxiliary technique, e.g., a strong pulse of light in the case of donors in silicon.²

For cases where thermal equilibrium cannot be brought about by "artificial" means and in which one must, therefore, rely on the internal T_1 process, it is necessary to provide some reference point in this process so that the electron populations at the start of T_i will be the same from cycle to cycle irrespective of the signal strength. This is done conveniently by equalizing the populations at the start of T_p by means of a strong pulse at the signal frequency.

If the received signals are low enough, or if a gain fluctuation from cycle to cycle is tolerable, a reference is not necessary and preparation will be greatly assisted by a second population inversion at the start of T_p . This will also reduce the heat given out by the system during T_p , a significant factor in helium cooled masers. In this method, of course, amplification periods follow alternate inversions. The receiver following the maser will have to be gated to be receptive only for a time T_a , within the period T_a , so as not to amplify the inverting and preparing radiation.

A possible superregenerative cycle (operating in the step-controlled linear mode) in which population inversion is achieved by a frequency sweep constituting adiabatic rapid passage, is shown in Fig. 1. For a material with $T_2=10^{-6}$ seconds, a frequency sweep rate of 10 mc per microsecond will be ample. Thus, a mode of a 3-cm klystron would be traversed in about 5 microseconds. For an inversion resulting in a 1 per cent transverse component of magnetic moment and for a sensitivity of 10^{-16} watts, T_d will

be 11 microseconds. For the case of a matched cavity with $Q_m = -Q_i/2$ (i.e., $Q_i = 2Q_m$) and $Q_i = 12,000$ (at low temperatures), the oscillation will build up with a characteristic time, τ , equal to $2 \cdot 10^{-7}$ seconds. The duration of T_a is just $n \cdot \tau$, where n will be between 10 and 20 for reasonable gains. Thus T_a will lie between 2 and 4 microseconds. Assuming a suitable paramagnetic material, preparation may be brought about by a light pulse which might be of 3-microsecond duration. The total time cycle, T , would then take 20 microseconds, and this would determine the response time of the instrument.⁷ The bandwidth for thermal radiation detection is, however, determined by τ and in this case will be about 1 mc.

When the above maser is used as a "noise amplifier," the time averaged power gain, g , is given by

$$g = (\tau/T) \exp^n = (\tau/T) 10^{0.43n} \text{ or } (4.3n - 20) \text{ db for } \tau/T = 0.01.$$

The dependence of gain on separate variations in the operating conditions is given by

$$dg/g \approx n dT_a/T_a \text{ or } 2ndQ_m/Q_m \text{ or } ndQ_i/Q_i.$$

For a continuous regenerative maser

$$g = Q_i^2(Q_i + Q_m)^{-2}$$

whence

$$dg/g = 2g^{1/2} dQ_m/Q_m \text{ or } 2g^{1/2} dQ_i/Q_i.$$

For a regenerative maser active for a time T_a in a total time T ,

$$dg/g = 2 \cdot g^{1/2} \cdot (T/T_a)^{1/2} \cdot dQ_m/Q_m.$$

A comparison of the sensitivity of gain to changes in operating conditions is shown in Fig. 2(a)-(g), for the cases of continuous re-

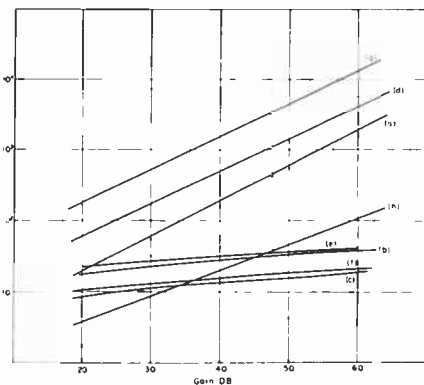


Fig. 2—(a)-(g) Variation of gain with changes in operating conditions. (a) $(d \ln g)/(d \ln Q_m)$ for regenerative maser operating continuously. (b) $(d \ln g)/(d \ln Q_m)$ for superregenerative maser with $\tau/T = 1$ per cent. (c) $(d \ln g)/(d \ln T_a)$ for superregenerative maser with $\tau/T = 1$ per cent. (d) $(d \ln g)/(d \ln Q_m)$ for regenerative maser with same T_a/T as (b) and (c). (e) $(d \ln g)/(d \ln Q_m)$ for superregenerative maser with $\tau/T = 0.1$ per cent. (f) $(d \ln g)/(d \ln T_a)$ for superregenerative maser with $\tau/T = 0.1$ per cent. (g) $(d \ln g)/(d \ln Q_m)$ for regenerative maser with same T_a/T as (e) and (f). (h) Relative power output at saturation, P_s/P_s , as a function of gain, for cases (b) and (d) above.

⁷ At power levels approaching the ultimate sensitivity of this maser, photon noise [due to fluctuations in the rate of arrival of radiation quanta at the antenna] becomes important and it is necessary to make several "samplings" of incident radiation to arrive at a reliable value for its intensity.

³ N. Bloembergen and R. V. Pound, "Radiation damping in magnetic resonance experiments," *Phys. Rev.*, vol. 95, pp. 8-12; July 1, 1954.

generation, superregeneration with $\tau/T = 0.01$ and 0.001 , and for regeneration with corresponding values of T_a/T . $1/|Q_m|$ is directly proportional to the net magnetization and therefore depends linearly on the magnetic field, on the temperature of the paramagnetic material, and, in a more complicated way, on the accuracy of inversion and preparation.

At high output levels the value of $1/|Q_m|$ and therefore of gain will become smaller as amplification proceeds. For a given cycling time and initial magnetization, and for the same allowable fall-off in gain over T_a , the ratio of superregenerative power output, P_s , to regenerative power output P_r , is given by

$$P_s/P_r = (gT/T_a)^{1/2} n^{-1}.$$

The variation of P_s/P_r with gain for Fig. 2(b) and (d) is plotted as Fig. 2(h). In Fig. 2(d), with $T = 20$ microseconds, the power input for a 10-per cent departure from linearity will be $\sim 5 \times 10^{-9}$ watts at 20-db gain and $\sim 5 \times 10^{-16}$ watts at 60-db gain.

For applications in radio astronomy and microwave radiometry, therefore, it would seem that a superregenerator, even in comparison with a continuous regenerative maser, has some advantage in the matter of stability, range of linearity, and stringency of inversion and preparation conditions, especially at high gains. Moreover, in cases where artificial shortening of T_1 cannot be used, and therefore in which the duty factor of a regenerative maser would be poor, the superregenerator compares favorably at lower gains.

The authors wish to acknowledge stimulating discussions with M. Menes.

P. F. CHESTER
AND D. I. BOLEF
Westinghouse Res. Labs.
Pittsburgh 35, Pa.

Maximum Efficiency of the Solid-State Maser*

In a recent paper Wittke¹ has estimated the efficiency of a maser amplifier operating in the linear amplification region and, not surprisingly, finds it to be very small. Most amplifiers have low efficiency when operated in the linear region. What is desired is an estimate of efficiency at saturation. Such a calculation can be made rather simply for the three-state maser of the type proposed by Bloembergen² if some simplifying assumptions are made regarding the transition probabilities.

Consider an amplifier utilizing a material with three energy levels (1, 2, 3) as envisaged by Bloembergen. Energy is supplied

to the crystal at ν_{31} , the driving frequency, saturating the (3, 1) transition and the population of level 3 is made larger than that of level 2. The device will now amplify at the signal frequency ν_{32} . Using Bloembergen's rate equations one can calculate the steady-state population difference ($n_3 - n_2$) and ($n_1 - n_2$). The power given up by the crystal at the signal frequency is

$$P_{\text{maser}} = (n_3 - n_2) h \nu_{32} W_{32}$$

and the power absorbed by the crystal at the driving frequency ν_{31} is

$$P_{\text{abs}} = (n_1 - n_2) h \nu_{31} W_{31}$$

where the W 's are the radiation induced transition probabilities. Imagine now that the (3, 2) transition has been saturated so that P_{maser} is a maximum. If it is assumed that each of the resonance lines is homogeneously broadened, then the two powers may be expressed as

$$P_{\text{maser}} = \frac{h^2 N \nu_{32}}{3kT} (w_{21} \nu_{21} - w_{23} \nu_{32})$$

$$P_{\text{abs}} = \frac{h^2 N \nu_{31}}{3kT} (w_{21} \nu_{21} + w_{13} \nu_{31})$$

where w_{nm} is the thermal transition probabilities from an initial state n to a final state m .

If the crystal were placed in a lossless cavity so that all the power supplied by it were delivered to the load, the limiting or *intrinsic* efficiency would be

$$\eta_i = \frac{P_{\text{maser}}}{P_{\text{abs}}} = \left(\frac{\nu_{32}}{\nu_{31}} \right) \frac{w_{21} \nu_{21} - w_{23} \nu_{32}}{w_{21} \nu_{21} + w_{13} \nu_{31}}$$

If we assume all the transition probabilities are equal, *i.e.*, all the spin-lattice relaxation times are equal, then, making use of the fact that $\nu_{31} = \nu_{32} + \nu_{21}$, we obtain a simple expression for the intrinsic efficiency.

$$\eta_i = \left(\frac{\nu_{32}}{\nu_{31}} \right) \frac{1 - 2 \left(\frac{\nu_{32}}{\nu_{31}} \right)}{2 - \left(\frac{\nu_{32}}{\nu_{31}} \right)} \quad (\text{all } w_{nm} \text{ equal}).$$

This efficiency shows a maximum when

$$\left(\frac{\nu_{32}}{\nu_{31}} \right) = 2 - \sqrt{3} = 0.268 \text{ which is}$$

$$\eta_{i \text{ max}} = 0.0718 \quad (\text{all } w_{nm} \text{ equal}).$$

Thus the three-state maser under these conditions could be expected to have at most an efficiency approaching 7.18 per cent.

The general relation for intrinsic efficiency suggests a method for obtaining considerably higher values than this. If we introduce another relaxation process whereby ions can make transitions between states 2 and 1, then we can increase the transition probability w_{21} . One such mechanism has been reported by Feher and Scovil³ who found that an additional impurity ion could under proper circumstances increase w_{21} by a factor of ten. (Scovil, Feher, and Seidel⁴

subsequently employed this effect in the first successful three-state maser.)

If, then, the transition probability w_{21} is increased considerably above w_{23} and w_{13} , the intrinsic efficiency approaches

$$\eta_i = \left(\frac{\nu_{32}}{\nu_{31}} \right) \quad (w_{21} \gg w_{23}, w_{13}).$$

Under these conditions, the three-state maser can exhibit very respectable efficiencies.

H. HEFFNER
Stanford University
Stanford, Calif.

The Phase-Shift Method of Single-Sideband Signal Reception*

The phase-shift method of SSB reception described in the above paper by Norgaard¹ appears to be the same as that employed by Hansell in his circuit for neutralizing the image frequency in a superheterodyne receiver.²

Briefly, if f_0 is the beating oscillator frequency and f_i is the intermediate frequency, then the incoming signal is, say, $(f_0 - f_i)$ and the image frequency is $(f_0 + f_i)$. The analogy to sidebands is evident. Two first detectors are employed, each supplied with a phase of quadrature-phase energy from the oscillator. The outputs of the detectors are given a uniform relative phase shift and then combined in the IF amplifier to provide cancellation of the image frequency.

HAROLD M. LEWIS
Professional Engineer
West Allenhurst, N. J.

* Received by the IRE, April 30, 1957.

¹ D. E. Norgaard, Proc. IRE, vol. 44, pp. 1735-1743; December, 1956.

² C. W. Hansell, British Patent 434902—Valve Circuits for Wireless Reception. Convention date, August 1, 1933. The number of the corresponding U. S. Patent is not at hand.

A Third Method of Generation and Detection of Single-Sideband Signals*

Earlier publications of the above method¹ by Madella, and by Tucker and MacDiarmid, have been cited by Frank and McPherson.² In view of their comments I trust that I may be pardoned if I call attention to a still earlier reference.³ Therein the heterodyne

* Received by the IRE, April 30, 1957.

¹ D. K. Weaver, Proc. IRE, vol. 44, pp. 1703-1705; December, 1956.

² R. L. Frank, and R. R. McPherson, "Discussion of the single-sideband issue," Proc. IRE, vol. 45, p. 539; April, 1957.

³ U. S. Patent 1964522—Phase Control System; June 26, 1934 (filed June 13, 1929).

* Received by the IRE, May 10, 1957.

¹ J. P. Wittke, "Molecular amplification and generation of microwaves," Proc. IRE, vol. 45, pp. 291-316; March, 1957.

² N. Bloembergen, "Proposal for a new type solid-state maser," Phys. Rev., vol. 104, pp. 324-327; October 15, 1956.

³ G. Feher and H. E. D. Scovil, "Electron spin relaxation times in gadolinium ethyl sulfate," Phys. Rev., vol. 105, pp. 760-762; January 15, 1957.

⁴ H. E. D. Scovil, G. Feher, and H. Seidel, "The operation of a solid-state maser," Phys. Rev., vol. 105, pp. 762-763; January 15, 1957.

method of providing a uniform relative phase shift of a band of frequencies is shown in a phase-control system of SSB generation.

In the patent mentioned,³ the location of the heterodyne carrier, to provide the uniform relative phase shift, is at the high end of the band and what Frank refers to as the "second distinct idea" of heterodyning in the center of the audio band is not shown. Most engineers who have studied circuits of this type have probably toyed with the idea of heterodyning in the center of a band of frequencies, generally with an idea of narrowing the band by folding it. So far as I know, the resulting mixture has been promptly abandoned as hopeless. It was, therefore, surprising to come upon Weaver's¹ use of this method in a practical system. Of course, he does not seek nor accomplish any band width reduction since, in the end, he must employ the two narrowed bands to resolve the mixture.

On the general subject of polyphase modulation, there is still an earlier patent.⁴

HAROLD M. LEWIS
Professional Engineer
West Allenhurst, N. J.

¹U.S. Patent 1898366—Frequency Transformation System, February 21, 1933.

Radar Echoes from Overdense Meteor Trails under Conditions of Severe Diffusion*

It has been shown recently¹ that the Lovell-Clegg scattering formula for meteor trails must be modified to a considerable extent when the wavelength of the radar is less than 2 m. An attenuation constant, η , was introduced for trails in which the electron density was less than the critical density n_c corresponding to the wavelength λ , and it was shown that under extreme conditions the attenuation approached a value of 40 db. To complete the theory it is necessary to consider trails in which the electron density is greater than n_c and to examine the behavior of these trails under conditions of severe diffusion.

The density of ions, n , produced behind a meteoroid at time t is cylindrically symmetric and is described by the expression

$$n = \frac{q}{(\pi r_0^2 + 4\pi Dt)} \exp \left[-\frac{r^2}{(r_0^2 + 4Dt)} \right] \quad (1)$$

where D is the ambipolar diffusion coefficient, r_0 is the initial diameter of the trail, and q is the number of ions per unit length

* Received by the IRE, May 13, 1957. This work originated at Sylvania Electric Products, Inc., under an Army Ordnance contract and was extended under contract AF19(122)-458, Subcontract No. 57.

¹G. S. Hawkins, "Radar echoes from meteor trails under conditions of severe diffusion," *Proc. IRE*, vol. 44, p. 1192; September, 1956.

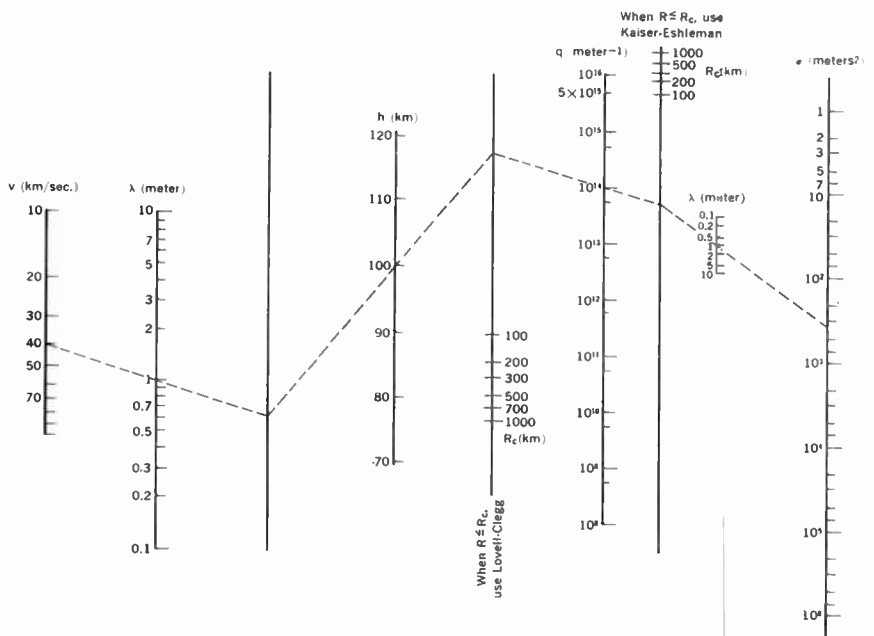


Fig. 2—Nomogram for computing radar cross section of diffuse meteor trails.

in the column. As a first approximation we may neglect r_0 and fit a paraboloid distribution to (1) by writing

$$n = \frac{q}{4\pi Dt} \left[1 - \frac{\gamma r^2}{4Dt} \right] \quad (2)$$

where $\gamma = 1 - \exp(-1)$. Eq. (2) applies over the region where $\gamma r^2 < 4Dt$ and fits (1) at a surface $r^2 = 4Dt$ when $r_0 = 0$. If the meteoroid, at position $(0, 0, Z)$, is moving in the positive direction along the z axis, as shown in Fig. 1, then $t = (Z - z)/v$, where v

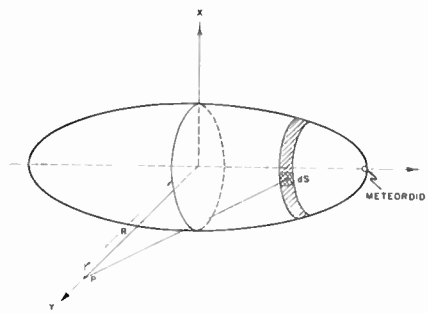


Fig. 1—Reflection from a spheroidal target.

is the meteoroid velocity, and we may write

$$n = \frac{qv}{4\pi D(Z - z)} \left[1 - \frac{\gamma r^2 v}{4D(Z - z)} \right] \quad (3)$$

By definition, a surface exists in the overdense meteor column where

$$n = n_c = \frac{4\pi^2 \epsilon_0 m c^2}{\lambda^2 e^2} = \frac{2\pi^{3/2}}{\lambda^2 \sigma_c^{1/2}} \quad (4)$$

The quantity

$$\frac{1}{4\pi} \left(\frac{e^2}{\epsilon_0 m c^2} \right)^2$$

will be recognized as the scattering cross section of a free electron, σ_e . This surface acts

as a perfect reflector and the dimensions of the radar target may be determined by substituting for n in (3). It is found that the surface is a spheroid described by

$$K_1(Z - z)^2 - (Z - z) + K_2 r^2 = 0 \quad (5)$$

where $K_1 = 8\pi^{5/2} D / \lambda^2 q v \sigma_c^{1/2}$ and $K_2 = \gamma v / 4D$. If we now put the meteoroid at the point $Z = 1/2K_1$, (5) takes the form

$$\frac{r^2}{a^2} + \frac{z^2}{b^2} = 1 \quad (6)$$

where $2a = (K_1 K_2)^{-1/2}$, $2b = 1/K_1$. Eq. (6) is the standard form for a prolate spheroid with center at the origin; the shape is represented in Fig. 1. It is interesting to note that the length of the target is the same function of v , λ , and D that was found previously for underdense trails.¹

To evaluate the field, v_p , scattered back to a radar on the y axis, we will adopt the Eikonal treatment of physical optics and write

$$v_p = \frac{v_0}{i\lambda} \int_S \frac{\exp \{ ik \{ R - 2(a - y) \} \}}{R + (a - y)} \cos \theta dS \quad (7)$$

where $k = 2\pi/\lambda$. The angle between the normal to the surface element and the range vector R is θ . The integral includes all sources, of amplitude v_0 , on the exposed surface S . Since $a \ll R$ and $\cos \theta dS = dx dz$, we may write

$$v_p = \frac{v_0}{i\lambda R} \exp \{ ik(R - 2a) \} \int_{-b}^{+b} \int_{-a}^{+a} \frac{\exp \{ 2iky \} dx dz}{\sqrt{1 - z^2/b^2} \sqrt{1 - x^2/a^2}} \quad (8)$$

If the substitutions

$$\begin{aligned} x &= a \sin \theta \cos \phi \\ y &= a \sin \theta \sin \phi \\ z &= b \cos \theta \end{aligned}$$

are made, (8) becomes

$$v_p = \frac{abv_0}{i\lambda R} \exp [ik(R - 2a)] \int_0^\pi \int_0^\pi \sin^2 \theta \sin \phi \cdot \exp [2aik \sin \theta \sin \phi] d\theta d\phi \quad (9)$$

which may be evaluated in terms of the Bessel functions J_0 and J_1 . It is found that

$$v_p = -\frac{\pi b v_0}{\lambda k R} \exp [ik(R - 2a)] \cdot \left\{ 1 - \frac{\sin 2ka}{ka} + \left(\frac{\sin ka}{ka}\right)^2 + \dots \right\}^{1/2} \quad (10)$$

The field v_0 is approximately constant over the target and $a \ll \lambda$ so that the scattered power p is given in terms of the antenna gain G and power output P of the radar by the following expression:

$$p = \frac{GP\lambda^2}{64\pi^3 R^4} \cdot \pi b^2 \quad (11)$$

It is interesting to note that the spheroid is an extremely efficient reflector; it is equivalent to a sphere with a diameter equal to the major axis of the spheroid. In terms of the constant K_1 , the scattering cross section of the overdense trail is

$$\sigma = \frac{\lambda^4 q^2 \sigma_e}{16^2 \pi^4 D^2} \quad (12)$$

This is identical with the scattering cross section of underdense trails when diffusion is severe.¹ Thus, in contrast to the two regimes of the early theories, we have a single formulation for all meteors: the echo power is proportional to $\lambda^6 q^2$ and is inversely proportional to the fourth power of the range. Scattering cross sections may be evaluated for certain values of q , λ , and height in the atmosphere, h , from the nomogram in Fig. 2. The value of D appropriate to a given height was computed from the relation of Greenhow and Neufeld.²

$$\log_{10} D = 0.0679 \times 10^{-3}h - 5.663. \quad (13)$$

The foregoing treatment has neglected r_0 , the initial diameter of the trail on formation, and the effect of fragmentation³ of the meteoroid. These phenomena are of importance in the coma which surrounds the meteoroid so that it is not possible to use the spheroid in calculating the scattering cross section along the z axis.

G. S. HAWKINS

Harvard College Observatory
Cambridge, Mass.

D. F. WINTER

Sylvania Electric Products, Inc.
Waltham, Mass.

and Harvard College Observatory

² J. S. Greenhow and E. L. Neufeld, "The diffusion and ionized meteor trails in the upper atmosphere," *J. Atmos. Terr. Phys.*, vol. 6, pp. 133-140; March, 1955.

³ L. G. Jacchia, "The physical theory of meteors VIII, fragmentation as the cause of the faint-meteor anomaly," *Astrophys. J.*, vol. 121, pp. 521-527; March, 1955.

The Theoretical Sensitivity of the Dicke Radiometer*

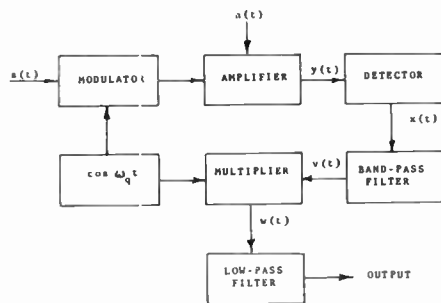
The microwave radiometer has attracted the attention of a number of investigators since Dicke devised a practical and sensitive circuit.¹ Today it is becoming one of the standard instruments of electronics. The results of a new analysis² are reported here along with comments on the recent remarks of Goldstein and Tucker.³

Prior analyses of the Dicke circuit^{1,4} were based upon the representation of the second detector by the expression $V_0 = kV_i^2$. Since a biased diode is almost universally used as a second detector it seems that a representation such as

$$V_0 = i(V_i - B)^N, \quad V_i > B \\ = 0, \quad V_i < B \quad (1)$$

should be used, or alternately, a justification of the simple relation offered. By the use of a relation equivalent to (1), the author achieved a more general treatment of the radiometer and found that the sensitivity was independent of the detector characteristic. The expression for the sensitivity agreed with that of Goldstein and Dicke (as corrected by Selove⁵). Only the assumptions and conclusions of the author's analysis will be described here.

Fig. 1 is a block diagram of the Dicke



Notes:

- 1) $s(t)$ and $n(t)$ are thermal noise voltages with average powers of $\sigma_s^2/2\omega_s$ and $\sigma_n^2/2\omega_n$ watts /radian.
- 2) The amplifier pass band is rectangular and of width ω_a centered at $\pm\omega$.
- 3) The band pass filter is rectangular and of width ω_b centered at $\pm\omega$.
- 4) The low-pass filter has a rectangular pass band extending from $-\omega_f$ to $+\omega_f$.

Fig. 1—Block diagram of the Dicke radiometer.

* Received by the IRE, April 25, 1957; revised manuscript received, May 15, 1957. The work described was performed at the Elec. Eng. Res. Lab., University of Texas.

¹ R. H. Dicke, "The measurement of thermal radiation at microwave frequencies," *Rev. Sci. Instr.*, vol. 17, pp. 268-275; July, 1946.

² L. D. Stross, "The theoretical sensitivity of the microwave radiometer," dissertation, Univ. of Texas; February, 1957 (available from University Microfilms, Ann Arbor, Mich.).

³ S. J. Goldstein, Jr., and D. G. Tucker, "A comparison of two radiometer circuits," *Proc. IRE*, vol. 45, pp. 365-366; March, 1957.

⁴ S. J. Goldstein, Jr., "A comparison of two radiometer circuits," *Proc. IRE*, vol. 43, pp. 1663-1666; November, 1955.

⁵ W. Selove, "A dc comparison radiometer," *Rev. Sci. Instr.*, vol. 25, pp. 120-124; February, 1954.

circuit with the major assumptions listed in the notes. With the exception of the description of the second detector, the assumptions of the author are essentially the same as those made by Goldstein. With properly chosen coefficients, a fifth-order polynomial has a curve that is a good model of the actual diode characteristic over a limited range. Indeed the curve

$$x(t) = \sum_{n=0}^5 a_n y^n(t), \quad -1 \leq y(t) \leq 1 \quad (2)$$

is superior to the curve of (1) in the vicinity of the origin. The fact that the polynomial is a valid model only within an interval is no liability. In most applications, and certainly in the radiometer, the signal applied to the diode is limited in the amplifier preceding the diode.

Sinusoidal modulation was assumed; the results for nonsinusoidal modulation can be obtained by resolving the complex modulation into its Fourier components. The input to the detector is

$$y(t) = s(t)\left(\frac{1}{2} + \frac{1}{2} \cos \omega_d t\right) + n(t) - B. \quad (3)$$

The spectral distribution of $y(t)$ is determined by the amplifier. Substitution of (3) into (2) produces the output signal, $x(t)$. The output autocorrelation function is computed from $x(t)$ by

$$R_x(\tau) = \lim_{T \rightarrow \infty} \frac{1}{T} \int_0^T x(t)x(t + \tau)dt. \quad (4)$$

After extensive simplification, $R_x(\tau)$ was reduced to 66 terms which were identified as autocorrelation and crosscorrelation terms of the input signal and noise. Completing the solution it was found that for small signals the power output of the radiometer was given by

$$P_0 = \frac{A^2}{32} \sigma_s^4 + A^2 \frac{\omega_y}{\omega} \sigma_n^4 \quad (5)$$

where

$$A = a_2 - 3a_3B + 6a_4B^2 - 10a_5B^3. \quad (6)$$

When the signal-to-noise ratio was computed and set equal to unity (following the usual method of defining sensitivity) the coefficient A^2 canceled out, indicating that the radiometer's sensitivity is independent of the second detector characteristic. If, instead of a fifth-order polynomial, an N th-order polynomial had been used for the diode, the calculation of the output power would be improved but the sensitivity relation would be unchanged. Expressed in terms of the minimum detectable temperature difference, this sensitivity is

$$\Delta T = NT_0 \sqrt{\frac{32\omega_y}{\omega_a}} \quad (7)$$

where N is the noise figure of the instrument with minimum insertion loss in the modulator and T_0 is the reference temperature used in computing the noise figure, usually 300°K. Experimental verification of these results for a variety of diodes and bias conditions was inherently inconclusive due to the nature of the signals. It was found that the measured sensitivity was about one

half as good as that calculated by (7) and that there was no significant change in sensitivity with a variety of diodes and bias conditions.

Since the above treatment establishes that the radiometer's sensitivity is independent of the detector characteristic, (7) should be identical to the results of the prior authors. The recent comment by Goldstein¹ revising his earlier result, which was the same as (7) above, is in error. Since Goldstein's treatment can be obtained as a special case of the present work, it was easy for the author to establish that his expression for the autocorrelation function of $v(t)$ reduced to Goldstein's $R_2(\tau)$,

$$R_2(\tau) = \frac{k^2}{8} \sigma_s^4 \cos \omega_q \tau + k^2 \left[\frac{17}{32} \sigma_s^4 + \frac{3}{2} \sigma_s^2 \sigma_n^2 + 2\sigma_n^4 \right] \frac{\cos \omega_q \tau \sin \frac{\omega \beta \tau}{2}}{\frac{\omega \alpha \tau}{2}} \quad (8)$$

The autocorrelation of $w(t)$, $R_3(\tau)$, can be obtained easily from $R_2(\tau)$. Since

$$w(t) = v(t) \cos \omega_q t, \quad (9)$$

$$\begin{aligned} R_3(\tau) &= \lim_{T \rightarrow \infty} \frac{1}{T} \int_0^T w(t)w(t+\tau) dt \\ &= \lim_{T \rightarrow \infty} \frac{1}{T} \int_0^T v(t)v(t+\tau) \cos \omega_q t \cos \omega_q (t+\tau) dt \\ &= \lim_{T \rightarrow \infty} \frac{1}{T} \int_0^T v(t)v(t+\tau) \frac{\cos \omega_q \tau}{2} dt \\ &+ \lim_{T \rightarrow \infty} \frac{1}{T} \int_0^T v(t)v(t+\tau) \frac{\cos \omega_q (2t+\tau)}{2} dt. \quad (10) \end{aligned}$$

The second integral on the right vanishes in the limit. Hence

$$R_3(\tau) = R_2(\tau) \frac{\cos \omega_q \tau}{2} \quad (11)$$

and thus

$$\begin{aligned} R_3(\tau) &= \frac{k^2 \sigma_s^4}{32} [1 + \cos 2\omega_q \tau] \\ &+ \frac{k^2}{2\omega_q \tau} \left[\frac{17}{32} \sigma_s^4 + \frac{3}{2} \sigma_s^2 \sigma_n^2 + 2\sigma_n^4 \right] \\ &\cdot \sin \frac{\omega \beta \tau}{2} [1 + \cos 2\omega_q \tau]. \quad (12) \end{aligned}$$

The contributions to the power spectrum by the $\cos 2\omega_q \tau$ terms lie outside the region of interest and are omitted. The correct statement for $R_3(\tau)$, deleted of terms that are subsequently filtered out, is just one half of Goldstein's original expression. Thus Goldstein's recent revision is correct but not complete. In computing the signal-to-noise ratio, the common factor of one half canceled out and the original result of Goldstein was correct although based upon a slightly incorrect autocorrelation function.

The use of a rectangular pass band for the output filter has been criticized by

Tucker.³ Since only the noise bandwidth of the output filter enters into the computation of sensitivity, this criticism appears trivial. On the other hand, the shape of the amplifier and band-pass response functions do enter into the problem since the autocorrelation functions are computed by evaluating the Fourier transforms of the signal leaving these stages. Fortunately, the error introduced is small and these convenient approximations can be used.

The author is indebted to a number of people at the University of Texas. In particular he would like to thank Drs. Straiton and Dueterhoeft for their aid and encouragement.

LELAND D. STROM
Texas Instruments, Inc.
Dallas, Texas

Prediction of Semiconductor Surface Response to Ambients by Use of Lewis Acid-Base Theory*

During the last few years, changes produced by ambient atmospheres, or ambients, in conductivity,^{1,2} surface conductance,^{3,4} contact potential,⁵ photoconductivity,⁶ and surface-recombination velocity^{7,8} of single-type semiconductors have been reported, as have the role of ambients in forming inversion layers, or channels, on diodes.^{9,10} Ambient-induced effects on reverse currents in a germanium diode¹¹ and on collector-base reverse saturation current, surface-breakdown voltage, and dc alpha of germanium alloy-junction transistors¹² have also been observed.

With two partial exceptions^{8,11} which may be associated with experimental error,

* Received by the IRE, May 23, 1957.

¹ C. Wagner, "The mechanism of the decomposition of nitrous oxide on zinc oxide as a catalyst," *J. Chem. Phys.*, vol. 18, pp. 69-71; January, 1950.

² E. N. Clarke, "Oxygen-induced surface conductivity on germanium," *Phys. Rev.*, vol. 91, pp. 756-757; August, 1953, and "Oxygen and the surface energy-level structure on germanium," *Phys. Rev.*, vol. 95, pp. 284-285; July, 1954.

³ S. R. Morrison, "Changes of surface conductivity of germanium with ambient," *J. Phys. Chem.*, vol. 57, pp. 860-863; November, 1953.

⁴ H. C. Montgomery and W. L. Brown, "Field-induced conductivity changes in germanium," *Phys. Rev.*, vol. 103, pp. 865-870; August, 1956.

⁵ W. H. Brattain and J. Bardeen, "Surface properties of germanium," *Bell Sys. Tech. J.*, vol. 32, pp. 1-41; January, 1953.

⁶ W. G. Schneider and T. C. Waddington, "Effect of gases on the photoconductivity of anthracene," *J. Chem. Phys.*, vol. 25, p. 358; August, 1956.

⁷ C. A. Hogarth, "On the measurement of minority carrier lifetimes in silicon," *Proc. Phys. Soc. (London)*, vol. B69, pp. 791-795; August, 1956.

⁸ B. H. Schultz, "Storage of injected carriers at surfaces of germanium," *Philips Res. Repts.*, vol. 12, pp. 82-96; February, 1957.

⁹ H. Christensen, "Surface conduction channel phenomena in germanium," *Proc. IRE*, vol. 42, pp. 1371-1376; September, 1954.

¹⁰ A. L. McWhorter and R. H. Kingston, "Channels and excess reverse current in grown germanium *p-n* junction diodes," *Proc. IRE*, vol. 42, pp. 1376-1380; September, 1954.

¹¹ W. T. Eriksen, H. Statz, and G. A. de Mars, "Excess surface currents on germanium and silicon diodes," *J. Appl. Phys.*, vol. 28, pp. 133-139; January, 1957.

¹² A. J. Wahl and J. J. Kleimack, "Factors affecting reliability of alloy junction transistors," *Proc. IRE*, vol. 44, pp. 494-502; April, 1956.

Lewis acid-base theory permits predicting all these ambient-induced changes.¹⁻¹² A *p*-type surface is considered a Lewis acid (electron-pair acceptor) and an *n*-type surface, a Lewis base (electron-pair donor). By their acceptor action, Lewis-acid ambients will decrease surface concentration of electrons and increase surface concentration of holes. Through their donor action, Lewis-base ambients will produce the opposite surface concentration changes. Hence, Lewis-acid ambients, such as oxygen, will decrease conductivity in an *n*-type surface and recombination velocity in a *p*-type surface while increasing conductivity in a *p*-type surface and recombination velocity in an *n*-type surface. While they are not Lewis acids, electronegative halogen atoms will act in the same way. On the other hand, Lewis-base ambients, such as ammonia, will produce exactly the opposite surface results. The extent to which these mechanisms are observed by the onset of ionic-like surface currents has yet to be determined.

From these considerations and Webster's data for germanium alloy-junction transistors,¹³ the following generalization can be made: An ambient-induced change in collector-base reverse saturation current in alloy-junction transistors, will move in the same direction as the change made by the ambient in base surface-recombination velocity and minority-carrier concentration in the base. In grown-junction transistors, ambient-induced changes in collector-base reverse saturation current, should be able to be predicted from expected changes in minority-carrier concentration and in surface-recombination velocity in the collector. In the case of dc alpha in germanium alloy-junction transistors, experimentally observed changes with ambient¹² can be accounted for by considering the competing changes produced by ambients in the first two terms in Webster's¹³ equations for $1/h_{fb}$.¹⁴ The first of these terms involves surface recombination in the base. The second contains the ratio of minority-carrier concentrations in the emitter and in the base. On applying these $1/h_{fb}$ equations to grown-junction transistors, it is found that the second term will probably be dominant for two reasons: 1) The trend toward reduction of surface-recombination in the base and 2) the fact that minority-carrier concentrations in both the emitter and base are large enough to show significant ambient-induced changes in opposite directions. The principles used in achieving these correlations should allow prediction of the change in electrical properties produced in any semiconductor surface by exposure to an ambient. Detailed treatment of the correlations mentioned here will be published elsewhere.

C. G. PEATTIE
AND J. R. MACDONALD
Texas Instruments, Inc.
Dallas 9, Tex.

¹³ W. M. Webster, "On the variation of junction-transistor current-amplification factor with emitter current," *Proc. IRE*, vol. 42, pp. 914-920; June, 1954.

¹⁴ The IRE Standards on Letter Symbols for Semiconductor Devices (*Proc. IRE*, vol. 44, pp. 934-937; July, 1956) are used here. In previous terminology, h_{fb} is α_{dc} .

Nonreciprocal Two-Port Measurement Based on an Averaging Technique*

In his communication on the measurement of nonreciprocal two-ports, Pippin¹ has suggested the use of the test setup, shown here again in Fig. 1, for the determination of the scattering matrix parameters.

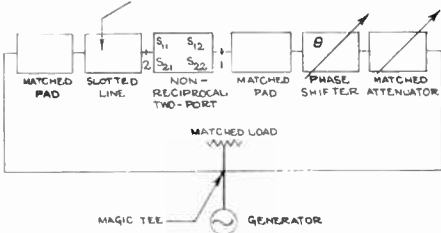


Fig. 1—Test setup as used to find S_{11} and S_{21} .

As already demonstrated by him, the reflection coefficients Γ_1 and Γ_2 can be measured with the slotted line where

$$\Gamma_1 = S_{11} + S_{12}e^{j\theta}, \quad \Gamma_2 = S_{22} + S_{21}e^{j\theta}$$

Here, θ is the phase shift due to the phase shifter within an additive constant.

It is interesting to note from these equations that the loci of $\Gamma_1(\theta)$ and $\Gamma_2(\theta)$ are circles in the reflection coefficient plane from which the scattering parameters can readily be abstracted, as shown in Fig. 2, for $\Gamma_2(\theta)$.

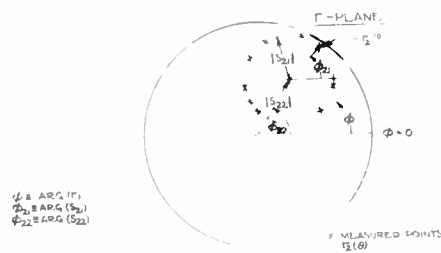


Fig. 2—Determination of S_{11} and S_{21} from locus of $\Gamma_2(\theta)$.

In order to improve precision, circle averaging techniques² can consequently be applied to the measurement of the scattering parameters of nonreciprocal two-ports. As in all such measurements, certain phases depend on single point reference measurements. In this instance, $\arg(S_{12})$ and $\arg(S_{21})$ correspond to $\Gamma_1(0)$ and $\Gamma_2(0)$. When indicated, additional care can be exercised to compensate for small variations (with θ) of the insertion loss of the uncalibrated phase shifter by elaborating on the basic circuit of Fig. 1.

HELMUT M. ALTSCHULER
Microwave Research Institute
Polytechnic Institute of Brooklyn
Brooklyn 1, N. Y.

* Received by the IRE, June 12, 1957.
¹ J. E. Pippin, "Scattering matrix measurements on nonreciprocal microwave devices," *Proc. IRE*, vol. 44, p. 110, January, 1956.
² H. M. Altschuler and A. A. Oliner, "A shunt technique for microwave measurements," *IRE TRANS.*, vol. MTT-3, pp. 24-30, July, 1955.

Signal Flow Graphs*

May I haste
To write Dr. Mason¹
That equations

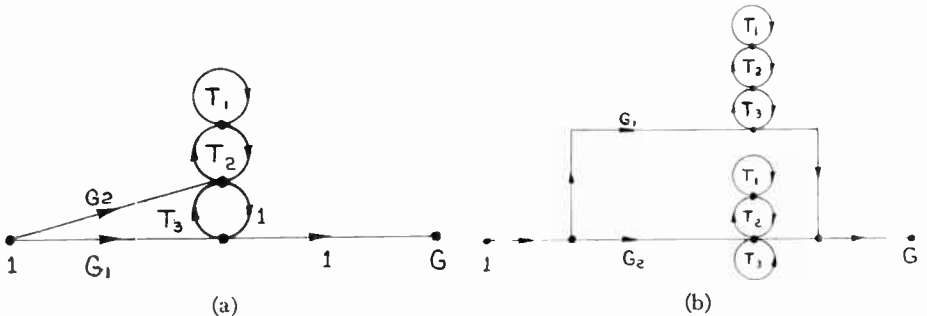


Fig. 1—The purpose of this communication is to point out that the rules given by Mason¹ for computing G may also be obtained from a series of flow graph transformations. The elimination of loops linking cascade paths is the first step in a series of successive transformations leading to a flow graph (Fig. 3) from which G can be evaluated at a glance.

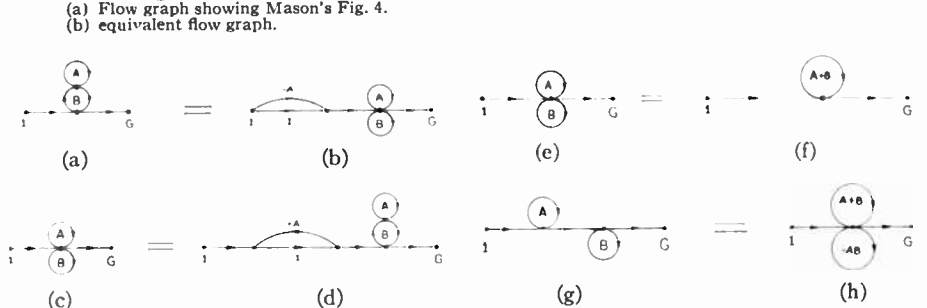


Fig. 2—Some transformation rules for loops. (a) and (b) are equivalent and illustrate how a loop not touching a cascade path may be replaced by a touching loop and a cascade path. (c) and (d) show that a touching loop is equivalent to a nontouching loop and a feedback path. (e) and (f) show that two loops touching each other are equivalent to a single loop. The value of the single loop is the sum of the individual loops. (g) and (h) demonstrate that two loops touching a cascade path but not each other, may be replaced by two touching loops: one equal to the sum of the isolated loops; the other equal to their product (with a change in sign).

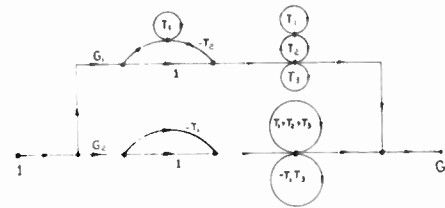


Fig. 3—Modification of Fig. 1. Nontouching loops are converted into equivalent touching loops using the transformation rules explained in Fig. 2(a)-(h). In the upper cascade path one subtracts a parallel cascade path, $G_1T_2/(1-T_1)$. In the lower cascade path one subtracts a parallel cascade path, G_2T_1 , and a self-loop, T_1T_3 .

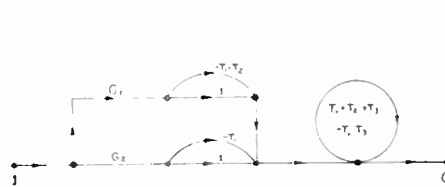


Fig. 4—Simplification of Fig. 3. Nontouching loops are eliminated and touching loops are added. This flow graph corresponds to Mason's (11).

Cause frustrations
When Topology
Needs no apology.
Eqs. (11), (12), and (13) amended
Pray author not offended.

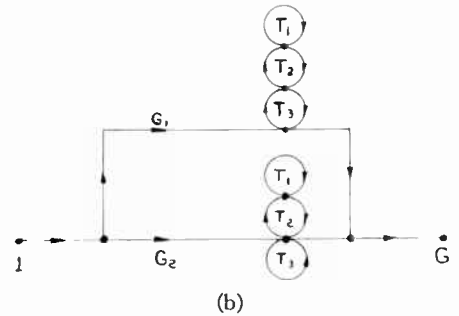


Fig. 5—Flow graph expressing formula for gain of the k th cascade path, corresponding to Mason's (12).

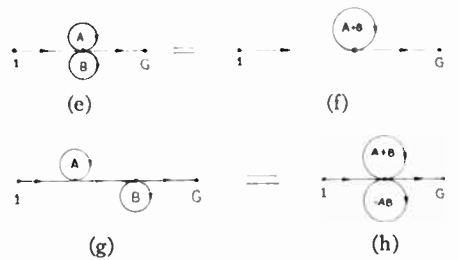


Fig. 6—One of several alternative forms of flow graph equivalent to Mason's (13a), obtained from his Fig. 7 by applying the transformation rules of Fig. 2. Note that all sets of loops occurring in Fig. 7(b) occur in the above graph as touching loops. Similarly, nontouching loops in Fig. 7(b), such as s_{12} and s_{21} , must appear in cascade in the above graph.

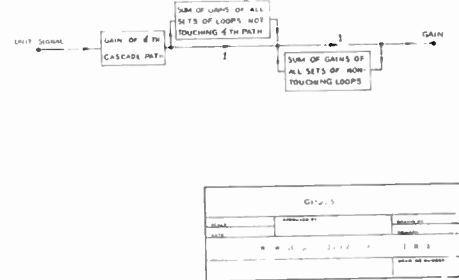


Fig. 7—Flow graph equivalent to Mason's (13a), obtained from his Fig. 7 by applying the transformation rules of Fig. 2. Note that all sets of loops occurring in Fig. 7(b) occur in the above graph as touching loops. Similarly, nontouching loops in Fig. 7(b), such as s_{12} and s_{21} , must appear in cascade in the above graph.

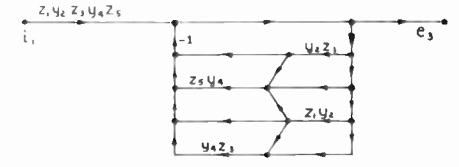


Fig. 8—Flow graph equivalent to Mason's (13a), obtained from his Fig. 7 by applying the transformation rules of Fig. 2. Note that all sets of loops occurring in Fig. 7(b) occur in the above graph as touching loops. Similarly, nontouching loops in Fig. 7(b), such as s_{12} and s_{21} , must appear in cascade in the above graph.

WILLIAM W. HAPP
Shockley Semiconductor Lab.
of Beckman Instruments, Inc.
Mountain View, Calif.

* Received by the IRE, July 30, 1956; revised manuscript received January 18, 1957.
¹ S. J. Mason, "Feedback theory—further properties of signal flow graphs," *Proc. IRE*, vol. 44, pp. 920-926, July, 1956. All references to equations and figures refer to this article.

Napierian Logarithms*

In some recent IRE publications, Napierian logarithms seem to be confused with natural logarithms. This is a very common error that is found in many books dealing with mathematical subjects.

I invite your attention to the following references which explain the distinction:

Encyclopaedia Britannica, vol. 14, 1942 ed., p. 303:

"*History of Logarithms.* Logarithms were invented independently by John Napier, a Scotsman, and by Joost Bürgi, a Swiss. The logarithms which they invented differed from each other and from the common and natural logarithms now in use. Napier's logarithms were published at Edinburgh,

in 1614, under the title, "Mirifici Logarithmorum Canonis Descriptio." When, in 1620, Bürgi's logarithms appeared at Prague under the title, "Arithmetische und Geometrische Progresstabulen," Napier's logarithms were already known and admired quite generally throughout Europe. To modern readers Napier's logarithms are a great curiosity, because of their singular properties and their strange mode of derivation . . ."

P. 304, (12):

$$\text{"Nap. log } y = 10^7 \log_e \left(\frac{10^7}{y} \right)\text{"}$$

"Since Napier, in 1614, did not take the logarithm of 1 to be 0, his logarithms, unmodified, do not admit of a base, *i.e.*, the relation of a number to its logarithm cannot be expressed by $b^l = n$."

Webster's New International Dictionary of the English Language, 1942 2nd ed., Unabridged. Under the word logarithm:

"Napierian logarithms are those calculated by John Napier, Laird of Merchiston, Scotland (1550-1617), who invented them and expounded them (1614) in his *Mirifici Logarithmorum Canonis Descriptio*. They are often confounded with natural logarithms, with which they are connected by the relation:

$$\text{"Nap. log } n = 10^7 \left\{ \text{nat. log } \left(\frac{10^7}{n} \right) \right\} \cdot \text{"}$$

It may be that the natural logarithms should be named in honor of Napier, but it does seem that the above-mentioned distinction should be stated.

M. S. CORRINGTON
Radio Corp. of America
Camden, N. J.

* Received by the IRE, June 17, 1957.

Contributors

H. G. Booker (SM'45-F'53) was born in Barking, Essex, England, in 1910. He was educated at Cambridge University, where he received the B.A. degree in 1933 and the Ph.D. degree in 1936. He was awarded the Smith's Prize in 1935 and became a Research Fellow of Christ's College in the same year.



H. G. BOOKER

During the war he was in charge of theoretical research at the Telecommunications Research Establishment in England. After the war he returned to Cambridge University as a lecturer, and in 1948 became a professor of electrical engineering at Cornell University.

❖

William C. Brown (A'39-VA'39-M'55) was born in Lewis, Iowa on May 22, 1916. He received the B.S. degree in electrical engineering from Iowa State College, Ames, Iowa in 1937. From 1937 to 1939, he was employed by the Radio Corporation of America. He received the M.S. degree from the Massachusetts Institute of Technology in 1941.



W. C. BROWN

Mr. Brown joined the Raytheon Manu-

facturing Company in 1940. Initially he was instrumental in developing new tube types for proximity fuses and subsequently worked on high-frequency triodes, which were used in radiosonde balloon transmitters. In 1943, Mr. Brown was placed in charge of the magnetron research and development laboratory. He was awarded the Naval Ordnance Development Award in 1945 and received the Certificate of Commendation for outstanding service during World War II. In 1953, he was made an assistant vice-president at Raytheon. He is currently in charge of the advanced development laboratory in the Microwave and Power Tube Operations.

Mr. Brown is a member of the honorary engineering societies, Tau Beta Pi and Eta Kappa Nu. He is also a member of the Advisory Group on Electron Tubes, serving as industry representative on the Working Group on Microwave Tubes.

❖

Donald G. Fink (A'35-SM'45-F'47), editor of PROCEEDINGS, was born on November 8, 1911, at Englewood, N. J. He received the B.S. degree in electrical engineering from the Massachusetts Institute of Technology in 1933 and the M.S. degree in electrical engineering from Columbia University in 1942.



D. G. FINK

During 1933-1934, Mr. Fink was a research assistant in the M.I.T. depart-

ments of electrical engineering and geology. From 1934 to 1952 he was on the editorial staff of *Electronics*, becoming Editor-in-Chief in November, 1946. Since 1952, he has been associated with the Philco Corp. as Director of Research for radio, television, and appliances.

Mr. Fink designed the standard Ioran transmitter in 1941-1943, when on leave to the Radiation Laboratory at M.I.T. In 1946, he was a civilian consultant of the Commander, Joint Task Force One, in charge of preparing damage reports on all electronic material and test facilities for the Bikini atom bomb tests.

He is a member of the Army Scientific Advisory Panel, Tau Beta Pi, Sigma Xi, Eta Kappa Nu, Fellow of the American Institute of Electrical Engineers and the Society of Motion Picture and Television Engineers.

❖

Donald W. Fraser (M'53-SM'55) was born on May 22, 1910. He attended the United States Naval Academy from which he received the B.S. degree in 1934. He did advanced work at the naval preradar and radar schools at Harvard and M.I.T. In 1948, he received the M.S. degree in electrical engineering from the Georgia Institute of Technology, Atlanta, Ga., and in 1955, he



D. W. FRASER

received the Ph.D. degree in electrical engineering.

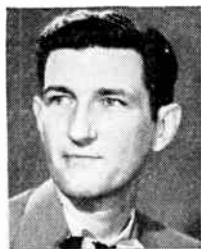
During World War II, Dr. Fraser served with the Electronic Field Service Group of the U. S. Navy, from June, 1942 until September, 1946. In the Korean War he became an electronics officer on Staff Commander Operational Development Force in the Navy, serving with this group from September, 1950 until January, 1953.

From 1946 until 1950, Mr. Fraser was assistant professor of electrical engineering and research associate at Georgia Tech., where he did research in high-frequency oscillators. He was also research engineer at the engineering experiment station of Georgia Tech from 1953 to 1955. He was director of projects on frequency control. At the present time he is the head of the Department of Electrical Engineering at the University of Rhode Island, Kingston, R. I.

Dr. Fraser is a member of Eta Kappa Nu, Tau Beta Pi, and Sigma Xi.



William E. Gordon (A'46-M'49) was born in Paterson, N. J., on January 8, 1918. He received the B.A. degree in mathematics from Montclair State Teachers' College in 1939, the M.S. degree in meteorology from the University of New York in 1946, and the Ph.D. degree from Cornell University in 1953.



W. E. GORDON

Dr. Gordon was in the Air Force during the war, engaged in radio-meteorological studies in association with the Committee on Propagation of NDRC. At the close of the war, he became associate director of the Electrical Engineering Research Laboratory, University of Texas. In 1948, he joined the staff of the school of electrical engineering, Cornell University, as research associate, becoming associate professor in 1953.

Dr. Gordon is Vice-Chairman of the USA National Committee, URSI, and a member of Tau Beta Pi, Sigma Xi, American Meteorological Society, and Joint Commission on Radio Meteorology, International Council of Scientific Unions.



John Hays Hammond, Jr. (A'12-M'14-SM'43) was born in San Francisco, Calif., on April 13, 1888. He received the B.S. degree from Yale University, Cambridge, Mass. in 1910 and the Sc.D. degree from George Washington University in 1919. He is president and treasurer of the Hammond Research Corporation and is a director of the RCA where he also serves as a consultant.



J. H. HAMMOND, JR.

Dr. Hammond has received over four hundred and twenty U. S. patents in a wide variety of fields. The U. S. Government has acquired rights in over ninety of these for radio-dynamic purposes, and RCA has acquired rights in over one hundred and sixty for radio-electronic purposes. He has also pioneered in the application of electronics in various other fields. Especially well known are the "Dynamic Amplifier" for expansion, compression, and noise reduction in audio systems; the "Accentor" for improving the tonal performance of pipe organs; and the "Telespot" for the momentary injection of a high-speed confidential facsimile service into a television channel with automatic reception, recording, processing and display.

Shortly after becoming an early member of the IRE, Dr. Hammond became a U. S. delegate to the International Radio-Telegraphic Conference of London in June, 1912; later he similarly served at the Washington Conference of 1927. He has also served on several advisory boards concerned with defense matters. In 1913-1914, he was treasurer of the IRE and was chairman of the special committees on membership and on finance. He also served the IRE for three years on its Board of Directors.



Claudius T. McCoy (A'37-SM'46) was born in Twin Falls, Idaho, on December 3, 1910. He attended Stanford University, Stanford, Calif., receiving the degree of Bachelor of Arts in physics in 1932. He joined the Philco Corp. in 1933, where for the past sixteen years he has been a member of the research division. He has worked on fm systems, vacuum-tube low-noise studies



C. T. MCCOY

afc analysis, storage tubes, microwave mixer networks, solid-state crystals for mixers and transistors; printed circuits in microwave, IF, and video, and molecular amplifiers. Mr. McCoy has applied for twelve patents, eight of which have been granted so far. He is at present a section engineer, acting as a staff consultant.



George C. Messenger (A'53) was born in Brattleboro, Vt. on July 20, 1930. He attended Worcester Polytechnic Institute, receiving the B.S. degree in physics in 1951. He received the M.S. degree in electrical engineering from the University of Pennsylvania in 1957. In 1951, Mr. Messenger went to work for the Philco Corp. as a member of the research division. He has worked



G. C. MESSENGER

primarily on the design of semiconductor devices, microwave mixer diodes, and on high-frequency transistors. He has published several papers related to these studies.

Mr. Messenger is a member of the APS.



Robert N. Noyce (M'56) was born in Burlington, Iowa on December 12, 1927. He received the B.A. degree in mathematics and physics from Grinnell College, Iowa, in 1949 and the Ph.D. degree from Massachusetts Institute of Technology in 1953 in physical electronics.



R. N. NOYCE

From 1953 to 1956, Dr. Noyce worked in the Research Department of Philco Corporation on problems in transistor design, semiconductor surface phenomena, and fabrication control.

For the past year he has been working on silicon transistor design and processing at the Shockley Semiconductor Laboratory, Mountain View, Calif.

Dr. Noyce is a member of the American Physical Society.



E. S. Purington (SM'47) was born in Mechanic Falls, Me., Oct. 13, 1891. He received the A.B. degree from Bowdoin College in 1912 and was granted the Everett graduate fellowship. He received the A.M. degree in physics and mathematics from Harvard University in 1913. After a year of teaching and another of further graduate work, he was laboratory assistant, assistant physicist, and



E. S. PURINGTON

associate physicist in the resistance, inductance, and capacitance, and the radio sections of the National Bureau of Standards. There he also did laboratory and field research for and with the armed forces in 1917-18, and later assisted in the post-war revision of the Signal Corps publication, "The Principles Underlying Radio Communication," used in military training.

Mr. Purington joined Hammond Laboratory in 1920, and has been connected with most of its subsequent developments in the radio-electronic field and is vice-president of the Hammond Research Corporation. He has received seventy U. S. patents, in which the U. S. Government has acquired rights to five and RCA to sixty-four. In addition to the many developments, he has been concerned with the application of electronics, especially well-known commercially is the "thermionic brake" method of rotary speed control used in transoceanic facsimile.

He is currently active in the IRE representation in the American Standards Association in matters pertaining to electric and magnetic magnitudes and units.

He is a member of Alpha Delta Phi and of Phi Beta Kappa.



Chih-Tang Sah (S'50-M'57) was born in Peiping, China, on November 10, 1932. He received B.S. degrees in engineering physics and in electrical engineering in 1953 from the University of Illinois.



C-T SAH

From 1953 to 1954, he was graduate fellow in electrical engineering at Stanford University and received the M.S. degree in 1954. From 1954 to 1956, he was a research assistant in the Electronics Research Laboratory at Stanford University. In 1956, he received the Ph.D. degree in electrical engineering, specializing in traveling-wave tubes. He joined the Shockley Semiconductor Laboratory in 1956 where he has worked on problems in semiconductor device physics and development.

Dr. Sah is a member of Sigma Xi, Phi Kappa Phi, Tau Beta Pi, Eta Kappa Nu, Pi Mu Epsilon, and the American Physical Society.



William Shockley (SM'51-F'55), one of three recipients of the 1956 Nobel Prize in Physics for his work on semiconductors and discovery of the transistor effect, was born in London, England, on February 13, 1910. He received the B.S. degree in 1932 from the California Institute of Technology. He continued his studies at Massachusetts Institute of Technology on a teaching fellowship, where he received the Ph.D. degree in physics in 1936.



W. SHOCKLEY

In September of that year he joined Bell Telephone Laboratories, where his work included vacuum-tube and electron-multiplier design, radar development, solid-state physics, magnetism, and semiconductors.

In 1942, Dr. Shockley was assigned to Columbia University Division of War Research as Director of Research for the Anti-submarine Warfare Operations Research Group. In 1944, he became a consultant to the Office of the Secretary of War.

Returning to Bell Telephone Laboratories in 1945, he became director of transistor physics, and in collaboration with W. H. Brattain and John Bardeen, worked on the development of the transistor.

At present, Dr. Shockley is director of the Shockley Semiconductor Laboratory of Beckman Instruments, Inc., Mountain View, Calif.

He was awarded the Presidential Medal for Merit in 1946 and the Morris Liebmann Award in 1952, and in 1951 was elected to the National Academy of Sciences. He received the honorary degree of Doctor of Science from the University of Pennsylvania in 1955 and from Rutgers University in 1956. He is a member of the American Physical Society, American Academy of Arts and Sciences, Tau Beta Pi, and Sigma Xi.



Otto J. M. Smith (M'44-SM'51) was born on August 6, 1917, in Urbana, Ill. He received the B.S. degree in chemistry from Oklahoma Agricultural and Mechanical College and the B.S. degree in electrical engineering from the University of Oklahoma in 1938. He was a research assistant at the H. G. Ryan High Voltage Laboratory at Stanford University from 1938 until 1941 when he received the Ph.D. degree in electrical engineering.



O. J. SMITH

Dr. Smith has taught and conducted research at Tufts College, Doble Engineering Company, Denver University, Westinghouse Research Laboratory, Summit Research and Development Laboratory, Shell Development Company, and Radio Interference Specialty Company. He has been at the University of California in Berkeley since 1947. From 1954 to 1956, while on leave from the University of California, he was a visiting professor of servomechanisms at the Instituto Tecnológico de Aeronáutica, São José dos Campos, Estado de São Paulo, Brasil. He also studied the educational system of Brasil, made recommendations, and taught advanced automatic control systems for the Brazilian government.

He is the author of "Feedback Control Systems," and the inventor of a low-frequency sine-function generator, an X-ray thickness gauge, dead-beat predictor controls for automatic systems, a constant-speed variable-frequency motor, a constant-frequency variable-speed generator, and a frequency-shift scaler. He has published research in the fields of magnetic amplifiers, magnetic frequency multipliers, semiconductors, phonograph recording, high-voltage corona, power-line fault locators, radiation instrumentation, counters, education, economic analogs, nonlinear feedback systems, and statistics.

Dr. Smith is a Fellow of the American Association for the Advancement of Science. He is active on editorial and review committees of the AIEE and IRE. He is a member of the American Society for Engineering Education, American Physical Society, American Institute of Physics, Sigma Xi, Phi Kappa Phi, Tau Beta Pi, Eta Kappa Nu, Phi Lambda Upsilon, Alpha Phi Omega, Kappa Tau Pi, Phi Eta Sigma, and Alpha Tau Omega.



Julius Tou (A'53-SM'56) was born in Shanghai, China on August 15, 1926. He received the B.S. degree in electrical engineering from Chiao-Tung University in 1947, the M.S. degree from Harvard in 1950, and the D.Eng. degree from Yale University in 1952.



J. TOU

At Harvard, he was a Gordon McKay scholar; at Yale, he did teaching and research at the Dunham Laboratory of Electrical Engineering. From 1952 to 1955, he was a project engineer of the research division of Philco Corporation. In February 1955, he joined the faculty of the Moore School of Electrical Engineering of the University of Pennsylvania, Philadelphia, Pa., as an assistant professor. In the Moore School, he worked on control and simulation problems and taught courses on feedback control theory and digital servomechanisms. Now he is an associate professor of electrical engineering at Purdue University, Lafayette, Ind.

Dr. Tou is a member of the American Institute of Electrical Engineers, the American Society for Engineering Education, and Sigma Xi.



IRE News and Radio Notes

FOUR EUROPEAN SCIENTISTS TO PARTICIPATE IN SYMPOSIUM

"Computers in Control" will be the theme of a symposium at the Chalfonte-Haddon Hall Hotel in Atlantic City, October 16-18, 1957. The conference, sponsored by the AIEE Feedback Control Systems Committee in conjunction with the IRE-PGAC and the ASME-IRD, will feature participation by J. Z. Tsytkin of Russia, M. Pelegrin of France, and P. F. Blackman of England. Special emphasis will be given to the use of digital and analog computers in design of and as elements of feedback control systems.

The opening session will be followed by a banquet on October 16th. Technical sessions the following day will culminate in a panel discussion on "Fitting Computers Into Control Systems," with Harold Chestnut of GE as moderator and Eugene Crabbe of Ramo-Wooldrige, T. James of DuPont, and John Moore of North American Automatic Division as panel members.

A portion of the papers to be presented at the conference are available in preprint form from the AIEE; Proceedings of the Conference will be published by the AIEE early in 1958. Conference arrangements have been made by a committee consisting of John Truxal, Polytechnic Institute of Brooklyn, Chairman; H. Chestnut; E. Grabbe; Adam Kegel, Westinghouse; and John Ragazzini, Columbia University.

The technical program will include the following papers from this country:

"Dynamic Programming and the Computation Solution of Feedback Control Design Problems," R. Bellman, Rand Corp.

"Compensation of Nonlinear and Time-Varying Systems by Computers," R. Booton M.I.T. and A. Rosenbloom, Ramo-Wooldrige.

"Real Time Computers for Control Systems," C. T. Leondes, UCLA.

"The Design of a Digital Computer for an Airborne Control System," J. T. Caulfield, J. V. B. Cooper, W. R. Maclay, and O. B. Shafer, IBM Military Products Div.

"System Considerations in Computer Control of a Semi-Continuous Chemical Process," T. M. Stout, Ramo-Wooldrige.

"A Stimulation Technique in the Synthesis of Automatic Flight Control Systems," Y. Nakada and S. J. Scroggs, Hughes.

"Control System Optimization Using Computers as Control System Elements," L. F. Kazda, University of Michigan.

"An Application of Root Locus Analysis to a Closed Loop Linear Control System Incorporating a Human Operator," J. Rodden and J. E. Mangelsdorf, Lockheed Missile Systems Div.

"Analog-Digital and Digital-Analog Conversion," A. K. Susskind, M.I.T.

"Differential Analyzer Aids Design of Computer Control System for Electric Utilities," L. K. Kirchmayer, GE.

"General Synthesis Procedure for Computer Control of Single and Multiloop Linear Systems," R. E. Kalman and J. E. Bertram, Columbia University.

Call for Papers

NOVEMBER 1 IS DEADLINE FOR 1958 IRE NATIONAL CONVENTION PAPERS

The 1958 IRE National Convention will be held at the Waldorf-Astoria Hotel and New York Coliseum, New York City, March 24-27, 1958.

Prospective authors are requested to submit all of the following by November 1, 1957:

- (1) 100-word abstract *in triplicate*, title of paper, name and address;
- (2) 500-word summary *in triplicate*, title of paper, name and address; and an indication of the technical field in which the paper falls.

The technical fields which may be covered are:

Aeronautical & Navigational Electronics	Engineering Management
Antennas and Propagation	Engineering Writing and Speech
Audio	Industrial Electronics
Automatic Control	Information Theory
Broadcast & Television Receivers	Instrumentation
Broadcast Transmission Systems	Medical Electronics
Circuit Theory	Microwave Theory & Techniques
Communications Systems	Military Electronics
Component Parts	Nuclear Science
Education	Production Techniques
Electron Devices	Reliability & Quality Control
Electronic Computers	Telemetry & Remote Control
	Ultrasonics Engineering
	Vehicular Communications

Address all material to:

G. L. Haller, Chairman
1958 Technical Program Committee
The Institute of Radio Engineers
1 East 79 St. New York 21, N. Y.

Calendar of Coming Events and Authors' Deadlines

- Special Technical Conference on Magnetic Amplifiers, Penn Sheraton Hotel, Pittsburgh, Pa., Sept. 4-5
- Industrial Electronics Symp., Morrison Hotel, Chicago, Ill., Sept. 24-25
- PGBTS Fall Symp., Willard Hotel, Wash., D. C., Sept. 27-28
- Nat'l Electronics Conference, Hotel Sherman, Chicago, Ill., Oct. 7-9
- Computers in Control Symp., Chalfonte-Haddon Hall Hotel, Atlantic City, N. J., Oct. 16-18
- IRE Canadian Convention Exhibition Park, Toronto, Can., Oct. 16-18
- Conf. on Eng. Writ. & Speech, Sheraton-McAlpin Hotel, New York City, Oct. 21-22
- International Conf. on UHF Circuits, Paris, France, Oct. 21-26
- East Coast Aero & Nav. Conf., Lord Baltimore Hotel & 5th Reg. Armory, Balt., Md., Oct. 28-30
- PGED Meeting, Shoreham Hotel, Wash., D. C., Oct. 31-Nov. 1 (DL*: Aug. 15, W. M. Webster, RCA, Somerville, N. J.)
- PGNS Annual Meeting, Henry Hudson Hotel, New York City, Oct. 31-Nov. 1
- Annual Symp. on Aero Commun., Hotel Utica, Utica, N. Y., Nov. 6-8
- Radio Fall Meeting, King Edward Hotel, Toronto, Can., Nov. 11-13
- PGI Conference, Atlanta-Biltmore Hotel, Atlanta, Ga., Nov. 11-13
- Mid-America Electronics Convention, Kan. City Mun. Audit., Kan. City, Mo., Nov. 13-14
- New England Radio Eng. Mtg., Mechanics Bldg., Boston, Mass., Nov. 15-16
- Conf. on Magnetism, Sheraton-Park Hotel, Wash., D. C., Nov. 18-20 (DL*: Aug. 15, L. R. Maxwell, U. S. Nav. Ordnance Lab., White Oak, Silver Springs, Md.)
- Elec. Computer Exhibition, Olympia, London, England, Nov. 28-Dec. 4
- PGVS Conf., Hotel Statler, Wash., D. C., Dec. 4-5
- Eastern Joint Computer Conf., Park-Sheraton Hotel, Wash., D. C., Dec. 9-13
- Nat'l Symp. on Reliability & Quality Control, Statler Hotel, Wash., D. C., Jan. 6-8, 1958
- Transistor-Solid State Circuits Conf., Phil., Pa., Feb. 20-21
- Nuclear Eng. and Science Congress, Palmer House, Chicago, Ill., Mar. 16-21
- IRE Nat'l Convention, N. Y. Coliseum and Waldorf-Astoria Hotel, New York City, Mar. 24-27 (DL*: Nov. 1)
- G. L. Haller, IRE Headquarters, New York City)
- Instruments & Regulators Conf., Univ. of Del., Newark, Del., Mar. 31-Apr. 2
- SW Regional Conf. & Show, Mun. Audit., San Antonio, Tex., Apr. 10-12
- Conf. on Automatic Techniques, Statler Hotel, Detroit, Mich., Apr. 14-16
- Elec. Components Symp., Los Angeles, Calif., Apr. 22-24
- * DL = Deadline for submitting abstracts

TWO NEW PROFESSIONAL GROUPS FORMED

**Professional Group
on
Education (PGE)**

Chairman: J. D. Ryder, Dean,
Michigan State University.

Assessment Fee: \$3.00.

The PGEWS plans to hold a conference at the Sheraton-McAlpin Hotel, New York City, October 21-22, 1957.

How to join either Group: Send your assessment fee to the Technical Secretary, IRE Headquarters, 1 E. 79 St., New York 21, N. Y., and ask that your name be added to the membership list.

**Professional Group
on
Engineering Writing and Speech (PGEWS)**

Chairman: D. J. McNamara, Department
of Publications, Sperry Gyroscope Co.

Assessment Fee: \$2.00.

**MILITARY ELECTRONICS GROUP
HOLDS FIRST NATIONAL
CONVENTION AT WASHINGTON**

Attendance at the First National Convention on Military Electronics June 17-19 far exceeded the PGMIL's preconvention estimate. Registration was over 2100 and viewers of the exhibits numbered nearly 5000. Approximately 80 technical papers were presented at 20 sessions, 5 of which were confidential. Efforts are now under way to publish the unclassified talks and make them available through IRE Headquarters.

The convention's theme, "Missiles and Electronics," was evident in the displays sponsored by seventy-eight exhibitors. These were highlighted by the first public showing of the Army's low-altitude ground-to-air missile, Hawk, whose prime contractor is Raytheon Manufacturing Company, and the Navy's Talos, an 80-100-mile surface-to-air guided missile built by Bendix Aviation Corporation. Other missile features were the Navy's surface-to-air Terrier, built by Convair Division of General Dynamics Corporation, and its air-to-air Sidewinder, built by Philco Corporation and General Electric. The Army's Missile Master, which directs and coordinates its Nike missile batteries also was displayed in miniature mockup style.

Social features at the convention included a luncheon sponsored by the Washington Chapter of the PGMIL at which Admiral W. F. Raborn, Bureau of Ordnance, spoke on "The Role of Missiles in the U. S. Navy." The annual banquet featured Lt. Gen. C. S. Irvine, Deputy Chief of Staff Materiel, Headquarters, U. S. Air Force, as guest speaker.

Among those responsible for convention arrangements were: Henry Randall, finance; L. D. Whitelock, exhibits; R. E. Frazier, program; J. W. Klotz, registration; and George Rappaport, public relations.

First PGMIL Convention A Success



Ralph Cole (left), chairman of the Washington Section, confers with R. C. Larson and convention officers Henry Randall and John Klotz at the recent PGMIL First National Convention.



At the banquet head table (left to right): Rear Adm. Rawson Bennett, Chief of Naval Research, John Henderson, IRE President, Rear Adm. W. F. Cleaves, Ret., Convention Chairman, Lt. Gen. C. S. Irvine, guest speaker.



Chris Engleman (right), National Chairman of PGMIL, talks with attendees.



Seated next to Admiral Cleaves (third from left) at the head table during the luncheon is Adm. W. F. Raborn, Bureau of Ordnance Navy Department who gave the luncheon address.

AVAILABLE BACK ISSUES OF IRE TRANSACTIONS

The following issues of TRANSACTIONS are available from the Institute of Radio Engineers, Inc., 1 East 79th Street, New York 21, New York, at the prices listed below:

Sponsoring Group	Publications	Group Mem- bers	IRE Mem- bers	Non- Mem- bers*
Aeronautical & Navigational Electronics	PGAE-5, October, 1952 (6 pages)	\$0.30	\$0.45	\$0.90
	PGAE-5, December, 1952 (10 pages)	0.30	0.45	0.90
	PGAE-8, June, 1953 (23 pages)	0.65	0.95	1.95
	PGAE-9, September, 1953 (27 pages)	0.70	1.05	2.10
	Vol. ANE-1, No. 2, June, 1954 (22 pages)	0.95	1.40	2.85
	Vol. ANE-1, No. 3, September, 1954 (27 pages)	1.00	1.50	3.00
	Vol. ANE-1, No. 4, December, 1954 (27 pages)	1.00	1.50	3.00
	Vol. ANE-2, No. 1, March, 1955 (41 pages)	1.40	2.10	4.20
	Vol. ANE-2, No. 2, June, 1955 (49 pages)	1.55	2.30	4.65
	Vol. ANE-2, No. 3, September, 1955 (27 pages)	0.95	1.45	2.85
	Vol. ANE-3, No. 2, June, 1956 (54 pages)	1.40	2.10	4.20
	Vol. ANE-3, No. 3, September, 1956 (39 pages)	1.05	1.55	3.15
	Vol. ANE-4, No. 1, March, 1957 (44 pages)	1.50	2.25	4.50
	Antennas and Propagation	Vol. AP-1, No. 1, July, 1953 (30 pages)	1.20	1.80
Vol. AP-1, No. 2, October, 1953 (31 pages)		1.20	1.80	3.60
Vol. AP-2, No. 1, January, 1954 (39 pages)		1.35	2.00	4.05
Vol. AP-2, No. 2, April, 1954 (41 pages)		2.00	3.00	6.00
Vol. AP-2, No. 3, July, 1954 (36 pages)		1.50	2.25	4.50
Vol. AP-3, No. 4, October, 1954 (36 pages)		1.50	2.25	4.50
Vol. AP-3, No. 1, January, 1955 (43 pages)		1.60	2.40	4.80
Vol. AP-3, No. 2, April, 1955 (47 pages)		1.60	2.40	4.80
Vol. AP-4, No. 1, January, 1956 (100 pages)		2.65	3.95	7.95
Vol. AP-4, No. 4, October, 1956 (96 pages)		2.10	3.15	6.30
Vol. AP-5, No. 1, January, 1957 (172 pages)		3.20	4.80	9.60
Vol. AP-5, No. 2, April, 1957 (72 pages)		1.75	2.60	5.25
Audio		PGA-7, May, 1952 (47 pages)	0.90	1.35
	PGA-10, November-December, 1952 (27 pages)	0.70	1.05	2.10
	Vol. AU-1, No. 6, November-December, 1953 (27 pages)	0.90	1.35	2.70
	Vol. AU-2, No. 1, January-February, 1954 (36 pages)	1.20	1.80	3.60
	Vol. AU-2, No. 3, May-June, 1954 (27 pages)	0.95	1.40	2.85
	Vol. AU-2, No. 4, July-August, 1954 (27 pages)	0.95	1.40	2.85
	Vol. AU-2, No. 5, September-October, 1954 (22 pages)	0.95	1.40	2.85
	Vol. AU-2, No. 6, November-December, 1954 (24 pages)	0.80	1.20	2.40
	Vol. AU-3, No. 1, January-February, 1955 (20 pages)	0.60	0.90	1.80
	Vol. AU-3, No. 3, May-June, 1955 (30 pages)	0.85	1.25	2.55
	Vol. AU-3, No. 5, September-October, 1955 (33 pages)	0.90	1.35	2.70
	Vol. AU-3, No. 6, November-December, 1955 (36 Pages)	0.95	1.40	2.85
	Vol. AU-4, No. 1, January-February, 1956 (27 pages)	0.75	1.10	2.25
	Vol. AU-4, No. 2, March-April, 1956 (17 pages)	0.55	0.80	1.65
	Vol. AU-4, No. 3, May-June, 1956 (34 pages)	0.80	1.20	2.40
	Vol. AU-4, No. 5, September-October, 1956 (31 pages)	0.60	0.90	1.80
	Vol. AU-4, No. 6, November-December, 1956 (36 pages)	0.60	1.20	2.40
Vol. AU-5, No. 1, January-February, 1957 (16 pages)	0.45	0.65	1.35	
Vol. AU-5, No. 2, March-April, 1957 (32 pages)	0.70	1.05	2.10	
Automatic Control	PGAC-2, February, 1957 (108 pages)	1.95	2.90	5.85
Broadcast Transmission Systems	PGBTS-1, March, 1955 (102 pages)	2.50	3.75	7.50
	PGBTS-2, December, 1955 (54 pages)	1.20	1.80	3.60
	PGBTS-4, March, 1956 (21 pages)	0.75	1.10	2.25
	PGBTS-5, September, 1956 (51 pages)	1.05	1.55	3.15
	PGBTS-6, October, 1956 (32 pages)	0.80	1.20	2.40
	PGBTS-7, February, 1957 (62 pages)	1.15	1.70	3.45
	PGBTS-8, June, 1957 (32 pages)	0.90	1.35	2.70
Broadcast and Television Receivers	PGSTR-1, July, 1952 (12 pages)	0.50	0.75	1.50
	PGSTR-5, January, 1954 (96 pages)	1.80	2.70	5.40
	PGSTR-7, July, 1954 (58 pages)	1.15	1.70	3.45
	PGSTR-8, October, 1954 (20 pages)	0.90	1.35	2.70
	Vol. BTR-1, No. 1, January, 1955 (68 pages)	1.25	1.85	3.75
	Vol. BTR-1, No. 2, April 1955 (40 pages)	0.95	1.45	2.85

* Public libraries, colleges and subscription agencies may purchase at IRE member rate.

(Continued on page 1300)

SPEAKERS AND TOPICS SET FOR INDUSTRIAL ELEC. SYMPOSIUM AT CHICAGO ON SEPT. 24-25

The Sixth Annual Symposium on Industrial Electronics, organized by the Professional Group on Industrial Electronics and co-sponsored by the Chicago Sections of the IRE and AIEE, is scheduled for the Morrison Hotel, Chicago, Ill., Sept. 24-25. Conference co-chairmen are E. A. Roberts and H. A. Garbarino. Eugene Mittelmann and Harold Chestnut are program co-chairmen and J. W. Grant is in charge of arrangements.

Richard Jenness of Northwestern University, Tomas Abbott of Standard Oil of Indiana, H. Cornelius of National Harvester Company, and Donald Arsen of Stewart Warner Electronics will act as moderators for the four sessions of the symposium.

Among papers scheduled for presentation are: *A Classification System for Measurement and Control*, E. A. Keller, Panellit Corp.; *Transmission of Torque Signals from High Speed Machinery*, E. S. Shepard, Air Research Mfg. Co.; *Photo-Electric Registration Control Systems*, J. C. Frommer, consulting engineer; *Industrial Digital Systems*, E. J. Otis, Daystrom Systems; *An Electronic Approach to Sortation Control*, R. W. Burtness, Stewart Warner Electronics; *Position Transducers for Machine Controls*, J. K. Snell, General Electric Co.; *Magnetic and Eddy Current Type Transducers for Use in Industrial Electronics*, D. L. Elam, Electro-Products Lab.; *Pulse Width Control of Transistors*, J. N. Van Seyoc and R. W. Bull, Armour Research Foundation; and *Accurate Volumetric Particle Size Determination by Electronic Techniques*, R. H. Berg, Process Control Services Co.

J. D. Ryder, Dean of Michigan State University, will speak at the luncheon meeting on September 24 on "Look, No Bounds." A. E. Sperry, President of Panellit Corp., will be the following day's luncheon speaker.

USAF RELEASES SEPTEMBER

RADIO BROADCAST SCHEDULE

The Air Force MARS Eastern Technical Net which broadcasts over the air every Sunday afternoon at 2 p.m. (EDT) on 3295 and 7540 kc announces the following guest speakers for September: Sept. 8—R. I. Colin, Federal Telecommunications Labs. Topic: TACAN—Aerial Navigation. Sept. 15—James Douglas, Yale Univ. Topic: Venus Calling. Sept. 22—Rear Adm. Rawson Bennett, Chief of Naval Research. Topic: What Research Has Done for Electronics. Sept. 29—Harry Wallace, Interference Associates. Topic: Radio Interference Reduction and Measurements.

IRE DIRECTORS APPROVE THE CREATION OF TWO SUBSECTIONS

At its meeting on June 21, the IRE Executive Committee approved the establishment of the Eastern North Carolina Subsection of the North Carolina-Virginia Section, and the Santa Barbara Subsection of the Los Angeles Section.

IRE SECTION HONORS MEMBERS

Five members of the Rome-Utica Section were honored for outstanding service recently. J. A. Thompson was cited for his contributions in promoting the advancement of IRE in the Rome-Utica area; R. C. Benoit, Jr., for his work as 1955-1956 publicity chairman; H. E. Webb, for his editorship of the Section's magazine; W. J. Kuehl, for his work as chairman of the first annual aeronautical communications symposium held in Utica last October; and R. S. Grisetti, for his part in founding the Rome-Utica Section.

CHICAGO SPONSORS LECTURES

The IRE Chicago Section is sponsoring a series of eight lectures on the theory and applications of the electronic transistor. This series will be patterned after the lecture series presented by the IRE Boston section last year.

The lectures will be of a survey nature, presented on a college senior level. They will be divided into two parts, the transistor—the device, and transistor circuit theory and applications. The lecture speakers for the series are as follows: Morton Prince, F. H. Blecher, Julius Hupert, G. R. Spencer, Donald Mogen, Leopold Sternlicht, R. M. Cohen, and Charles Simmons.

The lecture series will start September 30th and will consist of eight two-hour lectures presented on consecutive Monday evenings at Chicago Goodman Memorial Theatre. The total registration fee, which shall include published notes for each lecture, is \$6.00 for IRE members and students, and \$9.00 for nonmembers.

For registration or information contact Stuart McCarrell, 2900 W. 36th St., Chicago 32, Ill. Checks or money orders should be payable to the IRE Lecture Series.

INTERNATIONAL CONFERENCE SET

The Societé des Radioélectriciens of France is organizing an International Conference on Ultra-High Frequency Circuits and Antennas to be held in Paris October 21-26, 1957. Meetings will be held on the following general topics: circuit theory relating to waveguides and aerials, waveguides and lines, waveguide components, properties and use of anisotropic materials (ferrites), radiating aperture antennas, end-fire radiating antennas, special purpose antennas and antenna measurements. For further information contact M. Chabrol, 10 Avenue Pierre-Larousse-Malahoff (Seine), Paris, France.

OBITUARIES

Max L. Haas (A'50), a pioneer in the manufacture and marketing of radio and electronics components, died June 20. He was Chairman of the Board of Bud Radio, Inc., President of Cadillac Fabricators, Inc., and Treasurer of Radio Electronic Parts Corp.

Mr. Haas, who was 61, had been identified with radio, television and electronics industry since 1928 as a manufacturers' representative, a distributor and a manufacturer. His call letters as a radio amateur were W8VCC. He was a graduate of Cleveland Marshall Law School.

AVAILABLE BACK ISSUES OF IRE TRANSACTIONS

(Continued)

Sponsoring Group	Publications	Group Mem- bers	IRE Mem- bers	Non- Mem- bers*
	Vol. BTR-1, No. 3, July, 1955 (51 pages)	\$0.95	\$1.45	\$2.85
	Vol. BTR-1, No. 4, October, 1955 (19 pages)	0.95	1.40	2.85
	Vol. BTR-2, No. 1, April, 1956 (30 pages)	1.10	1.65	3.30
	Vol. BTR-2, No. 2, July, 1956 (21 pages)	0.85	1.25	2.55
	Vol. BTR, 2, No. 3, October, 1956 (32 pages)	1.05	1.55	3.15
	Vol. BTR-3, No. 1, June, 1957 (48 pages)	1.40	2.10	4.20
Circuit Theory	Vol. CT-2, No. 4, December, 1955 (88 pages)	1.85	2.75	5.55
	Vol. CT-3, No. 2, June, 1955 (74 pages)	1.60	2.40	4.80
	Vol. CT-3, No. 4, December, 1955 (104 pages)	1.90	2.85	5.70
	Vol. CT-4, No. 1, March, 1957 (28 pages)	0.65	0.95	1.95
	Vol. CT-4, No. 2, June, 1957 (32 pages)	0.70	1.05	2.10
Communications Systems	Vol. CS-2, No. 1, January, 1954 (83 pages)	1.65	2.50	4.95
	Vol. CS-2, No. 2, July, 1954 (132 pages)	2.25	3.35	6.75
	Vol. CS-2, No. 3, November 1954 (181 pages)	3.00	4.50	9.00
	Vol. CS-4, No. 2, May, 1956 (182 pages)	2.90	4.35	8.70
	Vol. CS-4, No. 3, October, 1956 (59 pages)	1.05	1.55	3.15
	Vol. CS-5, No. 1, March, 1957 (129 pages)	2.30	3.45	6.90
Component Parts	PGCP-3, April, 1955 (44 pages)	1.00	1.50	3.00
	Vol. CP-3, No. 2, September, 1956 (44 pages)	1.75	2.60	5.25
	Vol. CP-4, No. 1, March, 1957 (36 pages)	1.35	2.00	4.05
Electronic Computers	Vol. EC-4, No. 4, December, 1955 (40 pages)	0.90	1.35	2.70
	Vol. EC-5, No. 2, June, 1956 (46 pages)	0.90	1.35	2.70
	Vol. EC-5, No. 3, September, 1956 (72 pages)	1.05	1.55	3.15
	Vol. EC-6, No. 1, March, 1957 (72 pages)	1.15	1.70	3.45
	Vol. EC-6, No. 2, June, 1957 (72 pages)	1.05	1.55	3.15
Electron Devices	Vol. ED-1, No. 2, April, 1954 (75 pages)	1.40	2.10	4.20
	Vol. ED-1, No. 3, August, 1954 (77 pages)	1.40	2.10	4.20
	Vol. ED-1, No. 4, December, 1954 (280 pages)	3.20	4.80	9.60
	Vol. ED-2, No. 2, April, 1955 (53 pages)	2.10	3.15	6.30
	Vol. ED-2, No. 3, July, 1955 (27 pages)	1.10	1.65	3.30
	Vol. ED-2, No. 4, October, 1955 (42 pages)	1.50	2.25	4.50
	Vol. ED-3, No. 1, January 1956 (74 pages)	2.10	3.15	6.30
	Vol. ED-3, No. 2, April, 1956 (40 pages)	1.10	1.65	3.30
	Vol. ED-3, No. 3, July, 1956 (45 pages)	1.35	2.00	4.05
	Vol. ED-3, No. 4, October, 1956 (48 pages)	1.45	2.15	4.35
	Vol. ED-4, No. 1, January, 1957 (112 pages)	2.60	3.90	7.80
	Vol. ED-4, No. 2, April, 1957 (92 pages)	2.05	3.10	6.15
Engineering Management	PGEM-1, February, 1954 (55 pages)	1.15	1.70	3.45
	Vol. EM-3, No. 1, January, 1956 (29 pages)	0.95	1.40	2.85
	Vol. EM-3, No. 2, April, 1956 (15 pages)	0.55	0.80	1.65
	Vol. EM-3, No. 3, July, 1956 (37 pages)	0.90	1.35	2.70
	Vol. EM-4, No. 1, March, 1957 (44 pages)	1.00	1.50	3.00
	Vol. EM-4, No. 2, June, 1957 (44 pages)	1.00	1.50	3.00
Industrial Electronics	PGIE-1, August, 1953 (40 pages)	1.00	1.50	3.00
	PGIE-2, March, 1955 (81 pages)	1.90	2.85	5.70
	PGIE-3, March, 1956 (110 pages)	1.70	2.55	5.10
Information Theory	PGIT-3, March, 1954 (159 pages)	2.60	3.90	7.80
	PGIT-4, September, 1954 (234 pages)	3.35	5.00	10.00
	Vol. IT-1, No. 2, September, 1955 (50 pages)	1.90	2.85	5.70
	Vol. IT-1, No. 3, December, 1955 (44 pages)	1.55	2.30	4.65
	Vol. IT-2, No. 2, June, 1956 (51 pages)	1.65	2.45	4.95
	Vol. IT-2, No. 3, September, 1956 (224 pages)	3.00	4.50	9.00
	Vol. IT-2, No. 4, December, 1956 (64 pages)	1.85	2.75	5.55
	Vol. IT-3, No. 1, March, 1957 (84 pages)	2.20	3.30	6.60
Instrumentation	PGI-3, April, 1954 (55 pages)	1.05	1.55	3.15
	PGI-4, October, 1955 (182 pages)	2.70	4.05	8.10
	Vol. I-6, No. 1, March, 1957 (72 pages)	1.50	2.25	4.50
Medical Electronics	PGME-2, October, 1955 (39 pages)	0.85	1.25	2.55
	PGME-4, February, 1956 (61 pages)	1.95	2.90	5.85
	PGME-6, October, 1956 (72 pages)	1.28	1.65	3.75
	PGME-7, December, 1956 (49 pages)	1.00	1.50	3.00
	PGME-8, July, 1957 (48 pages)	0.95	1.40	2.85
Microwave Theory and Techniques	Vol. MTT-2, No. 3, September, 1954 (54 pages)	1.10	1.65	3.30
	Vol. MTT-3, No. 1, January, 1955 (47 pages)	1.50	2.25	4.50
	Vol. MTT-3, No. 4, July, 1955 (54 pages)	1.60	2.40	4.80

* Colleges, subscription agencies, and all libraries may purchase at IRE member rate.

(Continued on page 1301)

AVAILABLE BACK ISSUES OF IRE TRANSACTIONS

(Continued)

Sponsoring Group	Publications	Group Members	IRE Members	Non-Members*	
	Vol. MTT-3, No. 5, October, 1955 (59 pages)	\$1.70	\$2.55	\$5.10	
	Vol. MTT-4, No. 1, January, 1956 (63 pages)	1.65	2.45	4.95	
	Vol. MTT-4, No. 2, April, 1956 (89 pages)	1.70	2.55	5.10	
	Vol. MTT-4, No. 3, July, 1956 (54 pages)	1.25	1.85	3.75	
	Vol. MTT-4, No. 4, October, 1956 (84 pages)	1.85	2.75	5.55	
	Vol. MTT-5, No. 1, January, 1957 (80 pages)	1.75	2.60	5.25	
	Vol. MTT-5, No. 2, April, 1957 (92 pages)	1.90	2.85	5.70	
	Vol. MTT-5, No. 3, July, 1957 (52 pages)	1.15	1.70	3.45	
	Military Electronics	Vol. MIL-1, No. 1, March, 1957 (32 pages)	0.90	1.35	2.70
	Reliability and Quality Control	PGQC-2, March, 1950 (51 pages)	1.30	1.95	3.90
PGQC-3, February, 1954 (39 pages)		1.15	1.70	3.45	
PGQC-4, December, 1954 (56 pages)		1.29	1.80	3.60	
PGRQC-5, April, 1955 (56 pages)		1.15	1.75	3.45	
PGRQC-6, February, 1956 (66 pages)		1.50	2.25	4.50	
PGRQC-7, April, 1956 (52 pages)		1.10	1.65	3.30	
PGRQC-10, June, 1957 (68 pages)		1.20	1.80	3.60	
Nuclear Science	Vol. NS-1, No. 1, September, 1954 (42 pages)	0.70	1.00	2.00	
	Vol. NS-2, No. 1, June, 1955 (15 pages)	0.55	0.85	1.65	
	Vol. NS-3, No. 1, February, 1956 (40 pages)	0.90	1.35	2.70	
	Vol. NS-3, No. 2, March, 1956 (31 pages)	1.40	2.10	4.20	
	Vol. NS-3, No. 3, June, 1956 (24 pages)	1.00	1.50	3.00	
Production Techniques	Vol. NS-4, No. 1, March, 1957 (52 pages)	1.80	2.70	5.40	
	PGPT-2, April, 1957 (148 pages)	2.85	4.25	8.55	
Telemetry and Remote Control	PGRTRC-1, August, 1954 (16 pages)	0.85	1.25	2.55	
	PGRTRC-2, November, 1954 (24 pages)	0.95	1.40	2.85	
	Vol. TRC-1, No. 1, February, 1955 (24 pages)	0.95	1.40	2.85	
	Vol. TRC-1, No. 2, May, 1955 (24 pages)	0.95	1.40	2.85	
	Vol. TRC-1, No. 3, August, 1955 (12 pages)	0.70	1.05	2.10	
	Vol. TRC-2, No. 1, March, 1956 (22 pages)	1.00	1.50	3.00	
Ultrasonics Engineering	Vol. TRC-3, No. 2, May, 1957 (36 pages)	1.15	1.70	3.45	
	PGUE-1, June, 1954 (62 pages)	1.55	2.30	4.65	
Vehicular Communications	PGVC-5, June, 1955 (78 pages)	1.50	2.25	4.50	
	PGVC-6, July, 1956 (62 pages)	1.55	2.30	4.65	
	PGVC-8, May, 1957 (76 pages)	1.40	2.10	3.20	
	PGVC-9, June, 1957 (32 pages)	0.75	1.10	2.25	

* Colleges, subscription agencies, and all libraries may purchase at IRE member rate.

Frank A. Cowan (M'30-SM'43-F'55), a communications engineer and scientist, died recently after a short illness. He was 59.



F. A. COWAN

Mr. Cowan, Assistant Director of Operations for the Long Lines Department of American Telephone and Telegraph Company, had a score of inventions to his credit which contributed to the art of telephony.

Born in Escatawpa, Ala., and reared in the South, Mr.

Cowan was a graduate of the Georgia Institute of Technology. He graduated in 1919 with a B.S. degree in electrical engineering.

A few months after graduation, he joined Long Lines in Atlanta to begin a career with the Bell System. In 1922, he was transferred to New York and made his home here until his death. All of his years in the Bell System were devoted to engineering work.

Mr. Cowan's interest in scientific activities led to development of varistor type

modulators and demodulators, which are used today in communications systems. Another of his inventions, first built in his own workshop and now used throughout the Bell System, is a telegraph transmission measuring set.

Mr. Cowan also made several trips abroad on communications matters. He was the United States delegate at the meetings of the International Consulting Committee on Telephony in 1946, attending both the spring meeting in Paris and the plenary session held at Montreux, Switzerland the following fall.

Mr. Cowan was a fellow of the American Institute of Electrical Engineers. He had written a number of published papers on telephone subjects and, as a result of his accomplishments, was awarded the 1953 Lamme Gold Medal for outstanding contribution to long distance communication and development of transmission equipment.

William A. Tolson (A'28-SM'43-F'56), who was a member of the technical staff of RCA Laboratories for fourteen years, died recently in Florida after an illness of several months. He had been transferred last

November from the David Sarnoff Research Center in Princeton, N. J. to the Missile Test Project at Cocoa, Fla.



W. A. TOLSON

Mr. Tolson was born November 2, 1896, in San Angelo, Tex. He received his B.S.E.E. degree from A. & M. College of Texas and joined the General Electric Co. in Schenectady, New York, in 1923. In 1930, he transferred to RCA Victor Division in Camden, N. J., where he worked on

television development and then to the Princeton Labs. in 1942.

Mr. Tolson was one of the pioneers in television development; he was largely responsible for the synchronizing and deflection circuits used in substantially all modern television receivers, both black and white and color. "Doc," as he was called by his associates, was perhaps best known as the inventor of the universally used automatic synchronizing separator circuit, the picture linearity control circuit, and as the co-inventor with Roscoe Duncan of the blocking oscillator circuit which has enjoyed application in radar, as well as television. Included also in Mr. Tolson's forty-two issued U. S. patents is his contribution to the present-day standard television transmission system wherein the power line frequency is employed as the vertical or field scanning rate.

Mr. Tolson was active in the design of the equipment used in early 1930 television field tests. In 1940, he received the award of "Modern Pioneer" from the Radio Manufacturers' Association. He directed the design and installation of the first theater television projection system which was demonstrated at the New Yorker Theater in 1949. During World War II, Mr. Tolson was associated with development of radar fire-control and infrared systems.

TECHNICAL COMMITTEE NOTES

The following Technical Committee meetings were held recently:

June 18—Video Techniques Committee, S. Doba, Jr., Chairman, IRE Headquarters.

June 19—Industrial Electronics Committee, J. E. Eiselein, Chairman, IRE Headquarters.

—Antennas and Waveguides Committee, G. Deschamps, Chairman, IRE Headquarters.

June 21—Facsimile Committee, D. Frezzolini, Chairman, Times Building.

June 25—Audio Techniques Committee, I. Kerney, Chairman, IRE Headquarters.

June 27—Electronic Computers Committee, D. R. Brown, Chairman, IRE Headquarters.

June 28—Symbols Committee, H. R. Terhune, Chairman, IRE Headquarters.

July 11—Standards Committee, M. W. Baldwin, Chairman, Lexington Hotel.

Books

Transmission Circuits by E. M. Williams and J. B. Woodford, Jr.

Published (1957) by The Macmillan Co., 60 Fifth Ave., New York 11, N. Y. 140 pages+10 pages of appendix+6 index pages+ix pages. Illus. 9½×6¼. \$4.25.

This book is intended by the authors to be primarily used for teaching, rather than as a reference text, in a one-semester course for senior students majoring in electrical engineering. The seven chapters and two appendices bear the titles: Theory of the Generalized Transmission Circuit, Determination of Transmission Line Parameters, Power Transmission Lines in the Steady State, Signal Transmission Lines, High Frequency Transmission Lines and Distributed-Parameter Circuit Elements, Transients in Transmission Lines, and Lump Constants Transmission Networks; the appendices are titled Hyperbolic Functions, and Solutions of Transmission Circuit Problems by Means of Electric-Magnetic Field Theory. At the end of each chapter are given problems

(with no answers) relating to transmission lines and to four terminal networks.

The book starts with a statement of the usual partial differential equations for a distributed, constant parameter, transmission line, and goes on to the steady-state solutions of these equations in terms of characteristic impedance, propagation factor, and reflection coefficient. In the second chapter are given a number of formulas for the parameters of transmission lines with various geometries, including the coaxial. The authors should correct their misconception on page 31 that the equations for coaxial lines (leading to Bessel function solutions) are nonlinear differential equations; they are in fact linear. The fourth chapter on Signal Transmission Lines touching on information theory is weak and contains a number of statements which may mislead the student unless further explanation is given by the instructor. Circle and Smith chart diagrams are described briefly together with some

short comments on how v_{swr} is measured. The problem of transients in transmission lines is touched on briefly; consideration is given only in the case of an ideal nondissipative constant parameter line operated by a battery at the sending end and terminated in a resistance at the receiving end. The last chapter on lumped constant transmission networks considers only low-pass filters in a form too brief for design use.

In summary, a considerable amount of basic detail is intentionally avoided in this book and must be supplied by the instructor. This omission is apparently intentional and reflects the following objective of the authors quoted in their preface: "The wealth of detail which characterizes a reference work would jeopardize the educational objectives of the courses in which this text has been used."

M. J. DI TORO

Polytechnic Res. and Dev. Co.
Brooklyn, N. Y.

Professional Groups†

Aeronautical & Navigational Electronics—Joseph General, 6019 Highgate Dr., Baltimore 15, Md.
Antennas & Propagation—J. I. Bohnert, Code 5200, Naval Research Lab., Washington 25, D. C.
Audio—Dr. H. F. Olson, RCA Labs., Princeton, N. J.
Automatic Control—E. M. Grabbe, Ramo-Woolridge Corp., Box 45067, Airport Station, Los Angeles 45, Calif.
Broadcast & Television Receivers—L. R. Fink, Research Lab., General Electric Company, Schenectady, N. Y.
Broadcast Transmission Systems—C. H. Owen, 7 W. 66th St., N. Y. 23, N. Y.
Circuit Theory—W. H. Huggins, 2813 St. Paul St., Baltimore 18, Md.
Communications Systems—J. W. Worthington, Jr., Dawn Dr., Mounted Route, Rome, N. Y.
Component Parts—R. M. Soria, American

Phenolic Corp., 1830 S. 54 Ave., Chicago 50, Ill.
Education—J. D. Ryder, Dept. of Elec. Eng., Mich. State Univ., E. Lansing, Mich.
Electron Devices—T. M. Liimatainen, 5415 Connecticut Ave., N.W., Washington, D. C.
Electronic Computers—Werner Buchholz, IBM Engineering Lab., Poughkeepsie, N. Y.
Engineering Management—C. R. Burrows, Ford Instrument Co., 31-10 Thomson Ave., Long Island City 1, N. Y.
Engineering Writing and Speech—D. J. McNamara, Sperry Gyroscope Co., Great Neck, L. I., N. Y.
Industrial Electronics—W. R. Thurston, General Radio Co., 285 Massachusetts Ave., Cambridge 39, Mass.
Information Theory—W. B. Davenport, Jr., Garfield Rd., Concord, Mass.
Instrumentation—F. C. Smith, Jr., Southwestern Industrial Electronics Co., 2831

Post Oak Rd., Houston 19, Tex.
Medical Electronics—L. B. Lusted, M.D., Clinical Center, National Institute of Health, Bethesda 14, Md.
Microwave Theory and Techniques—W. L. Pritchard, Goodman Hill Rd., Sudbury, R.F.D., Mass.
Military Electronics—W. E. Cleaves, 3807 Fenchurch Rd., Baltimore 18, Md.
Nuclear Science—J. N. Grace, 112 Heather Dr., Pittsburgh 34, Pa.
Production Techniques—E. R. Gamson, Autonetics, 395-91, 12214 Lakewood Blvd., Downey, Calif.
Reliability and Quality Control—Victor Wouk, Beta Electric Corp., 333 E. 103rd St., New York 29, N. Y.
Telemetry and Remote Control—C. H. Doersam, Jr., 24 Winthrop Rd., Port Washington, L. I., N. Y.
Ultrasonics Engineering—C. M. Harris, 425 Riverside Dr., New York, N. Y.
Vehicular Communications—C. M. Heiden, 11 Pebble Hill Rd., S., DeWitt, N. Y.

† Names listed are Group Chairmen.

Sections*

Akron (4)—H. F. Lanier, 2220—27th St., Cuyahoga Falls, Ohio; Charles Morrill, 2248—16th St., Cuyahoga Falls, Ohio.
Alamogordo-Holloman (6)—V. J. Lynch, 1105 Maple Dr., Alamogordo, N. Mex.; R. B. Kleinman, Box 1054, Holloman AFB, N. Mex.

* Numerals in parentheses following section designate region number. First name designates Chairman, second name, Secretary.

Albuquerque-Los Alamos (7)—B. L. Basore, 2405 Parsifal, N.E., Albuquerque, N. Mex.; John McLay, 3369—48 Loop, Sandia Base, Albuquerque, N. Mex.
Atlanta (3)—W. B. Miller, 1369 Holly Lane, N.E., Atlanta 6, Ga.; W. H. White, 1454 S. Gordon St., S.W., Atlanta 10, Ga.
Baltimore (3)—M. R. Briggs, Westinghouse Elec. Corp., Box 746, Baltimore 3, Md.; B. Wolfe, Director of Eng'g., Station

WAAM-TV, 3725 Malden Ave., Baltimore 11, Md.
Bay of Quinte (8)—W. D. Ryan, Cavalry House, Royal Military College, Kingston, Ont., Canada; R. Williamson, R.R. 3, Belleville, Ont., Canada.
Beaumont-Port Arthur (6)—F. M. Crum, 1905 Prairie St., Beaumont, Tex.; H. K. Smith, 270 Canterbury Lane, Beaumont, Tex.

- Binghamton (1)**—Robert Nash, 12 Alice St., M.R. 97, Binghamton, N. Y.; Bruce Lockhart, R.D. 3, Binghamton, N. Y.
- Boston (1)**—C. J. Lahanas, 275 Massachusetts Ave., General Radio Co., Cambridge 39, Mass.; K. C. Black, 97 Lincoln Rd., Wayland, Mass.
- Buenos Aires**—J. M. Onativia, Bustamante 1865, Buenos Aires, Argentina; L. F. Rocha, Caseros 3321, D'TO. B., Buenos Aires, Argentina.
- Buffalo-Niagara (1)**—W. S. Holmes, Cornell Aeronautical Labs., 4455 Genesee St., Buffalo 21, N. Y.; R. B. Odden, 573 Allenhurst Rd., Buffalo, N. Y.
- Cedar Rapids (5)**—J. L. Dalton, 2900 E. Ave., N.E., Cedar Rapids, Iowa; S. M. Morrison, 2034 Fourth Ave., S.E., Cedar Rapids, Iowa.
- Central Florida (3)**—G. F. Anderson, Dynatronics, Inc., 717 W. Amelia Ave., Orlando, Fla.; J. W. Downs, 1020 Highland Ave., Eau Gallie, Fla.
- Central Pennsylvania (4)**—W. J. Leiss, 1173 S. Atherton St., State College, Pa.; P. J. Freed, Hallor, Raymond & Brown, State College, Pa.
- Chicago (5)**—R. M. Soria, 1830 S. 54th Ave., Chicago 50, Ill.; G. H. Brittain, 3150 Summit Ave., Highland Park, Ill.
- China Lake (7)**—C. F. Freeman, 100-B Halsey St., China Lake, Calif.; P. K. S. Kim, 200-A Byrnes St., China Lake, Calif.
- Cincinnati (4)**—F. L. Weidig, Jr., 3819 Davenant Ave., Cincinnati 13, Ohio; H. E. Hancock, R.R. 4, Branch Hill Box 52, Loveland, Ohio.
- Cleveland (4)**—W. G. Piwonka, 3121 Huntington Rd., Cleveland 20, Ohio; J. S. Hill, Smith Elec., Inc., 4900 Euclid Ave., Cleveland 3, Ohio.
- Columbus (4)**—R. L. Cosgriff, 2200 Homestead Dr., Columbus, Ohio; G. J. Falkenbach, Battelle Institute, Columbus 1, Ohio.
- Connecticut Valley (1)**—B. R. Kamiens, 94 Admiral Dr., New London, Conn.; J. D. Lebel, Benedict Hill Rd., New Canaan, Conn.
- Dallas (6)**—Frank Seay, Collins Radio Co., 1930 Hi-Line Dr., Dallas, Tex.; T. B. Moseley, 6114 Northwood Rd., Dallas 25, Tex.
- Dayton (4)**—N. A. Nelson, 101 Castle Dr., Dayton 9, Ohio; D. G. Clute, 2132 Merline Ave., Dayton 10, Ohio.
- Denver (6)**—R. C. Webb, 2440 S. Dahlia St., Denver 22, Colo.; S. B. Peterson, 1295 S. Jackson, Denver 10, Colo.
- Detroit (4)**—E. C. Johnson, 4417 Crooks Rd., Royal Oak, Mich.; G. E. Ryan, 5296 Devonshire Rd., Detroit 24, Mich.
- Egypt**—H. M. Mahmoud, Faculty of Engineering, Fouad I University, Giza, Cairo, Egypt; El Garhi I El Kashlan, Egyptian Broadcasting, 4, Shari Sherifein, Cairo, Egypt.
- Elmira-Corning (1)**—R. G. Larson, 220 Lynhurst Ave., Windsor Gardens, Horseheads, N. Y.; D. F. Aldrich, 1030 Hoffman St., Elmira, N. Y.
- El Paso (6)**—J. Crosson, 1100 Honeysuckle Drive, El Paso, Tex.; H. Markowitz, 700 E. Paisano Dr., El Paso, Tex.
- Emporium (4)**—H. S. Hench, Jr., Sylvan Heights, Emporium, Pa.; H. J. Fromell, Sylvania Elec. Prod. Inc., Emporium, Pa.
- Evansville-Owensboro (5)**—A. K. Miegler, 904 Kelsey Ave., Evansville, Ind.; M. Casler, Evansville College, Evansville, Ind.
- Florida West Coast (3)**—L. J. Link, 3216 Ninth St., North, St. Petersburg, Fla.; R. Murphy, 12112 N. Edison Ave., Tampa 4, Fla.
- Fort Huachuca (7)**—J. K. Oliver, Box 656, Ft. Huachuca, Ariz.; W. C. Shelton, Box 2919, Fort Huachuca, Ariz.
- Fort Wayne (5)**—T. L. Slater, 1916 Eileen Dr., Waynedale, Ind.; F. P. Smith, Windsor Rd., R.R. 15, Fort Wayne, Ind.
- Fort Worth (6)**—C. W. Macune, 3132 Forest Park Blvd., Fort Worth, Tex.; G. H. Robertson, 5749 Tracyne Drive, Fort Worth 14, Tex.
- Hamilton (8)**—C. N. Chapman, 40 Dundas St., Waterdown, Ont., Canada; C. J. Smith, Gilbert Ave., Dancaster Courts, Sub. Serv. 2, Ancaster, Ont., Canada.
- Hawaii (7)**—Vaughn Kelly, 99-1215 Aiea Hgts. Dr., Aiea, Hawaii; D. L. Grubb, 236 Paiko Dr., Honolulu, Hawaii.
- Houston (6)**—M. A. Arthur, Humble Oil & Refining Co., P.O. Box 2180, Houston 1, Tex.; C. G. Turner, Communications Engineering Co., P.O. Box 12325, Houston 17, Tex.
- Huntsville (3)**—T. L. Greenwood, 1709 La Grande St., Huntsville, Ala.; W. J. Robinson, 715 Wharton Rd., Huntsville, Ala.
- Indianapolis (5)**—N. G. Drilling, 3002 Ashland Ave., Indianapolis 26, Ind.; R. B. Flint, 4038 Evelyn St., Indianapolis 24, Ind.
- Israel**—Franz Ollendorf, Box 910, Hebrew Inst. of Technology, Haifa, Israel; M. Tkatch, 15 Ahad Haam, Haifa, Israel.
- Ithaca (1)**—W. E. Gordon, Phillips Hall, Cornell Univ., Ithaca, N. Y.; C. E. Ingalls, 106 Sheldon Rd., Ithaca, N. Y.
- Kansas City (6)**—P. C. Constant, Jr. 3014, E. Myer Blvd., Kansas City 30, Mo.; N. E. Vilander, 2509 W. 83rd St., Kansas City 15, Mo.
- Little Rock (6)**—J. D. Reid, 2210 Summit, Little Rock, Ark.; J. P. McRae, Route 1, Scott, Ark.
- London (8)**—E. R. Jarman, 13 King St., London, Ont., Canada; W. A. Nunn, Radio Station CFPL-TV, London, Ont., Canada.
- Long Island (2)**—E. G. Fubini, Airborne Instrument Labs., 160 Old Country Rd., Mineola, L. I., N. Y.; E. K. Stodola, 118 Stanton St., Northport, N. Y.
- Los Angeles (7)**—J. K. Gossland, 318 E. Calaveras St., Altadena, Calif.; R. G. Kuck, 914 Arroyo Dr., South Pasadena, Calif.
- Louisville (5)**—M. C. Probst, 5067 Poplar Level Rd., Louisville, Ky.; W. J. Ryan, 4215 N. Western Pkwy., Louisville, Ky.
- Lubbock (6)**—E. W. Jenkins, Jr., Shell Oil Co., Admin. Dept., Box 1509, Midland, Tex.; J. J. Criswell, 511 50th St., Lubbock Tex.
- Miami (3)**—W. H. Epperson, 5845 S.W. 108 St., Miami 43, Fla.; R. S. Rich, 7513 S.W. 54 Ct., S. Miami, Fla.
- Milwaukee (5)**—J. E. Jacobs, 6230 Hale Park Dr., Hales Corners, Wis.; F. J. Lofy, 2258 S. 56 St., West Allis 19, Wis.
- Montreal (8)**—R. E. Penton, 6120 Cote St., Luc Rd., Apt. 6, Montreal, Quebec, Canada; R. Lumsden, 1680 Lepine St., St. Laurent, Montreal 9, Quebec, Canada.
- Newfoundland (8)**—J. B. Austin, Jr., Hq. 1805th AACNS Wing, APO 862, c/o P.M. New York, N. Y.; J. A. Willis, Canadian Marconi Co., Ltd., Pinetree-NEAC Depot, Pepperrill AFB, St. John's Newfoundland, Canada.
- New Orleans (6)**—M. F. Chapin, 8116 Hampson St., New Orleans, La.; G. A. Hero, 1102 Lowerline St., New Orleans 18, La.
- New York (2)**—J. S. Smith, 3717 Clarendon Rd., Brooklyn, N. Y.; Joseph Reed, 52 Hillcrest Ave., New Rochelle, N. Y.
- North Carolina-Virginia (3)**—F. E. Brooks, Box 277, Colonial Ave., Colonial Beach Va.; E. S. Busby, Jr., 1608 "B" St., Portsmouth, Va.
- Northern Alberta (8)**—J. E. Sacker, 10235—103rd St., Edmonton, Alberta, Canada; Frank Hollingworth, 9619—85th St., Edmonton, Alberta, Canada.
- Northern New Jersey (2)**—A. M. Skellett, 10 Midwood Terr., Madison, N. J.; G. D. Hulst, 37 College Ave., Upper Montclair, N. J.
- Northwest Florida (3)**—G. C. Fleming, 579 E. Gardner Dr., Fort Walton Beach, Fla.; W. F. Kirlin, 67 Laurie Dr., Fort Walton Beach, Fla.
- Oklahoma City (6)**—Nicholas Battenburg, 2004 N.W. 30th St., Oklahoma City 6, Okla.; E. W. Foster, 5905 N.W. 42 St., Oklahoma City 12, Okla.
- Omaha-Lincoln (5)**—J. S. Petrik, c/o KLETV, 27 & Douglas Sts., Omaha, Neb.; H. W. Becker, 1214 N. 34 St., Omaha 3, Neb.
- Ottawa (8)**—L. H. Doherty, 227 Barclay Rd., Ottawa 2, Ont., Canada; R. S. Thain, 54 Rossland Ave., Box 474, City View, Ont., Canada.
- Philadelphia (3)**—Nels Johnson, Philco Corp., 4700 Wissahickon Ave., Philadelphia 44, Pa.; R. E. Robertson, General Electric Co., 3198 Chestnut St., Philadelphia 4, Pa.
- Phoenix (7)**—G. L. McClanathan, 509 E. San Juan Cove, Phoenix Ariz.; E. S. Shephard, 5716 N. 19 St., Phoenix, Ariz.
- Pittsburgh (4)**—Gary Muffly, 715 Hulton Rd., Oakmont, Pa.; H. R. Kaiser, WHIC-WWSW, Sherwyn Hotel, Pittsburgh 22, Pa.
- Portland (7)**—D. C. Strain, 7325 S.W. 35 Ave., Portland 19, Ore.; W. E. Marsh, 6110 S.W. Brigger St., Portland 19, Ore.
- Princeton (2)**—L. L. Burns, Jr., RCA Labs., Princeton, N. J.; Sylvan Fich, College of Eng'g., Rutgers Univ., New Brunswick, N. J.
- Regina (8)**—William McKay, 2856 Retailack St., Regina, Saskatchewan, Canada; J. A. Funk, 138 Leopold Crescent, Regina, Saskatchewan, Canada.
- Rio de Janeiro, Brazil**—M. P. De Britto Pereira, Caixa Postal 562, Rio de Janeiro, Brazil; J. A. Hertz, Caixa Postal 97 Lapa, Rio de Janeiro, Brazil.
- Rochester (1)**—B. L. McArdle, Box 54, Brighton Station, Rochester 10, N. Y.; L. D. Smith, 27 Landing Park, Rochester, N. Y.
- Rome-Utica (1)**—Edward R. Orear, Ch., 36 Herthum Rd., Harts Hill Heights, Whitesboro, N. Y.; Sidney Rosenberg, V. Ch., 907 Valentine Ave., Rome, N. Y.; Rob-

- ert A. Zachary, Jr., Sec., 11 Arbor Drive, New Hartford, N. Y.
- Sacramento (7)**—R. A. Poucher, Jr., 3021 Mountain View Ave., Sacramento 21, Calif.; X. W. Godfrey, 3220 Fulton Ave., Sacramento 21, Calif.
- St. Louis (6)**—C. E. Mosley, 8622 St. Charles Rock Rd., Overland 14, Mo.; R. D. Rodenroth, 7701 Delmont, Affton 23, Mo.
- Salt Lake City (7)**—V. E. Clayton, 1525 Browning Ave., Salt Lake City, Utah; A. L. Gunderson, 3906 Parkview Dr., Salt Lake City 17, Utah.
- San Antonio (6)**—W. H. Hartwig, Dept. of Elec. Eng., University of Texas, Austin 12, Tex.; E. L. Hixson, Dept. of Elec. Eng., University of Texas, Austin 12, Tex.
- San Diego (7)**—E. J. Moore, 3601 Eighth St., San Diego 3, Calif.; R. J. Cary, Jr., 4561 Normandie Place, La Mesa, Calif.
- San Francisco (7)**—Meyer Leifer, Electronic Defense Lab., Box 205, Mountain View, Calif.; V. B. Corey, 385 Gravatt Dr., Berkeley 5, Calif.
- Schenectady (1)**—A. E. Rankin, 833 Whitney Dr., Schenectady, N. Y.; Sec.-Treas. to be appointed later.
- Seattle (7)**—R. H. Hoglund, 1825 E. Lynn St., Seattle 2, Wash.; L. C. Perkins, Box 307, Des Moines, Wash.
- Shreveport (6)**—H. H. Moreland, Hq. 2nd Air Force, Barksdale AFB, La.; M. C. Benson, P.O. Box 1316, Shreveport, La.
- South Bend-Mishawaka (5)**—J. L. Colten, 149 E. Tasher, South Bend, Ind.; P. G. Cox, R.R. 2, 10251 Harrison Rd., Osceola, Ind.
- Southern Alberta (8)**—W. K. Allan, 2025 29th Ave., S.W., Calgary, Alta., Canada; R. W. H. Lamb, Radio Station CFCN, 12th Ave. and Sixth St. E., Calgary, Alberta, Canada.
- Syracuse (1)**—P. W. Howells, General Electric Co., H.M.E.E. Dept., Bldg. 3, Industrial Park, Syracuse, N. Y.; G. M. Glasford, Elec. Eng. Dept., Syracuse University, Syracuse 10, N. Y.
- Tokyo**—Yasujiro Niwa, Tokyo Elec. Engineering College, 2-2 Kanda-Nishikicho, Chiyoda-Ku, Tokyo, Japan; Fumio Minozuma, 16 Ohara-Machi, Meguro-Ku, Tokyo, Japan.
- Toledo (4)**—H. L. Nevert, 3534 Woodmont Rd., Toledo 13, Ohio; K. P. Herrick, 2516 Fulton St., Toledo 10, Ohio.
- Toronto (8)**—H. W. Jackson, 352 Laird Dr., Toronto 17, Ont., Canada; R. J. A. Turner, 66 Gage Ave., Scarborough, Ont., Canada.
- Tucson (7)**—P. E. Russell, Elec. Engrg. Dept., Univ. of Ariz., Tucson, Ariz.; C. L. Becker, 4411 E. Sixth St., Tucson, Ariz.
- Tulsa (6)**—R. L. Atchison, 415 E. 14 Pl., Tulsa 20, Okla.; B. H. Keller, 1412 S. Winston, Tulsa 12, Okla.
- Twin Cities (5)**—E. W. Harding, 5325 Colfax Ave., S., Minneapolis, Minn.; S. W. Schulz, 3132 Fourth St., S.E., Minneapolis 14, Minn.
- Vancouver (8)**—R. A. Marsh, 3873 W. 23 Ave., Vancouver, B. C., Canada; T. G. Lynch, 739 Edgewood Rd., North Vancouver, B. C., Canada.
- Washington (3)**—A. H. Schooley, 3940 First St., S.W., Washington 24, D. C.; J. E. Durkovic, 10316 Colesville Rd., Silver Spring, Md.
- Wichita (6)**—W. K. Klatt, 2625 Garland, Wichita 4, Kan., A. T. Murphy, Univ. of Wichita, Dept. of Elec. Engrg., Wichita 14, Kan.
- Williamsport (4)**—(No chairman at present); W. H. Bresee, 818 Park Ave., Williamsport, Pa.
- Winnipeg (8)**—C. J. Hopper, 332 Bronx Ave., Winnipeg 5, Man., Canada; T. J. White, Dept. of E.E., University of Manitoba, Ft. Garry, Man., Canada.

Subsections

- Berkshire (1)**—A. H. Forman, Jr., O.P. 1-203, M.O.S.D., General Electric Co., 100 Plastics Ave., Pittsfield, Mass.; E. L. Pack, 62 Cole Ave., Pittsfield, Mass.
- Buenaventura (7)**—M. H. Fields, 430 Roderrick St., Oxnard, Calif.; D. J. Heron, 1316 Ocean Dr., Oxnard, Calif.
- Charleston (3)**—A. Jonas, 105 Lancaster St., N. Charleston, S. C.; F. A. Smith, Route 4, Melrose Box 572, Charleston, S. C.
- East Bay (7)**—H. F. Gray, Jr., 2019 Mira Vista Dr., El Cerrito, Calif.; D. R. Cone, 6017 Chaboly Terr., Oakland 18, Calif.
- Eastern North Carolina (3)**—Henry Hulick, Sta. W.P.T.F., Insurance Bldg., Raleigh, N. C.; M. C. Todd, Todd Elec. Co., Wendell, N. C.
- Erie (1)**—J. D. Heibel, 310 W. Grandview, Erie, Pa.; D. H. Smith, 3025 State St., Erie, Pa.
- Gainesville (3)**—W. E. Lear, Dept. of Elec. Eng., Univ. of Fla., Gainesville, Fla. (Chairman)
- Hampton Roads (3)**—R. L. Lindell, WTAR Radio Corp., 720 Boush St., Norfolk 10, Va.; J. E. Eller, Waterview Apts., Apt. E-3, Portsmouth, Va.
- Kitchener-Waterloo (8)**—Jules Kadish, Raytheon Canada, Ltd., 61 Laurel St., Waterloo, Ont., Canada; G. C. Field, 48 Harber Ave., Kitchener, Ont., Canada.
- Lancaster (3)**—W. T. Dyall, 1415 Hillcrest Rd., Lancaster, Pa.; P. W. Kaseman, 405 S. School Lane, Lancaster, Pa.
- Las Cruces-White Sands Proving Grounds (6)**—Herbert Haas, Box 236, State College, N. M.; Michael Goldin, 1921 Calle DeSuenos, Las Cruces, N. M.
- Lehigh Valley (3)**—F. W. Smith, E.E. Dept., Lafayette College, Alumni Hall of Eng'g., Easton, Pa.; L. G. McCracken, Jr., 1774 W. Union Blvd., Bethlehem, Pa.
- Memphis (3)**—R. N. Clark, Box 227, Memphis State College, Memphis, Tenn. (Chairman)
- Mid-Hudson (2)**—Altman Lampe, Cramer Rd., R.D. 3, Poughkeepsie, N. Y.; M. R. Marshall, 208 Smith St., Poughkeepsie, N. Y.
- Monmouth (2)**—Edward Massell, Box 433, Locust, N. J.; Harrison Rowe, Box 107, Red Bank, N. J.
- Nashville (3)**—W. W. Stifer, Jr., Aladdin Electronics, Nashville 2, Tenn.; P. E. Dicker, Dept. of Elec. Engrg., Vanderbilt Univ., Nashville 5, Tenn.
- New Hampshire (1)**—M. R. Richmond, 55 Raymond St., Nashua, N. H.; R. O. Goodwin, 86 Broad St., Nashua, N. H.
- Northern Vermont (1)**—Charles Horvath, 15 Iby St., S. Burlington, Vt.; (secretary to be elected)
- Orange Belt (7)**—J. Tampico, 2709 N. Garey Ave., Pomona, Calif.; R. E. Beckman, 113 N. Lillie, Fullerton, Calif.
- Palo Alto (7)**—W. B. Wholey, 25044 La Loma Dr., Los Altos, Calif.; A. M. Peterson, 14846 Manuella Ave., Los Altos, Calif.
- Panama City (3)**—C. B. Koesy, 1815 Moates Ave., St. Andrew Station, Panama City, Fla.; M. H. Naeseth, 1107 Buena Vista Blvd., Panama City, Fla.
- Pasadena (7)**—J. L. Stewart, Assoc. Prof. of Elec. Engrg., Calif. Inst. of Tech., Pasadena, Calif.; J. E. Ranks, Electro-Data, Pasadena, Calif.
- Piedmont (3)**—H. H. Arnold, 548 S. Westview Dr., Winston-Salem, N. C.; C. A. Norwood, 830 Gales Ave., Winston-Salem, N. C.
- Quebec (8)**—R. E. Collin, 590 Avenue Mon Repos, Ste. Foy, Quebec, Can.; R. M. Vaillancourt, 638 Avenue Mon Repos, Ste. Foy, Quebec, Canada.
- Richland (7)**—R. E. Connally, 515 Cottonwood Dr., Richland, Wash.; R. R. Cone, 611 Thayer, Richland, Wash.
- San Fernando (7)**—J. J. Guarrera, 17160 Gresham Ave., Northridge, Calif.; C. C. Olsefsky, 8100 Aldea Ave., Van Nuys, Calif.
- Santa Barbara (7)**—G. J. Maki, 1417 Pacific Drive, Santa Barbara, Calif.; R. S. Hutcherson, 1714 Clearview Rd., Santa Barbara, Calif.
- USAFIT (4)**—LCdr. E. M. Lipsey, 46 Spinning Rd., Dayton 3, Ohio; Sec.-Treas. to be appointed later.
- Westchester County (2)**—D. S. Kellogg, 9 Bradley Farms, Chappaqua, N. Y.; M. J. Lichtenstein, 53 Beaumont Circle, Yonkers, N. Y.
- Western North Carolina (3)**—J. G. Carey, 1429 Lilac Rd., Charlotte, N. C.; R. W. Ramsey, Sr., 614 Clement Ave., Charlotte 4, N. C.

Seventh Annual IRE-PGBTS Fall Symposium

SEPTEMBER 27-28, 1957

WILLARD HOTEL, WASHINGTON, D. C.

Fourteen technical papers will be presented at the Seventh Annual Fall Symposium of the IRE-PGBTS on September 27-28 in Washington, D.C. In addition, the Group has scheduled a visit to Walter Reed Medical Center for a demonstration of its color television facilities by Dr. Paul W. Shafer. A cocktail party will precede the annual banquet on September 27th.

Edmund A. Laport of Radio Corporation of America, guest speaker at the banquet, will describe television and broadcasting practices in different parts of the world with particular emphasis on the unique phases which are generally unknown to American engineers. Mr. Laport has traveled extensively in his work of providing guidance and planning for broadcasting systems and practices. Raymond F. Guy will be toastmaster.

Registration will be held on the first morning of the meeting. Further information may be obtained from the Group chairman, Clure H. Owen, American Broadcasting Company, 7 West 66th Street, New York 23, N. Y.

Friday Morning, September 27

Moderator: E. W. Allen, Jr., Federal Communications Commission.

Transistor Regulated Power Supply for Video Circuits, M. Schorr, Technical Operations, Inc.

A Transistorized Intercom System, E. P. Vincent, American Broadcasting Company.

Microphone Pre-Amp with AGC (tentative), A. A. McGee, General Electric Company.

Television Film Quality Standards, K. B. Benson and J. R. Whittaker, CBS-TV.

Friday Afternoon, September 27

Visit to Walter Reed Medical Center, conducted by Dr. P. W. Schafer, Walter Reed Hospital.

Saturday Morning, September 28

Moderator: A. B. Chamberlain, CBS-TV.

Reduction of Image Retention in Image Orthicon Cameras, J. H. Roe, S. L. Bendell and K. Sa lashige, RCA.

Recent Developments in TV Camera Tubes, F. S. Veith, Radio Corporation of America.

TV Transmitter Operational Practices, R. N. Harmon, Westinghouse.

TV Transmitter Proof of Performance, J. E. Barr, FCC (tentative).

STL and Remote Pickup Experiences on 13,000 MC, F. W. Bailey, American Microwave Corp.

Saturday Afternoon, September 28

Moderator: P. B. Laeser, WTMJ-TV.

TASO Objectives and Progress, G. Town, TASO.

Progress Report on Video Test Signals During Vertical Blanking, R. M. Morris and J. Serafin, American Broadcasting Company.

Directional Antenna Maintenance, D. A. Peterson, A. E. Cullum, and J. G. Rountree, consulting engineers.

A Simplified 5-Megawatt Antenna for the UHF Broadcaster (tentative), R. E. Fisk, General Electric Company.

Automation Applied to Television Master Control Room and Film Room, J. L. Berryhill, KRON-TV.

1957 NATIONAL ELECTRONICS CONFERENCE

OCTOBER 7-9, 1957, HOTEL
SHERMAN, CHICAGO, ILLINOIS

October 7, Morning

TRANSISTOR CIRCUITS

Transistor Multiple Loop Feedback Amplifiers, F. H. Blecher, Bell Telephone Labs., Murray Hill, N. J.

Junction-Transistor Oscillators, M. A. Melehy and M. B. Reed, Michigan State Univ., East Lansing, Mich.

Some Advances in Transistor Modulators for Precise Measurement, A. J. Williams, Jr., J. U. Eynon and N. E. Polster, Leeds and Northrup Co., Philadelphia, Pa.

Unilateralized Common Collector Transistor Amplifier, L. M. Vallese, Polytechnic Institute of Brooklyn, Brooklyn, N. Y.

Transistor Push-Pull Audio Amplifier Theory, M. A. Melehy, Michigan State Univ., East Lansing, Mich.

COMMUNICATIONS

Magnetostrictive Delay Line for Video Signals, G. I. Cohn, L. C. Peach, M. Epstein and H. O. Sorensen, Ill. Inst. of Technology, Chicago, Ill.

Helical Folded Dipoles and Unipoles, R. E. Boim and T. Li, Northwestern Univ., Evanston, Ill.

Low Frequency Spectrum Output of a Noise Generator, S. K. Benjamin, S. King and P. Levy, General Precision Lab. Inc., Pleasantville, N. Y.

Packaged Electric Tuned 35-200 Mc Panoramic Receiver, Peter Pan, T. W. Butler, Jr., Univ. of Michigan, Ann Arbor, Mich.

Binary Decision Feedback Systems for Maintaining Reliability Under Conditions of Varying Signal Strength, B. Harris, A. Hauptschein, K. C. Morgan and L. S. Schwartz, New York Univ., University Heights, N. Y.

SERVOMECHANISM APPLICATIONS

New Electrohydraulic Servo, C. A. Stemmer and C. H. Willard, G.E. Co., Utica, N. Y.

Design of a Nonlinear High-speed Servo System for Instrumentation, J. Tou, Univ. of Pennsylvania, Philadelphia, Pa.

Iso-Parameter Contours for Airborne Fixed Fire Control Systems, Y. Chu and S. Haas, Westinghouse Electric Corp., Baltimore, Md.

Servomechanisms as Used on Variable Stability and Variable Control System Research Aircraft, J. V. Foster, NACA Ames Aeronautical Lab., Moffett Field, Calif.

AUDIO

Permanent Magnet in Audio Devices, R. J. Parker, General Electric Co.

A Transistorized Decade Amplifier for Low Level Audio Frequency Applications, A. B. Bereskin, Univ. of Cincinnati, Cincinnati, Ohio.

Comparative Tests on Light Weight High Power Sound System, F. C. Fischer and A. A. Gerlach, Cook Research Labs., Morton Grove, Ill.

Modern Practice in Noise Control, R. W. Benson, Armour Research Found., Chicago, Ill.

Luncheon Address

Afternoon

SEMICONDUCTOR DEVICES

Noise in Semiconductor Materials and Devices, J. H. Bell, McDonnell Aircraft Corporation, St. Louis, Mo.

On Thermistor Characteristics, E. K. Weise and B. P. Lathi, Univ. of Illinois, Urbana, Ill.

Transistor High Level Injection and High Current Switches, H. W. Henkels, Westinghouse Electric Corp., Youngwood, Pa.

Very High Frequency PNP Switching Transistor, F. B. Maynard and E. L. Steele, Motorola, Inc., Phoenix, Ariz.

MICROWAVES I

A Low Reflection Dielectric Waveguide Window for X-Band, H. Zucker and C. M. Knop, Armour Research Found., Chicago, Ill.

X-Band Triode Harmonic Amplifier, W. J. Dauksner, Airborne Instruments Lab. Inc., Mineola, N. Y.

Analogies in the Mathematics of Microwave Theory and Elasticity Theory, S. Malinowski, Motorola Inc., Chicago, Ill. and C. W. McMullen, Northwestern Univ., Evanston, Ill.

Recent Developments with Spark Gap Impulse Noise Generators, R. H. George and H. J. Heim, Purdue Univ., Lafayette, Ind.

CIRCUITS

Differentiated Bridge Networks, J. A. Connor, Hughes Aircraft Co.

Piezoelectric Ceramic Reed Filters, J. H. Denny and C. A. Rosen, General Electric Co., Syracuse, N. Y.

Circuit Standardization and Packaging Considerations of Crystal Oscillators, H. E. Gruen, Armour Research Found., Chicago, Ill.

Statistical Fluctuations and Stability Criteria in Oscillators, by J. B. Cicchetti, Hughes Aircraft Company, Culver City, Calif.

Factors in the Design of Pulse Synchronized Blocking Oscillators, R. W. Sonnenfeldt, RCA Victor Television Div., Cherry Hill, N. J.

RADIO ASTRONOMY

Interpretation of Experimental Results, E. McClain, Naval Research Lab., Washington, D. C.

Paper, J. G. Bolton, Calif. Inst. of Technology, Pasadena, Calif.

Paper, A. Maxwell, Harvard Radio Astronomy Station, Fort Davis, Tex.

October 8, Morning

TRANSISTORS AND TRANSISTOR APPLICATIONS

Transistor Characterization of VHF, R. J. Kirkpatrick and R. P. Abraham, Bell Tel. Labs., Inc., Murray Hill, N. J.

Some Useful Techniques for Transistor Power Gain Measurements, J. S. Brown, General Electric Co., Syracuse, N. Y.

The Use of Transistors in the Control and Protection of Aircraft Electrical Power Systems, D. A. Burt and C. A. Booker, Jr., Westinghouse Electric Corp., Pittsburgh, Pa.

A Temperature Stable Transistor Multiplex Terminal, P. W. Kiesling, Jr., Raytheon Manufacturing Co., Wayland, Mass.

Design Considerations of Transistor IF Amplifier for TV Receivers, W. F. Sands and H. K. Schlegelmich, RCA, Camden, N. J.

MICROWAVES II

On the Measurement of Resonant Cavity Q, M. G. Keeney, Michigan State Univ., East Lansing, Mich.

A New Property of the Turnstile Waveguide Junction, R. S. Potter, U. S. Naval Research Lab., Washington, D. C. and A. Sagar, Univ. of Pittsburgh, Pittsburgh, Pa.

A Reciprocal Ferrite Phase Shifter for X-Band, W. H. Hewitt, Jr., and W. H. von Anlock, Bell Telephone Labs., Inc., Whippany, N. J.

Analysis of a Lossy Transmission Line Filter, R. E. Saxe, Armour Research Found., Chicago, Ill.

COMPONENTS I

Prediction of Temperatures in Forced Convection-Cooled Equipment, L. Fried, General Electric Co., Utica, N. Y.

A New Concept in Temperature Rise Measurement of Transformers, S. F. Danko, Signal Corps Engineering Labs., Fort Monmouth, N. J.

Higher Voltages, Increased Ratings for Tantalum Capacitors, J. P. Holloway, H. T. Cannon and R. P. McManus, General Electric Co., Irmo, S. C.

Tubular Sintered Tantalum Anode Capacitors, S. W. Dubriski, D. Rogers, and W. W. Schroeder, Sprague Electric Co., North Adams, Mass.

SERVOMECHANISM THEORY

Root-Locus Delineations for Higher-Order Servomechanisms, H. Banerjee, Bengal Engineering College, Calcutta, India, and T. J. Higgins, Univ. of Wisconsin, Madison, Wis.

Phase Space Metrization for Relay Control of Two Time Constant Servomechanisms, E. J. Hagin, U. S. Air Force Academy, Lowry Field, Colo. and G. H. Fett, Univ. of Illinois, Urbana, Ill.

A General Criterion for Servo Performance, W. C. Schultz and V. C. Rideout, Univ. of Wisconsin, Madison, Wis.

Analysis of Sampled-Data Control Systems with Finite Sampling Duration, J. Tou, Univ. of Pennsylvania, Philadelphia, Pa.

Luncheon Address

Afternoon

SOLID STATE

Superconductivity and its Applications to Electronic Industry, A. E. Slade, A. D. Little Inc., Cambridge, Mass.

Electroluminescence, H. F. Ivey, Westinghouse Electric Co., Bloomfield, N. J.

Paper on electroluminescence, R. W. Peter and RCA, Princeton, N. J.

COMPUTERS

Transistorized Special Purpose Computer, J. D. Schmidt, H. N. Putschi and E. Keonjian, General Electric Co., Syracuse, N. Y.

Logical Organization of Tape Operations in the BIZMAC II Computer, H. Kleinberg and E. J. Schmitt, RCA, Camden, N. J.

A Transistorized Ferrite Plate Memory, V. L. Newhouse, N. R. Kornfield, M. M. Kaufman and T. E. Gilligan, RCA, Camden, N. J.

Magnetic Cores for Airborne Digital Computers, J. Reiner, General Electric Co., Utica, N. Y.

A Transistorized Magnetic Tape-to-Paper Tape Buffer Storage Unit, C. W. McMullen, Northwestern Univ., Evanston, Ill. and R. Aschenbrenner, Argonne National Labs., Lemont, Ill.

COMPONENTS II

An Investigation of the Effects of Humidity and Temperature on XXX-P Printed Wiring Boards, John Spalding, General Electric Co., Utica, N. Y.

The Magnetic Memory Switch or Madget, H. J. McCreary, General Telephone Labs. Inc., Chicago, Ill.

An Analytical Approach to the Vibration Design of Airborne Electronic Equipment, M. Gurtin, General Electric Co., Utica, N. Y.

Aircraft Motor Generator with Secondary Standard Frequency Output, L. J. Johnson, Hallamore Electronics Co., Anaheim, Calif. and S. E. Rauch, Univ. of California, Goleta, Calif.

RADAR AND RADIO NAVIGATION

An Application of the Principle of Least Squares in Automatic Radio Direction Finding, A. D. Bailey, Univ. of Illinois, Urbana, Ill.

A Target Simulator for Conical Scan Radars, L. W. Orr, Univ. of Michigan, Ann Arbor, Mich.

A Multi-Channel Radar Receiver Combining Etched R-F and I-F Circuits, W. B. Offutt and J. H. Hogan, Airborne Instruments Lab. Inc., Mineola, N. Y.

Interference Blanker for "Normal and MTI Video", H. Kurland, Airborne Instruments Lab. Inc., Mineola, N. Y.

Suppression of False Range Indications in High Pulse Repetition Rate Radars, G. I. Cohn, Ill. Inst. of Technology, Chicago, Ill., L. P. Elbinger, Sperry Gyroscope, Garden City, N. Y., and R. M. Leger, Convair-Astronautics, San Diego, Calif.

October 9, Morning

INSTRUMENTATION I

Electronic Time-of-Event Indicator, R. Winfield, D. H. Andrews and M. Turntine, Jr., Naval Material Lab., Brooklyn, N. Y.

The Digital Measurement of Pulse Width, J. Rarity, H. Roberts and L. Saporta, New York Univ., New York, N. Y.

An Incremental Hydrobarophone, J. H. Buehler, U. S. Dept. of State, E. L. Peters and M. S. Weinstein, U. S. Naval Ordnance Lab., White Oak, Silver Spring, Md.

Metallurgical Structure Analysis by Ultrasonics, H. A. Elion, RCA, Camden, N. J.

Ultrasonic Atomization of Liquids, J. N. Antonevich, Battelle Memorial Inst., Columbus, Ohio.

ELECTRON TUBES I

Use of the Potential-Shift Diagram for Analysis of the Operation of Display Storage Tubes, R. P. Stone, RCA, Lancaster, Pa.

The Wamoscope—A New Microwave Display Device, D. E. George, R. G. E. Hutter and L. R. Bloom, Sylvania Electric Prod. Inc., Bayside, N. Y.

Transient Response of Phosphors, G. I. Cohn, Ill. Inst. of Technology, Chicago, Ill. and H. M. Musal, Cook Research Lab.

The Effects of Beam-Landing Errors on Signal-Output and Dark-Current Uniformity of Vidicon-Type Camera Tubes, R. G. Neuhäuser and L. D. Miller, RCA, Lancaster, Pa.

New Image Orthicon Employing a Multi-Alkali Photocathode for Color Cameras, P. W. Kaseman, RCA, Lancaster, Pa.

CIRCUIT THEORY

The Segregate, A Generalization of Kirchhoff's Current Laws, M. B. Reed, Michigan State Univ., East Lansing, Mich.

A New Look at Impedance and Steady-State, M. B. Reed and G. B. Reed, Michigan State Univ., East Lansing, Mich.

Error Determination for Optimum Predicting Filters, T. R. Benedict and V. C. Rideout, Univ. of Wisconsin, Madison, Wis.

Compensation of Sampled-Data System, L. M. Benningfield and G. V. Lago, Univ. of Missouri, Columbia, Mo.

MAGNETIC AMPLIFIERS

Pulse Type Logic Element Industrial Control, C. J. Adams and R. E. Cooper, General Electric Co., Bloomington, Ill.

A Stable Three Phase Transistor-Core Power Inverter, W. E. Jewett and P. L.

Schmidt, Bell Tel. Labs., Whippany, N. J.
Design Considerations of a State Logic Annunciator, W. E. Guenther, D. N. Noreen and J. N. McNeill, Westinghouse Electric Corp., Pittsburgh, Pa.

Application of Magnetic Amplifiers in Aircraft Electrical Systems, A. Krausz, Jack and Heinz, Inc., Cleveland, Ohio.

A Transductor Summation System for Strip Plater, P. W. Covert and E. V. Weir, Magnetics Inc., Butler, Pa.

Luncheon Address

Afternoon

INSTRUMENTATION II

A New Method of Precise Phase and Amplitude Response Measurements on Physical Systems Utilizing Bridge Connected Transducers, J. J. Earshen, Bendix Aviation Corp., Ann Arbor, Mich.

High Speed Printing of Cathode Ray Tube Information by Electrostatic Photography Techniques, E. F. Mayer and V. E. Straughan, Horizons Inc., Cleveland, Ohio.

A Multi-Channel Tape Recording System for the Measurement of Transient Phenomena, J. F. Bamphfield, U. S. Naval Ordnance Lab., Silver Spring, Md.

A Step-Position Slave Unit for Recording Wind Direction, H. J. Dana, State College of Washington, Pullman, Wash.

Airborne Closed Loop TV System, A. F. Flacco, RCA, Camden, N. J.

ELECTRON TUBES II

10 Watt, CW, S-Band Traveling-Wave Tube with Periodic Permanent Magnets, E. Bliss and H. Pratt, RCA, Harrison, N. J.

Fast Operation Time in Subminiature Tubes, A. Blattel, Raytheon Manufacturing Co., Newton, Mass.

Advantages of Ceramics in Electron Tubes, J. A. Jolly, Eitel-McCullough, Inc., San Bruno, Calif.

Operation of a Specially Designed DC Differential Amplifier Tube, R. Wood and T. J. White, Raytheon Manufacturing Co., Newton, Mass.

NETWORK SYNTHESIS

Realization of Complex Zeros of Transmission by Means of RC Networks, S. L. Hakimi, Univ. of Illinois, Urbana, Ill. and S. Seshu, Syracuse Univ., Syracuse, N. Y.

Feedback Amplifier Design by Forward Equivalent Circuits, L. M. Vallese, Polytechnic Inst. of Brooklyn, Brooklyn, N. Y.

Transfer Function Synthesis with Active Elements, F. F. Kuo, Univ. of Illinois, Urbana, Ill.

A, B, C, D—Network Design Easy as Pie, L. Weinberg, Hughes Research Labs., Culver City, Calif.

IRE Canadian Convention

OCTOBER 16-18, 1957

AUTOMOTIVE BUILDING, EXHIBITION PARK, TORONTO, CANADA

The 1957 IRE Canadian Convention will be held in Toronto on October 16-18. One hundred fifty-seven Canadian, American, and overseas exhibitors have booked space in Exhibition Park for what General Chairman C. A. Norris has termed "the largest scientific event in the country." Attendance is expected to be over 10,000.

Dr. George Sinclair, Chairman of the Technical Program Committee, has announced that 116 papers, the majority by Canadian engineers, will be presented at 25 technical sessions. The feature session will be devoted to a description of Canada's part in the International Geophysical Year, with emphasis on the interests of the radio engineer. Another highlight will be a symposium on professional business management and the new concept of the professional manager.

A closely related symposium will include a demonstration on the techniques of idea generation by brainstorming as applied to specific problems in the electronics industry. Two sessions will describe Canada's role in the nucleonics field.

The opening sessions on October 16th will be followed by the All-Industry cocktail party. The convention banquet will be held on Thursday evening, October 17th in the King Edward Hotel and will feature Dr. Marcus Long, professor of philosophy, University of Toronto, as guest speaker. Headquarters for ladies' activities will be the Royal York Hotel.

Advance registration and reservations can be arranged by contacting Grant Smedmor, convention manager, 745 Mount Pleasant Road, Toronto 7, Canada. Registration fee to IRE members and registered professional engineers is \$1.00, and to all others, \$1.50.

Wednesday Afternoon, October 16

ELECTRONICS FOR GUIDED MISSILES

Electrical Power Supply Units for Guided Missile-Borne Electronic Equipment, D. B. Cannon, The De Havilland Aircraft of Canada Ltd., Toronto.

Space Stabilization of Small Tracking Systems for Missile Guidance, P. A. Lapp, De Havilland Aircraft, Toronto.

A Simple CRT Presentation for a Flight Simulator, A. B. Johnson, Canadair Ltd., Montreal.

The Importance of Simulators in the Design and Checkout of Guided Missiles, J. E. A. Mortimer, Canadair Ltd., Montreal, Quebec.

A Rugged Telemetry System for Ballistic Ranges, D. L. Duff, Canadian Westinghouse Co. Ltd., Hamilton.

TELEVISION RECEIVER TECHNIQUES

A Television Signal Strength Meter of Novel Design, S. J. Gabzdyl, Canadian Radio Manufacturing Co., Toronto.

A Television Pattern Generator, A. B. Johnson, Canadair Ltd., Montreal.

Design Considerations for a 21-Inch Color TV Receiver, W. Kurz, Canadian Radio Manufacturing Co., Toronto.

The Application of 110-Degree Picture Tubes, S. F. Love, Radio Valve Co. Ltd., Toronto.

The Property of Television Sync Separator Without and With Interference Pulses in the Composite Signal, E. Luedicke, RCA Victor Co. Ltd., Montreal.

HUMAN ENGINEERING

Information Rates on Keyboards—Part A—Human Factors in the Design of Keyboards, M. Humphries and J. C. Ogilvie, Defence Research Medical Laboratories, Toronto.

Information Rates on Keyboards—Part B—Experiments With a Ten-Key Keyboard, D. K. Ritchie, Ferranti Electric Ltd., Toronto, and H. C. Ratz, Fischer and Porter, Toronto.

Transfer Function Models for Human Operators, J. M. Ham, University of Toronto, Toronto, Ont.

Changes in Parameters of an Equation Representing Human Perceptual-Motor Performance with Changes in Direction of Movement of Controls, A. H. Shephard, Dept. of Psychology, University of Toronto, Toronto.

HIGH FREQUENCY COMPONENTS

Small Size Microwave Duplexers and Fillers for Airborne Equipment, B. Vural and J. A. Smitke, Canadian General Electric Co. Ltd., Toronto.

Some Considerations on the Development and Design of Wide-Band Microwave Mixers Using Microstripline Components, B. Vural and J. Cappon, Canadian General Electric Co. Ltd., Toronto.

Microwave Modulator Using Polarization Rotation, J. E. Bryden, Canadian Marconi Company, Montreal.

Video Ferrite Delay Line—Ferrite Phase Modulator, J. MacHill, General Electric Company, Auburn, N. Y.

Graphical Method of Calculating Cascaded Microwave Networks, C. Adkar, Aircraft Div., Canadair Ltd., Montreal.

PROPAGATION

Investigation of Horizontal Drifts in the E Region of the Ionosphere in Relation to Random Fading of Radio Waves, B. Ramachandra Rao, Ionosphere Research Laboratories, Andhra University, India, and M. Spiramo Rao, Nat'l. Res. Council, Ottawa.

Effect on Short Wave Propagation of the Nature of Reflecting Ground, M. P. Bachynski, RCA Victor Company, Ltd., Montreal.

Diffraction of Short EM Waves by Natural Obstacles with Smooth Crests, H. E. J. Neugebauer and M. P. Bachynski, RCA Victor Co. Ltd., Montreal.

Path-Loss Testing of the Trans-Canada TD-2 Route, W. Von Hagen, A. N. MacDiarmid and L. V. Goldenberg, The Bell Telephone Co. of Canada, Montreal.

Measurement and Shielding of Electromagnetic Fields, J. Miedzinski, Department of National Defence, Ottawa, formerly British Electrical and Allied Industries Research Association (ERA).

Thursday Morning, October 17

CANADA'S PART IN THE INTERNATIONAL GEOPHYSICAL YEAR

The International Geophysical Year, F. T. Davies, Defence Research Board, Ottawa.

The IGY Auroral Program in Canada, P. M. Millman, National Research Council, Ottawa.

The Canadian Ionospheric Physics Program for the IGY, P. A. Forsyth, Defence Research Board, Ottawa.

The IGY Radio Astronomy Program in Canada, D. A. MacRae, Dept. of Astronomy, University of Toronto, Toronto.

COMPUTERS AND DATA PROCESSING

An Analog Memory, W. S. Kozak, Canadian Westinghouse Co. Ltd., Hamilton.

New Components of Datatron System: Cardatron and Datafile and Their Applications, G. Glinski, Burroughs Adding Machine of Canada Ltd., Ottawa.

Allrec, S. Gould, Canadian Marconi Co., Montreal.

A Hysteresigraph for Testing Magnetic Materials Using Analog Computer Techniques, G. A. Charasz and T. J. F. Pavlasek, Dept. of Electrical Engineering, McGill University, Montreal.

The TACAN Data Link, J. F. Sullivan, Standard Telephones & Cables Mfg. Co., Montreal.

DESIGN FOR MANUFACTURE

Design for Manufacture, M. Conklin, Canadian Gen. Elec. Co. Ltd., Toronto.

What's Another Engineering Change?, G. L. King, Canadian General Electric Co. Ltd., Toronto.

An Effective Material and Standards Program Is a Management Responsibility, M. J. McKerrow, Canadian Westinghouse Co. Ltd., Hamilton.

Some Fundamental Considerations in Starting a Quality Control Program, J. B. Pringle, Bell Telephone Co. of Canada, Montreal.

The Obtaining of Maximum Customer Acceptance of Electronic Equipment, B. E. Davies, Canadian General Electric Co. Ltd., Toronto.

MEDICAL ELECTRONICS I

Electronic Recording of Sensory Responses Resulting from Stimulation of the Organs of Balance, W. H. Johnson, Defence Research Medical Laboratories, Toronto.

An Electronic Heart-Beat Simulator and a Cardiac Tachometer, O. Z. Roy, National Research Council, Ottawa.

Oximetry, W. Paul, University of Toronto, Toronto.

ELECTRONIC TUBES

Factors Contributing to the Increase in Life Expectancy of Gaseous Discharge Visual Devices, J. McCauley, Burroughs Corporation, Plainfield, N. J.

The Characteristics of Evaporated CdS and CdSe Photoconductive Cells, D. A. Anderson, Canadian Marconi Company, Montreal.

Applications of Photoconductive Cells in the Visible Light Range, Z. Szepezi, Canadian Marconi Company, Montreal.

A Direct Method of Investigating Pulsed Magnetron Stability, N. J. Taylor, Aircraft Div., Canadair Ltd., Montreal.

High Power Klystrons for Single Sideband Operation, G. M. W. Badger, Eitel-McCullough Inc., San Bruno, Calif.

Thursday Afternoon, October 17

PANEL DISCUSSION ON ENGINEERING EDUCATION

Panel Members: J. D. Ryder, Dean of the College of Engineering, Michigan State University, East Lansing, Mich.; F. Noakes, Head of the Dept. of Electrical Engineering, University of British Columbia, Vancouver, B. C.; K. F. Tupper, Ewbank and Partners (Canada) Ltd., Toronto, Ont.; G. F. Tracy, Head of the Dept. of Electrical Engineering, University of Toronto, Toronto, Ont.

COMMUNICATION SYSTEMS

The Status of Radio in Canada in the Common Carrier Telephone Field, S. Bonneville, Bell Tel. Co. of Can., Montreal

The Use of Radio To Provide Telephone Service in Bush Country, E. O. Tunman, Bell Tel. Co. of Can., Montreal.

Restricted Common Carrier Mobile Radio Telephone Service, R. Fortier, The Bell Telephone Company of Canada, Montreal.

Diversity Reception in UHF and Microwave Radio Systems, A. J. Dinnin, The Bell Telephone Company of Canada, Montreal.

Practical Considerations of Combining Television and Telephone Signals on a Broadband Microwave Channel, U. C. P. Strahlehdorf and A. J. Wade, The Bell Telephone Company of Canada, Montreal.

SYMPOSIUM ON NUMERICAL CONTROL OF MACHINE TOOLS

Null-Track Control System, F. Brouwer, Canadian Westinghouse Co. Ltd., Hamilton.

A Numerically Controlled Machine-Tool System, E. C. Johnson and R. C. Sims, Bendix Aviation Corporation, Detroit, Mich.

A New Numerical Control Concept for Data Reduction in Aircraft Design, D. E. Nuttall, Ferranti Electric Ltd., Toronto.

Numerical Control in the Canadian Aircraft Industry, co-authors to be announced.

MEDICAL ELECTRONICS II

A New Six-Channel Electromyograph for Studies on Muscle, J. V. Basmajian, Dept. of Anatomy, University of Toronto, Toronto.

The Application of Transistors to a Portable Electrocardiograph, R. S. Richards, National Research Council, Ottawa.

A Sensitive System for Measurement of Brain Responses in the Intact Human, J. F. Davis, Dept. of Electrophysiology, Allan Memorial Institute, Montreal.

ANTENNAS

Duplexers or Decoupled Antennas?, A. H. Secord and W. V. Tilston, Sinclair Radio Laboratories Ltd., Toronto.

Dual Polarization Feed Horn, D. J. LeVine and L. A. Juhas, Standard Telephones and Cables Mfg. Co. (Canada) Ltd., Montreal.

A Slotted Waveguide Antenna for Marine Radar Applications, M. Katchky, Canadian Arsenals Limited, Toronto.

The Radiation Characteristics of a Zig-Zag Antenna, D. Sengupta, University of Toronto, Toronto.

A Two-Dimensional Array of Circular Holes, G. C. McCormick, National Research Council, Ottawa.

Friday Morning, October 18

AUDIO AND ACOUSTICS

Measurement of Audio Amplifier Internal Resistance, W. H. Anderson, Toronto.

A New High Impedance Audio Output Circuit, J. R. de Miranda, Phillips, Eindhoven, Holland.

A New Approach to Program Sound Systems for Schools, Hospitals and Industry, R. H. Tanner, Northern Electric Co. Ltd., Belleville, Ont.

The Acoustical Design of the Permanent Stratford Theatre, R. H. Tanner, Northern Electric Co. Ltd., Belleville, Ont.

Acoustical Design of the Alberta Jubilee Auditoria, T. D. Northwood, Div. of Building Research, National Research Council, Ottawa.

SYMPOSIUM ON PROFESSIONAL BUSINESS MANAGEMENT

The Changing Concept of the Professional Manager, W. A. Dimma, Asst. to Pres., National Carbon Company, Div. of Union Carbide (Canada) Ltd., Toronto.

The Skill of Functional Management, C. R. Miner, Mgr. Monochrome TV. Product Engineering, General Electric Company, Syracuse, N. Y.

Selecting Potential Professional Managers, H. Moore, Ph.D., Director, Psychological Service Centre, Toronto.

The Kind of Management Which Stimulates Professional Growth, P. Humeniuk, Manager, Radio and TV. Operation, Canadian Gen. Elect. Co. Ltd., Toronto.

RADIO ASTRONOMY

Solar Radio Astronomy, A. E. Covington, National Research Council, Ottawa.

Lunar Radar Echoes, B. C. Blevins, D.R.B., Defence Research Telecommunications Establishment, Shirley Bay, Ottawa.

Scintillation Measurements, W. D. Ryan, Royal Military College of Canada, Kingston, Ont.

The Design and Construction of a K-Band Spectrometer for the Measurement of Absolute Intensity, J. A. Fulford and J. H. Blackwell,

Dept. of Physics, University of Western Ontario, London, Ont.

RADIO TECHNIQUES

Video Recording Tape, L. F. Bennett, Department of National Defence, Ottawa.

System Design of Large Television Stations, A. L. Reeve, Canadian General Electric Co. Ltd., Toronto.

Modular TV Transmitter Design, M. L. Falk and C. C. Nicholson, Canadian General Electric Co. Ltd., Toronto.

The Vapotron, H. G. Towlson, General Electric Co., Syracuse, N. Y.

Design of Single-Layer Coils for Transmitters, J. Soul, Canadian General Electric Co. Ltd., Toronto.

NUCLEONICS I

Characteristics of an Electron Synchrotron for Atomic Research, H. Janzen, Queen's University, Kingston, Ont.

Electronics of the McGill Synchrocyclotron, W. M. Martin, Radiation Laboratory, McGill University, Montreal.

Proposed Experimental Use of a 10-MEV Tandem-Style Van De Graaf Accelerator, H. E. Gove, Atomic Energy of Canada Ltd., Chalk River, Ont.

Electronics in Reactor Operations, A. Pearson, Atomic Energy of Canada Ltd., Chalk River, Ont.

The Δ Atomichron: An Atomic Frequency Standard, J. H. Holloway, National Company, Inc., Malden, Mass.

Friday Afternoon, October 18

SYMPOSIUM ON BRAINSTORMING

Panel discussion under C. Watt, Canadian General Electric Co., Toronto, Ont.

TRANSISTOR ELECTRONICS

The Equivalent Circuit of the Drift Transistor, J. Almond, RCA Victor Company Ltd., Montreal.

A Transistor Controlled Susceptance, M. L. Blostein and H. W. Baumans, Canadian Marconi Company, Montreal.

A Transistorized Regulated Power Supply Design, D. J. McLean, G. E. Reesor and S. V. Soanes, Ferranti Electric Ltd., Mount Dennis, Ont.

A Regenerative Type Frequency Divider Using Semiconductor Devices, D. P. Henderson, Defence Research Board, Ottawa.

The Design of a Transistorized 60-Watt Low-Frequency Amplifier, D. G. W. Mace and R. N. Blunt, Canadian Westinghouse Co. Ltd., Hamilton, Ont.

NUCLEONICS II

Some Gas-Filled Radiation Counters Used in Reactor Instrumentation, I. L. Fowler, Atomic Energy of Canada Ltd., Chalk River, Ont.

An Automatic Sample Changer and Printing Scaler, W. D. Howell, Atomic Energy of Canada Ltd., Chalk River, Ont.

Some Applications of an Analog Computer in Nuclear Reactor Studies, J. G. Bayly, Atomic Energy of Canada Ltd., Chalk River, Ont.

A Fast Gray Wedge Analyzer for High Input Rates, J. T. Flynn and F. A. Johnson, D. R. B. Suffield Experimental Station, Suffield, Alberta.

Fault Analysis of Nucleonic Equipment, R. B. Shields, Atomic Energy of Canada Ltd., Chalk River, Ont.

MICROWAVE MEASUREMENT TECHNIQUES

A Broadband Standing Wave Ratio Analyzer, S. Presentey, T.M.C. (Canada) Ltd., Ottawa.

Laboratory Method of Constructing Lossy Microwave Components, A. Staniforth, National Research Council, Ottawa.

Absolute Microwave Power Measurement in the Milliwatt Ranges, R. F. Clark, National Research Council, Ottawa.

An Automatic Phase Plotter for the Measurement of Microwave Fields, T. J. F. Pavlasek, Dept. of Electrical Engineering, McGill University, Montreal.

A Method of Calculating the Characteristic Impedance of a Microstripline to a Given Degree of Accuracy, R. G. deBuda, Canadian General Electric Co. Ltd., Toronto.

COMPONENTS

Gina—An Automatic Test and Recording Apparatus for Rotational Noise of Variable Resistors, F. J. F. Osborne and H. J. Moody, Canadian Marconi Company, Montreal.

Performance and Reliability of Fixed Carbon Composition Resistors, H. J. Moody and F. J. F. Osborne, Canadian Marconi Company, Montreal.

A New Metal Film Precision Resistor, R. C. Langford, Weston Electrical Instrument Corp., Newark, N. J.

Quartz Crystal Units in Glass HC-6/u Style Holders for Improved Performance and Reliability, D. M. Eisen, Canadian Radio Manufacturing Corp. Ltd., Leaside, Toronto.

Automatic Electronic Boiler Control, M. Gladden, Newfoundland Section of Institute of Radio Engineers, St. John's, Nfld.



1957 IRE WESCON Convention Record

All available papers presented at the 1957 IRE WESCON Convention will appear for the first time in an IRE WESCON CONVENTION RECORD to be published in late Fall. The IRE WESCON CONVENTION RECORD will be issued in ten Parts, with each Part devoted to related subjects. The papers for each session are listed on pages 1156-1160 of the August issue.

Instructions on Ordering

1. If you are a member of a Professional Group and have paid the group assessment by September 30, you will automatically receive, free of charge, that Part of the IRE WESCON CONVENTION RECORD pertaining to the field of interest of your group, as indicated in the chart below.

2. If you are not a member of an IRE Professional Group, IRE WESCON CONVENTION RECORD Parts may be purchased at the prices listed in the chart below. Orders must be accompanied by remittance, and to assure prompt delivery, should be sent immediately to The Institute of Radio Engineers, 1 East 79 Street, New York 21, N. Y.

IRE WESCON CONVENTION RECORD

Part	Subject	Free to paid members of following IRE Professional Groups	Prices for members (M) College & Pub. Libraries & Sub. Agencies (L) Non-Members (NM)		
			M	L	NM
1	Microwave; Antennas & Propagation Sessions: 2, 8, 12, 18, 20, 31, 46	Antennas & Propagation Microwave Theory & Techniques	\$ 3.25	\$ 7.80	\$ 9.75
2	Circuit Theory; Information Theory Sessions: 1, 6, 7, 26, 32	Circuit Theory Information Theory	2.75	6.60	8.25
3	Electron Devices Sessions: 13, 19, 27, 33, 39	Electron Devices	2.25	5.40	6.75
4	Computers; Automatic Control Sessions: 3, 9, 15, 21, 24, 28, 40	Automatic Control Electronic Computers	5.00	12.00	15.00
5	Instrumentation; Telemetry Sessions: 29, 35, 41, 47	Instrumentation Telemetry & Remote Control	2.00	4.80	6.00
6	Components; Production; Industrial Electronics Sessions: 4, 10, 22, 37, 43	Component Parts Industrial Electronics Production Techniques	2.00	4.80	6.00
7	Audio; Broadcast Sessions: 23, 38, 45	Audio Broadcast & TV Receivers Broadcast Transmission Systems	2.00	4.80	6.00
8	Aeronautical; Communications; Military Sessions: 14, 16, 17, 36, 42	Aeronautical & Navigational Electronics Communication Systems Military Electronics Vehicular Communications	2.75	6.60	8.25
9	Ultrasonics; Nuclear; Medical Sessions: 25, 34, 44, 48	Medical Electronics Nuclear Science Ultrasonics Engineering	1.50	3.60	4.50
10	Quality Control; Engineering Management Sessions: 5, 11, 30	Engineering Management Reliability & Quality Control	1.50	3.60	4.50
	Complete Set (10 Parts)		\$25.00	\$60.00	\$75.00



Abstracts of IRE Transactions

The following issues of "Transactions" have recently been published, and are not available from the Institute of Radio Engineers, Inc., 1 East 79th Street, New York 21, N. Y. at the following prices. The contents of each issue and, where available, abstracts of technical papers are given below.

Sponsoring Group	Publication	Group Members	IRE Members	Non-Members*
Electronic Computers	Vol. EC-6, No. 2	\$1.05	\$1.55	\$3.15
Medical Electronics	PGME-8	0.95	1.40	2.85
Microwave Theory & Techniques	Vol. MTT-5, No. 3	1.15	1.70	3.45
Ultrasonics Engineering	PGUE-5	1.50	2.25	4.50

* Public libraries and colleges may purchase copies at IRE Member rates.

Electronic Computers

VOL. EC-6, No. 2, JUNE, 1957

The IRE "Affiliate" Plan—A New Venture^e in Engineering Society Structure and Service—W. R. G. Baker (p. 71)

A Time Sequential Tabular Analysis of Flip-Flop Logical Operation—G. W. Arant (p. 72)

In examining flip-flop response the principal concern of the logical designer is to find what input signals must be applied to the flip-flop in order to produce the output conditions that are desired. Equation methods of analysis and a time-sequential tabular method of analysis are described, and some advantages of the tabular method are pointed out.

Dynamic Accuracy as a Design Criterion of Linear Electronic-Analog Differential Analyzers—A. Nathan (p. 74)

A frequency error analysis of computing elements is presented which leads to a definition of their dynamic accuracy.

The concept of a computing transfer function is introduced for this purpose, permitting the evaluation of an effective bandwidth, the latter being connected with the variance of the output for wideband inputs. Limited bandwidth is considered as equivalent to finite resolution and thus to an additional effective error. Single frequency errors are dealt with separately and are shown to be of minor importance. Suitable optimization of dynamic accuracy yields parameters of design and performance such as optimum computing time and required base amplifier gain.

The theory is applied to integrators and adders with base amplifiers of direct and of capacitive coupling.

Trigonometric Resolution in Analog Computers by Means of Multiplier Elements—R. M. Howe and E. G. Gilbert (p. 86)

A method of generating sine and cosine functions in analog computers by means of multiplier elements and integrators is discussed. Static accuracy of the method is analyzed and found to be essentially equal to the accuracy of the multipliers employed. The system accepts $d\theta/dt$ as the input and generates output voltages of $\sin \theta$ and $\cos \theta$. Amplitude-stabilizing loops are employed to maintain $\sin^2 \theta + \cos^2 \theta = 1$. Advantages of the method include representation of unlimited range in angles, dynamic capabilities far beyond that of the multipliers alone, and possibility of employing electronic multipliers. The method has been successfully used to compute Euler angles in analog computer solutions of the three-dimensional flight equations.

Minimization of the Partially-Developed Transfer Tree—M. P. Marcus (p. 92)

A transfer tree is a particular type of multi-terminal network having a single input which may be connected to any one of a number of outputs.

An n -relay transfer tree is partially developed if it has less than the 2^n possible output terminals. Rearrangement of a partially-developed tree can lead to a reduction in the total number of transfers required.

This paper presents a method of obtaining a required partially-developed transfer tree with the minimum number of transfers.

A New Diode Function Generator—T. Miura, H. Amemiya, and T. Numakura (p. 95)

With the diode function generators that are currently in use, generation of functions is made by combining straight lines. The main drawback of these function generators is that the slope of the line segment cannot be changed independently. With the new function generator described in this paper, functions are generated by connecting independent line segments. Accordingly, the slope of each segment is given independently and also quantitatively. It is possible to approximate any desired function without recourse to an oscilloscope for inspection. These advantages are realized by using ganged potentiometers differentially. The operating principle and a practical generator experimentally built are described.

An Electronic Analog Multiplier—D. C. Kalbfell (p. 100)

This multiplier uses the variable pulse area principle, but employs phase sensitive circuitry to operate naturally in all four quadrants without bias voltages. The output is zero if either input is zero. The X and Y channels are separately linearized with independent feedback loops. The circuitry is simple and lends itself to either transistors or vacuum tubes.

An Algorithm for Determining Minimal Representations of a Logic Function—B. Harris (p. 103)

For each logic function, or Boolean algebraic expression, there corresponds an appropriate computer circuit. However, the minimization of the appearances of the Boolean variables does not necessarily lead to the most economical circuit. A general approach to the problem therefore requires the development of techniques for the simple and rapid generation of a variety of near-minimal forms.

This paper describes such a method for constructing the minimal representations of a logic function given as a truth table or in one of its canonical forms. The minimal representations achieved are either sums of products, or products of sums, such that no term contains super-

fluous variables and such that no term is superfluous. The utility of the method lies in the conciseness of notation, which permits the handling of a large number of variables and simplifies the process for machine computation.

Computing Techniques for the Sampling Parametric Computer—C. J. Hirsch and F. C. Hallden (p. 108)

This paper describes novel calculating techniques suitable for an electronic analog computer using exponential discharges to simulate the logarithmic scales of the slide rule. Among others, the device can perform the following operations: $z = xy$; $z = x/y$; $z = xy^a$; $\log_a x$; a^x ; and evaluate such series as $y = Ax^a + Bx^b + Cx^c + \dots$ where the exponents can be fractional and z, x , and y can be time variables. The problems can be solved explicitly or implicitly; thus in the above series y (or x) can be determined with equal ease if x (or y) are given. The appendix describes an actual computer which gave accuracies of 1 to 2 per cent of full range from 0 to 95 per cent of full range and 4 per cent from 95 to 100 per cent of full range without recalibration for different groups of problems. The accuracy can be increased by calibrating the device for a specific group of problems.

Correspondence (p. 120)

Contributors (p. 124)

PGEC News (p. 126)

Review of Current Literature (p. 129)

Medical Electronics

PGME-8, JULY, 1957

(Paper Presented at WESCON, Los Angeles, Calif., Aug. 21-24, 1956)

Xeroradiography—D. B. Slauson (p. 1)

(Papers Presented at the Canadian IRE Convention, Toronto, Can., Oct. 1-3, 1956)

Electronic Applications in Cardiovascular Surgery—J. A. Hoppes (p. 6)

The role of electronics for diagnostic and therapeutic use in heart surgery at lowered body temperature (hypothermia) is discussed. The current trend of lowered-temperature anesthesia offers distinct advantages to the cardiovascular surgeon in reducing anesthetic shock and extending tolerance to interrupted oxygenated blood circulation. However, lowered body temperatures impose critical demands on monitoring instruments and on equipment for countering ventricular fibrillation or cardiac arrest. A cardiac resuscitation unit has been designed and built for diagnostic and treatment use in the operating room. The equipment includes an electrocardiograph with both cathode-ray and pen-recorder displays, a heart-rate meter, pacemaker stimulator, defibrillator, thermistor thermometer, blood-pressure monitor and oxygen resuscitator. The application of other electronic techniques in cardiovascular surgery is outlined briefly.

Electronics in Medicine—W. E. Hodges (p. 15)

(Paper Presented at the National Electronics Conference, Chicago, Ill., Oct. 1-3, 1956)

A New Approach to Signal Analysis in Electroencephalography—Bernard Saltzberg, N. R. Burch, M. A. McLennan and E. G. Correll (p. 24)

This paper describes the theoretical aspects of the work done in an Air Force research program on the analysis of electroencephalographic waveforms (brain waves). An analytical characterization of an electroencephalographic (eeg) time series is presented and a neurophysiological model is discussed for relating eeg waveshape to the response of neural populations. The mathematical theory is based on a statistical representation of the eeg signal. A

system of signal analysis which may be implemented by measuring the location of zeros, extremals and points of inflection results from treating the individual rectified sections of the eeg signal as statistical distributions.

(*Papers Presented at the Ninth Annual Conference on Electrical Techniques in Medicine and Biology, New York City, Nov. 7-9, 1956*)

An Electronic Computer for Vector Electrocardiography—Robert DeCote and W. J. Horvath (p. 31)

The Sonic Valve Pressure Gauge—F. W. Noble (p. 38)

An Analog Computer Employing Network Analogy Techniques—G. E. Kaufer (p. 46)

Microwave Theory and Techniques

VOL. MTT-5, No. 3, JULY, 1957

Sergei A. Schelkunoff (p. 172)

Microwaves and Mathematics—S. A. Schelkunoff (p. 173)

Well Done, Ted—H. F. Englemann (p. 174)

A Modified Equal-Element Band-Pass Filter—R. Bawer and G. Kefalas (p. 175)

A method is presented whereby considerable improvement in the frequency response of a five-stage, equal-element waveguide filter can be realized while preserving nearly all the structural simplicity of this realization. It is shown that by increasing the loaded Q of the center resonant element of a five-stage, equal-element filter, the pass band ripple can be appreciably reduced and the skirt selectivity improved. The modified design also provides a simple means of bandwidth adjustment.

Application of Rayleigh-Ritz Method to Dielectric Steps in Waveguides—R. E. Collin and R. M. Vaillancourt (p. 177)

The Rayleigh-Ritz method is applied to obtain approximations to the first N eigenfunctions and corresponding eigenvalues in an inhomogeneously filled rectangular waveguide. These approximate eigenfunctions are then used to obtain a solution for the reflection and transmission coefficients at the junction of an empty and partially filled waveguide. Theoretical and experimental results are given for a dielectric slab which extends completely across the broad dimension of the guide, but only partially across the narrow dimension. The experimental values are within the experimental error of the computed values obtained by considering the dominant mode and only two evanescent modes.

Coupling Through an Aperture Containing an Anisotropic Ferrite—D. C. Stinson (p. 184)

Coupling through an aperture containing anisotropic ferrites is investigated theoretically by a simple extension of Bethe's small-hole coupling theory to include the dipole moment of the body in the aperture. The magnetic dipole moment of the ferrite body is ordinarily a vector but becomes a tensor upon the application of a magnetostatic field. This new theory is applicable to any situation where Bethe's small-hole coupling theory is valid. Experimental verification was quite satisfactory and was obtained on two Bethe-hole type couplers; one with the waveguides parallel, and the other with the waveguides perpendicular.

An Adjustable Sliding Termination for Rectangular Waveguide—R. W. Beatty (p. 192)

A new adjustable sliding termination for rectangular waveguide has been developed. The termination is of simple design and can easily be adjusted to have reflection coefficients from zero to nearly unity in magnitude and any desired phase. In addition to the usual applications of adjustable sliding terminations for rectangular waveguide, it provides a suitable design for an adjustable transfer of secondary standard of impedance for rectangular waveguide systems.

Field Displacement Isolators at 4, 6, 11, and

24 KMC—S. Weisbaum and H. Boyet (p. 194)

Performance of ferrite field displacement isolators at various frequency bands is described. Single and double-slab isolators have been constructed in rectangular waveguide. Four single-slab isolators are reported in the following frequency bands: 3700-4200 mc; 5925-6425 mc; 10,700-11,700 mc and 23,500-24,470 mc; one double-slab isolator is described in the frequency range 10,700-11,700 mc.

A Method of Reducing Broad-Band Circular Polarization Employing an Anisotropic Dielectric—H. S. Kirschbaum and S. Chen (p. 199)

A procedure is described whereby it is possible to design circular polarizers for both waveguides and in window form to be used over a broad band of frequencies. The difference in phase constants for two mutually orthogonal E fields, while propagating in an anisotropic dielectric is combined with the effect due to guide wall spacing to obtain a reasonably constant differential phase constant for the two fields over a broad frequency band. By properly choosing the length of the anisotropic dielectric in the direction of propagation, and orienting this dielectric properly with respect to an incident linearly-polarized wave, the transmitted wave is circularly polarized over a correspondingly broad band of frequencies.

Errors in a Magic-Tee Phase Changer—R. M. Vaillancourt (p. 204)

This paper recalls the basic properties of a magic-tee and how it can be used as a linear phase changer. An analysis of the symmetrical magic-tee phase changer is made, which shows that non-linearities of the phase shift and amplitude modulation are second and higher order effects caused by small mismatches of the structure. Also, some qualitative comments are made on the errors of an asymmetrical phase changer. Measurements on a phase changer assembled from ordinary laboratory equipment show that the phase shift is linear to better than 1°.

Excess Noise in Microwave Crystal Diodes Used as Rectifiers and Harmonic Generators—J. M. Richardson and J. J. Faris (p. 208)

Excess noise produced by microwave excitation of silicon crystal diodes was studied for operation of the crystal as a detector and as a microwave harmonic generator. The noise appears at the detector terminals and also as noise sidebands of the microwave harmonic, thus degrading the spectral purity of the harmonic relative to that of the fundamental. Possible models of the processes involved are presented. Difficulties and technique of measurement are discussed. Observations for 1N26 crystals, used as detectors, doublers, and triplers, and excited by X-band power in the range 8 to 100 mw are presented, showing limitations on spectral purity set by the process of noise production during harmonic generation.

Exponential Transmission Lines as Resonators and Transformers—R. N. Ghose (p. 213)

An attempt has been made to analyze the theory of an exponential transmission line from its complex reflection coefficient's standpoint and to indicate how the characteristics of an exponential line can be completely represented for any frequency with the help of the Smith chart. It is shown that the optimum design parameters of an exponential transmission line which may be used as a transformer, with a frequency-sensitive load at one end, can be determined with the help of the Smith chart and some derived equations. This paper also includes a study of the coaxial type exponential line which can be used as a series or parallel resonator. Theoretical expressions for the attenuation constant, stored energy, and Q for such types of resonator have been derived. Also indicated in this paper is the possibility of replacing the uniform-line coaxial-type resonators in many microwave and uhf wave filters by the ex-

ponential-line resonators, particularly when a large power-handling capacity is warranted.

Correction (p. 217)

Correspondence (p. 218)

Contributors (p. 219)

Ultrasonic Engineering

PGUE-5, AUGUST, 1957

A High Performance Magnetostriction-Sonic Delay Line—H. Epstein, O. B. Stram (p. 0)

The magnetostriction-sonic delay line described can be used to definite advantage in applications where extremely short resolution time is unnecessary. This inexpensive, high-performance line consists of transducer coils and thin-walled nickel tubing. The construction and design result in a rugged delay line with a relatively small insertion loss; a comparatively long, continuously adjustable delay; and a relatively small temperature dependence.

A simplified theory of operation is discussed and a laboratory model incorporating the features of the delay line is described. Consideration is given to optimal design of the components and some applications are offered.

Use of High Frequency Ultrasound for Determining the Elastic Moduli of Small Specimen—H. J. McSkimin (p. 25)

Many materials, such as single crystals, are available only in small sizes. For specimens having linear dimensions of the order of 2 or 3 mm, a phase comparison technique employing high frequency ultrasonic waves for determining elastic moduli has proved successful.

In order to minimize and evaluate the effects of dispersion due to diffraction, transducer coupling, and to reflection of energy from lateral boundaries, it was found necessary to make measurements over a wide frequency range extending to 200 mc/sec.

A description of the experimental methods and of the apparatus used is given, including the construction of units suitable for measurements over a temperature range. Results for single crystal indium antimonide are given.

Current Developments in Ultrasonic Equipment for Medical Diagnosis—J. M. Reid and J. J. Wild (p. 44)

This paper reviews developmental equipment currently being used for cancer diagnosis by ultrasonic echo-ranging. Results of clinical trials conducted to date are summarized from an engineering viewpoint. First pictures taken with a new instrument which scans the lower bowel are shown.

Current work on systems development is described, based on the clinical results and leading toward improvement of diagnostic accuracy and extension to detection. The operation of the system is limited by two fundamental considerations, attenuation and random noise. The design of systems producing optimum results within these limitations is considered using conventional means. Present systems are limited primarily by transducer aperture, and means of increasing the aperture are considered. A transducer producing an electrically moveable focused spot is described.

Precision Calibration of Ultrasonic Fields by Thermoelectric Probes—Floyd Dunn and W. J. Fry (p. 59)

The highly stable, small and readily constructed ultrasonic probe, developed and in use at this laboratory for the past five years, is discussed from the point of view of construction, calibration and operation.

This transient type thermoelectric probe yields information concerning the pressure amplitude, particle velocity amplitude and intensity of the ultrasonic field in which it is placed. If the field characteristics are known, the principle of operation of the probe provides a method for determining the absorption coefficient of minute quantities of material.

Abstracts and References

Compiled by the Radio Research Organization of the Department of Scientific and Industrial Research, London, England, and Published by Arrangement with that Department and the *Electronic and Radio Engineer*, incorporating *Wireless Engineer*, London, England

NOTE: The Institute of Radio Engineers does not have available copies of the publications mentioned in these pages, nor does it have reprints of the articles abstracted. Correspondence regarding these articles and requests for their procurement should be addressed to the individual publications, not to the IRE.

Acoustics and Audio Frequencies.....	1313
Antennas and Transmission Lines.....	1314
Automatic Computers.....	1314
Circuits and Circuit Elements.....	1315
General Physics.....	1316
Geophysical and Extraterrestrial Phenomena.....	1318
Location and Aids to Navigation.....	1318
Materials and Subsidiary Techniques..	1319
Mathematics.....	1322
Measurements and Test Gears.....	1322
Other Applications of Radio and Electronics.....	1323
Propagation of Waves.....	1323
Reception.....	1323
Stations and Communication Systems..	1324
Subsidiary Techniques.....	1324
Television and Phototelegraphy.....	1324
Transmission.....	1325
Tubes and Thermionics.....	1325
Miscellaneous.....	1326

The number in heavy type at the upper left of each Abstract is its Universal Decimal Classification number and is not to be confused with the Decimal Classification used by the United States National Bureau of Standards. The number in heavy type at the top right is the serial number of the Abstract. D.C numbers marked with a dagger (†) must be regarded as provisional.

ACOUSTICS AND AUDIO FREQUENCIES

- 534.2** **2312**
Disk-Loaded Torsional Wave Delay Line: Part 1—Construction and Test—P. Andreatch, Jr. and R. N. Thurston. (*J. Acoust. Soc. Amer.*, vol. 29, pp. 16-19; January, 1957.) Two delay lines constructed of brass gave delays of 43 μ s/cm-length and 114 μ s/cm-length compared with 4.5 μ s/cm-length for a uniform diameter line. The former was loaded with 0.02-inch-thick disks spaced at 0.02 inch having a diameter four times that of the uniform line; the latter with 0.015-inch-thick disks spaced at 0.015 inch, with a 5:1 diameter ratio.
- 534.2** **2313**
Disk-Loaded Torsional Wave Delay Line: Part 2—Theoretical Interpretation of Tests and Design Information—R. N. Thurston. (*J. Acoust. Soc. Amer.*, vol. 29, pp. 20-25; January, 1957.)
- 534.25-16-8** **2314**
Ultrasonic Double Refraction in Single Crystals—P. C. Waterman and L. J. Teutonico. (*J. Appl. Phys.*, vol. 28, pp. 266-270; February, 1957.) The phenomenon, methods of observation using pulse reflection, and two causes are described. Double refraction effects were observed in three Ge single crystals.
- 534.26** **2315**
Scattering in an Inhomogeneous Medium—E. Skudrzyk. (*J. Acoust. Soc. Amer.*, vol. 29, pp. 50-60; January, 1957.) "The standard mathematical procedure formally describes scattering by the superposition of a scattered pressure on the unscattered sound field. At low frequencies, because of the irregular dis-

The Index to the Abstracts and References published in the PROC. IRE from February, 1956 through January, 1957 is published by the PROC. IRE, May, 1957, Part II. It is also published by *Electronic and Radio Engineer*, incorporating *Wireless Engineer*, and included in the March, 1957 issue of that journal. Included with the Index is a selected list of journals scanned for abstracting with publishers' addresses.

tribution of the inhomogeneities, the phases of the scattered waves are at random and scattering is an interference phenomenon. As the frequency increases, scattering becomes highly collimated in the forward direction and the phase differences decrease to zero. At this point, ray theory starts to apply. The scattered pressure, then, essentially describes only a phase change caused by the different sound velocities and the focusing and defocusing by the lens action of the patches. The medium in the neighborhood of the receiver can be shown to contribute only by focusing, the medium farther away only by interference fluctuations. Focusing leads to normally distributed amplitude fluctuations. The distribution of the interference fluctuations, however, passes from normal to Rayleigh with increasing values of range."

- 534.612** **2316**
Acoustic Radiation Pressure—P. J. Westervelt. (*J. Acoust. Soc. Amer.*, vol. 29, pp. 26-29; January, 1957.)
- 534.613** **2317**
The Torque on an Infinite Strip Exposed to Plane Sound Waves—H. Levine. (*Proc. Camb. Phil. Soc.*, vol. 53, pp. 234-247; January, 1957.)
- 534.7** **2318**
Inapplicability of the Threshold Concept to Detection of Signals in Noise—R. R. McPherson. (*J. Acoust. Soc. Amer.*, vol. 29, p. 151; January, 1957.) Brief discussion of the concept which considers that a response occurs only if the variable is larger than a certain magnitude.
- 534.7** **2319**
Some Results of Research on Speech Perception—A. M. Liberman. (*J. Acoust. Soc. Amer.*, vol. 29, pp. 117-123; January, 1957.) "Recent experiments with synthetic speech have succeeded in isolating some of the acoustic cues which underlie the perception of speech. This paper describes, and attempts to interpret, some of the research in that area."
- 534.78** **2320**
Information Conveyed by Vowels—P. Ladefoged and D. E. Broadbent. (*J. Acoust. Soc. Amer.*, vol. 29, pp. 98-104; January, 1957.)
- 534.78** **2321**
Acoustic Properties of Stop Consonants—M. Halle, G. W. Hughes, and J. P. A. Radley. (*J. Acoust. Soc. Amer.*, vol. 29, pp. 107-116; January, 1957.)

- 534.844.1** **2322**
A Reverberation-Time Meter—G. Odin. (*Hochfreq. und Elektroak.*, vol. 65, pp. 86-91; November, 1956.) The instrument described automatically measures and records the decay time of sound in rooms; tests can be made repetitively.
- 534.846** **2323**
Acoustics at the Rochester (New York) War Memorial Auditorium—B. Olney and R. S. Anderson. (*J. Acoust. Soc. Amer.*, vol. 29, pp. 94-98; January, 1957.) This arena type auditorium has a volume of 3.24×10^6 cubic feet and a reverberation time of 2.5 s at 500 cps when unoccupied, and 1.9 s with two-thirds of the audience. Design features are discussed.
- 534.846.6** **2324**
Investigation of the Acoustic Shock Wave-Form Used for Pulse Measurement of Room Acoustics—H. Niese. (*Hochfreq. und Elektroak.*, vol. 65, pp. 98-108; November, 1956.) The conditions are examined which must be fulfilled by the sound source and the pulse shape so that consistent results are achieved for the measurement of audibility at any test point, on a subjective basis. The directivity of a sound source reproducing speech was determined to find a means of measuring intelligibility. A loudspeaker specially designed to meet the requirements is shown (see also 3267 of 1956).
- 534.846.6.001.57** **2325**
Electroacoustic Measurements on Room Models—W. Kraak. (*Hochfreq. und Elektroak.*, vol. 65, pp. 91-98; November, 1956.) The assumptions necessary for measurements on a model are investigated with reference to the various conditions which have to be simulated, such as wall absorption and reflection, the presence of an audience, etc. Methods using sound pulses with a frequency spectrum around 1 kc extending over about 3 octaves appear most suitable. See also 2324 above.
- 621.395.612.45.1** **2326**
Bigradient Uniaxial Microphone—H. F. Olson, J. Preston, and J. C. Bleazey. (*RCA Rev.*, vol. 17, pp. 522-533; December, 1956.) Two uniaxial microphones (see 2199 of 1953) are connected in series opposition to form a second-order unidirectional microphone. The improved directional efficiency of this assembly makes it usable for a pickup distance three times that of a nondirectional microphone.
- 621.395.616:534.612.4** **2327**
Apparatus for the Calibration of Condenser Microphones—A. Bressi. (*Alta Frequenza*, vol.

25, pp. 505-519; December, 1956.) Description of equipment for the absolute calibration of microphones by the pistonphone and reciprocity methods.

621.395.625.3:655.3 2328

Printed Magnetic Recording Tapes—H. Schiesser. (*Elektrotech. Z., Edn B.*, vol. 8, pp. 473-475; December 21, 1956.) A method of copying tapes is outlined in which variable-area recording based on the boundary-displacement process [1963 of 1952 (Daniels)] is used. Prints are made in color containing suspended magnetic particles and the recording can be reproduced photoelectrically. After being magnetized to saturation the tape can be used for magnetic reproduction. Advantages and difficulties are briefly discussed; economic mass production of magnetic tape recordings may thus be feasible.

621.395.625.3:778.5 2329

Magnetic 16-mm Single-System Sound-on-Film Recording Camera Equipment—W. Bach, E. M. Berndt, A. N. Brown, and R. L. George. (*J. Soc. Mol. Pict. Telev. Eng.*, vol. 65, pp. 603-605; November, 1956.) Discussion p. 605.)

681.84:534.851 2330

Limiting Factors in Gramophone Reproduction—D. A. Barlow. (*Wireless World*, vol. 63, pp. 228-230, 290-294; May/June, 1957.) Considers the deformation and wear of groove walls, the mechanical design of the pick-up, types of styli, and tracing distortion with particular reference to playing speeds and recording characteristics.

681.892:61 2331

Acoustic Mapping within the Heart—J. D. Wallace, J. R. Brown, Jr., D. H. Lewis, and G. W. Deitz. (*J. Acoust. Soc. Amer.*, vol. 29, pp. 9-15; January, 1957.) A miniature bariumtitanate transducer in conjunction with amplifier and recording equipment was used for intracardiac acoustic mapping. The equipment and some of the results obtained are described.

ANTENNAS AND TRANSMISSION LINES

621.3.091 2332

The Definition of Cymomotive Force—G. Barzilai. (*Poste e Telecomunicazioni*, vol. 5, pp. 796-798; November/December, 1956.) The use of the term cymomotive force (cmf) for defining the properties of radiating systems in free space has been adopted by the CCIR. The definition given is that contained in Document 386-E of May 24, 1956 presented at the 8th Plenary Assembly of the CCIR in Warsaw, 1956, to point out that the cmf is independent of frequency. For an application of this concept, see 29 of 1957 (Micheletta) where it is termed "radiative force."

621.315.2.013.78:621.317.332 2333

The Measurement of the Coupling [surface-transfer] Impedance of Cable Screens at High Frequencies—H. Jungfer. (*Nachrichtentech. Z.*, vol. 9, pp. 553-560; December, 1956.) General equations are derived and a suitable test arrangement is described. A comparison of results obtained by alternative methods in the frequency range 10-1000 mc shows satisfactory agreement and an approximately linear increase of transfer impedance with frequency.

621.315.212 2334

Screening Effect of the Outer Conductors of Flexible Coaxial Cables—L. Krügel. (*Telefunken Ztg.*, vol. 29, pp. 256-266; December, 1956. English summary, p. 293.) Tests were made on cables with braided, single, and double layer-wound screens to assess the effect of the number of wires or strands, their thickness, and lay. Results are given in graphical form and discussed in detail.

621.372.2:621.317.34 2335

Investigations on Helical Lines—K. Hübener. (*Nachrichtentech. Z.*, vol. 9, pp. 581-584; December, 1956.) Inhomogeneities, such as kinks, bends, and variations in pitch, are treated as lossless or lossy quadrupoles. The reflection coefficients are calculated from measurements made by means of the apparatus described.

621.372.2.029.6 2336

Theory of Twin-Helix Coaxial Line—V. S. Mikhalevski. (*Radiotekhnika i Elektronika*, vol. 1, pp. 1309-1316; October, 1956.) The dispersion in twin-helix lines is calculated, assuming perfect conductors and the possibility of substituting for the helices equivalent cylindrical surfaces conducting only along a helical path. Helices wound in the same sense and in opposite senses are considered.

621.372.8 2337

Propagation Characteristics of Low-Loss Tubular Waveguides—H. E. M. Barlow and H. G. Effemy. (*Proc. IEE*, Part B, vol. 104, pp. 254-260; May, 1957.) The propagation of the H_{01} mode in straight lengths of circular waveguide was studied at a frequency of 35 kmc. Lengths of copper and aluminium tube manufactured to commercial tolerances were found to give attenuations about 30 per cent above the theoretical values. Launching arrangements are discussed, and possible applications of the method to trunk communication and high-power transmission are pointed out.

621.372.8 2338

A New Type of Waveguide with Diaphragms—R. G. Mirimanov and G. I. Zhileiko. (*Radiotekhnika i Elektronika*, vol. 1, pp. 1374-1377; October, 1956.) Coaxial waveguides with diaphragms are discussed theoretically.

621.372.8 2339

A New Form of Hybrid Junction for Microwave Frequencies—P. D. Lomer and J. W. Crompton. (*Proc. IEE*, Part B, vol. 104, pp. 261-264; May, 1957.) Performance details are given for a branch-waveguide directional coupler in which the voltage coupling coefficients of the branch waveguides are proportional to the coefficients in a binomial expansion.

621.372.8:621.318.134 2340

Ferrite Slabs in Transverse Electric Mode Waveguide—H. Seidel. (*J. Appl. Phys.*, vol. 28, pp. 218-226; February, 1957.) A qualitative description of the nonreciprocal properties of ferrite-loaded waveguides is developed showing that a suitably loaded coaxial line may have nonreciprocal properties. The treatment is extended to gyromagnetic resonance.

621.396.67 2341

Calculation of the Current along a Cylindrical Antenna—R. Dematte. (*Ann. Télécommun.*, vol. 11, pp. 280-287; December, 1956.) The author details the calculation of the numerical results used to illustrate the method developed by Poincelot (980 of 1956) who introduces the paper.

621.396.677.029.6 2342

The Gain of Highly Directive Antennas Used for Scatter Propagation—A. Chinni and G. C. Corazza. (*Poste e Telecomunicazioni*, vol. 5, pp. 804-809; November/December, 1956.) A formula is derived on the basis of Booker and Gordon's theory of tropospheric scattering (1757 of 1950) for the change in gain as a function of aperture angle and effective scattering area. The importance of the law assumed for the distribution with height of local fluctuations of the dielectric constant is discussed.

621.396.677.029.64 2343

Microwave Helical Antennas—T. G. Hame. (*Electronic Eng.*, vol. 29, pp. 181-183; April,

1957.) Dielectric-enclosed helical antennas are effective up to 10,000 mc, if the design allows for the detuning effect of the dielectric.

621.396.677.32 2344

Reduction of Side Lobes in Directional Antennas—S. Manczarski. (*Arch. Elektrotech.*, vol. 5, pp. 325-337; 1956. English summary, pp. 340-341.) Discussion of rhombic, broadside, and end-fire arrays for sw communication followed by a description of the Type-j/8DD/1 end-fire array designed for the Polish Radio. The array comprised eight double-dipole elements spaced at $\lambda/4$ with a 90° phase-difference between adjacent elements. A radiation polar diagram is given.

AUTOMATIC COMPUTERS

681.142 2345

A High-Speed Data Processing System—M. L. Klein, R. B. Rush, and H. C. Morgan. (*Electronic Eng.*, vol. 29, pp. 158-163; April, 1957.) Data from 20-100 independent channels, at a full-scale level of 100 mv, are taken at a rate of 100 kc and recorded digitally on a magnetic tape together with the source information and time.

681.142 2346

The "Bizmac" Digital Data Processing System—J. C. Hamerton. (*Electronic Eng.*, vol. 29, pp. 174-180; April, 1957.) As used at the central agency for American military supply depots.

681.142 2347

500,000,000-Bit Random-Access Memory—G. E. Comstock. (*Instrum. & Automation*, vol. 29, pp. 2208-2211; November, 1956.) The machine described combines mechanical and electrical techniques to store and have accessible within less than a second 64×10^6 8-bit characters. Magnetic recording tape about 60 miles long is used as storage medium.

681.142 2348

Possibilities and Developments of the Method of Rheoelectric Analogues—L. Malavard. (*Onde Elect.*, vol. 36, pp. 829-837 and 1046-1052; October and December, 1956.) Continuation and conclusion of a paper published in the computer issue *ibid.*, August/September, 1956 (see 997 of 1957). A detailed review of the principles and experimental techniques with 200 references.

681.142 2349

Application of Computers in Automatic Systems—A. A. Fel'dbaum. (*Avtomatika i Telemekhanika*, vol. 17, pp. 1046-1056; November, 1956.) A survey. Twenty-six references including several to Russian literature.

681.142:517.948.34 2350

On the Continuous Solution of Integral Equations by an Electronic Analogue: Part I—M. E. Fisher. (*Proc. Camb. Phil. Soc.*, vol. 53, pp. 162-174; January, 1957.) "A scheme is proposed for solving a class of integral equations by electronic analog computing techniques in times as short as one-tenth of a second. The scheme utilizes a recently developed high-speed analog function store for carrying out a special iterative procedure which is shown to be more efficient than the classical Neumann process. The problem of the kernel generation at high repetition rates is considered and a novel method based on pivotal function generators is described. Likely errors are analyzed and an over-all accuracy of the order of 1 per cent is shown to be attainable with known techniques."

681.142:621.318.57 2351

Counters Select Magnetic Drum Sectors—A. J. Strassman and R. E. King. (*Electronics*, vol. 30, pp. 161-163; April 1, 1957.) A test instrument for "writing" a predetermined

binary pattern on any selected sector of a magnetic drum memory system.

CIRCUITS AND CIRCUIT ELEMENTS

- 621.3.049.75:621.396.6.002.2 2352
The "Asmodular" Process, a New Assembly Technique for Electronic Equipment—M. L. Paternault. (*Onde élect.*, vol. 36, pp. 1031-1039; December, 1956.) Description of the modular design technique [see 693 of 1954 (Henry and Rayburn)] developed in the U.S.A., with particular reference to its adoption by the French electronic industry for mechanized mass production.
- 621.372:681.142 2353
Theory on Nonlinear Operational Elements using a Piecewise Linear Approximation—B. Ya. Kogan. (*Avtomatika, i Telemekhanika*, vol. 17, pp. 1081-1091; December, 1956.) A function generator is considered to be an operational amplifier with nonlinear conductances in the feedback circuit. Fundamental relations are derived and examples are given of the synthesis of a function generator using diode-circuit elements.
- 621.372.4 2354
Novel Method of Realizing Two-Pole Functions by Canonical Circuits or Circuits without Coupling Elements—R. Unbehauen. (*Nachrichtentech. Z.*, vol. 9, pp. 565-572; December, 1956.) An outline is given of a generalized form of Brune's method of network synthesis by canonical circuits, which permits a reduction in transformer elements. By means of another method, transformerless networks can be realized which have fewer reactive elements than those given by Bott and Duffin (1108 of 1951). See also Reza (47 of 1955).
- 621.372.41:621.372.8 2355
Resonator in the Form of a Cut-Off Waveguide—I. V. Lebedev and E. M. Gutsait. (*Radiotekhnika i Elektronika*, vol. 1, pp. 1303-1308; October, 1956.) The input impedance of a uniform waveguide operating below cutoff frequency is calculated. The feasibility of synthesizing a resonator, with characteristics similar to a parallel tuned circuit, from the waveguide and a reactive diaphragm is shown. The resonator Q is low.
- 621.372.413 2356
The Use of Lossy Material to Suppress Unwanted Modes in Cavity Resonators—M. Y. El-Ibiary and J. Brown. (*Proc. IEE*, Part C, vol. 104, pp. 25-34; March, 1957.) A ring of lossy material in a groove at the junction between an end wall and the cylindrical wall does not affect the H_{01n} mode but may suppress others. Analysis is given and confirmed by measurements.
- 621.372.413:621.318.134 2357
An Exact Solution for a Cylindrical Cavity containing a Gyromagnetic Material—H. E. Bussey and L. A. Steinert. (*Proc. IRE*, vol. 45, pp. 693-694; May, 1957.)
- 621.372.5 2358
The Equivalent Transmission Line of a Linear Four-Terminal Network. Calculations with Cascade-Connected Four-Terminal Networks—C. G. Aurell. (*Ericsson Tech.*, vol. 12, pp. 107-145; 1956.) The transmission-line analogy is applied to nonsymmetrical and nonreciprocal quadripoles (see also 2861 of 1955). Different formulas are derived without the use of exponential or hyperbolic functions. Steady state conditions are assumed.
- 621.372.5 2359
Synthesis of Transmission Systems in Terms of Tandem-Connected Quadripoles—P. W. Seymour and S. Døssing. (*Proc. IEE*, Part C, vol. 104, pp. 62-80; March, 1957.)
- Theoretically derived formulas aid the rapid solution of some practical transmission problems.
- 621.372.5:621.376.3:621.3.018.78 2360
Frequency-Modulation Distortion in Linear Networks—A. S. Gladwin; R. F. Brown. (*Proc. IEE*, Part B, vol. 104, p. 264; May, 1957.) Comment on 1581 of 1957 and author's reply.
- 621.372.512 2361
A Method for the Approximate Determination of the Impulse Response of a Number of Identical Circuits in Cascade—K. F. Sander. (*Proc. IEE*, Part C, vol. 104, pp. 13-24; March, 1957.) The method of steepest descents is used to obtain approximate analytical expressions for various values of time. These are tested against two networks for which exact solution is possible.
- 621.372.54 2362
Outline of a Generalized Filter Theory—E. Henze. (*Arch. elekt. Übertragung*, vol. 10, pp. 541-551; December, 1956.) This treatment of ideal linear filters by the use of function-space techniques is based on the work of Zadeh and Miller (2147 of 1952). Examples of practical applications are briefly discussed.
- 621.372.54 2363
New Types of Sections for Zig-Zag Filters—T. Laurent. (*Ericsson Tech.*, vol. 12, pp. 147-164; 1956.) Continuation of an earlier paper (83 of 1954). Zig-zig and zag-zag sections, in which both attenuation peaks lie above or below the pass band, respectively, instead of having a peak on either side of the band, are derived and their application is discussed.
- 621.372.54 2364
Practical Methods of Formulating the Hurwitz Polynomial in Filter Synthesis—F. Bauhuber. (*Nachrichtentech. Z.*, vol. 9, pp. 573-580; December, 1956.) The application of several methods [see, e.g., 3679 of 1955 (Bauer)] is discussed and a new direct iteration method is described with numerical examples. Twenty-one references.
- 621.372.54 2365
Quartz Crystal Filters with Sharp Cut-Off and Large Bandwidth in Branch Networks—W. Poschenrieder. (*Nachrichtentech. Z.*, vol. 9, pp. 561-565; December, 1956.) Ladder-type networks of improved efficiency and an example of their application at about 100 kc are briefly described.
- 621.372.54 2366
Tables of Frequency Transformation and Band-Pass Filters—H. Weber and J. Martony. (*Tech. Mitt. schweiz. Telegr.-Teleph. Verw.*, vol. 34, pp. 499-502; December 1, 1956. In French and German.) The tables are based on Laurent's theory of combined impedance and frequency transformation (see 723 of 1957). The characteristics and design parameters of band-pass filter half-sections are tabulated.
- 621.372.543.2 2367
Figure of Merit of Band-Pass Filters with a Tchebycheff Characteristic—J. Lenkowski. (*Arch. Electrotech.*, vol. 5, pp. 365-373; 1956. English summary, pp. 375-377.)
- 621.372.543.2 2368
Filter Circuits with Two Coupled Resonators for Wide Relative Pass Bands—F. Carassa. (*Alla Frequenza*, vol. 25, pp. 451-481; December, 1956.) The amplitude and phase characteristics of double-tuned filters are examined for the case where the pass band width is great relative to the mid-frequency.
- 621.372.543.2 2369
A Survey of the Design of Lossy Filters using the Insertion-Loss Method with Special
- Reference to "Zig-Zag" Band-Pass Filters**—C. Kurth. (*Frequenz*, vol. 10, pp. 391-396; December, 1956; vol. 11, pp. 12-19, 43-53; January/February, 1957.)
- 621.372.543.2 2370
Design of Three-Resonator Dissipative Band-Pass Filters having Minimum Insertion Loss—J. J. Taub and B. F. Bogner. (*Proc. IRE*, vol. 45, pp. 681-687; May, 1957.) Universal design curves are given.
- 621.373:621.316.729 2371
Theory of Synchronization of Nonsinusoidal Oscillations—I. I. Minakova and K. F. Teodorovich. (*Radiotekhnika i Elektronika*, vol. 1, pp. 1317-1324; October, 1956.)
- 621.373.029.42 2372
A Two-Phase Low-Frequency Oscillator: Part 1—E. F. Good. (*Electronic Eng.*, vol. 29, pp. 164-169; April, 1957.) Two series-connected integrating circuits with over-all feedback give oscillations of stable amplitude and low harmonic content. Two outputs are available with 90° phase difference.
- 621.373.029.62/63 2373
Generation of Electromagnetic Oscillations by means of a Travelling-Wave Valve with a Twin-Helix Coaxial Line—V. S. Mikhalevski, A. G. Dolganov, and V. D. Ivanova. (*Radiotekhnika i Elektronika*, vol. 1, pp. 1383-1393; November, 1956.) An experimental verification of theoretical results (2336 above) is reported. Results indicate that the theory may be used for approximate calculations.
- 621.373.029.64:538.569.4 2374
Maser Oscillators—Helmer. (See 2431.)
- 621.373.421:621.376.3 2375
Frequency-Modulated Quartz Oscillators for Broadcasting Equipment—W. S. Mortley. (*Proc. IEE*, Part B, vol. 104, pp. 239-249; May, 1957. Discussion pp. 249-253.) "An fm system is described which employs a directly-frequency-modulated quartz-crystal oscillator, the design of the circuit and of the crystal plate being treated in some detail."
- 621.373.43 2376
Nonsinusoidal Oscillations. Investigation of Continuous Solutions—L. Sideriades. (*C.R. Acad. Sci., Paris*, vol. 244, pp. 1330-1333; March 4, 1957.) Experimental verification of analysis outlined in 1369 of 1957.
- 621.373.43 2377
Controllable Relaxation Oscillator using a Glow Discharge Tube—S. V. Svechnikov. (*Avtomatika i Telemekhanika*, vol. 17, pp. 1029-1034; November, 1956.) A simple neon-lamp relaxation oscillator with a linear relation between the output frequency and the input voltage is described. In the particular case considered a CdS photoresistor control element was used.
- 621.373.43 2378
A Square-Wave Converter with Feedback Control of Mark-to-Space Ratio—J. B. Earnshaw. (*Electronic Eng.*, vol. 29, pp. 170-173; April, 1957.) Operates with sinusoidal, sawtooth, or triangular input waveforms.
- 621.373.431.2 2379
The Blocking Oscillator—(*Wireless World*, vol. 63, pp. 285-289; June, 1957.) An analysis of the operation of this type of circuit.
- 621.373.431.2 2380
Millimicrosecond Blocking Oscillators—J. M. Smith. (*Electronic Eng.*, vol. 29, pp. 184-186; April, 1957.) A circuit designed to deliver pulses up to 200-v amplitude to a low-impedance load such as a coaxial cable.
- 621.373.444:621.314.7 2381
Investigation of Transient Processes in a

- Point-Contact Semiconductor-Triode Trigger Circuit and the Forming of Pulses from a Sinusoidal Voltage**—V. A. Kuz'min. (*Radiotekhnika i Elektronika*, vol. 1, pp. 1406-1412; November, 1956.) The transistor switching circuit previously considered by Lebov and Baker (2592 of 1954) is further analyzed. A method is presented of calculating the leading edge of the output pulses and part of the trailing edge corresponding to the transition of the circuit through the active region under the action of a negative voltage jump. The forming of pulses, using a sinusoidal input voltage, is considered and results of an experimental verification of the theory are briefly reported.
- 621.373.444.1:621.397.621** 2382
C.R.T. Deflection Circuit has High Efficiency—W. B. Guggi. (*Electronics*, vol. 30, pp. 172-175; April 1, 1957.) A transistor time-base generator for magnetic deflection. A technique of switching the paths followed by circulating currents reduces power consumption to one third.
- 621.373.52** 2383
Junction-Transistor Bootstrap Linear-Sweep Circuits—K. P. P. Nambiar and A. R. Boothroyd. (*Proc. IEE*, Part B, vol. 104, pp. 293-306; May, 1957. Discussion, pp. 333-336.) The principles are discussed and analyzed. A basic circuit employing two $p-n-p$ junction transistors is given, and improvement of linearity by feedback is considered. Monostable and astable forms, and a blocking-oscillator comparator for precision timing, are given. Sweep amplitudes are small, but larger values should be possible using existing transistors, with sweep durations $< 1 \mu s$.
- 621.373.52:621.376.3** 2384
Semiconductor-Triode High-Frequency RC Oscillator—L. N. Kaptsov. (*Radiotekhnika i Elektronika*, vol. 1, pp. 1413-1418; November, 1956.) Analysis is presented of a circuit generating almost harmonic oscillations at frequencies of the order of the critical frequency. Experimental results indicate the feasibility of frequency modulating the oscillations.
- 621.374.32** 2385
A Decade Pulse Counting System with Circulating Storage in a Delay Line—D. Maeder. (*Helv. Phys. Acta*, vol. 29, pp. 459-462; In German.) Brief description of equipment which uses a Ni-wire delay line; the display is in the form of a raster on a cr tube screen.
- 621.374.33:531.76** 2386
Gate Tube Generates Interleaved Pulse Chain—D. Kushner. (*Electronics*, vol. 30, pp. 186-187; April 1, 1957.) A Type-6BN6 gated beam tube is employed to generate spaced pulses by means of ringing circuits at the anode and second grid.
- 621.375.012** 2387
An Extension of the Noise-Figure Definition—H. A. Haus and R. B. Adler. (*Proc. IRE*, vol. 45, pp. 690-691; May, 1957.) An extension of previous analysis (see 1956 IRE CONVENTION RECORD, part 2, pp. 53-67). A new concept, the exchangeable power of a source, is suggested to overcome difficulties which arise in the use of the notion of available power when negative resistance is involved.
- 621.375.121.2:621.396.621.22** 2388
Distributed Amplifiers as Antenna Multipliers—E. T. Pfund, Jr. (*Electronics*, vol. 30, pp. 176-179; April 1, 1957.) Describes tests of a Telefunken equipment employing push-pull distributed amplifiers to feed up to six receivers from one antenna. This principle gives less intermodulation than conventional systems.
- 621.375.132:621.396.822** 2389
Noise in Negative Feedback Amplifiers—C. N. W. Litting. (*Electronic Radio Eng.*, vol. 34, pp. 219-223; June, 1957.) The improvement in signal/noise ratio obtained by the use of feedback is discussed and the conditions under which it is most effective are deduced.
- 621.375.2:621.3.018.78** 2390
Grid-Circuit Distortion—E. Watkinson. (*Electronic Radio Eng.*, vol. 34, pp. 207-214; June, 1957.) The effects of control-grid currents between 10^{-6} and 10^{-9} A are analyzed. It is shown that recommended operating conditions may lead to grid-circuit distortion comparable with that produced in the anode circuit.
- 621.375.2:621.317.733** 2391
Intermodulation in Bridge Detector Amplifiers—G. J. Johnson and A. M. Thompson. (*Proc. IEE*, Part C, vol. 104, pp. 217-221; March, 1957.) A discussion of the effects of intermodulation and methods for its reduction, with special reference to a practical amplifier for use at 1 and 1.6 kc.
- 621.375.4.018.7** 2392
Nonlinear Distortion in Transistor Amplifiers at Low Signal Levels and Low Frequencies—N. I. Meyer. (*Proc. IEE*, Part C, vol. 104, pp. 208-216; March, 1957.) An analytical method is presented for calculating the nonlinear distortion of sinusoidal signals in the input and output circuits. A considerable reduction of the output distortion at low frequencies in the simple common-emitter amplifier can be obtained by arranging that the input and output distortions cancel each other. The expressions derived have been verified experimentally.
- 621.375.4.029.5** 2393
Voltage Amplification of Point-Contact Semiconductor Triodes in Tuned Amplifiers—E. F. Vorob'eva. (*Radiotekhnika i Elektronika*, vol. 1, pp. 1394-1405; November, 1956.) The amplification factor of the grounded-base tuned amplifier at frequencies up to $1.5f_a$ is expressed by $K = SR_n$, where R_n is the collector load impedance at resonance and S is a parameter calculated in terms of the I_f parameters of the transistor and f_a . Curves are given for calculating the amplification at frequencies up to $1.5f_a$ with various feedback and collector load factors. The experimental verification on four transistors shows fair agreement with calculations.

GENERAL PHYSICS

- 53** 2394
Replacement of a Nonstationary Random Process by a Stationary Process—V. I. Tikhonov. (*Zh. Tekh. Fiz.*, vol. 26, pp. 2057-2059; September, 1956.) The nonstationary random process $\eta(t) = A\xi(t) \sin(\omega t + \phi)$, where $\xi(t)$ is a stationary random process is considered. Expressions are given for the correlation function for $\eta(t)$, using a) statistical means and b) a mean over a period ξ/ω . The conditions in which b) can be used and their physical meaning are discussed. Application to fluctuations in a tube oscillator is considered.
- 530.1** 2395
On a Solution of Field Equations in Einstein's Unified Field Theory: Part 1—N. N. Ghosh. (*Progr. Theor. Phys.*, vol. 16, pp. 421-428; November, 1956.)
- 530.145.6:538.566** 2396
Multiple Scattering by Quantum-Mechanical Systems—K. M. Watson. (*Phys. Rev.*, vol. 105, pp. 1388-1398; February 15, 1957.) In addition to a general treatment of the problem, specific calculations are made of the refractive index of a medium which is "polarized" by the scattered particle and also of a medium which has correlated structure.
- 531.3:621.396.822** 2397
Influence of Non-normal Fluctuations on Linear Systems—V. I. Tikhonov and A. A. Tolkachev. (*Bull. Acad. Sci. U.R.S.S., Tech. Sci.*, no. 12; pp. 48-56; December, 1956. In Russian.) The influence of fluctuations is considered, the characteristics of which do not appreciably differ from a normal (e.g., Rayleigh-type) characteristic.
- 533.7:537.56** 2398
A Relativistic Form of Boltzmann's Transport Equation in the Absence of Collisions—P. C. Clemmow and A. J. Willson. (*Proc. Camb. Phil. Soc.*, vol. 53, pp. 222-225; January, 1957.)
- 534.01** 2399
On an Error in the Theoretical Analysis of Ferroresonance Phenomena at a Frequency Equal to One Third of the Frequency of the Applied Force—A. N. Valkhrameev. (*Zh. Tekh. Fiz.*, vol. 26, p. 1862; August, 1956.) Comment on paper by Hayashi (2953 of 1953).
- 534.01+538.56]:517.9** 2400
On the Short-Wave Asymptotic Theory of the Wave Equation ($\nabla^2 + k^2$) $\phi = 0$ —F. Ursell. (*Proc. Camb. Phil. Soc.*, vol. 53, pp. 115-133; January, 1957.) "The present work appears to be the first practical and rigorous solution of a short-wave problem in optics or acoustics when a solution in closed form is not available. It is suggested that the technique (suitably combined with formal expansions) may be applicable to a wider class of radiation and diffraction problems."
- 535.215+537.533** 2401
On the Additivity of Photo-emission and Secondary-Electron Emission of Metals—L. I. Ekertova. (*Zh. Tekh. Fiz.*, vol. 26, pp. 1665-1668; August, 1956.) Contrary to the assertion of a number of authors that the two effects are nonadditive, it is shown theoretically, as well as experimentally, that this is not the case.
- 535.222** 2402
A New Effort to Measure the Velocity of Light—R. Gerharz. (*J. Electronics*, vol. 2, pp. 416-424; March, 1957.) A preliminary report is given of apparatus being developed to measure the group velocity of light pulses originating from the dynodes of an electron-multiplier as visible fluorescent radiation.
- 535.223:621.372.413** 2403
Accuracy of a Microwave Resonant-Cavity Measurement of the Velocity of Light—D. H. Janney. (*Phys. Rev.*, vol. 105, pp. 1138-1140; February 15, 1957.) Unless the surface reactance and resistance of the cavity are known, the uncertainty of the measurement is limited to a value greater than 2 parts in 10^6 .
- 535.34:535.37** 2404
Universal Relation between the Absorption and Luminescence Spectra of Complex Molecules—B. I. Stepanov. (*C.R. Acad. Sci. U.R.S.S.*, vol. 112, pp. 839-841; February 11, 1957. In Russian.)
- 535.376** 2405
Build-Up of Electroluminescent Brightness—C. H. Haake. (*J. Appl. Phys.*, vol. 28, pp. 245-250; February, 1957.) This build-up is compared with that of photoluminescence under various conditions affecting the electron population in traps. A qualitative exploration is proposed for the mechanism.
- 537.2/3:621.3.013** 2406
The Approximate Solution of Electric-Field Problems with the Aid of Curvilinear Nets—L. Tasny-Tschiasny. (*Proc. IEE*, Part C, vol. 104, pp. 116-129; March, 1957.)

- 537.31 2407
The Length of the Free Path of an Electron in Liquid and Amorphous Conductors [and semiconductors]—A. I. Gubanov. (*Zh. Tekh. Fiz.*, vol. 26, pp. 1651-1656; August, 1956.) The free path of an electron is determined taking into account the scattering of electrons at defects of the quasi-crystalline structure and the effect of thermal oscillations.
- 537.311 2408
Oscillographic Determination of the Energy of the Electric Explosion of Wires—I. F. Kvartskhava, V. V. Bondarenko, A. A. Plyutto, and A. A. Chernov. (*Zh. Eksp. Teor. Fiz.*, vol. 31, pp. 745-751; November, 1956.) An oscillographic method is described. Results indicate that at high voltages the resistance of the wire is not determined uniquely by the magnitude of the energy introduced.
- 537.311.1 2409
Transport Processes in Conductors taking into account Nonlinear Effects—V. P. Shabanski. (*Zh. Eksp. Teor. Fiz.*, vol. 31, pp. 657-671; October, 1956.) Relaxation processes in the electron-lattice system are analyzed and equations are obtained for the heating of the electron gas in strong electric fields. The kinetic equations are solved for particular cases and galvanomagnetic and thermoelectric phenomena are discussed. The theory is applicable to semiconductors in the region of conduction electron degeneracy.
- 537.311.1:536.3:621.396.822 2410
Thermal Fluctuations in Conductors—N. L. Balazs. (*Phys. Rev.*, vol. 105, pp. 896-899; February 1, 1957.) The spectrum of current fluctuations is derived for a conductor in thermal equilibrium with the surrounding radiation field, in terms of the conductor's absorptive power. For low frequencies the result reduces to Nyquist's relation, but for high frequencies the fluctuations are proportional to the skin resistance and depend on the shape of the conductor.
- 537.311.31 2411
On the Connection between Electrical Resistivity and Potential Energy in Pure Metals—G. Borelius. (*Ark. Fys.*, vol. 11, pp. 291-294; 1956.) Results suggest that the zero-point energy, which at zero temperature makes no contribution to the resistivity, at higher temperatures co-operates with the thermal potential energy to maintain the lattice disturbances causing resistivity.
- 537.312.8:538.632 2412
The Interdependence and Independence of Galvanomagnetism and of Magnetothermoelectricity—A. Perrier. (*Helv. Phys. Acta*, vol. 29, pp. 419-423; December 15, 1956. In French.) The relation between Hall and Nernst-Ettingshausen effects is discussed.
- 537.52 2413
The Demonstration of Single Electron Avalanches and their Secondary Processes in Gases—J. K. Vogel and H. Raether. (*Z. Phys.*, vol. 147, pp. 141-147; December 15, 1956.) A method of obtaining voltage oscillograms of electron avalanches in pure gases is described. The need for adding vapor is eliminated by using high pressure and an electrode gap of 2 cm. Typical results are illustrated and discussed.
- 537.533.7:621.384.612 2414
On the Relativistic Motion of Electrons in Magnetic Fields when Quantum Effects are taken into Account—A. Sokolov. (*Nuovo Cim.*, vol. 3, supplement no. 4, pp. 743-759; In English.) Summary of theoretical results with 35 references, mainly to Russian authors.
- 537.533.71 2415
Reflection of Plane-Polarized, Electromagnetic Radiation from an Echelette Diffraction Grating—W. C. Meecham and C. W. Peters. (*J. Appl. Phys.*, vol. 28, pp. 216-217; February, 1957.)
- 537.534.8 2416
Theory of the Reflection of Positive Ions at Metal Surfaces—O. v. Ross. (*Z. Phys.*, vol. 147, pp. 184-209, December 15, 1956.) The theory developed yields results which are in satisfactory agreement with experiments on Mo surfaces described by Brunnée (2517 below).
- 537.534.8 2417
Theory of the Kinetic Emission of Secondary Electrons Released by Positive Ions—O. v. Ross. (*Z. Phys.*, vol. 147, pp. 210-227; December 15, 1956.) See also 2416 above, and for experimental verification 2517 below.
- 537.56:538.56 2418
Oscillations of Electron Plasma in a Magnetic Field—A. G. Sitenko and K. N. Stepanov. (*Zh. Eksp. Teor. Fiz.*, vol. 31, pp. 642-651; October, 1956.) Plasma oscillations at frequencies which are multiples of the gyrofrequency are considered on the basis of kinetic theory. The refractive indices for the ordinary, extraordinary, and plasma waves propagated at an angle θ to the magnetic field are calculated. At the frequencies considered, the plasma wave is strongly attenuated at $\theta < \pi/2$; at $\theta \approx \pi/2$ these plasma waves cannot be propagated.
- 537.56:538.566 2419
Note on Waves in a Homogeneous Magnetically Active Plasma—B. N. Gershman. (*Zh. Eksp. Teor. Fiz.*, vol. 31, pp. 707-709; October, 1956. Note on papers by Piddington (e.g., 91 and 753 of 1956).)
- 537.56:538.63 2420
Development of a General Solution for Boltzmann's Transport Equation in the Presence of an Electric and Magnetic Field—R. Jancel and T. Kahan. (*C.R. Acad. Sci., Paris*, vol. 244, pp. 1333-1336; March 4, 1957.) The general equation derived covers results previously obtained by these and other authors (see e.g., 1318 of 1955).
- 538.221 2421
On the Magnetic Interaction in a System of Doublets—G. Karpman. (*C.R. Acad. Sci., Paris*, vol. 244, pp. 1336-1339; March 4, 1957.) The interaction energy is equivalent to that postulated by Herring and Kittel in their spin-wave theory (*Phys. Rev.*, vol. 81, pp. 869-880; March, 1951) for a ferromagnetic medium.
- 538.3 2422
Nonlinear Field Theory—K. Bechert. (*Z. Naturf.*, vol. 11a, pp. 177-182; March, 1956.) New formulation of the electrodynamic theory previously developed (see 84 of 1956 and back references).
- 538.3:521 2423
Theory of Magnetohydrodynamic Waves—E. Richter. (*Z. Naturf.*, vol. 11a, p. 251; March, 1956.) Brief note on applications to astrophysical problems.
- 538.566+534.2 2424
General Theorems on the Equivalence of Group Velocity and Energy Transport—M. A. Biot. (*Phys. Rev.*, vol. 105, pp. 1129-1137; February 15, 1957.) It is shown that under very general conditions there is a rigorous identity between the group velocity and the velocity of energy transport in nonhomogeneous media, with or without anomalous dispersion.
- 538.566:535.42 2425
The Diffraction of an Electromagnetic Wave by a Circular Aperture—R. F. Millar. (*Proc. IEE*, Part C, vol. 104, pp. 87-95; March, 1957.) The diffraction theory previously developed (2366 of 1956) is used to calculate interaction effects in a plane, perfectly conducting screen, by asymptotic evaluation of the first-order aperture field.
- 538.566.029.6 2426
Methods of Microwave Optics—K. Bochenek and J. Plebański. (*Arch. Elektrotech.*, vol. 5, pp. 293-322; 1956. English summary, pp. 322-323.) Two approximation methods developed on the basis of geometrical optics are proposed for the treatment of em fields. In the first method a solution of the wave equation is sought in the form $u = A \exp(ik_0 L)$. The expression $[1 + (1/k_0^2)(\Delta A/A)]^\dagger$ stands for an effective coefficient of refraction and can be determined to a high accuracy. This interpretation is analogous to the quantum mechanical interpretation of Bohm (*Phys. Rev.*, vol. 85, pp. 166-193; January 15, 1952). The boundary-value problem for the wave equation is transformed into a Cauchy problem for the set of equations for the successive terms of the expansion of A and L in k_0^{-1} . The second method takes the Wentzel-Krammer-Brillouin approximation as a starting point. Both methods are illustrated by examples.
- 538.569.4:538.221 2427
Dependence of the Ferromagnetic Resonance Line Width on the Shape of the Specimen—A. D. Berk. (*J. Appl. Phys.*, vol. 28, pp. 190-192; February, 1957.) A discussion of the relation between the line width and the damping term in the equation of motion of the magnetization.
- 538.569.4:538.221:539.23 2428
Ferromagnetic Resonance Absorption by Thin Conducting Films in Cavities—J. O. Artman. (*J. Appl. Phys.*, vol. 28, p. 277; February, 1957.) Two cases are briefly considered corresponding to film deposited on a metal and a dielectric substratum, respectively.
- 538.569.4:538.222 2429
Some Problems of Paramagnetic Resonance—S. A. Al'tsuler (Al'tshuler) and B. M. Kozyrev. (*Nuovo Cim.*, vol. 3, supplement no. 4, pp. 614-628; 1956. In English.) Brief survey and discussion of acoustic paramagnetic resonance and paramagnetic resonance in iron-group salt solutions. Fifty-two references, mainly to Russian authors.
- 538.569.4:539.152.1:621.317.4 2430
Proton Resonance and the Measurement of Magnetic Fields—(*Electronic Radio Eng.*, vol. 34, pp. 215-218; June, 1957.)
- 538.569.4:621.373.029.64 2431
Maser Oscillators—J. C. Helmer. (*J. Appl. Phys.*, vol. 28, pp. 212-215; February, 1957.) The experimental behavior of one maser under various operating conditions has been observed, using a second maser as a reference standard. Results are compared with theory obtained from a new analysis including the velocity distribution in the beam. See also 100 of 1955 (Gordon, et al.).
- 539.15:538.56 2432
Generalized Theory of Relaxation—F. Bloch. (*Phys. Rev.*, vol. 105, pp. 1206-1222; February 15, 1957.) A further generalization of an earlier theory (*ibid.*, vol. 89, pp. 728-739; February 15, 1953 (Wangness and Bloch)), the energy of the spin system now being freed from restrictions.
- 539.15:548.0 2433
Interaction of an Electron Hole with Lattice Oscillations in a Homopolar Crystal—K. B. Tolpygo and A. M. Fedorchenko. (*Zh. Eksp. Teor. Fiz.*, vol. 31, pp. 845-853; November, 1956.) The motion of a hole in a diamond-type

homopolar crystal is considered on the basis of the multi-electron Schrödinger equation.

- 621.3.081.5 2434
Differences of Opinion about Dimensions—R. O. Kapp. (*Proc. IEE*, Part B, vol. 104, pp. 198–204; May, 1957. Discussion, pp. 205–209.) An exposition of the views of different schools.

GEOPHYSICAL AND EXTRA-TERRESTRIAL PHENOMENA

- 523.16:621.396.822 2435
Discrete Sources of Cosmic Radio Noise at 18.3 and 10.5 Mc/s—G. R. Ellis and G. Newstead. (*J. Atmos. Terr. Phys.*, vol. 10, pp. 185–193; 1957.) Six discrete sources were observed at 18.3 mc and 10.05 mc using similar interferometers with a 7λ base-line. Four of these sources have been observed at 100 mc by other workers, enabling noise flux densities in the range 10–100 mc to be compared. It appears that two of the sources show noise peaks at 20 mc, while the remaining two peak near 10 mc.
- 523.746:538.56.029.63 2436
Observation of Polarization of Radio Wave Emission from Sunspots at a Wavelength of 3.2 cm.—N. L. Kaidanovskii, D. V. Korol'kov, N. S. Soboleva, and S. E. Kliaikin. (*C. R. Acad. Sci. U.R.S.S.*, vol. 112, pp. 1012–1015; February 21, 1957. In Russian.)
- 523.752 2437
The Nature of a Type of Radio Emission associated with certain Eruptions from the Chromosphere—A. Boisshot. (*C. R. Acad. Sci., Paris*, vol. 244, pp. 1326–1329; March 4, 1957.) Report on observations at a frequency of 169 mc by means of the interferometer at Nançay [see also 3644 of 1956 (Blum, Boisshot, and Ginat)].
- 550.384 2438
Linear Secular Oscillation of the Northern Magnetic Pole—E. R. Hope. (*J. Geophys. Res.*, vol. 62, pp. 19–27; March, 1957.) "Modern data seem to support the thesis (van Bemmelen, 1899) that the secular motion of the northern magnetic pole is a nearly linear oscillation. This oscillation is along the axis of a great magnetic anomaly in the arctic. Except for the constraint of the anomaly, the motion would probably be circular or quasi-circular, as suggested by the historical declination-dip curves."
- 550.384 2439
Rotation, Pulse-Disturbance, and Drift in the Geomagnetic Secular Variation—E. R. Hope. (*J. Geophys. Res.*, vol. 62, pp. 29–42; March, 1957.) A strong pulse disturbance which occurred between 1880 and 1920 in the relative rotation of the terrestrial core, and, therefore, in the westward drift of surface geomagnetic patterns, is shown to affect the 480-year rotation in a manner which helps to clarify the relations.
- 550.385 2440
On Sudden Commencements of Magnetic Storms at Higher Latitudes—S. Matsushita. (*J. Geophys. Res.*, vol. 62, pp. 162–166; March, 1957.) Forty-four sudden commencements are described; in 21 a small negative impulse preceded the main positive impulse in the horizontal field, in 14 a positive impulse preceded a negative impulse, while in nine the normal low-latitude single-impulse type was observed.
- 550.385 2441
Comparison between the Ionized-Cloud Theory of Chapman and Ferraro and the Recording of the Start of a Magnetic Storm—J. L. Bureau. (*C. R. Acad. Sci., Paris*, vol. 244, pp. 1396–1398; March 4, 1957.) Brief analysis of the sudden commencement of a magnetic storm on October 21, 1952 recorded in French West Africa.
- 551.51 2442
Upper Air Pressure and Density Measurements from 90 to 220 Kilometers with the Viking 7 Rocket—R. Horowitz and H. E. LaGow. (*J. Geophys. Res.*, vol. 62, pp. 47–78; March, 1957.) The approximate ratios of "Viking 7" measurements to corresponding "Rocket Panel" values (*Phys. Rev.*, vol. 88, pp. 1027–1932; December 1, 1952) were: pressure at 90 to 105 km, one quarter; pressure at 220 km, two; densities at 120 to 185 km, one quarter to one half; density at 220 km, one; derived scale height above 140 km, two.
- 551.510.535 2443
The Ionospheric F₂ Layer over Ahmedabad, Delhi and Tiruchirapalli during the Sunspot Minimum Period (1953–54)—K. M. Kotadia. (*J. Sci. Industr. Res.*, vol. 15A, pp. 543–550; December, 1956.)
- 551.510.535:523.74 2444
The Electron Density in the F₂ Layer and its Correlation with the Solar Activity—F. Mariani. (*J. Atmos. Terr. Phys.*, vol. 10, pp. 239–242; 1957.) The minimum electron density is shown to be a function not only of sunspot number R, but also of the areas of hydrogen filaments and flocculi, A_f and A_φ. The relative contribution of these quantities is different for the F₂ layer in the northern and southern geomagnetic hemispheres.
- 551.510.535:523.78 2445
Ionospheric Changes at Singapore during the Solar Eclipse of 20 June 1955—C. M. Minnis. (*J. Atmos. Terr. Phys.*, vol. 10, pp. 229–236; 1957.) From vertical-incidence measurements on the eclipse and control days, it is deduced that there was a bright source of ionizing radiation in the sun's southern hemisphere probably associated with an observed group of sunspots. An F_{1.6} layer appeared during the eclipse, indicating a rearrangement of electrons in the lower part of the F₂ layer.
- 551.510.535:550.385:523.16 2446
The Correlation of Radio-Star-Scintillation Phenomena with Geomagnetic Disturbances and the Mechanism of Motion of the Ionospheric Irregularities in the F Region—M. Dagg. (*J. Atmos. Terr. Phys.*, vol. 10, pp. 194–203; 1957.) F-region drift velocities and the magnitude of variations in the earth's magnetic field are closely correlated, while occasional correlation also exists between scintillation amplitude and magnetic variations. These results are shown to agree with Martyn's theory, ascribing F-region phenomena to the interaction of the earth's magnetic field with an electric field communicated from the dynamo region.
- 551.510.535:550.523.16 2447
Diurnal Variations of Radio-Star Scintillations, Spread F, and Geomagnetic Activity—M. Dagg. (*J. Atmos. Terr. Phys.*, vol. 10, pp. 204–214; 1957.) Scintillation measurements of the radio-star in Cassiopeia for the period August, 1954–July, 1955 are compared month by month with the occurrence of spread F at Inverness and with K indices at Lerwick or Eskdalemuir.
- 551.510.535:621.396.11 2448
Geographical Distribution in High Latitudes of the Anomalous Absorption of Radio Waves in the Ionosphere—A. P. Nikol'ski. (*C. R. Acad. Sci. U.R.S.S.*, vol. 112, pp. 628–631; February 1, 1957. In Russian.) Discussion based on data from North American ionospheric observatories and Kiruna, Tromsø, Reykjavik, Spitzbergen, and Bukhta Tikhaya.
- 551.510.535:621.396.11.029.45 2449
Calculations of Ionospheric Reflection
- Coefficients at Very Low Radio Frequencies**—J. R. Wait and L. B. Perry. (*J. Geophys. Res.*, vol. 62, pp. 43–56; March, 1957.) "A set of calculated curves are presented for the reflection coefficients at a sharply-bounded homogeneous ionized medium with a superimposed magnetic field. The results are plotted parametrically to permit general comparisons with experimental data. Both steady-state and transient cases are considered."
- 551.594.5:621.396.11.029.62 2450
The Frequency Dependence of Radio Reflections from Aurora—P. A. Forsyth and E. L. Vogan. (*J. Atmos. Terr. Phys.*, vol. 10, pp. 215–228; 1957.) It is concluded that within small regions of the aurora the ionization is often sufficient to cause complete reflection at four frequencies in the range 30–50 mc over a distance of 860 km. Absorption may contribute significantly to observed frequency dependence.
- 551.594.6 2451
Some Statistical Properties of Atmospherics—Ya. I. Likhter. (*Radiotekhnika i Elektronika*, vol. 1, pp. 1295–1302; October, 1956.) An experimental determination of the amplitude probability distribution is reported; a block diagram of the apparatus and the simplified circuit-diagram of a ten-channel statistical analyzer are shown. Results of measurements at 50 kc (bandwidth 750 cps) indicate that the probability distribution function is given approximately by the relation $P(V) = (1-c) \exp(-aV^2) + c \exp(-bV^2)$, where a , b , and c are constants.

LOCATION AND AIDS TO NAVIGATION

- 621.396.9 2452
The Expected Error of a Least-Squares Solution of Location from Direction-Finding Equipment—B. Harkin. (*Aust. J. Appl. Sci.*, vol. 7, pp. 263–272; December, 1956.) "Formulas are derived for the error variances and covariances of the coordinate components of an unweighted least-squares solution for the location of a missile simultaneously reported by a number of optical or electronic direction-finding stations. Practical applications of the formulas are suggested."
- 621.396.932 2453
An Investigation of the Sensitivity of the Direction Finder Telegon III with and without Rectification—K. Baur. (*Telefunken Ztg.*, vol. 29, pp. 288–290; December, 1956. English summary, pp. 295–196.) In the direction-finder Telegon III [see also 1455 of 1957 (Troost)] signal strength is indicated by a vertical trace on a "magic-eye" crt. Three methods of applying the signal to the indicator, one direct and two using rectification, are compared to determine their merits regarding the indication of low-signal levels. Results are inconclusive.
- 621.396.96:621.396.934 2454
Subminiature Beacon for Guided Missiles—M. Cohen and D. Arany. (*Electronics*, vol. 30, pp. 144–147; April 1, 1957.) A transponder for installation in a missile to assist radar tracking. The transponder, which uses transistors, also provides an audio command channel to the missile.
- 621.396.969.3:538.569.4.029.6 2455
Investigation of Radar Absorption Materials—A. Giger and F. Tank. (*Schweiz. Arch. angew. Wiss. Tech.*, vol. 22, pp. 414–416; December, 1956.) Brief discussion of theory of centimeter-wave absorption by dissipative dielectric layers on a conductive metallic base. Reflection-coefficient/depth-of-coating curves are given for an iron-dust material for 3 and 10 cm λ and theoretical curves are given for materials with typical dielectric constants and loss tangents.

MATERIALS AND SUBSIDIARY TECHNIQUES

- 535.215:546.482.21 2456
The Properties of Cadmium Sulphide Photoresistors Irradiated with γ and β Rays—S. V. Svechnikov. (*Zh. Tekh. Fiz.*, vol. 26, pp. 1646–1650; August, 1956.) The voltage current characteristics of the photoresistors and the build-up and decay of photocurrent characteristics were determined. Results are presented graphically.
- 535.215:546.817.231 2457
Photoconductivity in Lead Selenide: Theory of the Dependence of Sensitivity on Film Thickness and Absorption Coefficients—J. N. Humphrey and R. L. Petritz. (*Phys. Rev.*, vol. 105, pp. 1192–1197; February 14, 1957.) The wavelength-dependence of the absorption-coefficient of a photoconductor calculated from the photoconductive spectral response of thin films, is consistent with that predicted from the theory of indirect main-band transitions.
- 535.215:546.863.221:621.397.331.2 2458
Semiconductor Photosensitive Layers for Photoresistance Television Tubes—Ya. A. Oksman. (*Radiotekhnika i Elektronika*, vol. 1, pp. 1340–1343; October, 1956.) The experimental determination of the characteristics of Sb_2S_3 layers for use in vidicon-type tubes is described and results are presented graphically.
- 535.215.2:[546.817.221+546.56.231] 2459
External Photoeffect in Lead Sulphide and Copper Selenide—P. S. Popov. (*Radiotekhnika i Elektronika*, vol. 1, pp. 1334–1339; October, 1956.) Measurements on stable PbS and CuSe photocathodes gave the following results: cut-off wavelength (2919 ± 10) Å and ($2950 + 10$) Å for two PbS specimens, and (3172 ± 10) Å for CuSe; contact potential difference to Au in high vacuum: 0.350 v and 0.470 v for PbS and CuSe, respectively. PbS specimens with different energy gaps δ between the filled zone and the Fermi level had equal thermionic work functions. The width of the forbidden zone, ΔE , calculated from the results of measurements, was 0.30 eV and 0.39 eV for the two specimens of PbS, respectively; these values agree with that predicted by Bell, *et al.* (2037 of 1953). Results of measurements are presented graphically.
- 535.215.2:546.863.36 2460
Some Results of an Investigation of the Energy Distribution of Photoelectrons from an Antimony-Cesium Cathode—N. M. Politova. (*Radiotekhnika i Elektronika*, vol. 1, pp. 1325–1333; October, 1956.) The photoelectric work function of Cs_3Sb , determined from measurements of the red-threshold wavelength of the photoeffect was found to be greater than ϕ_F , the work function determined from retardation potential measurements. ϕ_F is only slightly greater than the thermionic work function and its value increases with $h\nu$. These results are discussed.
- 535.37 2461
Impurity-Activated Crystalline Phosphors: their Production and Thermoluminescence Curves—A. Wizesinska. (*Acta Phys. Polon.*, vol. 15, pp. 151–162; 1956. In English.)
- 535.37 2462
Tungstate-Silicate Mixed Phosphors—H. Witzmann and W. Plamann. (*Naturwiss.*, vol. 43, p. 580; December, 1956.) Brief preliminary report of investigations on the luminescence of the following systems activated by ultraviolet light: a) $CaWO_4-CaSiO_3$; b) $CaWO_4-CaSiO_3$; (Mn, Pb); c) $ZnWO_4-ZnO-Zn_2SiO_4$; (Mn).
- 535.37 2463
Luminescence of Potassium Iodide—K. J. Teegarden. (*Phys. Rev.*, vol. 105, pp. 1222–1227; February 15, 1957.) The excitation and emission spectra are presented.
- 535.37:538.569.4 2464
Paramagnetic Resonance Spectrum of Manganese in Cubic MgO and CaF_2 —W. Low. (*Phys. Rev.*, vol. 105, pp. 793–800; February 1, 1957.) Experimental results at 1.2 and 3.3 cm λ .
- 535.37:538.569.4 2465
Paramagnetic Resonance and Optical Absorption Spectra of Cr^{3+} in MgO —W. Low. (*Phys. Rev.*, vol. 105, pp. 801–805; February 1, 1957.)
- 535.376 2466
Aging Characteristics of Electroluminescent Phosphors—S. Roberts. (*J. Appl. Phys.*, vol. 28, pp. 262–265; February, 1957.) A discussion of the decay of brightness with time, and of the rate of aging with varying voltage and frequency.
- 535.376 2467
Low-Field Electroluminescence in Insulating Crystals of Cadmium Sulphide—R. W. Smith. (*Phys. Rev.*, vol. 105, pp. 900–904; February 1, 1957.) Report of measurements of green electroluminescence obtained with field strength about 1 kv/cm at the emitting centers. The associated abrupt increase of current through the crystal is attributed to the injection of free carriers from the electrodes.
- 535.376:537.311.33:546.26-1 2468
Electroluminescence of Semiconducting Diamonds—R. Wolfe and J. Woods. (*Phys. Rev.*, vol. 105, pp. 921–922; February 1, 1957.) Light, whose spectrum consists of a single broad band centered at 4400 Å, is emitted in the vicinity of a negatively biased point-contact electrode. Voltage and frequency characteristics of the phenomenon are described.
- 537.226+537.311.33 2469
Dipole Moments of Dielectric and Semiconductor Particles—D. V. Kuz'min. (*Zh. Tekh. Fiz.*, vol. 26, pp. 1880–1883; September, 1956.) Dipole moments of solid particles with various permittivities and conductivities are calculated both for constant and for alternating electric fields.
- 537.226/.227:546.431.824-31 2470
Neutron Diffraction Study of Orthorhombic $BaTiO_3$ —G. Shirane, H. Danner, and R. Pepinsky. (*Phys. Rev.*, vol. 105, pp. 856–860; February 1, 1957.)
- 537.226/.227:546.431.824-31 2471
Symmetry of the Low-Temperature Phase of $BaTiO_3$ —F. Jona and R. Pepinsky. (*Phys. Rev.*, vol. 105, pp. 861–864; February 1, 1957.)
- 537.226/.227:546.431.824-31 2472
Electrostatic Considerations in $BaTiO_3$ Domain Formation during Polarization Reversal—R. Landauer. (*J. Appl. Phys.*, vol. 28, pp. 227–234; February, 1957.) An analysis of Merz's concept (445 of 1955) of spike-shaped domains of reversed polarization, with special consideration of the electrostatic aspects.
- 537.226/.227:546.824-31 2473
Anomalous Polarization of Polycrystalline Titanum Dioxide—N. P. Bogoroditski, I. D. Fridberg, and N. M. Tsvetkov. (*Zh. Tekh. Fiz.*, vol. 26, pp. 1890–1901; September, 1956.) An experimental investigation of the effect of Group II, III, and V oxide impurities. Results of measurements of the dielectric constant and the loss tangent at rf are tabulated and the temperature characteristics are presented graphically. A phase diagram for the Ti- TiO_2 system is also given.
- 537.226:546.87.824-31 2474
Dielectric Properties of Bismuth Titanates—G. I. Skanavi and A. I. Demeshina. (*Zh. Eksp. Teor. Fiz.*, vol. 31, pp. 565–468; October, 1956.) The properties of nonferroelectric dielectrics of composition $TiO_2:Bi_2O_3$ between 22.3:1 and 1:1 were investigated and results are tabulated and partly presented graphically. The dielectric constant at a temperature of 20°C and a frequency of 2 mc lies between 68 and 121, $\tan \delta$ between 0.0015 and 0.0054 and the temperature coefficient of ϵ between -540×10^{-6} and $+590 \times 10^{-6}$.
- 537.226:621.315.61 2475
The Aging of the Insulation of Ceramic Materials at High Temperatures—I. E. Balygin and K. S. Porovski. (*Zh. Tekh. Fiz.*, vol. 26, pp. 1714–1722; August, 1956.) Experiments are reported on the effects of aging in specimens of ultra-porcelain, radio-porcelain, steatite, and spinel at a temperature of 380°C in steady electric fields between about 0.4 and 1.3 kv/mm. For the investigation of the electrolytic processes, some of the experiments were carried out at a temperature of approximately 700°C.
- 537.226:621.315.61 2476
An Investigation into the Dielectric Polarization and Losses of Polytrifluoromonoethylene—G. P. Mikhailov and B. I. Sazhin. (*Zh. Tekh. Fiz.*, vol. 26, pp. 1723–1729; August, 1956.) The permittivity and the loss angle of the material were investigated over a frequency range from 50 to 10^7 cps and a temperature range from -100 to $+230^\circ C$. Two types of relaxation polarization were observed.
- 537.226.3 2477
Dielectric Losses in Glasses: Parts 2 & 3. N. M. Verebeichik and V. I. Odolevski. (*Zh. Tekh. Fiz.*, vol. 26, pp. 1696–1703, 1704–1713; August, 1956.) In Part 2 results are given of an experimental investigation of the electrical properties, thermal expansion, density, and refractive index of aluminosilicate sodium glasses. A theoretical interpretation of these results is given. In Part 3 the various existing theories of the "high-temperature" relaxation dielectric losses in alkali glasses are reviewed and their insufficiency is pointed out. A structural model of this type of glass is proposed and a theory is developed which explains the peculiar role which is played by aluminium atoms in these glasses. A report is also presented on an experimental investigation the results of which confirm the theory. For Part 1, see *Zh. Tekh. Fiz.*, vol. 22, pp. 12–15; January, 1952 (Verebeichik, *et al.*).
- 537.226.3 2478
Dependence of Dielectric Losses in Ceramic Materials on the Strength of the Electric Field—I. E. Balygin and A. I. Obratsov. (*Zh. Tekh. Fiz.*, vol. 26, pp. 1917–1923; September, 1956.) Experimental investigation of $\tan \delta$ of several Russian ceramic materials at a frequency of 50 cps.
- 537.226.31 2479
Nature of the Temperature Dependence of Dielectric Losses in the Polarization of Ionic Compounds—N. P. Bogoroditski and I. D. Fridberg. (*Zh. Tekh. Fiz.*, vol. 26, pp. 1884–1889; September, 1956.) The temperature dependence of $\tan \delta$ at a frequency of 1 mc was experimentally investigated in borate and silicate glasses and in several ceramic materials; results are presented graphically. The dielectric losses are probably due to phenomena of a) relaxation during polarization, b) relaxation during electrical conduction, and c) ionization (usually of the free or distributed gas in the solid); a) and b) are connected with the thermal motion of particles.
- 537.227 2480
Behaviour of Ferroelectrics in Strong Electric Fields—V. A. Bokov. (*Zh. Tekh. Fiz.*, vol. 26, pp. 1902–1911; September, 1956.) Investigation of the coefficient of nonlinear distortion K and of ϵ_1 in $Ba(Ti, Sn)O_3$, $Ba(Ti, Zr)O_3$ and $(Ba, Sr)TiO_3$ in electric fields of fre-

quency 70 cps. Maximum nonlinearity, at room temperature, was observed in Ba ($Ti_{0.9}, Sn_{0.1}O_3$) and Ba ($Ti_{0.9}, Zr_{0.1}O_3$).

537.227 2481

Causes of Formation of a Curie Region in some Ferroelectric Solid Solutions—V. A. Isupov. (*Zh. Tekh. Fiz.*, vol. 26, pp. 1912–1916; September, 1956.) The spread of Curie temperature in specimens of ferroelectric materials can largely be accounted for by fluctuations in the composition, assuming that the "Kanzig regions" decrease with an increase in nonferroelectric content.

537.3:621.315.6 2482

An Investigation of the Electrical Conductivity of Insulating Materials Prior to, During and After Irradiation—I. M. Rozman and K. G. Tsimmer. (*Zh. Tekh. Fiz.*, vol. 26, pp. 1681–1688; August, 1956.) A new and simple method based on the use of a capacitor ionization chamber is described, and results are given of measurements on pressed amber, polystyrene, polymethylmetacrylate, polythene, and polymonochlorotrifluorethylene.

537.311:536.2.08 2483

The Thermal and Electrical Conductivities of Metals at High Temperatures—M. R. Hopkins. (*Z. Phys.*, vol. 147, pp. 148–160; December 15, 1956. In English.) In the method described simultaneous measurements of electrical potential and maximum temperature are made on a short current-carrying wire; observations can be extended into the molten range.

537.311.33 2484

The Properties and Structure of Ternary Semiconductor Systems: Part 3—Conductivity and Photoconductivity of Systems based on the Sulphides of Thallium, Antimony and Bismuth—N. A. Goryunova, B. T. Kolomiets, and A. A. Mal'kova. (*Zh. Tekh. Fiz.*, vol. 26, pp. 1625–1633; August, 1956.) Experimental results show that the $xTl_2S \cdot (1-x)Sb_2S_3$ system has a very complex structure, and that within this system there exists a new ternary compound. The materials of which this system is made up are semiconductors with a photoconductivity not exceeding that of the initial binary compounds. The $xSb_2S_3 \cdot (1-x)Bi_2S_3$ system forms a series of semiconductor materials based on solid solutions of the substitution type. Materials with a considerably lower conductivity than that of the initial materials, and with the maximum of spectral sensitivity displaced towards longer waves can be obtained in this system. By introducing an excess of sulphur, materials of a considerably higher absolute sensitivity can be obtained. Part 2: 3417 of 1956 (Goryunova and Kolomiets).

537.311.33 2485

Bipolar Diffusion in Semiconductors at Heavy Currents—A. I. Gubanov and L. L. Makovski. (*Zh. Tekh. Fiz.*, vol. 26, pp. 2126–2128; September, 1956.) Comment on 1752 of 1956 (Tolpygo and Zaslavskaya) and author's reply.

537.311.33 2486

The Stability of Vertical Fusion Zones—W. Heywang. (*Z. Naturf.*, vol. 11a, pp. 238–243; March, 1956.) Mathematical treatment of the stability conditions for stationary zones [see also 1381 of 1955 (Heywang and Ziegler)]. The validity of simplifying assumptions is discussed.

537.311.33 2487

One-Dimensional Treatment of the Effective Mass in Semiconductors—I. Adawi. (*Phys. Rev.*, vol. 105, pp. 789–792; February 1, 1957.) The width of the forbidden band and the effective mass of electrons are calculated as a function of the atomic spacing and potential asymmetry, using a Kronig-Penney model of a one-dimensional semiconductor. Contrary to

the result of Seraphin (1379 of 1955), the effective mass, for a specific average potential, is found to increase monotonically with potential asymmetry.

537.311.33 2488

Hall and Drift Mobilities; their Ratio and Temperature Dependence in Semiconductors—F. J. Blatt. (*Phys. Rev.*, vol. 105, pp. 1203–1205; February 15, 1957.) It is shown that the temperature-dependence of the Hall and drift mobilities in the impurity-scattering temperature range should be less rapid than $T^{3/2}$. The conclusion is in agreement with experiment.

537.311.33:535.215 2489

Theory of Atomic Semiconductors—A. G. Samoilovich and V. M. Kondratenko. (*Zh. Eksp. Teor. Fiz.*, vol. 31, pp. 596–608; October, 1956.) Problems in the theory of absorption of light and the theory of photoconductivity are considered on the basis of the polar crystal model of Shubin and Vonsovski. *C. R. Acad. Sci. U.R.S.S.*, vol. 1, p. 449; 1934, taking into account excitons.

537.311.33:535.215 2490

The Determination of Volume- and Surface-Recombination of Charge Carriers in Semiconductors—W. Heywang and M. Zerbst. (*Z. Naturf.*, vol. 11a, pp. 256–257; March, 1956.) A photoconductivity method for determining separately the bulk lifetime and surface recombination velocity is outlined and some typical results are briefly discussed.

537.311.33:535.215 2491

Influence of Vapours and Gases on the Internal Photoeffect in Oxide Semiconductors and Sensitization by Chlorophyll—E. K. Putseiko. (*Radiotekhnika i Elektronika*, vol. 1, pp. 1364–1373; October, 1956.) The effect of oxygen, water vapor, and other gases and vapors on the photoeffect in ZnO, HgO, and PbO was investigated. In the presence of O_2 , thermal activation up to 100°C increases the photoemf of HgO and increases the sensitivity of the photo-emf of PbO to long-wave light. The sensitization of ZnO and HgO by chlorophyll and its analogs is discussed.

537.311.33:535.215:538.61 2492

Spectral Distribution of the Photomagneto-electric Effect in Semiconductors: Theory—W. Gärtner. (*Phys. Rev.*, vol. 105, pp. 823–829; February 1, 1957.) An extension of the theory of the photomagnetolectric (pme) effect to cover its dependence on the wavelength of the incident light. The pme response is shown graphically as a function of absorption coefficient, with bulk lifetime, surface recombination velocities, and slab thickness as parameters.

537.311.33:536.21.022 2493

On Thermal Conduction in Semiconductors—A. F. Ioffe. (*Nuovo Cim.*, vol. 3, supplement no. 4, pp. 702–715; 1956. In English.) Brief review and discussion of the results of recent investigations mainly by Russian authors.

537.311.33:[538.63+538.66 2494

Theory of Isothermal Galvano- and Thermo-magnetic Phenomena in Semiconductors—F. G. Bass and I. M. Tsidal'kovski. (*Zh. Eksp. Teor. Fiz.*, vol. 31, pp. 672–683; October, 1956.) The phenomena are considered theoretically for the case of magnetic fields at which $(uH/c)^2 \approx 1$ or $\gg 1$, where H is the magnetic field strength, u the mobility of charge carriers, and c the velocity of light.

537.311.33:[546.23+546.24 2495

Electronic Band Structure of Selenium and Tellurium—J. R. Reitz. (*Phys. Rev.*, vol. 105, pp. 1233–1240; February 15, 1957.) The band structure of Se and Te has been calculated according to the tight-binding scheme in which only nearest-neighbor interactions are presumed to be important.

537.311.33:546.24 2496

The Effect of Impurities and Heat Treatment on the Electrical Properties of High-Purity Tellurium—H. Kronmüller, J. Jauermann, and K. Seiler. (*Z. Naturf.*, vol. 11a, pp. 243–250; March, 1956.) The influence of small additions of As, Sb, Br, and I on the Hall effect and conductivity was investigated in the temperature range -140 to 300°C . Results are shown graphically and discussed.

537.311.33:546.28 2497

Ionization Rates for Holes and Electrons in Silicon—S. L. Miller. (*Phys. Rev.*, vol. 105, pp. 1246–1249; February 15, 1957.) "The ionization rates for holes and electrons in silicon at high electric fields have been evaluated from data on the multiplication of reverse-biased junctions. In Si, electrons have a higher ionization rate than holes. The variation of ionization rate with field strength is in good agreement with theory."

537.311.33:546.28 2498

Properties of Gold-Doped Silicon—C. B. Collins, R. O. Carlson, and C. J. Gallagher. (*Phys. Rev.*, vol. 105, pp. 1168–1173; February 15, 1957.) Measurements of the temperature-dependence of resistivity and Hall coefficient show an acceptor level at 0.54 eV from the conduction band and a donor level at 0.35 eV from the valence band. Concentrations of these levels are equal within experimental accuracy.

537.311.33:[546.28+546.289]:534.13-8 2499

Ultrasonic Attenuation in Germanium and Silicon—F. J. Blatt. (*Phys. Rev.*, vol. 105, pp. 1118–1119; February 1, 1957.) It is suggested that measurements of ultrasonic attenuation would throw light on the intervalley scattering of electrons and might permit a direct determination of the relevant coupling constant.

537.311.33:546.289 2500

Determination of Germanium in some Italian Coals—G. Leonardi and E. Mariani. (*Poste e Telecomunicazioni*, vol. 5, pp. 799–803; November/December, 1956.)

537.311.33:546.289 2501

Surface Electrical Conductivity of Germanium—V. I. Lyashenko and T. N. Sytenko. (*Zh. Eksp. Teor. Fiz.*, vol. 31, pp. 905–907; November, 1956.) Experimental results indicate the existence of surface zone conductivity in the specimens investigated.

537.311.33:546.289 2502

Energy of Ionization by Electrons in Germanium Crystals—V. S. Vavilov, L. S. Snirnov, and V. M. Patskevich. (*C. R. Acad. Sci. U.R.S.S.*, vol. 112, pp. 1020–1022; February 21, 1957. In Russian.) An experimental determination of the mean energy of ionization ϵ in Ge bombarded by 5–15-keV electron beams; results indicate that $\epsilon = 3.7 \pm 0.4$ eV in this range.

537.311.33:546.289 2503

Experimental Evidence of the Anisotropy of Hot Electrons in n-Type Germanium—V. Sasaki and M. Shibuya. (*J. Phys. Soc. Japan.*, vol. 11, pp. 1202–1203; November, 1956.) Brief note on experimental technique used and results obtained. For a statement of the problem, see 464 of 1956 (Shibuya.)

537.311.33:546.289 2504

Effect of Annealing in Various Gases on the Bulk Lifetime of Germanium—K. Weiser. (*J. Appl. Phys.*, vol. 28, pp. 271–272; February, 1957.) The lifetime was increased markedly by annealing in oxygen having a trace of water vapor. A decrease, after a period of no change, was observed for dry oxygen, wet nitrogen, helium, argon, and hydrogen.

537.311.33:546.289 2505

The Influence of Omnidirectional Pressure

- on the Drift Mobility of Holes in Germanium—G. Landwehr. (*Z. Naturf.*, vol. 11a, p. 257; March, 1956.) Brief account of measurements at pressures up to 10,000 kg/cm² at 22°C, which show that drift mobility is not affected and that the surface recombination velocity increases with pressure.
- 537.311.33:546.289 2506
Effect of Impurities on Free-Hole Infrared Absorption in p-Type Germanium—R. Newman and W. W. Tyler. (*Phys. Rev.*, vol. 105, pp. 885–886; February 1, 1957.) The spectrum structure becomes less pronounced with increasing carrier and total impurity concentration. The effects are consistent with changes in the Fermi level and with nonvertical transitions induced by charged impurity centers.
- 537.311.33:546.289 2507
K X-Ray Adsorption Spectrum of a Single Crystal of Germanium—D. G. Doran and S. T. Stephenson. (*Phys. Rev.*, vol. 105, pp. 1156–1157; February 15, 1957.)
- 537.311.33:546.289 2508
The Breakdown of p-n Junctions in Germanium by a Voltage Impulse—A. P. Shotov. (*Zh. Tekh. Fiz.*, vol. 26, pp. 1634–1645; August, 1956.) Junctions prepared by alloying indium with n-germanium and diffusing of antimony in p-germanium were investigated. The specific resistance of the initial germanium varied between 0.15 and 50 Ω·cm. The breakdown voltage was measured with 10⁻⁶–10⁻⁶-s pulses. It was established that the breakdown of all junctions investigated is caused by shock ionization. The breakdown voltage increases with temperature owing to the dependence of the ionization coefficient on temperature. For junctions prepared by alloying indium with germanium, the value of the ionization coefficient is determined.
- 537.311.33:546.289;537.533.9 2509
Formation of Crystal Lattice Defects in Germanium under Bombardment by Fast Electrons—V. S. Vavilov, L. S. Smirnov, G. N. Galkin, A. V. Spitsyn, and V. M. Patskevich. (*Zh. Tekh. Fiz.*, vol. 26, pp. 1865–1869; September, 1956.) The dependence of the defect-formation cross section on irradiation electron energy was investigated experimentally by measurement of the electrical conductivity of monocrystalline n-type Ge films bombarded with 400–1000-keV electrons. No effects were observed at energies below 500 ± 20 keV.
- 537.311.33:546.289;537.534.9 2510
Work-Function Studies of Germanium Crystals Cleaned by Ion Bombardment—J. A. Dillon, Jr., and H. E. Farnsworth. (*J. Appl. Phys.*, vol. 28, pp. 174–184; February, 1957.) Measurements of the effects of adsorption of gases, strong electric fields, and intense illumination upon the work functions of single germanium crystals are reported and discussed.
- 537.311.33:546.289;538.63 2511
Magnetoelectricity in p-Type Germanium—C. Goldberg, E. N. Adams, and R. E. Davis. (*Phys. Rev.*, vol. 105, pp. 865–876; February 1, 1957.) "Measurements of the Hall coefficient and resistivity of p-type germanium have been made as a function of magnetic field, temperature, and carrier concentration between 77°K and 300°K. An attempt is made to interpret the data quantitatively using a two-carrier model, but no completely satisfactory quantitative interpretation is possible."
- 537.311.33:546.482.21 2512
Connection between Changes in Electrical Conductivity and Redistribution of Electron Density in a Cadmium Sulphide Crystal—Yu. N. Shuvalov. (*Zh. Tekh. Fiz.*, vol. 26, pp. 1870–1879; September, 1956.) An X-ray crystallographic investigation is reported.
- 537.311.33:546.682.86 2513
Interband Magneto-optic Effects in Semiconductors—E. Burstein and G. S. Picus. (*Phys. Rev.*, vol. 105, pp. 1123–1125; February 1, 1957.) With magnetic fields as low as 15,000 oersted the absorption spectrum shows several peaks, which move to higher photon energies with increasing field. Tentative mechanisms for the absorption peaks are suggested, in terms of the energy bands as affected by the magnetic field.
- 537.311.33:546.682.86 2514
Elastoresistance Constants of p-Type InSb at 77°K—A. J. Tuzzolino. (*Phys. Rev.*, vol. 105, pp. 1411; February 15, 1957.) Report of a preliminary experiment.
- 537.311.33:546.811–17 2515
On Factors Influencing the Transformation of White Tin into Grey Tin—A. I. Bykhovski. (*Zh. Tekh. Fiz.*, vol. 26, pp. 1799–1801; August 1956.) A brief review of the literature is presented and the effect of impurities and of their redistribution during heating on the transformation of white tin into grey tin ('tin plague') is discussed.
- 537.533:[546.289+546.56+546.811] 2516
Secondary-Electron Emission of Copper, Germanium and Tin in Solid and Liquid States—V. G. Bol'shov and V. K. Seleznev. (*Zh. Tekh. Fiz.*, vol. 26, pp. 1657–1664; August, 1956.) Experimental results show that when the temperature is increased from room temperature to 232°C (in the case of tin) and to 1033°C (in the case of copper) σ_{\max} varies by not more than 1 per cent. In the case of Ge, when temperature is increased to 959°C, σ_{\max} decreases by approximately 5–6 per cent. As a result of melting σ changes abruptly in the same direction for the whole range of energies of primary electrons from 100 to 1500 eV, viz., in the case of copper σ_{\max} decreases by 5 per cent, in the case of tin and germanium it increases by 14 per cent and 9 per cent, respectively. The energy distribution of secondary electrons for solid and liquid tin has also been considered.
- 537.534.8 2517
The Ion Reflection and Secondary Electron Emission at the Impact of Alkali Ions on Clean Molybdenum Surfaces—C. Brunnee. (*Z. Phys.*, vol. 147, pp. 161–183; December 15, 1956.) Report and detailed discussion of measurements in the energy range 0.4–4 keV. Over sixty references.
- 537.534.9:[546.74+546.883] 2518
Disintegration of Tantalum and Nickel in the Form of Ions under Bombardment by Positive Caesium Ions—V. I. Veksler and J. B. Ben'yamovich. (*Zh. Tekh. Fiz.*, vol. 26, pp. 1671–1680; August, 1956.) In a mass-spectrometer investigation of the products of the secondary emission of Ta and Ni targets, positive ions of these two metals were observed in quantities greatly exceeding the theoretical values.
- 537.583:546.883 2519
Autoelectron [thermionic] Emission of Tantalum—M. I. Elinson and G. F. Vasil'ev. (*Zh. Tekh. Fiz.*, vol. 26, pp. 1669–1679; August, 1956.)
- 538 2520
Conference on the Physics of Magnetic Phenomena [Moscow, 23rd–31st May, 1956]—S. V. Vonsovski. (*Uspekhi Fiz. Nauk*, vol. 60, pp. 709–722; December, 1956.) Review of papers presented at the conference.
- 538.22 2521
Magnetic Susceptibility of Dilute Alloys of Nickel in Copper between 2.5°K and 295°K—E. W. Pugh, B. R. Coles, A. Arrott, and J. E. Goldman. (*Phys. Rev.*, vol. 105, pp. 814–818; February 1, 1957.)
- 538.221 2522
New Magnetic Anisotropy—W. H. Meiklejohn and C. P. Bean. (*Phys. Rev.*, vol. 105, pp. 904–913; February 1, 1957.) Report and discussion of measurements relating to 'exchange anisotropy' (see 3803 of 1956.)
- 538.221 2523
Effect of a Cavity on a Single-Domain Magnetic Particle—W. F. Brown, Jr. and A. H. Morrish. (*Phys. Rev.*, vol. 105, pp. 1198–1201; February 15, 1957.) A detailed investigation of the effect of internal cavities in single-domain particles on the coercive force, shows that they may account, at least in part, for the low values sometimes encountered.
- 538.221:538.245 2524
On the Statistical Nature of the Remagnetization of Ferromagnetics—F. V. Bunkin. (*Zh. Tekh. Fiz.*, vol. 26, pp. 1782–1789; August, 1956.) A mathematical investigation of the phenomenon is presented, on the assumption that all domains have an equal probability of remagnetization during each cycle of the field variation. It is shown that the probability of the transitions of a domain into a new state at a given value of the magnetizing field is proportional to the rate of the increase in the magnetization of the specimen at this value of the field. Formulas are also derived for determining the scatter of transition instants.
- 538.221:538.245 2525
Noise due to the Cyclic Remagnetization of Ferromagnetics—F. V. Bunkin. (*Zh. Tekh. Fiz.*, vol. 26, pp. 1790–1798; August, 1956.) A general expression is derived for the spectral intensity of the induction emf during the cyclic remagnetization of a ferroelectric specimen. The signal/noise ratio in transformers is also determined.
- 538.221:546.74–3 2526
Crystal Structure of Ferromagnetic Nickel Oxide—Y. Shimoura, M. Kojima, and S. Saito. (*J. Phys. Soc. Japan*, vol. 11, pp. 1136–1146; November, 1956.)
- 538.221:621.318.12 2527
Structure and Magnetic Properties of Permanent-Magnet Alloys during Isothermal Precipitation Hardening: Part 2—The Process of Segregation and the Interpretation of Magnetic Behaviour—E. Biedermann and E. Kneller. (*Z. Metallkunde*, vol. 47, pp. 760–774; December, 1956.) Further analysis of investigations made on Cu-Ni-Fe and Cu-Ni-Co alloys. Part 1: 202 of 1957.
- 538.221:621.318.134 2528
Formation of Manganese Ferrite by Solid-State Reaction—H. H. Kedesdy and A. Tauber. (*J. Amer. Ceram. Soc.*, vol. 39, pp. 425–431; December, 1956.) The effect of four different firing cycles on the formation of the ferrite is investigated, and the magnetic properties are compared for toroidal specimens subjected to three different forms of heat treatment.
- 538.221:621.318.134 2529
Low Loss Magnesium Manganese Ferrites—L. C. F. Blackman. (*J. Electronics*, vol. 2, pp. 451–456; March, 1957.) These are prepared by thermal decomposition of mixed nitrates. The normalized energy-loss-factor for the Q band is 0.04 ± 0.02 db.
- 538.221:621.318.134:538.566 2530
Effects of Zero Ferrite Permeability on Circularly Polarized Waves—B. J. Duncan and L. Swern. (*Proc. IRE*, vol. 45, pp. 647–655; May, 1957.) If the imaginary part of the effective permeability of a ferrite is negligible, the ferrite can be made to exhibit zero permeability to a wave with positive sense of circular polariza-

tion. The application of this to a rod placed axially in a circular waveguide propagating the TE_{11} circularly-polarized mode is examined theoretically and experimentally. It is shown that the ferrite can be made to expel practically all microwave energy from its interior, and this behavior can be used to obtain large nonreciprocal attenuations.

538.221:621.318.134:538.6 2531

Microwave Frequency Doubling from 9 to 18 kMc/s in Ferrites—J. L. Melchor, W. P. Ayers, and P. H. Vartanian. (*Proc. IRE*, vol. 45, pp. 643-646; May, 1957.) The theory of the process is given and it is found experimentally that conversion efficiency depends markedly on the geometry of the ferrite; efficiencies as high as -6 db have been observed. See also 2138 of 1956 (Ayles, *et al.*)

438.632:539.23:546.87 2532

The Hall Effect in Thin Bismuth Films—A. Colombani and P. Huet. (*C. R. Acad. Sci., Paris*, vol. 244, pp. 1344-1347; March 4, 1957.) Experimental results are given in graphical form for fields up to 34,300 oersted and thicknesses between 60 and 6000 Å. See also 2225 and 2226 of 1957.

538.652:546.74 2533

Theory of Magnetostriction of Single Crystals of Nickel—W. F. Brown, Jr. and N. S. Akulov. (*C. R. Acad. Sci. U.R.S.S.*, vol. 112, pp. 827-839; February, 11, 1957. In Russian.) Comment on 2143 of 1956 comparing the theory with Heisenberg's theory of magnetostriction, and author's reply.

548.5:537.228.1 2534

Properties of Synthetic Quartz Oscillator Crystals—C. S. Brown and L. A. Thomas. (*Proc. IRE*, Part C, vol. 104, pp. 174-184; March, 1957.) A process for the growing of well formed crystals weighing about 135 g is described. The crystals possess electrical and mechanical properties which closely resemble those of the natural Brazilian quartz. Comparative measurements on oscillator crystals cut from natural and synthetic quartz are also described.

621.315.6 2535

The Electrical Properties and Structure of Silicone Polymers—K. A. Andrianov and G. E. Golubkov. (*Zh. Tekh. Fiz.*, vol. 26, pp. 1689-1695; August, 1956.) The electrical properties of polydimethylsiloxanes and polydiethylsiloxanes were studied at various temperatures and frequencies, as well as the variation of their thermal properties in the process of cooling and heating.

621.318.134:621.318.424 2536

Ferrite Thermomagnets—L. I. Rabkin and B. Sh. Epshtein. (*Radiotekhnika i Elektronika*, vol. 1, pp. 1357-1363; October, 1956.) Temperature-sensitive ferrite core materials suitable for temperature compensation of inductors are described.

621.79:621.3.049.001.4 2537

Leakage Testing of Sealed Electronic Enclosures—D. C. Bedwell and E. A. Meyer. (*Elec. Mfg.*, vol. 56, pp. 127-133; December, 1955.) Methods of testing electronic components suitable for airborne applications are reviewed, and an evaluation of the qualities of various types of seals based on a series of tests is given in tabular form.

MATHEMATICS

512.3:621.372 2538

An Elimination Technique for Certain Impedance Equations—C. D. Allen. (*Electronic Eng.*, vol. 29, pp. 187-188; April, 1957.) "A set of linear simultaneous equations of a type which frequently arises in the analysis of linear networks is considered. A short method of per-

forming the elimination necessary to obtain the impedance equations of the network is proved."

512.831:621.372 2539

Some Matrix Theorems—W. Proctor Wilson. (*Electronic Radio Eng.*, vol. 34, pp. 229-231; June, 1957.) A theorem relating to the n th power of a matrix and another having particular relevance in the study of tapered networks are included.

517 2540

Limiting Properties of Mathieu Functions—M. A. Jaswon. (*Proc. Camb. Phil. Soc.*, vol. 53, pp. 111-114; January, 1957.) A new analysis is made of the coefficients appearing in periodic Mathieu functions and this is applied to establish the limiting properties of certain solutions of the equation $r(d/dr)[r(d/dr)y - (a + \alpha^2 r^2 + \beta^2 r^{-2})y] = 0$, where a , α , and β are parameters.

517.512.2 2541

The Closed-Form Summation of some Common Fourier Series—C. C. Chao. (*Quart. J. Mech. Appl. Math.*, vol. 9, pp. 508-512; December, 1956.) "A method is presented for the summation in closed form of Fourier series whose coefficients are ratios of polynomials of certain types frequently encountered in practice. The result is obtained as the solution of a linear differential equation with constant coefficients, which can be solved by elementary methods."

MEASUREMENTS AND TEST GEARS

531.76:621.372.632 2542

Millimicrosecond Time Analyser—C. Cottini and E. Gatti. (*Nuovo Cim.*, vol. 4, pp. 1550-1557; December 1, 1956. In English.) A fuller account is given of the arrangement for measurement of time intervals discussed by Cottini, *et al.* (219 of 1957).

621.3.087 2543

A Method of Measuring Integrated Values with Very High Time Constants—G. Bartels and R. Steinert. (*Nachr.-Tech.*, vol. 6, pp. 500-502; November, 1956.) The application is briefly discussed of a high-resistance tube-voltmeter circuit using electrometer or 'inverted' tubes for recording average values of variables with time constants up to several hours. A circuit for usw fields strength measurements with a time constant of 900 s is shown together with a typical record made by it.

621.317.3:621.314.63 2544

Dynamic Methods of Testing Semiconductor Rectifier Elements and Power Diodes: Part 1—A. H. B. Waiker and R. G. Martin. (*Electronic Eng.*, vol. 29, pp. 150-157; April, 1957.) In full dynamic tests the forward and reverse characteristics of the diode are measured simultaneously. The forward voltage is measured by a low-range voltmeter unaffected by the reverse half cycle, and the reverse current by an ammeter of substantially zero impedance, unaffected by the forward current. The design and performance of negative-feedback amplifiers which provide these characteristics are fully described.

621.317.3.029.6 2545

Single-Oscillator Microwave Measuring System—D. H. Ring. (*Bell Lab. Rec.*, vol. 34, pp. 465-468; December, 1956.) A simplified version of the continuous waveguide phase-shifter described by Fox (1255 of 1948) is used to obtain a 2°-phase shift for each degree of rotation of the motor-driven middle section. By passing a microwave signal through the waveguide and rotating the section at, e.g., 4500 rpm a frequency change of ± 150 cps is obtained so that measurements can be made at the IF of 150 cps. The advantages of the conventional two-oscillator circuit are thus com-

bined with the stability of the single-oscillator system.

621.317.3/.41/.029.64:621.318.134 2546

New Method of Measuring the Parameters of Magnetized Ferrites at Centimetre Wavelengths—V. N. Vasil'ev. (*Radiotekhnika i Elektronika*, vol. 1, pp. 1444-1460; November, 1956.) The ferrite specimen in the form of a lamina is placed along the axis of a rectangular resonator; using H_{210} and H_{310} modes and varying the direction of the steady magnetic field in a specified way, the resulting changes of the resonance frequency and the Q of the resonator will be functions of only one or two parameters of the ferrite. The required formulas are given. The method is suitable for the 0.8-20-cm- λ range. Results of measurements at 3 cm λ are presented graphically.

621.317.328:621.396.822 2547

Logarithmic Amplifier measures Noise—J. D. Wells. (*Electronics*, vol. 30, pp. 169-171; April 1, 1957.) An equipment for recording atmospheric noise level is described in which the logarithm of the voltage equalled or exceeded for 50 per cent of the time is determined.

621.317.33+[621.317.39:531.71 2548

Regenerative Measuring Pickups—L. L. Dekabrun. (*Avtomatika i Telemekhanika*, vol. 17, pp. 1114-1122; December, 1956.) Analysis is presented of devices for measuring rf conductivity or linear displacement by means of the damping effect on a tuned circuit.

621.317.334:621.362 2549

Inductance-Type Thermocouple Tester—P. R. Morris. (*Instrum. & Automation*, vol. 29, pp. 2217-2219; November, 1956.) A battery-operated inductance bridge and 1.5-mc oscillator are used to detect short-circuits, four or more inches from the hot junction of a 5-foot thermocouple.

621.317.335.3.029.64:537.226.2 2550

Waveguide Method of Measuring the Dielectric Properties of Materials at Elevated Temperatures—V. I. Aksenov and M. Ya. Borodin. (*Radiotekhnika i Elektronika*, vol. 1, pp. 1435-1443; November, 1956.) Application of the short-circuit and open-circuit waveguide methods of determining the dielectric properties of materials at a wavelength of 3.2 cm and temperatures of 20-200°C is discussed. Formulas are given for calculating ϵ' and ϵ'' and the results of determinations of ϵ' and $\tan \delta$ of some high molecular-weight materials are tabulated and presented graphically.

621.317.36:621.385.029.6 2551

The Measurement of Magnetron Frequency Pulling—Twisleton. (See 2645.)

621.317.38.029.6 2552

Hall Effect and its Counterpart, Radiation Pressure, in Microwave Power Measurement—H. E. M. Barlow. (*Proc. IEE*, Part C, vol. 104, pp. 35-42; March, 1957.) Theory shows the close link between high-frequency Hall effect and radiation pressure. It predicts an equivalent Hall emf in a dielectric and offers a possible new approach in exploration of properties of dielectrics. Aspects of applications for microwave power measurement are discussed.

621.317.729.1 2553

A New Form of Electrolytic Tank—K. F. Sander and V. G. Yates. (*Proc. IEE*, Part C, vol. 104, pp. 81-86; March, 1957.) Measurements with capillary probes in a plane defined by an insulating surface eliminate meniscus effects with probes in a free surface.

621.317.733:621.375.2 2554

Intermodulation in Bridge Detector Amplifiers—Johnson and Thompson. (See 2391.)

621.317.755:621.397.001.4:535.623 2555
The Vectorscope—Parker Smith and Matley. (See 2602.)

621.317.784.029.64 2556
An Absolute Microwave Wattmeter—A. Macpherson. (PROC. IRE, vol. 45, pp. 688-689; May, 1957.) The wattmeter is of the calorimetric type and versions for X band and K band use are described. The estimated least detectable power is about 0.1 w at K band and 0.01 w at X-band frequencies.

OTHER APPLICATIONS OF RADIO AND ELECTRONICS

621.384.6 2557
Theory of Betatron Oscillations of Particles in Magnetic Field Systems—A. A. Kolomenski. (Zh. Tekh. Fiz., vol. 26, pp. 1969-1990; September, 1956.)

621.384.612 2558
Synchrotron Oscillations in Strong-Focusing Accelerators: Part 1—Linear Theory—L. L. Gol'din and D. G. Koshkarev. (Zh. Eksp. Teor. Fiz., vol. 31, pp. 803-814; November, 1956.)

621.384.613 2559
Stereo-betatron—V. A. Moskalev. (Zh. Tekh. Fiz., vol. 26, pp. 2060-2061; September, 1956.) Brief note with a section drawing of a 10-nev stereo-betatron for flaw detection in materials.

621.384.622.2 2560
A Theoretical and Experimental Investigation of Anisotropic-Dielectric-Loaded Linear Electron Accelerators—R. B. R. Shersby-Harvie, L. B. Mullett, W. Walkinshaw, J. S. Bell, and B. G. Loach. (Proc. IEE, Part B, vol. 104, pp. 273-290; May, 1957. Discussion, pp. 290-292.) The theory of waveguides loaded with closely-spaced dielectric disks is given, and the shunt loss is derived. Advantages over the conventional corrugated waveguides are discussed. Details of practical construction and measurements using titanium-oxide disks are given; excess attenuation at high rf power probably being due to deposits of carbon from the oil-diffusion pumps, the use of mercury pumps is suggested. Forty references.

621.385.833 2561
The Treatment of the Transition Regions by the Parabola Method and Similar Computation Techniques—P. Schiske. (Optik, Stuttgart, vol. 13, pp. 529-536; December, 1956.) Methods of approximating the third-order electron trajectories in electrostatic systems are compared and discussed.

621.385.833 2562
The Electron-Microscope Transmission Factor of Thin Films—W. Lippert. (Optik, Stuttgart, vol. 13, pp. 506-515; November, 1956.)

621.385.833 2563
The Lower Limit of the Aperture Error in Magnetic Electron Lenses—W. Tretner. (Optik, Stuttgart, vol. 13, pp. 516-519; November, 1956.) Addition to earlier work (236 of 1955 and 539 of 1956.)

621.385.833:535.317.3 2564
The Lower Limit of the Chromatic Aberration of Magnetic Lenses for a Given Maximum Field Strength—P. Schiske. (Optik, Stuttgart, vol. 13, pp. 502-505; November, 1956.)

621.385.833:537.533.73 2565
The Treatment of Electron-Optical Aberrations by Diffraction Theory—J. Picht. (Optik, Stuttgart, vol. 13, pp. 494-501; November, 1956.)

PROPAGATION OF WAVES

538.566 2566
Reflection of Waves by an Isotropic Inhomogeneous Layer—A. G. Zharkovski and O. M. Todes. (Zh. Eksp. Teor. Fiz., vol. 31, pp. 815-818; November, 1956.) An approximate method of calculating the reflection coefficient of an isotropic inhomogeneous layer for a plane wave is developed for media whose permittivity and permeability are functions of a single space coordinate.

538.566:537.56 2567
On the Interaction of Electromagnetic Waves with Charged Particles and on the Oscillations of the Electronic Plasma—A. Ahiezer (Akhiezer). (Nuovo Cim., vol. 3, supplement no. 4, pp. 591-613; 1956. In English.) Survey of theoretical work in this field with thirty-four references, mainly to Russian authors.

538.566:537.56 2568
A Property of the Field of an Electromagnetic Wave Propagated in an Inhomogeneous Plasma—N. G. Denisov. (Zh. Eksp. Teor. Fiz., vol. 31, pp. 609-619; October, 1956.) The growth of the field in the region where the plasma permittivity tends to zero is investigated theoretically. The influence of absorption is clarified. The connection between field growth and plasma resonance is established.

621.396.11 2569
Radio Propagation over a Discontinuity in the Earth's Electrical Properties: Part 1.—T. B. A. Senior. (Proc. IEE, Part C, vol. 104, pp. 43-53; March, 1957.) A method avoiding the analytical complications of rigorous theory is developed using known results for diffraction at a straight edge. Solutions reveal all the important features of mixed-path propagation and are suitable for numerical application.

621.396.11 2570
Radio Propagation over a Discontinuity in the Earth's Electrical Properties: Part 2—Coastal Refraction—T. B. A. Senior. (Proc. IEE, Part C, vol. 104, pp. 139-147; March, 1957.) By adopting a model for the coastal region, analysis of Part 1 (2569 above) provides expressions for the angle of refraction appropriate to various positions of a transmitter and receiver relative to the coast.

621.396.11:550.372 2571
Influence of a Ridge on the Low-Frequency Ground Wave—J. R. Wait and A. Murphy. (J. Res. Nat. Bur. Stand., vol. 58, pp. 1-5; January, 1957.) "The problem of a plane wave incident on a semielliptical boss on an otherwise perfectly conducting flat ground plane is considered. A solution in terms of elliptic wave functions is obtained. Numerical values of the field on the near and far side of this idealized ridge are given for a base width of about two-thirds of a wavelength and various ellipticity ratios."

621.396.11:551.510.52 2572
Scatter-Field Strengths and Large-Ion Concentration—S. C. Coroniti and N. C. Gerson. (J. Atmos. Terr. Phys., vol. 10, pp. 237-239; 1957.) The authors suggest that the concentration of large ions may be more sensitive than refractive index as an indicator of the more basic atmospheric parameters which influence forward-scatter signal strength.

621.396.11:551.510.535 2573
Doppler Effect in Ionospheric Propagation—S. Borowski, S. Jasiński, and S. Mańczarski. (Arch. Elektrotech., vol. 5, pp. 343-351; 1956. English summary, pp. 352-353.) A mathematical analysis of the general problem and an analysis of experimental evidence is presented. A formula expressing the frequency variation due to motion of the ionosphere is derived on

the basis of geometrical optics; calculations made using this formula predict a small frequency change only. The formula applies at frequencies not too near the muf where the ionosphere behaves like a selective low-pass filter, for waves returning to the earth, with constantly changing filter parameters. The returning signal is analyzed. The treatment presented provides an explanation of the correlation between the Doppler effect and the variability of the angle of arrival of ionospheric waves.

621.396.11.029.4:551.510.535 2574
Multiple Reflections between the Earth and the Ionosphere in V.L.F. Propagation—J. R. Wait and A. Murphy. (Geofis. Pura Appl., vol. 35, pp. 61-72, September-December, 1956. In English.) The ionosphere is treated as a sharply bounded ionized medium and, using geometrical-optical methods, reflection coefficients are calculated for very low-radio frequencies. The amplitudes and phase delays of the sky waves are derived, and the computed field-strength/distance curves for 16 kc are compared with experimental values for an all-sea path.

621.396.11.029.62 2575
Long-Distance Propagation at 94.35 Mc/s over the North Sea—R. A. Rowden and J. W. Stark. (Proc. IEE, Part B, vol. 194, pp. 210-212; May, 1957.) Measurements over long sea paths suggest that higher field strengths are reached for a given percentage of the over-all time than for overland paths.

621.396.11.029.62:551.510.535 2576
Radio-Frequency and Scattering-Angle Dependence of Ionospheric Scatter Propagation at V.H.F.—A. D. Wheelon. (J. Geophys. Res., vol. 62, pp. 93-112; March, 1957.) "The weak and fluctuating radio signals observed at distances of 1500 km on uhf are attributed to scattering from E-region turbulence. It is noted that propagation constants $k = 4\pi/\lambda \sin(\theta/2)$, corresponding to the experimental frequencies (28 to 108 mc), just straddle the viscosity cut-off wave-number $k_c = (2 \text{ meters})^{-1}$ of the region: thereby giving a qualitative explanation for the curious dichotomy found in the experimental data. The two competitive turbulence theories are then developed in detail near the viscosity transition range." It is concluded that both theories explain recent experimental results quite well, and that therefore more precise, simultaneous measurements will be required.

621.396.11.029.63:523.5 2577
Meteor Echoes at Ultra High Frequencies—W. A. Flood. (J. Geophys. Res., vol. 62, pp. 79-91; March, 1957.) "It is proposed that, at ultra-high frequencies, underdense meteor echoes have an effective scattering length L , which is much less than a Fresnel zone. Consequently, uhf meteoric echoes may be analyzed in terms of Fraunhofer diffraction theory, resulting in a relaxation of the requirement that a meteor trail be perpendicular to the radar line-of-sight before an echo can be received. Formulas for the back-scattered power, time duration, and echo rate are deduced."

RECEPTION

621.396.621:621.3.018.41 2578
The Effect on a Radio Receiver of an Input Voltage with an Instantaneous Frequency with Sawtooth Variation—P. Poincelot. (Ann. Télécommun., vol. 11, pp. 262-266; December, 1956.) The input voltage is expressed as a Fourier integral and a numerical example is given to show that erroneous results will arise from the incorrect application of the concept of instantaneous frequency. See also 2908 of 1953.

- 621.396.621:621.314.7 2579
Tetrajunction Transistor Simplifies Receiver Design—R. J. Farber, A. Proudfit, K. M. St. John, and C. R. Wilhelmson. (*Electronics*, vol. 30, pp. 148-151; April 1, 1957.) "Dual-triode transistor, with emitter of one unit and collector of the other section of same germanium region, provides performance of two triode units with considerable reduction of circuit components when compared to two individual units. Superheterodyne receiver in which first four stages are replaced with two tetrajunction units is described."
- 621.396.621:621.376.33 2580
Limiters and Discriminators for F. M. Receivers: Part 4—G. G. Johnstone. (*Wireless World*, vol. 63, pp. 275-280; June, 1957.) The operating principles and practical design of the gated beam discriminator, the synchronizer, and the counter circuit are described. Part 3: 2277 of 1957.
- 621.396.621:621.376.33 2581
Methods of Compensating Quasi-static and Dynamic Distortions in the I.F. Section of F.M. Receivers—E. G. Woschini. (*Nachr. Tech.*, vol. 6, pp. 488-491; November, 1956.) Brief outline of possibilities of eliminating nonlinear distortion by appropriate filter design.
- 621.396.621.22:621.375.121.2 2582
Distributed Amplifiers as Antenna Multi-couplers—Pfund, Jr. (See 2388.)
- 621.396.621.59 2583
Reception of Pulse Trains of Arbitrary Shape by a Superregenerator—L. R. Yavich. (*Radiotekhnika i Elektronika*, vol. 1, pp. 1419-1427; November, 1956.) Theory.
- 621.396.621.59 2584
Analysis of Superregenerator Circuit with Quenching causing Frequency Modulation—F. Wiñiewski. (*Arch. Elektrotech.*, vol. 5, pp. 263-289; 1956. English summary, pp. 290-292.)
- 621.396.8 2585
The Effect of Fading on Communication Circuits Subject to Interference—M. E. Bond and H. F. Meyer. (*Proc. IRE*, vol. 45, pp. 636-642; May, 1957.) The statistical performance of such circuits is analyzed for the cases where either the desired or undesired signal or both are subject to Rayleigh fading over the propagation path and the improvement which dual diversity reception offers is discussed.
- 621.396.812.029.62 2586
Observations of Long-Distance Reception in the 3-m Broadcast Band—L. Klinker. (*Hochfreq. und. Elektroak.*, vol. 65, pp. 77-86; November, 1956.) Analysis of field-strength measurements for eight transmission paths of 100 to 500 km length made at Kühlungsborn since 1951 [see also 248 and 538 of 1955 (Lauter and Klinker)] confirms the validity of the CCIR curves for the Central European area. Diurnal field-strength variations have a mean amplitude of 10 db in summer, and seasonal propagation changes are only noticeable for a sea path with slight improvement during early summer. Fading range, day-by-day changes, and the mean amplitude of diurnal variations reach a maximum for about 200 km path length; day-by-day changes are greatest in winter.
- 621.396.812.3 2587
The Effect of the Correlation between the Received Field Strengths and Diversity Reception—K. H. Schmelovsky. (*Hochfreq. und Elektroak.*, vol. 65, pp. 74-76; November, 1956.) A formula is derived for calculating approximately the probability that the field strengths at two spaced antennas will drop simultaneously below a given value in cases of low to medium correlation between the two signals.
- 621.396.822 2588
The Influence of Threshold Action on the R.M.S. Value of Input Gaussian Noise—R. D. Teasdale and A. H. Benner. (*Proc. IRE*, vol. 45, p. 697; May, 1957.)
- 621.396.822:621.317.328 2589
Logarithmic Amplifier measures Noise—Wells. (See 2547.)
- STATIONS AND COMMUNICATION SYSTEMS**
- 621.376.3:621.3.018.78:621.372.5 2590
Frequency-Modulation Distortion in Linear Networks—A. S. Gladwin; R. F. Brown. (*Proc. IEE*, Part B, vol. 104, p. 264; May, 1957.) Comment on 1581 of 1957 and author's reply.
- 621.396.3 2591
Binary Data Transmission Techniques for Linear Systems—M. L. Doelz, E. T. Heald, and D. L. Martin. (*Proc. IRE*, vol. 45, pp. 656-661; May, 1957.) Problems associated with utilizing fully the binary data transmission potential of an ssb voice channel, including stability of the propagation media and multipath reception, are discussed. Equipment designed to transmit 3000 bits/second is described.
- 621.396.3 2592
The Frequency [of occurrence] of Errors in Al- and Fl-Telegraphy Transmission Systems, particularly in the Presence of White Noise—H. Beger. (*Telefunken Ztg.*, vol. 29, pp. 245-255; December, 1956. English summary, p. 294.) Report of investigations carried out to compare the performance of on-off and frequency-shift keying systems. Tests were made on teleprinter systems to determine the influence of transmission bandwidth, modulation index, and limiting level. For transmissions at constant level with white-noise interference both methods of modulation are almost equivalent. The importance of maintaining the optimum limiting level to minimize errors is shown during fading this is only possible for F1 operation. Stability and accurate alignment of transmitter and receiver are necessary to secure the maximum advantage of the F1 system.
- 621.396.71.029.55(43) 2593
Modern High-Power Transmitting Stations for the Short-Wave Overseas Service—A. Heilmann. (*Telefunken Ztg.*, vol. 29, pp. 225-236; December, 1956. English summary pp. 292-283.) A survey with details of the telegraphy transmitter of the German Post Office near Frankfurt (Main).
- 621.396.712:621.376.3 2594
The B.B.C. Sound Broadcasting Service on Very High Frequencies—E. W. Hayes and H. Page. (*Proc. IEE*, Part B, vol. 104, pp. 213-224; May, 1957. Discussion, pp. 249-253.) This paper describes the developments leading to the inauguration of BBC sound broadcasting in the band 87.5-100 mc. The need for the use of vhf and the choice of frequency modulation are explained. By 1958, 96 per cent of the population of Great Britain and Ireland will be covered by this service. The experience of the first year's operation is described, with special reference to the performance of commercial receivers.
- 621.396.712.029.55 2595
New Short-Wave Transmitters for Single-Sideband Telephony—W. Burkhardtmaier. (*Telefunken Ztg.*, vol. 29, pp. 236-244; December, 1956. English summary, p. 293.) Description and some design and test data of the 20/100-kw transmitters for the 3.3-26.4-mc frequency range installed at Usingen by the West-German Post Office.
- 621.396.73:621.396.6 2596
Superregenerative Transistor Transceiver—W. F. Chow. (*Electronics*, vol. 30, pp. 180-182; April 1, 1957.) The transceiver which employs three transistors uses a tetrode transistor as a 52-mc oscillator for transmission and as a 'forced quench' superregenerative detector for reception. The range of communication is $\frac{1}{2}$ mile.
- 621.396.933 2597
Aircraft Radiophone speeds Communications—B. R. Rashkow. (*Electronics*, vol. 30, pp. 164-168; April 1, 1957.) The increase of transoceanic air traffic has necessitated the replacement of w/t by r/t. The article discusses the operational, equipment, and propagation problems involved.
- SUBSIDIARY TECHNIQUES**
- 621-52 2598
The Describing-Function Analysis of a Nonlinear Servomechanism Subjected to Stochastic Signals and Noise—P. N. Nikiforuk and J. C. West. (*Proc. IEE*, Part C, vol. 104, pp. 193-203; March, 1957.) A method is given for evaluating the response of a specific type of nonlinear mechanism to random signals, and to sinusoidal and random signals contaminated by noise.
- 621.314.5:621.373.52 2599
Design Considerations of Junction-Transistor Oscillators for the Conversion of Power from Direct to Alternating Current—F. Oakes. (*Proc. IEE*, Part B, vol. 104, pp. 307-317; May, 1957. Discussion, pp. 333-336.) Basic principles and graphical methods of design are given. The design of a Class-B oscillator is described in detail and illustrated by means of a practical numerical example. Calculated data agreed well with practical measurements.
- 621.316.726:621.376.3 2600
A New Control Element for Automatic Frequency Retuning—A. Karaminkov. (*Nachr. Tech.*, vol. 6, pp. 497-500; November, 1956.) The device described performs the function of reactance tube and motor in automatic tuning control equipment for usw fm transmitters or receivers. It consists of a suitably damped moving-coil instrument assembly, without control springs, which drives the vane of an air capacitor. The frequency stability is claimed to be of the order of 1 part in 10⁶.
- TELEVISION AND PHOTOTELEGRAPHY**
- 621.397:621.39.001.11 2601
Bandwidth Compression of a Television Signal—G. G. Gouriet. (*Proc. IEE*, Part B, vol. 104, pp. 265-272; May, 1957.) "Two sets of data are fundamentally required to describe a television picture, one giving the significant changes of brightness, and the other the positions of such changes. The total information content is calculated according to Shannon, and the means are discussed for reducing bandwidth by redistributing the data in time so as to achieve a constant rate of transmission."
- 621.397.001.4:535.623:621.317.755 2602
The Vectorscope—N. N. Parker Smith and C. J. Matley. (*Electronic Radio Eng.*, vol. 34, pp. 198-296; June, 1957.) The instrument displays as a pattern of vectors the chrominance component of the NTSC type of signal in which the component is transmitted by means of a subcarrier modulated both in amplitude and phase.
- 621.397.331.2:535.215:546.863.221 2603
Semiconductor Photosensitive Layers for Photoresistance Television Tubes—Oksman (See 2458.)
- 621.397.5 2604
High Definition on 405 Lines—(*Wireless World*, vol. 63, pp. 254-255; June, 1957.) Spot wobble at a frequency of 6 mc is synchronized in frequency and phase between camera and monitor cr tube. Primarily suggested for sup-

pressed-frame telerecording, it could be used for a high-definition service compatible with the existing 405-line standard.

621.397.5:621.396.41 2605
Bilingual Television by Pulse-Multiplex System—B. Pouzols. (*Électronique, Paris*, no. 121, pp. 21–25; December, 1956.) Outline of a single-channel multiplex system with pam for providing alternative sound transmissions. The circuits described are suitable for French standards. Tests show that crosstalk is negligible and only small modifications to normal receivers are required. See also 2300 of 1957 (Dubec).

621.397.5.001.4:535.623 2606
Test Signal for Measuring "On-the-Air" Colour-Television System Performance—R. C. Kennedy. (*RCA Rev.*, vol. 17, pp. 553–557; December, 1956.) Description of a signal used by the NBC which provides a reference level for the amplitude adjustment of the various video signals and permits the measurement of differential gain and phase distortion.

621.397.61 2607
Transistorized Television Cameras using the Miniature Vidicon—L. E. Flory, G. W. Gray, J. M. Morgan, and W. S. Pike. (*RCA Rev.*, vol. 17, pp. 469–502; December, 1956.) Description of miniature camera and portable outside-broadcasting equipment. See also 1925 of 1957 and 2610 below.

621.397.61 2608
A Video Automatic-Gain-Control Amplifier—J. O. Schroeder. (*RCA Rev.*, vol. 17, pp. 558–570; December, 1956.) Design and performance data of an amplifier successfully used by the NBC are discussed.

621.397.611:535.623 2609
Camera Tubes for Colour-Television broadcast Service—R. G. Neuhauser. (*J. Soc. Mot. Pict. Telev. Eng.*, vol. 65, pp. 636–642; December, 1956.) The general characteristics required for color-television tubes are discussed and compared with the characteristics of the vidicon and image orthicon.

621.397.611.2 2610
A Miniature Vidicon of High Sensitivity—A. D. Cope. (*RCA Rev.*, vol. 17, pp. 460–468; December, 1956.) The experimental tube described is 3 inches long; its diameter is $\frac{1}{2}$ inch. A photoconductive layer of increased sensitivity is used covering a range from 400 to 800 m μ with a maximum near 600 m μ . For applications of this tube, see 2607 above.

621.397.62 2611
Television Receiver for Metre Wavelengths—V. Biggi. (*Onde élect.*, vol. 36, pp. 1021–1030; December, 1956; vol. 37, pp. 55–67; January, 1957.) The design and application are discussed of a receiver capable of driving a relay transmitter for long-range television transmission. A special agc circuit for positive modulation systems is described.

621.397.62:539.234:546.45 2612
The Properties of Thin Beryllium Foils, and their Application to Light Modulation and Television—M. Auphan. (*Onde élect.*, vol. 36, pp. 1040–1045; December 1956.) A method is described of obtaining foils of Be 200 to 1000 Å thick tightly drawn across a supporting graticule in close proximity of a glass screen. Electrostatic charges deposited on such a screen inside a crt will result in local deflections of the foil, thus providing a means of modulating light by reflection. The application to monochrome television is outlined; experiments have been made using a foil specially corrugated to suit the optical system. Color television methods are discussed, including a compatible projection system with two tubes using foil screens:

one low-definition tube reproduces color, the other provides the high-definition luminance detail.

621.397.62:621.3.049.7 2613
Mechanized Production of TV Wiring Boards—J. Markus. (*Electronics*, vol. 30, pp. 138–143; April 1, 1957.) Description of the latest semi-automatic machines and assembly lines for manufacturing printed circuits in use by the Philco Corporation. This article brings up to date an earlier report (3811 of 1955).

621.397.62:621.373.4 2614
Analytical Approaches to Local-Oscillator Stabilization—W. Y. Pan and D. J. Carlson. (*RCA Rev.*, vol. 17, pp. 534–552; December, 1956.) The analytical treatment of frequency stability under complex thermal conditions indicated by Yau (593 of 1956) is applied to two commercial television receiver circuits. Results show that satisfactory stabilization even for frequencies beyond 1 kmc can be achieved with conventional temperature-sensitive devices.

621.397.621:621.373.444.1 2615
C.R.T. Deflection Circuit has High Efficiency—Guggi. (See 2382.)

621.397.621.2:535.623:621.385.832 2616
Methods of Local [post-deflection] Spot Position Control for Electron Beams—U. Pellegrini. (*Alta Frequenza*, vol. 25, pp. 482–504; December, 1956.) Two methods of accurately focusing the beam in a color cr tube are analyzed; in one a wire grid close to the phosphor screen is used, as; e.g., in the post-deflection-focus color kinescope [3894 of 1956 (Carpenter)], in the other the screen consists of separate aluminized strips. Differential equations are derived for the electron trajectories, and the equipotential contours and lines of flux are plotted.

621.397.8 2617
Television Interference from Sea Reflections—J. K. S. Jowett. (*Wireless World*, vol. 63, pp. 262–266; June, 1957.) A possible explanation of the flutter experienced at certain localities served by the North Hessian Tor transmitter. Quasi-specular reflection at oblique incidence may occur from sea wave fronts and beat with the direct signal attenuated by local hills. The flutter frequency is consistent with the sea wave velocity.

621.397.8 2618
Reduction of Co-channel Television Interference by Precise Frequency Control of Television Picture Carriers—W. L. Behrend. (*RCA Rev.*, vol. 17, pp. 443–459; December, 1956.) In offset carrier-frequency operation interference minima occur at some offset frequencies which are multiples of the frame frequency. To assess the importance of precise frequency control, subjective tests were made of interference visibility and the results of field tests with experimental equipment are reported.

621.397.81 2619
A Method of Predicting the Coverage of a Television Station—J. Epstein and D. W. Peterson. (*RCA Rev.*, vol. 17, pp. 571–582; December, 1956.) A method of estimating the median field strength along a radial line from the transmitter is described. The estimate is based on the plotted elevation profile and the use of theoretical and empirical curves resulting from the analysis of extensive field surveys and investigations (see; e.g., 2423 of 1953). The entire vhf and uhf spectrum is covered and the accuracy so far achieved is adequate for surveys involving large numbers of stations.

621.397.813 2620
Frequency-Dependent Equalization of Gradation for Television Signals—H. Schönfelder. (*Arch. elekt. Übertragung*, vol. 10, pp. 512–534;

December, 1956.) By limiting the equalization to the lower frequencies of the video signal, a picture of acceptable quality can be obtained; the signal/noise ratio in the dark portions is considerably improved in comparison with that for uniform equalization of gradation. An upper limiting frequency of about 3 mc is chosen according to system conditions and the amount of distortion tolerable. The design of a suitable equalizing circuit is detailed and experimental results are illustrated by oscillograms and reproductions of test pictures.

TRANSMISSION

621.376.3:621.373.421 2621
Frequency-Modulated Quartz Oscillators for Broadcasting Equipment—Mortley. (See 2375.)

621.396.712:621.376.3 2622
Frequency-Modulated V.H.F. Transmitter Technique—A. C. Beck, F. T. Norbury, and J. L. Storr-Best. (*Proc. IEE*, Part B, vol. 104, pp. 225–238; May, 1957. Discussion, pp. 249–253.) The general planning and design of the complete vhf transmitting equipment used by the BBC on its sites is surveyed, including problems of unattended operation, automatic phasing of paralleled amplifiers, and 3-program common-antenna working; special reference is made to a current 10-kw fm transmitter operating in Band II (87.5–100 mc.)

TUBES AND THERMIONICS

621.314.63 2623
The Apparent Contact Potential of a Pseudo-Abrupt p - n Junction—H. Kroehmer. (*RCA Rev.*, vol. 17, pp. 515–521; December, 1956.) Junctions are studied which have constant impurity densities on both sides without abrupt transition. A finite region of transition within the space-charge region is assumed. The difference between the "apparent" contact potential found from capacitance measurements and the true potential calculated from the impurity densities provides quantitative information about the internal structure of the junction.

621.314.63 2624
On the Tail in the Transient Behaviour of Point-Contact Diodes—H. L. Armstrong. (*Proc. IRE*, vol. 45, pp. 696–697; May, 1957.) Although the main part of the transient response of small hemispherical p - n junctions is almost independent of lifetime, there is a "tail" which is almost exponential and is determined by the lifetime.

621.314.63:537.311.33 2625
Minority-Carrier Storage in Semiconductor Diodes—J. C. Henderson and J. R. Tillman. (*Proc. IEE*, Part B, vol. 104, pp. 318–333; May, 1957. Discussion, pp. 333–336.) Transient reverse-current effects in planar and hemispherical diodes of n -type base material are analyzed under various conditions, although the extent to which the analyses apply to point-contact diodes remains debatable. Experiments to test the theory and to deduce the hole lifetimes are given.

621.314.63:537.311.33 2626
Rectification Properties of Metal/Silicon Contacts—E. C. Wurst, Jr and E. H. Borneman. (*J. Appl. Phys.*, vol. 28, pp. 235–240; February, 1957.) The rectifying properties of metal/silicon contacts are related to the work function of the metal. The measured reverse saturation currents of metal/silicon diodes are greater than predicted values; the discrepancy is not yet explained.

621.314.632 2627
Strain-Energy Calculations in the Design of Cat's Whiskers for Semiconductor Devices—S. J. Morrison. (*Proc. IEE*, Part C, vol. 104,

pp. 148-153; March, 1957.) A general theory of contact pressures and deflections is derived and experiments on large-scale whisker models have shown close agreement with theory.

621.314.632:546.289 2628

A Millisecond Relaxation Process in the Reverse Current of Germanium Point-Contact Diodes—R. E. Burgess. (*Brit. J. Appl. Phys.*, vol. 8, pp. 62-63; February, 1957.) When a reverse voltage is suddenly applied to a diode initially having zero bias, a decrease of current to the final steady-state is usually found, the relaxation time being about 1 ms. It is suggested that redistribution of surface charge is the most likely cause.

621.314.7 2629

Transistor Junction Temperatures as a Function of Time—K. E. Mortenson. (*Proc. IRE*, vol. 45, pp. 504-513; April, 1957.) The step and impulse temperature responses are obtained for a one-dimensional heat-flow model and the junction temperature determined for periodic rectangular pulse excitation. The maximum, average, and minimum temperatures are plotted in terms of duty cycle, prf, and thermal time constant, and the theoretical results confirmed experimentally. The maximum junction temperature can be several times the average at low duty cycles and repetition rates.

621.314.7 2630

Temperature Dependence of Junction Transistor Parameters—W. F. Gartner. (*Proc. IRE*, vol. 45, pp. 662-680; May, 1957.) Four representative types of transistor are considered, namely Ge *p-n-p* alloy, Ge *n-p-n* grown, Ge *n-p-n* rate-grown, and Si *n-p-n* grown types. The temperature dependence of their characteristics is calculated from existing theories of transistor performance and the known temperature behavior of the semiconductor properties. The results are expressed in terms of the four-pole and equivalent-circuit parameters.

621.314.7 2631

Point-Contact Transistor Studies using Radioactive Collectors—D. Haneman and A. J. Mortlock. (*Proc. Phys. Soc.*, vol. 70, pp. 145-147; January 1, 1957.) Pile-activated pure antimony points containing ¹²⁵Sb in contact with single crystals of *n*-type Ge were formed. The activity transferred and the surface distribution were then measured.

621.314.7 2632

The Characteristics and the Charge Carrier Distribution of Alloy Junction Transistors—W. Engbert. (*Telefunken Ztg.*, vol. 29, pp. 277-287; December, 1956. English summary, p. 295.) The distribution of carrier and hole densities and potentials in the *p-n-p* regions is derived from the transistor characteristics and the amount of doping.

621.314.7:621.396.621 2633

Tetrajunction Transistor Simplifies Receiver Design—Farber, Proudfit, St. John, and Wilhelmsen. (See 2579.)

621.314.7.012.8 2634

The Effect of Non-Ideal Emitter Junctions on the Behaviour of Junction Transistors—E. Baldinger, W. Czaja and M. Nicolet. (*Helv. Phys. Acta*, vol. 29, pp. 428-430; December 15, 1956. In German.) In the transistor equivalent circuit [see, e.g., 1193 of 1955 (Giacoletto)] the emitter "lead" resistance R_e , introduced to allow for the difference between theory and experimental behavior, varies according to the operating point. By modifying the slope S by a

factor m between 0.5 and 1, a value of R_e constant over the whole range can be assumed.

621.383.2:621.385.83 2635

Shutter Image-Converter Tubes—B. R. Linden and P. A. Snell. (*Proc. IRE*, vol. 45, pp. 513-523, April, 1957.) A triode type is described which uses a mesh, near the cathode, to gate the photoelectron emission. The electron-optical theory is presented for electrostatically and magnetically focused types and illustrated by practical results.

621.383.27 2636

Optical Feedback in Photomultipliers—R. Gerharz. (*J. Electronics*, vol. 2, pp. 409-415; March, 1957.) The optical feedback to the photo-cathode, arising from electro-fluorescence induced by the dark-current, has been investigated for commercial photomultipliers Types 1P21 and 931A.

621.383.27(47) 2637

Commercial Types of Multistage Photomultipliers—I. Ya. Breido, B. M. Glukhovskoi, and L. G. Leiteizen. (*Radiotekhnika i Elektronika*, vol. 1, pp. 1344-1356; October, 1956.) Description of Russian "commercial" types with characteristic curves and tabulated data.

621.383.42.011.4 2638

On the Capacitance of Selenium Photocells—M. Bichara. (*C. R. Acad. Sci., Paris*, vol. 244, pp. 742-744; February 4, 1957.) Results of measurements on forty-six samples are tabulated.

621.383.5:537.311.33 2639

A New Semiconductor Photocell using Lateral Photoeffect—J. T. Wallmark. (*Proc. IRE*, vol. 45, pp. 474-483; April, 1957.) A non-uniform illumination produces a lateral voltage parallel to a germanium-indium junction. The output voltage is a linear function of the position of the light spot and the sensitivity is approximately 200 $\mu\text{A/lumen}$. The spot position and the direction of the light beam can be measured to less than 100 Å and 0.1 seconds of arc, respectively.

621.385-71 2640

Vapotron Technique—C. Beurtheret. (*Rev. Tech. Comp. franç. Thompson-Houston*, no. 24, pp. 53-83; December, 1956.) The development of this method of cooling high-power transmitting tubes is outlined (see also 542 of 1952) together with the underlying theory of heat transfer. Results of tests on various forms of anode dissipating surface and for various metals are discussed. Illustrations show the evolution of the vapotron from 1950 to date, including associated equipment. Thirty-two references.

621.385:621.317.331 2641

A New Method for the Detection of Thin Conducting Films in Thermionic Valves—F. H. Reynolds and M. W. Rogers. (*Proc. IEE*, Part B, vol. 104, pp. 337-340; May, 1957.) A system of three electrodes is painted on the outside of the bulb over the region where the film is to be detected, and connected to an impedance bridge.

621.385:621.318.57.032.2 2642

Improved Keep-Alive Design for T. R. Tubes—L. Gould. (*Proc. IRE*, vol. 45, pp. 530-533; April, 1957.) By insulating the cone wall and using a stainless-steel cathode a life in excess of 100 h is possible.

621.385.029.6 2643

International Congress on Microwave Valves—(*Onde élect.*, vol. 36, pp. 866-996;

November, 1956.) Selection of papers presented at the 1956 Congress in Paris. See 1267 of 1957.

621.385.029.6 2644

The Assembly of Microwave Valves by Brazing—R. Paliès. (*Rev. tech. Comp. franç. Thompson-Houston*, no. 24, pp. 41-51; December, 1956.) The method of brazing by resistance heating is described and illustrated by two examples of its application.

621.385.029.6:621.317.36 2645

The Measurement of Magnetron Frequency Pulling—J. R. G. Twisleton. (*Proc. IEE*, Part C, vol. 104, pp. 8-12; March, 1957.) The theoretical frequency pulling when multiple reflected waves exist in the output feeder is estimated and the performance of a typical testing waveguide system is examined.

621.385.029.6:621.396.822 2646

Experiments on Noise Reduction in Backward-Wave Amplifiers—M. R. Currie and D. C. Forster. (*Proc. IRE*, vol. 45, p. 690; May, 1957.) Using a tube with a gun structure which produces an annular electron beam noise figures approaching the theoretical ones were obtained.

621.385.029.65 2647

Backward-Wave Oscillator Experiments at 100 to 200 Kilomegacycles—A. Karp. (*Proc. IRE*, vol. 45, pp. 496-503; April, 1957.) The circuit structure consists of a ridged waveguide with transverse slots in the broad wall. For electron beam velocities between 650 and 2700 v and current densities between 3 and 10 a/cm^2 , probable power outputs of a few tenths of a milliwatt were obtained.

621.385.032.3 2648

High-Temperature Properties of Tungsten which Influence Filament Temperatures, Lives and Thermionic-Emission Densities—R. N. Bloomer. (*Proc. IEE*, Part B, vol. 104, pp. 153-157; March, 1957.) Calculations using reliable published data are compared with experimental results.

621.385.3 2649

On the Amplification Factor of the Triode—E. B. Moullin. (*Proc. IEE*, Part C, vol. 104, pp. 222-232; March, 1957.) A new treatment of the characteristic of the triode, as expressed by the equation $I_a = f(V_a + \mu V_g)$. The limitations in the conventional method are discussed. See also 1985 of 1957 (Hammond).

621.385.5:621.373.422 2650

Transitron Negative Resistance—A. G. Bogle. (*Electronic Radio Eng.*, vol. 34, pp. 170-174; May, 1957.) A detailed investigation shows that the negative resistance is approximately inversely proportional to the cathode current within ± 10 per cent over the range 3-90 kΩ.

MISCELLANEOUS

621.3.002.2 2651

Electronic Subminiaturization Techniques—(*Tech. News Bull. Nat. Bur. Stand.*, vol. 41, pp. 3-5; January, 1957.) Techniques developed in connection with the program for the U. S. Navy Bureau of Aeronautics are discussed; items mentioned include a commutator-type gain control using a tape resistor on a glass tube carrying longitudinal stripes of conducting paint, a temperature-compensated permeability-tuned inductor, high-temperature litz wire, and IF transformers with ferrite sleeve and tuning screw.

